ENVIRONMENTAL CHAMBER STUDIES OF MAXIMUM INCREMENTAL REACTIVITIES OF VOLATILE ORGANIC COMPOUNDS

by

**William P. L. Carter, John A. Pierce,
Irina L. Malkina, Dongmin Luo, William D. Long**

Report to

**Coordinating Research Council, Inc.
Project No. ME-9**

**California Air Resources Board
Contract no. A032-0692**

**South Coast Air Quality Management District
Technical Services Agreement Carter-88
Contract No. C91323**

**United States Environmental Protection Agency
Cooperative Agreement No. CR-814396-01-0**

**University Corporation of Atmospheric Research
Contract No. 59166**

Dow Corning Corporation

April 1, 1993

**Statewide Air Pollution Research Center
University of California
Riverside, CA 92521**

PREFACE

The report describes work carried out at the Statewide Air Pollution Research Center (SAPRC) at the University of California at Riverside under funding from six different contracts or agreements. The major funding for this work, covering the preparation of this report and most of the experiments carried out in 1991 and 1992, was provided jointly by the California Air Resources Board (CARB) through contract number A032-0962 and the Coordinating Research Council, Inc. (CRC), through project number ME-9. The National Aerosol Association (NAA) provided funding to the CRC project for the experiments with propane, isobutane, and dimethyl ether, and the Chemical Manufacturers Association (CMA) provided funding to the CRC project for the experiments with acetone. The initial experiments and methods development were funded by the United States EPA through cooperative agreement CR-814396-01-0. The experiments with ethanol, isopropanol, MTBE, ethoxyethanol, and carbitol were funded by the California South Coast Air Quality Management District (SCAQMD) through Technical Services Agreement No. Carter-88. The experiments with isoprene were funded as part of the EPA's Southern Oxidant Study through University Corporation of Atmospheric Research (UCAR) Contract No. 59166. The experiments with the siloxanes were funded by the Dow Corning Corporation. Finally, the California SCAQMD provided funding for the modular building where all the experiments in 1992 were carried out. Dr. William P. L. Carter of SAPRC was Principal Investigator on all these contracts except for the UCAR contract, where Dr. Roger Atkinson of SAPRC was co-Principal Investigator with Dr. Carter.

ABSTRACT

The effects of 36 representative volatile organic compounds (VOCs) and CO on ozone formation, NO oxidation, and OH radical levels were measured in a series of environmental chamber experiments representing conditions where VOCs have the greatest effect on photochemical ozone formation. The experiments consisted of repeated 6-hour indoor chamber irradiations of a simplified mixture of ozone precursors with NO_x in excess, alternating with runs with varying amounts of a test VOC added. The VOCs studied included representative alkanes, alkenes, aromatic hydrocarbons, aldehydes, alcohols, ethers, alcohol ethers, and siloxanes. CO, Acetone and 2-chloromethyl-3-chloropropene were also studied. Reactions of formaldehyde, acetone, the methylbenzenes and the alkenes had the largest positive effects on OH radical levels, and because of this they caused the most NO oxidation and ozone formation per molecule reacted. Reactions of the siloxanes and the C_{6+} n-alkanes had the most inhibiting effects on radicals, causing them to inhibit NO oxidation and ozone formation under the conditions of these experiments. The other compounds had smaller and usually negative effects on OH radicals, and had moderate but positive effects on ozone formed and NO oxidized. Information was also obtained on amounts of NO oxidation caused directly by the reactions of the added VOCs or their products.

The results are compared with model calculations using a detailed atmospheric photochemical reaction mechanism, and new or refined mechanisms for isobutene, isooctane, MTBE and alcohol ethers were developed. The model fit the data to within the experimental uncertainties for approximately half the VOCs, and generally predicted the observed qualitative reactivity trends. However, the results indicate that refinements to the mechanisms for alkenes and aromatics are needed. Additional data needs, some of which we will be addressing in the next phase of our ongoing studies, are discussed.

ACKNOWLEDGEMENTS

The authors wish to acknowledge the project officers for the contracts funding this research and other representatives of the funding agencies for their support and assistance in carrying out this work and related projects. These include Mr. Bart Croes of the CARB; Drs. Alan Lloyd, Chung Liu, Henry Hogo and Julia Lester of the SCAQMD; Mr. Timothy Belian of the CRC, Dr. Harry McCain of Aeropres Corporation (representing the NAA); Dr. David Morgott of Eastman Kodak (representing the CMA); Dr. Cecil Frye of Dow Corning Corporation, and Drs. Basil Dimitriades, Joseph J. Bufalini, and Marcia Dodge of the EPA. We also wish to thank the members of the CRC/APRAC committee who took the time to review the first draft of this report and provide us with useful comments.

The authors also acknowledge Dr. Roger Atkinson of SAPRC for many helpful discussions, and for assistance in carrying out these experiments and administering the above-referenced contracts. We also acknowledge Ms. Patricia McElroy, who conducted a major portion of the experimental work prior to June of 1990. Ms. Sara Aschmann and Dr. Ernesto Tuazon also provided occasional valuable assistance in carrying out these experiments, and Ms. Minn Poe provided assistance with computer programming in the data collection and analysis. Ms. Kathalena M. Smihula and Mr. Armando D. Avallone of the UCR College of Engineering, Center for Environmental Research and Technology (CE-CERT) assisted in carrying out the later experiments in this study. We thank Dr. Joseph Norbeck, director of CE-CERT, for supporting Ms. Smihula and Mr. Avallone during this period.

EXECUTIVE SUMMARY

Background

The formation of ground-level ozone is caused by the gas-phase interactions of emitted volatile organic compounds (VOCs) and oxides of nitrogen (NO_x) in the presence of sunlight. Reducing emissions of both these ozone precursors is necessary to achieve ozone air quality standards. Traditionally VOC control strategies to reduce ozone have focused on reducing the total mass of VOC emissions, but not all VOCs are equal in the amount of ozone formation they cause. Control strategies which take into account these differences in "reactivities" of VOCs might provide a means for additional ozone reduction which could supplement mass-based controls. Examples of such control strategies include conversion of motor vehicles to alternative fuels and solvent substitutions. However, before reactivity-based VOC strategies can be implemented, there must be a means to quantify VOC reactivity which is sufficiently reliable that it can be used in regulatory applications.

The most direct quantitative measure of the degree to which a VOC contributes to ozone formation in a photochemical air pollution episode is its "incremental reactivity". This is defined as the amount of additional ozone formation resulting from the addition of a small amount of the compound to the emissions in the episode, divided by the amount of compound added. Incremental reactivities of VOCs in the atmosphere cannot be measured experimentally because it is not feasible to duplicate in the laboratory all the environmental factors which affect reactivity. But they can be calculated using computer airshed models, given a model for airshed conditions and a mechanism for the VOCs atmospheric chemical reactions. For example, a set of models for airshed conditions throughout the U.S. and a detailed chemical mechanism were used to calculate a "Maximum Incremental Reactivity" (MIR) scale which has been adopted by the California Air Resources Board (ARB) for the derivation of reactivity adjustment factors for use in vehicle emissions standards.

However, such calculations can be no more reliable than the chemical mechanisms upon which they are based. To be minimally suitable for this purpose. such mechanisms need to be evaluated by comparing their predictions with experimental measurements of VOC reactivity. Although the MIR scale gives reactivity factors for over 100 compounds, prior to this study the mechanisms for less than a dozen have been tested against results of environmental chamber experiments, and only a few of these experiments could be considered to be incremental reactivity experiments.

Scope

This report describes the results of the first phase of a program to obtain experimental data needed to reduce the chemical mechanistic uncertainties in models used to calculate ozone reactivities of VOCs. In this phase of the program, we have focused on obtaining data to test model predictions of reactivities of VOCs under the relatively high NO_x conditions (or low ROG/NO_x ratios) where ozone yields are determined primarily by how rapidly ozone is formed and where VOCs have their greatest effect on ozone formation. This reflects the environmental conditions used to calculate the MIR scale. Although a complete assessment requires data concerning reactivities under all conditions, obtaining maximum reactivity data is of particular importance because it reflects conditions where VOC controls are the most effective ozone reduction strategy, and because maximum reactivity has been shown to be a good predictor of reactivity with respect to exposure to integrated ozone levels. Such data also have immediate practical regulatory interest, since as indicated above California ARB has adopted the MIR scale for its vehicle regulations. The specific VOCs which were studied are given on Table EX-1.

Approach

The approach consisted of carrying out a series of repeated 6-hour irradiations of a simplified mixture representing photochemical smog precursors in an indoor environmental chamber, alternating with irradiations of the same mixture with varying amounts of the test VOCs added. The amount of test VOC

Table EX-1. List of Compounds Studied.

Alkanes	Aromatics	Ethers
ethane	benzene	dimethyl ether
propane	toluene	methyl-t-butyl ether (MTBE)
n-butane	o-xylene	2-ethoxyethanol
n-hexane	m-xylene	2-(2-ethoxyethoxy)-ethanol (carbitol)
isobutane	p-xylene	
n-octane	ethylbenzene	
334-trimethyl pentane (isooctane)	123-trimethylbenzene	Others
	135-trimethylbenzene	carbon Monoxide
Alkenes	124-trimethylbenzene	acetone
ethene		
propene	Alcohols	Siloxanes
trans-2-butene	methanol	hexamethyldisiloxane
isobutene	ethanol	octamethyltetracyclo-siloxane
isoprene	isopropanol	
2-chloromethyl-3-chloropropene	Aldehydes	decamethylpentacyclo-silocane
	formaldehyde	pentamethyldisiloxanol
	acetaldehyde	

added was generally such that its addition caused at least a 30-60% change in the sum of amount of NO consumed plus the amount of ozone formed in six hours. (Thus the amount of VOC added was roughly inversely proportional to its effect on the system.) The photochemical smog precursor mixture consisted of a reactive organic gas (ROG) "mini-surrogate" containing ethene, n-hexane and m-xylene, together with oxides of nitrogen (NO_x) in air, in concentration levels appropriate to represent maximum incremental reactivity conditions. Although the ROG mini-surrogate is a simplification of the complex mixture of ROGs present in the atmosphere, model calculations showed that its use in chamber experiments could give reasonably good correlations with maximum reactivities in the atmosphere, except that its use tends to give a more sensitive measure of the effects of VOCs on ozone formation and radical levels than use of more complex mixtures. This latter characteristic is more of an advantage than a disadvantage, since it makes the experiments a more sensitive test of the chemical mechanisms.

Results.

Approximately 250 mini-surrogate - NO_x - air experiments were carried out in this study, including approximately 120 experiments where CO or one of the 35 test VOCs was added, alternating with ~130 repeated standard or "base case" experiments. Thus at least two, and usually three or more, experiments were carried out to test the reactivities of each of the test compounds. Appropriate characterization, control and actinometry experiments were also conducted in conjunction with these runs, to characterize the conditions of the runs for model evaluations. In addition, data were obtained concerning the OH radical rate constants for many of the added VOCs, including the first published measurements of the OH radical rate constant for carbitol.

Measures of Reactivity. The results of the experiments with added VOCs, together with the results of the repeated standard runs, were analyzed to yield three measures of reactivity:

- The effect of the added VOC on the amount of NO reacted plus the amount of ozone formed at each hour in the experiment, divided by the added VOC which reacted up to that hour. This is referred to as "ozone mechanistic reactivity".

- The effect of the added VOC on integrated OH radical levels (abbreviated IntOH) relative to the amount of added VOC which reacted. This is referred to as the IntOH mechanistic reactivity.

- A quantity which approximates the amount of NO oxidation and ozone formation caused directly by the added VOC's reactions, as opposed to the

change in NO oxidation and ozone formation caused by the effects of the VOC on the reactions of the other VOCs. This is referred to as the "conversion factor".

The ozone mechanistic reactivity provides a direct measure of the effect of the VOC on the reactions responsible for ozone formation, while the IntOH reactivities and the conversion factors provide a means of testing the various aspects of the mechanism which affect a VOC's reactivity in greater detail than would otherwise be the case.

Note that ozone mechanistic reactivities are not the same as incremental reactivities, which have been proposed as a basis for evaluating relative effects of VOC emissions on ozone formation. Incremental reactivities refer to the effects of the VOCs relative to the amount added, while the mechanistic reactivities refer to the effects of the VOCs relative to the amount reacted. For example, while methanol has a relatively low incremental reactivity because it reacts fairly slowly in the atmosphere, it has a very high mechanistic reactivity because once it does react it has a large effect on ozone formation because it forms a highly reactive oxidation product, i.e., formaldehyde. Although incremental reactivities are more relevant in terms of ozone control strategies, the mechanistic reactivities are the more useful to compare with model simulations because they depend on the most uncertain aspects of the VOCs reaction mechanism. They also provide a means to compare the effects of differences in reaction mechanisms for the various types of VOCs, with the (often much larger) effects of differences in their reaction rates being, at least to some extent, factored out.

Data Obtained. The data obtained are consistent with results of previous experimental and computer modeling studies in showing that different VOCs have significantly different effects on ozone formation, even after differences in reaction rates are taken into account. The measure which has the most direct relationship to the effect of a VOC's reactions on ozone formation is its ozone mechanistic reactivity. This quantity, expressed as moles O_3 formed + NO oxidized per mole carbon reacted, ranged in these experiments from a high of approximately 1.5 for 1,3,5-trimethylbenzene, formaldehyde, and acetone to lows of -1 to -1.5 for the siloxanes for the conditions of these experiments. Other compounds found to have high mechanistic reactivities on a per carbon basis were ethane, all the alkenes, all the other alkylbenzenes (but not benzene itself), methanol and dimethyl ether. These are the compounds with the greatest efficiency in promoting ozone formation once they react. Propane, n-butane, isobutane, isooctane, benzene, acetaldehyde, and the C3+ alcohols and ethers also promote ozone formation in these experiments, but with much less efficiency, with the efficiency being lowest for isooctane, benzene and carbitol. The C6+

n-alkanes and the siloxanes inhibit NO oxidation and ozone formation in our experiments.

Approximately half the compounds studied tended to enhance OH radical levels under the conditions of these experiments, with the rest tending to inhibit them to various degrees. All the VOCs which enhanced OH radicals had high ozone mechanistic reactivities. These included formaldehyde, acetone, methanol, the alkenes and the alkylbenzenes. Most other VOCs tend to suppress radicals, though some to much greater extents than others. Most of these radical suppressing compounds still had positive ozone reactivities under the conditions of our experiments. In these cases the additional ozone formation caused by the VOC's direct reactions is sufficient to counter their effects on reducing ozone formation from other VOCs. But, as one would expect, the efficiency of ozone formation decreases as the tendency to suppress radicals increased, and when the suppression becomes sufficiently large, it overwhelms the positive effect on ozone formation of the VOC's direct reactions, making the compound a net ozone inhibitor (i.e., having a negative ozone reactivity). This is the case for the siloxanes and the C_{6+} n-alkanes under the conditions of our experiments.

Note, however, that this balance between positive and negative effects for these compounds may be different in atmospheric conditions, and compounds which were negatively reactive towards ozone in these experiments may be positively reactive in the atmosphere. Thus the primary utility of these data are to test the ability of the chemical mechanisms to predict reactivity, rather than directly measure what reactivity would be in the atmosphere. Nevertheless, at least for maximum reactivity conditions, one would expect the relative general reactivity trends in the atmosphere to be similar to those observed in these experiments.

Comparison with Model Predictions.

The results of these experiments were compared with predictions of an updated version of the SAPRC detailed chemical mechanism which has been used previously to calculate reactivity scales. A small adjustment had to be made to the mechanism for m-xylene because the model otherwise tended to underpredict the rate of ozone formation in most of the base case runs. This was done to avoid biases being introduced in model predictions on effects of the added VOCs which might result if the model did not correctly simulate the base case run, though for most VOCs the reactivity predictions were found to be insensitive to this adjustment. Except as noted, no other adjustments were made to the model when simulating the experimental reactivities of these VOCs.

The performance of the updated SAPRC mechanism in simulating the ozone mechanistic reactivities is shown on Figure EX-1, which gives plots of the experimental vs calculated ozone mechanistic reactivities for most of the VOCs which were studied. (Acetone and formaldehyde, which are off scale on the positive side, and the volatile siloxanes, which are off scale on the negative side, are not shown.) This figure also shows the wide range of values of ozone mechanistic reactivities which were measured and calculated for the species which were studied.

In general, as can be seen from Figure 1, the model was found to simulate the ozone reactivities to within the experimental uncertainties for approximately half the VOCs studied, and generally correctly predicted the observed reactivity trends. However, a number of discrepancies were observed. The model over-predicted the reactivity of formaldehyde in the initial stages of the experiments, and overpredicted the reactivity of acetone. A large discrepancy was observed in the prediction of the reactivity of iso-octane, which was found to be probably due to ignoring steric effects when estimating its mechanism. The model tended to underpredict the reactivities of alkenes, and incorrectly predicted how their reactivities vary with time. The model somewhat under-predicted the incremental reactivities of most, though not all, the aromatics, and did not account for observed reactivity differences among xylene and

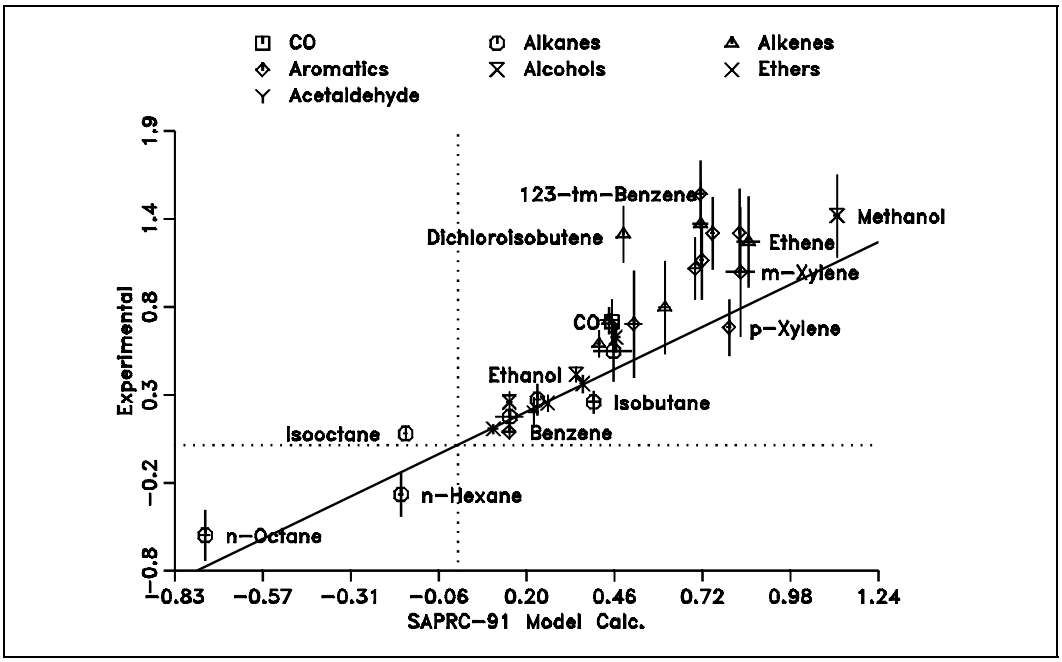

Figure EX-1. Plot of averages of the experimental ozone mechanistic reactivities against averages of results of model simulations of the experiments using the SAPRC-91 mechanism. (Units are ppm ozone formed and NO oxidized per ppmC VOC reacted.)

trimethylbenzene isomers, nor did it explain the observation of negative conversion factors for benzene.

The results of these experiments were used to adjust or refine the chemical mechanisms for methyl t-butyl ether (MTBE) and the alcohol ethers ethoxyethanol and carbitol. The model could fit the reactivity data if it is assumed that these ethers have significantly lower organic nitrate yields, i.e., are less radical inhibiting, than similarly sized alkanes. Thus, these data indicate these compounds are somewhat more reactive towards ozone formation than one might estimate *a-priori*.

Conclusions.

We believe that this study was successful in its objective of providing the type of data needed for reducing the chemical mechanistic uncertainties in maximum reactivity scales for ozone formation in the atmosphere. Data were obtained which can test model predictions of maximum reactivities of a wide variety of VOCs, many of which have never been studied previously in environmental chamber experiments suitable for mechanism evaluation. For example, this study has provided the only data available concerning the ozone reactivities of representative ethers, alcohol ethers, and siloxanes, has provided the most useful presently available data concerning ozone reactivities of alkanes, and has provided a unique and valuable addition to the existing data for the other VOCs, most of which have not been previously studied in this way.

The ultimate practical benefit of these data for evaluating mechanisms will come when the mechanisms used to calculate VOC reactivity scales are updated to take these results into account. The preliminary evaluation of the SAPRC mechanisms which was carried out as part of this study showed that while the mechanism performs reasonably well in simulating the general reactivity trends and rankings among the VOCs, there are a number of discrepancies which will need to be addressed. These will be taken into account when the mechanism is updated.

It is important to recognize, however, that this study does not provide all the data needed to adequately evaluate the chemical mechanisms for predicting atmospheric reactivities. The present experiments are not suitable for testing mechanisms under low NO_x conditions, and no information was obtained on the effect of changing the base ROG mixture on measured VOC reactivities. The next phase of this study should address at least some of these additional data needs.

TABLE OF CONTENTS

	Page
EXECUTIVE SUMMARY	iv
LIST OF TABLES	xiii
LIST OF FIGURES	xiv
GLOSSARY OF TERMS, SYMBOLS AND ACRONYMS	xvii
I. INTRODUCTION AND BACKGROUND	1
A. Introduction	1
B. Quantification of Reactivity	2
C. Objectives and Approach of This Study	5
1. Reactivities Relative to Ozone Formation and NO Oxidation	6
2. Reactivity with Respect to OH Radical Levels	8
3. Direct and Indirect Reactivities and Conversion Factors	9
4. Measurement of OH Radical Rate Constants	13
II. EXPERIMENTAL METHODS	14
A. Chamber	14
B. Experimental Procedures	15
C. Analytical Methods	16
1. Gas Chromatograph Analyses	16
2. Continuous Monitoring Instruments	20
3. Formaldehyde Analysis	22
D. Characterization of the Light Source in the Chamber	23
E. Other Characterization Experiments	24
III. EXPERIMENTAL RESULTS	26
A. Derivation of OH Radical Rate Constant Ratios, and Estimates of Chamber Dilution Rates	26
1. Derivation of Dilution Rate.	34
2. Discussion of Kinetic Data Obtained.	40
3. Effect of 2-Chloromethyl-3-chloropropene on the Apparent n-Hexane/ m-Xylene Rate Constant Ratio.	41
B. Results of Mini-Surrogate Runs: Variations of Run Conditions	43
1. Variations in Light Intensity.	52
2. Variations in Temperature.	53
3. Variations in Initial Reactant Concentrations.	54
C. Results of the Mini-Surrogate Runs: Derivation of Reactivities	56

Page

1. Experimental Results Used to Quantify Reactivity . . . 56
2. Derivation of Base Case Results 62
3. Measured VOC Reactivities 68

IV. MODEL SIMULATIONS 76
A. Chemical Mechanisms 76
1. The SAPRC-90 Mechanism 76
2. The SAPRC-91 Mechanism 77
3. VOCs Added to the Mechanisms 80
a. Ethoxyethanol and Carbitol. 81
b. 2-Chloromethyl-3-chloropropene. 85
B. Chamber Characterization Model 85
C. Results of Model Simulations of Base Case Experiments, and Modifications to Base ROG Mechanism 87
D. Model Simulations of Reactivity Experiments 89
1. Results for VOCs with Adjusted or Modified Mechanisms . 90
a. Ethers 94
b. Isobutane 97
c. Isooctane 99
d. Siloxanes 102
2. Results for Unadjusted Mechanisms 102

V. DISCUSSION 105
A. General Reactivity Trends 105
B. Mechanism Performance Evaluation 109
1. Utility of Data Base 109
2. Performance of the SAPRC Detailed Mechanisms 111
a. Alkanes. 112
b. Alkenes. 114
c. Aromatics 115
d. Aldehydes and Ketones. 116
e. Alcohols and Ethers. 118
f. Siloxanes. 119

VI. CONCLUSIONS 120

VII. REFERENCES 122

APPENDIX A. DETAILED DATA TABULATIONS AND PLOTS A-1

APPENDIX B. EXAMPLE OF DATA CALCULATIONS: ETC-226 . . . . . B-1

LIST OF TABLES

Number		page
1.	Chronological Listing of Environmental Chamber Experiments.	27
2.	OH Radical Rate Constants Derived from the Mini-Surrogate Chamber Runs Compared with Literature Values, and Dilution Rate Estimates Derived Using the Literature Rate Constant Ratios.	35
3.	Conditions and Selected Results of the Mini-Surrogate Runs used for Reactivity Assessment	44
4.	Results of Regression Analysis of Effects of Run Conditions on Results of Standard Runs, and Regression Parameters Used to Estimate Base Case Results for Conditions of the Added VOC Runs.	66
5.	Summary of Reactivity Results for the Test VOC Experiments. (Quantities in parentheses are uncertainty estimates.)	70
6.	Optimized Aromatic Product Parameters in the SAPRC-90 and SAPRC-91 Mechanisms.	80
7.	Averages of the Experimental and Calculated 6-hour d(O_3-NO) Reactivities for all the VOCs studied.	91
8.	Averages of the Experimental and Calculated 6-hour IntOH Reactivities for all the VOCs studied.	92
9.	Averages of the Experimental and Calculated 6-hour Conversion Factors for all the VOCs studied.	93
10.	Estimated and Adjusted Organic Nitrate Yields for all Ethers Studied in this Program.	95
A-1	Derivation of Reactivities with Respect to Hourly Ozone Formation and NO Oxidation for all Test VOC Experiments.	A-2
A-2	Derivation of Reactivities with Respect to Hourly Integrated OH Radical Levels for all Test VOC Experiments.	A-18
A-3	Derivation of Conversion Factors for all the Test VOC Experiments.	A-34

LIST OF FIGURES

Number		page
1.	Diagram of the SAPRC Indoor Teflon Chamber #2 (ETC), and associated instrumentation.	14
2.	Plots of Equation (XIX) for n-hexane from all the mini-surrogate experiments conducted after the computer GC data system was installed.	36
3.	Plots of Equation (XIX) for the alkylbenzenes from the added alkylbenzene mini-surrogate experiments.	37
4.	Plots of Equation (XIX) for dimethyl ether, ethoxyethanol, carbitol and 2-chloromethyl-3-chloropropene from the mini-surrogate experiments where they were present.	38
5.	Plot of Equation (XX) for representative runs.	40
6.	Plots of Equation (XIX) for n-hexane data from the mini-surrogate experiments with ~100 ppb added 2-chloromethyl-3-chlorobutene.	43
7.	Concentration - time plots of the major species in the representative Set 1 standard mini-surrogate run ETC-087.	49
8.	Concentration - time plots of the major species in the representative Set 2 standard mini-surrogate run ETC-137.	50
9.	Concentration - time plots of the major species in the representative Set 3 standard mini-surrogate run ETC-292.	51
10.	Plot of measured NO2 photolysis rates against ETC run number.	53
11.	Plot of average temperature of the mini-surrogate experiments against ETC run number.	54
12.	Plots of initial reactant concentrations against run number for all the standard mini-surrogate experiments.	55
13.	Representative plots of -ln[m-Xylene] against time and d(O3-NO), showing best fit lines or quadratic regression curves.	59
14.	Plots of the t=2, 4, and 6-hour d(O3-NO) results against ETC run number for all the base case experiments.	63
15.	Plots of the t=2, 4, and 6-hour IntOH results against ETC run number for all the base case experiments.	63
16.	Plots of the 6-hour ConvR results against ETC run number for all the base case experiments.	64
17.	Concentration - time plots of ozone, NO, and NO_2 for the mini-surrogate runs where benzene was added.	74
18.	Plots of experimental and calculated 6-hour d(O_3-NO) and IntOH mechanistic reactivities against amount of VOC added for the ethoxyethanol experiments.	96
19.	Plots of experimental and calculated 6-hour d(O_3-NO) and IntOH mechanistic reactivities against amount of VOC added for the carbitol experiments.	96

Number page

20. Plots of selected experimental and calculated reactivity results for isobutane. 98

21. Plot of averages of the experimental 6-hour d(O3-NO) mechanistic reactivities against averages of results of model simulations of the experiments using the SAPRC-91 mechanism. 103

22. Plot of averages of the experimental 6-hour IntOH mechanistic reactivities against averages of results of model simulations of the experiments using the SAPRC-91 mechanism. 103

23. Plot of averages of experimental 6-hour Conversion Factors against averages of results of model simulations of the experiments using the SAPRC-91 mechanism. 104

A-1 Plots of reactivity results for Ethane. A-38
A-2 Plots of reactivity results for Propane. A-39
A-3 Plots of reactivity results for n-Butane. A-40
A-4 Plots of reactivity results for Isobutane. A-41
A-5 Plots of reactivity results for n-Hexane. A-42
A-6 Plots of reactivity results for n-Octane. A-43
A-7 Plots of reactivity results for Isooctane. A-44
A-8 Plots of reactivity results for Ethene. A-45
A-9 Plots of reactivity results for Propene. A-46
A-10 Plots of reactivity results for Isobutene. A-47
A-11 Plots of reactivity results for trans-2-Butene. A-48
A-12 Plots of reactivity results for Isoprene. A-49
A-13 Plots of reactivity results for 2-Chloromethyl-3-Chloropropene. . A-50
A-14 Plots of reactivity results for Benzene. A-51
A-15 Plots of reactivity results for Toluene. A-52
A-16 Plots of reactivity results for Ethylbenzene. A-53
A-17 Plots of reactivity results for o-Xylene. A-54
A-18 Plots of reactivity results for m-Xylene. A-55
A-19 Plots of reactivity results for p-Xylene. A-56
A-20 Plots of reactivity results for 135-trimethyl Benzene. A-57
A-21 Plots of reactivity results for 124-trimethyl Benzene. A-58
A-22 Plots of reactivity results for 123-trimethyl Benzene. A-59
A-23 Plots of reactivity results for Methanol. A-60
A-24 Plots of reactivity results for Ethanol. A-61
A-25 Plots of reactivity results for Isopropanol. A-62
A-26 Plots of reactivity results for Dimethyl Ether. A-63
A-27 Plots of reactivity results for MTBE. A-64
A-28 Plots of reactivity results for Ethoxyethanol. A-65
A-29 Plots of reactivity results for Carbitol. A-66
A-30 Plots of reactivity results for Formaldehyde. A-67
A-31 Plots of reactivity results for Acetaldehyde. A-68
A-32 Plots of reactivity results for Acetone. A-69

Number page

A-33 Plots of reactivity results for Hexamethyldisiloxane. A-70
A-34 Plots of reactivity results for Octamethylcyclotetrasiloxane. . . A-71
A-35 Plots of reactivity results for Decamethylcyclopentasiloxane. . . A-72
A-36 Plots of reactivity results for Pentamethyldisiloxanol A-73
A-37 Plots of reactivity results for Carbon Monoxide A-74

GLOSSARY OF TERMS, SYMBOLS AND ACRONYMS

Adjusted Base Xylene Mechanism Mechanisms with the parameters in the m-xylene mechanism re-optimized so the model would better fit the results of the Set 3 base case experiments.

Base Case or **Base Case Experiment** The atmospheric or experimental condition for which the VOC reactivity is being determined. In the context of this study, the base case experiment is the standard 6-hour mini-surrogate - NO_x - air irradiation in the ETC Chamber.

Base ROG Surrogate The mixture of reactive organic gases used in the base case experiment to represent the mixture of all reacting organics emitted into the atmosphere. In these experiments, the base ROG surrogate is the "mini-surrogate" consisting of ethene, n-hexane, and m-xylene.

CARB California Air Resources Board.

Carbitol 2-(2-ethoxyethoxy)-ethanol.

Characterization Experiments Experiments conducted for the purpose of determining chamber effects or assuring that the chamber characteristics are normal.

Chlorobutene Refers to 2-Chloromethyl-3-chloropropene in the context of this report.

CMA Chemical Manufacturers Association.

Conversion Factor (ConvF) The direct reactivity of the VOC relative to the amount of VOC reacted, or the number of molecules of NO converted (oxidized) and ozone formed from the reactions of the radicals formed when one molecule of the VOC reacts. Also called the "Direct Mechanistic Reactivity". Note that the "ConvF" derived from the experimental data using Equation (XVI) is only an approximation of the true conversion factor.

Conversion Ratio (ConvR) The ratio of $d(O_3\text{-}NO)^{base}$ to $IntOH^{base}$. This is measured in the base case experiments to provide a means to estimate $d(O_3\text{-}NO)^{base\ rog(test)}$ from $IntOH^{test}$.

CRC Coordinating Research Council, inc.

D The dilution rate, or first order rate of reduction of concentrations of species due to dilution.

Direct Reactivity The amount of NO oxidation and ozone formation in an added test VOC experiment which is caused directly by reactions of radicals formed from the reactions of the test VOC or one of its oxidation products. It does not count the effect of the VOC on how much ozone is formed from radicals formed the reactions of the components of the base ROG surrogate or its products, even though in general the VOC may affect this.

Direct Incremental Reactivity (IR^{direct}) The direct reactivity of the VOC relative to the amount of VOC added. Given by $d(O_3\text{-}NO)^{voc}$ divided by the amount of VOC added.

Direct Mechanistic Reactivity (MR^{direct}). The direct reactivity of the VOC relative to the amount of VOC reacted. Given by $d(O_3\text{-}NO)^{voc}$ divided by the amount of VOC reacted. Also called the "conversion factor" (or ConvF), since it reflects the number of molecules of NO converted (oxidized) when one molecule of the VOC reacts. Note that the "ConvF" derived from the experimental data is only an approximation of the true direct mechanistic reactivity.

$d(O_3\text{-}NO)$ The sum of the amount of ozone formed and the amount of NO reacted during the experiment, or $\Delta[O_3]\text{-}\Delta[NO]$. Directly related to the chemical processes responsible for ozone formation.

$d(O_3\text{-}NO)^{base}$ The $\Delta[O_3]\text{-}\Delta[NO]$ measured in a base case experiment, or estimated for a hypothetical base case experiment if it were carried out under the same conditions as a particular added VOC experiment.

$d(O_3\text{-}NO)^{base\ rog(test)}$ The amount of NO oxidation and ozone formation in an experiment with a test VOC added which can be attributed to the reactions of radicals formed from the reactions of a component of the base ROG mixture or one of its oxidation products. Estimated by the product of the Conversion Ratio and $IntOH^{test}$.

$d(O_3\text{-}NO)^{test}$ The $\Delta[O_3]\text{-}\Delta[NO]$ measured in an experiment where a test VOC was added.

$d(O_3\text{-}NO)^{voc}$ The amount of NO oxidation and ozone formation which can be attributed to the reactions of radicals formed directly from the reactions of the VOC or one of its oxidation products. Estimated by $d(O_3\text{-}NO)^{test}$-$d(O_3\text{-}NO)^{base\ ROG(test)}$.

EPA United States Environmental Protection Agency.

ETC The SAPRC Indoor Teflon Chamber #2, or "Ernie's Teflon Chamber". (Named after Ernesto Tuazon, who originally designed this chamber.) This chamber was used for all experiments in this report.

Ethoxyethanol Always 2-ethoxyethanol in the context of this report.

GC Gas Chromatography.

Incremental Reactivity (IR) The change in an experimental or calculated photochemical smog manifestation caused by adding a VOC to a base case experiment or episode, divided by the amount of VOC added. In the context of airshed modeling, it is defined for the case where the amount of VOC added approaches zero. In the context of this report, it is defined for the actual amounts of VOC added in the experiment, and thus in general may depend on the amount of VOC added. In this report, the manifestation could be ozone formed, ozone formed + NO oxidized, integrated OH radical levels, or direct reactivity.

Indirect Reactivity The effect of the VOC on ozone formation and NO oxidation due to its effect on the reactions of the components of the base ROG surrogate or their oxidation products, either relative to the amount of VOC added (**Indirect Incremental Reactivity** or **$IR^{indirect}$**) or relative to the amount of VOC reacted (**Indirect Mechanistic Reactivity**, or **$MR^{indirect}$**). Under the conditions of these experiments, it is determined primarily by the effects of the VOC on radical levels.

IntOH The integral of the OH radical concentrations over time during the experiment or episode.

$IntOH^{base}$ The integrated OH radical concentrations in a base case experiment, or IntOH levels estimated for a hypothetical base case experiment if it were carried out under the same conditions as a particular added VOC experiment.

$IntOH^{test}$ The integrated OH radical concentrations in an experiment where a VOC was added.

Isooctane 2,2,4-trimethylpentane.

ITC The SAPRC Indoor Teflon Chamber #1, which is similar in design, but slightly larger than, the "ETC" chamber used in this study.

k_1 The NO_2 photolysis rate. A measurement of the light intensity in the experiments.

Kinetic Reactivity The fraction of initially present (or emitted) VOC which reacts.

kOH^{voc} The rate constant for the reactions of OH radicals with the VOC.

Mechanistic Reactivity (MR) The change in an experimental or calculated photochemical smog manifestation caused by adding a VOC to a base case experiment or episode, divided by the amount of VOC which reacted during the experiment or the episode. In the context of airshed modeling, it is defined for the case where the amount of VOC added approaches zero. In the context of this report, it is defined for the actual amounts of VOC added in the experiment, and thus in general may depend on the amount of VOC added. In this report, the manifestation could be ozone formed, ozone formed + NO oxidized, integrated OH radical levels, or direct reactivity.

Mini-Surrogate A simplified mixture of compounds used to represent the reactive organic gases emitted into urban atmospheres. In these experiments, the mini-surrogate mixture consisted of ethene, n-hexane, and m-xylene.

Mini-Surrogate Runs Any of the runs where the mini-surrogate - NO_x - air mixture is irradiated. Includes both "base case" and "test" experiments.

MTBE Methyl t-butyl ether.

NAA National Aerosol Association.

Nitrate yields The total amount of organic nitrates formed from the reactions of organic peroxy radicals with NO in the oxidation of the VOC in the presence of NO_x.

NO_2+Nitrates Compounds causing a response in the "NO_2" mode of commercial NO-NO_x analyzers which monitor NO_2 by using a heated catalyst to convert it to NO. Includes PAN, organic nitrates, and (non-quantitative) nitric acid for the experiments reported here.

NO_x NO and NO_2.

Ozone Formation Efficiency The amount of ozone formation which can result when a VOC reacts. In the context of this report, it is the same as the mechanistic reactivity relative to $D(O_3\text{-}NO)$.

Ozone Formed and NO Oxidized [$d(O_3\text{-}NO)$] The sum of the amount of ozone formed and the amount of NO reacted during the experiment, or $\Delta[O_3]\text{-}\Delta[NO]$. Directly related to the chemical processes responsible for ozone formation.

Overall Reactivity The sum of the direct and indirect reactivity with respect to ozone or ozone formed + NO oxidized (incremental or mechanistic, depending on context).

Reactivity A general term referring to the magnitude of the effects of the reactions of a VOC on some manifestation of the photochemical smog system, which in this report could be ozone formation, ozone formed + NO oxidized, or integrated OH radical levels. (Reactivities with respect to ozone formation and with respect to ozone formation + NO oxidation are sometimes used interchangeably, since they are determined by the same chemical factors.) Incremental reactivities measure the effects of the VOC relative to the amount added or emitted, mechanistic reactivities measure the effects relative to the amount of VOC which reacts, and kinetic reactivities measure the fraction of the emitted or added VOC which reacts. If the term "reactivity" is used without qualifier, the specific meaning depends on the context of the discussion. If the context is VOC emissions and VOC control strategies, it refers to incremental reactivities with respect to ozone, defined for the limit as the amount of VOC added approaches zero. If the context is interpreting the results of these experiments, it refers to mechanistic reactivities with respect to NO oxidation and ozone formation, defined for the amount of test VOC actually added in the experiment.

Reactivity Experiments Experiments where the effect of adding a VOC to the reactions of a mixture of the other VOCs are determined. These consist of standard or "base case" experiments and repeats of the same experiment with a test VOC added.

ROG Reactive organic gases. In the context of this report, it usually refers to the mixture of reactive organic gases in the base case experiment, or the "mini-surrogate".

SAPRC Statewide Air Pollution Research Center at the University of California at Riverside. This is where these experiments were carried out and where the SAPRC mechanisms were developed.

SAPRC Mechanism The gas-phase atmospheric chemical mechanism developed at SAPRC and documented by Carter (1990), or an updated version of that mechanism.

SAPRC-90 Mechanism The version of the SAPRC mechanism as documented by Carter (1990) with some updates in the representations of individual VOCs.

SAPRC-91 Mechanism The SAPRC-90 mechanism with updated kinetics for PAN formation, updated formaldehyde absorption cross sections, and minor changes in the aromatic mechanisms.

SCAQMD California South Coast Air Quality Management District.

Test Experiment An experiment where a test VOC was added to the base case mixture to determine the VOC’s reactivity.

Test VOC A VOC whose reactivity is being determined.

Siloxanes In the context of this report, refers to hexamethyldisiloxane [$(CH_3)_3SiOSi(CH_3)_3$], octamethylcyclotetrasiloxane [$(-(CH_3)_2SiO-)_4$], decamethylcyclopentasiloxane [$-(CH_3)_2SiO-)_5$], or pentamethyldisiloxanol [$(CH_3)_3SiOSi(CH_3)_2OH$].

Standard Runs Same as "base case" experiments.

VOC Volatile organic compound.

I. INTRODUCTION AND BACKGROUND

A. Introduction

The formation of ground-level ozone is caused by the gas-phase interactions of emitted volatile organic compounds (VOCs) and oxides of nitrogen (NO_x) in the presence of sunlight. Reducing emissions of both these ozone precursors is necessary to achieve ozone air quality standards. NO_x controls reduce the ultimate amount of ozone which can be formed, and thus have the greatest effects on ozone downwind of the source areas, while VOC controls reduce the rate at which ozone is formed and thus have the greatest effects on the concentrations of ozone nearer the source areas. Traditionally, VOC control strategies to reduce ozone have focused on reducing the total mass of VOC emissions. However, not all VOCs are equal in the amount of ozone formation they cause. These differences are referred to as the "reactivities" of the VOCs. Since significant further reductions of VOC emissions from most of the major sources will be difficult and costly, control strategies involving reducing the reactivity of VOC emissions are receiving increasing attention. Examples of such control strategies are conversion of motor vehicles to alternative fuels, and solvent substitutions.

Before reactivity-based VOC strategies can be implemented there must be a means to quantify VOC reactivity which is sufficiently reliable that it can be used in regulatory applications. VOC reactivities can be quantified and calculated using computer models (e.g., see Carter, 1991), but such calculations can be no more reliable than the chemical mechanisms upon which they are based. To be minimally suitable for this purpose, such mechanisms need to be evaluated by comparing their predictions with experimental measurements of VOC reactivity.

This report describes the results of the first phase of a program to obtain experimental data needed to reduce the chemical mechanistic uncertainties in models used to calculate ozone reactivities of VOCs. Data was obtained concerning the reactivities of a total of 35 VOCs, including representatives of the major classes species of interest in assessing alternative fuel use or solvent substitution strategies. The specific compounds studied were:

- Ethane ... the most reactive compound exempted as "unreactive" by the EPA and thus the informal standard the EPA uses to determine if a compound is of negligible reactivity;
- Propane and butanes ... present in vehicle exhausts but mainly of interest because they are solvents and propellants in aerosol products;

- Representative higher alkanes ... present in current vehicle fuels, vehicle exhaust and the major components of petroleum based solvents;
- Representative aromatic hydrocarbons ... present in current vehicle fuels, vehicle exhaust and (to a lesser extent) petroleum based solvents;
- Ethylene and representative higher olefins ... important contributor to the reactivity of vehicle exhausts;
- Formaldehyde and acetaldehyde ... present in vehicle exhausts, and important contributors to the reactivities of exhausts from fuels containing methanol or ethanol, respectively;
- Ethanol ... important both as a solvent and as a component of some current and alternative fuels;
- Acetone ... an important solvent compound;
- Methyl t-butyl ether (MTBE) ... an important component of many reformulated fuels;
- Dimethyl ether ... a solvent and propellant of some types of aerosol products;
- Ethoxyethanol and carbitol [2-(2-ethoxyethoxy)-ethanol] ... representative of the types of solvents present in water-based coatings; and
- Representative volatile silicone compounds .. solvents in personal care products and other products which are being considered for classification as unreactive.

Before describing the specific work carried out and presenting the results, it is necessary to discuss how reactivity is quantified, the uncertainties involved, the objectives of this study and how it is designed to address these uncertainties. This is given in the following section.

B. Quantification of Reactivity

The most direct quantitative measure of the degree to which a VOC contributes to ozone formation in a photochemical air pollution episode is its "incremental reactivity". This is defined as the amount of additional ozone formation resulting from the addition of a small amount of the compound to the emissions in the episode, divided by the amount of compound added. It can be expressed either as moles ozone formed per mole carbon VOC emitted or as grams ozone formed per gram VOC emitted. The latter is probably more appropriate for regulatory purposes where VOC emissions are quantified by mass, but the former will be used in this report because it is more directly related to the fundamental chemistry. Incremental reactivities are defined as the limit as the amount of compound added approaches zero to remove the dependence on the amount of VOC added (Carter and Atkinson, 1987, 1989a). This has the additional advantages that incremental reactivities of mixtures can be calculated from linear summations of incremental reactivities of the components.

Incremental reactivities for VOCs in the atmosphere cannot be measured experimentally except by making changes in emissions and observing the resulting changes in air quality under similar meteorological conditions. However, they can be calculated using computer airshed models if the VOC's atmospheric reaction mechanism is known or can be estimated (e.g., see Dodge, 1984; Carter and Atkinson, 1989a; Chang and Rudy, 1990; Carter, 1991; Russell, 1990). But such calculations are no more accurate than the model for the VOCs' atmospheric chemical reactions. Therefore, some method is needed either to directly relate experimentally measurable quantities to atmospheric reactivity, or to experimentally test the chemical mechanisms used in the model to predict reactivity.

The best method is to carry out fundamental kinetic and mechanistic studies on the atmospheric reactions of the VOC and its major photooxidation products and use the results to derive detailed mechanisms for the VOCs. These mechanisms should then be tested by carrying out a wide variety of environmental chamber experiments with the VOCs to see if the model can accurately predict their results. However, this is a major, multi-year effort, and it is not feasible to apply this approach for all of the many types of VOCs which are emitted.

The approach we have employed in this study is to conduct a more limited set of experiments to provide the data of most direct relevance to the factors affecting a VOC's reactivity. For this purpose, it is useful to consider a VOC's reactivity as being a product of two separate factors: their "kinetic reactivity" and their "mechanistic reactivity" (Carter and Atkinson, 1989a; Carter, 1991). The kinetic reactivity is defined as the fraction of the emitted VOC which undergoes chemical reaction in the pollution scenario being considered,

$$\text{Kinetic Reactivity} = \text{Fraction Reacted} = \frac{\text{VOC Reacted}}{\text{VOC Emitted}}$$

and the mechanistic reactivity is the amount of ozone formed relative to the amount of VOC which reacts in that scenario.

$$\text{Mechanistic Reactivity} = \frac{\text{Ozone Formed}}{\text{VOC Reacted}}$$

The product of these two quantities then gives the overall incremental reactivity.

$$\frac{\text{Ozone Formed}}{\text{VOC Emitted}} = \frac{\text{VOC Reacted}}{\text{VOC Emitted}} \times \frac{\text{Ozone Formed}}{\text{VOC Reacted}}$$

$$\text{Incremental Reactivity} = \text{Kinetic Reactivity} \times \text{Mechanistic Reactivity}$$

Each of these components of reactivity is affected by different aspects of the VOCs reaction mechanism, and different types of experiments provide the most useful data concerning them. The kinetic reactivity is a function of how rapidly the VOC reacts, so measurement of the rate constants of the atmospherically important reactions of the VOC provides the most relevant data needed to estimate this. Atmospherically important rate constant measurements have been made for most VOCs emitted in significant quantities, including those present in the major alternative fuels being considered. Reaction with hydroxyl (OH) radicals is the most important atmospheric removal process for most VOCs, and is the only significant atmospheric reaction for alkanes, aromatic hydrocarbons, alcohols, and ethers. Atkinson (1989) gives an extensive review of the available data concerning OH radical kinetics, and describes a method for estimating the OH radical rate constant for compounds where it has not been measured (Atkinson, 1987, 1989). Alkenes are also consumed by reaction with ozone and NO_3 radicals, and aldehydes are also consumed by photolysis, and information is available concerning the kinetics of these reactions as well (Carter and Atkinson, 1984; Atkinson et al., 1989; DeMore et al. 1990; Atkinson, 1990; 1991a). Thus the kinetic reactivities for most VOCs of interest can be readily estimated given overall atmospheric radical, ozone, and light levels.

The mechanistic reactivity of a VOC is the amount of ozone formation caused by the VOC once it reacts. This depends on a number of aspects of the VOCs reaction mechanism, such as the number of molecules of NO which it oxidizes when it reacts, whether its reactions enhance or inhibit radical levels or the rate of NO_x removal, and — often most importantly — the reactivity of the VOC's organic oxidation products. Mechanistic reactivities are also strongly dependent on environmental conditions, particularly the relative levels of NO_x. Under high NO_x conditions, ozone yields are determined by how rapidly ozone is formed, and therefore aspects of the mechanism affecting overall radical levels tend to be most important. Under conditions where ozone formation is NO_x-limited, aspects of the mechanism involving NO_x sinks become more important.

Because of the complexity and uncertainties in the atmospheric reaction mechanisms of most VOCs, the mechanistic reactivity is the most uncertain of the two components of reactivity. Although there is no single laboratory experiment which would yield all the information needed to determine mechanistic reactivities under all conditions, they can be measured for a given set of conditions in environmental chamber experiments. Such experiments involve adding the VOC to

environmental chamber irradiations of Reactive Organic Gas (ROG) - NO_x - air mixtures simulating photochemical smog precursors, and determining the effect of the added VOC on ozone formation. But because conditions of chamber experiments are not the same in all respects as in the atmosphere, measured mechanistic reactivities will be different from those in the atmosphere, even if NO_x conditions are similar. Therefore, modeling is necessary to relate the experimental results to atmospheric conditions. Thus the utility of experimental mechanistic reactivity measurements is that they provide a means to test the ability of chemical mechanisms to predict mechanistic reactivities in the chamber and thus in the atmosphere.

C. Objectives and Approach of This Study

This report describes the results of the first phase of a program to measure the mechanistic reactivities of representative VOCs, to reduce the uncertainties of model predictions of their reactivities in the atmosphere. In this phase of the program, we have focused on obtaining data concerning the maximum reactivities of the VOCs, i.e., on their reactivities under conditions of relatively high NO_x levels (or low ROG/NO_x ratios) where the ozone yields are determined primarily by how rapidly ozone formation occurs. Although a complete assessment requires data concerning reactivities under all conditions, obtaining maximum reactivity data is of particular importance because it reflects conditions where VOC controls are the most effective ozone reduction strategy, and because maximum reactivity has been shown to be a good predictor of reactivity with respect to exposure to integrated ozone levels (Carter, 1991; Russell, 1990). Such data also have immediate practical regulatory interest, since the California Air Resources Board has adopted maximum reactivity as the criterion for emissions standards from alternatively fueled vehicles (CARB, 1991).

The specific experiments carried out in this study consisted of repeated 6-hour environmental chamber irradiations of a simplified mixture representing photochemical smog precursors at low ROG/NO_x ratios, alternating with irradiations of the same mixture with varying amounts of a test VOC added. These are referred to as the "base case" and the "test" experiments, respectively. The mixture used in the base case experiment consisted of 3.5 to 4.5 ppmC of a ROG "mini-surrogate" containing 35% (as carbon) ethene, 50% n-hexane, and 15% m-xylene, together with ~0.5 ppm of NO_x in air. Although this mixture is a significant oversimplification of those present in the atmosphere (see, for example, Lurmann et al., 1992, Jeffries et. al., 1989), and employs higher total NO_x levels than usually present in the atmosphere during ozone pollution episodes, our model calculations show that its use in the chamber experiments gave similar correlations with maximum atmospheric reactivities as compared to

use of more complex and realistic mixtures. The n-hexane and m-xylene were chosen to be representatives of the alkane and aromatic hydrocarbons emissions, respectively, with their relative amounts approximately representing the relative amounts of these two classes of compounds in the atmosphere. The ethene in the mixture, which forms high yields of formaldehyde when it reacts, was used to represent the effects of both the olefins and the aldehydes. Its relative amount was based on model calculations comparing predicted incremental reactivities of VOCs in chamber experiments with those predicted for atmospheric conditions with more realistic mixtures.

The amount of test VOC added in the test experiments varied depending on its reactivity, being determined so that its addition caused a 40-80% change in the amount of NO oxidized and ozone formed. (At least 40% change is needed to yield a precise measurement of the effect of the added VOC on the system, but too large of a change would result in a poor approximation to the concept of incremental reactivity.) The results of the experiments with added test VOC, together with the results of the repeated base case runs, were analyzed to yield three measures of reactivity for the VOC which represent three different factors which must be accurately predicted by models that are used to assess reactivity in the atmosphere. These are then compared to the predictions of the detailed chemical mechanism (Carter, 1990) used to predict the maximum reactivity scale adopted by the CARB (1991), to determine the extent to which the mechanism is consistent with these results, and the extent to which the mechanism needs improvement. These three measures of reactivity, their utility, and the methods used to measure them in our experiments, are discussed in the following sections.

1. Reactivities Relative to Ozone Formation and NO Oxidation

Since the objective of this study is to test estimates of the effects of VOCs on ozone, obviously the reactivity with respect to ozone is a relevant quantity to measure. However, as discussed elsewhere (e.g., Johnson, 1983; Carter and Atkinson, 1987; Carter and Lurmann, 1990, 1991) the sum of NO oxidized plus ozone formed (or the change in $[O_3]$-[NO]) provides a more useful and general measure of ozone formation potential than simply ozone formed. This is because ozone formation is caused by the oxidation of NO by the peroxy radicals formed when the VOCs react, with these processes being manifested by NO consumption when NO is in excess and then by ozone formation after most of the NO has been consumed. It is a more generally applicable measure of ozone formation potential because it provides a meaningful measure of the processes ultimately responsible for ozone formation even for conditions when NO is in excess and ozone is not formed.

In the subsequent discussion, the amount of ozone formed plus the amount of ozone consumed at time t in an experiment, or $\Delta[O_3]_t - \Delta[NO]_t$, will be designated as $d(O3\text{-}NO)_t$. The experimental incremental reactivity with respect to this quantity, $IR[d(O_3\text{-}NO)]_t^{voc}$, is then given by,

$$IR[d(O_3\text{-}NO)]_t^{voc} = \frac{d(O_3\text{-}NO)_t^{test} - d(O_3\text{-}NO)_t^{base}}{[VOC]_0} \qquad (I)$$

and the mechanistic reactivity, $MR[d(O_3\text{-}NO)]_t^{voc}$, is given by

$$MR[d(O_3\text{-}NO)]_t^{voc} = \frac{d(O_3\text{-}NO)_t^{test} - d(O_3\text{-}NO)_t^{base}}{(VOC\ reacted)_t} \qquad (II)$$

where $d(O_3\text{-}NO)_t^{test}$ is the $d(O_3\text{-}NO)$ measured at time t from the experiment where the VOC was added, $d(O_3\text{-}NO)_t^{base}$ is the corresponding value from the "base case" experiments where the VOC was not present, $[VOC]_0$ is the initial VOC concentration in the experiment where it was added (i.e., the amount added), and $(VOC\ reacted)_t$ is the amount which has reacted at time t.

Note that in our previous discussions of incremental and mechanistic reactivity, these quantities have been defined as the limit as the amount of VOC added approaches zero (Carter and Atkinson, 1987; 1989a; Carter, 1991). However, in the context of this report, we will use these terms to refer to the reactivities defined for the actual amounts of VOCs added in the experiments, as shown above in Equations (I) and (II). This notation is used to avoid having to introduce new terms for these quantities.

Note also that if ozone is in excess in both the base case and the added test VOC experiments then reactivity with respect to $d(O_3\text{-}NO)$ is equivalent to reactivity with respect to ozone alone. This is because if ozone is in excess, essentially all of the initially present NO is oxidized, and this is the same in both the base case and the added VOC experiment. However, at early periods of the run when no significant ozone formation has occurred, reactivity with respect to ozone is not a particularly meaningful quantity. Quantifying reactivity in terms of $d(O_3\text{-}NO)$ provides a measure which is useful throughout the experiment, allowing for tests of model predictions of how relative ozone formation potential of a VOC varies with time. The reactivities with respect to $d(O_3\text{-}NO)$ are reported for each hour of the six hour experiments.

The quantities $d(O_3\text{-}NO)_t^{test}$ and the amounts of test VOC added and reacted can be obtained from each experiment where the test VOC is added, so each such experiment gives a separate set of incremental and mechanistic reactivities for that VOC. The quantities $d(O_3\text{-}NO)_t^{base}$ are estimates of what the result of the experiment would be if the VOC was not added. If there were no experimental

variability, this could simply be obtained by running a single "base case" experiment and using it to obtain the $d(O_3\text{-}NO)_t^{base}$ values for all the reactivity experiments. However, in practice there is run-to-run variability in the conditions of the experiments, causing variabilities in $d(O_3\text{-}NO)_t$ and other measures of reactivity. To address this, many repeated base case runs need to be conducted to obtain reliable estimates of base case results, and how they depend on experimental variables such as temperature, light intensity, and variations in amounts of initial NO_x and ROG mini-surrogate components injected. These dependencies could then be used to derive appropriate estimates of $d(O_3\text{-}NO)_t^{base}$ to associate with the conditions of each added test VOC experiment.

2. Reactivity with Respect to OH Radical Levels

The second measure of reactivity obtained in this study is the effect of the VOC on overall OH radical concentrations in the experiment. This is an important factor affecting reactivity because radical levels affect how rapidly all VOCs present, including the base ROG components, react to form ozone. An experimental measure of this would provide a useful means to directly test how well mechanisms represent this important factor affecting a VOCs reactivity.

The overall OH radical levels in an experiment is quantified by the integrated OH radical concentration, which is designated by the abbreviation "IntOH" in the subsequent discussion.

$$IntOH_t = \int_0^t [OH]_\tau d\tau \qquad \text{(III)}$$

If the experiment contains a VOC which reacts only with OH radicals, if the VOC reacts sufficiently rapidly that the amount which reacts can be precisely measured, and if dilution can be neglected or corrected for, then IntOH can be estimated from the amount of VOC which reacts and the rate constant for its reaction. M-xylene is used for this purpose in most of our experiments because it is present in all experiments as a base ROG surrogate component, because its reaction with OH radicals is its only significant means of consumption under atmospheric conditions (Atkinson, 1989), and because it reacts sufficiently rapidly that its rate of consumption could be measured with a reasonable degree of precision. In a few later experiments, including those where the presence of p-xylene as the test VOC prevented analysis of the m-xylene, trace amounts of 2-chloromethyl-3-chloropropene were added to the experiments to determine the integrated OH radical levels.

The incremental and mechanistic reactivities of the VOC relative to IntOH is calculated in a manner entirely analogous to that discussed above for reactivities relative to $d(O_3\text{-}NO)$, i.e.,

$$IR[IntOH]_t^{voc} = \frac{IntOH_t^{test} - IntOH_t^{base}}{[VOC]_0} \quad \text{(IV)}$$

$$MR[IntOH]_t^{voc} = \frac{IntOH_t^{test} - IntOH_t^{base}}{(VOC\ reacted)_t} \quad \text{(V)}$$

In this case, only reactivities relative to the final, six-hour IntOH levels are discussed, though the detailed data tabulations in the appendix give hourly MR[IntOH] values as well.

3. Direct and Indirect Reactivities and Conversion Factors

The reactivity of a test VOC with respect to $d(O_3\text{-NO})$ measures both the direct effects of the reactions of the radicals formed from the test VOC and its products, and the indirect effect of the test VOC on NO oxidation and ozone formation from the reactions of the other VOCs which are present. In the case of the compounds whose reactions have significant effects on overall radical levels -- i.e., large positive or negative IntOH reactivities -- it is the indirect effect which is the dominant factor affecting reactivity. Because of this, for many compounds model predictions of the $d(O_3\text{-NO})$ reactivity are not highly sensitive to their representation of the direct effects of the intermediates formed from the VOC and its oxidation products. Thus these aspects of the reaction mechanisms for the test VOCs can not be well tested using model predictions of this measure of reactivity. However, a more sensitive test of this can be obtained by comparing model predictions with experimental measurements of a third measure of reactivity which can be derived from reactivity experiments, which we call the "conversion factor". This is defined and derived as discussed below.

All peroxy radicals which oxidize NO and cause ozone formation in a ROG-NO_x-air photooxidation system can be traced back to an initially present or emitted VOC (Jeffries and Crouse, 1991). Therefore, the total amount of ozone formed and NO oxidized in a base case ROG-NO_x-air experiment where a test VOC is added can be expressed as the sum of ozone formed and NO oxidized due to radicals formed from the reacting test VOC or its products, designated $d(O_3\text{-NO})^{voc}$, plus the ozone formed and NO oxidized from radicals formed from reactions of the components of the base ROG surrogate and their products, designated as $d(O_3\text{-NO})^{base\ rog(test)}$.

$$d(O_3\text{-NO})^{test} = d(O_3\text{-NO})^{voc} + d(O_3\text{-NO})^{base\ rog(test)} \quad \text{(VI)}$$

Note that $d(O_3\text{-NO})^{base\ rog(test)}$ is not the same as $d(O_3\text{-NO})^{base}$, since the former refers to the $d(O_3\text{-NO})$ from the base ROG reactions when the test VOC is present, while the latter refers to $d(O_3\text{-NO})$ formed in the absence of the test VOC. Dividing both sides of this equation by $[VOC]_0$, the amount of VOC added, and combining the result with Equation (I), the definition of incremental reactivity, yields:

$$IR[d(O_3\text{-NO})]^{voc} = IR^{direct}[d(O_3\text{-NO})]^{voc} + IR^{indirect}[d(O_3\text{-NO})]^{voc} \quad \text{(VII)}$$

where

$$IR^{direct}[d(O_3\text{-NO})]^{voc} = \frac{d(O_3\text{-NO})^{voc}}{[VOC]_0} \quad \text{(VIII)}$$

and

$$IR^{indirect}[d(O_3\text{-NO})]^{voc} = \frac{d(O_3\text{-NO})^{base\ rog(test)} - d(O_3\text{-NO})^{base}}{[VOC]_0} \quad \text{(IX)}$$

Likewise, dividing Equation (VI) by the amount of VOC reacted and combining the result with Equation (III) yields:

$$MR[d(O_3\text{-NO})]^{voc} = MR^{direct}[d(O_3\text{-NO})]^{voc} + MR^{indirect}[d(O_3\text{-NO})]^{voc} \quad \text{(X)}$$

where

$$MR^{direct}[d(O_3\text{-NO})]^{voc} = \frac{d(O_3\text{-NO})^{voc}}{(VOC\ reacted)} = ConvF^{voc} \quad \text{(XI)}$$

and

$$MR^{indirect}[d(O_3\text{-NO})]^{voc} = \frac{d(O_3\text{-NO})^{base\ rog(test)} - d(O_3\text{-NO})^{base}}{(VOC\ reacted)} \quad \text{(XII)}$$

Thus the incremental and mechanistic reactivity of a VOC can be considered to be the sum of a "direct" reactivity term, reflecting the ozone formed and NO oxidized from the radicals formed from the VOC, and an "indirect" term, reflecting the change in ozone formed and NO oxidized from the base ROG components caused by adding the VOC.

In the subsequent discussion, the quantity $MR^{direct}[d(O_3\text{-NO})]^{voc}$ will be referred to as the "conversion factor" for the VOC, and abbreviated "ConvF" on the equations and tabulations. This quantity can be directly related to elementary process in the reactions of the VOC because if each peroxy radical is completely efficient in converting NO and forming ozone, it is equal to the number of peroxy radicals which are formed (either from the VOC or from the subsequent reactions of a product) when one molecule of the VOC reacts. Peroxy radicals tend to be reasonably efficient in converting NO under maximum reactivity conditions (Carter and Atkinson, 1989), so measurements of this

quantity under maximum reactivity conditions give a fairly direct indication of the number of peroxy radicals formed when a VOC reacts. Therefore, comparing this quantity with model predictions gives a good test of this aspect of the VOC's mechanism.

Unfortunately, neither $d(O_3\text{-NO})^{voc}$ nor $d(O_3\text{-NO})^{base\ rog(test)}$ are measured directly, and they have to be estimated. However, estimates of these quantities can be derived if it is assumed (1) that the amount of base ROG surrogate component and their products which react in any experiment (whether base or added test VOC) is proportional to the integrated OH radical levels, and (2) that the number of molecules of NO oxidized and ozone formed from the reactions of a given amount of ROG surrogate components or products is unaffected by the addition of the test VOC. From these two assumptions it follows that the ratio of the amount of NO oxidized and ozone formed from the reactions of the base ROG surrogate to the IntOH, which we designate as the "conversion ratio" for the base ROG (or $ConvR^{base}$), is the same in the added test VOC run as it is in the base experiment, i.e.,

$$ConvR^{base} = \frac{d(O_3\text{-NO})^{base}}{IntOH^{base}} \cong \frac{d(O_3\text{-NO})^{base\ rog(test)}}{IntOH^{test}} \qquad \text{(XIII)}$$

or

$$d(O_3\text{-NO})^{base\ rog(test)} \cong ConvR^{base}\ IntOH^{test} \qquad \text{(XIV)}$$

This can be combined with Equations (IX) and (XI) to yield

$$IR^{direct}[d(O_3\text{-NO})]^{voc} \cong \frac{d(O_3\text{-NO})^{test} - ConvR^{base}\ IntOH^{test}}{[VOC]_0} \qquad \text{(XV)}$$

and

$$ConvF^{voc} \cong \frac{d(O_3\text{-NO})^{test} - ConvR^{base}\ IntOH^{test}}{(\text{VOC reacted})}, \qquad \text{(XVI)}$$

respectively. Since all the quantities on the right sides of Equations (XV) and (XVI) are measurable, they provide a means to obtain experimental estimates of the direct reactivity components.

The extent to which the direct incremental reactivity and conversion factors derived from equations (XV) and (XVI) reflect the elementary processes depend on the validity of the two assumptions upon which the derivation is based. The first assumption, that the amount of base ROG reacted is proportional to IntOH, is only strictly true for VOCs which react relatively slowly and only with

OH radicals, but is probably good to within the precision of experimental incremental reactivity data. The second assumption, that the addition of a VOC will not affect the amount of NO conversion and thus ozone formation from reactions of a given amount of other VOCs, is based on the facts that (1) the addition of one VOC should not affect the number of peroxy radicals formed from the other VOCs as long as NO_x levels are sufficiently high that cross reactions of radicals from different VOCs are not important, and (2) under the relatively high NO_x levels of maximum reactivity conditions the major fate of most peroxy radicals should be reaction with NO regardless of which other VOCs are present. However, this assumption is only applicable under maximum reactivity conditions because if ozone is NO_x limited then the addition of VOCs which remove NO_x will reduce NO conversion and ozone formation from all the radicals present. This assumption also neglects the fact that the distribution of ROG components which react will change with the extent of reaction, and this would be affected by the presence of the VOCs which affect radicals. Thus the extent to which the quantities derived from Equations (XV) and (XVI) reflect elementary processes becomes more approximate as the magnitude (whether positive or negative) of the IntOH reactivity increases.

Note that assuming that the presence of the test VOC does not affect the net conversion factor for the ROG surrogate components is equivalent to assuming that the direct component of the VOC's reactivity is due entirely to its effect on radical levels. This can be seen, for example, by plugging Equation (XIV) into Equation (IX), which yields,

$$IR^{indirect}[d(O_3\text{-}NO)]^{voc} = ConvR^{base} \left(\frac{IntOH^{test} - IntOH^{base}}{[VOC]_0} \right)$$

and then combining the result with equation (IV), the definition of IntOH incremental reactivity, to yield

$$IR^{indirect}[d(O_3\text{-}NO)]^{voc} = ConvR^{base}\ IR[IntOH]^{voc} \qquad \text{(XVII)}$$

An exactly analogous result is obtained for mechanistic reactivities by plugging Equation (XIV) into (XII), and combining the result with Equation (V):

$$MR^{indirect}[d(O_3\text{-}NO)]^{voc} = ConvR^{base}\ MR[IntOH]^{voc} \qquad \text{(XVIII)}$$

This approximation implies that for any VOC the indirect $d(O_3\text{-}NO)$ reactivity is directly proportional to its IntOH reactivity, with the proportionality constant being a function only of the base case experiment. This is obviously not true under NO_x limited conditions when aspects of a VOC's mechanisms involving NO_x

sinks can have an important affect on the conversion factors for the reacting components of the base ROG surrogate, and thus the VOC's indirect reactivity. However, this is consistent with results of model calculations of mechanistic factors affecting reactivities under higher NO_x, maximum reactivity conditions (Carter and Atkinson, 1989).

Equations (XVII) and (XVIII) provide a means to convert IntOH reactivities into units which can be directly compared with $d(O_3\text{-}NO)$ reactivities and [in the case of (XVIII)] conversion factors. This is useful for comparing the relative importance of direct and indirect components in determining the overall reactivities of the various VOCs.

4. Measurement of OH Radical Rate Constants

Since reaction with OH radicals is a major atmospheric consumption process for most VOCs, it is obviously an important factor affecting its reactivity. The OH radical rate constants for most of the VOCs whose reactivities are assessed in this work have already been measured, in many cases by a number of different laboratories (Atkinson, 1989). Therefore, determining OH radical rate constants was not a focus of this study. However, no OH radical rate constants have been reported for carbitol, and this needs to be measured to assess its reactivity. Fortunately, the simultaneous measurement of the rates of decay of m-xylene and the various test compounds employed in this study which react primarily with OH radicals permitted a number of OH radical rate constant ratios involving m-xylene to be determined, including those for carbitol and ethoxyethanol. The data for carbitol provide the first available kOH measurement for this compound, and the data for the other compounds can be compared with literature values, to serve as a consistency check for the measurements obtained in this study.

II. EXPERIMENTAL METHODS

A. Chamber

All experiments in this study were conducted using the ~3000 liter SAPRC indoor Teflon chamber #2, which is called the "ETC". This chamber is shown schematically in Figure 1. The chamber consisted of a 2-mil thick FEP Teflon reaction bag fitted inside an aluminum frame of dimensions of 8 ft x 4 ft x 4 ft. The light source for the chamber consisted of two diametrically opposed banks of 30 Sylvania 40-W BL blacklamps, one above and the other below the chamber. Pure dry air for these experiments prior to January 1992 was provided by an air purification system that has been described in detail previously (Doyle et al., 1977). After January 1992, an AADCO air purification system was employed. The air was not humidified for these experiments, and is estimated to have a relative humidity of approximately 5%. Dry air was used because it tends to reduce chamber wall effects and improve reproducibility. The temperature in the chamber when the lights ranged from 298 to 304 K.

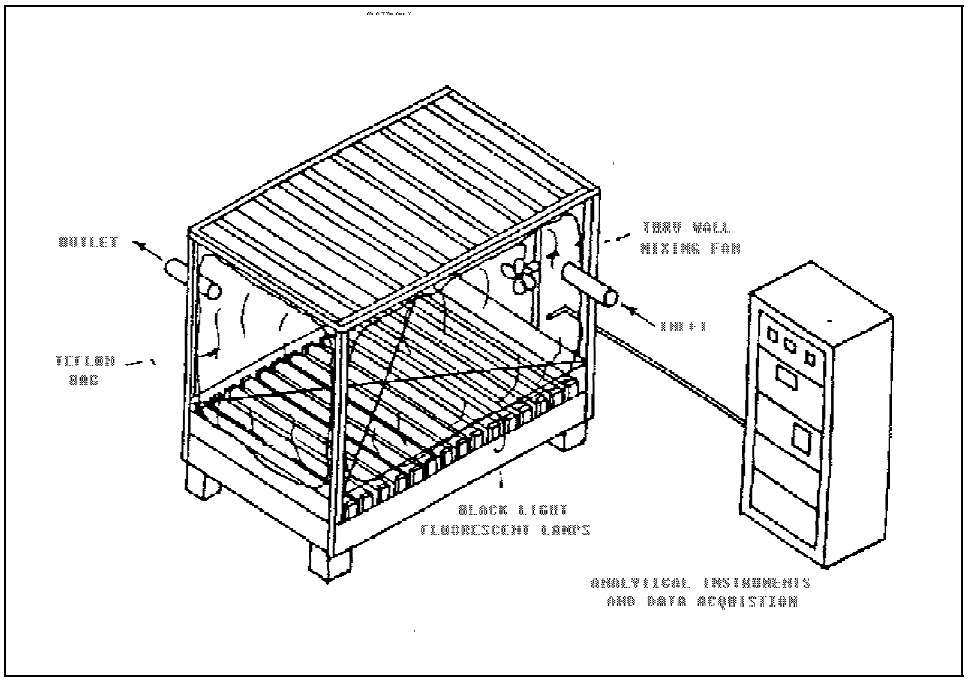

Figure 1. Diagram of the SAPRC Indoor Teflon Chamber #2 (ETC), and associated instrumentation.

The chamber is similar in design and characteristics to the SAPRC ~6400-liter Indoor Teflon Chamber #1 (designated the "ITC") which is described in detail in previous SAPRC reports (Carter et al. 1984, 1986a, 1987; Carter, 1987). The same air purification system (prior to 1992) and a similar light source is employed in both of these chambers.

B. Experimental Procedures

Before each experiment, the chamber was flushed with purified air for at least 6 hours with the lights on and then for at least 3 hours with the lights off. The NO/NO_x monitors were zeroed with zero air prior to being connected to the chamber. The monitors for ozone and NO/NO_x were connected to the chamber approximately 1.5 hours before the start of the irradiation. Temperature was monitored prior to as well as during the experiments. Space heaters were turned on prior to the experiments to bring the chamber to the approximate temperature attained when the lights are on. The reactants were injected as described below, with the NO and NO_2 being injected last, approximately 15 minutes before the lights are turned on. Samples were then analyzed on the appropriate gas chromatograph (GC) before irradiation began. A measurement for CO was also taken. The irradiation began by turning on both banks of blacklights, and most irradiations lasted for 6 hours. Data from the continuous monitoring instruments (ozone, NO, NO_x, and temperature) were recorded every 15 minutes using a PC-based computer data acquisition system. GC samples were taken hourly for monitoring organic reactants.

The methods used to inject the reactants for the standard experiment varied somewhat throughout the study. Prior to run ETC-90, NO and ethene were injected into the chamber by measuring the desired volume using all-glass gas-tight hypodermic syringes, diluting it with dry N_2, and flushing it into the chamber with N_2. NO_2 was prepared by diluting NO with O_2 in the syringe prior to injecting it into the chamber. After run ETC-90, NO, NO_2, and (later) ethene were prepared for injection into the chamber using a vacuum rack. In the case of ethene and NO, the appropriate pressure of the reactant, measured using a MKS Baratron Gauge, was expanded into an evacuated 2000-ml bulb, and was then diluted with dry N_2. The NO_2 was prepared by expanding the appropriate amount of NO in a 500 ml bulb, then diluting it with dry O_2. The contents of the bulb was then flushed into the chamber using dry N_2, for approximately 5 minutes.

In the case of the surrogate components n-hexane and m-xylene, which are liquid at room temperature and pressure, the desired volume of liquid was injected using a microsyringe into a 2-liter Pyrex bulb, and the contents of the bulb were then injected into the chamber by heating the bulb with a heat gun while flushing it with N_2 for at least 5 minutes. In many runs, a pre-prepared

liquid mixture of m-xylene and n-hexane was used to inject both reactants simultaneously. This allowed for improved reproducibility in the injections of m-xylene, to which the results of the runs were sensitive.

The methods for injecting the test compound depended on the compound. Compounds which were gaseous at room temperature were injected using glass syringes as discussed above for ethene and NO prior to ETC-90. Compounds which were liquid were injected as discussed above for n-hexane and m-xylene, except that longer flushing times were employed for the less volatile compounds such as the alcohol ethers or siloxanes.

A mixing fan was turned on in the chamber to insure proper mixing when the reactants were injected. The fan was turned off prior to the start of the irradiation.

The runs terminated after 6 hours of irradiation. The chamber was flushed with pure air to remove the contents and prepare for the next run.

C. Analytical Methods

1. Gas Chromatograph Analyses

Organic reactants and products were monitored using several different GC systems, each suitable for a particular set of compounds. Samples for chromatographic analyses were withdrawn from the chamber either using 100 ml gas-tight, all-glass syringes or by collecting the 100 ml sample from the chamber onto Tenax-GC solid adsorbent cartridges. In the former case, the syringes were flushed at least three times with the sample gas before the sample for analysis was taken. A syringe was attached to the sample port of the chamber to withdraw a sample. The sample port was a ca. 18 in. x 0.25 in. Pyrex tube with a Becton-Dickinson stainless steel lever-lok stopcock manifold. Depending on the particular GC system used and the concentration range of the compound(s) being monitored, the contents of the syringe were either flushed through a 2 ml or 3 ml stainless steel loop (maintained at room temperature) and subsequently injected onto the column by turning a gas sample valve, or condensed in a trap cooled with liquid argon and then injected onto the column by simultaneously turning the gas sample valve and heating the loop with boiling water or ice water. In the analyses using the Tenax cartridge system, the sample was placed in series with the GC column, thermally desorbed at 220 C for 2 min. and cryofocused on the column.

The various GC systems used and the compounds that they monitored are described below.

1) The mini-surrogate components n-hexane and m-xylene, as well as the test compounds, acetaldehyde, acetone, ethylbenzene, isopropanol, octane, o-xylene, toluene, 1,2,3-trimethylbenzene, 1,3,5-trimethylbenzene and 1,2,4-trimethylbenzene were monitored using the "C-600" GC. This system consisted of a Varian 1400 GC with a flame ionization detector (FID) and a 10 ft x 0.125 in. stainless steel column packed with 10% Carbowax 600 on C-22 Firebrick (30/60 mesh). The flow through this column was set at 50 ml min^{-1}, and, as was the case for most of the Varian GC's, the carrier gas was nitrogen. The hydrogen flow was kept at 45 ml min^{-1}, and the oxygen, used in place of air to enhance sensitivity, was set at 250 ml min^{-1}. The detector was heated to 200 C, and the column was maintained at 75 C. The 100 ml samples that were drawn from the chamber were trapped by pushing the gas sample through a 10 in. x 0.125 in. stainless steel tube packed with glass beads (80 mesh) and immersed in liquid argon. The sample was carried onto the column by then immersing the trap in boiling water and simultaneously actuating the gas sampling valve which was heated to 125 C to prevent adsorption of compounds. The mv response was measured from the strip chart recording and used to quantitate the amount of compound present. Starting with run ETC-254 and onwards the peak area was measured with an Hewlett-Packard (HP) analog-to-digital converter and HP Chemstation software. This yielded a significantly improved quantification for all compounds, especially n-hexane.

2) The other mini-surrogate component, ethene, and a test compound, ethane, were monitored using the "PN" GC which consisted of a Varian 1400 GC with an FID detector maintained at 200 C and a 5 ft. x 0.125 in. stainless steel column packed with Porapak N, 80/100 mesh. The nitrogen carrier flow was set at 80 ml min^{-1}, the hydrogen at 60 ml min^{-1}, and the oxygen at 400 ml min^{-1}. The column was kept at 60 C, while the detector was heated to 200 C. When a sample was to be analyzed, 100 ml of gas was pushed through a 2 ml stainless steel loop and injected onto the column by actuating the gas sampling valve. The mv response was measured from the strip chart recording and used to quantitate the amount of compound present. Starting with run ETC-254 and onwards the peak area was measured with an Hewlett-Packard analog-to-digital converter and HP Chemstation software.

3) Two test compounds MTBE and hexamethyldisiloxane were monitored using the "C-20M" GC which consisted of a Varian 1400 GC with an FID detector maintained at 200 C and a 20 ft. x 0.125 in. stainless steel column packed with 5% DC703/C20M on 100/120 AW, DMCS Chromosorb G. The nitrogen carrier flow was set at 50 ml min^{-1}, the hydrogen at 45 ml min^{-1}, and the oxygen at 300 ml min^{-1}. The column was kept at 60 C, while the detector was heated to 200 C. When a sample was to be analyzed, 100 ml of gas was pushed through a 3 ml stainless steel loop and injected onto the column by actuating the gas sampling valve.

The mv response was measured from the strip chart recording and used to quantitate the amount of compound present.

4) The test compounds ethoxyethanol, carbitol, octamethylcyclotetrasiloxane and decamethylcyclopentasiloxane were monitored on a modified HP 5880A GC using the Tenax cartridge sampling system. The GC was fitted with a 15 m DB-5 (5% phenyl-methylsilicone) megabore column and the samples detected with an FID maintained at 200 C . The column would be kept at -10 C while the sample desorbed from the Tenax cartridge (ca. 2 min.), then a temperature ramp of 8 C min^{-1} would be applied up to a final oven temperature of 200 C. The nitrogen carrier flow was set at 10 ml min^{-1}, the hydrogen flow at 30 ml min^{-1}, and the oxygen flow at 150 ml min^{-1}. Peak areas were measured and used to quantitate the amount of compound present.

5) The test compounds n-butane, trans-2-butene, dimethyl ether, ethane, isobutane, isobutene, isoprene, propane, propene and (for some runs) the mini-surrogate component ethene were monitored using the "GSQ" GC. This consisted of a Varian 1400 GC with an FID detector maintained at 200 C and a 30 m x 0.53 mm megabore gas-solid porous polymer GSQ column. The helium carrier flow was set at 3 ml min^{-1}, the makeup at 30 ml min^{-1}, the hydrogen at 58.1 ml min^{-1}, and the oxygen at 210 ml min^{-1}. In most cases, a 100 ml sample was trapped onto a stainless steel loop immersed in liquid argon as described above, or the sample was collected in a 3 ml stainless steel loop and injected as described previously. Generally, the initial column temperature was 75 C and held for 1 minute, then a temperature ramp of 20 C min^{-1} was applied up to a final temperature of 120 C. In the cases when both ethane and ethene were analyzed simultaneously the column was maintained isothermally at 50 C. The mv response was occasionally used to quantitate the amount of compound present, whereas, in most cases, an integrator was used to quantify the peak area. Beginning with run ETC-326 and onwards the peak area was measured with an Hewlett-Packard analog-to-digital converter and HP Chemstation software.

6) A Hewlett-Packard 5890 Series II GC with an FID detector maintained at 300 C and a 15 m x 0.53 mm megabore DB-5 column was used to supplement (from run ETC-288 onwards) and then later (from run ETC-325 onwards) replace the "C-600" GC described above. As such, the compounds analyzed were identical to those detected on the "C-600" GC with the exceptions that only methanol was analyzed on the HP GC, and that t-2-butene was analyzed on the HP GC, as well as the "GSQ" GC. The helium carrier flow was set at 10 ml min^{-1}, the helium makeup gas at 20 ml min^{-1}, the hydrogen at 30 ml min^{-1}, and the oxygen at 150 ml min^{-1}. A 100 ml sample was taken and injected into the trap while immersed in liquid argon as described above. Initially the column was maintained at subzero temperatures (usually -15 C) while the sample flowed onto the column during desorption (trap immersed in boiling water). After which a temperature ramp was applied (15 C

min^{-1}) up to 125 C. The HP chemstation software allowed for quantitation by peak area.

6) PAN was analyzed beginning with run ETC-223 through run ETC-250 on a Varian Aerograph GC with an electron capture detector (ECD) maintained at room temperature (ca. 21 C) and a packed 5% C-400 24" x 1/8" column, also at room temperature. The nitrogen carrier flow was 75 ml min^{-1}. A 2.2 ml sample loop was used to contain the sample prior to injection, and the signal was quantified by peak height (mv). A fresh batch of PAN was synthesized according to the method of Stephens et al. (1965) prior to calibration. (The PAN data will not be discussed in this report.)

8) A second Hewlett-Packard 5890 Series II GC outfitted with an ECD maintained at 50 C and a 5 m x 0.53 mm megabore HP-1 column was also used to analyze for PAN (from run ETC-268 until ETC-321). The helium carrier flow was set at 10 ml min^{-1} while the 5% methane/argon makeup gas was set at 60 ml min^{-1}. A ca. 2 ml Teflon loop maintained at 25 C was used to contain the sample prior to injection. Initially the column was maintained at subzero temperatures (usually -30 C) while the sample flowed onto the column, after which a temperature ramp was applied (15 C min^{-1}) up to 35 C. The HP chemstation software allowed for quantitation by peak area. A fresh batch of PAN was synthesized according to the method of Stephens and Burleson (1965) prior to calibration.

9) The HP 5890 GC used to monitor PAN had a second detector and column; these were used to monitor 2-chloromethyl-3-chloropropene and carbon tetrachloride. The ECD detector was maintained at 250 C and the column was a 15m x 0.53 mm DB-5. The helium carrier flow was set at 9 ml min^{-1} while the 5% methane/argon makeup gas was set at 94 ml min^{-1}. The sampling valve was maintained at 120 C, with the sampling loop at a somewhat lower temperature. The column had a similar temperature program as the HP-1 column, except that the temperature was ramped up to 150 C. The HP chemstation software was used.

Calibrations of all GC’s were performed at intervals of two months or less and were carried out in a similar manner. First, all gas flows were measured to verify that no changes had occurred which would indicate that previous measurements were erroneous. After measuring these flow rates, a calibration mixture was made up using one of two methods. The calibration mixture, composed of known quantities of various compounds, was then injected into the appropriate GC and the elution time and height of each peak recorded.

For gaseous compounds, two ca. 2000 ml flasks (volumes determined by measuring with water) were flushed with nitrogen for 20 minutes and then 2 ml of each pure gas was injected into the first flask with a 5 ml syringe. This flask

was allowed to mix for 20 minutes, and then 2 ml from this flask was transferred into the second flask. The contents of this second flask were allowed to mix for an additional 20 minutes. This resulted in a concentration of ca. 1 ppm of the gas in the second flask. 100 ml of gas was then removed from the second flask and placed into the loop for quantitation. Trap calibrations were accomplished by diluting a 5 ml sample from the second flask with nitrogen in a 100 ml syringe, and passing the contents of the syringe through the trap. For a flask containing 1 ppm of the compound, this method was equivalent to sampling 100 ml of gas containing 50 ppb of the compound.

Calibration of relatively volatile compounds that were liquid at room temperature and pressure was carried out using a ca. 50 l all-glass carboy, which was first cleaned by being heated from the inside with a heat gun, then cooled with the heat gun with the heat off until the carboy reached room temperature, and finally flushed with nitrogen for one hour. The carboy was then dosed with 1 microliter of each pure liquid to be calibrated with a 10 microliter syringe. These were allowed to mix for one hour prior to any samples being taken. Trap and loop calibrations were both accomplished in a similar fashion. A 1 ml sample was taken from the carboy using a 100 ml syringe and then diluted with 99 ml of nitrogen. The samples were injected in the manner described previously. The exact concentration of each compound was calculated by knowing the amount of liquid injected and its density.

The various siloxanes and ethers studied, which possess a relatively lower vapor pressure, were all calibrated by using the ETC chamber itself. First, the chamber bag was flushed using the same procedure as for each run (see above), and then an appropriate amount of each sample was injected as described above for the introduction of reactants. Since the exact bag volume is not known, ethene was also injected, and by the known calibration value for its detection a volume for the bag could be determined. The samples were injected into the appropriate GC's in the manner described previously. The concentration of each component was calculated by knowing the amount of liquid injected, its density, and the calculated bag volume. Generally speaking, the ETC chamber was used whenever possible to perform calibrations.

2. Continuous Monitoring Instruments

Ozone, nitrogen oxides, and temperature were monitored continuously using the instruments described below. Samples for analysis were taken from a probe inserted directly into the chamber (ca. 18 in.) using Teflon or Pyrex sampling lines (See Figure 1). The output of these instruments were connected to a computer data acquisition system, which recorded their measurements in 15 minute

intervals, with averaging times of 30 seconds. The output was also connected to strip chart recorders.

Ozone was monitored using a Dasibi Model 1003AH ozone monitor. Calibrations were carried out against a Dasibi ozone monitor transfer standard which in turn was routinely calibrated by the California Air Resources Board. Calibration factors for individual runs were determined by least squares fit to the calibrations to the instruments carried out since early 1989.

Nitric oxide and total oxides of nitrogen (NO_x + organic nitrates) were monitored using a Columbia Scientific Industries Series 1600 and a Teco Model 14B. Calibrations were done using a National Bureau of Standards cylinder of NO in nitrogen. The dilution gas was Liquid Carbonic Co. Zero Air. The analyzer was first zeroed using Zero Air, then calibrated for NO by diluting NO in Zero Air and measuring the flow of each gas with a bubble flowmeter. The converter efficiency was checked by setting up a NO concentration of ca. 0.30 ppm and then reacting this with a lesser concentration of ozone. If the converter was operating properly, the NO_2 would equal the difference in NO. Calibration factors for individual runs were determined based on results of calibrations carried out before and after the run. The calibration factor for NO_2 included a correction for the converter efficiency, which was generally in the range of 95% or better, except as noted below. (However, the calibration factor for NO_x does not include the correction for NO_2 converter efficiency.)

Ocatamethylcyclotetrasiloxane, decamethylcyclopentasiloxane and (to a lesser extent) hexamethyldisiloxane were found to "poison" the converter used for NO_2 and NO_x analysis in both the Teco and the Columbia NO-NO_x analyzer. This resulted in the NO_2 data taken during experiments containing those compounds, and the experiments immediately following, being highly questionable or invalid. After this effect was noticed, steps were taken to avoid exposure of the converters to the siloxanes, so NO_2 data was not taken during most runs where these compounds were present. In the case of the Teco instrument, the ocatamethylcyclotetrasiloxane exposure caused the NO_2 converter efficiency to be reduced to 30%, but it gradually recovered to ~85%. In the case of the Columbia, the efficiency was reduced to about 65%. The affected converters were subsequently replaced.

Fortunately, NO_2 data is not required for the analyses of the reactivity results; its primary utility is determining whether the proper amount of NO_2 was injected in the run. Experience with the repeated runs throughout this and the previous program indicated relatively little run-to-run variability of initial NO_2 concentrations during the experiments.

Temperature was monitored with an Analogic Model AN 2572 Digital thermocouple indicator. The temperature probe was located about twelve inches into the chamber, near the center of the chamber wall.

3. Formaldehyde Analysis

Formaldehyde was not monitored except for the last several runs in this study, which included the runs where formaldehyde was added. For this purpose, a diffusion scrubber system was constructed following the description given by Dasgupta and co-workers (Dasgupta et al. 1988, 1990; Dong and Dasgupta, 1987). The system is similar to that used with the University of North Carolina outdoor chamber (Jeffries et al. 1990) and the help and cooperation of Drs. K.G. Sexton and H.E. Jeffries of UNC was instrumental in constructing this system.

Except as indicated, the system was designed as described in the references above. The formaldehyde scrubber is 40 cm. in length and differs from the Dasgupta unit only in the end treatment of microporous tube connections and support. The system uses a 1/4 inch stainless-steel Ultra-Torr tee, to form the inlet-outlet connections. Teflon tubing (1/4 inch o.d.) connects the two tees and with the hydrophobic membrane tubing stretched inside the 1/4 inch tubing. Sample air is drawn through the annular space into and out of the side arm of the tees. HPLC grade water is pumped through the scrubber by a Gilson Minipuls peristaltic pump. After the scrubber, a micro-bore stainless steel tee brings the reagent and water together before passing through 80 cm of 0.508 mm i.d. stainless steel tubing maintained at 95 degrees C in a heated bed. The detector is a Fluoromonitor III model 1311 fluorometer, with a 30 micro-liter volume flow cell. The source was changed to a 406 nm lamp with a 400 nm primary filter and a 500 nm emission filter. Liquid waste is collected directly from the flow cell outlet, without any added restricted.

An in-house formaldehyde permeation-tube-based formaldehyde generator was constructed to allow calibration checks as desired. The permeation tube (VICI Metronics) is maintained at 70 deg. C. Mass flow controllers (Tylan model FC280) are used for the permeation tube flush air, dilution air and sample air flow. Digital outputs of these three flow rates are constantly monitored. Permeation tube oven temperature and heated bed temperature can also be monitored constantly. The formaldehyde calibrator and measurement system are mounted together on a small laboratory cart. The choice of zero air, calibration or sample measurement cycle can be manually selected or remotely controlled by timers or the data acquisition system.

Initial system calibration was performed by sampling from the SAPRC Evacuable Chamber. Known volumes of formaldehyde were injected into the SAPRC

chamber and measured with the in-situ FTIR instrument. This calibration procedure, coupled with the permeation tube weight loss history (which was not well established at the time these experiments were conducted) has given an operating span factor. With an air sample flow rate of 1.75 lpm and the Fluoromonitor range at 200, a full scale response of about 1 ppm results. At present a strip chart recorder monitors the instrument response, but the system is being interfaced to the data acquisition computer for future experiments. Instrument response time is approximately 10 minutes.

D. Characterization of the Light Source in the Chamber

The light intensity in the chamber experiments was measured by carrying out NO_2 actinometry experiments at various times throughout the series of experiments. A slightly modified version of the quartz tube technique of Zafonte et al. (1977) was employed for this purpose. In this technique, the reactor cell consisted of a 100 cm segment of 25 mm (nominal) quartz tubing with 0.25 in. o.d. extensions at each end. The volume of the flow tube exposed to the light was 295 ml for most of the experiments discussed here. A mixture of 1.95 ppm of NO_2 in nitrogen was flowed through the tube with a flow rate of 1 liter min^{-1}. The NO and NO_2 in the mixture flowing from the tube were measured using a Columbia $NO\text{-}NO_x$ analyzer both with the lights on and with the lights off.

As discussed by Zafonte et al. (1977) the NO_2 photolysis rate (k_1) is given by

$$k_1 = \frac{[NO]^{light} - [NO]^{dark}}{[NO_2]^{light} + \frac{1}{2}\left([NO]^{light} - [NO]^{dark}\right)} \times \frac{F}{V} \times \frac{1}{\Phi}$$

where $[NO]^{light}$ and $[NO_2]^{light}$ are the NO and NO_2 concentrations from the tube with the lights on, $[NO]^{dark}$ is the NO concentration with the light off, F is the flow rate, V is the volume of the tube exposed to the light, and Φ is an "effective quantum yield" factor which takes into account the kinetics of the reactions involved in converting NO_2 to NO when it is photolyzed in N_2. As indicated above, for these experiments, F = 1 liter min^{-1}, and V = 0.295 liters. Φ was calculated by Zafonte et al (1977), but we re-calculated it more recently using updated rate constants and a plug-flow model for the reaction tube and the relevant reactions and rate constants from the SAPRC detailed mechanism (Carter, 1990). We found that Φ was in the range of 1.74-1.76 for the conditions of our actinometry experiments, so a value of Φ = 1.75 was used in our data analyses. This is approximately 9% higher than the value given by Zafonte et al (1977).

In order to calculate the rates of photolysis reactions when carrying out model simulations of the chamber experiments, it is necessary to know the

spectral distribution of the light source as well as the absolute light intensity. Since this chamber uses the same type of blacklights as does the SAPRC ITC, it was assumed to have the same relative spectral distribution. The similarities of the relative spectral distributions of light sources in these two chambers was confirmed by several spectral distribution measurements carried out in this chamber and the ITC using SPEX and LiCor radiometers. The ITC spectral distribution, which was used in our model simulations of the conditions of these ETC experiments, is given elsewhere (e.g., Carter and Lurmann, 1990, 1991). Spectral distributions of light sources in SAPRC chambers are being investigated as part of a separate study we are carrying out in conjunction with Jeffries and co-workers at the University of North Carolina, but a discussion of this is beyond the scope of this report.

For most of the actinometry experiments during this study the NO and NO_2 data were taken with the Columbia NO_x analyzer, since experience in our laboratories indicat that Columbia instruments perform somewhat better when sampling mixtures in N_2 for extended periods of time. However, the Teco was employed in one critical actinometry experiment (ETC-322) carried out just prior to moving the chamber to the new modular building, following an extended period when no NO_2 actinometry experiments were conducted. Both instruments were used in most of the subsequent actinometry experiments. In all these experiments the k_1 measured by the Teco is consistently lower than that measured by the Columbia, by approximately 5% on the average.

Although this apparent dependence of k_1 on NO_x instrument used was not a large effect, it complicates attempts to assess relative trends in light intensity. As will be seen later, determination of trends in chamber conditions is important in the analysis of results of reactivity experiments. Although we do not know that the data from the Columbia are necessarily more accurate, to place all the results on a consistent basis for determining trends in light intensity, the few k_1's determined using the Teco were corrected by a factor of 1.05 to make them consistent with the larger body of data obtained using the Columbia. Although this correction increases the precision of trend data, the possibility that it decreases the accuracy cannot be ruled out, and the absolute k_1 levels should be considered to be uncertain by at least 10%.

E. Other Characterization Experiments

The other characterization runs carried out in this chamber consisted of pure air irradiations, NO_x-air irradiations with small amounts of (~10 ppb) isobutene and n-butane present as radical tracers, n-butane-NO_x-air runs, and propene-NO_x-air runs. These runs are used primarily to characterize chamber effects needed for conducting model simulations of these experiments, and to

assure that the chamber characteristics are as expected based on previous runs (see Carter and Lurmann, 1990; 1991; Carter et al. 1986b, and references therein).

Perhaps the most important type of control run for this study is the standard mini-surrogate-NO_x experiment. Many repeats of this same experiment were carried out prior to, during, and subsequent to this study. The reproducibility of the results tended to serve as a monitor for the chamber effects which might affect the results of this study. This is discussed in detail in the following section.

III. EXPERIMENTAL RESULTS

A chronological listing of all experiments carried out in this study is given in Table 1. These consist primarily of the 244 mini-surrogate - NO_x - air experiments, including a total of 115 experiments where one of the 35 test VOCs were added, alternating with 129 repeated standard or "base case" experiments. Several characterization and control runs, and a number of NO_2 actinometry experiments were also conducted, and their results are discussed where relevant in the appropriate sections below. Comments and footnotes to the table indicate occurrences of special problems or changes in run conditions which occurred during the course of these experiments.

In the sections below, we will first discuss the analysis of the mini-surrogate experiments to obtain kinetic data and information concerning dilution in the chamber. This is useful for evaluating the consistency of our results with literature data, and provides the first reported measurement of the OH radical rate constant for carbitol, one of the VOCs whose reactivities were assessed. It is also useful for deriving estimates of dilution rates in the chamber experiments, which is needed in the reactivity analysis. The reactivity results of the mini-surrogate experiments are then discussed in Sections III-B and III-C. Section III-B gives a discussion of the variability of run conditions observed when carrying out the large set of repeated mini-surrogate experiments. The methods used to take this variability in conditions into account when deriving reactivity information from these runs, and the results obtained, are given in Section III-C.

A. Derivation of OH Radical Rate Constant Ratios, and Estimates of Chamber Dilution Rates

Reaction with OH radicals is a major if not the only significant consumption process for most VOCs in the atmosphere, and a knowledge of its rate constant (kOH) is essential for assessing a compound’s reactivity. Since these rate constants are known for most VOCs used in this study except for carbitol (Atkinson, 1989), measuring these is not an objective of this study. However, in principle, ratios of OH radical rate constants can be obtained from the results of these experiments from the relative rates of consumptions of the added VOCs, provided that (1) the VOCs react significantly only with OH radicals, and (2) dilution during these experiments is either known or negligible. 27 of the 35 test VOCs studied and two of the components of the base ROG surrogate (n-hexane and m-xylene) are expected to react primarily with OH radicals under

Table 1. Chronological Listing of Environmental Chamber Experiments.

RunNo	Date	Description	Comments
		Runs ETC-42 through 118 were conducted for EPA Cooperative Agreement no. CR-814396. Initial Characterization and Conditioning.	
42		O_3 Decay	O_3 decay rate = 2.23%/hour
43		NO_2 Actinometry	k_1 = 0.446 min^{-1}
44	10/25/89	Propene-NO_x Conditioning	
45a	10/26/89	Pure Air Photolysis	71 ppb O_3 formed in 6 hours
45b	10/26/89	NO_2 Actinometry	k_1 = 0.401 min^{-1}
46	11/17/89	Tracer-NO_x	Radical source characterization
		Start of Set 1 Runs.	
47	11/20/89	Mini-Surg.	
48a		NO_2 Actinometry	k_1 = 0.413 min^{-1}
48b		NO_2 Actinometry	k_1 = 0.416 min^{-1}
49	11/22/89	Ethane-NO_x	Control run for modeling
50	11/27/89	Mini-Surg.	
51	11/29/89	Mini-Surg. + 2.4 ppm n-Butane	
52	12/ 6/89	Mini-Surg.	
53	12/ 7/89	Mini-Surg. + 5.2 ppm n-Butane	
54	12/ 8/89	n-Butane-NO_x	Control run for modeling
55		NO_2 Actinometry	k_1 = 0.405 min^{-1}
57	1/ 9/90	Pure Air	52 ppb O_3 formed in 6 hours
56	12/20/89	Tracer-NO_x	Radical source characterization
58	1/12/90	Mini-Surg.	
59	1/17/90	Mini-Surg. + 1.8 ppm n-Butane	
60	1/18/90	Mini-Surg.	
61	1/19/90	Mini-Surg. + 0.16 ppm Toluene	
62	1/23/90	Mini-Surg. + 18. ppm Ethane	
63	1/24/90	Mini-Surg.	
64	1/25/90	Mini-Surg. + 0.055 ppm Toluene	
65	1/26/90	Mini-Surg. + 0.087 ppm Propene	
66	1/29/90	NO_2 Actinometry	k_1 = 0.356 min^{-1}
67	1/31/90	Mini-Surg.	
68	2/ 1/90	Mini-Surg. + 10.0 ppm Ethane	
69	2/ 8/90	Mini-Surg. + 0.087 ppm Toluene	
70	2/ 9/90	Tracer-NO_x	Radical source characterization
71	2/13/90	Mini-Surg.	
72	2/15/90	Mini-Surg. + 0.123 ppm Propene	
73	2/16/90	Mini-Surg. + 18. ppm Ethane	
74		NO_2 Actinometry	k_1 = 0.363 min^{-1}
75	2/21/90	Mini-Surg.	
76	2/22/90	Tracer-NO_x	Radical source characterization
77	2/23/90	Mini-Surg.	
78		(aborted run) [a]	
79	2/28/90	Mini-Surg. + 18. ppm Ethane	
80	3/ 2/90	Mini-Surg.	
81	3/ 6/90	Mini-Surg.	
82	3/ 7/90	Mini-Surg. + 6.7 ppm n-Butane	
83	3/ 8/90	Mini-Surg.	
84		NO_2 Actinometry	k_1 = 0.367 min^{-1}
85	3/13/90	(aborted run) [a]	
86	3/14/90	Mini-Surg. + 6.9 ppm n-Butane	
87	3/15/90	Mini-Surg.	
88	3/20/90	Mini-Surg. + 24. ppm Ethane	
89	3/21/90	Mini-Surg.	
		Start of Set 2 runs. NO_x injected from vacuum rack from this point on.	
90	3/22/90	Mini-Surg.	
91	3/29/90	Mini-Surg.	
92	3/30/90	Mini-Surg. + 17. ppm Ethane	
93	4/ 3/90	Mini-Surg.	
94	4/ 5/90	Mini-Surg. + 7.2 ppm n-Butane	
95	4/ 6/90	Mini-Surg.	
96		NO_2 Actinometry	k_1 = 0.334 min^{-1}
97	4/19/90	Mini-Surg. + 6.2 ppm n-Butane	
98	4/20/90	Mini-Surg.	
99	4/24/90	Mini-Surg. + 18. ppm Ethane	
100	4/27/90	Mini-Surg.	
101	5/ 1/90	Mini-Surg. + 0.16 ppm Toluene	
102	5/ 3/90	Mini-Surg.	
103	5/ 4/90	Mini-Surg. + 0.16 ppm Toluene	
104	5/ 9/90	Mini-Surg.	
105		NO_2 Actinometry	k_1 = 0.339 min^{-1}
106	5/11/90	Mini-Surg. + 0.084 ppm Propene	
107	5/17/90	Mini-Surg.	
108	5/18/90	Mini-Surg. + 0.085 ppm Propene	

Table 1 (continued)

RunNo	Date	Description	Comments
109	5/22/90	Mini-Surg.	
110	5/24/90	Mini-Surg. + 0.077 ppm Propene	
111		NO_2 Actinometry	k_1 = 0.329 min^{-1}
112	5/30/90	Tracer-NO_x	Radical source characterization
113	5/31/90	Mini-Surg.	
114	6/13/90	Mini-Surg.	
115	6/15/90	Mini-Surg.	
116	6/18/90	Rejected Mini-Surg. [b]	
117	6/19/90	Mini-Surg.	
118	6/20/90	Mini-Surg. + 0.148 ppm Propene	
		Runs ETC-119 through ETC-176 were carried out for the 1987-1991 SCAQMD program.	
119	6/21/90	Rejected Mini-Surg. [b]	
121		NO_2 Actinometry	k_1 = 0.329 min^{-1}
120	6/22/90	Mini-Surg. + 2.0 ppm Methyl t-Butyl Ether	
122	6/26/90	Mini-Surg.	
123	6/27/90	Mini-Surg. + 3.0 ppm Methyl t-Butyl Ether	
124	6/28/90	Mini-Surg.	
125	6/29/90	Mini-Surg. + 2.5 ppm Methyl t-Butyl Ether	
126	7/ 2/90	Mini-Surg.	
127	7/ 3/90	Mini-Surg. + 2.5 ppm Methyl t-Butyl Ether	
128	7/ 5/90	Mini-Surg.	
129	7/ 6/90	Mini-Surg.	
130	7/16/90	Mini-Surg.	
131	7/17/90	Mini-Surg. + 3.1 ppm Ethanol	
132	7/18/90	Mini-Surg.	
133	7/19/90	Mini-Surg. + 2.9 ppm Ethanol	
134	7/20/90	Mini-Surg.	
135	7/24/90	Mini-Surg. + 6.1 ppm n-Butane	
136		NO_2 Actinometry	k_1 = 0.326 min^{-1}
137	7/26/90	Mini-Surg.	
138	7/27/90	Mini-Surg. + 3.0 ppm Ethanol	
139	7/30/90	Mini-Surg.	
140		NO_2 Actinometry	k_1 = 0.319 min^{-1}
141	10/23/90	Pure Air Photolysis	158 ppb O_3 formed in 22 hours
142		(aborted run)	
143	10/31/90	Rejected Mini-Surg. [b]	
144		(aborted run)	
145	11/ 2/90	Mini-Surg.	
146		(aborted run)	
147	11/ 7/90	Mini-Surg.	
148	11/ 9/90	Mini-Surg. + 4.0 ppm Isopropyl Alcohol	
149	11/12/90	Mini-Surg.	
150	11/16/90	m-Xylene	Control run for modeling
151	1/ 7/91	Pure Air	134 ppb O_3 formed in 15.5 hours
152		(aborted run)	
		Start of Set 3. Initial base ROG increased by approximately 40%	
153	1/ 9/91	Mini-Surg.	
154	1/10/91	Mini-Surg.	
155	1/11/91	Mini-Surg. + 1.7 ppm Isopropyl Alcohol	
156	1/14/91	Mini-Surg.	
157	1/16/91	Mini-Surg. + 1.26 ppm Isopropyl Alcohol	
158	1/17/91	Mini-Surg.	
159	1/18/91	Mini-Surg. + 1.6 ppm Isopropyl Alcohol	
160	1/22/91	Mini-Surg.	
161	1/24/91	Mini-Surg.	
162	1/28/91	Mini-Surg.	
163	1/31/91	Mini-Surg. + 0.82 ppm 2-Ethoxy-Ethanol	
164	2/ 1/91	Mini-Surg.	
165	2/ 6/91	Mini-Surg.	
166	2/ 7/91	Mini-Surg. + 0.51 ppm Carbitol [c]	
167		NO_2 Actinometry	k_1 = 0.322 min^{-1}
168	2/12/91	Mini-Surg.	
169	2/13/91	Mini-Surg. + 0.41 ppm Carbitol	
170	2/14/91	Mini-Surg.	
171	2/20/91	Mini-Surg. + 0.71 ppm 2-Ethoxy-Ethanol	
172	2/21/91	Mini-Surg.	
173	2/22/91	Mini-Surg. + 0.94 ppm Carbitol	
174	2/25/91	Mini-Surg.	
175	2/26/91	Mini-Surg. + 0.41 ppm 2-Ethoxy-Ethanol	
176	2/27/91	Mini-Surg.	
		Runs ETC-177 through ETC-195 were carried out for the Dow Corning Corporation. Problems with NO_2 analysis [d]	
177	3/19/91	Mini-Surg. [e]	

Table 1 (continued)

RunNo	Date	Description	Comments
178	3/20/91	Mini-Surg. [e]	
179	3/21/91	Mini-Surg. + 9.4 ppm Hexamethyldisiloxane	
181	3/26/91	Mini-Surg. + 10.1 ppm D4 Cyclosiloxane [f]	
182	3/27/91	Mini-Surg.	
183	3/28/91	Mini-Surg. + 6.7 ppm Hexamethyldisiloxane	
184	3/29/91	Mini-Surg.	
185	4/ 2/91	Mini-Surg. + 4.4 ppm D4 Cyclosiloxane	
186	4/ 3/91	Mini-Surg.	
187	4/ 4/91	Mini-Surg. + 4.9 ppm D5 Cyclosiloxane [g]	
189	4/12/91	Mini-Surg.	
190	4/15/91	Mini-Surg. + 1.5 ppm D5 Cyclosiloxane	
191	4/16/91	Mini-Surg.	
192	4/17/91	Mini-Surg. + 1.9 ppm D5 Cyclosiloxane	
193	4/18/91	Mini-Surg.	
194	4/19/91	Mini-Surg. + 2.1 ppm D4 Cyclosiloxane	
195	4/22/91	Mini-Surg.	
		Except where noted all runs after ETC-195 were carried out for the Joint ARB, CRC, SCAQMD Reactivity Program.	
196	4/23/91	Mini-Surg. + 0.057 ppm m-Xylene [h]	
197	4/25/91	Rejected Mini-Surg. [i]	
198	4/26/91	Mini-Surg.	
199	4/29/91	Mini-Surg. + 0.39 ppm Ethene [h]	
200	4/30/91	Mini-Surg.	
201	5/ 1/91	Mini-Surg. + 1.17 ppm n-Hexane [h]	
202	5/ 2/91	Mini-Surg.	
203	5/ 7/91	Mini-Surg. + 0.22 ppm Ethene [h]	
204	5/ 8/91	Mini-Surg.	
205	5/ 9/91	Pure Air Photolysis	61 ppb O_3 formed in 14.5 hours
206	5/ 9/91	NO_2 Actinometry	$k_1 = 0.322\ min^{-1}$
207	5/10/91	Mini-Surg. + 0.038 ppm m-Xylene	
208	5/14/91	Mini-Surg. [j]	
209	5/15/91	Mini-Surg. + 1.58 ppm n-Hexane	
210	5/16/91	Mini-Surg.	
		Runs ETC-211 through 222 were conducted primarily as control runs for modeling	
211	5/17/91	Rejected Tracer-NO_x [k]	
212	5/22/91	Rejected Tracer-NO_x [k]	
213	5/22/91	Tracer-NO_x	Characterization of radical sources
214	5/23/91	n-Butane-NO_x	
215	5/24/91	Mini-Surg. [l]	
216	5/30/91	Propene-NO_x	
217	5/31/91	Mini-Surg. with 1/2 normal NO_x	
218	6/ 3/91	(M-Xylene + Ethene)-NO_x	
219	6/ 4/91	Mini-Surg. with 1/2 normal NO_x	
220	6/ 6/91	Ethene-NO_x	
221	6/ 7/91	Ethene-NO_x	
222	6/10/91	M-Xylene-NO_x	
223	6/12/91	Mini-Surg.	
224	6/13/91	Mini-Surg. + 10.0 ppm n-Butane	
225	6/14/91	Rejected Mini-Surg. [m]	
226	6/17/91	Mini-Surg. + 11.2 ppm Propane	
227	6/18/91	Mini-Surg.	
228	6/19/91	Mini-Surg. + 2.7 ppm Isobutane	
229	6/20/91	Mini-Surg.	
230	6/21/91	Mini-Surg. + 28. ppm Propane	
231	6/24/91	Mini-Surg.	
232	6/25/91	Mini-Surg. + 21. ppm Isobutane	
233	6/26/91	Mini-Surg.	
		The chamber was relocated to another room. [n]	
234	7/10/91	Mini-Surg.	
235	7/11/91	Mini-Surg. + 42. ppm Ethane	
236	7/12/91	Mini-Surg.	
237	7/15/91	Mini-Surg. + 1.7 ppm n-Octane	
238	7/16/91	Mini-Surg.	
239	7/18/91	Mini-Surg. + 1.6 ppm n-Octane	
240	7/19/91	Mini-Surg.	
241	7/22/91	Mini-Surg. + 10.3 ppm Isobutane	
242	7/23/91	Mini-Surg.	
243	7/24/91	Mini-Surg. + 0.85 ppm Acetone	
244	7/26/91	Mini-Surg.	
245	7/29/91	Mini-Surg. + 2.2 ppm Acetone	
246	7/30/91	Mini-Surg.	
247	7/31/91	Mini-Surg. + 4.3 ppm Acetone	
248	8/ 1/91	Rejected Mini-Surg. [m]	

Table 1 (continued)

RunNo	Date	Description	Comments
		Use of the GC computer data system begins with ETC-249. [p]	
249	8/ 2/91	Mini-Surg. + 0.046 ppm 1,3,5-Trimethyl Benzene	
250	8/ 6/91	Mini-Surg.	
251	8/ 6/91	Mini-Surg. + 0.044 ppm 1,3,5-Trimethyl Benzene	
252	8/ 7/91	Mini-Surg.	
253	8/ 9/91	Mini-Surg. + 0.21 ppm Isobutene	
254	8/12/91	Rejected Mini-Surg [m]	
255	8/13/91	Mini-Surg. + 0.19 ppm Isobutene	
256	8/14/91	Rejected Mini-Surg [m]	
257	8/15/91	Mini-Surg. + 0.108 ppm Isobutene	
258	8/16/91	Mini-Surg.	
259	8/19/91	Mini-Surg. + 0.063 ppm o-Xylene	
260	8/20/91	Mini-Surg.	
261	8/21/91	Mini-Surg. + 0.065 ppm o-Xylene	
262	8/22/91	Mini-Surg.	
263	8/23/91	Mini-Surg. + 6.8 ppm Benzene	
264	8/26/91	Mini-Surg.	
265	8/27/91	Mini-Surg. + 5.8 ppm Benzene	
266	8/28/91	Mini-Surg.	
267	8/29/91	Mini-Surg. + 0.037 ppm 1,2,4-Trimethyl Benzene	
268	9/ 3/91	Rejected Mini-Surg [m]	
269	9/ 4/91	Mini-Surg. + 0.041 ppm 1,2,4-Trimethyl Benzene	
270	9/ 5/91	Mini-Surg.	
		The runs with Isoprene were carried out for the EPA/SOS project.	
271	9/10/91	Mini-Surg. + 0.15 ppm Isoprene	
272	9/11/91	Mini-Surg.	
273	9/13/91	Mini-Surg. + 0.138 ppm Isoprene	
274	9/16/91	Mini-Surg.	
275	9/17/91	Mini-Surg. + 0.108 ppm Isoprene	
276	9/18/91	Mini-Surg.	
277	9/19/91	Mini-Surg. + 0.076 ppm Isoprene	
278	9/20/91	Mini-Surg.	
279	9/23/91	Mini-Surg. + 4.0 ppm Dimethyl Ether	
280	9/24/91	Mini-Surg.	
281	9/25/91	Mini-Surg. + 3.4 ppm Dimethyl Ether	
282	9/26/91	Mini-Surg.	
283	9/27/91	Mini-Surg. + 2.1 ppm Dimethyl Ether	
284	9/30/91	Mini-Surg.	
285	10/ 1/91	Mini-Surg. + 7.7 ppm Methanol	
286	10/ 3/91	Mini-Surg.	
287	10/ 4/91	Mini-Surg. + 0.83 ppm Methanol	
288	10/ 8/91	Mini-Surg.	
289	10/ 9/91	Mini-Surg. + 2.4 ppm Methanol	
290	10/10/91	Mini-Surg.	
291	10/11/91	Mini-Surg. + 10.1 ppm 2,2,4-Trimethyl Pentane	
292	10/14/91	Mini-Surg.	
293	10/15/91	Mini-Surg. + 10.7 ppm 2,2,4-Trimethyl Pentane	
294	10/16/91	Mini-Surg.	
295	10/17/91	Mini-Surg. + 2.1 ppm Dimethyl Ether	
296	10/18/91	Mini-Surg.	
297	10/21/91	Mini-Surg. + 0.043 ppm 1,2,3-Trimethyl Benzene	
298	10/22/91	Mini-Surg.	
299	10/23/91	Mini-Surg. + 0.036 ppm 1,2,3-Trimethyl Benzene	
300	10/24/91	Mini-Surg.	
301	10/25/91	Mini-Surg. + 0.054 ppm m-Xylene [h]	
302	10/28/91	Mini-Surg.	
303	10/29/91	Mini-Surg. + 6.6 ppm Isobutane	
304	10/30/91	Mini-Surg.	
305	10/31/91	Mini-Surg. + 20. ppm Propane	
306	11/ 4/91	Mini-Surg.	
307	11/ 5/91	Mini-Surg. + 0.095 ppm trans-2-Butene	
308	11/ 6/91	Mini-Surg.	
309	11/ 7/91	Mini-Surg. + 0.071 ppm trans-2-Butene	
310	11/ 8/91	Mini-Surg.	
311	11/11/91	Mini-Surg. + 0.096 ppm Ethyl Benzene	
312	11/12/91	Mini-Surg.	
313	11/13/91	Mini-Surg. + 0.092 ppm Ethyl Benzene	
314	11/15/91	Mini-Surg.	
315	11/18/91	Mini-Surg. + 0.22 ppm Ethyl Benzene	
316	11/19/91	Mini-Surg.	
317	11/20/91	Tracer-NO_x	Characterization of radical sources
318	11/21/91	Butane-NO_x	Control run for modeling
319	11/22/91	Acetaldehyde-Air	Characterization of NO_x offgasing
320	11/25/91	Pure air	30 ppb O_3 formed in 6 hours

Table 1 (continued)

RunNo	Date	Description	Comments
321	11/26/91	Propene-NO_x	Control run for modeling
322	12/ 2/91	NO_2 Actinometry	Teco used for first time for an NO_2 actinometry run. k_1 = 0.285 min^{-1}
		The chamber was moved to the new SCAQMD-funded modular building next to the site of the outdoor chamber A series of standard runs were conducted initially to assure consistency of results.	
323	1/17/92	Mini-Surg. [m,q]	
324	1/21/92	Mini-Surg. [m,r]	
325	1/22/92	Mini-Surg.	
326	1/24/92	Mini-Surg.	
327	2/ 3/92	Mini-Surg.	
328	2/ 4/92	Mini-Surg.	
329	2/ 5/92	Mini-Surg.	
330	2/ 6/92	Mini-Surg.	
331	2/ 7/92	Mini-Surg.	
332	2/10/92	Mini-Surg. + 20. ppm Ethane [s]	
333	2/11/92	Mini-Surg. + 21. ppm Ethane [s]	
334	2/12/92	Mini-Surg.	
335	2/14/92	Mini-Surg. + 0.70 ppm Acetaldehyde	
336	2/18/92	Mini-Surg.	
337	2/19/92	NO_2 Actinometry	Teco used. k_1 = 0.347 min^{-1}
338	2/19/92	Mini-Surg. + 1.31 ppm Acetaldehyde	
		Starting with Run ETC-339, approximately 2 ppb of 2-chloromethyl-3-chloropropene was added to the runs to serve as an OH radical tracer.	
339	2/20/92	Mini-Surg.	
340	2/21/92	NO_2 Actinometry	k_1 using Columbia = 0.328 min^{-1}. k_1 using Teco = 0.300 min^{-1}
341	2/21/92	NO_2 Actinometry	k_1 using Columbia = 0.324 min^{-1} k_1 using Teco = 0.306 min^{-1}
342	2/25/92	Mini-Surg. + 0.107 ppm Chlorobutene [t]	
343	2/26/92	Mini-Surg. + 0.102 ppm Chlorobutene	
344	2/27/92	Mini-Surg. + 0.081 ppm m-Xylene [h]	Two lights had to be replaced.
345	3/ 2/92	Mini-Surg.	
346	3/ 3/92	Mini-Surg. + 0.080 ppm p-Xylene [u]	
		Formaldehyde was monitored starting with ETC-347	
347	3/ 4/92	Mini-Surg.	
348	3/ 5/92	Mini-Surg. + 0.075 ppm p-Xylene [u]	
349	3/ 6/92	Mini-Surg.	
350	3/ 9/92	Mini-Surg. + 0.108 ppm Chlorobutene	
351	3/10/92	Mini-Surg.	
352	3/11/92	Mini-Surg. + 0.104 ppm Formaldehyde	
353	3/12/92	Mini-Surg.	
354	3/13/92	Dark Surrogate run	Monitor dark losses and dilution [v]
		Starting with run ETC-355, CCl_4 added to monitor dilution [w]	
355	3/17/92	Dark Surrogate run	Monitor dark losses and dilution
356	3/18/92	Mini-Surg.	
357	3/19/92	Mini-Surg. + 0.27 ppm Formaldehyde	
359	3/25/92	NO_2 Actinometry	k_1 using Columbia = 0.356 min^{-1} k_1 using Teco = 0.338 min^{-1}
	4/22/92	New reaction bag installed.	Contaminants from pure air system made data from runs 358 through 368 (except the actinometry experiments) invalid. The reaction bag was replaced and medical air was used until the pure air system was repaired.
369	4/22/92	NO_2 Actinometry	k_1 using Columbia = 0.414 min^{-1}; Teco = 0.393 min^{-1}. Results not used. [x]
370	4/23/92	Pure-air irradiation	
371	4/23/92	Ozone decay	Result in normal range. (Contamination had caused abnormally high ozone decays.)
372	4/27/92	Mini-Surg. (not used) [y]	
373	4/28/92	Mini-Surg. (not used) [y]	
374	5/12/92	Pure-air irradiation	
375	5/18/92	Propene-NO_x	
376	5/19/92	Standard Mini-Surg.	
377	5/20/92	Ethene-NO_x	
378	5/21/92	Formaldehyde - NO_x	
379	5/22/92	Formaldehyde-air	
380	5/26/92	Tracer-NO_x	
381	5/27/92	Ethene-NO_x	

Table 1 (continued)

RunNo	Date	Description	Comments
382	5/28/92	Acetaldehyde-air	
383	6/ 2/92	Mini-Surg.	
384	6/ 3/92	Mini-Surg.	
385	6/ 8/92	Formaldehyde-air	
		A series of runs were carried out for another program, or for the second phase of this program, which are beyond the scope of this report.	
394		NO_2 Actinometry	k_1 using Columbia = 0.325 min^{-1} k_1 using Teco = 0.339 min^{-1}.
408	7/20/92	Mini-Surg.	
409	7/21/92	Mini-Surg. + 2.2 ppm MDOH [z]	
410	7/22/92	Ozone dark decay run	
411	7/23/92	Mini-Surg.	
412	7/24/92	Mini-Surg. + 0.7 ppm MDOH	
413	7/27/92	Mini-Surg.	
414	7/29/92	Mini-Surg. + 138 ppm CO	Probable CO contamination [aa]
415	7/31/92	Mini-Surg.	
416	8/ 4/92	Mini-Surg. + 130 ppm CO	
417	8/ /92	Mini-Surg. (not used) [bb]	
418	8/10/92	Mini-Surg. + 110 ppm CO	
419	8/ /92	Mini-Surg.	
448		NO_2 Actinometry	k_1 using Columbia = 0.328 min^{-1} k_1 using Teco = 0.333 min^{-1}.

[a] Leak in chamber.
[b] Run rejected because initial reactant concentrations not within acceptable range.
[c] "Carbitol" is 2-(2-ethoxyethoxy) ethanol
[d] NO_2 data invalid, missing or questionable in runs ETC-179 through 188, 190, 192, and 194 because the siloxanes were found to "poison" the catalyst used for NO_2 analysis. Once this problem was recognized, the catalyst was replaced, and NO_2 was not monitored when siloxanes were present in the chamber.
[e] Small amounts of siloxane contaminants seen in the chamber.
[f] "D4" is octamethylcyclotetrasiloxane
[g] "D5" is decamethylcyclopentasiloxane
[h] Initial amount of a component of the base ROG was increased to determine its reactivity. The nominal "amount added" used for reactivity assessment is the difference between the initial concentration in the run and the average initial concentration for the Set 3 runs where this component was not increased. The "amount reacted" in the reactivity calculations was the (total amount reacted) x (nominal amount added) / (total amount added).
[i] Run is anomalously reactive because of methyl nitrite contamination in error in NO_x injection procedure.
[j] Run not used in reactivity data analysis because of problems with the O_3 analysis
[k] Problems with syringes used for injection
[l] This run was conducted for control purposes and was not used in the reactivity data analysis.
[m] Run rejected because of anomalous results.
[n] Somewhat greater difficulties in maintaining temperature control on a day to day basis was observed in this location.
[p] This system permitted integration of GC peaks, resulting in improved precision in GC analyses, especially for n-hexane.
[q] Anomalously high ozone formation. Reason unknown
[r] Anomalously low ozone formation. Reason unknown
[s] These runs (especially ETC-332) had unexpectedly high reactivity for ethane, especially initially. Probable contaminant in ethane sample used.
[t] "Chlorobutene" is 2-(chloromethyl)-3-chloropropene
[u] P-xylene and m-xylene cannot be monitored separately because they could not be separated in our GC analysis. Initial concentrations determined by injecting them sequentially, and measuring the change in the total peak area.
[v] Anomalously high dilution (4%/hour) observed in this run. Because of questions concerning dilution, an inert tracer (CCl_4) was added for the subsequent runs.
[w] Essentially no dilution observed in runs ETC-335 and ETC-336. Approximately 1%/hour observed in runs ETC-337 and ETC-338
[x] The k_1 values measured in this run were amomalously high compared to the results of the other actinometry determinations, and were not used when computing the average k_1 for the runs in the new building.
[y] These runs had unusually high temperatures.
[z] "MDOH" is pentamethyldisiloxanol.
[aa] This run had anomalously high IntOH values, and a theoretically unreasonable ConvF result. Probably due to CO contamination, since the CO was not purified, and since subsequent runs, with CO purified by passing through molecular sieves, gave lower IntOH reactivities and more chemically reasonable ConvF results.
[bb] Run had no valid temperature data.

the conditions of these experiments, and thus in principle rate constant ratios for these compounds can be measured. For the majority of compounds whose rate constants are available from the literature, measuring these rate constant ratios provides a useful cross-check on the conditions of these experiments (and in some cases on the literature rate constants), and in the case of carbitol this provides information necessary to assess its reactivity.

In this analysis, m-xylene is used as the reference compound against which the relative rate constants for the other VOCs are determined. It is used because it reacts significantly only with OH radicals, has a reasonably well known OH radical rate constant (Atkinson, 1989), reacts relatively rapidly, is present in all the mini-surrogate experiments, and was measured with reasonably good precision in most experiments. N-hexane, the other mini-surrogate component which reacts significantly only with OH radicals, is less suitable because it reacts slower and because it was not measured with as good precision as the m-xylene until around ETC-254, when the HP Chemstation software was used.

If m-xylene and another VOC are present in the same experiment and are consumed significantly only by dilution or reaction with OH radicals, then their rates of consumption are given by,

$$\frac{d\ ln[m\text{-}Xyl]}{dt} = kOH^{m\text{-}xyl}\ [OH]_t + D$$

$$\frac{d\ ln[VOC]}{dt} = kOH^{voc}\ [OH]_t + D$$

where $kOH^{m\text{-}xyl}$ and kOH^{voc} are the OH radical rate constants for m-xylene and the VOC, respectively, $[OH]_t$ is the OH radical concentration at time t, and D is the dilution rate. Combining and re-arranging these equations to eliminate $[OH]_t$ yields

$$\left(-\frac{d\ ln[VOC]}{dt} - D \right) = \left(\frac{kOH^{voc}}{kOH^{m\text{-}xyl}} \right) \left(\frac{d\ ln[m\text{-}Xyl]}{dt} - D \right)$$

and integrating both sides and re-arranging yields:

$$\left\{ ln\left(\frac{[VOC]_0}{[VOC]_t} \right) - D \right\} = \left(\frac{kOH^{voc}}{kOH^{m\text{-}xyl}} \right) \left\{ ln\left(\frac{[m\text{-}Xyl]_0}{[m\text{-}Xyl]_t} \right) - Dt \right\} \qquad (XIX)$$

where $[VOC]_0$, $[VOC]_t$, $[m\text{-}Xyl]_0$, and $[m\text{-}Xyl]_t$ are the measured initial and time t values of the VOC and m-xylene, respectively. Plots of $ln([VOC]_0/[VOC]_t)$-Dt vs $ln([m\text{-}Xyl]_0/[m\text{-}Xyl]_t$-Dt should give a straight line with a slope equal to the ratio of rate constants. This is a standard method for determining OH radical

rate constants using the relative rate technique (Atkinson, 1986, and references therein).

Dilution is expected to be small in these experiments since a flexible reaction bag is used which can collapse as samples are withdrawn. However, the possibility that a small amount of leakage or exchange is occurring during the six hours of an experiment cannot be ruled out. Because this might be non-negligible, this possibility needs to be considered in the data analysis, both when deriving OH radical rate constants and when deriving mechanistic reactivities.

The rate constants derived from the results of our experiments are summarized on Table 2, where they are compared with literature values. Plots of $\ln([VOC]_0/[VOC]_t)$ vs $\ln([m\text{-}Xyl]_0/[m\text{-}Xyl]_t)$ are shown on Figures 2-4 for those VOCs whose rate constants could be determined with a (one σ) standard deviation of less than 15%. (Except for the top plot on Figure 2, the plots on the figures are derived assuming D = 0.5%/hour, based on the considerations discussed below.) The rate constants on Table 2 are placed on an absolute basis using the $kOH^{m\text{-}xyl}$ recommendation of Atkinson (1989), which is

$$kOH^{m\text{-}xyl} = 2.36 \times 10^{-11} \text{ cm}^3 \text{ molec}^{-1} \text{ s}^{-1}$$

independent of temperature over the range 250-315 K, with an estimated overall (two σ) uncertainty of ± 25%. Except where indicated, the rate constants for the other VOCs shown on Table 2 are also those recommended by Atkinson (1989), with his estimated (two σ) uncertainties also being given.

1. Derivation of Dilution Rate.

The data in the "D=0" column on Table 2 were calculated assuming dilution is negligible in the chamber. Note that the rate constants in this column are higher than the literature value by more than the standard deviation of the measurement for all compounds which react slower than toluene, except for n-butane. This is particularly true for n-hexane, whose rate constant derived assuming no dilution is 24% lower than the literature value, but whose apparent rate constant relative to m-xylene is measured with a standard deviation of only 1%. This is because of the large number of experiments where both compounds are present. This systematic discrepancy suggests that dilution occurring in these experiments, since dilution would have a greater effect on the rates of decay of the slower reacting compounds than the more rapidly reacting ones.

Table 2. OH Radical Rate Constants Derived from the Mini-Surrogate Chamber Runs Compared with Literature Values, and Dilution Rate Estimates Derived Using the Literature Rate Constant Ratios.

VOC	Lit. kOH [a]	kOH (S.Dev) [Diff] [b] D=0			kOH (S.Dev) [Diff] [b] D=0.5			Adjusted D (%/hour) [c]	
Ethane	0.274 (20%)	[d]			[d]			0.3	(0.2)
Propane	1.16 (30%)	[d]			[d]			0.2	(0.3)
n-Butane	2.56 (20%)	2.03	(24%)	[-21%]	0.98	(76%)	[-62%]	0.1	(0.3)
Isobutane	2.36 (25%)	3.86	(11%)	[64%]	2.75	(27%)	[17%]	0.6	(0.2)
n-Hexane	5.63 (25%)	6.97	(1%)	[24%]	6.50	(4%)	[15%]	1.2	(1.0)
2,2,4-Trimethyl Pentane	3.72 (20%)	5.40	(36%)	[45%]	2.94	(88%)	[-21%]	0.4	(0.4)
n-Octane	8.79 (20%)	12.7	(9%)	[45%]	10.6	(17%)	[21%]	0.8	(0.3)
Benzene	1.29 (30%)	2.00	(12%)	[55%]	1.51	(24%)	[17%]	0.6	(0.4)
Toluene	5.91 (25%)	6.14	(2%)	[4%]	5.65	(5%)	[-4%]	0.4	(1.3)
Ethyl Benzene	7.1 (35%)	6.62	(3%)	[-7%]	5.95	(7%)	[-16%]	[e]	
o-Xylene	13.7 (25%)	12.6	(4%)	[-8%]	12.3	(4%)	[-10%]	[e]	
1,3,5-Trimethyl Benzene	57.5 (35%)	60.4	(1%)	[5%]	61.3	(2%)	[7%]	[e]	
1,2,4-Trimethyl Benzene	32.5 (35%)	27.8	(2%)	[-14%]	27.9	(3%)	[-14%]	[e]	
1,2,3-Trimethyl Benzene	32.7 (35%)	35.1	(4%)	[7%]	35.3	(5%)	[8%]	[e]	
Methanol	0.940 (25%)	1.65	(32%)	[75%]	1.03	(62%)	[10%]	0.7	(0.4)
Ethanol	3.28 (20%)	[d]			[d]				
Isopropyl Alcohol	5.20 (40%)	6.32	(14%)	[21%]	5.72	(17%)	[10%]	0.8	(1.6)
Dimethyl Ether	3.01 (25%)	4.13	(9%)	[37%]	3.51	(14%)	[17%]	0.8	(0.6)
Methyl t-Butyl Ether	2.84 (35%)	2.99	(13%)	[5%]	1.81	(41%)	[-36%]	0.2	(0.4)
2-Ethoxy-Ethanol	23.6 [f]	21.6	(5%)	[41%]	21.5	(6%)	[41%]		
2-(2-Ethoxyethoxy) Ethanol	[g]	49.2	(10%)		50.8	(11%)			
Hexamethyldisiloxane	1.38 [h]								
D4 Cyclosiloxane	1.01 [h]								
D5 Cyclosiloxane	1.55 [h]								
2-(Cl-methyl)-3-Cl Propene	33.5 [i]	31.4	(1%)	[-6%]	31.6	(1%)	[-6%]		
Carbon Tetrachloride	0.0							0.7	(0.2)

[a] Literature values (in units of 10^{-12} cm^3 $molec^{-1}$ s^{-1}) from review of Atkinson (1989), for T=300K. Quantities in parentheses are Atkinson's (1989) estimated uncertainty in the recommended absolute rate constant. If no recommendation is given, footnote gives source of literature kOH used.

[b] kOH (in units of 10^{-12} cm^3 $molec^{-1}$ s^{-1}) calculated assuming no dilution (D=0), and assuming D = 0.48±0.24 %/hr (D=0.5). Measured values of kOH_{voc} placed on an absolute basis using $kOH_{m\text{-}xyl}$ 2.36 x 10^{-11} cm^3 $molec^{-1}$ s^{-1} (Atkinson, 1989). Quantities in parenthesis are (one σ) standard deviations. Standard deviations for D=0.5 values include uncertainty in dilution. Quantities in brackets are differences between kOH values from this work and literature values.

[c] Dilution rate adjusted so kOH derived from the chamber data is the same as the literature value. Quantities in parenthesis is (one σ) standard deviation of derivation. Standard deviation includes effect of uncertainty in literature kOH.

[d] Measurement data too scattered for kOH determination.

[e] Reacts too rapidly to be sensitive to dilution.

[f] The two published kOH measurements disagree, and Atkinson (1989) gives no recommendation. Value shown is from Daguat et al (1988). Value from Hartmann et al (1987) (1.2 x 10^{-11} cm^3 $molec^{-1}$ s^{-1}) is assumed to be less reliable because of poor agreement with the other two determinations.

[g] kOH not measured previously.

[h] From Atkinson (1990).

[i] From Tuazon et al. (1988).

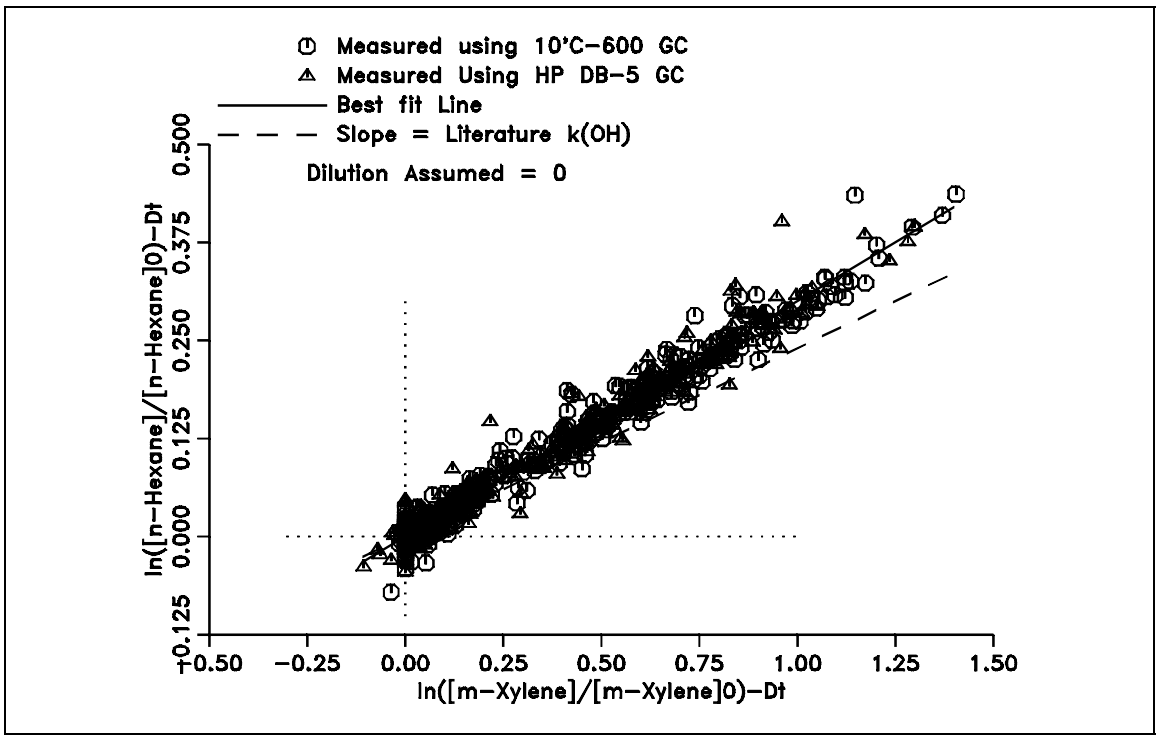

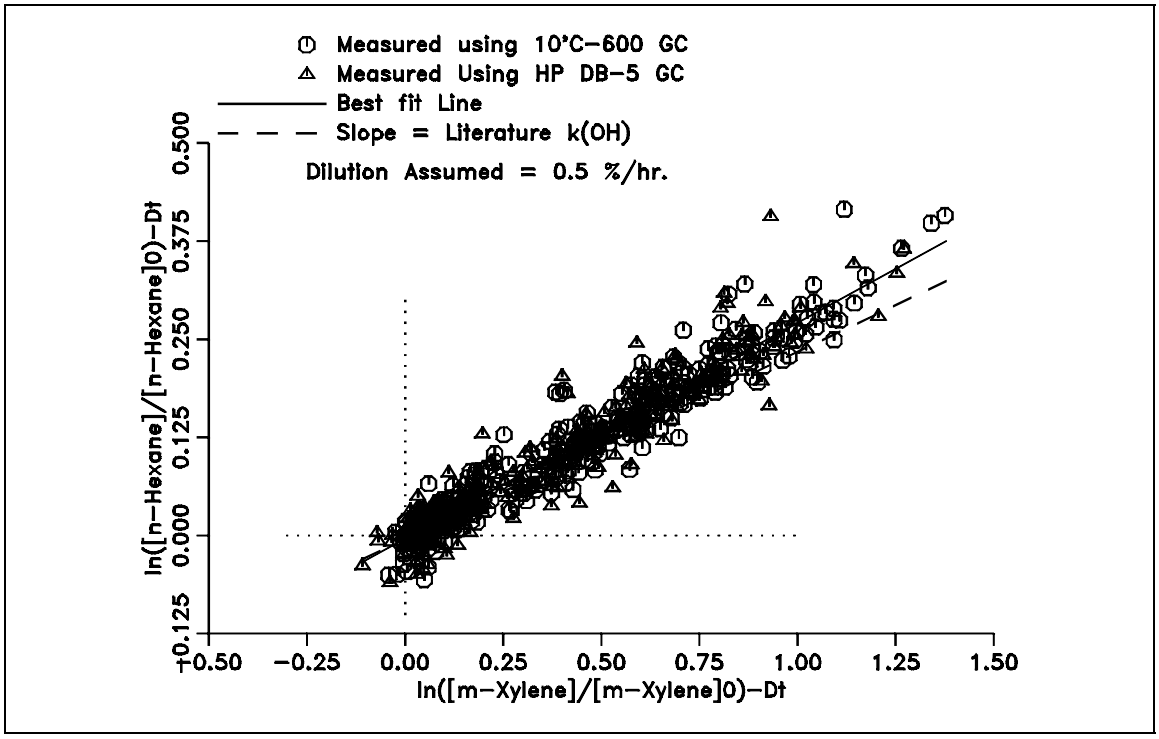

Figure 2. Plots of Equation (XIX) for n-hexane from all the mini-surrogate experiments conducted after the computer GC data system was installed. (Runs with ~100 ppb added 2-chloromethyl-3-chloropropene are excluded. See Text).

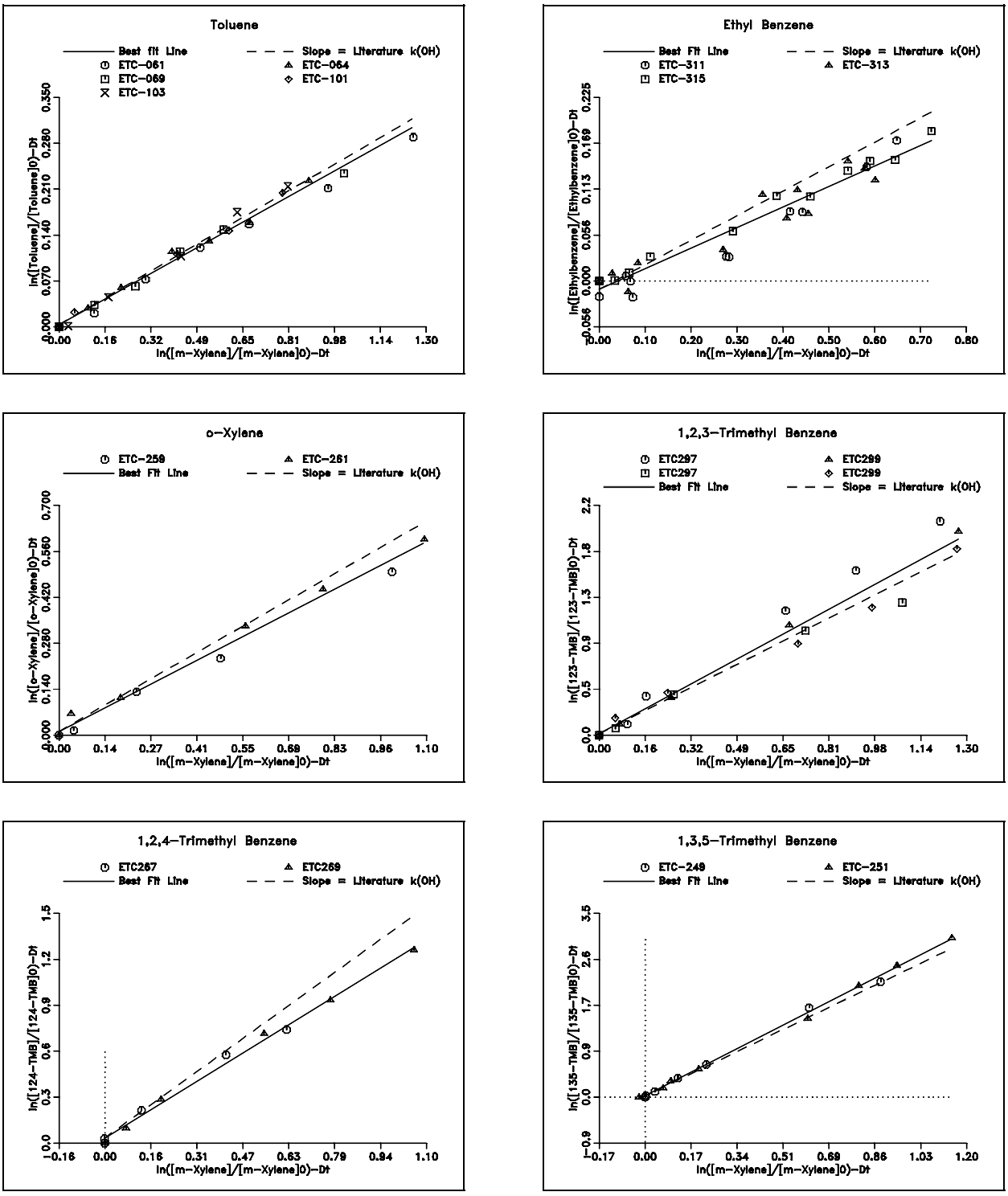

Figure 3. Plots of Equation (XIX) for the alkylbenzenes from the added alkylbenzene mini-surrogate experiments. Plots derived assuming dilution = 0.5%/hour.

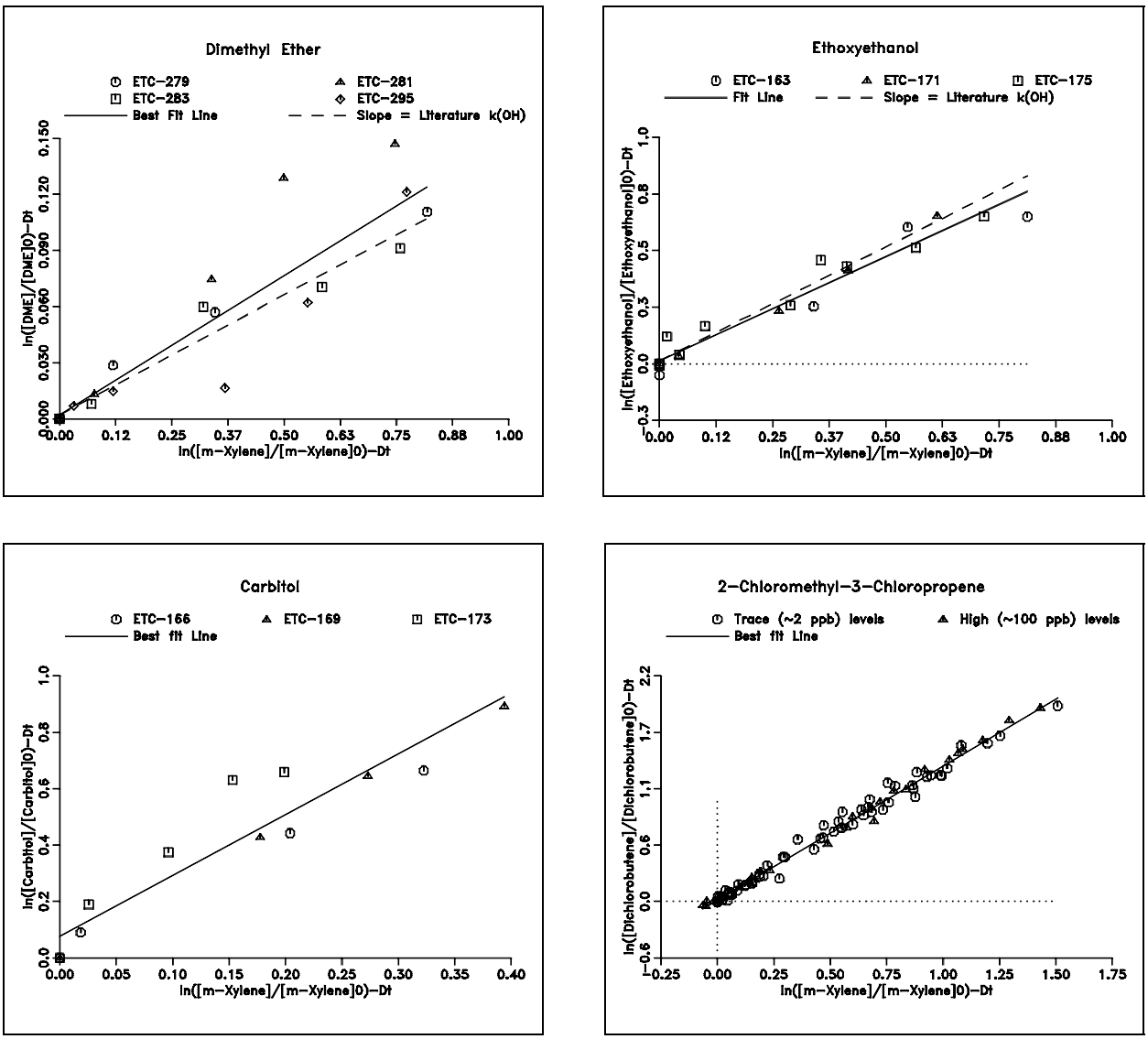

Figure 4. Plots of Equation (XIX) for dimethyl ether, ethoxyethanol, carbitol and 2-chloromethyl-3-chloropropene from the mini-surrogate experiments where they were present. Plots derived assuming dilution = 0.5%/hour.

Because of this evidence for dilution (which did not become apparent until around the end of the study) small amounts of CCl_4 was added in several of the later mini-surrogate runs. The results indicated that dilution occurs but it may be variable, with the CCl_4 data indicating no dilution, 0.8%/hour, and 1%/hour dilution in runs ETC-356, 357 and 358, respectively. Unfortunately, there was no inert tracer present in any of the other experiments, and dilution in these latter runs may not be representative because they had additional sample withdrawal due to the analysis of formaldehyde, which was not employed prior to

run ETC-347. (Also, the results of run ETC-358 were anomalous in some respects and probably should not be taken as being representative.) Therefore, all that can be concluded from these data is that dilution may be occurring up to a rate of 1%/hour, though it may be less.

Fortunately, an indication of the dilution rate can be obtained from the rates of decay of the less reactive components if their literature OH radical rate constants are assumed to be correct. If m-xylene and the other VOC reacts only with OH radicals, their rates of consumption are given by,

$$\frac{d[\text{m-Xyl}]}{dt} = kOH^{\text{m-xyl}} [OH]_t + D$$

$$\frac{d[\text{VOC}]}{dt} = kOH^{\text{voc}} [OH]_t + D$$

which can be combined and integrated to yield:

$$\frac{kOH^{\text{m-xyl}} \ln\left(\frac{[\text{VOC}]_0}{[\text{VOC}]_t}\right) - kOH^{\text{voc}} \ln\left(\frac{[\text{m-Xyl}]_0}{[\text{m-Xyl}]_t}\right)}{kOH^{\text{m-xyl}} - kOH^{\text{voc}}} = Dt \qquad \text{(XX)}$$

Thus, plots of the quantity on the right of Equation (XX) vs time should yield a straight line with intercept D. The dilution rates derived using this method are given on Table 2, and examples of plots of Equation (XX) are shown on Figure 5. The standard deviations of the estimated dilution rates include the uncertainty in the OH radical rate constant ratios; the uncertainty estimates given by Atkinson (1989), shown on Table 2, were used for this purpose.

The dilution estimates obtained by using Equation (XX), the literature kOH values, and the experiments with the slower-reacting test compounds are generally consistent with the measured CCl_4 decay rates, indicating a dilution rate of 0.2-1%/hour. The weighed least squares average of the dilution rate estimates (including the CCl_4 decay measurements) yield D=0.48 $\pm$ 0.25 %/hour. This "best estimate" dilution rate was assumed in all the data analysis of the data discussed in this report, and was used in generating the lower plot on Figure 2, and all the plots on Figures 3 and 4.

Table 2 gives (under the "D=0.5" column) the OH radical rate constants derived using this best estimate dilution rate. It can be seen that except for n-hexane, the rate constants for the slower reacting compounds are consistent with the literature values within the standard deviation of the kOH derivation (which includes the effect of a 0.25%/hour uncertainty in D). The discrepancy

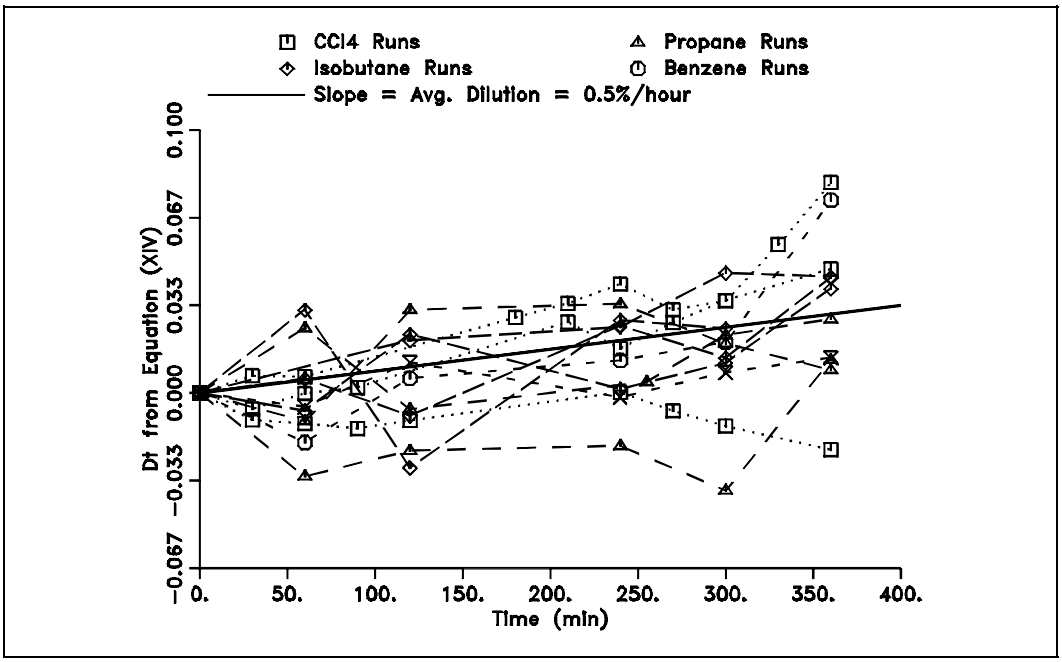

Figure 5. Plot of Equation (XX) for representative runs.

in the case of n-hexane may be due to uncertainties in the literature kOH, analytical problems, other unknown processes causing consumption of n-hexane, or the dilution being higher than our assumed 0.5%/hour. However, the weight of evidence with the other VOCs do not indicate as high a dilution rate as indicated by the n-hexane data. In any case, our n-hexane rate constant agrees with the value recommended by Atkinson (1989) within his estimated 25% uncertainty level.

2. Discussion of Kinetic Data Obtained.

Because of their sensitivity to random scatter in the measurement data as well as to uncertainties in the dilution, the rate constant determinations for the slower reacting compounds are imprecise and not particularly useful as kinetic data. However, the rate constant ratios for the alkylbenzenes, ethoxyethanol, carbitol, and 2-chloromethyl-3-chloropropene were determined with high levels of precision, and the results are not sensitive to the uncertainties in dilution. The results for the alkylbenzenes agree with the values recommended by Atkinson (1989) within the estimated level of uncertainty, and these data are probably as useful as any of the relative rate data in the literature. The results for ethoxyethanol are in good agreement with the kOH determined by Daguat et al (1988), but not with the value of Hartmann et al (1987). The results for 2-chloromethyl-3-chloropropene is in good agreement with the recent determination of Tuazon et al (1988).

Since 2-chloromethyl-3-chloropropene is an alkene, the possibility of non-negligible consumption by reaction with ozone, NO_3 radicals, or $O(^3P)$ atoms also needs to be considered. However, the rate constant for the reaction of this compound with ozone has been measured to be only 3.9×10^{-19} cm^3 $molec^{-1}$ sec^{-1} (Tuazon et al. 1984), making it negligible under the conditions of these experiments. The rate constant for the reaction with NO_3 has not been measured, but Atkinson (personal communication, 1992) estimates it to be 10^{-15} cm^3 $molec^{-1}$ sec^{-1} based on the measured rate constant for NO_3 + allyl chloride (Atkinson, 1991a). The rate constant for the $O(^3P)$ reaction is also unknown, but it is probably no larger than the rate constant for isobutene. Model simulations of our experiments incorporating these estimates for the NO_3 and $O(^3P)$ rate constants indicate that these two reactions are not important. Note that if these reactions were non-negligible, one might expect curvature in plots of Equation (XIX), which is not seen (see Figure 4) despite the relatively high precision of the data.

This work is the first reported measurement of the OH radical rate constant for carbitol. The value obtained, 5.1×10^{-11} cm^3 $molec^{-1}$ sec^{-1}, is approximately 75% higher than that estimated using the group additivity technique of Atkinson (1987), though it agrees to within the factor of 2 uncertainty of this estimation technique. For comparison purposes, we note that the measured rate constant for ethoxyethanol is approximately 40% higher than the group additivity estimate. Therefore, the group additivity method appears to somewhat underestimate the rate constants for these alcohol ethers.

The SAPRC chemical mechanism used in the model simulations discussed in Section IV of this report was updated to incorporate our measured rate constant for carbitol, and the ethoxyethanol rate constant was changed to be that of Daguat et al (1988), which is consistent with our data. In both cases, the previous mechanism used kOH values estimated by the group additivity method. (In the case of ethoxyethanol, the estimated value was used because it was within the range of the two discrepant measurements). Although it might be appropriate to use these data to refine the rate constants for some of the aromatics, the recommended values were retained for the time being, since the new data are not inconsistent with these recommendations.

3. Effect of 2-Chloromethyl-3-chloropropene on the Apparent n-Hexane/m-Xylene Rate Constant Ratio.

Since n-hexane and m-xylene were present together in all mini-surrogate experiments conducted in this study, in principle all these experiments amounted to a determination of this rate constant ratio. In practice, sufficiently precise n-hexane data for kinetic analyses were obtained only after the

computerized GC data system was acquired. However, this still involves over 100 runs, roughly half being standard runs and the rest being runs with various test VOCs added. With one notable exception, all of the runs with the added VOCs yielded essentially equivalent apparent n-hexane/m-xylene rate constant ratios as the standard runs, as one would expect based on the expectation that none of these VOCs are expected to form products or intermediates which react with these compounds.

The exception is the three runs with the added ~100 ppb 2-chloromethyl-3-chloropropene. As shown on Figure 6, the rate of decay of n-hexane relative to m-xylene is ~25% higher than in all the other runs, which is well outside the range of experimental variability. This can be attributed to the formation of chlorine atoms in the chlorobutene photooxidation process. Chlorine atoms are known to react very rapidly with alkanes (Atkinson and Aschmann, 1985), with much higher rate constants relative to aromatics than is the case for OH radicals. Thus if a sufficient amount of Cl is formed in this system that it will contribute to significantly to the consumption of n-hexane, the result would be a higher rate of reaction of n-hexane relative to m-xylene than would otherwise be the case. This is apparently occurring in the runs with the added ~100 ppb 2-chloromethyl-3-chloropropene. The data from these runs were therefore not used in the derivation of the n-hexane/m-xylene rate constant ratios shown on Table 2.

If chlorine atoms are formed when 100 ppb of the chlorobutene is added, it gives concern about the use of the chlorobutene as a radical tracer. However, only ~2 ppb or less of the chlorobutene is used when it is added as a radical tracer. When present at this level, the n-hexane/m-xylene relative decay rate was the same, within experimental uncertainty, as in the runs where it was absent. (Indeed, the relative decay rate was ~1% lower, the opposite direction one would expect.) The addition of the chlorobutene at the ~2 ppb level also had no apparent effect on the amount of ozone formed, m-xylene consumed, or other results of the standard run. Therefore, we conclude that the amount of chlorine atom formation occurring when ~2 ppb or less chlorobutene is present is not enough to measurably affect the results of the experiments, so we continue to use it as a radical tracer compound. However, clearly it should not be added at levels much greater than this, or Cl atom formation will affect the results.

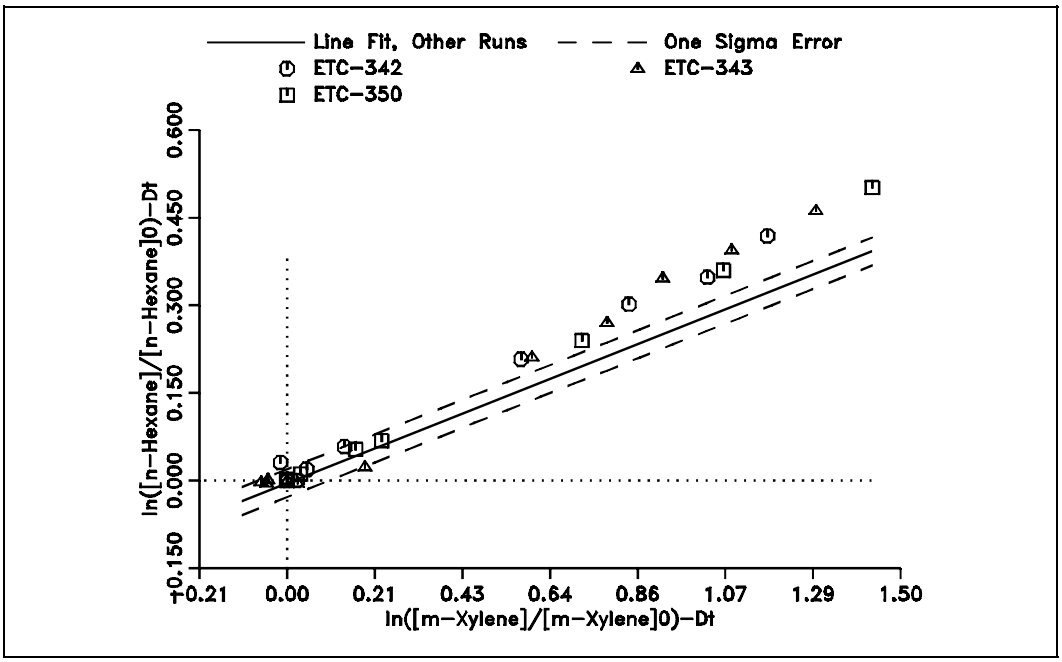

Figure 6. Plots of Equation (XIX) for n-hexane data from the mini-surrogate experiments with ~100 ppb added 2-chloromethyl-3-chlorobutene. The solid line shows the best fit to the data for all the other mini-surrogate experiments, and dotted lines show the (one σ) standard deviation of the fit. A dilution rate of 0.5 %/hour is assumed.

B. Results of Mini-Surrogate Runs: Variations of Run Conditions

The conditions and selected results of the mini-surrogate experiments are summarized on Table 3. As indicated on Table 1, the initial reactant concentrations or reactant preparation method for the standard mini-surrogate experiments changed three times during this study. Table 3 shows that these changes resulted in significant differences in the results of the standard experiments. Therefore, for the purpose of data analysis the mini-surrogate runs are grouped into three separate sets, as indicated below:

Set 1 consists of runs ETC-47 through ETC-89. These runs employed 3.5 ppm of the mini-surrogate, and the NO_x was injected using glass syringes. A typical standard run in this series produced 0.22 ppm O_3 in six hours. An Example of the results of a base case experiment in this group is shown on Figure 7. Results of model simulations of this experiments are also shown; these are discussed later in Section IV. Note that ozone formation is just starting to occur when the run is terminated after 6 hours of irradiation, so the final ozone yield is

Table 3. Conditions and Selected Results of the Mini-Surrogate Runs used for Reactivity Assessment

Run	Added (ppm)	Avg.T (K)	k_1 (min^{-1})	Initial Conc (ppb) NO	NO2	n-C_6	Ethe.	m-Xyl	d(O_3-NO) (ppb) t=2	t=4	t=6	IntOH [a] (ppt-min)	Meth	ConvR [b] (10^3 min^{-1})
Set 1														
Standard Runs														
47	----	301.6	0.417	373	163	352	738	86.6	247	445	725	24.5 (9%)	t2m	29.6
50	----	301.4	0.409	389	128	306	728	90.5	235	460	696	26.0 (7%)	t2m	26.7
52	----	301.2	0.404	388	132	282	716	87.6	205	429	650	26.1 (7%)	t3m	24.9
58	----	300.8	0.389	375	131	289	806	71.5	192	406	640	22.2 (9%)	d3m	28.9
60	----	300.5	0.385	386	124	293	755	88.0	192	422	662	23.9 (7%)	t3m	27.7
63	----	300.3	0.379	389	124	281	732	88.0	180	406	622	22.3 (8%)	t3m	27.9
67	----	300.4	0.372	384	125	293	677	90.8	189	410	611	24.0 (7%)	t2m	25.5
71	----	300.7	0.366	375	129	267	676	85.5	193	416	649	23.6 (7%)	t3m	27.5
75	----	300.5	0.361	386	128	285	688	82.4	142	345	538	17.5 (9%)	d2m	30.8
77	----	302.6	0.358	382	126	282	673	81.1	139	361	572	20.3 (8%)	t3m	28.2
80	----	301.4	0.354	392	119	290	666	83.4	204	428	668	22.4 (8%)	d3m	29.9
81	----	301.3	0.353	393	125	289	678	79.9	163	363	563	19.2 (9%)	d2m	29.4
83	----	301.4	0.351	379	129	283	682	79.6	199	413	621	22.0 (8%)	d3m	28.2
87	----	300.9	0.347	388	129	286	672	81.3	162	364	550	20.3 (8%)	d3m	27.1
89	----	301.9	0.345	386	139	284	680	78.7	166	356	546	19.7 (9%)	t3m	27.7
Ethane														
62	17.6	300.2	0.381	386	128	286	811	94.1	279	553	882	20.7 (9%)	d3m	42.6
68	10.0	300.2	0.371	376	132	276	748	92.1	222	446	675	21.7 (9%)	t2m	31.2
73	18.1	300.2	0.363	385	125	282	713	83.6	213	448	696	17.0 (10%)	t3m	41.0
79	17.6	300.9	0.356	386	127	293	644	87.8	243	477	724	18.3 (10%)	d2m	39.6
88	24.4	302.6	0.346	398	132	283	682	82.2	297	558	881	18.5 (9%)	d3m	47.5
n-Butane														
51	2.31	301.2	0.406	369	134	303	771	93.3	225	494	830	17.8 (10%)	d2m	46.6
53	5.21	302.0	0.401	398	118	303	677	79.3	229	518	878	19.2 (10%)	d3m	45.8
59	1.82	300.4	0.387	388	121	261	755	75.6	223	471	761	18.4 (12%)	d3m	41.3
82	6.75	301.3	0.352	403	118	277	660	83.3	208	461	775	10.5 (16%)	d2m	74.0
86	7.00	301.0	0.348	387	133	288	687	80.7	225	472	813	10.5 (16%)	t3m	77.7
Propene														
65	0.083	300.6	0.376	397	119	295	760	85.2	223	494	776	25.5 (6%)	t3m	30.4
72	0.120	300.1	0.365	377	128	284	663	89.2	180	432	695	24.1 (8%)	d2m	28.9
Toluene														
61	0.174	300.5	0.383	388	126	286	733	92.1	298	624	1041	36.2 (5%)	d3m	28.8
64	0.061	300.5	0.378	421	136	293	801	93.0	205	454	702	25.1 (7%)	d3m	27.9
69	0.095	300.6	0.369	381	122	281	732	85.4	224	487	785	29.7 (8%)	d2m	26.4
Set 2														
Standard Runs														
90	----	301.6	0.344	404	148	292	731	81.1	90	270	465	15.9 (5%)	d2m	29.2
91	----	301.3	0.344	381	132	287	649	80.1	89	267	433	16.0 (5%)	t3m	27.0
93	----	301.6	0.342	388	132	287	656	80.9	108	296	473	16.4 (4%)	t3m	28.8
95	----	301.7	0.340	379	135	286	694	78.0	92	278	463	16.6 (4%)	d2m	27.9
98	----	301.4	0.338	387	130	276	658	76.3	103	290	445	17.7 (4%)	t3m	25.2
100	----	301.1	0.337	384	132	275	658	76.5	91	270	449	17.1 (4%)	t3m	26.3
102	----	300.9	0.336	377	134	288	664	76.7	119	291	482	16.9 (4%)	d2m	28.6
104	----	300.9	0.335	376	128	275	662	73.5	96	267	439	17.6 (4%)	d2m	24.9
107	----	300.5	0.333	382	125	288	738	73.0	124	306	475	17.4 (4%)	d3m	27.2
109	----	301.1	0.332	393	130	284	686	68.6	78	236	406	15.6 (5%)	d3m	26.0
113	----	300.4	0.330	387	126	283	691	72.8	87	259	419	14.9 (5%)	d2m	28.0
114	----	300.8	0.330	366	124	294	646	76.5	80	255	411	16.1 (5%)	d2m	25.5
115	----	300.6	0.329	408	131	284	631	78.1	76	241	402	15.2 (5%)	d2m	26.5
117	----	301.9	0.328	396	131	304	627	78.5	87	270	434	17.4 (4%)	t3m	24.9
122	----	304.3	0.326	396	137	289	540	76.7	92	284	478	18.0 (4%)	d3m	26.5
124	----	303.4	0.326	380	128	295	540	76.8	84	273	452	17.1 (4%)	d3m	26.4
126	----	302.6	0.325	396	133	304	538	79.4	83	265	426	17.1 (4%)	d3m	24.9
128	----	301.8	0.325	400	137	320	537	78.8	78	242	404	16.5 (4%)	d3m	24.5
129	----	301.7	0.324	396	136	308	539	77.0	73	244	408	15.6 (5%)	d2m	26.1
130	----	302.2	0.324	393	130	301	529	76.8	81	257	427	16.1 (4%)	d2m	26.5
132	----	302.6	0.323	407	138	317	522	75.1	74	243	426	16.9 (4%)	t3m	25.2
134	----	303.1	0.323	404	132	303	521	77.0	77	253	433	16.6 (4%)	d3m	26.1
137	----	300.9	0.322	396	134	288	518	70.6	81	236	392	15.4 (5%)	d2m	25.5
139	----	301.4	0.322	403	130	298	534	75.3	85	247	412	16.0 (5%)	d2m	25.7
145	----	301.6	0.321	391	122	262	505	61.5	77	230	387	15.2 (5%)	d3m	25.4
147	----	301.5	0.320	379	124	266	495	60.6	82	233	384	15.3 (5%)	d2m	25.1
149	----	302.2	0.320	384	129	267	494	61.8	75	242	404	15.6 (5%)	d2m	25.8
Ethane														
92	17.1	301.4	0.343	383	134	285	689	80.6	131	345	581	14.8 (9%)	t3m	39.2
99	16.6	300.8	0.338	380	129	283	676	77.4	140	347	562	14.7 (11%)	d2m	38.3

Table 3. (continued)

Run	Added (ppm)	Avg.T (K)	k_1 (min^{-1})	Initial Conc (ppb) NO	NO2	n-C_6	Ethe.	m-Xyl	d(O_3-NO) (ppb) t=2	t=4	t=6	IntOH [a] (ppt-min)	Meth	ConvR [b] (10^3 min^{-1})
n-Butane														
94	7.16	301.3	0.341	359	127	273	612	78.3	127	330	574	9.5 (10%)	t3m	60.7
97	6.12	301.2	0.339	377	131	275	660	75.4	144	347	618	8.6 (20%)	d2m	72.2
135	6.06	301.6	0.323	389	134	303	513	72.6	109	312	534	9.5 (20%)	d2m	56.3
Propene														
106	0.081	300.8	0.333	386	134	294	685	80.4	142	390	655	21.1 (5%)	d2m	31.0
108	0.085	300.5	0.332	398	131	301	697	74.8	143	366	596	19.0 (5%)	d3m	31.4
110	0.070	300.7	0.331	396	132	260	671	72.9	132	363	624	17.7 (16%)	d3m	35.3
118	0.148	302.4	0.328	375	130	298	604	83.0	145	395	702	22.9 (9%)	t3m	30.7
Toluene														
101	0.170	300.7	0.336	376	133	270	656	79.2	128	395	647	23.1 (4%)	t3m	28.0
103	0.174	301.4	0.335	385	136	278	650	78.7	138	396	680	23.3 (5%)	d2m	29.1
Ethanol														
131	3.15	302.6	0.324	408	137	310	531	72.9	138	370	598	14.4 (6%)	t3m	41.4
133	2.92	303.0	0.323	403	138	280	529	66.2	128	375	600	14.9 (8%)	d3m	40.3
138	3.01	301.0	0.322	403	140	303	521	75.1	124	345	553	14.0 (9%)	t3m	39.6
Isopropyl Alcohol														
148	3.63	302.5	0.320	392	123	257	494	63.6	185	472	816	18.3 (5%)	t3m	44.7
Methyl t-Butyl Ether														
120	2.04	302.0	0.327	395	139	---	562	81.3	119	325	555	13.2 (7%)	d3m	42.2
123	2.98	305.6	0.326	383	138	---	551	74.3	160	437	812	17.1 (6%)	t3m	47.5
125	2.49	302.3	0.325	388	132	---	550	79.3	104	314	552	12.0 (10%)	d2m	45.9
127	2.51	302.2	0.325	396	142	---	543	74.4	121	338	579	11.4 (8%)	t3m	50.9
Set 3														
Standard Runs														
153	----	300.9	0.319	407	119	361	---	95.4	174	448	717	24.8 (8%)	t3m	28.9
154	----	300.4	0.319	391	113	401	---	89.6	152	398	631	23.1 (8%)	t3m	27.3
156	----	300.8	0.319	396	111	377	720	94.6	164	432	688	24.0 (8%)	d3m	28.7
158	----	300.7	0.319	383	114	379	716	92.2	139	369	604	22.2 (9%)	d3m	27.2
160	----	300.7	0.319	390	114	431	799	96.6	161	422	677	22.8 (8%)	d3m	29.6
161	----	301.6	0.318	406	114	413	785	96.3	156	426	692	23.0 (8%)	t3m	30.0
162	----	301.5	0.318	387	111	403	786	93.9	152	430	694	22.1 (9%)	d3m	31.4
164	----	301.6	0.318	389	115	420	---	95.2	141	397	654	22.2 (9%)	d3m	29.5
165	----	303.7	0.318	387	116	470	747	97.9	164	453	789	24.3 (8%)	d3m	32.5
168	----	301.6	0.318	404	117	428	617	99.7	163	444	729	19.8 (10%)	d3m	36.8
170	----	301.5	0.318	395	118	417	663	100.6	154	426	719	20.8 (9%)	d3m	34.6
172	----	301.1	0.317	384	120	409	769	100.6	140	396	677	20.1 (9%)	d3m	33.7
174	----	299.6	0.317	381	116	435	735	108.0	132	395	668	19.2 (10%)	d3m	34.8
176	----	299.3	0.317	384	111	447	728	105.7	122	376	630	20.4 (9%)	d3m	30.9
177	----	298.9	0.317	394	116	362	685	100.1	136	383	642	15.1 (13%)	d2m	42.5
178	----	298.7	0.317	386	110	405	597	102.5	142	525	655	18.7 (10%)	d3m	35.1
182	----	299.4	0.317	370	---	382	739	103.5	141	406	688	20.0 (10%)	d3m	34.4
184	----	298.8	0.317	377	---	368	732	102.1	118	361	602	16.1 (12%)	d3m	37.4
186	----	299.7	0.316	373	---	366	760	100.1	117	364	640	19.6 (10%)	d3m	32.6
189	----	300.7	0.316	410	141	377	729	106.4	159	439	726	19.5 (10%)	t3m	37.3
191	----	299.9	0.316	343	120	337	741	100.8	136	383	683	20.8 (9%)	d2m	32.8
193	----	299.4	0.316	326	118	338	717	101.2	108	332	615	21.0 (10%)	d2m	29.3
195	----	300.7	0.316	346	117	343	861	103.8	138	389	674	21.4 (9%)	d2m	31.5
198	----	300.5	0.316	390	115	358	787	132.6	138	400	658	24.7 (8%)	t2m	26.6
200	----	300.4	0.316	378	115	322	752	93.9	136	391	671	21.4 (9%)	d2m	31.3
202	----	300.2	0.316	393	109	344	749	99.7	145	404	678	23.5 (8%)	d3m	28.8
204	----	301.2	0.316	406	114	403	778	103.6	168	447	746	23.3 (8%)	d3m	32.0
210	----	300.1	0.315	406	111	423	691	109.0	134	409	671	19.1 (10%)	d3m	35.2
223	----	300.6	0.315	395	112	427	651	105.4	172	449	727	20.0 (10%)	t3m	36.3
227	----	300.4	0.315	392	119	421	763	106.7	125	379	632	18.9 (10%)	t3m	33.4
229	----	300.8	0.315	408	115	399	769	101.7	125	383	642	19.9 (10%)	d3m	32.2
231	----	299.9	0.315	392	118	417	741	104.1	136	395	650	19.3 (10%)	t3m	33.7
233	----	300.9	0.315	413	113	397	768	128.3	117	387	659	23.3 (9%)	t3m	28.3
234	----	302.1	0.315	386	118	384	674	97.6	147	425	727	23.1 (8%)	d3m	31.5
236	----	302.0	0.315	386	116	382	676	93.2	142	408	705	22.6 (8%)	t3m	31.1
238	----	301.3	0.315	371	108	408	670	92.3	136	399	693	20.9 (9%)	d3m	33.2
240	----	300.9	0.315	363	109	374	668	90.8	115	353	628	19.9 (10%)	d2m	31.6
242	----	301.8	0.315	352	100	393	665	95.1	146	403	724	23.6 (8%)	d2m	30.7
244	----	302.2	0.315	384	100	379	651	91.6	134	407	707	21.2 (9%)	d3m	33.4
246	----	302.2	0.315	391	105	384	667	100.1	142	417	737	23.6 (8%)	t3m	31.2
250	----	299.9	0.315	391	108	410	743	93.2	142	428	746	20.3 (9%)	d2m	36.8
252	----	300.4	0.315	385	113	336	759	96.0	135	389	683	21.0 (9%)	d3m	32.6
258	----	302.0	0.315	373	111	388	729	92.1	161	445	775	23.7 (8%)	d3m	32.7
260	----	300.7	0.315	372	112	391	732	94.3	149	416	711	21.8 (9%)	t3m	32.6
262	----	302.5	0.315	369	105	379	708	94.1	167	445	771	23.7 (8%)	d2m	32.5
264	----	301.5	0.315	368	120	385	718	96.5	175	456	768	25.8 (7%)	t3m	29.8
266	----	300.6	0.315	356	107	392	700	95.3	170	434	743	23.1 (8%)	d3m	32.1
270	----	301.2	0.315	382	105	384	681	96.1	163	442	762	22.8 (8%)	d3m	33.5
272	----	301.2	0.315	376	119	394	665	103.4	163	458	787	23.8 (8%)	t3m	33.0

Table 3. (continued)

Run	Added (ppm)	Avg.T (K)	k_1 (min^{-1})	Initial Conc (ppb) NO	NO2	n-C_6	Ethe.	m-Xyl	d(O_3-NO) (ppb) t=2	t=4	t=6	IntOH [a] (ppt-min)	Meth	ConvR [b] (10^3 min^{-1})
274	----	302.3	0.315	397	112	381	659	103.3	159	479	839	23.2 (8%)	t3m	36.2
276	----	302.3	0.315	382	113	365	648	98.9	163	468	819	25.6 (7%)	t3m	32.0
278	----	302.8	0.315	394	119	364	635	98.9	153	456	826	23.3 (8%)	d3m	35.4
280	----	303.4	0.315	388	116	378	655	99.0	160	473	862	24.7 (8%)	d3m	35.0
282	----	303.0	0.315	387	117	358	627	100.8	157	463	833	23.5 (8%)	t3m	35.4
284	----	302.7	0.315	383	114	369	638	104.5	167	477	855	24.7 (8%)	d3m	34.6
286	----	303.3	0.315	382	109	356	656	104.4	155	476	871	24.9 (8%)	t3m	35.0
288	----	304.0	0.315	381	116	325	646	98.2	164	494	906	26.7 (7%)	d2m	34.0
290	----	304.1	0.315	386	113	390	641	105.4	172	519	932	31.4 (6%)	t3m	29.7
292	----	301.6	0.315	393	109	363	632	108.1	164	479	817	23.3 (8%)	d3m	35.0
294	----	302.2	0.315	394	102	366	629	102.1	159	479	832	21.9 (9%)	d2m	38.0
296	----	302.1	0.315	383	105	368	614	104.9	166	495	861	22.4 (9%)	t3m	38.4
298	----	302.6	0.315	392	105	374	647	118.3	188	532	923	26.9 (7%)	d3m	34.3
300	----	301.1	0.315	386	105	368	651	116.9	172	487	833	25.6 (8%)	d3m	32.5
302	----	300.3	0.315	381	102	405	644	89.4	108	353	604	18.8 (10%)	d3m	32.0
304	----	301.2	0.315	384	91	393	618	91.7	104	342	602	19.3 (10%)	d2m	31.2
306	----	301.3	0.315	386	148	366	623	87.3	110	363	627	17.8 (11%)	d2m	35.3
308	----	301.8	0.315	388	137	382	644	90.5	120	383	661	18.6 (10%)	d3m	35.4
310	----	299.7	0.315	391	126	393	645	92.3	107	339	581	17.1 (11%)	t3m	33.9
312	----	297.6	0.315	381	130	379	656	98.9	93	315	548	16.0 (12%)	d2m	34.3
314	----	298.5	0.315	392	137	372	642	99.3	112	351	594	16.7 (12%)	t3m	35.7
316	----	298.9	0.315	378	120	365	619	96.5	119	367	611	17.0 (11%)	t3m	35.9
325	----	302.9	0.336	411	113	404	788	99.4	182	496	813	22.8 (8%)	d3m	35.6
326	----	303.0	0.336	417	113	393	773	102.3	217	531	861	22.4 (9%)	d3m	38.4
327	----	303.0	0.336	394	105	358	878	89.1	201	525	894	24.8 (8%)	d3m	36.0
328	----	303.1	0.336	414	108	377	775	92.5	178	524	801	21.8 (9%)	t3m	36.8
329	----	303.2	0.336	419	113	394	770	101.9	188	512	845	23.3 (8%)	d3m	36.3
330	----	303.4	0.336	399	107	391	765	100.5	204	531	886	25.1 (8%)	d3m	35.3
331	----	303.5	0.336	402	111	396	734	97.1	183	491	821	22.9 (8%)	d3m	35.8
334	----	303.3	0.336	408	116	387	777	101.4	190	498	836	23.6 (8%)	d3m	35.4
336	----	303.6	0.336	420	110	391	764	105.2	201	519	865	25.1 (8%)	d3m	34.5
339	----	303.4	0.336	406	117	409	809	104.8	216	554	928	27.8 (7%)	t3c	33.3
345	----	303.7	0.336	412	118	389	752	99.1	214	565	919	27.0 (7%)	d3c	34.0
347	----	303.6	0.336	407	107	399	747	95.6	201	528	864	26.5 (7%)	d3c	32.6
349	----	304.1	0.336	397	109	398	755	87.9	216	558	916	28.1 (7%)	d3c	32.6
351	----	304.0	0.336	451	120	387	767	94.1	180	493	782	22.1 (9%)	d3c	35.4
353	----	303.5	0.336	400	111	390	788	95.2	184	494	840	26.0 (7%)	d3m	32.3
356	----	303.0	0.336	394	118	361	784	75.2	167	473	773	25.1 (8%)	d3c	30.8
408	----	300.4	0.336	406	102	418	717	104.7	161	406	647	23.8 (8%)	t3c	27.1
411	----	300.4	0.336	442	107	429	759	114.2	172	461	717	23.8 (8%)	d3c	30.1
413	----	299.9	0.336	410	116	424	740	107.6	157	408	647	20.8 (9%)	t3c	31.1
415	----	299.2	0.336	462	98	405	765	102.2	127	387	622	22.8 (9%)	t3c	27.3
419	----	299.8	0.336	437	108	419	772	114.9	149	420	662	17.5 (11%)	d3m	37.8
Carbon Monoxide														
414	138	299.7	0.336	418	106	422	741	108.1	480	910	1356	28.8 (7%)	d3c	47.2
416	130	298.9	0.336	443	133	412	848	108.8	402	770	1238	16.1 (12%)	d2m	76.7
418	110	300.1	0.336	412	98	417	832	110.9	269	644	1120	17.4 (11%)	t3m	64.4
Ethane														
235	43.7	302.0	0.315	382	112	383	752	95.3	236	586	1006	17.7 (11%)	d2m	56.9
332	20.0	303.3	0.336	413	110	382	750	101.2	320	708	1115	22.8 (8%)	d3m	48.8
333	21.0	303.4	0.336	414	88	380	---	99.9	501	910	1299	28.4 (7%)	t3m	45.8
Propane														
226	11.6	300.0	0.315	372	113	403	729	101.7	146	408	736	12.0 (16%)	d3m	61.5
230	28.8	300.5	0.315	413	109	413	740	98.1	249	648	1180	10.5 (18%)	d3m	112.4
305	20.1	301.3	0.315	388	152	368	612	87.4	191	530	1018	12.1 (16%)	d2m	84.4
n-Butane														
224	9.76	300.3	0.315	394	114	408	721	111.2	197	532	953	8.7 (22%)	t2m	109.8
Isobutane														
228	2.72	300.2	0.315	402	114	420	763	103.9	140	412	739	13.6 (14%)	d2m	54.5
232	20.9	300.0	0.315	407	114	428	743	106.1	210	642	1373	7.7 (46%)	d2m	179.1
241	10.2	301.2	0.315	359	99	396	686	94.0	164	533	1209	12.3 (16%)	d3m	98.6
303	6.62	301.2	0.315	380	100	387	620	87.8	136	443	937	15.1 (32%)	d2m	62.0
n-Hexane														
201	1.17	300.4	0.316	391	110	387	765	97.6	110	313	558	4.4 (86%)	d2m	126.9
209	1.58	300.0	0.315	405	112	387	684	98.5	102	284	480	7.3 (26%)	d3m	65.3
n-Octane														
237	1.66	301.6	0.315	366	118	394	660	95.3	59	180	345	4.8 (40%)	d2m	71.8
239	1.55	301.7	0.315	414	119	391	682	92.3	60	175	334	3.3 (58%)	t2m	101.2
2,2,4-Trimethyl Pentane														
291	10.135	303.5	0.315	398	117	336	636	102.5	131	449	1060	5.5 (35%)	d2m	193.8
293	10.644	302.3	0.315	395	109	348	654	111.4	131	438	1033	6.8 (31%)	d2m	152.0

Table 3. (continued)

Run	Added (ppm)	Avg.T (K)	k_1 (min^{-1})	Initial Conc (ppb) NO	NO2	n-C_6 Ethe.	m-Xyl		d(O_3-NO) (ppb) t=2	t=4	t=6	IntOH [a] (ppt-min)	Meth	ConvR [b] (10^3 min^{-1})
Ethene														
199	0.386	301.3	0.316	370	116	334	713	101.9	237	653	1198	32.7 (9%)	d3m	36.6
203	0.217	301.4	0.316	398	119	364	713	107.7	201	538	956	28.0 (7%)	d3m	34.1
Isobutene														
253	0.207	301.9	0.315	369	109	405	678	96.0	293	832	1259	38.1 (5%)	t3m	33.0
255	0.195	303.0	0.315	386	95	386	722	94.3	294	816	1246	39.3 (5%)	t3m	31.7
257	0.108	301.3	0.315	373	113	386	731	90.2	217	578	998	29.1 (7%)	d3m	34.2
trans-2-Butene														
307	0.087	301.1	0.315	398	149	385	640	91.6	531	833	1126	32.5 (8%)	d3m	34.6
309	0.069	301.6	0.315	395	123	365	621	85.0	441	761	1079	29.8 (7%)	t3m	36.2
Isoprene														
271	0.157	300.1	0.315	377	115	387	674	99.4	303	788	1207	28.6 (7%)	t3m	42.3
273	0.139	301.7	0.315	389	108	376	653	103.9	334	840	1262	30.3 (8%)	t3m	41.7
275	0.109	302.2	0.315	392	114	363	647	98.0	297	765	1217	30.8 (8%)	d3m	39.6
277	0.076	303.1	0.315	390	113	364	645	98.8	268	701	1167	29.9 (6%)	t3m	39.0
2-(Cl-methyl)-3-Cl-Propene														
342	0.108	303.7	0.336	430	117	367	587	89.5	308	833	1335	34.9 (6%)	t3c	38.2
343	0.103	303.5	0.336	368	178	402	631	98.7	288	786	1260	40.0 (5%)	t3c	31.5
350	0.113	304.3	0.336	417	112	413	795	98.7	341	922	1386	43.2 (5%)	t3c	32.1
Benzene														
263	6.86	303.4	0.315	367	105	367	719	90.1	244	836	983	36.2 (10%)	t3m	27.2
265	5.78	301.1	0.315	366	112	384	707	95.9	226	675	989	34.2 (14%)	t3m	28.9
m-Xylene														
207	0.038	299.9	0.316	403	110	322	810	99.9	213	590	977	25.8 (16%)	d3m	37.9
301	0.053	300.6	0.315	374	104	396	647	99.9	198	585	1014	29.0 (7%)	d3m	34.9
344	0.081	303.8	0.336	413	116	415	597	99.9	411	983	1329	28.0 (13%)	d2m	47.4
196	0.057	300.3	0.316	342	122	363	783	99.9	175	518	892	27.1 (7%)	d2m	33.0
o-Xylene														
259	0.064	301.0	0.315	367	113	375	725	92.9	208	554	962	27.8 (9%)	d3m	34.6
261	0.064	301.9	0.315	360	112	376	716	95.5	212	579	1028	30.2 (11%)	d2m	34.1
p-Xylene														
346	0.080	303.8	0.336	357	108	418	767	100.8	252	684	1130	32.6 (6%)	d3c	34.7
348	0.075	303.9	0.336	406	108	437	757	99.3	233	626	1066	31.4 (6%)	t3c	33.9
Ethyl Benzene														
311	0.098	297.7	0.315	365	131	386	649	104.3	108	354	608	18.1 (11%)	d3m	33.6
313	0.092	298.5	0.315	366	144	368	629	98.7	124	377	649	17.6 (11%)	t3m	36.9
315	0.215	298.7	0.315	396	134	357	645	97.0	141	457	806	19.0 (10%)	d3m	42.4
1,2,3-Trimethyl Benzene														
297	0.044	302.1	0.315	380	102	371	652	117.2	364	897	1273	41.0 (5%)	t3m	31.0
299	0.035	301.7	0.315	390	109	368	633	117.7	311	794	1221	35.7 (5%)	d3m	34.2
1,2,4-Trimethyl Benzene														
267	0.037	301.0	0.315	366	111	402	706	91.3	203	539	952	26.0 (7%)	d3m	36.6
269	0.041	302.3	0.315	371	105	382	675	98.4	224	600	1049	30.5 (6%)	t3m	34.4
1,3,5-Trimethyl Benzene														
249	0.047	301.6	0.315	389	110	403	835	90.4	353	871	1305	40.8 (6%)	t3m	32.0
251	0.045	299.6	0.315	395	107	396	757	88.9	278	677	1029	33.2 (6%)	t3m	31.0
Formaldehyde														
352	0.104	303.5	0.336	403	125	405	755	100.8	350	715	1110	34.6 (6%)	d3c	32.0
357	0.267	303.4	0.336	409	123	390	822	95.2	461	866	1206	42.5 (5%)	t3c	28.4
Acetaldehyde														
335	0.696	303.7	0.336	415	126	390	763	102.2	410	709	1036	18.5 (10%)	d3m	55.9
338	1.31	303.3	0.336	392	129	383	737	103.1	459	734	1020	13.1 (15%)	d3m	77.9
Acetone														
243	0.847	301.8	0.315	361	102	384	657	94.0	161	447	770	25.5 (8%)	d3m	30.2
245	2.19	302.3	0.315	395	109	421	673	97.2	222	521	886	26.2 (10%)	d2m	33.8
247	4.15	301.9	0.315	375	122	371	666	95.7	253	564	942	27.7 (7%)	t3m	34.1
Methanol														
285	7.65	303.5	0.315	399	121	362	623	106.4	239	721	1302	31.0 (6%)	d3m	41.9
287	0.815	303.2	0.315	393	132	356	640	103.5	174	500	886	24.5 (8%)	d3m	36.1
289	2.29	304.4	0.315	386	129	367	623	109.7	205	606	1093	28.5 (7%)	d3m	38.4
Isopropyl Alcohol														
155	1.74	301.1	0.319	394	108	411	705	94.8	219	545	927	24.3 (8%)	d3m	38.2
157	1.26	300.9	0.319	398	117	373	738	88.1	186	463	774	22.6 (18%)	d2m	34.2
159	1.61	301.4	0.319	390	114	424	728	93.2	183	472	811	24.0 (8%)	t3m	33.8

Table 3. (continued)

Run	Added (ppm)	Avg.T (K)	k_1 (min^{-1})	Initial Conc (ppb) NO	NO2	n-C_6	Ethe.	m-Xyl	d(O_3-NO) (ppb) t=2	t=4	t=6	IntOH [a] (ppt-min)	Meth	ConvR [b] (10^3 min^{-1})
Dimethyl Ether														
279	4.039	303.1	0.315	393	116	365	633	101.4	283	769	1361	24.4 (8%)	t3m	55.8
281	3.408	303.3	0.315	393	119	361	632	101.7	248	677	1248	23.1 (8%)	t3m	54.0
283	2.102	303.4	0.315	390	117	372	645	105.5	238	659	1196	23.6 (8%)	d3m	50.6
295	2.119	302.0	0.315	393	105	357	623	110.0	221	591	1069	22.3 (9%)	d3m	47.8
2-Ethoxy-Ethanol														
163	0.859	302.2	0.318	382	112	440	---	104.0	272	798	1424	24.1 (20%)	t3m	59.0
171	0.731	301.1	0.317	374	120	362	734	84.8	214	616	1208	18.7 (10%)	t3m	64.7
175	0.401	299.2	0.317	392	115	435	673	103.3	177	486	905	17.3 (11%)	t3m	52.3
2-(2-Ethoxyethoxy) Ethanol														
166	0.503	304.8	0.318	391	118	407	753	90.8	191	556	1109	14.3 (14%)	d3m	77.8
169	0.412	301.0	0.318	402	114	434	653	94.3	164	438	817	10.5 (18%)	d3m	77.8
173	0.946	300.6	0.317	395	120	407	738	101.3	151	423	871	6.7 (29%)	t3m	130.9
Hexamethyldisiloxane														
179	9.13	298.6	0.317	400	---	441	781	104.9	82	179	257	3.5 (55%)	d2m	73.4
183	6.71	299.3	0.317	366	---	370	734	113.6	83	184	282	5.7 (34%)	t3m	49.2
Octamethylcyclotetrasiloxane														
181	10.1	299.4	0.317	389	---	368	703	92.5	46	111	183	1.6(>100%)	d2m	112.7
185	4.31	298.9	0.316	387	---	378	730	98.9	67	179	278	7.7 (25%)	t2m	36.0
194	2.16	300.7	0.316	344	---	354	783	95.4	83	232	387	10.1 (19%)	d2m	38.2
Decamethylcyclopentasiloxane														
187	4.93	300.6	0.316	361	---	334	759	107.4	38	123	211	3.5 (55%)	t2m	60.2
190	1.55	300.1	0.316	328	---	344	778	105.5	52	146	257	6.8 (30%)	d2m	37.8
192	1.85	299.8	0.316	332	---	348	722	102.5	55	158	271	7.1 (28%)	t2m	37.9
Pentamethylsiloxanol														
409	2.18	300.1	0.336	432	---	414	714	100.6	88	232	370	12.8 (15%)	t3m	29.0
412	0.712	299.6	0.336	402	113	407	739	109.3	124	330	526	18.6 (10%)	t3c	28.3

[a] IntOH = 6-hour integrated OH radicals, computed from the m-Xylene or 2-chloromethyl-3-chloropropene data. Method codes: "tnm" = IntOH computed from rate of decay of m-Xylene, where [m-xyl](t) computed by fitting the experimental m-xylene data to a linear (n=2) or quadratic (n=3) function of time; "dnm" = same as above, but [m-xyl](t) computed by fitting m-xylene data to functions of d(O_3-NO); "tnc", "dnc": Same as "tnm" or "dnm", respectively, except 2-chloromethyl-3-chloropropene used instead of m-xylene. Quantity in parentheses is standard deviation from fit to data, and does not include uncertainty in the OH radical rate constant.

[b] ConvR is the ratio of the 6-hour d(O_3-NO) to the 6-hour IntOH. It is assumed to have the same relative uncertainty as the IntOH.

[c] This is a ROG surrogate component. Amount added is increase over average initial concentration for other runs in this set.

highly sensitive to the ozone formation rate. This is an appropriate type of experiment to assess maximum reactivities of VOCs, since these largely reflect their effects on ozone formation rates.

The Set 1 experiments were characterized by relatively high rates of initial NO oxidation compared to the later experiments in this study. This suggests that nitrous acid (HONO) may be present as a contaminant in these experiments, since its photolysis would cause an initially high rate of NO oxidation (Carter et al., 1982; Carter and Lurmann; 1990, 1991). This can be introduced either as a contaminant in the NO used to prepare the NO_x injections, or by the heterogeneous hydrolysis of NO_2 when it is being prepared for injection. Tracer-NO_x-air experiments, which consist of irradiation of NO and NO_2 with trace amounts of a rapidly reacting VOC — isobutene in this case — to monitor OH radicals from their rates of consumption, are useful control experiments for characterizing chamber radical sources such as initial HONO

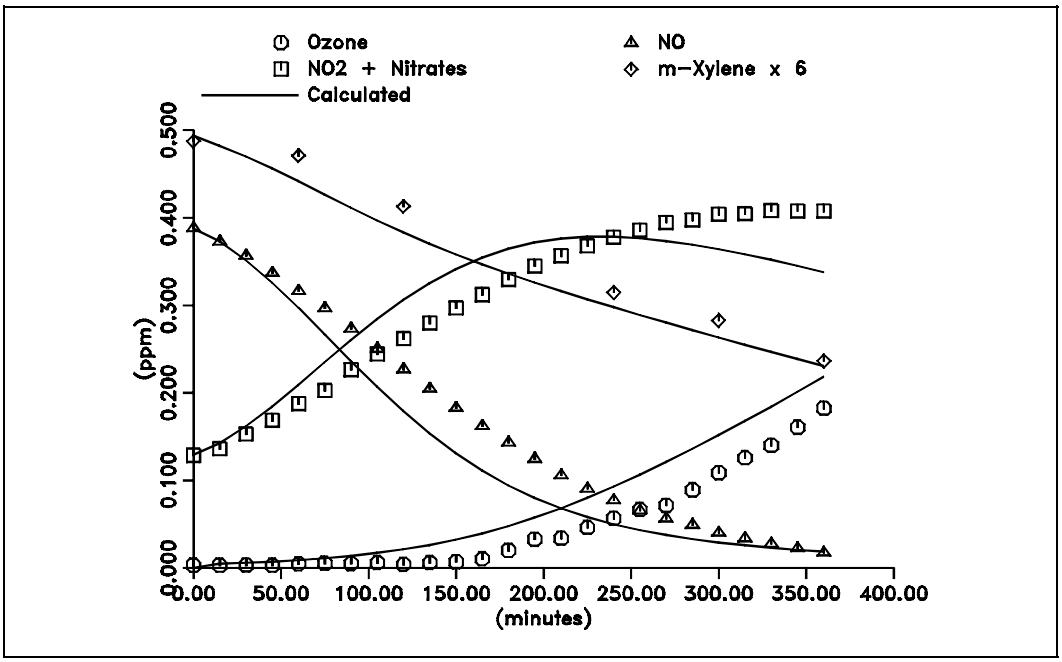

Figure 7. Concentration - time plots of the major species in the representative Set 1 standard mini-surrogate run ETC-087. Results of model simulations of the experiments are also shown (see Section IV).

(Carter et al., 1982). Model simulations could not fit the observed rate of consumption of isobutene in the tracer-NO_x runs ETC-46 and ETC-47 unless it is assumed that approximately 1.5% of the initial NO_2 is converted to HONO. Although this is a lower apparent HONO/NO_2 ratio than derived from analysis of similar runs carried out in the SAPRC evacuable chamber, it is greater than derived from runs in the ~6000-liter SAPRC Indoor Teflon Chamber (see "note added in proof" in Carter and Lurmann, 1991). This initial HONO is undesirable because it can be a source of run-to-run variability, and because the initial HONO must be treated as an adjustable parameter in model simulations.

Set 2 consists of runs ETC-90 through ETC-149. These employed the same initial reactant concentrations as Set 1, but steps were taken to reduce the amount of HONO contamination in the experiments. The NO_x was prepared for injection using vacuum techniques to minimize exposure of NO_2 to humidity, and the NO used for the NO and NO_2 injections was purified prior to use by passing through molecular sieves. This procedure clearly had an effect, as can be seen by comparing the results of a typical standard run in this set, shown on Figure 8, with the results of the representative Set 1 run shown on Figure 7. The change in NO_x injection procedure resulted in a significant reduction in the initial rate of NO oxidation, with the slower rate of initial NO oxidation resulting in much less ozone being formed by the end of the run. The tracer-NO_x

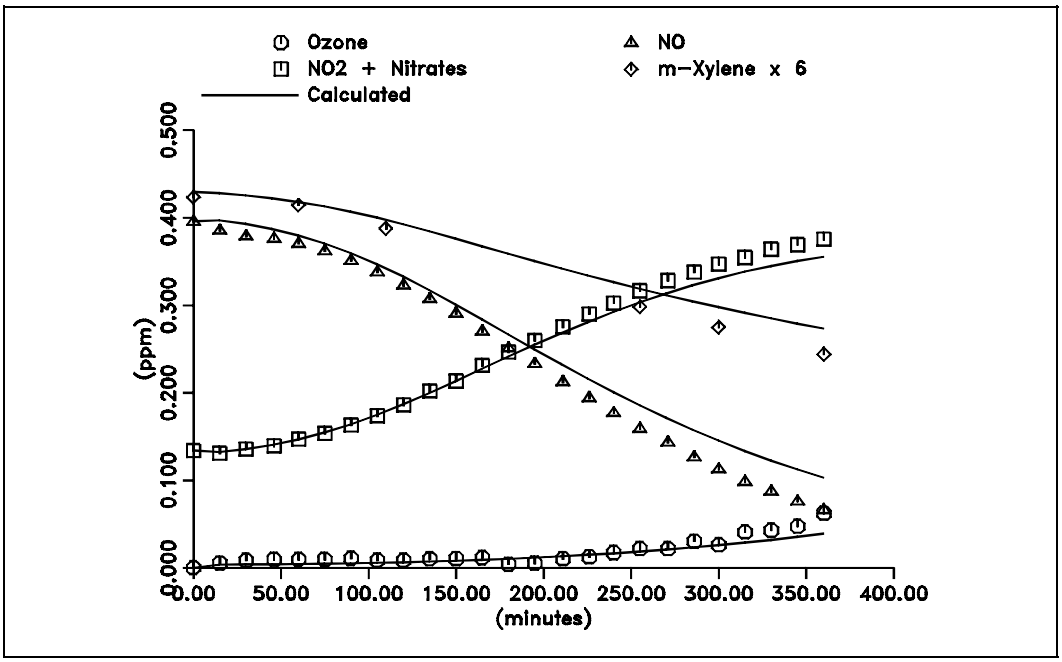

Figure 8. Concentration - time plots of the major species in the representative Set 2 standard mini-surrogate run ETC-137. Results of model simulations of the experiment are also shown (see Section IV).

run ETC-112 also indicated that HONO is essentially eliminated by this procedure, since the isobutene decay rate in that run could be fit in model simulations assuming that HONO is not initially present in these experiments.

The change in the NO_x injection procedure resulted in a standard run with very little ozone being formed because NO is not consumed until around the end of the run. Such an experiment can still provide useful information concerning ozone reactivities of VOCs, since the chemical processes which cause NO to be consumed when it is in excess are the same as those which cause ozone formation once the NO has reacted. However, this run does not adequately represent chemical effects resulting from reactions of ozone, and thus the conditions were subsequently modified to give higher ozone yields.

Set 3 consists of runs ETC-153 and all following runs, the majority of the experiments in this study. The initial concentration of the mini-surrogate components was increased from ~3.5 to ~4.5 ppm to increase the amount of ozone formed in the base case experiment, while still remaining in maximum reactivity conditions. The six-hour ozone formed in the experiment depended on the average temperature in the run (see below), but was typically ~0.30 ppm. Results of a typical standard and a typical added ROG experiment in this group are shown on Figure 9.

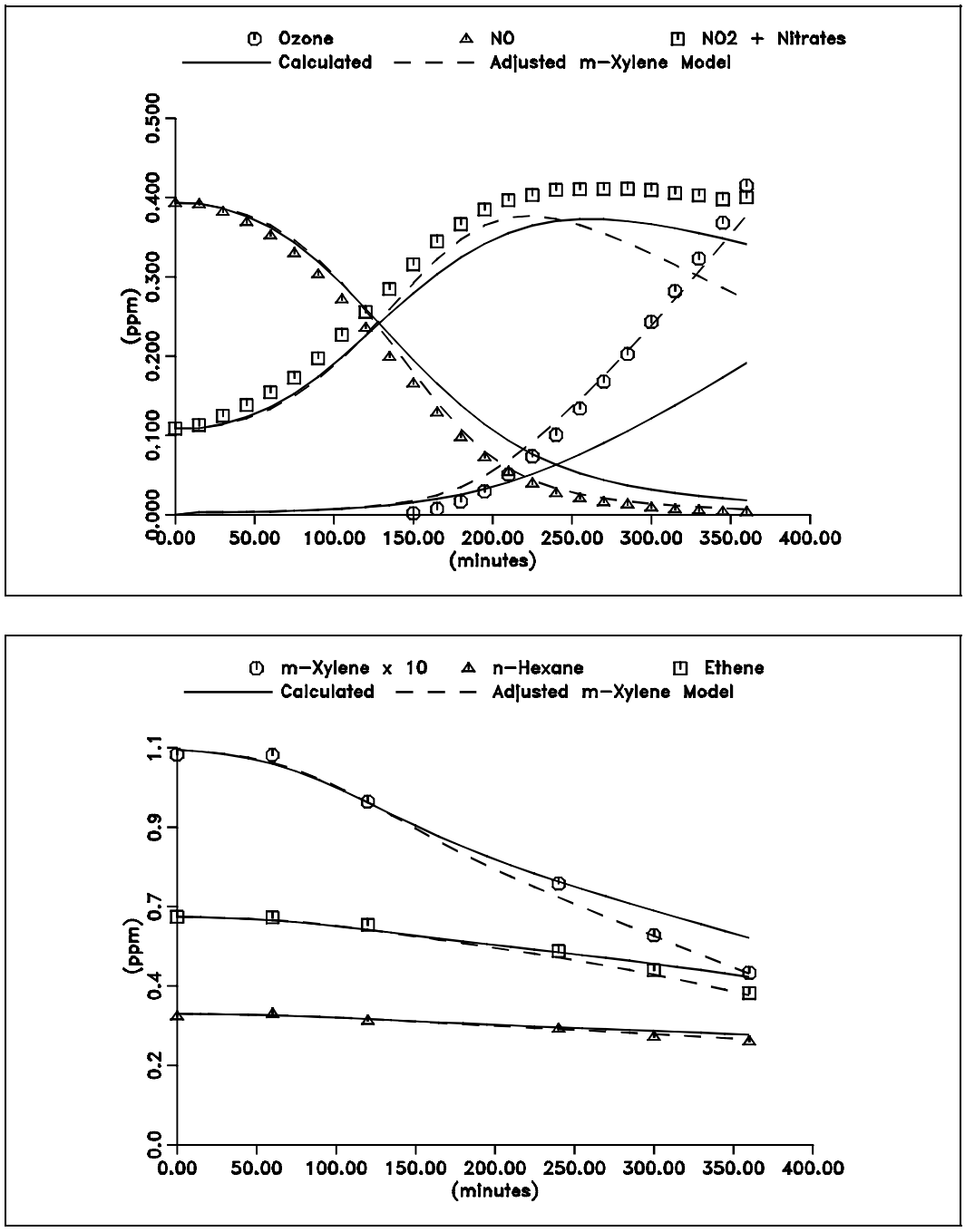

Figure 9. Concentration - time plots of the major species in the representative Set 3 standard mini-surrogate run ETC-292. Results of model simulations using the standard SAPRC-91 mechanism (solid lines) and a the mechanism with optimized mechanistic parameters for m-xylene (dashed lines) are also shown (see Section IV).

1. Variations in Light Intensity.

The results of the periodic NO_2 actinometry experiments (given on Table 3) indicate that the light intensity as measured by the NO_2 photolysis rate (designated "k_1" in the Table and the subsequent discussion) was not constant during all these experiments. This is shown on Figure 10, which gives a plot of the measured NO_2 photolysis rate against run number. The measured NO_2 photolysis rate (k_1) decreased with time during the initial experiments, then apparently stabilized at a relatively constant value until the chamber was moved to the new building after run ETC-322, after which it apparently increased by approximately 7%.

The decrease in light intensity as measured by k_1 can be attributed to the fact that new blacklights were employed around the beginning of the study, which decrease in intensity for a period until they are "burned in". This has been observed in previous indoor chamber studies using this light source (Carter et al., 1984). Unfortunately, there were relatively few NO_2 actinometry runs during most of the Set 3 experiments, so there is some uncertainty in the variation of light intensity for this set. However, the previous behavior of this light source (Carter et al., 1984) and the results of the subsequent actinometry experiments indicate that it is reasonable to expect the light intensity had leveled off during most of the period of set 3.

The slight increase in light intensity after the chamber was moved to the new facility can be attributed to the fact that the lights were cleaned when the chamber was moved.

To assess the effects of this decrease in k_1 on the results of the experiments, and to take it into account in the reactivity analysis, it is necessary to associate a k_1 value to each experiment. For the runs prior to the move to the new facility, this was done by fitting the actinometry to the following empirical exponential decay function:

$$k_1(\text{RunNo}) = 0.315 + 0.396\ e^{-0.0287\ \text{RunNo}}$$

where RunNo is the ETC run number. (The fit was determined with the measurement in Run ETC-322 being increased by 7% to put it on a consistent basis with the other measurements, as discussed in Section II-D.) This is essentially an arbitrary parameterization, but is based on an assumed model of exponential decay to a constant, non-zero value over time. The curve defined by this equation is shown on Figure 10, and can be seen to fit the time-dependence of the data to within their level of uncertainty.

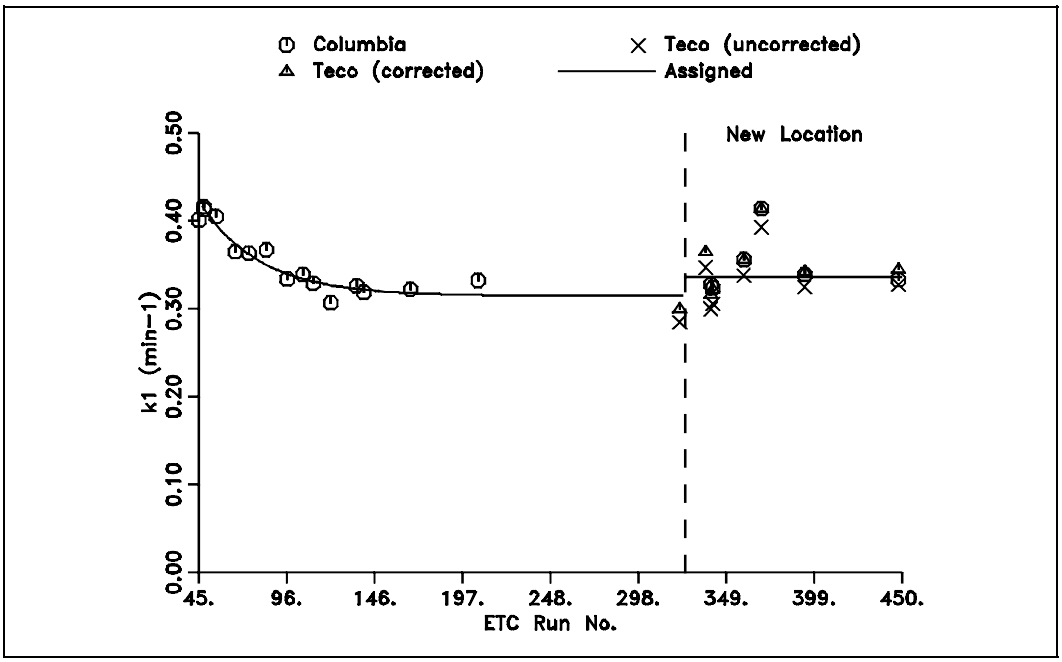

Figure 10. Plot of measured NO2 photolysis rates against ETC run number. The lines show the fit or average value used to assign an NO2 photolysis rate to each experiment.

The light intensity was assumed to be constant after the move to the new facility, since the lights were well "burned in", and since there are insufficient data to indicate any trend in any case. For these runs, the average of the k_1 measurements using the Columbia NO_x analyzer was used for all runs (with the results from run ETC-369, which had an anomalously high value, not being used). The line on figure 10 for the runs in this time period shows this average value.

2. Variations in Temperature.

Although every effort is made to minimize temperature variations from run to run, the chamber is not insulated from the daily variations in the building air conditioning, and the average temperatures for the runs fluctuated somewhat during the runs and from day to day. Occasional room air conditioning or heating problems resulted in average temperatures as high as 305 K or as low as 297 K in a few experiments. Figure 11 shows plots, against run number, of the average temperature for each experiment, also showing the standard deviations of these averages. Although the fluctuation usually appeared to be random, there were periods where some trends could be seen. This variation was also taken into account in the analysis of the data as discussed later in Section III-C.

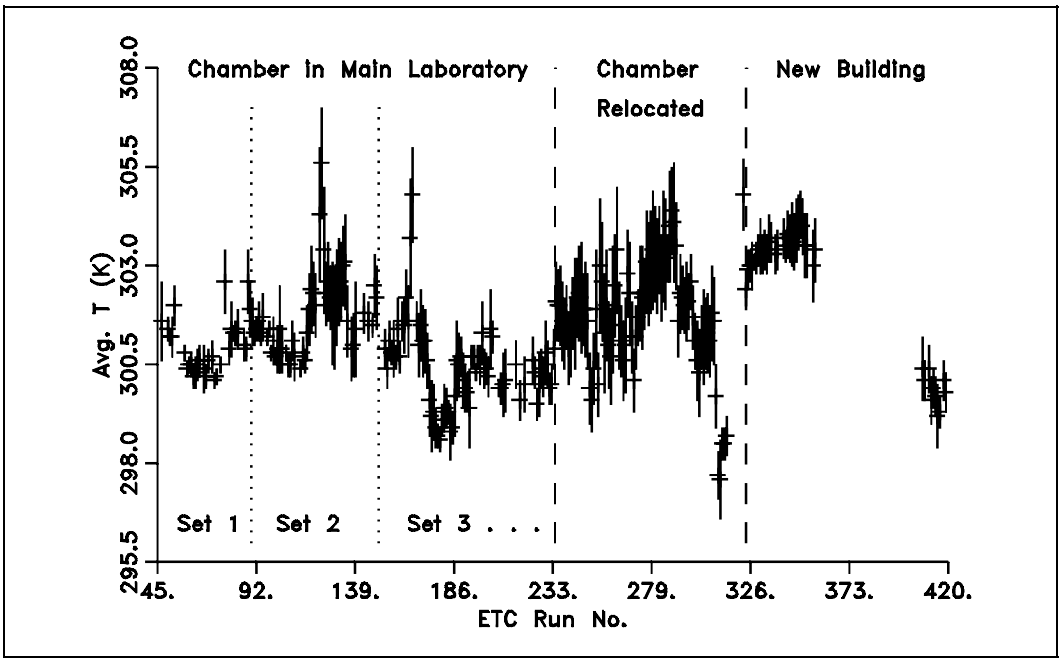

Figure 11. Plot of average temperature of the mini-surrogate experiments against ETC run number. The "error bars" show the standard deviations of these averages.

3. Variations in Initial Reactant Concentrations.

All the mini-surrogate runs were intended to have the same initial concentrations of NO, NO_2 and the mini-surrogate components, except for a few runs where one of the mini-surrogate components was varied, and except for the fact that the levels of the mini-surrogate components was increased in Set 3 relative to Sets 1 and 2. However, in practice there was some variation in these levels, as is shown in Figure 12, which gives plots of initial reactant concentrations against run number in all the mini-surrogate runs except those where the reactant was deliberately varied.

Some of this scatter in initial measured reactant concentrations can be attributed to analytical variability. The ethene data for runs ETC-265 through ETC-221 are of low quality because the instrument did not maintain consistent calibrations from day to day. The quality of all the GC data increased after around the ETC-220's because of the use of a new computer data system allowed quantification of peaks by area. However, the m-xylene measurements were of relatively high precision during most of this program, so the observed variations in its initial concentrations are probably real. The discontinuity in m-xylene at run ETC-302 is due to use of a new n-hexane, m-xylene mixture for injecting

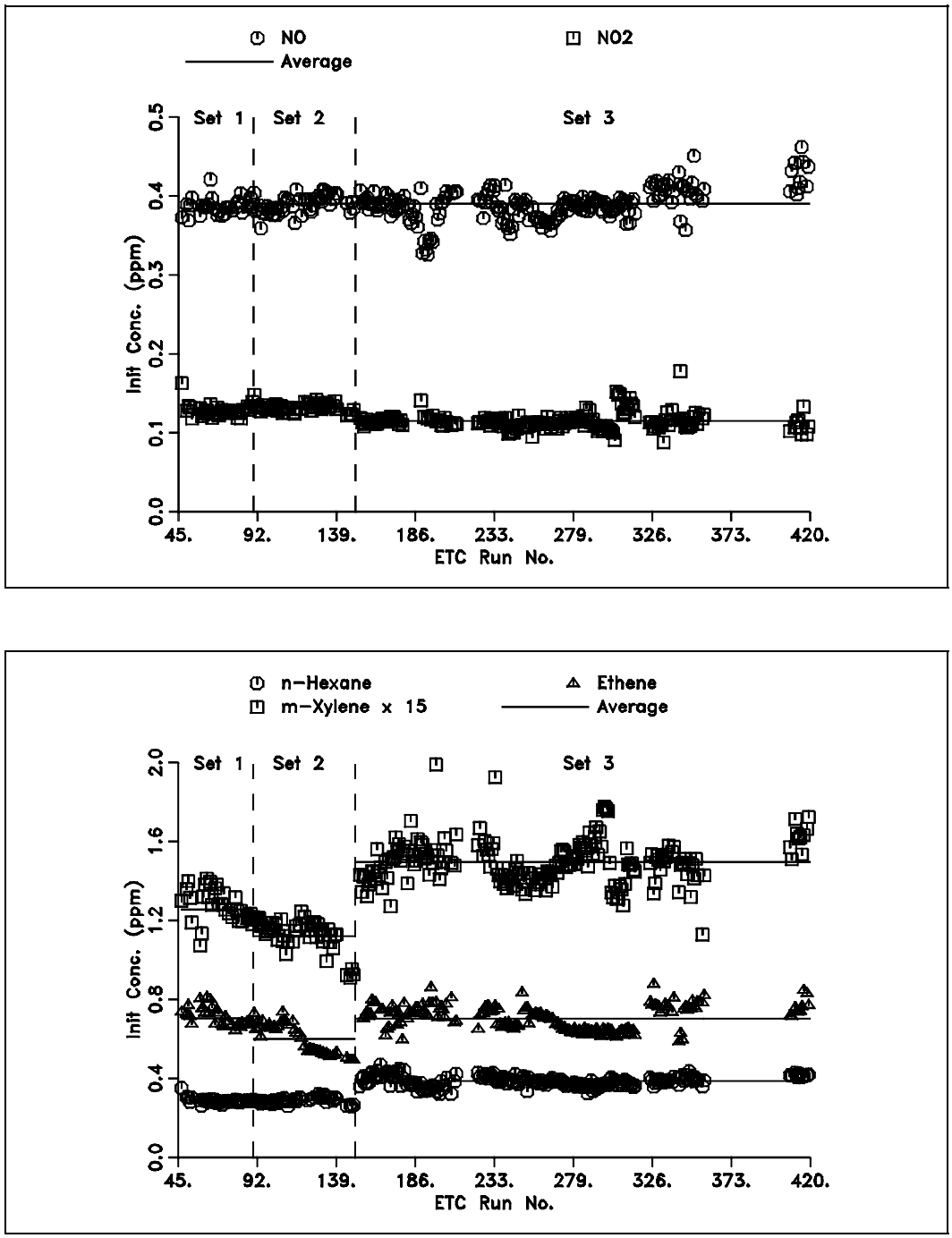

Figure 12. Plots of initial reactant concentrations against run number for all the standard mini-surrogate experiments.

these compounds. The effect of these variations on the results is discussed in the following section.

C. Results of the Mini-Surrogate Runs: Derivation of Reactivities

The main purpose of conducting these mini-surrogate experiments is to determine the effects of the added VOCs on the amount of NO consumed and ozone formed [$d(O_3\text{-}NO)$], on the integrated OH radical levels (IntOH), and on the conversion ratio (ConvR), i.e., the ratio of IntOH to $d(O_3\text{-}NO)$. The incremental reactivities of the VOCs are the changes caused by adding the VOC divided by the amount of VOC added, and the mechanistic reactivities are the changes divided by the amount of VOC reacted. Determining these measures of reactivity requires determining, for each added VOC experiment, (1) the $d(O_3\text{-}NO)$, IntOH, and ConvR values in the added VOC experiment; (2) "base case" values of these quantities which correspond to the conditions of the added VOC experiment; (3) the amount of test VOC which reacted at various times during the experiment; and (4) estimates of uncertainties of all these steps and the overall uncertainty in the measure of reactivity which was derived. These various steps, and the results obtained, are discussed in this section.

1. Experimental Results Used to Quantify Reactivity

In this section, we discuss the specific methods used to derive the various experimental quantities used in the reactivity determinations, and to estimate their uncertainties. These include, for each experiment, the quantities $d(O_3\text{-}NO)$, IntOH, and ConvR, and, for the experiments with an added test VOC, the amount of VOC reacting during the experiment.

Ozone Formed and NO Reacted. The quantity $d(O_3\text{-}NO)$ measures the total amount of ozone formed and NO consumed in the experiment, and is the most direct indicator of ozone formation potential. It is derived directly from the ozone and NO data, i.e., from $([O_3]_t\text{-}[NO]_t) - ([O_3]_0\text{-}[NO]_0)$. Although O_3 and NO data are taken every 15 minutes, only hourly data are used in this analysis. In some experiments the data are not taken exactly on the hour, in those cases, the hourly value is estimated by linear interpolation. Table 3 gives the t = 2, 4, and 6-hour $d(O_3\text{-}NO)$ values, and all the hourly values are given in Table A-1 in Appendix A.

Although there is some uncertainty in the ozone and NO measurements due to calibration uncertainties (estimated to be 5% or less), this is small compared to the uncertainty due to run-to-run variability of the results (discussed later), and is ignored in our uncertainty analysis.

Integrated OH Radical Levels. Estimates of the integrated OH levels, IntOH, are derived from the rate of consumption of either m-xylene or (for a few of the latest experiments) 2-chloromethyl-3-chloropropene. If a VOC reacts only with OH radicals, then its rate of consumption is determined only by its OH radical rate constant, kOH^{voc}, the OH radical concentration, and the dilution rate, D, in the chamber:

$$\frac{d[VOC]}{dt} = (kOH^{VOC}[OH] - D) [VOC]_t \qquad \text{(XXI)}$$

This can be integrated and re-arranged to yield:

$$IntOH_t = \frac{\ln\left(\frac{[VOC]_0}{[VOC]_t}\right) - Dt}{kOH^{VOC}} \qquad \text{(XXII)}$$

The kOH value used when deriving IntOH from the m-xylene data was 2.36×10^{-11} cm^3 $molec^{-1}$ sec^{-1}, based on the recommendation of Atkinson (1989). In the case of the runs using the 2-chloromethyl-3-chloropropene as the OH tracer, the kOH^{tracer} used was 3.16×10^{-11} cm^3 $molec^{-1}$ sec^{-1} cm^3, based on our measurements of $kOH^{tracer}/kOH^{m\text{-}xyl}$ discussed above.

Although dilution should be small in these experiments because the reaction chamber was designed to collapse as samples are withdrawn for analysis, as discussed above the rates of consumption of the less reactive VOCs in our experiments indicate a dilution rate of D= 0.48 $\pm$ 0.25 %/hour, and this was used in our analysis. The dilution correction amounted to approximately 0.8 ppt-min for the 6-hour IntOH derived from runs using m-xylene as the OH tracer, and 0.6 ppt-min for the runs using the chlorobutene tracer. Since the IntOH levels in the Set 1 and 3 standard runs were approximately 20-25 ppt-min and were approximately 15 ppt-min for the Set 2 standard runs, this amounted to an approximately 4-5% correction for these runs. The relative importance of the dilution correction was larger in runs with added VOCs which are radical inhibitors and smaller in runs with added radical initiators.

To reduce the sensitivity of the IntOH results to scatter in individual m-xylene or 2-chloromethyl-3-chloropropene measurements, and to provide a more precise estimate for IntOH for conditions where only relatively small amounts of m-xylene or the chlorobutene have reacted, the data were smoothed by fitting $\ln([m\text{-}Xyl]_t)$ or ln([chlorobutene]) to either linear or quadratic functions of either time or $d(O_3\text{-}NO)(t)$, i.e., to

$$\ln[VOC]_t = a_1 + b_1\, t \qquad \text{(method code = "t2")} \qquad \text{(XXIII)}$$

or

$$\ln[VOC]_t = a_2 + b_2\, t + c_2\, t^2, \qquad \text{(code = "t3")} \qquad \text{(XXIV)}$$

or

$$\ln[VOC]_t = a_3 + b_3\, d(O_3\text{-}NO)_t, \qquad \text{(code = "d2")} \qquad \text{(XXV)}$$

or

$$\ln[VOC]_t = a_4 + b_4\, d(O_3\text{-}NO)_t + c_4\, d(O_3\text{-}NO)t^2 \qquad \text{(code = "d3")} \qquad \text{(XXVI)}$$

and using the fit which gives the lowest standard deviation in estimated initial VOC concentrations. (The codes are those used in Table 3 to indicate the method employed.) Quadratic fits giving local minima or maxima were rejected. Fits against $d(O_3\text{-}NO)$ were not used for the few experiments where an ozone maximum occurred, i.e., where $d(O_3\text{-}NO)$ was not a monotonically increasing function of time. The regressions of ln([VOC]) against $d(O_3\text{-}NO)$ were usually somewhat better fit by a straight line than those against time. Representative plots of the xylene data and the curves fitting them are shown on Figure 13. (Plots of the chlorobutene data are similar.)

Table 3 gives the 6 hour IntOH values for these experiments, and also gives codes indicating which data were used to derive IntOH and the method used to fit these data. The hourly IntOH results are given in Table A-2 in Appendix A. The tables also give the estimated (one σ) uncertainties in values derived. These uncertainty estimates are based on the uncertainties in the initial and time=t m-xylene or tracer values from the regression used and the 0.25%/hour uncertainty in the dilution, but do not include possible systematic errors due to uncertainties in the m-xylene OH radical rate constant used. Note that an error in $kOH^{m\text{-}xyl}$ would affect all the IntOH data by an equal factor, since the kOH for this compound was derived relative to the value we used for m-xylene.

As discussed in Sections III-A-3 there is evidence for non-negligible formation of Cl atoms in the runs with 2-chloromethyl-3-chloropropene added as the test compound. Although this effect most obviously manifests itself as an anomalously high consumption rate of n-hexane, the possibility of Cl atoms also contributing non-negligibly to the amount of m-xylene or chlorobutene reacting cannot be ruled out. If this is occurring, then Equation (XXII) may be giving an overestimate of the true IntOH concentration in the experiment. Because of this, the IntOH measured in experiments with the 2-chloromethyl-3-chloropropene added as the test compound must be considered to be upper limits. This does not apply to runs where it is present only as a radical tracer, since in those cases the amount added is too small to have a measurable effect on the n-hexane data. (Since it does not measurably affect the n-hexane data, the effect on m-xylene or 2-chloromethyl-2-chloropropene consumption would be totally negligible.)

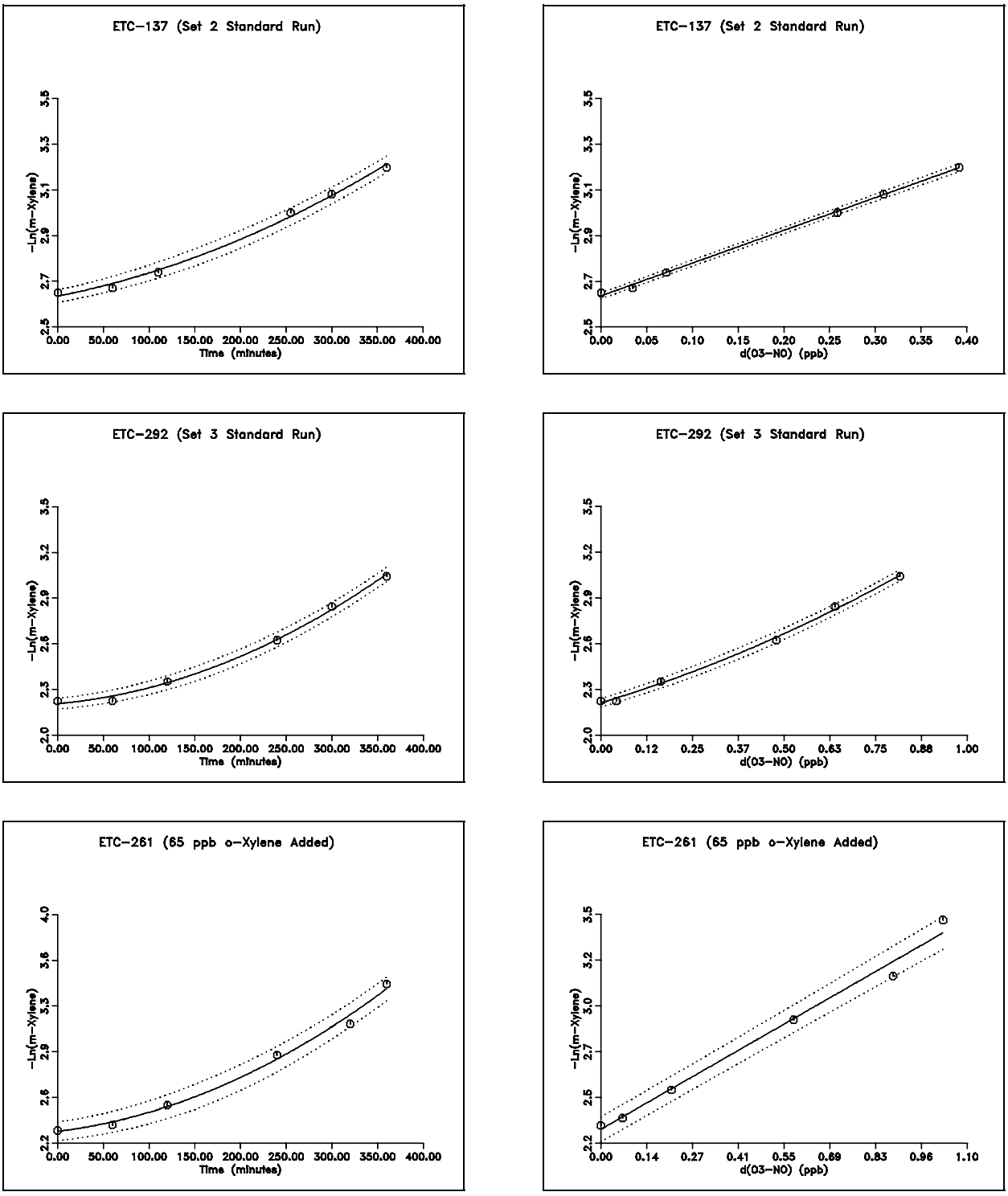

Figure 13. Representative plots of -ln[m-Xylene] against time and d(O3-NO), showing best fit lines or quadratic regression curves. Dotted lines are (one σ) error limits of fits.

Conversion Ratios. The conversion ratio, ConvR, is simply the ratio of the 6-hour IntOH to the 6-hour $d(O_3\text{-NO})$ from the base case experiments. As discussed in Section I-C-3, these are used for estimating direct and indirect components of reactivity. The values obtained from the individual experiments are listed in Table 3. The conversion ratios tended to be less variable from run to run than either IntOH or $d(O_3\text{-NO})$, and thus more precise estimates of conversion ratios for conditions of the test runs could be obtained by using the dependence of ConvR on run conditions than using the ratios of the separately estimated IntOH and $d(O_3\text{-NO})$ values for the conditions of the test runs. Since the uncertainties in the individual $d(O_3\text{-NO})$ measurements are ignored in our analysis, the relative uncertainties in the ConvR values are the same as the relative uncertainty given for the 6-hour IntOH.

Note that the key assumption involved in using base case conversion ratios to estimate direct and indirect reactivity components is that the ratio of NO oxidized and ozone formed from the reactions of the base ROG components to the amounts of base ROG components reacted is approximately independent of the extent of reaction. If the amount of base ROG components reacted is approximately proportional to IntOH, this would imply that the ConvR should also be approximately constant, i.e., that plots of $d(O_3\text{-NO})_t$ vs $IntOH_t$ should be linear. The examples of such plots shown on the right side of Figure 13, above, are typical of the runs in this study. It can be seen that the points are best fit by a straight line in runs ETC-137 and ETC-261, and that although there is a slight curvature in the plot for ETC-292, the points can also be fit by a straight line to within their uncertainty limits. There were no base case runs and only a few test runs which had significantly more curvature in their $d(O_3\text{-NO})_t$ vs $IntOH_t$ plots than shown for ETC-292. This tends to support our assumption that the ratios of NO oxidized and ozone formed to VOC reacted are approximately constant under the conditions of these experiments.

Amounts of Test VOC Reacted. The derivation of mechanistic reactivities requires determining the concentrations of the test VOCs at various times during the experiments. To reduce the effects of measurement scatter in these determinations, the test VOC data were also fitted to the regressions of Equations (XXIII) - (XXVI), and the regression giving the lowest mean square error of the estimate of the initial concentration was used to estimate the concentrations as a function of time. The standard deviations of estimates from the regressions were also compared with the standard deviation of a simple average of all the measurements, and if the standard deviation of the average was lowest, or if the linear regression predicted the VOC increased with time, the simple average was used for estimating the initial VOC concentration. In the latter case, the direct VOC measurements were not used to estimate the amount of VOC reacting during the experiment.

If the VOC reacted sufficiently rapidly, the amount of VOC reacting up to time t was estimated by

$$(\text{VOC reacted})_t = [\text{VOC}]_0 - [\text{VOC}]_t - D \int_0^t [\text{VOC}]\, dt \qquad \text{(XXVII)}$$

where $[\text{VOC}]_0$ and $[\text{VOC}]_t$ are the estimated VOC concentrations derived from the best fit regression, and the last term is the amount of amount VOC lost due to dilution up to time t. The uncertainty in this estimate can be derived from the uncertainties in the [VOC] values predicted by the regression, and the from the uncertainty in D.

The above method has high uncertainties for VOCs which react so slowly that the estimated amount reacted is comparable to the uncertainties in the measurements of the VOC. However, if the VOC reacts only with OH radicals, there is an alternative method which can give more precise estimates of amounts reacted for slower reacting VOCs. If the VOC is consumed only by dilution or reaction with OH radicals, its concentration at time t is given by

$$[\text{VOC}]_t = [\text{VOC}]_0\, e^{- kOH^{VOC}\, IntOH_t - Dt}, \qquad \text{(XXVIII)}$$

which is derived by integrating and rearranging Equation (XXI). Plugging this into Equation (XXVII) yields

$$(\text{VOC reacted})_t = [\text{VOC}]_0 \left(1 - e^{- kOH^{VOC}\, IntOH_t - Dt} - D \int_0^t e^{- kOH^{VOC}\, IntOH_\tau - D\tau}\, d\tau \right)$$

If we make the approximation that [OH] is approximately constant during the experiments, i.e., that $IntOH_t \cong [OH]^{avg}\, t$, then the integral in the last term can be evaluated to yield

$$(\text{VOC reacted})_t \cong [\text{VOC}]_0 \frac{kOH^{VOC}\, IntOH_t}{kOH^{VOC}\, IntOH_t + Dt} \left(1 - e^{- kOH^{VOC}\, IntOH_t - Dt} \right) \qquad \text{(XXIX)}$$

The uncertainty in this estimate would depend on the uncertainties in $[\text{VOC}]_0$, IntOH, and D, but not in $[\text{VOC}]_0 - [\text{VOC}]_t$, as is the case with the estimates using the more direct method [i.e., using Equation (XXVII)]. However, unlike the more direct method, the amounts of VOC reacted estimated using Equation (XXIX) are affected by uncertainties in kOH^{VOC}. The kOH^{VOC} values used are given in Table 2, above.

If the amount of VOC reacting could be derived from both approaches, the approach giving the lower estimated uncertainty was used. A 20% uncertainty in the kOH^{voc} (actually in $kOH^{voc}/kOH^{m\text{-}xyl}$) was included when deriving the uncertainty in the estimate using Equation (XXIX) for the purpose of comparing it with the uncertainty of the estimate using Equation (XXVII), but was not used otherwise.

The amounts of VOC reacting in each added VOC experiment and their estimated uncertainties are given in Tables A-1 and A-2 in Appendix A. Table A-1 also gives codes indicating the method used to estimate these quantities.

2. Derivation of Base Case Results

Since the purpose of this study is to determine the effect of adding a test VOC to a standard experiment, it is obviously important to establish the baseline against which the effect of the addition of the test VOC is compared. If there were no run-to-run variability in our chamber experiments, a single experiment would be sufficient for this purpose. However, such variability is an inherent part of environmental chamber experiments, and must be taken into account when determining the appropriate base case result corresponding to the conditions of each added test VOC run. Because of this, a large number of replicates of the same base case experiment was carried out during the course of this program. Although every effort was made to hold conditions constant from run to run in the various sets (other than the addition of the test compound), Table 3 shows that there was variability in the results of the many replicated standard base case experiments. This is shown perhaps more clearly on Figures 14-16, which give plots of the final $d(O_3\text{-}NO)$, IntOH, and ConvR, respectively, against ETC run number.

Some of the most obvious trends and variabilities in the results shown on Figures 14-16 can be explained by known changes in run conditions or experimental conditions. The abrupt changes in the $d(O_3\text{-}NO)$ and IntOH results between Sets 1 and 2 is due to changing the NO_x injection procedure; this apparently had no significant effect on the ConvR's. However, the change in initial base ROG concentration between Sets 2 and 3 changed all three of these types of results. (The apparent smooth transition in the change in ConvR results in the first runs of Set 3 as shown on Figure 16 is difficult to understand, and is presumed to be simply coincidence.) The consistent decline in $d(O_3\text{-}NO)$ and IntOH results in the Set 1 and (to a much lesser extent) the Set 2 experiments is due to a gradual decrease in light intensity, as indicated by results of NO_2 actinometry measurements (discussed below). The sharp fluctuations in the $d(O_3\text{-}NO)$ and IntOH results around the time of ETC-300 are attributed to failures in the temperature control system around that time, with unusually high $d(O_3\text{-}NO)$ and IntOH results

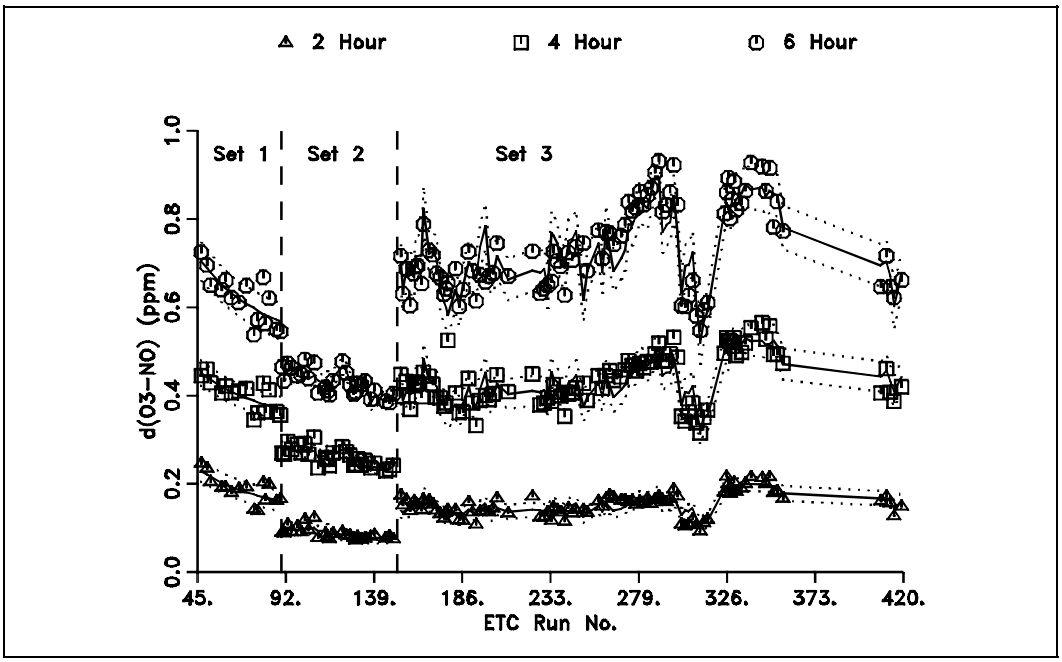

Figure 14. Plots of the t=2, 4, and 6-hour d(O3-NO) results against ETC run number for all the base case experiments. Solid lines show the values estimated using the regression fits, and dotted lines show the (one σ) uncertainty ranges of the estimates for each run.

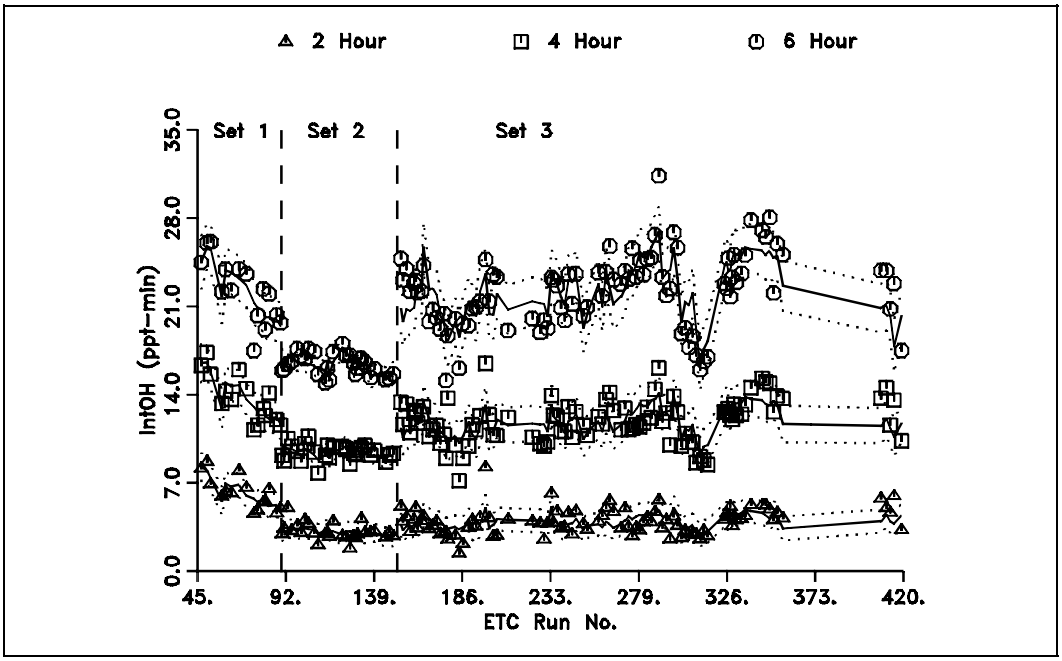

Figure 15. Plots of the t=2, 4, and 6-hour IntOH results against ETC run number for all the base case experiments. Solid lines show the values estimated using the regression fits, and dotted lines show the (one σ) uncertainty ranges of the estimates for each run.

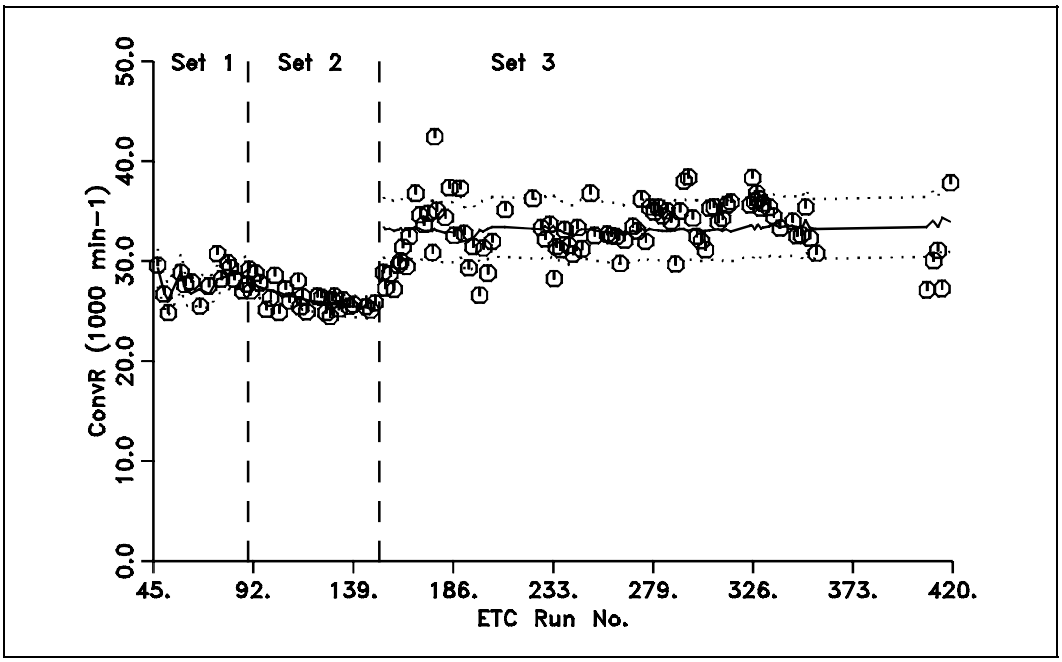

Figure 16. Plots of the 6-hour ConvR results against ETC run number for all the base case experiments. Solid lines show the values estimated using the regression fits, and dotted lines show the (one σ) uncertainty ranges of the estimate for each run.

being observed in high temperature runs, and vise-versa. The ConvR is apparently not dependent on temperature, since it remains relatively constant around the time when the large temperature fluctuations were observed.

A linear multiple regression analysis was used to determine the extent to which these and other known variations in run conditions can account for this variability in the results of the repeated standard experiments. First, the SAS "STEPWISE" procedure with the "forward selection" option (SAS, 1985) was run to determine the extent to which the known variability in the average temperature, assigned k_1, and initial reactant concentrations could account for the variability observed for the 6-hour d(O_3-NO), IntOH, and ConvR in the standard runs. In this procedure, the program starts with no variables in the regression model, and then determines, for each variable, the F statistic measuring its contribution to the model if it is included (Snedecor and Cochran, 1967; SAS, 1985). The variable with the largest F statistic is then added to the model, and the program then determines which of the remaining variables has the largest F statistic when added to the model, etc. In addition, the SAS "RSQUARE" procedure was run with all possible combinations of including or excluding regression variables to determine which combination gave the lowest mean square error (Snedecor and Cochran, 1967; SAS, 1985).

The results of the forward selection regression analysis are given on Table 4. The results indicate that the known variations in run conditions could account for approximately 73-80% of the variation in $d(O_3\text{-}NO)$ in all three sets, ~75% of the variations in IntOH in Sets 1 and 3, ~50% of the variation the IntOH in Set 2, ~50% of the variations in ConvR in Sets 1 and 2, and only ~30% of the variations of ConvR in Set 3. In general, $d(O_3\text{-}NO)$ and IntOH appear to be sensitive to both temperature and light intensity (k_1), with the relatively large changes in k_1 during Set 1 accounting for most of the variability in these results for this set, and with the large daily fluctuations in temperature during Set 3 accounting for most of the variability in the $D(O_3\text{-}NO)$ and IntOH results for that set. In the case of Set 2, variations in k_1 are more important in accounting for the variability in $d(O_3\text{-}NO)$, while variations in temperature are more important in accounting for the variability in IntOH. Unlike $d(O_3\text{-}NO)$ and IntOH, the ConvR appears to be relatively insensitive to temperature, and it appears to have only a relatively weak dependence on variations in light intensity. Presumably because of this the ConvR was less variable from run to run than the other measures of reactivity, and what variability was observed for ConvR is less clearly attributable to any particular set of run conditions.

Since this regression analysis indicates that up to 75% of the variability of the base case results could be accounted for by the known variability of run conditions, a regression with the appropriate set of variables can be used to estimate, for each run with an added test VOC, what the results of a standard experiment would be if it were carried out with the exact same temperature, light intensity, and initial concentrations of other reactants as the added VOC run. Table 4 indicates the set of variables which gave the lowest mean square error of the estimates, and indicates the set of variables which were actually used and their corresponding regression coefficients. The percent root mean square errors of the estimates are also shown.

The sets of parameters used were those giving the lowest mean square error, except that k_1 was included among the set of parameters used to estimate $d(O_3\text{-}NO)$ for the Set 2 runs, and the initial NO_2 and n-hexane were not used for the Set 3 estimates. K_1 was used for the Set 2 $d(O_3\text{-}NO)$ estimates because the "stepwise" analysis indicated it is the most important single variable, and the results of the Set 1 runs clearly indicate that it is reasonable to expect it to be a significant factor. Including it only causes a 1.5% increase in the root mean square error. The initial NO_2 and ethene concentrations are not available for some of the added VOC Set 3 experiments, so they were not used in the estimates. Excluding them caused about a 5% increase in the root mean square uncertainty estimate for $d(O_3\text{-}NO)$ and IntOH, and about a 10% increase for ConvR.

The ability of the minimum (or near-minimum) mean square error regressions to predict the results of the base case experiments are shown on Figures 14-16.

Table 4. Results of Regression Analysis of Effects of Run Conditions on Results of Standard Runs, And Regression Parameters Used to Estimate Base Case Results for Conditions of the Added VOC Runs.

Set	Parameter	Value	Stepwise Regression [b]			Estimatimation Coefficient [c]	Root MSE [d]	
		Avg. (sdev)	Partial R^2	Total R^2	F	Value (unc.)	Minimum	Set Used
1	* Intercept					0.621 (0.009)	5.9%	5.9%
	* k1	0.327 (0.024)	0.613	0.613	20.54	1.9 (0.4)		
	NO	0.384 (0.006)	0.012	0.625	0.39			
	m-Xylene	0.084 (0.005)	0.025	0.649	0.77			
	NO2	0.130 (0.010)	0.011	0.660	0.31			
	n-Hexane	0.291 (0.019)	0.056	0.716	1.78			
	Avg Temp.	301.0 (0.6)	0.012	0.728	0.35			
	Ethene	0.704 (0.040)	0.000	0.728	0.00			
2	* Intercept					0.431 (0.003)	3.7%	3.8%
	k1	0.330 (0.008)	0.419	0.419	18.04	0.6 (1.0)		
	* Avg Temp.	301.7 (0.9)	0.210	0.629	13.54	0.021 (0.005)		
	* Ethene	0.600 (0.079)	0.088	0.717	7.15	0.25 (0.09)		
	* NO	0.390 (0.011)	0.010	0.727	0.83	-0.5 (0.4)		
	* m-Xylene	0.075 (0.006)	0.016	0.743	1.32	0.9 (0.8)		
	NO2	0.131 (0.005)	0.004	0.747	0.29			
	n-Hexane	0.290 (0.015)	0.008	0.755	0.65			
3	* Intercept					0.736 (0.005)	6.3%	6.4%
	* Avg Temp.	301.4 (1.5)	0.724	0.724	207.67	0.056 (0.004)		
	* m-Xylene	0.100 (0.008)	0.042	0.766	13.98	2.9 (0.6)		
	* n-Hexane	0.387 (0.027)	0.008	0.774	2.64	-0.4 (0.2)		
	* NO2 [e]	0.114 (0.009)	0.006	0.780	2.09			
	* k1	0.321 (0.009)	0.005	0.785	1.78	1.3 (0.8)		
	* Ethene[e]	0.713 (0.062)	0.010	0.795	3.46			
	* NO	0.391 (0.020)	0.005	0.800	1.84	-0.4 (0.3)		
6-Hour IntOH								
1	* Intercept					22.3 (0.4)	11.2%	11.2%
	* k1	0.327 (0.024)	0.591	0.591	18.79	80 (25)		
	* m-Xylene	0.084 (0.005)	0.084	0.675	3.19	150 (90)		
	* n-Hexane	0.291 (0.019)	0.028	0.703	1.04	-30 (30)		
	NO	0.384 (0.006)	0.017	0.720	0.62			
	Avg Temp.	301.0 (0.6)	0.017	0.737	0.56			
	NO2	0.130 (0.010)	0.014	0.751	0.46			
	Ethene	0.704 (0.040)	0.000	0.751	0.00			
2	* Intercept					16.4 (0.1)	4.1%	4.1%
	* m-Xylene	0.075 (0.006)	0.190	0.190	5.86	40 (30)		
	* Avg Temp.	301.7 (0.9)	0.126	0.316	4.43	0.6 (0.2)		
	* NO	0.390 (0.011)	0.119	0.435	4.85	-20 (15)		
	* Ethene	0.600 (0.079)	0.050	0.485	2.15	4. (3.)		
	k1	0.330 (0.008)	0.014	0.500	0.60			
	NO2	0.131 (0.005)	0.002	0.502	0.09			
	n-Hexane	0.290 (0.015)	0.000	0.502	0.00			
3	* Intercept					22.3 (0.2)	7.0%	7.3%
	* Avg Temp.	301.4 (1.5)	0.589	0.589	113.39	1.6 (0.14)		
	* m-Xylene	0.100 (0.008)	0.052	0.642	11.34	84 (26)		
	* NO	0.391 (0.020)	0.062	0.703	16.04	-16 (10)		
	* Ethene[e]	0.713 (0.062)	0.022	0.725	5.97			
	* NO2 [e]	0.114 (0.009)	0.013	0.737	3.58			
	n-Hexane	0.387 (0.027)	0.003	0.740	0.76			
	k1	0.321 (0.009)	0.000	0.740	0.09			
6-Hour ConvR								
1	* Intercept					28.0 (0.4)	4.9%	4.9%
	* m-Xylene	0.084 (0.005)	0.222	0.222	3.71	-130 (80)		
	* n-Hexane	0.291 (0.019)	0.117	0.339	2.12	50 (25)		
	* k1	0.327 (0.024)	0.084	0.423	1.60	-30 (20)		
	NO2	0.130 (0.010)	0.043	0.466	0.80			
	Avg Temp.	301.0 (0.6)	0.025	0.491	0.43			
	Ethene	0.704 (0.040)	0.004	0.494	0.06			
	NO	0.384 (0.006)	0.002	0.496	0.02			

Table 4 (continued)

Set	Parameter	Value	Stepwise Regression [b]			Estimatimation Coefficient [c]		Root MSE [d]	
		Avg. (sdev)	Partial R^2	Total R^2	F	Value	(unc.)	Minimum	Set Used
2	* Intercept					26.3	(0.2)	3.8%	3.8%
	* k1	0.330 (0.008)	0.400	0.400	16.65	105	(25)		
	NO2	0.131 (0.005)	0.019	0.419	0.80				
	Ethene	0.600 (0.079)	0.017	0.436	0.69				
	n-Hexane	0.290 (0.015)	0.022	0.458	0.90				
	Avg Temp.	301.7 (0.9)	0.007	0.466	0.29				
	m-Xylene	0.075 (0.006)	0.002	0.468	0.09				
	NO	0.390 (0.011)	0.001	0.469	0.03				
3	* Intercept					33.2	(0.3)	7.1%	7.8%
	* NO	0.391 (0.020)	0.109	0.109	9.63	17	(15)		
	* Ethene[e]	0.713 (0.062)	0.104	0.213	10.32				
	* k1	0.321 (0.009)	0.051	0.263	5.28				
	* NO2 [e]	0.114 (0.009)	0.023	0.286	2.49				
	* Avg Temp.	301.4 (1.5)	0.012	0.299	1.28				
	n-Hexane	0.387 (0.027)	0.002	0.300	0.16				
	m-Xylene	0.100 (0.008)	0.000	0.300	0.00				

[a] Dependent parameters are listed in order of significance as determined by the SAS "STEPWISE" program. Parameters with a "*" are in the set which gave the lowest mean square error of the estimate.
[b] Results of stepwise addition of most significant parameter to regression, using the SAS "STEPWISE" procedure with the "FORWARD" option. Total R^2 is the R^2 statistic for the parameter and the more significant parameters listed above it (if any). Partial R^2 is difference between total R^2 and R^2 from the previous step before this parameter was added. F is the F statistic for the parameter. (Some corrections were made to the data and some Set 3 runs were added after the stepwise regression analyses were carried out, the results shown here are expected to be a good approximation of an analysis of the final data base.)
[c] Coefficients for the parameter used to estimate the "base case" result for the conditions of the test runs, where the coefficient is multiplied by the difference between the parameter value for the run and the average parameter value for the set, then added to the "intercept" and the terms for the other parameters to obtain the estimate. (The "intercept" is the same as the average value from the standard runs.) The set of parameters used is that which gives the minimum mean sum of squares error, except as indicated in the text. If no coefficient is given, then this parameter was not used to estimate this result for this set. The parameters correspond to $d(O_3\text{-NO})$ in units of ppm, IntOH in units of ppt-min, ConvR in units of 10^{-3} min^{-1}, T in K, k_1 in min^{-1}, and initial concentrations in ppm.
[d] Lowest root mean square error (as percent of average) of the estimate, and root mean square with the set of parameters used, if different. (Derived from the same data base as used for the stepwise analysis. See footnote [b].)
[e] This parameter could not be used for estimation purposes because it is unknown for some of the added VOC runs in the set.

Except for a few anomalous runs, the regressions appear to be reasonably successful in fitting the results of these experiments.

The uncertainty levels of the estimates of these regressions are important because they provide a measure of the run-to-run variability which cannot be accounted for by known variabilities of conditions. Since the runs with the added test VOC would be expected to have similar run-to-run variability due to the same unmeasured factors, for the purpose of estimating uncertainties of incremental reactivities the results of the added test VOC run was assumed to have the same relative uncertainty as the estimate for the corresponding base case result. Thus the absolute uncertainty in the change in $d(O_3\text{-NO})$, IntOH, or ConvR caused by the addition of the test VOC was estimated to be $\sqrt{2}$ times the absolute uncertainty in the estimate for the base run. For example, the uncertainties of the estimates of the 6-hour $d(O_3\text{-NO})$ results for the standard Set 3 runs were typically 6%, and typically the addition of a test VOC causes a

40% increase in $d(O_3\text{-NO})$. If this uncertainty is assumed to be due to run-to-run variability due to unknown factors which is the same in both the standard and the added VOC run, this would correspond to a 21% estimated uncertainty in the change in $d(O_3\text{-NO})$ caused by adding the VOC, and thus at least this much uncertainty in the reactivity. Although the amount of test VOC added and reacted also contributed to the uncertainties of the reactivity estimates, as well imprecisions in measurements in IntOH (in the case of reactivities relative to IntOH or conversion factors), the run-to-run variability due to unmeasured factors was the dominant source of uncertainty in most of the reactivity measurements reported here.

3. Measured VOC Reactivities

The detailed results of the reactivity determinations are given in the tables and figures in Appendix A to this report. Table A-1 gives, for each experiment where a test VOC was added, the amounts of test VOC estimated to have reacted at the end of each hour in the experiment and their estimated uncertainties; the hourly $d(O_3\text{-NO})$ measured in the experiment ("Test"); the corresponding value estimated, using the regression parameters given on Table 4, for a base case experiment if it were carried out under the same conditions ("Base Fit"); the difference between the results of the added VOC experiment and the estimate for the base experiment ("Change"); the hourly incremental and mechanistic reactivities and their uncertainties. Table A-2 gives similar results for the hourly IntOH data, and Table A-3 gives the test run and base fit conversion ratio results and their uncertainties, and the conversion factors which were derived from them, and their uncertainties. Table A-1 also includes codes indicating how the amounts of test VOC reacted were estimated. The uncertainties on the tables results reflect the uncertainties in the measured or estimated amounts of VOC added or reacted, the run to run variabilities as discussed in the previous section, and (for IntOH and ConvR) the uncertainties in the measurements of IntOH.

Appendix B provides an illustration of how all the experimentally derived quantities were calculated for a selected added test VOC experiment. This includes calculations of the 6-hour $d(O_3\text{-NO})$, IntOH, amount of test VOC reacted, base case results, the incremental and mechanistic $d(O_3\text{-NO})$, IntOH, and direct reactivities, and the estimated uncertainties in all these quantities. The appendix was generated using the Mathcad 3.1 computer program (MathSoft, 1992). The example run chosen was added propane run ETC-226, where the amount reacted was estimated using the IntOH method.

Appendix A also includes various plots showing how the measured $d(O_3\text{-NO})$ and IntOH reactivities and conversion factors vary with amount of test VOC added,

how the d(O_3-NO) reactivities vary with time in the experiment, and how the amount of test VOC reacted varied with amount added. The plots also include results of computer model simulations of these data which are discussed in later sections.

Table 5 gives a summary of the major reactivity results, including, for each experiment where a test VOC was added, the estimated or measured amount of VOC reacting in the run, the 6-hour d(O_3-NO) incremental and mechanistic reactivities and their estimated uncertainties, and the estimated direct and indirect components of the d(O_3-NO) mechanistic reactivities. Note that the "direct" component of the d(O_3-NO) mechanistic reactivity is the same as the Conversion Factor (ConvF), and was derived using Equation (XI) as indicated on Table A-3. The "indirect" component of the d(O_3-NO) reactivity shown on Table 5 was derived from the IntOH reactivities from Table A-2 and the Conversion Ratios from Table A-3 using Equation (XVIII). Footnotes to the table indicate special conditions or problem runs; these are discussed in more detail below.

Experimental mechanistic reactivities could not be determined for acetone and formaldehyde because the amounts reacted could not be estimated for these VOCs. The direct method (Equation XXVI) could not be used for acetone because it reacts too slowly for changes in its concentration to be reliably measured, and it could not be used for formaldehyde because formaldehyde is formed from the reactions of the base ROG surrogate. The IntOH method (Equation XXVIII) could not be used for either compound because both are consumed to a non-negligible extent by photolysis. For these compounds, Tables A-1 and A-2 give only incremental reactivities, and the plots in Appendix A give incremental reactivities instead of mechanistic reactivities. (In addition, incremental rather than mechanistic reactivities are shown on the reactivity vs time plots for the highly radical-inhibiting VOCs such as n-octane and the siloxanes, because when IntOH is low the estimates of amounts reacted are highly uncertain at the shorter reaction times.) However, to allow for comparisons with mechanistic reactivities for other VOCs, Table 5 gives estimates of mechanistic reactivities for these compounds derived from the experimental incremental reactivities and amounts reacted estimated from computer model calculations. Note that the model calculation affects only the comparison of the magnitudes of the mechanistic reactivities with those for the other VOCs, and not the results in terms of the relative importance of the direct vs indirect reactivity components for formaldehyde and acetone. Note also that the model calculation for the amount of formaldehyde reacted is unlikely to be significantly in error, since most of the added formaldehyde is expected to react. The possible error in the case of acetone is greater, but given the level of agreement between model calculated and experimental 6-hour reactivities for this compound (see Section IV), it is unlikely to be off by more than a factor of 2.

Table 5. Summary of Reactivity Results for the Test VOC Experiments. (Quantities in parentheses are uncertainty estimates.)

Set	Run		Added (ppm)	Reacted (ppm)	Reactivity: Incremental (mol O_3-NO/ mol added)	Reactivity: Mechanistic (mol O_3-NO/mol reacted) Overall	Indirect [a]	Direct [b]
Carbon Monoxide								
3	418		110.	0.662 (6%)	0.0039 (16%)	0.6 ± 0.1	-0.2 ± 0.1	0.8 ± 0.1
3	416		130.	0.726 (6%)	0.0048 (11%)	0.9 ± 0.1	-0.1 ± 0.1	0.9 ± 0.1
3	414	[c]	138.	1.370 (5%)	0.0050 (10%)	0.5 ± 0.1	0.2 ± 0.1	0.3 ± 0.1
Ethane								
1	68		10.01	0.086 (7%)	0.0057 (97%)	0.7 ± 0.7	-0.7 ± 0.8	1.2 ± 0.7
1	79		17.6	0.127 (6%)	0.0077 (42%)	1.1 ± 0.4	-0.7 ± 0.6	1.7 ± 0.5
1	62		17.6	0.144 (5%)	0.0139 (23%)	1.7 ± 0.4	-0.7 ± 0.5	2.4 ± 0.4
1	73		18.1	0.122 (6%)	0.0052 (60%)	0.8 ± 0.5	-1.1 ± 0.5	1.8 ± 0.4
1	88		24.4	0.178 (6%)	0.0127 (19%)	1.7 ± 0.3	-0.3 ± 0.4	2.0 ± 0.3
2	99		16.6	0.096 (13%)	0.0071 (22%)	1.2 ± 0.3	-0.5 ± 0.5	1.7 ± 0.5
2	92		17.1	0.100 (10%)	0.0069 (22%)	1.2 ± 0.3	-0.6 ± 0.4	1.7 ± 0.4
3	332	[c]	20.0	0.180 (5%)	0.0129 (26%)	1.4 ± 0.4	-0.4 ± 0.5	1.9 ± 0.5
3	333	[c]	21.0	0.235 (4%)	0.0209 (15%)	1.9 ± 0.3	0.5 ± 0.4	1.5 ± 0.5
3	235		43.7	0.306 (6%)	0.0058 (26%)	0.8 ± 0.2	-0.6 ± 0.3	1.4 ± 0.3
Propane								
3	226		11.57	0.231 (8%)	0.0068 (85%)	0.3 ± 0.3	-1.2 ± 0.4	1.5 ± 0.3
3	305		20.1	0.405 (15%)	0.0160 (21%)	0.8 ± 0.2	-0.7 ± 0.3	1.5 ± 0.3
3	230		28.8	0.505 (10%)	0.0183 (13%)	1.0 ± 0.2	-0.7 ± 0.2	1.6 ± 0.2
n-Butane								
1	59		1.82	0.120 (6%)	0.0619 (50%)	0.9 ± 0.5	-1.0 ± 0.7	2.2 ± 0.6
1	51		2.31	0.148 (8%)	0.0630 (41%)	1.0 ± 0.4	-1.5 ± 0.5	2.4 ± 0.4
1	53	[c]	5.21	0.357 (9%)	0.0390 (29%)	0.6 ± 0.2	-0.3 ± 0.2	0.9 ± 0.2
1	82		6.75	0.257 (10%)	0.0286 (30%)	0.8 ± 0.2	-1.1 ± 0.3	1.9 ± 0.3
1	86		7.00	0.266 (12%)	0.0341 (24%)	0.9 ± 0.2	-1.0 ± 0.3	1.9 ± 0.3
2	135		6.06	0.209 (20%)	0.0217 (19%)	0.6 ± 0.2	-0.8 ± 0.3	1.4 ± 0.4
2	97		6.12	0.191 (20%)	0.0278 (15%)	0.9 ± 0.2	-1.2 ± 0.4	2.0 ± 0.5
2	94		7.16	0.247 (10%)	0.0173 (25%)	0.5 ± 0.1	-0.8 ± 0.2	1.3 ± 0.2
3	224		9.76	0.309 (17%)	0.0269 (26%)	0.8 ± 0.3	-1.4 ± 0.4	2.2 ± 0.4
4	393		3.46	0.226 (8%)	[d]			
4	389		3.60	0.256 (10%)	[d]			
Isobutane								
3	228		2.72	0.123 (12%)	0.0304 (81%)	0.7 ± 0.5	-1.9 ± 0.8	2.3 ± 0.7
3	303		6.62	0.333 (31%)	0.0378 (27%)	0.8 ± 0.3	-0.6 ± 0.5	1.3 ± 0.6
3	241		10.21	0.418 (8%)	0.0488 (14%)	1.2 ± 0.2	-0.8 ± 0.2	1.9 ± 0.2
3	232		20.9	0.539 (45%)	0.0347 (9%)	1.3 ± 0.6	-0.8 ± 0.4	2.1 ± 1.0
n-Hexane								
3	201		1.168	0.041 (**%)	-0.0935 (60%)	-2.7 ± 3.4	-13.0 ±15.1	10.0 ±11.7
3	209		1.58	0.092 (16%)	-0.101 (42%)	-1.7 ± 0.8	-4.5 ± 1.3	2.6 ± 0.9
Isooctane								
3	291		10.14	0.294 (34%)	0.0188 (36%)	0.6 ± 0.3	-2.3 ± 0.9	3.0 ± 1.0
3	293		10.64	0.382 (31%)	0.0195 (33%)	0.5 ± 0.2	-1.5 ± 0.6	2.1 ± 0.7
n-Octane								
3	239		1.55	0.064 (28%)	-0.243 (18%)	-5.9 ± 2.0	-9.7 ± 3.2	3.5 ± 1.4
3	237		1.66	0.098 (19%)	-0.235 (17%)	-4.0 ± 1.0	-5.9 ± 1.5	1.9 ± 0.8
Ethene								
3	203		0.217	0.086 (29%)	0.912 (35%)	2.3 ± 1.0	2.0 ± 1.2	0.3 ± 1.2
3	199		0.386	0.172 (20%)	1.14 (17%)	2.5 ± 0.6	1.9 ± 0.8	0.7 ± 0.8
Propene								
1	65		0.083	0.067 (22%)	1.80 (41%)	2.2 ± 1.0	1.2 ± 1.0	1.0 ± 0.9
1	72		0.120	0.090 (6%)	0.742 (63%)	1.0 ± 0.6	0.4 ± 0.8	0.5 ± 0.7
2	110		0.070	0.045 (22%)	2.84 (18%)	4.4 ± 1.1	1.1 ± 1.7	3.4 ± 1.9
2	106		0.081	0.057 (7%)	2.61 (13%)	3.7 ± 0.5	2.1 ± 0.6	1.6 ± 0.6
2	108		0.085	0.057 (5%)	1.98 (16%)	3.0 ± 0.5	1.5 ± 0.6	1.6 ± 0.6
2	118		0.148	0.108 (6%)	1.63 (12%)	2.2 ± 0.3	1.3 ± 0.5	1.0 ± 0.5
Isobutene								
3	257		0.108	0.104 (2%)	2.73 (23%)	2.8 ± 0.6	2.4 ± 0.9	0.4 ± 1.0
3	255		0.195	0.192 (12%)	2.27 (19%)	2.3 ± 0.4	2.6 ± 0.6	-0.3 ± 0.7
3	253		0.207	0.205 (7%)	2.46 (15%)	2.5 ± 0.4	2.4 ± 0.5	0.0 ± 0.6

Table 5 (continued)

Set	Run	Added (ppm)	Reacted (ppm)	Reactivity: Incremental (mol O_3-NO/ mol added)	Reactivity: Mechanistic (mol O_3-NO/mol reacted) Overall	Radical	Direct
trans-2-Butene							
3	309	0.069	0.068 (11%)	5.47 (21%)	5.5 ± 1.2	4.2 ± 1.5	1.3 ± 1.6
3	307	0.087	0.086 (35%)	5.09 (38%)	5.1 ± 1.9	4.5 ± 2.0	0.5 ± 1.5
Isoprene							
3	277	0.076	0.075 (2%)	4.44 (20%)	4.5 ± 0.9	2.2 ± 1.2	2.3 ± 1.5
3	275	0.108	0.108 (2%)	4.06 (15%)	4.1 ± 0.6	2.3 ± 1.0	1.8 ± 1.2
3	273	0.139	0.138 (3%)	3.59 (14%)	3.6 ± 0.5	1.7 ± 0.7	1.9 ± 0.9
3	271	0.157	0.150 (5%)	3.49 (13%)	3.6 ± 0.5	1.8 ± 0.6	1.8 ± 0.7
2-Chloromethyl-3-chloropropene							
3	343	0.103	0.085 (5%)	3.77 (19%)	4.5 ± 0.9	5.4 ± 1.2	-0.6 ± 1.6
3	342	0.108	0.085 (3%)	4.55 (14%)	5.8 ± 0.8	4.2 ± 1.2	1.8 ± 1.5
3	350	0.113	0.096 (7%)	4.37 (15%)	5.1 ± 0.8	5.9 ± 1.2	-0.7 ± 1.5
Benzene							
3	265	5.78	0.357 (14%)	0.0479 (24%)	0.8 ± 0.2	1.1 ± 0.5	-0.4 ± 0.5
3	263	6.86	0.447 (11%)	0.0224 (44%)	0.3 ± 0.2	0.8 ± 0.3	-0.5 ± 0.4
Toluene							
1	64	0.061	0.011 (16%)	1.16 (78%)	6.2 ± 5.0	2.5 ± 6.1	2.6 ± 5.6
1	69	0.095	0.020 (14%)	1.80 (33%)	8.7 ± 3.1	10.1 ± 4.3	-1.5 ± 4.0
1	61	0.175	0.043 (11%)	2.30 (14%)	9.3 ± 1.7	7.2 ± 1.8	2.0 ± 1.7
2	101	0.170	0.030 (16%)	1.22 (13%)	6.9 ± 1.4	5.9 ± 1.5	0.8 ± 1.2
2	103	0.174	0.034 (15%)	1.34 (11%)	7.0 ± 1.3	5.3 ± 1.4	1.6 ± 1.3
Ethylbenzene							
3	313	0.092	0.015 (7%)	0.738 (99%)	4.5 ± 4.4	-0.9 ± 5.9	4.7 ± 5.5
3	311	0.098	0.017 (8%)	[d]			
3	315	0.215	0.031 (21%)	1.06 (30%)	7.3 ± 2.7	1.4 ± 3.0	5.6 ± 3.0
o-Xylene							
3	259	0.064	0.024 (14%)	4.11 (26%)	10.9 ± 3.2	8.7 ± 4.6	2.2 ± 4.9
3	261	0.064	0.027 (11%)	4.18 (25%)	10.0 ± 2.7	8.5 ± 4.8	1.6 ± 5.3
m-Xylene							
3	207	0.038	0.023 (16%)	8.24 (24%)	13.7 ± 3.7	8.9 ± 6.7	5.1 ± 6.8
3	301	0.053	0.033 (20%)	6.16 (23%)	9.9 ± 2.8	7.7 ± 3.2	1.8 ± 3.3
3	196	0.057	0.034 (11%)	3.41 (36%)	5.7 ± 2.1	5.4 ± 2.8	0.5 ± 3.1
3	344	0.081	0.049 (33%)	5.70 (23%)	9.3 ± 3.3	1.6 ± 2.9	7.8 ± 4.0
p-Xylene							
3	348	0.075	0.036 (3%)	2.63 (35%)	5.5 ± 1.9	5.1 ± 2.6	0.4 ± 3.2
3	346	0.080	0.039 (3%)	2.93 (31%)	6.0 ± 1.9	4.9 ± 2.4	1.7 ± 3.0
135-trimethyl-Benzene							
3	251	0.045	0.042 (7%)	9.78 (17%)	10.4 ± 1.8	11.6 ± 2.6	-1.7 ± 2.8
3	249	0.047	0.045 (11%)	12.8 (16%)	13.3 ± 2.1	14.0 ± 3.0	-1.1 ± 3.3
124-trimethyl-Benzene							
3	267	0.037	0.023 (5%)	7.14 (25%)	11.4 ± 2.9	6.6 ± 3.9	4.3 ± 4.3
3	269	0.041	0.028 (5%)	6.49 (25%)	9.3 ± 2.4	7.7 ± 3.2	1.7 ± 3.9
123-trimethyl-Benzene							
3	299	0.035	0.028 (13%)	12.0 (19%)	14.8 ± 3.0	13.4 ± 3.9	1.4 ± 4.4
3	297	0.044	0.033 (3%)	10.1 (15%)	13.3 ± 2.1	15.8 ± 3.3	-2.4 ± 4.3
Methanol							
3	287	0.816	0.027 (7%)	[d]			
3	289	2.29	0.087 (6%)	0.0695 (43%)	1.8 ± 0.8	0.2 ± 1.1	1.7 ± 1.2
3	285	7.64	0.316 (6%)	0.0564 (16%)	1.4 ± 0.2	0.5 ± 0.3	0.8 ± 0.4
Ethanol							
2	133	2.91	0.199 (9%)	0.0606 (16%)	0.9 ± 0.2	-0.2 ± 0.2	1.1 ± 0.2
2	138	3.01	0.193 (11%)	0.0552 (17%)	0.9 ± 0.2	-0.2 ± 0.2	1.0 ± 0.2
2	131	3.15	0.208 (7%)	0.0565 (14%)	0.9 ± 0.1	-0.2 ± 0.1	1.1 ± 0.2
Isopropanol							
2	148	3.63	0.466 (10%)	0.113 (10%)	0.9 ± 0.1	0.1 ± 0.1	0.8 ± 0.1
3	157	1.26	0.212 (17%)	0.0796 (67%)	0.5 ± 0.3	0.4 ± 0.7	0.1 ± 0.7
3	159	1.61	0.265 (7%)	0.0685 (61%)	0.4 ± 0.3	0.3 ± 0.3	0.1 ± 0.4
3	155	1.74	0.290 (9%)	0.135 (29%)	0.8 ± 0.2	0.3 ± 0.3	0.4 ± 0.3

Table 5 (continued)

Set	Run	Added (ppm)	Reacted (ppm)	Reactivity: Incremental (mol O_3-NO/ mol added)	Reactivity: Mechanistic (mol O_3-NO/mol reacted) Overall	Radical	Direct
Dimethyl Ether							
3	283	2.10	0.206 (8%)	0.159 (20%)	1.6 ± 0.4	-0.4 ± 0.4	2.0 ± 0.5
3	295	2.12	0.197 (5%)	0.126 (25%)	1.4 ± 0.3	-0.3 ± 0.5	1.7 ± 0.5
3	281	3.41	0.326 (6%)	0.117 (17%)	1.2 ± 0.2	-0.2 ± 0.3	1.5 ± 0.3
3	279	4.04	0.407 (7%)	0.130 (13%)	1.3 ± 0.2	0.0 ± 0.2	1.4 ± 0.3
MTBE							
2	120	2.04	0.108 (7%)	0.0610 (20%)	1.2 ± 0.3	-0.8 ± 0.3	2.0 ± 0.3
2	125	2.49	0.120 (10%)	0.0473 (22%)	1.0 ± 0.2	-1.0 ± 0.3	2.0 ± 0.3
2	127	2.51	0.115 (9%)	0.0626 (16%)	1.4 ± 0.2	-1.1 ± 0.3	2.5 ± 0.3
2	123	2.98	0.202 (6%)	0.104 (11%)	1.5 ± 0.2	-0.2 ± 0.2	1.8 ± 0.2
Ethoxyethanol							
3	175	0.401	0.178 (17%)	0.761 (23%)	1.7 ± 0.5	-0.3 ± 0.5	1.9 ± 0.6
3	171	0.730	0.342 (8%)	0.713 (13%)	1.5 ± 0.2	-0.2 ± 0.3	1.7 ± 0.3
3	163	0.859	0.480 (10%)	0.758 (25%)	1.4 ± 0.3	0.0 ± 0.4	1.3 ± 0.4
Carbitol							
3	169	0.412	0.239 (4%)	0.353 (46%)	0.6 ± 0.3	-1.5 ± 0.4	2.0 ± 0.3
3	166	0.503	0.289 (6%)	0.439 (31%)	0.8 ± 0.2	-1.4 ± 0.4	2.2 ± 0.3
3	173	0.946	0.365 (11%)	0.201 (35%)	0.5 ± 0.2	-1.3 ± 0.3	1.8 ± 0.3
Formaldehyde							
3	352	0.104	(0.078 [e])	2.37 (27%)	3.2 ± 0.9	3.9 ± 1.2	-0.6 ± 1.6
3	357	0.267	(0.209 [e])	1.35 (19%)	1.7 ± 0.3	2.9 ± 0.5	-1.0 ± 0.7
Acetaldehyde							
3	335	0.696	0.261 (7%)	0.226 (43%)	0.6 ± 0.3	-0.9 ± 0.4	1.6 ± 0.3
3	338	1.31	0.444 (8%)	0.113 (46%)	0.3 ± 0.2	-0.9 ± 0.2	1.3 ± 0.2
Acetone							
3	243	0.847	(0.010 [e])	[d]			
3	245	2.19	(0.028 [e])	0.0591 (52%)	4.5 ± 2.4	3.3 ± 3.7	0.5 ± 4.0
3	247	4.14	(0.058 [e])	0.0446 (36%)	3.2 ± 1.1	2.7 ± 1.6	0.5 ± 1.8
Hexamethyldisiloxane							
3	183	6.71	0.076 (17%)	-0.0579 (18%)	-5.1 ± 1.2	-6.3 ± 1.7	1.2 ± 0.9
3	179	9.13	0.064 (45%)	-0.0338 (22%)	-4.8 ± 2.4	-7.7 ± 3.8	2.2 ± 1.4
4	396	2.83	0.091 (14%)	-0.0757 (51%)	-2.3 ± 1.2	-3.7 ± 1.6	1.2 ± 1.2
4	391	3.99	0.072 (14%)	-0.0822 (33%)	-4.6 ± 1.6	-6.6 ± 2.3	1.9 ± 1.3
Octamethylcyclotetrasiloxane							
3	194	2.15	0.032 (19%)	-0.150 (25%)	-10.2 ± 2.9	-11.7 ± 3.7	1.9 ± 2.3
3	185	4.31	0.048 (21%)	-0.0731 (22%)	-6.5 ± 2.0	-7.3 ± 2.5	0.5 ± 1.4
3	181	10.08	0.024 (63%)	-0.0419 (16%)	-17.7 ±11.5	-23.5 ±15.5	5.4 ± 4.4
4	406	1.35	0.037 (6%)	-0.152 (53%)	-5.5 ± 2.9	-7.6 ± 3.8	1.8 ± 3.0
4	402	1.77	0.044 (5%)	-0.154 (42%)	-6.3 ± 2.7	-7.2 ± 3.4	0.7 ± 2.6
4	398	2.62	0.008(100%)	-0.122 (35%)	-38.0 ±43.1	-72.1 ±80.2	33.1 ±37.4
Decamethylcyclopentasiloxane							
3	190	1.55	0.023 (18%)	-0.296 (16%)	-19.5 ± 4.7	-20.4 ± 5.7	1.7 ± 2.9
3	192	1.85	0.029 (21%)	-0.225 (22%)	-14.1 ± 3.8	-15.0 ± 4.6	1.4 ± 2.3
3	187	4.93	0.039 (27%)	-0.107 (13%)	-13.7 ± 4.1	-15.7 ± 5.0	2.5 ± 1.8
Pentamethyldisiloxanol							
3	412	0.712	0.036 (5%)	-0.202 (48%)	-4.0 ± 2.0	-1.4 ± 2.6	-2.6 ± 2.4
3	409	2.17	0.075 (12%)	-0.132 (24%)	-3.8 ± 1.0	-3.1 ± 1.3	-0.8 ± 1.0
4	404	1.20	0.040 (6%)	-0.214 (38%)	-6.4 ± 2.4	-10.1 ± 3.8	3.4 ± 2.6
4	400	2.70	0.066 (11%)	-0.146 (30%)	-6.0 ± 1.9	-7.2 ± 2.4	1.1 ± 1.4

[a] Estimated using $MR^{indirect}[d(O_3\text{-NO})] \approx ConvR^{base}$ MR[IntOH] (Equation XVIII).
[b] MR^{direct} = ConvF. Calculated using Equation (XII).
[c] Data from this run appear to be anomalous and were not used for computing average reactivities. See text.
[d] Uncertainty is greater than magnitude of reactivity.
[e] The amounts of formaldehyde and acetone reacted could not be determined. The amounts reacted used to derive the mechanistic reactivities were estimated using model calculations of fractions reacted. The model calculations used the SAPRC-91 mechanism (with adjusted base ROG surrogate) as discussed in Section IV. Uncertainty estimates in mechanistic reactivities do not include uncertainty in amounts reacted.

At least two, and usually more, reactivity determinations were carried out for each VOC, though not all experiments provided useful data. This is because some experiments had insufficient test VOC added for its effect to be significantly above run-to-run variability. Because of this, data from only one useful experiment each are available for n-hexane and ethylbenzene.

As can be seen from the figures in Appendix A, the results of most of the experiments were reasonably consistent with each other given the experimental uncertainties and variabilities, with the exception of a CO run and several ethane, n-butane and propene runs. In the case of CO, the CO was not purified in the first run (ETC-414) carried out for that compound, and the resulting run had a theoretically unreasonable ConvF, presumably due to an anomalously high IntOH. The subsequent runs, where the CO was purified, gave lower IntOH reactivities and more reasonable ConvF values. In the case of ethane (see Figure A-1), three of the nine runs gave higher reactivities than the other runs, with run ETC-333 being clearly anomalous, having much higher initial reactivities than seen in the other runs or predicted by the model. This might be due to contamination by some reactive impurity in the ethane sample -- because of its low rate of reaction relatively large amounts of ethane (over 20 ppm in the case of the most anomalous run) have to be added to yield a useful reactivity measurement. In the case of n-butane (see Figure A-3), one run had an anomalously high IntOH reactivity, causing an anomalously high conversion factor and fraction reacted, and another had an anomalously high conversion factor, compared to the other seven runs carried out with this compound. In the case of propene (see Figure A-9) two of the Set 2 runs had 6-hour d(O_3-NO) reactivities which were about twice as high as indicated by the results of the two Set 1 runs or the Set 2 run with the most precise reactivity measurement. The two most anomalous ethane runs (ETC-332 and ETC-333) and the most anomalous n-butane run (ETC-53) were not used in computing the average reactivities for the purpose of evaluating model predictions, but the data from the other runs mentioned above were not rejected.

Reactivities with respect to IntOH derived for 2-chloromethyl-3-chlorobutene must be considered to be upper limits because of the evidence, discussed above, of significant Cl atom formation in the runs where more than trace amounts of this compound were added. However, given the relatively rapid rate of reaction of this compound with OH radicals compared to n-hexane, consumption of the chlorobutene by Cl atoms may be minor, and the IntOH and ConvR determinations may not be significantly in error. But since this cannot be quantified, these values must be considered to be suspect.

The runs with added benzene were somewhat unique in that these were the only runs where a "true" ozone maximum was observed. This can be seen on Figure 17, which gives concentration-time plots for ozone, NO, and uncorrected NO_2 for

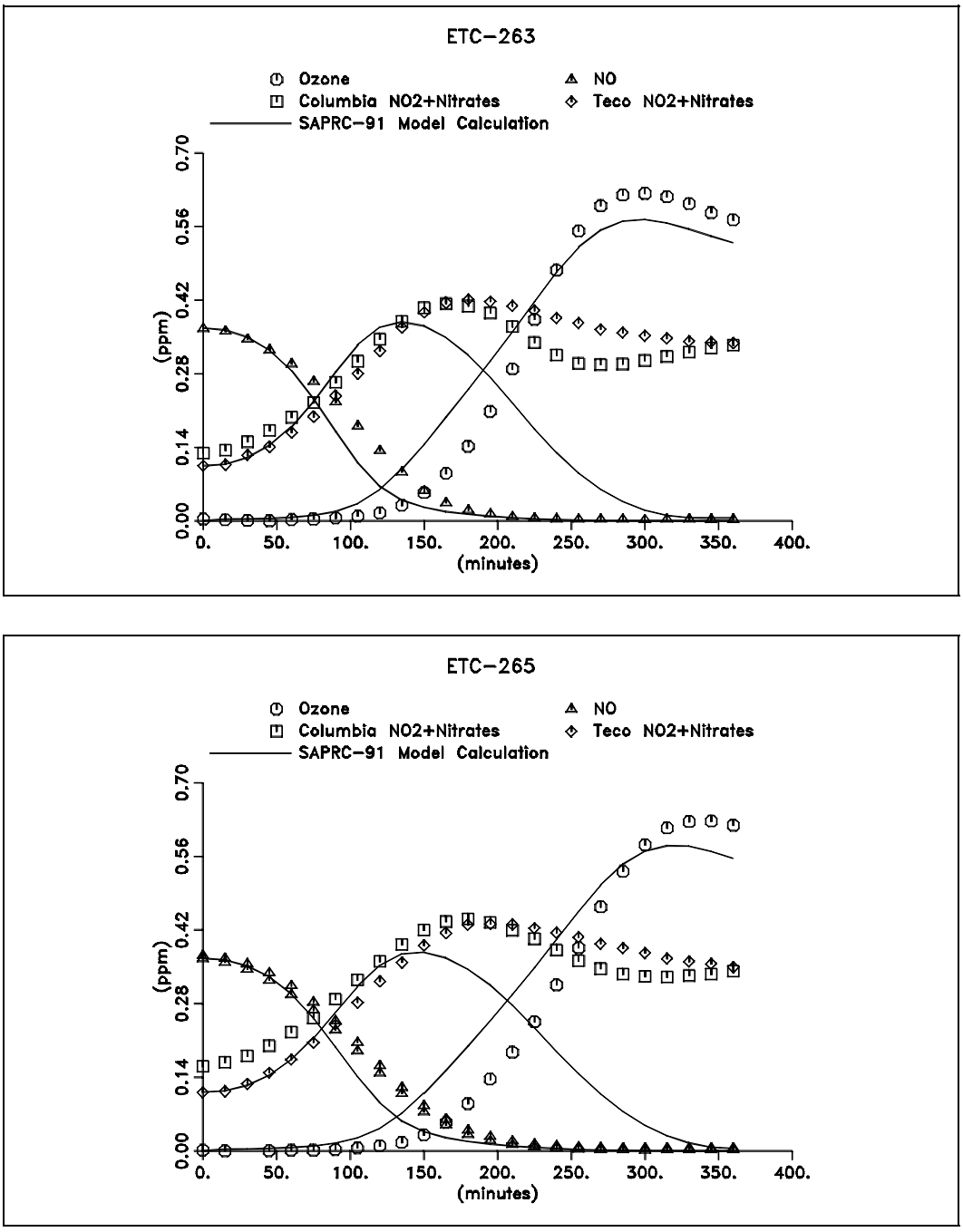

Figure 17. Concentration - time plots of ozone, NO, and NO_2 for the mini-surrogate runs where benzene was added. The experimental NO_2 data are not corrected for nitrate interferences. Results of model simulations using the SAPRC-91 mechanism (with the adjusted base m-xylene mechanism) are also shown.

the two added benzene runs. (The NO and uncorrected NO_2 data from both the Columbia and the Teco NO_x analyzers are shown.) The decline in the ozone concentration could be due either to NO_x being consumed, ending ozone formation (since NO_x is required for ozone formation), or to benzene forming some product which reacts with ozone in a manner which does not cause NO oxidation (and thus ozone regeneration). Note that the fact that the uncorrected NO_2 data do not give a good indication of whether NO_x is consumed, since the instrument also responds to organic nitrates and (non-quantitatively) HNO_3. However, the response of the Teco and Columbia to these interferences generally tend to differ, so the fact that they agree around the end of these runs suggests (though certainly does not prove) that significant amounts of NO_2 may still remain. On the other hand, the model calculation, which successfully predicts that ozone maxima occur in these experiments, predicts that most of the NO_2 is consumed, and thus that ozone formation is NO_x limited. If this is the case then the assumptions involved in the derivation of Equation (XVI) are not valid for these added benzene runs, and thus the reported ConvF is not a true indication of the actual amount of NO oxidized by the elementary reactions of benzene or its oxidation products. However, benzene was the only VOC studied where this was observed; for all other added VOC runs the production of ozone was still occurring at a significant rate at the end of the 6-hour runs, indicating that ozone formation is not NO_x limited in any of the other experiments.

The implications of these results concerning the atmospheric reactions and reactivities of these VOCs are discussed later in this report, after the results of the model simulations of these experiments are presented.

IV. MODEL SIMULATIONS

One of the primary objectives of this study is to provide data to test the ability of chemical mechanisms used in airshed models to correctly predict VOC reactivities. Although a complete mechanism evaluation and update using these data is beyond the scope of the present report, model calculations were carried out to determine the extent to which the predictions of the current (Carter, 1990) and a preliminary updated version (Carter, unpublished results) of the detailed SAPRC mechanism are consistent with these new data. The performance of this mechanism is of particular interest because it has been designed specifically for use in reactivity predictions, and it has been used to derive the reactivity adjustment factors incorporated in the California ARB's Clean Fuels/Low Emissions Vehicles regulations (CARB, 1991). The mechanisms and approach used to simulate the chamber experiments, and the results obtained, are discussed in this section.

A. Chemical Mechanisms

Two different versions of the SAPRC detailed mechanism were used in this study. The first, designated "SAPRC-90", is the mechanism which was used to derive factors adopted by the CARB (1991), and is a slightly updated and expanded version of the Carter (1990) mechanism. The second, designated "SAPRC-91" for the purpose of this discussion, is a preliminary updated version of the SAPRC-90 mechanism, incorporating corrections concerning formaldehyde photolysis and the kinetics of PAN formation. In addition, representations for carbitol, ethoxyethanol, 2-chloromethyl-3-chloropropene and preliminary representations for the siloxanes were added to the mechanism, as discussed in the following sections.

1. The SAPRC-90 Mechanism

The mechanism designated "SAPRC-90" is documented by Carter (1990) and the updates to it concerning ethanol, dimethyl ether, MTBE and ETBE are documented by Carter (1991). This mechanism was evaluated extensively against chamber data (Carter and Lurmann, 1991), though the presently available data are sufficient for evaluating reactivity predictions for only a few VOCs. This mechanism was used to calculate the reactivity scales given by Carter (1991).

Prior to calculating the reactivity scale for the ARB's regulations, the ARB contracted Gery to conduct a review of the SAPRC-90 mechanism, and he made

some suggestions for updates (Gery, 1991), and we also re-reviewed this mechanism during that time period, and found some needs for corrections and updates. Some of the recommended updates could not be implemented in the time required by the CARB for the reactivity scale because they required a complete reevaluation of the mechanism against the chamber data, but updates concerning representations of individual VOCs whose mechanisms are not well tested by the available chamber data could be implemented. The updates and corrections made to the SAPRC-90 mechanisms prior to the calculation of the reactivity scale for the ARB, and the calculations described in this report, are as follows:

- A minor error found by Gery (1991) in the computer algorithm for computing mechanistic parameters for branched alkanes was corrected.

- Several additional classes of representative alkanes were added based on Gery's suggestions.

- Errors found in assignments for 2-butanol and isobutyl alcohol were corrected.

- The rate constants for the reactions of NO_3 radicals with the alkenes were updated so they were consistent with the results of Atkinson's recent review (Atkinson, 1991a).

- The method used for representing the cycloalkene reactions was modified so their ozone reactions would be predicted to have the same yields of radicals and fragmentation products as other internal alkenes.

These changes did not require reevaluation of the mechanism because either there were no experiments involving the affected VOCs in the SAPRC-90 evaluation data base (Carter and Lurmann, 1991), or the rate constant changes had no significant affect on the results of the evaluation simulations. A number of simulations of the evaluation experiments were conducted to verify this, and to assure errors were not introduced when these modifications were implemented.

2. The SAPRC-91 Mechanism

The mechanism designated "SAPRC-91" is the same as the SAPRC-90 mechanism except that it has been updated to incorporate recent data concerning formaldehyde photolysis and the kinetics of PAN formation. The aromatics mechanism was modified slightly and reoptimized, but no changes were made in the representations of any of the other VOCs. The specific updates and modifications are as follows:

(1) The formaldehyde absorption cross-sections were updated based on the recent data of Cantrell et al. (1990) and Rogers (1989). The data of Cantrell et al. (1990) was used for wavelength above 300 nm, while those of Rogers (1989) were used for the lower wavelengths for which Cantrell et al. (1990) had no data. These yield somewhat higher formaldehyde photolysis rates than the Carter (1990) mechanism, which used averages of the data of Bass et al. (1980) and Moortgat et al. (1983). The newer data indicate that the lower values of Bass et al. (1980) are probably incorrect. The recommendation to use the Cantrell et al. (1990) cross sections will be incorporated in the upcoming IUPAC data evaluation (Atkinson, personal communication, 1992).

(2) The kinetics for the reactions of the acetyl peroxy radical with NO and NO_2, which are involved in the formation and decomposition of PAN, and the kinetics of the thermal decomposition of PAN, were updated based on recent experimental results of Tuazon et al. (1991a) and Bridier et al. (1991). This will also be incorporated in the IUPAC data evaluation (Atkinson, personal communication, 1992). This modification causes the model to predict somewhat higher ozone formation rates than the 1990 mechanism.

(3) The SAPRC mechanisms for aromatic hydrocarbons uses two highly photoreactive model species, designated "AFG1" and "AFG2", to account for the fact that the reactivities of these compounds are higher than can be attributed to known aromatic products. The yields and photolysis rates of these compounds are adjusted based on simulations of aromatic - NO_x - air chamber experiments carried out using different light sources (Carter 1990). The changes to the PAN kinetics affected the results of simulations of the chamber runs used to optimize the aromatic mechanisms, so this change necessitated re-optimizing these parameters. Since the aromatics mechanism had to be reoptimized in any case, we used this opportunity to make the spectral response (absorption cross section, quantum yield product) of AFG1 and AFG2 more chemically reasonable. These are discussed below.

The SAPRC-90 mechanism used a somewhat arbitrary spectral response function which was derived to be the simplest possible representation which fit the data from chambers using different light sources. Some features of this response function gave Gery (1990) and Jeffries and Crouse (1991) concerns that it might not accurately extrapolate to ambient lighting conditions. However, we found that this spectral response function gives essentially equivalent changes in photolysis rates with light source as those calculated using the measured absorption cross sections of acrolein (Gardner et al., 1987), a compound with a structure much like what would be expected for aromatic fragmentation products. Since the spectral response function for acrolein is less arbitrary and more justifiable than the simplified adjusted function used in the SAPRC-90 mechanism, it was used for AFG1 and AFG2 in the SAPRC-92 mechanism. If we assume that AFG1

has quantum yields of 0.1 at all wavelengths and that AFG2 has quantum yields of 1, then their photolysis rates are calculated to closely corresponded to those in the previous mechanism, with the ratios of SAPRC-91/SAPRC-90 AFG photolysis rates being respectively 0.93, 0.97 and 0.88 for blacklight, xenon arc, and direct overhead sunlight irradiation, respectively. Although this is still an arbitrary adjustment to fit chamber data, the use of absorption cross sections for a real compound, and one which might be chemically similar to the actual aromatic fragmentation products, makes this parameterization somewhat more chemically justifiable than it was previously.

The reoptimized AFG1 and AFG2 yields for the various classes of aromatics in the SAPRC-91 mechanism are given in Table 6, where they can be compared with the values from the previous mechanism. This change did not significantly affect the quality of the fits of model simulation to chamber experiments or ambient conditions, but as indicated above gives a more chemically reasonable model. The main factor causing the change in optimized AFG yields in the two mechanisms is the use of the new rate constants for PAN formation.

The updates concerning formaldehyde photolysis and PAN formation kinetics addressed the major areas which Gery (1991) regarded as "necessary updates" which could not be incorporated into the SAPRC-90 mechanism prior to the calculation of the reactivity scale for the CARB. These updates were not incorporated because a preliminary evaluation of this SAPRC-91 mechanism, using the same experiments and approach as used to evaluate the SAPRC-90 mechanism (Carter and Lurmann, 1991) showed that it gave a slightly worse performance in simulating the chamber data than did the previous mechanism. In particular, the SAPRC-90 mechanism had a slight (~15%) bias towards overpredicting maximum ozone yields in the surrogate mixture experiments, which Carter and Lurmann (1991) considered to be acceptable given the approximately 30% run-to-run variability in the overall model performance in fitting these chamber data. However, when the SAPRC-91 mechanism was used to simulate the same experiments (with the same chamber effects and chamber operations models), this positive bias increased to ~25%, which, though still less than the run to run variability, is no longer considered acceptable. This bias can probably be reduced by refining the various uncertain areas of the mechanisms, and/or by re-adjusting the parameters in the models for the various chamber effects and operating conditions which affect the simulations of chamber runs. This process takes time and has not been completed.

Because of this, the SAPRC-91 mechanism is considered to be preliminary and not yet suitable for use in modeling applications which will be applied to control strategy development. However, since it incorporates potentially important updates which are missing in the SAPRC-90 mechanism, it is of obvious interest to determine if it gives different reactivity predictions or is more consistent with these new chamber data.

Table 6. Optimized Aromatic Product Parameters in the SAPRC-90 and SAPRC-91 Mechanisms.

Parameter	Optimized Value SAPRC-90	SAPRC-91
100 x Photolysis Rates/k_1 [a]		
AFG1	0.86	0.23
AFG2	8.6	8.0
AFG2 from m-Xylene in Set 3 base ROG [b]	2.01	1.89
AFG1 Yields		
Benzene	0.49	1.75
AFG2 Yields		
Monoalkyl Benzenes	0.41	0.39
Dialkyl Benzenes	0.67	0.63
Trialkyl Benzenes	0.60	0.60
m-Xylene in Set 3 base ROG [b]	2.0	2.0

[a] Ratios of photolysis rate constants for AFG2 or AFG1 relative to the photolysis rate of NO_2 for the black-light light source used in the chamber. The ratios for direct overhead sunlight are approximately 65% of these.

[b] Adjustment to the mechanism for m-xylene in the base ROG surrogate used to improve fits of model simulations to the standard Set 3 mini-surrogate experiment. Not used for calculating m-xylene reactivity or for simulations of Set 1 or 2 experiments.

3. VOCs Added to the Mechanisms

Among the VOCs studied in this program are ethoxyethanol, carbitol, 2-chloromethyl-3-chloropropene and various siloxanes, which have not been previously incorporated in the SAPRC mechanisms. The mechanisms for the siloxanes are still under development (Carter et al., 1992), and a detailed discussion of these is beyond the scope of this report. However, new kinetic and mechanistic assignments were developed so that ethoxyethanol, carbitol, and the chlorobutene can be represented using the SAPRC-90 and SAPRC-91 mechanisms, so the predictions using these mechanisms can be compared with these new data. These assignments are discussed in this section.

a. Ethoxyethanol and Carbitol.

The data files developed for processing emissions for the SAPRC mechanisms included mechanistic assignments for ethoxyethanol and carbitol, but these assignments have not been documented, and have been updated and modified for this program. These compounds are both expected to be consumed primarily by reaction with OH radicals, and the kinetic data for these reactions are discussed above in Section III-A. As indicated there, the kOH used for ethoxyethanol in the updated mechanism is 2.36 x 10^{-11} cm^3 $molec^{-1}$ sec^{-1}, as reported by Hartmann et al. (1987), and confirmed by our data, and the kOH used for carbitol is 5.1 x 10^{-11} cm^3 $molec^{-1}$ sec^{-1}, as derived from our experiments.

The mechanisms for ethoxyethanol and carbitol can be estimated by using the estimation method of Atkinson (1987) to derive relative rates of reaction at various positions in the molecule, and by using analogies with known mechanisms for alcohols and ethers which have been studied. In the case of ethoxyethanol, the major initial reactions are expected to be as follows:

$$CH_2CH_2OCH_2CH_2OH + OH \dashrightarrow CH_3CH_2OCH_2\dot{C}HOH \quad (a)$$

$$\dashrightarrow CH_3CH_2O\dot{C}HCH_2OH \quad (b)$$

$$\dashrightarrow CH_3\dot{C}HOCH_2CH_2OH \quad (c)$$

with pathways (a), (b), and (c) estimated, using the method of Atkinson (1987) to occur 23%, 43%, and 33% of the time, respectively. (An estimated 1% reaction at the methyl group is neglected). The subsequent reaction expected following pathway (a) is analogous to that seen for other alcohols (Carter and Atkinson, 1985 and references therein), i.e.,

$$CH_3CH_2OCH_2\dot{C}HOH \xrightarrow{O_2} CH_3CH_2OCH_2\overset{O}{\overset{\|}{C}}H$$

The reactions of the radicals formed in pathways (b) and (c) can be estimated by analogy with the mechanism for diethyl ether (Wallington and Japar, 1991), where similar radicals are formed. In the case of (b), the expected reactions are,

$$CH_3CH_2O\dot{C}HCH_2OH \xrightarrow{O_2} CH_3CH_2O\overset{OO\cdot}{\overset{|}{C}}HCH_2OH \xrightarrow[NO_2]{NO} CH_3CH_2O\overset{O\cdot}{\overset{|}{C}}HCH_2OH \dashrightarrow$$

$$\dashrightarrow CH_3CH_2O\overset{O}{\overset{\|}{C}}H + \cdot CH_2OH \xrightarrow{O_2} CH_3CH_2O\overset{O}{\overset{\|}{C}}H + H\overset{O}{\overset{\|}{C}}H + HO_2$$

and in the case of (c) the reactions are,

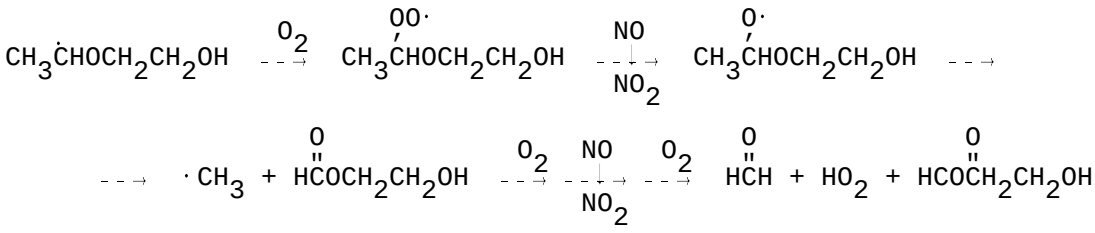

Isomerizations of the alkoxy radicals by 1,4-H migration are the most likely competing process which would complicate the mechanisms shown for (b) and (c). However, these are estimated to be unimportant in this system since the analogous reaction apparently does not occur in the diethyl ether case, and this can be rationalized by the fact that decomposition and the competing O_2 reactions are estimated to be more thermochemically favored for these ethers than is the case for the alkanes, where isomerization tends to be more important (see discussion in Atkinson and Carter, 1991). On the other hand, isomerization of the radical formed in Pathway (c) is expected to be thermochemically more favorable than the analogous process in the dimethyl ether system, so the possibility that isomerization is occurring in this case cannot be ruled out.

These pathways, and their estimated relative importance, can be combined and re-cast in terms of the radical "operators" in the SAPRC mechanism to yield the following overall process:

$$\begin{aligned} \text{OH + Ethoxyethanol} \longrightarrow\ & 0.76\ \text{HCHO} + 0.43\ CH_3CH_2OCHO \\ & + 0.33\ HOCH_2CH_2OCHO + 0.24\ CH_3CH_2OCH_2CHO \\ & + 0.75\ \text{RO2-R}\cdot + 0.24\ HO_2 + 0.33\ \text{R2O2}\cdot \end{aligned}$$

As discussed elsewhere (Carter, 1990), "RO2-R·" and "R2O2·" are "chemical operators" used to simplify the representation of reactions of VOCs in the SAPRC mechanism. The operator RO2-R· represents the effects of radicals which convert NO to NO_2 and generate HO_2, and R2O2· represents the extra NO to NO_2 conversions caused by multi-step mechanisms resulting from alkoxy radical decompositions or isomerization.

In the case of carbitol [2-(2-ethoxy)-ethoxy ethanol] the reactions are entirely analogous, though the system is more complex because the initial reaction can occur at five different positions in the molecule (again neglecting the minor reaction at the methyl group). These reactions, and the subsequent reactions expected for the radicals formed, are listed below. The relative percentages for the various pathways are derived using the estimation method of Atkinson (1987), and the subsequent reactions are analogous to those discussed above for ethoxyethanol.

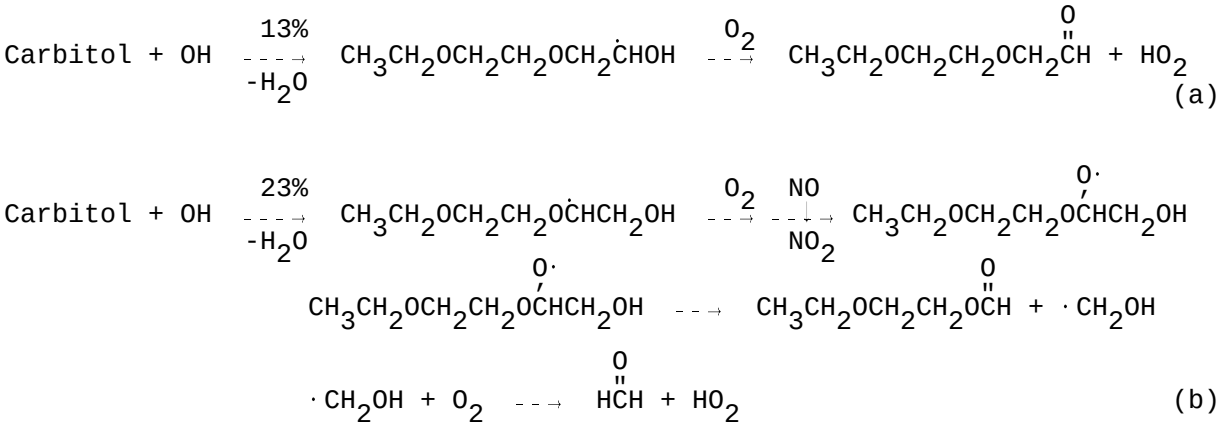

(a)

(b)

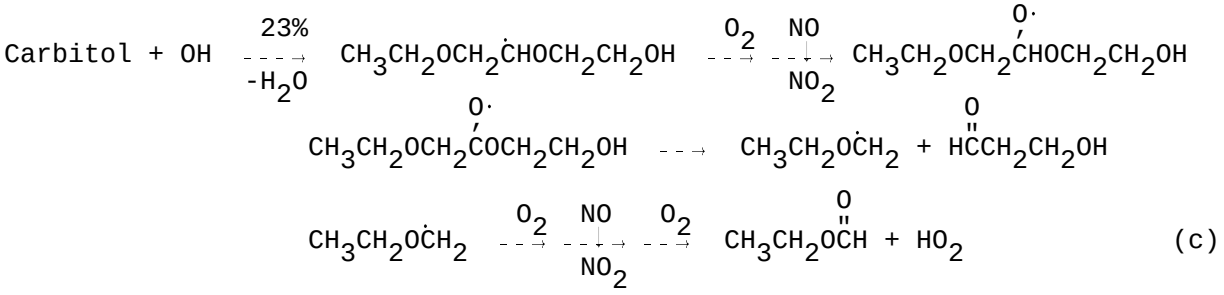

(c)

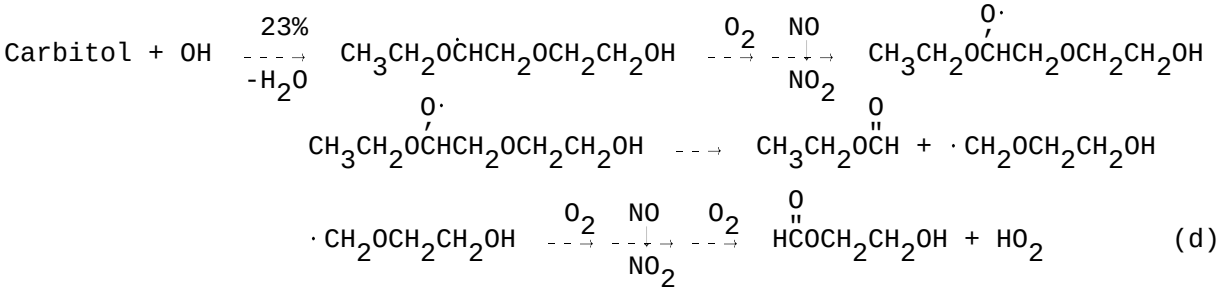

(d)

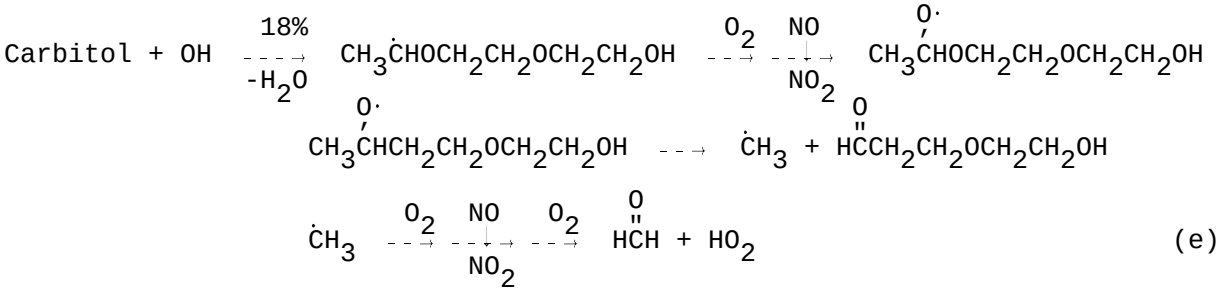

(e)

When combined and recast in terms of radical operators in the SAPRC mechanism, the above reactions yield the following overall process:

$$\text{Carbitol + OH} \dashrightarrow 0.41\ \text{HCHO} + 0.46\ CH_3CH_2OCHO + 0.46\ HOCH_2CH_2OCHO$$
$$+ 0.23\ CH_3CH_2OCH_2CH_2OCHO + 0.18\ HOCH_2CH_2OCH_2CH_2OCHO$$
$$+ 0.13\ CH_3CH_2OCH_2CH_2OCH_2CHO + 0.13\ HO_2 + 0.87\ \text{RO2-R}\cdot$$
$$+ 0.64\ \text{R2O2}\cdot$$

The SAPRC mechanism does not have explicit representations for the organic products predicted for the ethoxyethanol or carbitol reactions other than formaldehyde, and thus these products have to be represented by model species in the mechanism using the "surrogate species" approach. The approach used to represent alkane products in the SAPRC mechanism is to use "RCHO" (propionaldehyde) to represent all aldehydes which are formed, and MEK (methyl ethyl ketone) to represent the remaining C4+ oxygenated product carbon (Carter, 1990). (Although the SAPRC mechanism does not have any species designed to represent formates, MEK provides a closer approximation to their expected reactivities than any of the other product species in the mechanism.) Adopting the approach used for the alkane products for these two alcohol ethers, the overall processes written above can be represented in terms of the SAPRC model species as follows:

$$\text{OH + Ethoxyethanol} \dashrightarrow 0.76\ \text{HCHO} + 0.24\ \text{RCHO} + 0.63\ \text{MEK}$$
$$+ 0.24\ HO_2 + 0.76\ \text{RO2-R}\cdot + 0.33\ \text{R2O2}\cdot$$

$$\text{OH + Carbitol} \dashrightarrow 0.41\ \text{HCHO} + 0.13\ \text{RCHO} + 1.30\ \text{MEK}$$
$$+ 0.13\ HO_2 + 0.87\ \text{RO2-R}\cdot + 0.64\ \text{R2O2}\cdot$$

The above reactions do not include possible organic nitrate formation from the reactions of organic peroxy radicals with NO, which is an important factor affecting the reactivities of the higher molecular weight alkanes (Carter and Atkinson, 1985, 1989a, 1989b). In the case of the n-alkanes, the alkyl nitrate yield at room temperature increases monotonically from ~0% for C_1 up to ~35% for n-octane, with the nitrate yields tending to be lower in the branched alkanes (Carter and Atkinson, 1985; 1989b). There are no data concerning how the presence of O-atoms will affect the relative importance of the analogous reactions of the radicals formed in the alcohol ethers. Model simulations of effects of alternative assumptions in this regard were carried out to determine the nitrate yields which best fit the results of these experiments. The results of these simulations, and the ethoxyethanol and carbitol mechanisms which best fit these data, are discussed in Section IV-D, below.

b. 2-Chloromethyl-3-chloropropene.

Although the only purpose for conducting reactivity experiments with this compound was to assess its suitability as an OH radical tracer, it is of interest to determine if the SAPRC mechanisms can also predict the reactivity of this compound, which is the only chlorinated alkene studied. The SAPRC mechanisms represent reactions of alkenes with OH radicals, ozone, $O(^3P)$ atoms, and NO_3 radicals using the appropriate rate constants for the compound and a generalized reaction scheme based on the structure of the molecule. As discussed in Section III-A, above, the OH radical rate constant for this compound has been measured previously, but the most precise measurement is probably from this work, where a kOH of 3.16×10^{-11} cm^3 $molec^{-1}$ sec^{-1} was obtained. The ozone rate constant used was 3.9×10^{-19} cm^3 $molec^{-1}$ sec^{-1} (Tuazon et al., 1984). The rate constants for the $O(^3P)$ and NO_3 reactions have not been measured. Atkinson (personal communication, 1992) estimates the NO_3 rate constant to be $\sim 1 \times 10^{-15}$ cm^3 $molec^{-1}$ sec^{-1} based on the rate constant for NO_3 + allyl chloride (Atkinson, 1991a), and for preliminary modeling purposes we assume it has the same $O(^3P)$ rate constant as isobutene (Atkinson and Pitts, 1977), i.e., 1.5×10^{-11} cm^3 $molec^{-1}$ sec^{-1} at 300K.

We made no attempt to derive an explicit representation for this compound or account for any special effects on reactivity which might be caused by the presence of the chlorine atoms (other than their effects on the rate constants of the initial reactions). Therefore, the general method described by Carter (1990) for representing the alkene reactions based on its structure around the double bond was employed for this compound. Since this compound has the same structure around the double bond as isobutene, it was represented in the model as forming the same products as the model uses in the analogous reactions of isobutene.

B. Chamber Characterization Model

The testing of a chemical mechanism against environmental chamber results requires including in the model appropriate representations for chamber-dependent effects such as wall reactions and characteristics of the light source used during the experiments. The methods used to represent them in this study are based on those discussed in detail by Carter and Lurmann (1991), adapted for these specific sets of experiments as indicated below. Where possible, the parameters were derived based on analysis of results of characterization experiments carried out in conjunction with these runs. In cases where no data are available for this specific chamber, the parameters used by Carter and Lurmann (1991) for model simulations of runs carried out in the SAPRC ITC were used. The SAPRC ITC is similar in construction to the SAPRC ETC used for this study; both are indoor chambers consisting of 2-mil thick FEP Teflon reaction

bags with blacklight light source. The specific chamber-dependent parameters used in chamber model simulations for this study, and their derivations are as follows:

Light Characterization: The characterization of the light intensity, as measured by the NO_2 photolysis rate (k_1), was discussed in Section II-D, above. The spectral distribution of the blacklight light source was the same as that used by Carter and Lurmann (1990, 1991) for the SAPRC ITC, which has the same type of light source. Measurements of the spectral distribution of the ETC confirm that it is essentially the same as in the ITC.

Temperature: The average temperatures for these experiments are given on Table 3. The temperature also varied with time within an experiment, but was assumed to be constant at the average value in the model simulations.

Humidity: Unhumidified air was used in these experiments because it minimizes chamber effects and improves reproducability. Measurements made previously indicate the unhumidified output of the SAPRC pure air system typically has humidities of approximately 5%. This corresponds to approximately 5000 ppm of H_2O, which was used in the model simulations.

Initial Nitrous Acid: Nitrous acid (HONO) can sometimes be introduced into the chamber during NO_x injection (Carter and Lurmann, 1990, 1991), and if present can affect rates of NO oxidation at the beginning of the run because of its rapid photolysis to form OH radicals. As discussed above, HONO contamination was apparently occurring during the Set 1 experiments, and model simulations of tracer-NO_x-air runs ETC-46 and 47 indicated that 1.5% of the initial NO_2 is converted to HONO. Vacuum methods were used to inject NO_x into the chamber for the Sets 2 and 3 runs, and this procedure apparently resulted in significantly reduced initial HONO. Model simulations of the tracer-NO_x-air runs (e.g., ETC-112) are best fit if initial HONO is assumed to be negligible. This was assumed in simulations of all the Sets 2 and 3 experiments.

Continuous Chamber Radical Source: As discussed previously (Carter et al., 1982; Carter and Lurmann, 1990, 1991) there is a continuous chamber-dependent radical source which must be accounted for in model simulations of environmental chamber experiments. This can be determined by model simulations of radical tracer-NO_x-air experiments (Carter et al., 1982), or alkane-NO_x-air experiments. The simulations of the tracer-NO_x-air experiments ETC-46 and 47 were best fit by assuming an OH radical input rate of 0.12 ppb x k_1, and this was used in the model simulations of all the Set 1 runs. This is slightly lower than the range of radical input rates used for the SAPRC-ITC (Carter and Lurmann, 1991). However, results of other Set 1 characterization runs indicated that the initial HONO and continuous radical source was variable from run to run. The change in

NO_x injection procedure beginning with Set 2 apparently somehow also caused the continuous radical input rate to be reduced, since the tracer-NO_x-air run ETC-112 was fit by a relatively low rate of 0.02 ppb x k_1. This lower rate was assumed in simulations of all Set 2 and 3 experiments.

NO_x Offgasing Rate: A light-dependent offgasing of NO_x also occurs in environmental chamber experiments. The NO_x offgasing rate used in the simulations of these runs was 0.11 ppb x k_1. This is based on model simulations of a pure air irradiation carried out before these experiments were conducted. This parameter only affects simulations of low-NO_x experiments. Since relatively high levels of NO_x were employed in all experiments modeled in this study, this is not an important parameter in this case.

NO Conversion Due to Background VOCs. The effect of background organics is represented by a conversion of HO to HO_2 at a rate adjusted to fit pure air experiments (Carter and Lurmann, 1990, 1991). These simulations used the same rate as derived for the SAPRC ITC, or 250 min^{-1}. The simulations of the mini-surrogate runs are insensitive to this parameter.

Ozone Decay Rate: An ozone dark decay rate of 3.7 x 10^{-4} min^{-1}, measured in run ETC-42, was used for these experiments.

N_2O_5 Hydrolysis: The rate of the heterogeneous hydrolysis of N_2O_5 was not measured in this chamber. The same rate as used by Carter and Lurmann (1990, 1991) in modeling the ITC runs was used in modeling the ETC runs for this study. This process is of significance only in model simulations of runs where ozone formation stops because most of the initial NO_x was consumed, which was not the case for most of the experiments in this study.

Dilution: A dilution rate of 0.5 %/hour was used in the simulations of these experiments, derived as discussed above in Section III-A-1.

Carter and Lurmann (1990, 1991) should be consulted for details concerning how these chamber effects are represented in the model, and for a discussion of the uncertainties involved and their effects on model simulations.

C. Results of Model Simulations of Base Case Experiments, and Modifications to Base ROG Mechanism

Representative results of model simulations of base case experiments, using both the SAPRC-90 and the SAPRC-91 mechanisms, are shown in Figures 7-9, above. (The SAPRC-90 and SAPRC-91 mechanisms gave essentially the same results for the compounds plotted, so only one set of curves is shown for both.) The mechanisms

slightly overpredict the rates of reaction in the Set 1 run and slightly underpredict them in the set 2 run, but generally fit the results for these two sets to within the experimental variability. (The simulation of the Set 1 run could be made to fit if the initial nitrous acid is adjusted to within its variability; the simulation shown uses the default value derived from adjusting the model to fit a tracer - NO_x - air run, not the value which best fits the run shown.) However, the unadjusted model underpredicts the rates of reaction to a much larger extent in Set 3 standard runs, with the calculated six-hour ozone being only approximately half that which is experimentally observed for the representative run shown. The results of simulations of the other runs are similar. This discrepancy is outside the range of run to run variability, and no reasonable adjustment of uncertain chamber effects parameters significantly improves the results of the simulations. This indicates a problem in the base ROG mechanisms.

Although this discrepancy in the simulation of the Set 3 standard runs is not large in view of the overall performance of the mechanism in simulating individual chamber runs (Carter and Lurmann, 1991), it is of concern in this application because an error in simulating the base case experiment may introduce biases in predictions of effects of adding VOCs which may have nothing directly to do with errors in the mechanisms of the VOCs being tested. For example, if a test VOC has high reactivity because it reacts with ozone to form radicals, and the model underpredicts ozone in simulating the base case experiment, the contribution to reactivity due to this reaction will be underpredicted even if the mechanism used for the VOC is correct. The model must at least be able to simulate the overall features of the base case experiment to provide a useful test of whether it can correctly predict the reactivities of the added VOCs.

Of the three VOCs present in the base case experiment, m-xylene has by far the most uncertain mechanism, and test calculations show that its uncertainties have the greatest effect on the model simulations of these experiments. As discussed above, in order to simulate the relatively high reactivities observed for aromatics, the model must include the formation and reactions of unknown photoreactive ring fragmentation products whose yields and photolysis rates are adjusted to fit simulations of aromatic-NO_x-air runs (Carter, 1990). It was found that decreasing the photolysis rate of the unknown m-xylene fragmentation product AFG2 (Carter, 1990), and increasing its yield, significantly improved the results of the model simulations to the experiments. This is shown on Figure 9, where the dashed lines give the model predictions calculated using the reoptimized aromatics model. The adjusted parameter values which fit the Set 3 runs are given in Table 6.

Unfortunately, although this optimization improved the fits to the Set 3 runs, it resulted in overpredictions of reaction rates in simulations of the Set

1 and 2 runs, and exacerbated the tendency of the xylene mechanism to under-predict rates of ozone formation in xylene - NO_x - air irradiations carried out at high ROG/NO_x ratios. In other words, no single set of adjusted parameters for the xylene-NO_x-air mechanism yields acceptable fits to all the available experiments involving this compound.

Clearly the mechanisms for xylenes and other aromatics need to be improved so that the available experiments can be fit by a single mechanism. Updates to the aromatics mechanism are being investigated, but this process is not complete and a discussion of this is beyond the scope of this report. For this work, the model simulations of the Set 3 runs were carried out using the adjusted mechanism for m-xylene in the base ROG surrogate. The standard mechanism was used in the simulations of the Set 1 and 2 experiments, and also to represent the added m-xylene in the runs carried out to measure its reactivity. (In that case, the m-xylene added above the base case amount was represented using a different model species, which had the standard SAPRC-90 or SAPRC-91 m-xylene mechanism.) This approach was adopted to provide a means to assess model predictions of reactivity the Set 3 runs without the complications and biases which might result from errors in simulating the base case experiment. For comparison purposes, model simulations of Set 3 reactivity runs were also carried out using the unadjusted SAPRC-91 mechanism.

D. Model Simulations of Reactivity Experiments

Modeling the reactivity experiments consisted of simulating the effects of adding varying amounts of the test VOCs to calculations representing averaged conditions for each of the three sets of standard experiments. The initial reactant concentrations, temperature, and light intensity used in the simulations for each set were the averages of all the standard runs in the set. No attempt was made to simulate exactly the conditions of each individual experiment except for the amount of test VOC added. Although the run-to-run variations of conditions will affect the results of any given experiment, the effects of these variations on the reactivities (i.e., on the relative changes caused by adding the VOCs) is expected to be much smaller and is neglected in this analysis. Such an effect undoubtedly exists, but in most if not all cases they should be small compared to the experimental uncertainties of the reactivity measurements.

Unless noted otherwise, the SAPRC-90 and SAPRC-91 model calculations of reactivities in the Set 3 runs were carried out using the mechanism for the m-xylene in the Set 3 base ROG surrogate which was adjusted so the model would correctly simulate the base case experiments. Note that this adjustment does not affect simulations of Set 1 or 2 experiments, or in simulations of the added m-xylene in the experiments where the initial m-xylene was increased to assess

its reactivity. To show the effect of this adjustment on the calculated reactivities, simulations of the Set 3 reactivities were also carried out using the unadjusted SAPRC-91 mechanism. These are designated as "Set 3na" on the data tabulations and plots, and as the "unadjusted base xylene model" in the subsequent discussion.

Tables 7 - 9 show the overall performance of the SAPRC-90 and SAPRC-91 mechanisms in simulating the average experimental mechanistic reactivities for the VOCs, and the plots in Appendix A include plots of results of the SAPRC-91 model simulations, where they can be compared with the experimental data. Table 7 gives, for each VOC, the averages of the experimental 6-hour $d(O_3\text{-}NO)$ mechanistic reactivities weighed by the reciprocal square of the experimental uncertainties (excluding the anomalous runs discussed above), and the corresponding averages predicted by the SAPRC-90 and SAPRC-91 model calculations. Tables 8 and 9 give similar data for the 6-hour IntOH reactivities and the conversion factors, respectively. The weighting factor for the calculated results are the same as used for the experiments, to place them on a comparable basis. The "var" columns included with the model simulation results on Tables 7-9 give the variations in mechanistic reactivities calculated for the experiments with differing amounts of test VOC added. The plots in Appendix A show calculations for each run set where a run involving the VOC was carried out, but the run sets are shown separately on Table 7 only if the model predicts significant differences in reactivities among the run sets. Results of SAPRC-91 calculations for Set 3 runs are shown using both the adjusted ("Calc Set 3") and unadjusted ("Calc Set 3na") base xylene model, while the SAPRC-90 Set 3 calculations are shown only using the adjusted model.

For some VOCs results of additional calculations are shown on the plots in Appendix A. These are discussed in the appropriate sections below.

1. Results for VOCs with Adjusted or Modified Mechanisms

While the mechanisms for most VOCs were not changed in any way to fit these data, the mechanisms for several were modified or adjusted based on the simulations of these experiments, either because (in the cases of MTBE, ethoxyethanol and carbitol) these data are used in developing the mechanisms, or because (in the cases of isobutane or isooctane) the SAPRC mechanisms performed exceptionally poorly in simulating these experiments, and modifications were found which resulted in significant improvement. These are discussed in this section.

Table 7. Averages of the Experimental and Calculated 6-hour d(O_3-NO) Reactivities for All the VOCs studied.

Compound	Runs	d(O_3-NO) Mechanistic Reactivity (mol/mol C) [a]											
		Experimental		SAPRC-90 Calc			SAPRC-91 Calc			SAPRC-91 (na) Calc		
		Avg.	(Sdev.)	Avg.	(Var.)	(Fit.)	Avg.	(Var.)	(Fit.)	Avg.	(Var.)	(Fit.)
Carbon Monoxide	2	0.75	18%	0.46	0%	-39%	0.45	0%	-40%	0.52	1%	-31%
Ethane (Set 1)	5	0.67	36%	0.45	1%	-33%	0.50	1%	-25%	0.51	0%	-25%
(Set 2)	2	0.60	17%	0.48	0%	-20%	0.48	0%	-21%	0.53	0%	-12%
(Set 3)	1	0.41	27%	0.34	0%	-17%	0.37	0%	-10%	0.48	0%	15%
Propane	3	0.28	33%	0.23	5%	-18%	0.23	4%	-16%	0.29	5%	3%
n-Butane (Set 1)	4	0.21	20%	0.19	7%	-10%	0.21	5%	-2%	0.21	5%	-2%
(Set 2)	3	0.15	28%	0.15	1%	-1%	0.14	1%	-9%	0.17	1%	9%
(Set 3)	1	0.21	30%	0.07	0%	-68%	0.07	0%	-66%	0.12	0%	-44%
Isobutane [b]	4	0.27	25%	0.40	4%	51%	0.40	5%	50%	0.34	4%	27%
n-Hexane	2	-0.30	44%	-0.15	4%	50%	-0.17	4%	44%	-0.18	3%	38%
Isooctane [b]	2	0.07	35%	-0.15	3%	-0.22	-0.15	3%	-0.23	-0.10	2%	-0.17
n-Octane	2	-0.55	28%	-0.68	2%	-24%	-0.74	2%	-36%	-0.83	2%	-51%
Ethene	2	1.24	22%	0.82	3%	-34%	0.85	4%	-31%	1.08	4%	-13%
Propene	6	0.84	33%	0.60	4%	-29%	0.61	3%	-28%	0.66	4%	-21%
Isobutene	3	0.62	13%	0.39	1%	-37%	0.41	1%	-33%	0.48	0%	-22%
trans-2-Butene	2	1.35	19%	0.60	3%	-56%	0.71	3%	-47%	0.78	2%	-42%
Isoprene	4	0.76	11%	0.37	5%	-52%	0.44	5%	-42%	0.53	4%	-30%
Dichlorisobutene	3	1.29	13%	0.46	0%	-64%	0.49	0%	-62%	0.54	0%	-58%
Benzene	2	0.08	49%	0.08	18%	-6%	0.15	10%	84%	0.27	5%	0.18
Toluene	5	1.08	17%	0.70	2%	-35%	0.70	2%	-35%	0.75	2%	-31%
Ethylbenzene	3	0.74	44%	0.49	4%	-34%	0.52	5%	-30%	0.64	4%	-13%
o-Xylene	2	1.30	20%	0.77	0%	-40%	0.83	0%	-36%	1.03	0%	-21%
m-Xylene	4	1.06	37%	0.78	4%	-26%	0.83	5%	-22%	1.02	4%	-3%
p-Xylene	2	0.72	24%	0.75	1%	4%	0.80	1%	11%	0.99	1%	38%
135-tm-Benzene	2	1.29	17%	0.69	1%	-46%	0.75	1%	-42%	0.90	0%	-31%
124-tm-Benzene	2	1.13	21%	0.66	1%	-41%	0.72	1%	-37%	0.87	1%	-23%
123-tm-Benzene	2	1.53	13%	0.66	1%	-57%	0.71	2%	-53%	0.86	1%	-44%
Methanol	3	1.40	18%	1.09	0%	-22%	1.11	1%	-20%	1.35	0%	-3%
Ethanol	3	0.43	10%	0.35	0%	-19%	0.35	0%	-20%	0.40	0%	-9%
Isopropanol	4	0.26	24%	0.15	5%	-42%	0.15	5%	-42%	0.16	4%	-39%
Dimethyl Ether	4	0.66	13%	0.47	3%	-29%	0.46	3%	-30%	0.50	4%	-24%
MTBE [c]	4	0.26	19%	0.26	2%	2%	0.26	2%	3%	0.28	2%	8%
Ethoxyethanol [c]	3	0.38	14%	0.21	2%	-45%	0.37	2%	-3%	0.45	2%	20%
Carbitol [c]	3	0.10	28%	-0.28	21%	-0.38	0.10	14%	2%	0.15	10%	45%
Formaldehyde (IR) [d]	2	1.90	29%	2.22	18%	17%	2.27	20%	19%	2.57	12%	35%
Acetaldehyde	2	0.20	44%	0.11	4%	-47%	0.22	6%	11%	0.44	7%	0.24
Acetone (IR x 100) [d]	3	1.14	34%	1.73	12%	52%	1.87	13%	63%	2.19	11%	92%
MM Siloxane [d,e]	2	-0.84	22%									
D4 Cyclosiloxane [d,f]	3	-0.99	34%									
D5 Cyclosiloxane [d,g]	3	-1.54	22%									
Pentamethyldisiloxanol	2	-0.77	23%									

[a] Terms used: "Avg" = average for all runs, weighed by (Experimental Sdev)$^{-2}$. "Var" = standard deviation of calculated average. Indicates variation of calculated reactivity due to variation of amount of VOC added. "Fit" = [(calculated reactivity) - (experimental reactivity)]/(experimental reactivity). Given as percentage unless magnitude > 100%. "SAPRC-90 Calc", "SAPRC-90 Calc" = calculated using the SAPRC-90 or SAPRC-91 mechanism using adjusted base Xylene mechanism for Set 3 runs. "SAPRC-91 (na) Calc" = calculated using the SAPRC-91 mechanism with the base xylene mechanism not adjusted for Set 3 runs.
[b] Calculated using the standard mechanism. Much better fits are obtained if modified as discussed in the text.
[c] Mechanism adjusted to fit these data.
[d] Mechanistic reactivity could not be determined. Incremental reactivities are given.
[e] MM = Hexamethyldisiloxane
[f] D4 = Octomethylcyclotetrasiloxane.
[g] D5 = Decamethylcyclopentasiloxane.

Table 8. Averages of the Experimental and Calculated 6-hour IntOH Reactivities for All the VOCs studied.

Compound	Runs	IntOH Mechanistic Reactivity (ppt-min/ppmC) [a]											
		Experimental		SAPRC-90 Calc			SAPRC-91 Calc			SAPRC-91 (na) Calc			
		Avg.	(Sdev.)	Avg.	(Var.)	(Fit.)	Avg.	(Var.)	(Fit.)	Avg.	(Var.)	(Fit.)	
Carbon Monoxide	2	-4.	77%	-9.	1%	-5.	-9.	1%	-5.	-8.	3%	-92%	
Ethane	8	-10.	47%	-16.	2%	-56%	-15.	6%	-45%	-13.	8%	-33%	
Propane	3	-8.	31%	-10.	5%	-27%	-9.	5%	-23%	-8.	7%	-8%	
n-Butane	8	-9.	20%	-13.	9%	-41%	-13.	12%	-40%	-12.	9%	-34%	
Isobutane [b]	4	-6.	40%	-3.	7%	46%	-3.	7%	49%	-6.	8%	-5%	
n-Hexane	2	-23.	31%	-17.	0%	24%	-17.	0%	23%	-19.	0%	18%	
Isooctane [b]	2	-7.	32%	-14.	1%	-8.	-14.	1%	-8.	-13.	0%	-7.	
n-Octane	2	-25.	29%	-31.	1%	-21%	-32.	1%	-27%	-35.	1%	-40%	
Ethene	2	30.	33%	15.	2%	-50%	16.	3%	-46%	22.	2%	-27%	
Propene	6	17.	42%	9.	6%	-46%	10.	10%	-42%	11.	7%	-34%	
Isobutene	3	19.	14%	8.	3%	-55%	9.	2%	-50%	11.	4%	-41%	
t-2-Butene	2	32.	27%	16.	4%	-51%	19.	4%	-41%	21.	3%	-36%	
Isoprene	4	11.	24%	5.	7%	-53%	8.	8%	-33%	10.	5%	-13%	
Dichloroisobutene [c]	3	39.	19%	7.	0%	-83%	8.	0%	-81%	9.	0%	-76%	
Benzene	2	5.	33%	0.	0.	-92%	-1.	41%	-5.	2.	13%	-53%	
Toluene	5	32.	24%	19.	4%	-41%	19.	6%	-41%	21.	5%	-36%	
Ethylbenzene	3	4.	10.	13.	2%	9.	14.	3%	10.	17.	3%	13.	
o-Xylene	2	33.	38%	23.	0%	-31%	24.	0%	-27%	29.	0%	-11%	
m-Xylene	4	19.	61%	23.	3%	23%	25.	4%	30%	30.	3%	57%	
p-Xylene	2	19.	34%	22.	0%	17%	23.	0%	23%	29.	0%	50%	
135-tm-Benzene	2	42.	17%	22.	0%	-49%	23.	0%	-44%	27.	0%	-36%	
124-tm-Benzene	2	25.	34%	19.	0%	-22%	21.	0%	-16%	25.	0%	0%	
123-tm-Benzene	2	50.	17%	19.	1%	-62%	21.	1%	-59%	25.	1%	-51%	
Methanol	3	15.	62%	11.	0%	-29%	12.	1%	-21%	19.	0%	23%	
Ethanol	3	-4.	51%	-7.	0%	-77%	-7.	0%	-84%	-6.	0%	-44%	
Isopropanol	4	2.	52%	-4.	3%	-6.	-4.	3%	-6.	-4.	3%	-5.	
Dimethyl Ether	4	-3.	3.	-9.	5%	-6.	-9.	5%	-6.	-8.	8%	-6.	
MTBE [d]	4	-5.	66%	-4.	6%	14%	-4.	6%	17%	-4.	7%	23%	
Ethoxyethanol [d]	3	-1.	2.	-4.	9%	-2.	-1.	11%	50%	2.	5%	3.	
Carbitol [d]	3	-7.	14%	-20.	9%	-13.	-7.	7%	-6%	-6.	8%	9%	
Acetaldehyde	2	-14.	20%	-18.	3%	-33%	-14.	0%	-3%	-9.	4%	36%	
MM Siloxane [e]	2	-33.	23%										
D4 Siloxane [f]	3	-34.	39%										
D5 Siloxane [g]	3	-52.	22%										
Pentamethyldisiloxanol	2	-16.	49%										

[a] Terms used: "Avg" = average for all runs, weighed by (Experimental Sdev)$^{-2}$. "Var" = standard deviation of calculated average. Indicates variationof calculated reactivity due to variation of amount of VOC added. "Fit" = [(calculated reactivity) - (experimental reactivity)]/(experimentalreactivity). Given as percentage unless magnitude > 100%. "SAPRC-90 Calc","SAPRC-90 Calc" = calculated using the SAPRC-90 or SAPRC-91 mechanism using adjusted base Xylene mechanism for Set 3 runs. "SAPRC-91 (na) Calc" =calculated using the SAPRC-91 mechanism with the base xylene mechanism not adjusted for Set 3 runs.
[b] Calculated using the standard mechanism. Much better fits are obtained if modified as discussed in the text.
[c] Experimental IntOH reactivity may be high because of Cl atom interferences.
[d] Mechanism adjusted to fit these data.
[e] MM = Hexamethyldisiloxane
[f] D4 = Octomethylcyclotetrasiloxane.
[g] D5 = Decamethylcyclopentasiloxane.

Table 9. Averages of the Experimental and Calculated 6-hour Conversion Factors for All the VOCs studied.

Compound	Runs	Conversion Factor [a]											
		Experimental		SAPRC-90 Calc			SAPRC-91 Calc			SAPRC-91 (na) Calc			
		Avg.	(Sdev.)	Avg.	(Var.)	(Fit.)	Avg.	(Var.)	(Fit.)	Avg.	(Var.)	(Fit.)	
Carbon Monoxide	2	0.88	13%	0.75	0%	-15%	0.75	0%	-15%	0.77	0%	-13%	
Ethane	8	1.73	20%	1.76	2%	2%	1.78	2%	3%	1.78	2%	3%	
Propane	3	1.57	11%	1.65	1%	5%	1.65	1%	5%	1.67	1%	6%	
n-Butane	8	1.66	24%	2.06	3%	24%	2.08	3%	25%	2.08	3%	25%	
Isobutane [b]	4	1.91	16%	2.03	3%	6%	2.01	3%	5%	2.21	1%	16%	
n-Hexane	2	2.59	39%	2.53	0%	-2%	2.53	0%	-2%	2.55	0%	-2%	
Isooctane [b]	2	2.37	29%	2.65	0%	12%	2.65	0%	12%	2.66	0%	12%	
n-Octane	2	2.26	41%	2.72	0%	21%	2.71	0%	20%	2.66	0%	18%	
Ethene	2	0.59	0.71	0.66	6%	13%	0.63	7%	7%	0.74	6%	27%	
Propene	6	1.23	49%	1.02	11%	-17%	0.98	9%	-20%	1.03	11%	-16%	
Isobutene	3	-0.02	0.49	0.45	11%	0.47	0.41	12%	0.43	0.50	11%	0.52	
t-2-Butene	2	0.87	1.18	0.31	4%	-64%	0.27	5%	-69%	0.41	3%	-53%	
Isoprene	4	1.86	27%	0.93	3%	-50%	0.92	3%	-51%	1.01	2%	-46%	
Dichloroisobutene [c]	3	0.23	1.46	0.96	0%	0.73	0.93	0%	0.70	0.96	0%	0.74	
Benzene	2	-0.42	72%	0.38	3%	0.81	1.06	2%	1.49	1.16	2%	1.58	
Toluene	5	1.24	85%	1.19	15%	-4%	1.07	11%	-14%	1.23	18%	-1%	
Ethylbenzene	3	4.48	67%	0.40	18%	-91%	0.38	21%	-91%	0.67	11%	-85%	
o-Xylene	2	1.90	3.60	0.16	0%	-92%	0.13	0%	-93%	0.50	0%	-74%	
m-Xylene	4	2.92	3.45	-0.10	86%	-3.03	-0.16	61%	-3.08	0.25	41%	-91%	
p-Xylene	2	1.12	2.27	0.08	13%	-93%	0.04	26%	-96%	0.42	3%	-62%	
135-tm-Benzene	2	-1.45	2.16	-0.28	4%	81%	-0.39	3%	73%	0.11	13%	1.56	
124-tm-Benzene	2	2.86	3.19	0.20	6%	-93%	0.16	10%	-95%	0.54	2%	-81%	
123-tm-Benzene	2	-0.59	3.60	0.19	16%	0.79	0.15	24%	0.74	0.54	6%	1.13	
Methanol	3	0.93	48%	0.73	0%	-22%	0.71	1%	-24%	0.74	0%	-21%	
Ethanol	3	1.08	10%	1.09	0%	1%	1.11	0%	3%	1.11	0%	3%	
Isopropanol	4	0.68	33%	0.79	1%	16%	0.79	1%	16%	0.80	1%	17%	
Dimethyl Ether	4	1.51	18%	1.53	0%	1%	1.52	0%	1%	1.55	0%	3%	
MTBE [d]	4	2.01	14%	1.92	0%	-5%	1.91	0%	-5%	1.92	0%	-4%	
Ethoxyethanol [d]	3	1.62	18%	1.32	2%	-19%	1.55	2%	-5%	1.60	2%	-2%	
Carbitol [d]	3	1.96	12%	2.32	0%	18%	2.11	1%	8%	2.13	1%	8%	
Acetaldehyde	2	1.38	15%	1.44	2%	4%	1.41	2%	2%	1.46	3%	6%	
MM Siloxane [f]	2	1.51	58%										
D4 Siloxane [g]	3	1.18	1.75										
D5 Siloxane [h]	3	2.00	69%										
Pentamethyldisiloxanol	2	-1.11	1.15										

[a] Terms used: "Avg" = average for all runs, weighed by (Experimental Sdev)$^{-2}$. "Var" = standard deviation of calculated average. Indicates variation of calculated reactivity due to variation of amount of VOC added. "Fit" = [(calculated reactivity) - (experimental reactivity)]/(experimental reactivity). Given as percentage unless magnitude > 100%. "SAPRC-90 Calc", "SAPRC-90 Calc" = calculated using the SAPRC-90 or SAPRC-91 mechanism using adjusted base Xylene mechanism for Set 3 runs. "SAPRC-91 (na) Calc" = calculated using the SAPRC-91 mechanism with the base xylene mechanism not adjusted for Set 3 runs.
[b] Calculated using the standard mechanism. Much better fits are obtained if modified as discussed in the text.
[c] Experimental conversion factor may be low because of Cl atom interferences on IntOH determination.
[d] Mechanism adjusted to fit these data.
[e] Fractions reacted used to derive experimental ConvF were derived from SAPRC-91 model calculations.
[f] MM = Hexamethyldisiloxane
[g] D4 = Octomethylcyclotetrasiloxane.
[h] D5 = Decamethylcyclopentasiloxane.

a. Ethers

As discussed above, a major uncertainty in the photooxidation mechanisms for higher molecular weight ethers and alcohol ethers is the extent of organic nitrate formation from the reactions of NO with the intermediate O-substituted peroxy radicals formed. Product data on the NO_x-air reactions of the alkanes indicate that nitrate formation via this route becomes increasingly important as the size of the molecule increases (Carter and Atkinson, 1985, 1989b), and modeling indicates that this is an important factor affecting alkane reactivity (e.g., see Carter and Atkinson, 1989a). It reduces reactivity under maximum reactivity conditions because it is a radical terminating process, and reduces reactivity under maximum ozone or NO_x limited conditions because it also removes NO_x from the system (Carter, 1990). Most other aspects of the ether/alcohol ether photooxidation mechanisms can be estimated based on considerations such as discussed above in Section IV-A-3. However, beyond the fact that Tuazon et al. (1991b — see also Carter et al., 1991) observed IR bands attributed to unidentified nitrate(s) in an MTBE/NO_x product study, there are no data concerning the yields of organic nitrates from these compounds, and no basis for estimating these yields other than the yields from the photooxidations of the alkanes.

There are two ways nitrate yields for ethers and alcohol ethers can be estimated from those of alkanes. They can be assumed to be the same as the nitrate yield as the most closely corresponding alkane with the same number of carbons, or they can be derived from the corresponding alkane with the same approximate molecular weight (i.e., the same number of carbons as C's + O's in the ether). Table 10 shows these estimates for all the ethers and alcohol ethers studied in this program. The table also shows the nitrate yield for MTBE derived based on model simulations of these experiments which have been discussed previously (Carter et al., 1991). In the case of MTBE, the nitrate yield which fit these data is less than half that of the lower of the two estimates based on the alkanes, and 7.5 times lower than the higher estimate. This suggests that the nitrate should also be lower than the alkane estimates for the other ethers.

In the case of dimethyl ether, the "best fit" organic nitrate yield is zero, since the mechanism assuming this slightly underpredicts the reactivity of this compound (see Tables 7 and 8 and figure A-26). Assuming a nonzero organic nitrate yield will make this discrepancy worse. The effects of assuming either no nitrate formation or the lower of the two alkane estimates on the predicted 6-hour d(O_3-NO) and IntOH reactivities for ethoxyethanol and carbitol are shown on Figures 18 and 19, respectively. It can be seen that, consistent with the results with the other ethers, the estimates based on the alkane data cause

Table 10. Estimated and Adjusted Organic Nitrate Yields for All Ethers Studied in this Program.

Ether	Total Organic Nitrate Yield (%)		
	Best Fit Model	Estimated from Alkanes	
		Same C's	Same size
CH_3OCH_3	0 [a]	0	4
$(CH_3)_3COCH_3$	2 [b]	5	15
$HOCH_2CH_2OCH_2CH_3$	0	8	19
$HO(CH_2CH_2O)_2CH_2CH_3$	9	19	37

[a] The mechanism with no nitrate formation slightly overpredicts the reactivity of dimethyl ether.
[b] See Carter et al. (1991) for a discussion of the adjustments to the MTBE mechanism.

significant underprediction of the reactivities of these two compounds. Assuming no organic nitrate formation in the ethoxyethanol system gives good fits to these data, so Table 10 gives zero as the "best fit" nitrate yield for this compound. This is slightly lower than one would expect based on the modeling of the MTBE data. On the other hand, assuming no nitrate formation causes significant overprediction of the reactivity of carbitol, and the best fit to these data are obtained assuming a yield of ~9%. This is approximately half the yield in the "low" alkane estimate, as is the case with the MTBE model.

Based on these results, we conclude that it is reasonable to assume organic nitrate yields of respectively 0% and 9% in the representations of the reactions of ethoxyethanol and carbitol in airshed models. Combining these with the other estimates for the mechanism for these compounds discussed above in Section IV-A-3 gives rise to the following representations for ethoxyethanol and carbitol in terms of the model species in the SAPRC-90 and SAPRC-91 mechanisms:

$$\text{OH + Ethoxyethanol} \dashrightarrow 0.76\ \text{HCHO} + 0.24\ \text{RCHO} + 0.63\ \text{MEK} + 0.24\ HO_2 + 0.76\ \text{RO2-R}\cdot + 0.33\ \text{R2O2}\cdot$$

$$\text{OH + Carbitol} \dashrightarrow 0.37\ \text{HCHO} + 0.12\ \text{RCHO} + 1.18\ \text{MEK} + 0.12\ HO_2 + 0.79\ \text{RO2-R}\cdot + 0.58\ \text{R2O2}\cdot + 0.09\ \text{RO2-N}\cdot + 0.10\ \text{"lost carbon"},$$

Note that "RO2-N·" is the operator representing the formation of peroxy radicals which eventually react with NO and form organic nitrates. The model species used in the SAPRC mechanisms to represent organic nitrates has five carbons, and this is reflected in the "lost carbon" yield in the carbitol mechanisms. These

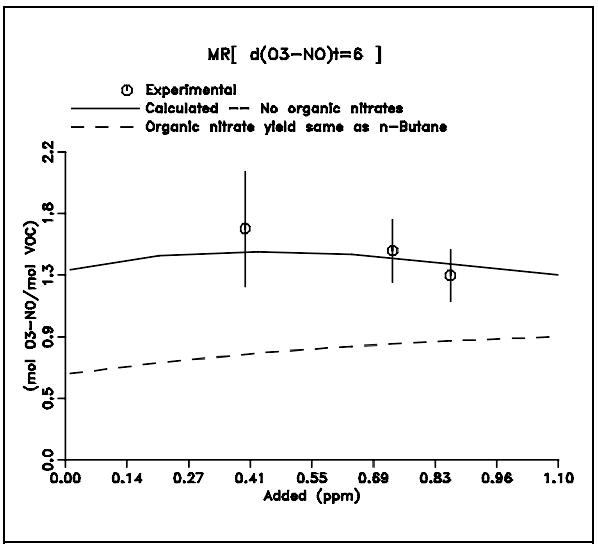

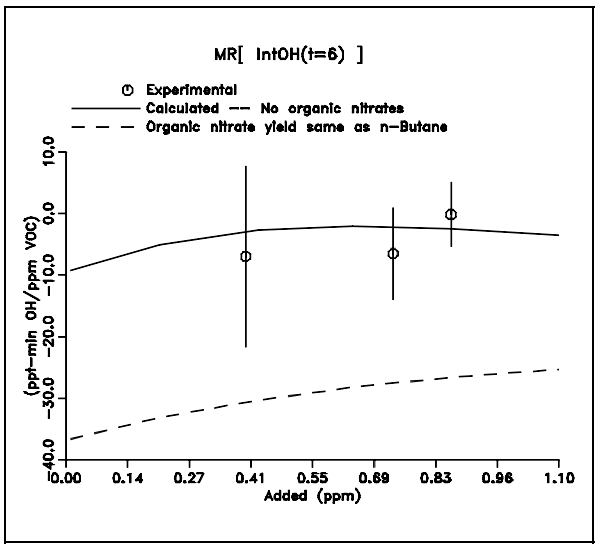

Figure 18. Plots of experimental and calculated 6-hour d(O_3-NO) and IntOH mechanistic reactivities against amount of VOC added for the ethoxyethanol experiments. The calculations show effects of two assumptions concerning organic nitrate yields from ethoxyethanol.

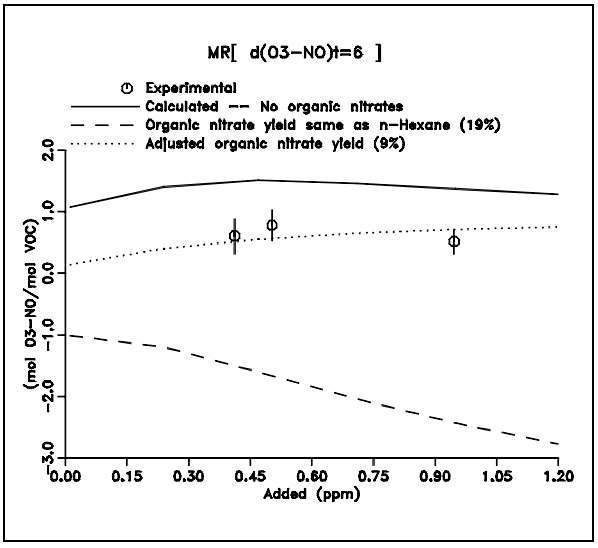

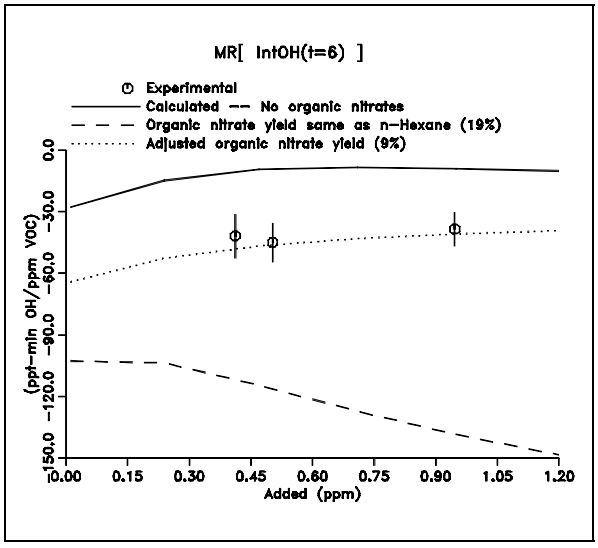

Figure 19. Plots of experimental and calculated 6-hour d(O_3-NO) and IntOH mechanistic reactivities against amount of VOC added for the carbitol experiments. The lines show effects of various assumptions concerning organic nitrate yields from carbitol.

representations have been incorporated in the SAPRC mechanism, and were used in the model simulations for these compounds shown on Table 10 and Figures A-28 and A-29.

b. Isobutane

Figures 20 and A-4 show that the isobutane reactivity predictions of the SAPRC mechanisms do not agree well with these data, particularly for the initial stages of the experiment. This can be attributed to radical termination from the reactions of alkoxy radicals with NO_2, which is neglected in the SAPRC mechanism because it is usually of negligible importance under atmospheric conditions, but may be important in this system. Although alkoxy radicals react with NO_2 with relatively high rate constants (Atkinson, 1990 and references therein) most alkoxy radicals also either react with O_2 or undergo unimolecular reactions at sufficiently rapid rates that the NO_2 reaction is of negligible importance under atmospheric conditions. Neglecting this reaction in the mechanism permits mathematical condensation approximations which remove the requirement to include alkoxy radical species in the model, significantly reducing the size and complexity of the model. Because of this, the approximation of neglecting alkoxy + NO_2 reactions is incorporated in almost all mechanisms used in airshed models, even the relatively detailed SAPRC (Carter, 1990) and RADM-2 (Stockwell et al., 1990) mechanisms.

However, this approximation breaks down in the case of isobutane reacting under the relatively high NO_x conditions of these experiments. OH radicals can react with isobutane at two positions, with the more important process, estimated (Atkinson, 1987) to occur 75% of the time, ultimately giving rise to 2-butoxy radicals in the presence of NO_x:

$$OH + \text{Isobutane} \xrightarrow[-H_2O]{25\%} (CH_3)_2\dot{C}HCH_2 \xrightarrow{O_2} \xrightarrow[NO_2]{NO} \xrightarrow{O_2} (CH_3)_2CHC(=O)H + HO_2$$

$$OH + \text{Isobutane} \xrightarrow[-H_2O]{75\%} (CH_3)_3C\cdot \xrightarrow{O_2} \xrightarrow[NO_2]{NO} (CH_3)_3CO\cdot$$

The t-butoxy radical lacks abstractable α- or δ- hydrogens, so the only process competing with the reaction with NO_2

$$(CH_3)_3O\cdot + NO_2 \xrightarrow{M} (CH_3)_3ONO_2$$

is decomposition:

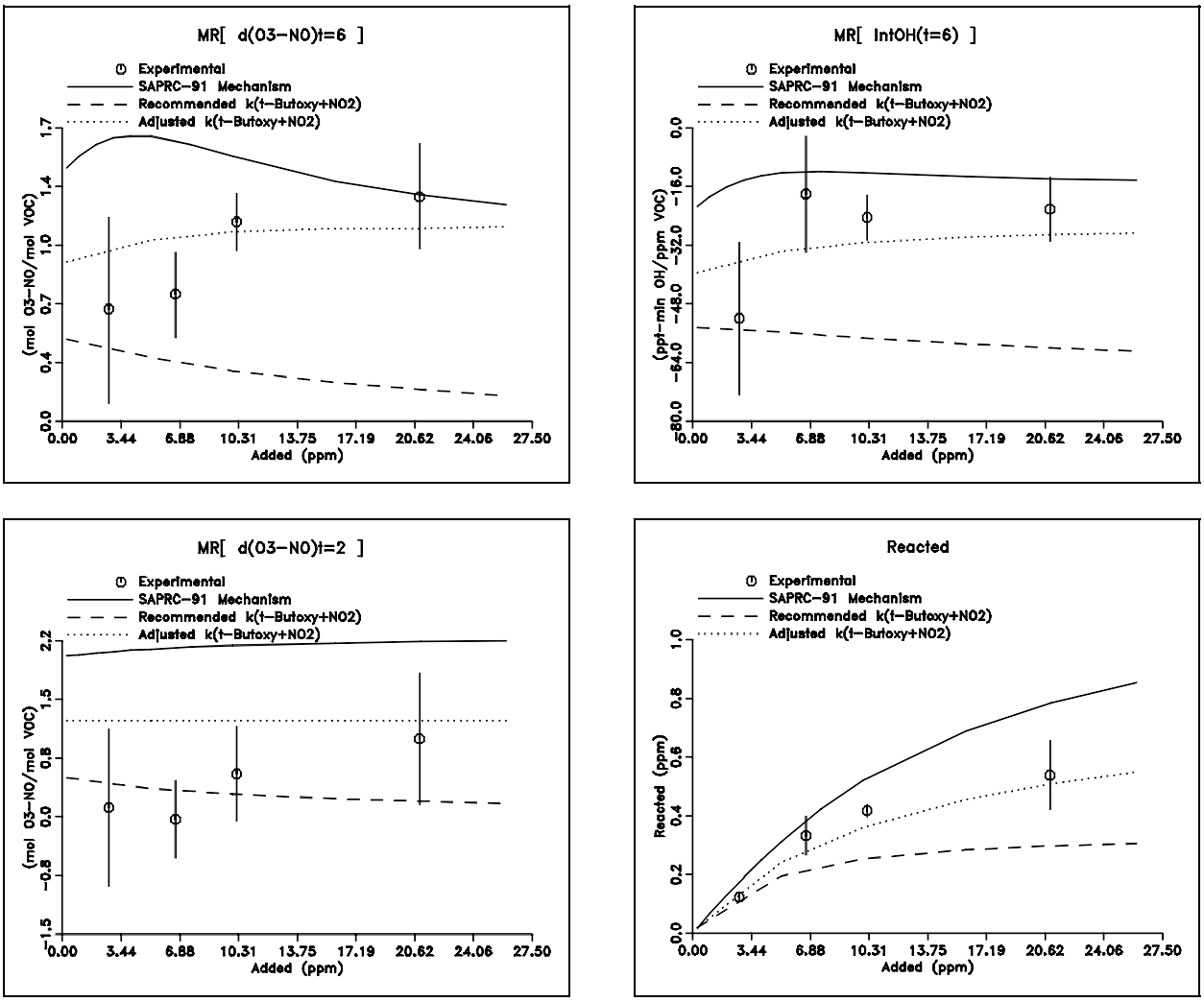

Figure 20. Plots of selected experimental and calculated reactivity results for isobutane. The adjusted t-butoxy + NO2 rate constant is a factor of 2 lower than the recommended estimate.

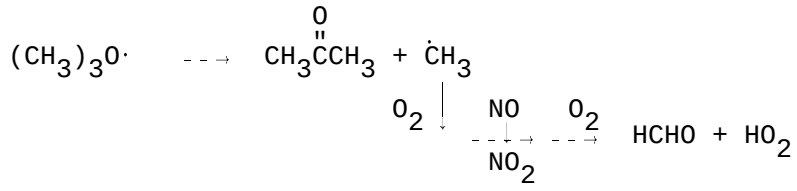

The representation of isobutane in the SAPRC mechanism in effect assumes that the decomposition (process b) dominates. However, the high pressure limit for the decomposition reaction is $1.1 \times 10^{+14}\ e^{-7519/T}$ cm^3 $molec^{-1}$ sec^{-1}, and at 298K RRKM calculations indicate that the atmospheric rate constant is 79% of the high pressure limit (Batt et al., 1989). The rate constant for the NO_2 reaction has not been

measured for isobutoxy radicals, but based on measurements for other alkoxy radicals, Atkinson (1992) estimates that it is 2.3 x 10^{-11} $e^{+150/T}$ cm^3 $molec^{-1}$ sec^{-1}. Under typical conditions of our experiments (301 K and [NO_2] = ~0.2 ppm), these rate constants predict that the NO_2 reaction will occur 12% of the time. This is not negligible for a radical termination process such as this.

Figure 20 shows the results of selected model simulations using the SAPRC-91 mechanism modified as discussed above to explicitly represent t-butoxy reactions, where they can be compared with the experimental results and the predictions of the unmodified mechanism. (All calculations use the adjusted base Xylene model appropriate for Set 3 runs.) This figure shows that using the modified model with the recommended rate constants significantly underpredicts the reactivity of isobutane. Thus, the experimental data suggest that while the t-butoxy + NO_2 reaction may not be negligible, it may not be as important as predicted using the recommended t-butoxy rate constants discussed above. Since the t-butoxy + NO_2 rate constant has not been measured directly but was estimated from reactions of other alkoxy radicals, it may not be inappropriate to adjust it slightly to improve fits to these data. Our data are best fit if it is assumed that this rate constant is one half its recommended value, as is shown by the "adjusted" model calculations shown on Figures 20 and A-4.

It is unclear whether a factor of 2 adjustment in the rate constant is within the acceptable uncertainty range for the t-butoxy + NO_2/decomposition rate constant ratio. However, until more direct data are available concerning this rate constant ratio, we adopt this adjustment in our "best estimate" model for the atmospheric reactions of isobutane.

c. Isooctane

The compound represented in the standard SAPRC mechanism where the model performed most poorly is isooctane (2,2,4-trimethyl pentane). As shown on Table 7 and Figure A-7, the model predicts that isooctane would have a significantly negative mechanistic reactivity with respect to 6-hour d(O_3-NO), while the measured reactivity is actually positive by about the same amount, and Table 8 shows that the model predicts that isooctane inhibits IntOH by approximately twice as much as observed experimentally. While there are no data directly concerning the reactions and products of this specific compound, there are sufficient data for related compounds to have allowed estimation techniques to be developed from which most aspects of its mechanism can be derived (Carter and Atkinson, 1985; Atkinson, 1987, 1990; Carter and Atkinson, 1989b). Because of this grossly unacceptable model performance, we examined the basis of the derivation of the mechanism for this compound to determine the possible source of this apparent failure of these estimation techniques.

The reason that the model predicts that isooctane is so negatively reactive is that it incorporates the estimate that alkyl nitrate formation from peroxy + NO reactions occurs ~18% of the time — a very significant fraction for a radical termination process. (An even larger fraction is estimated for n-octane, but in this case the model predictions are reasonably consistent with the data.) These estimates arise by utilizing the estimation methods of Atkinson (1987) to estimate ratios of reactions of the OH radical at various sites in the molecule to form the various possible peroxy radicals, then using the estimation methods of Carter and Atkinson (1989b) to determine the relative importance of alkyl nitrate formation from these peroxy radicals. (As discussed previously [Carter, 1990], we assume that alkyl nitrate formation occurs only from the initially formed peroxy radicals and not from those formed following 1,5-H shift isomerization based on model simulations of previous experiments, and indeed the discrepancy in this case would be even worse if this were not assumed.) The experimental data clearly indicate that the reactivity of isooctane is far less negative than this model predicts, which means that the overall nitrate yield from this compound must be significantly lower than the estimated 18%

Although there are no data concerning alkyl nitrate yields from isooctane or any of the specific peroxy radicals expected to be formed when it reacts, such data are available for a variety of other primary, secondary, and tertiary alkyl peroxy radicals. These data indicate that at a given temperature and pressure the alkyl nitrate yields depend on the number of carbon atoms in the radical and on whether the radical is primary, secondary or tertiary, but not to a large extent on whether the radical is branched or straight chain (Carter and Atkinson, 1985, 1989b). Most of the available data are for secondary radicals, and the empirical formula of Carter and Atkinson (1989b) predicts that C_8 secondary peroxy radicals react with NO to form C_8 nitrates 34% of the time at 300 K. The more limited data for primary and tertiary radicals indicate that they have significantly lower nitrate yields, and Carter and Atkinson (1989b) derived scaling factors of 0.4 ± 0.05 and 0.3 ± 0.15 for primary and tertiary peroxy radicals, respectively, relative to secondary radicals. This gives rise to 14% and 10% nitrate yields for primary and secondary C_8 peroxy radicals, respectively. This means that in the case of isooctane, which can form any of the three types of peroxy radicals depending on where the OH reacts, the predicted nitrate yield is critically dependent on the relative amount of secondary peroxy radical formation which can occur.

Secondary peroxy radicals can be formed only when OH reacts at the 3-position of the 2,2,4-trimethylpentane molecule, and thus the extent of reaction at this position is the critical parameter affecting predictions of its overall alkyl nitrate yields. The structure-reactivity analysis derived by Atkinson (1987) from OH radical rate constants for a wide variety of alkanes predicts that reaction at this position will occur approximately 30% of the time.

Reaction at the 4-position, yielding tertiary radicals is estimated to occur ~50% of the time, with the remaining 20% of the reaction being at a methyl group forming a primary radical. Although the secondary radical is estimated to be formed less than 1/3 the time, because of its high nitrate yield it accounts for over 1/2 the overall nitrate formation predicted for isooctane.

The structure-reactivity estimate of Atkinson (1987) for the rate of reaction at the 3-position is based primarily on OH radical rate constants for n-alkanes, where the radical has a relatively unhindered access to the abstracted hydrogen. On the other hand, the secondary hydrogens in the isooctane molecule are surrounded by three methyl groups on the neighboring carbons, so one would expect steric hinderance to inhibit, at least to some extent, reaction at this position. Although the extent to which these steric effects inhibit this reaction is unknown, it is reasonable to conclude -- independently of our chamber data -- that the 30% reaction at the 3-position is an overestimate.

To determine whether the model could be made consistent with our data if this steric effect were assumed to be significant, we derived an isooctane mechanism based on the assumption that the steric effect is sufficiently important that reaction at the 3-position, i.e., secondary radical formation, can be neglected. If this is assumed, then it is estimated that the tertiary radical is formed 71% of the time and that primary radicals are formed the remaining 29% of the time, giving rise to an estimated alkyl nitrate yield of 11%. If the other reactions of these radicals are estimated using the standard procedure for deriving alkane mechanisms in the SAPRC-90 model (Carter, 1990; Carter and Atkinson, 1985 — updated as discussed by Carter and Atkinson, 1989b and Carter, 1990), and the standard SAPRC-90 for representing alkane photooxidation products is adopted, then the resulting isooctane mechanism in terms of SAPRC model species is:

$$\text{OH + Isooctane} \dashrightarrow \begin{aligned} &0.89\ \text{RO2-R}\cdot + 0.11\ \text{RO2-N}\cdot + 0.79\ \text{R2O2}\cdot + \\ &0.89\ \text{RCHO} + 1.11\ \text{MEK} + 0.34\ \text{"lost C"}. \end{aligned}$$

Figure A-7 shows results of selected model simulations using the isooctane mechanism modified as discussed above, where they can be compared with the experimental results and the predictions of the standard mechanism. This new mechanism does a remarkably better job in simulating the data, fitting almost all the results to within the experimental uncertainty. Although this mechanism was not adjusted to fit these data in any way, it should be regarded as an adjusted mechanism since if it had overpredicted the reactivity of isooctane, we would have adjusted the fraction reacted at the 3-position (i.e., the relative importance of steric inhibition) to fit these data. The model assuming no reaction at the 3-position, i.e., very strong steric inhibition by the neighboring methyl groups, clearly fits these data the best.

d. Siloxanes

The mechanisms for the atmospheric reactions of the volatile siloxanes are unknown, but the results of these experiments indicate that they are strong radical inhibitors, since they have the most negative $d(O_3\text{-NO})$ and IntOH mechanistic reactivities of all the VOCs studied. These compounds are not represented in the current SAPRC90 or SAPRC91 mechanisms, so model simulations of their reactivity measurements are not shown here. A detailed discussion of possible atmospheric reaction mechanisms of siloxanes, including giving results of experiments carried out at lower NO_x concentrations and higher ROG/NO_x ratios, and showing results of model simulations of all the available siloxane reactivity experiments, is given elsewhere (Carter et al., 1992).

2. Results for Unadjusted Mechanisms

The mechanisms used for all the other VOCs were not adjusted based on these data, and thus these model simulations provide an independent test of the SAPRC mechanisms, and of the estimation techniques used to derive them. The ability of the model to simulate how reactivities depend on amount of VOC added or on reaction time can be seen from the plots in Appendix A, and from Tables 7-9, above. Tables 7-9 give summaries of the performance of the SAPRC-90 and of the two versions of the SAPRC-91 mechanisms in fitting the averages of the 6-hour reactivities from the various runs. The performance of the SAPRC-91 mechanism (with the adjusted base xylene mechanism used for the Set 3 runs) in fitting the averages of the 6-hour reactivities is shown graphically on Figures 21-23, which gives plots of calculated vs experimental 6-hour mechanistic reactivities for $d(O_3\text{-NO})$, IntOH, and the conversion factor, respectively.

The results show that in most cases the model predictions are not grossly inconsistent with these experiments. The model fits the data to within the experimental uncertainties for approximately half the VOCs, and generally predicts the observed reactivity trends. However, there are a number of cases where the model predictions are outside the estimated experimental uncertainty ranges. The implications of these results concerning the reliability of VOC reactivity predictions of current mechanisms are discussed in the following section.

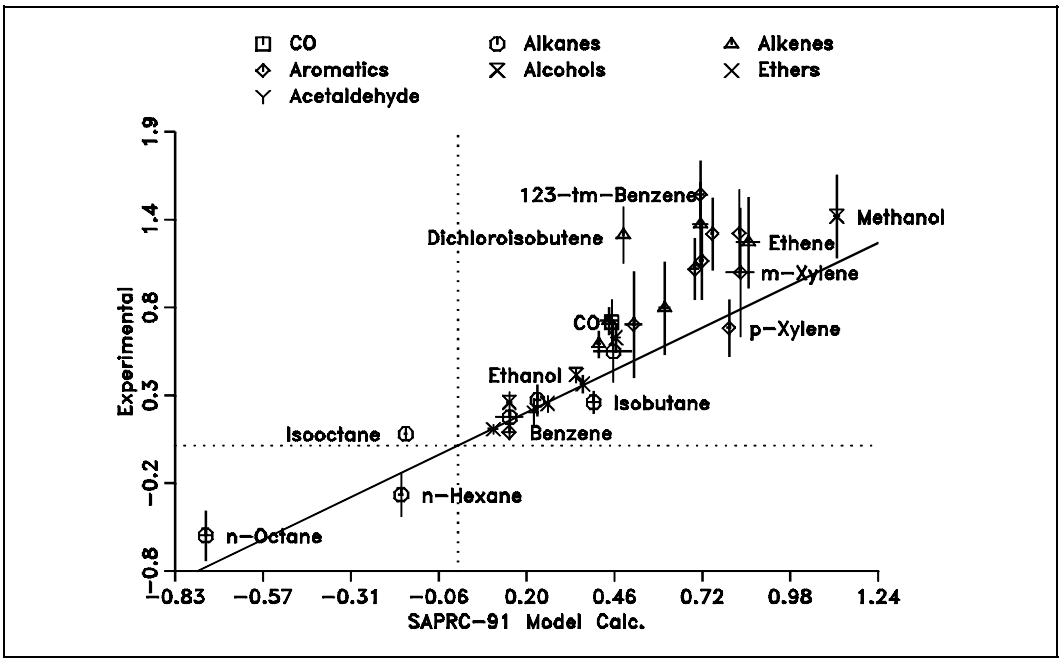

Figure 21. Plot of averages of the experimental 6-hour d(O3-NO) mechanistic reactivities against averages of results of model simulations of the experiments using the SAPRC-91 mechanism. (Units are ppm O3-NO per ppmC VOC reacted.)

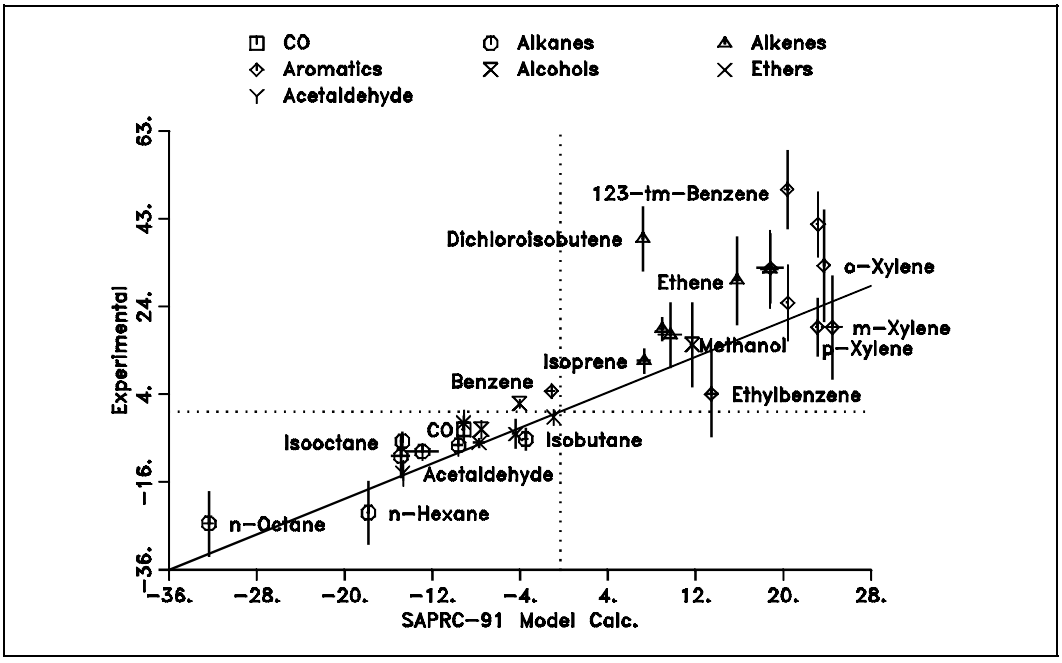

Figure 22. Plot of averages of the experimental 6-hour IntOH mechanistic reactivities against averages of results of model simulations of the experiments using the SAPRC-91 mechanism. (Units are ppb-min IntOH per ppmC VOC reacted.)

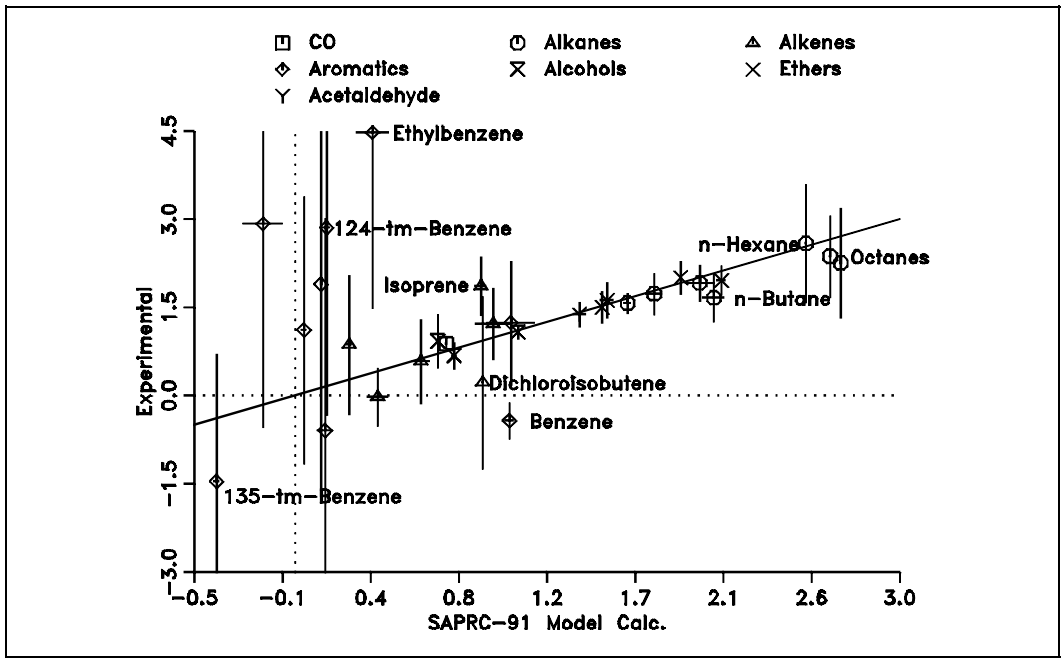

Figure 23. Plot of averages of experimental 6-hour Conversion Factors against averages of results of model simulations of the experiments using the SAPRC-91 mechanism.

V. DISCUSSION

A. General Reactivity Trends

The results of these experiments are consistent with previous experimental (Carter and Atkinson, 1982) and computer modeling (e.g., Dodge, 1984; Carter and Atkinson, 1989a; Chang and Rudy, 1990; Carter, 1991) results in showing that different VOCs have significantly different effects on ozone formation, even after differences in reaction rates are taken into account (Carter and Atkinson, 1989a; Carter, 1991). The measure which has the most direct relationship to the effect of a VOC's reactions on ozone formation is its mechanistic reactivity with respect to d(O_3-NO). This quantity, expressed as moles O_3 formed + NO oxidized per mole carbon reacted, ranges from a high of approximately 1.5 for 1,3,5-trimethylbenzene, formaldehyde, and acetone to lows of -1 to -1.5 for the siloxanes (see Table 7). Other compounds found to have high mechanistic reactivities on a per carbon basis were ethane, all the alkenes, all the other alkylbenzenes (but not benzene itself), methanol and dimethyl ether. These are the compounds which cause the most ozone formation once they react. Propane, n-butane, isobutane, isooctane, benzene, acetaldehyde, and the C3+ alcohols and ethers also promote ozone formation, but with much less efficiency, with the efficiency being lowest for isooctane, benzene and carbitol. The C6+ n-alkanes and the siloxanes inhibit NO oxidation and ozone formation in our experiments.

The processes by which VOCs promote or inhibit ozone formation are complex and involve the interaction of a number of factors. VOCs promote ozone formation by reacting to form peroxy radicals which react to oxidize NO and shift the NO, NO_2, ozone photostationary state towards higher ozone levels. The maximum amount of ozone formation which can be directly caused by a VOC's reactions is the amount of NO it oxidizes when it reacts. However, VOCs also affect ozone formation indirectly, by affecting how much ozone is formed from the reactions of all other VOCs. If the reactions of a VOC enhances or inhibits overall radical levels, it would affect how rapidly all VOCs present react and form ozone. This is important in affecting maximum reactivities for VOCs, since these reflect primarily how a VOC affects ozone formation rates (Carter, 1991). The presence of NO_x is required for ozone formation to occur, and if the reactions of a VOC enhance the rate of removal of NO_x from the system, it will reduce the maximum ozone formation potential from reactions of all VOCs. This affects reactivities only when ozone is NO_x limited, which is not the case for the experiments discussed here.

The measurements of conversion factors provide an indication of the amount of ozone formation caused directly by the reaction of the VOCs, independently (to a first approximation) of how the VOC's reactions affect the reactions of other VOCs. Unfortunately, experimental uncertainties tend to dominate the derivation of this quantity for compounds with large positive reactivities with respect to radical levels, and the conversion factors derived for the alkylbenzenes have high uncertainties and are probably not particularly meaningful. Also the assumption that the VOC is not affecting ratios of amounts of ozone directly formed to amounts of ROG reacted for the base ROG components may break down when the test VOC has a large effect on the radicals in the system, because the test VOC would also have a large effect on the extent of reaction of the base ROG components. This assumption is clearly not valid for the added benzene runs, where ozone is apparently NO_x limited. However, useful information concerning conversion factors were obtained for the alkanes, alcohols, and ethers. In most (but not all) cases, the results were consistent with our understanding of the atmospheric reactions of these VOCs.

For example, the major processes consuming both ethane and ethanol involve formation of acetaldehyde, but two NO to NO_2 conversions are involved in the ethane mechanism, while only one is involved for ethanol (excluding the estimated 10% reaction at the methyl group):

$$OH + C_2H_6 \xrightarrow[-H_2O]{O_2} C_2H_5OO\cdot \xrightarrow[NO_2]{NO} C_2H_5O\cdot \xrightarrow[CH_3CHO]{O_2} HO_2 \xrightarrow[NO_2]{NO} OH$$

$$OH + C_2H_5OH \xrightarrow[-H_2O]{} CH_3\dot{C}HOH \xrightarrow[CH_3CHO]{O_2} HO_2 \xrightarrow[NO_2]{NO} OH$$

Thus, the expected conversion factors are 2 for ethane and 1 ethanol. These are consistent with the observed values of 1.7 $\pm$ 0.3 and 1.0 $\pm$ 0.1, respectively. The other alcohols are expected to have similar mechanisms as ethanol, and indeed they also have relatively low conversion factors compared to the alkanes. CO is also expected to have a conversion factor of ~1, and this is indeed what is observed (except for the experiment where the CO was not purified). The factors for the alkanes are in the 1.5 - 2.5 range, tending to increase with the size of the molecule. The higher alkanes have the highest conversion factors of all the VOCs studied. This is expected because higher alkanes have an increased tendency to have alkoxy radical decompositions and isomerization which cause multi-step mechanisms involving additional NO oxidations.

Formaldehyde and benzene are unusual in that their conversion factors are measured to be negative even after the uncertainties are taken into account. In the case of benzene, this result is probably largely due to the fact that the benzene runs appear to be NO_x limited, unlike the runs with any of the other

added VOCs. Under NO_x limited conditions the assumptions involved in deriving ConvF from our data are not valid, i.e., the measured ConvF, while still sensitive to direct NO oxidations caused by reactions of benzene or its products, is also significantly influenced by other mechanistic factors. In the case of formaldehyde, the large effect on radical levels, and thus the extent of reaction of the other VOCs, may also be having a significant influence on the ConvF value derived from our data.

Note that the conversion factor by itself gives a poor prediction of a VOC's overall reactivity. For example, despite having the highest conversion factors, the higher alkanes form little ozone or are ozone inhibitors in these experiments. The effect of the VOCs on radical levels, which are directly measured by the IntOH reactivities (and also by the "indirect" reactivities), appears to be a more important factor. This is shown on Table 5, above, where it can be seen that for many VOCs the indirect reactivities, which reflect effects on radical levels under the conditions of these experiments, are higher in magnitude than the direct reactivities. Without exception, the VOCs which are the highest in IntOH reactivities also have the highest in $d(O_3\text{-NO})$ reactivities, and those with the most negative IntOH reactivities are also the strongest ozone inhibitors. Thus the major factor accounting for extremes in reactivity is not the amount of ozone the VOC forms directly, but the extent to which it affects how much ozone is formed from other VOCs.

Approximately half the compounds studied tended to enhance radical levels under the conditions of these experiments, with the rest tending to inhibit radicals to various degrees. All the VOCs which enhanced radicals had high mechanistic reactivities towards forming ozone. These included formaldehyde, acetone, methanol, the alkenes and the alkylbenzenes. The enhancement caused by formaldehyde and acetone are attributed to their direct photolysis to form radicals, while in the case of methanol and the aromatics the enhancement is attributed to the formation of radical initiating products. In the case of methanol the radical initiating product is formaldehyde, while in the case of the aromatics the known radical initiating products are α-dicarbonyls such as methyl glyoxal. Aromatics also apparently form other photoreactive products which have not been identified as such, since only models which assume this (or which use unrealistically high α-dicarbonyl yields) can account for the high reactivities of aromatics. In the case of the alkenes, radical formation can come directly from the reaction of the alkene with ozone, or indirectly from the formation of photoreactive products such as formaldehyde and acetaldehyde.

Most other VOCs tend to suppress radical levels. In the case of the alkanes and the higher molecular weight ethers, this is attributed to removal of peroxy radicals by reactions with NO to form alkyl nitrates, while in the case of the acetaldehyde and ethanol (which forms acetaldehyde), this is attributed

to the removal of acetyl peroxy radicals by reaction with NO_2 to form PAN. In the case of isobutane, removal of alkoxy radicals by reaction with NO_2 to form a nitrate also appears to be significant under the conditions of these experiments, though this is expected to be less important in the atmosphere because the NO_2 levels are generally lower. However, the inhibition by the peroxy + NO reactions in the other alkane systems or the PAN formation from acetaldehyde are expected to be of comparable importance in the atmosphere as they are in these experiments, since the relative importance of these reactions are not dependent on total NO_2 levels (though it does depend on the NO_2/NO ratio). The siloxanes are the strongest radical inhibitors of all the compounds studied under the conditions of these experiments, but the mechanism for this inhibition, and how it depends on NO_x levels, is unknown.

It is interesting to note that CO also has a slight tendency to suppress radicals, despite the fact that no radical terminations are involved in its photooxidation. Its only reaction is to convert OH to HO_2, and it forms no reactive products. Thus, simply converting NO to NO_2 (as results when HO_2 reacts with NO to regenerate OH) must cause at least some suppression of integrated radical levels in these experiments. This is probably due to the enhanced reactions of OH with NO_2 resulting from the more rapid increase of NO_2 caused by this conversion. Since essentially all VOCs have some reactions which convert NO to NO_2, they would all inherently have this slight tendency to reduce radicals, even if they or their products did not have direct radical termination reactions.

Most of the compounds which suppress radical levels still have positive d(O_3-NO) reactivities, i.e., still cause enhanced NO oxidation and ozone formation under the conditions of our experiments. In these cases the additional ozone formation caused by the VOC's direct reactions is sufficient to counter their effects on reducing ozone formation from other VOCs (see Table 5, above). In the case of acetaldehyde, direct radical formation from its photolysis would also counter inhibition due to PAN formation, though apparently the latter is more important under the conditions of these experiments, since it has a negative IntOH reactivity. But, as one would expect, the efficiency in ozone formation (i.e., the d(O_3-NO) mechanistic reactivities) decrease as the tendency to suppress radicals increased, and when the suppression becomes sufficiently large, it overwhelms the positive effect on ozone formation of the VOC's direct reactions, making the compound a net ozone inhibitor. This is the case for the siloxanes and the C_{6+} n-alkanes under the conditions of our experiments,.

Thus for VOCs which are radical inhibitors, there is a balance between opposing effects of the VOC causing additional ozone formation from its direct reactions and its causing lower radicals and thus less ozone formation from other VOCs. Which effect is more important can vary depending on conditions. Model

simulations suggest that this balance is somewhat different under atmospheric conditions than in these experiments, since n-hexane and n-octane, which are correctly predicted by the model to have negative reactivities in these experiments, are predicted by the same model to have positive (though small) maximum reactivities in the atmosphere (Carter, 1991). Apparently effects on radicals are somewhat less important in affecting ozone reactivities in the atmosphere, or in the presence of the more complex atmospheric mixtures, than in these experiments. However, the small magnitudes of the atmospheric reactivities of these radical inhibiting VOCs indicate that the radical inhibition is still significantly suppressing their reactivities in the atmosphere.

B. Mechanism Performance Evaluation

1. Utility of Data Base

The major utility of the data obtained in this study is to test the ability of chemical mechanisms used in airshed models to predict maximum reactivities of VOCs. Previous mechanism evaluations (e.g., Gery et al., 1988, Carter and Lurmann, 1990, 1991) have focused primarily on the ability of mechanisms to simulate results of single VOC NO_x-air chamber runs. This is because such runs have been the principal means to test aspects of the VOC's mechanism independently of uncertainties in mechanisms of other VOCs. This type of test is obviously critical, but it should be recognized that such runs represent a chemical environment far different from those most VOCs encounter when they react in the atmosphere. The results of these experiments (as well as modeling studies [e.g., Carter and Atkinson, 1989a; Jeffries and Crouse, 1991]) show that in many cases the effect of a VOC on the reactions of other VOCs (e.g., through providing or removing radicals) is a more important component of a VOC's reactivity than its direct effect on ozone. Mixture runs represent a potentially more realistic chemical environment, but most mixture runs do not provide a means to unambiguously test mechanisms of a single VOC. If a model does not perform adequately in simulating such a run, it is often not clear where the error lies. Reactivity experiments such as these provide a means to address both these problems. The VOC is reacting in a fairly realistic chemical environment, and yet if the base case condition is well established, the effect of the single VOC on the system can at least to some extent be isolated.

Another advantage that reactivity experiments have over single compound runs is that the effects on model simulations of uncertainties in chamber characterization is reduced, in some cases significantly so. Since the measurement of interest in a reactivity experiment is the difference between experiments conducted under similar chamber conditions, inaccuracies in the chamber effects model will to some extent (though obviously not completely)

cancel when modeling these differences. This advantage is most significant when evaluating mechanisms for compounds, such as alkanes, alcohols, and ethers, which do not have significant internal radical sources, or are radical inhibitors. NO_x-air irradiations of such compounds by themselves are totally dominated by chamber radical sources, since those are the major sources of radicals initiating these systems. Since chamber radical sources are uncertain and tend to vary from run to run, this represents a significant uncertainty in the evaluation of mechanisms for these compounds using such data (e.g., see Carter and Lurmann, 1991). Because of this, it can be argued that the mechanisms for alkanes and other such compounds have never been adequately tested. Thus these experiments provide the first real test for mechanisms for alkanes and other non-radical-initiating VOCs.

Of course, mechanism evaluations using reactivity experiments is not without compounding effects of uncertainties in the mechanisms for the VOCs present in the base case mixture. If the mechanism cannot accurately simulate the result of the base case experiment, it cannot be expected to be successful in simulating the effect of adding a test VOC without compensating errors. If it simulates the base case experiment but does so with compensating errors, these errors may influence model predictions of the effects of the added VOC, especially if the presence of the VOC and its reactions changes the balance between these compensating errors. Thus reactivity experiments will never eliminate the need for testing mechanisms with single compound runs.

Compensating errors are almost certainly occurring in the simulations of the base case experiments discussed in this report. This must be the case because the mechanism was unable to successfully simulate the Set 3 base case runs without being adjusted in a way which makes it less consistent with results of other runs. The use of the highly simplified ROG surrogate is advantageous in this regard because it made the probable source of error more evident. We believe the error is in the m-xylene mechanism because it is the most reactive compound in the mixture, it has the most uncertain mechanism, and because adjusting uncertain parameters in its mechanism can result in good fits. Unfortunately, the same set of parameters cannot fit all runs, including the other two types of base case runs in this study. Clearly, the m-xylene mechanism needs to be reformulated. Until this mechanism is corrected, simulations of all experiments with this compound must have some compensating errors. In modeling VOC reactivities we had no choice but to use different m-xylene mechanisms when simulating different base case systems, in order that the model represent, at least in its major observable features, the chemical environment in which the test VOCs are reacting.

In an attempt to obtain some information concerning the magnitude of the effect on reactivity predictions of the errors in the m-xylene mechanism, we

simulated the Set 3 experiments both with and without adjusting the mechanism for m-xylene in the ROG surrogate to fit the base case runs. This provides a comparison of reactivity predictions using a model which underpredicts ozone in the base case run (and thus also in the runs with the added VOC, if the mechanism for the VOC is correct), with using a model which correctly predicts ozone in the base case run, but with compensating errors. Fortunately, in most cases the two models give reactivity predictions which agree with each other to within the experimental uncertainty. (See the summary of experimental and calculated average reactivities on Tables 7-9, and the plots of experimental and calculated reactivity results in Appendix A.) Indeed, the unadjusted mechanism gave slightly better predictions of reactivities of most VOCs, though the difference may not be significant. (One major exception was that the adjusted model fit the reactivity of acetaldehyde while the unadjusted model overpredicted it [see Figure A-31], presumably because the unadjusted model underpredicted the extent of PAN formation in the experiments. The adjusted and unadjusted models are also quite different in predictions of benzene reactivity, both fitting the data poorly in different ways.) This suggests (though obviously does not prove) that although there are compensating errors in the model representations of the base ROG reactions, the model predictions of incremental or mechanistic reactivity may not necessarily be sensitive to these errors.

2. Performance of the SAPRC Detailed Mechanisms

The detailed SAPRC mechanism (Carter, 1990) is a prime example of the type of mechanism that these experiments are designed to test. It includes representations for the NO_x-air reactions of approximately 100 types of VOCs, which in most cases are based on untested extrapolations of mechanisms of a subset of compounds which are presumed to be representative. These data provide a means to test the validity of at least some of these extrapolations. In addition, although the mechanisms for many of the representative VOCs used as the basis for the extrapolations have been tested against a variety of environmental chamber experiments (Carter and Lurmann, 1991), most of them have never been tested in quite this way.

The performance of the SAPRC mechanisms in simulating these experiments is shown on Tables 7-9 and in the plots in Appendix A. The results for the various classes of VOCs, and implications concerning the overall performance and reliability of the mechanisms, are discussed below.

a. Alkanes.

As discussed above, these data provide the first good environmental chamber test for alkane mechanisms. The major parameter in the alkane mechanisms affecting predictions of their reactivities is the overall alkyl nitrate yield. Although apparently anomalous results were seen in some runs employing ethane and n-butane, the model performs reasonably well in simulating the 6-hour reactivities of the n-alkanes, including n-hexane and n-octane. This may not seem surprising since alkyl nitrate yields have been directly measured from these compounds, but the measured yields only concern alkyl nitrate formation from the initially formed peroxy radicals. Long chain alkanes such as n-hexane and n-octane are also predicted to form nitrates from reactions of the OH-substituted peroxy presumed to be formed following 1,5-H shift isomerization. For example, the reactions below are expected to occur in the n-hexane system following reaction at the 2-position:

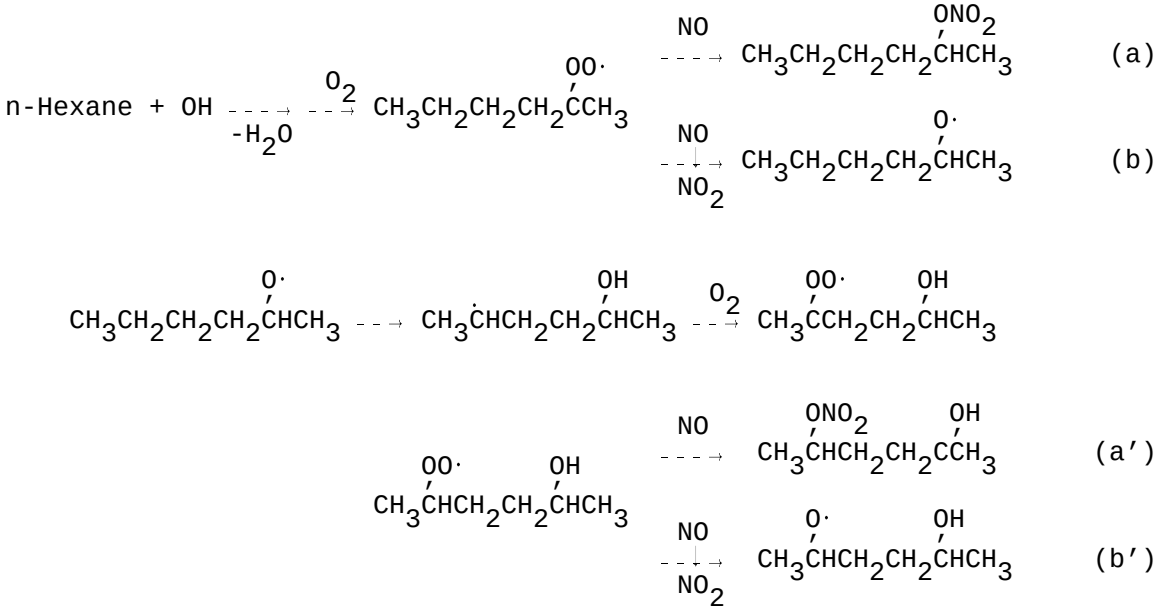

If the nitrate yields (e.g., $k'_a/k'_a+k'_b$) from these reactions were the same as in the corresponding unsubstituted radical (e.g., k_a/k_a+k_b), the overall nitrate yield from the alkane would be increased by almost a factor of two. This would significantly affect predictions of the alkane's reactivity. The SAPRC mechanism assumes that nitrate formation from this source is not important based on model simulations of single alkane-NO_x-air experiments, but simulations of such experiments are uncertain because of their extreme sensitivity to chamber radical sources. These experiments provide much stronger support for this assumption, clearly indicating that this cannot be an important process, since otherwise the mechanism would grossly overpredict radical inhibition by these compounds.

The apparently low nitrate yield from the reactions of NO with OH-substituted peroxy radicals is consistent with the results with the ethers and alcohol ethers, discussed in the previous section. These data indicate that O-substituted peroxy radicals, which includes those formed following isomerization reactions in the alkane system as well as in reactions of ethers and alcohol ethers, have much lower nitrate yields than the corresponding unsubstituted radicals formed in the initial reactions of the alkanes. Perhaps electron withdrawing substituents decrease the importance of alkyl nitrate formation in the peroxy + NO reaction.

The model performance in the simulations of the runs for the two branched alkanes studied, isobutane and isooctane, was remarkably poor, and for two quite different reasons (see Sections IV-D-1-b and IV-D-1-c, above). However, in both cases the discrepancies could be attributed to approximations in the general alkane mechanism which could be resolved by using less approximate, more chemically detailed representations which are consistent with our current theories. In the case of isobutane, a type of reaction (alkoxy + NO_2) which is normally unimportant in atmospheric systems — and which is generally ignored in models because it allows significant simplification in implementation — was found to be non-negligible under the conditions of these experiments. This type of reaction, which is unimportant for most other alkanes, will be less important under most atmospheric conditions, when NO_2 concentrations are lower than in these experiments. However, the reaction may be non-negligible near NO_x sources, and it becomes increasingly important as the temperature is reduced, because the competing decomposition reaction is highly temperature dependent (Batt et al. 1989).

In the case of isooctane, the discrepancy can be attributed to steric effects which are not accounted for in the general alkane estimation methods used to derive the mechanism for this compound (Carter and Atkinson, 1985; Atkinson, 1987). The sensitivity of predictions of isooctane reactivity to assumptions at this level of detail indicate that mechanisms for other branched alkanes need to be examined on a case by case basis. In particular, the reactivity predictions are highly sensitive to estimates concerning fractions of reactions involving formation of secondary vs primary or tertiary radicals, which may vary widely among alkane isomers. Isooctane may provide an extreme example of steric effects, but it is probably not the only branched alkane where such considerations may be important.

b. Alkenes.

The mechanism correctly predicts that the alkenes tend to be radical initiators and thus have high mechanistic reactivities. However, the mechanism has a tendency to underptedict alkene reactivities, particularly for the C_{4+} alkenes. In the cases of ethene (Figure A-8) and propene (Figure A-9), the underprediction may be within experimental uncertainty or run-to-run variability. However, the underprediction of reactivity is outside the experimental uncertainty for the C_{4+} alkenes, with the 6-hour IntOH and d(O_3-NO) reactivities for isobutene, trans-2-butene and isoprene being underpredicted by 40-50%. The model also incorrectly predicts how the reactivities of these alkenes change with time, with the model fitting the early experiment reactivity of trans-2-butene, and overpredicting the early experiment reactivities of isobutene and isoprene.

The worst performance is for isoprene and (especially) 2-chloromethyl-2-chloropropene. Poor performance for isoprene is not unexpected since it forms types of products which are not well represented in the SAPRC mechanisms. Note that this is the only alkene where the model predictions of the conversion factors are outside the uncertainty ranges of the measurements. The need to improve the SAPRC isoprene mechanism was apparent from the original evaluation of that mechanism (Carter and Lurmann, 1991).

Poor performance for the chlorobutene is also not unexpected since no attempt was made to represent the effects of the formation of chlorine atoms, which are apparently involved in this system. The chlorine causes a significantly higher fraction of n-hexane to react than would otherwise be the case, and this effect is not represented in the model. However, this should be manifested primarily by the model underpredicting the conversion factor, but in fact the conversion factor is only slightly underpredicted, and the worst discrepancy is in the predictions of the IntOH reactivates. This may be due to the model underestimating photodecomposition rates of the Cl-containing products. Note that the ozone reaction is unimportant for this compound, so errors in this aspect of the mechanism are unlikely to be significant contributors to this problem.

The reasons for the model predictions being also outside the experimental uncertainty ranges for trans-2-butene and isobutene are less readily explained, but it should be noted that the model performance is also not totally satisfactory in simulating single compound runs with these VOCs (Carter and Lurmann, 19901). One probable source of error is the representation of the ozone + olefin reactions, which is highly uncertain (Atkinson, 1990; Carter, 1990). Recently, Atkinson et al. (1992) found evidence for evidence for relatively large OH radical yields in ozone + alkene reactions, which is not consistent with the current representation in the SAPRC mechanism (Carter, 1990). It is clear that

modifications are needed to the mechanisms for these alkenes to improve model performance in simulating these and other chamber data.

c. Aromatics

The mechanism correctly predicts that the alkylbenzenes, like the alkenes, are strong radical initiators and thus have high d(O_3-NO) reactivities. This is not surprising since the mechanisms were adjusted to simulate this behavior. Since the SAPRC alkylbenzene mechanisms were developed based on model simulations of toluene, m-xylene and 135-trimethylbenzene runs, one would expect it to perform best in simulating reactivities of these compounds. However, the mechanism underpredicted, by 20-50%, the d(O_3-NO) reactivities of all three compounds, and also underpredicted the radical initiating reactivities of toluene and 1,3,5-trimethylbenzene.

The SAPRC mechanisms assume that the other xylene and trimethylbenzene isomers react like m-xylene or 1,3,5-trimethylbenzene, but the data show that the mechanistic reactivities for the different isomers can differ by up to a factor of 2. However, the isomer used in the SAPRC mechanism as being representative turned out to be the middle compound in reactivity in both cases, so the worst discrepancies in terms of model predictions were on the order of 60%.

The model performance in simulating the benzene data suggests other problems with the aromatics mechanisms. Although the model did not perform particularly poorly in simulating the d(O_3-NO) or IntOH reactivities, and also correctly predicted the fact that ozone peaked in these added benzene runs (see Figure 17), it significantly underpredicted the conversion factor. The conversion factors for the other aromatics are also not well predicted, but the relatively high experimental uncertainty in determining conversion factors for the alkylbenzenes makes the significance of this uncertain. However, the results for benzene, which forms less reactive products than do the alkylbenzenes, suggest that the initial reactions of the aromatics involve fewer NO to NO_2 conversions than assumed in the SAPRC mechanism. (As discussed above, the benzene conversion factor derived from our data would also be sensitive to the NO_x sinks in the benzene mechanism. However, this aspect of the mechanism appears to be reasonably well represented, given the success of the model in predicting the ozone maxima in these experiments, as seen on Figure 17.) In the case of the other aromatics, the NO to NO_2 conversions caused by the reactions of the more reactive products these compounds form may be the major contributor to the conversion factors, making the effect of the initial reactions of the aromatic compound relatively less important.

Thus, while the mechanism can predict the major overall reactivity characteristics for the aromatics, there are clearly problems with the aromatics mechanisms which need to be addressed. This is in addition to the fact that the results of the Set 3 standard experiments could not be simulated by models using the standard SAPRC m-xylene mechanism adjusted based on simulations of other experiments. The SAPRC aromatics mechanism is in the process of being modified, but a version with significantly improved performance in this regard has not yet been developed.

d. Aldehydes and Ketones.

The SAPRC-91 mechanism is reasonably successful in simulating the reactivity data for acetaldehyde and the 6-hour reactivities of formaldehyde, but overpredicts the reactivity of formaldehyde at earlier times in the experiment, and overpredicts the reactivities of acetone at all times, particularly earlier in the runs (See Figures A-30 through A-32). The results for the SAPRC-90 mechanism are also shown on the plots in Figures A-30 - A-32, because the changes in SAPRC-91 relative to SAPRC-90 are expected to affect these compounds more than the other VOCs. The SAPRC-90 mechanism uses slightly lower photolysis quantum yields for formaldehyde, which in fact causes a slightly better simulation of the formaldehyde reactivities, though the difference is relatively minor (see Figure A-30). The SAPRC-90 mechanism also uses different rate constants for PAN formation reactions, predicting more PAN formation from its precursors, and thus lower reactivities for PAN precursors such as acetaldehyde and acetone. (This is because PAN formation is a radical termination process). This results in significantly lower predicted mechanistic reactivities for acetaldehyde, and much poorer fits to the data for the SAPRC-91 mechanism. On the other hand, the change in PAN kinetics has a relatively small effect on the simulations of the acetone reactivities.

It is difficult to account for the reason for the overprediction of the formaldehyde reactivity early in the experiment, since the formaldehyde mechanism is now considered to be reasonably well established. The possibility of the model incorrectly predicting the formaldehyde photolysis rate because of chamber light characterization problems cannot be totally ruled out, because the model also overpredicts the rate of consumption of formaldehyde when it is irradiated by itself in our chamber. However, we consider it unlikely that the problem is due to light intensity inputs in our model since this would mean the model is using values which are too high. If this would be the case, the model should consistently overpredict the rates of reaction in other types of runs. In fact, no such overprediction is observed in simulations of the propene or ethene-NO_x control experiments, and, as discussed above, the unadjusted model underpredicts the rates of reaction in the Set 3 base case experiments. The light spectra in

our chamber have been measured by two different spectrometers which give the same results, making it unlikely that the discrepancy is due to the model using an incorrect spectral distribution when calculating the formaldehyde and other photolysis rates.

A similar type of discrepancy is observed in the case of acetone, though the acetone reactivity is overpredicted at all times in the experiments, and not just initially. However, the likelihood that this discrepancy is due to errors in the quantum yields in the model is somewhat greater in the case of acetone than is (presumably) the case for formaldehyde. The acetone quantum yields in the SAPRC mechanism are based on the data of Meyrahn et al. (1986), who used PAN yields measured in photolyses of high concentrations of acetone in the presence of NO_2 at various wavelengths with monochromatic light sources to determine the quantum yields for the photodecomposition reaction. This is a somewhat indirect determination, and its validity is based on the assumption that the photolysis reaction is the only source of PAN precursors in this system. Since PAN can also be formed following the reaction of OH radicals with acetone, and the photolysis reactions lead to OH radical formation, we carried out model simulations of the experimental system of Meyrahn et al. (1986) to determine whether there may be problems with the interpretations of these data. The results of our simulations tended to support their analyses except at 330 nm, the longest wavelength studied, where the model predicts they may be overestimating the quantum yield of the elementary reaction. The quantum yield they report for that wavelength (0.033) is also high based on what one would expect from the trend of quantum yields measured at the lower wavelengths. An exponential extrapolation of the quantum yields measured at the shorter wavelengths suggests a 330 nm quantum yield of ~0.018 is more reasonable. However, making that change only causes a 15% reduction in the calculated acetone photolysis rate in our chamber. This is not sufficient to account for the discrepancy in the model prediction, since a reduction of the photolysis rate by a factor of 2 is required for the model to fit the experimental reactivity results.

An additional possibility which should be considered is that the discrepancy concerning formaldehyde reactivity could be due to a problem with the base ROG reactions being less sensitive to radical input processes at the early stages of the experiments than predicted by this model. This could be the case if both radical initiation and radical terminating processes in the base ROG mechanism were stronger than assumed in this model. This explanation would also account for the overprediction of the acetone reactivities. However, the adjustment of the base xylene mechanism does not strongly affect the predictions of initial reactivities of formaldehyde, acetone, or the strongly radical inhibiting compounds. Perhaps more significantly, additional runs we have carried out very recently, where the effects of adding formaldehyde or acetone to ethylene-NO_x-air runs, yielded essentially the same discrepancies between

experimental results and model predictions (unpublished results from this laboratory). Since the modeling of latter experiments does not have the uncertainties in the aromatics mechanism, these data suggest that problems with the base ROG mechanism is not the explanation.

In contrast to acetone and formaldehyde, the model successfully predicts the reactivity of acetaldehyde in the initial as well as in the final stages of the experiment. However, photolysis is a less important factor in accounting for acetaldehyde reactivity than is the case for formaldehyde or acetone, because the OH radical reaction is relatively more important. This is indicated by its low IntOH mechanistic reactivity in the initial stages of the experiment, when termination by PAN formation is relatively unimportant (see Table A-2). Thus, if the model is giving an incorrect prediction of the response of the base ROG reactions to radical input, it would not significantly affect predictions of acetaldehyde reactivity. On the other hand, acetaldehyde reactivity is highly sensitive to predictions of PAN formation, as indicated by the significant differences between the predictions of the SAPRC-90 and the SAPRC-91 mechanisms.

e. Alcohols and Ethers.

The mechanism performed reasonably well in simulating the reactivities of methanol and ethanol (see Figures A-23 and A-24), as one would expect since the mechanisms for these compounds are considered to be well established. Since they are not strong radical initiators or inhibitors, problems with the base ROG mechanism involving sensitivity to radicals would not affect reactivity predictions for these compounds. Methanol has a relatively high mechanistic reactivity because its major product is formaldehyde, which is highly reactive. Although the model tends to overpredict the initial reactivity of formaldehyde, it gives a reasonably good simulation of the reactivity of methanol.

The model simulation of the reactivity of isopropanol is not as good as for the other alcohols, with the model predicting isopropanol to be a moderate radical inhibitor while in fact it appears to be a moderate radical initiator under the conditions of these experiments (see Figure A-25). Isopropanol should have a relatively simple mechanism, with the main process being OH abstracting the tertiary hydrogen and forming acetone + HO_2 in a single step. The SAPRC mechanism ignores reaction at a methyl group, which is predicted to ultimately form formaldehyde and acetaldehyde with an additional NO to NO_2 conversion, since it is estimated (Atkinson, 1987) to occur only ~5% of the time. Including this step at the 5% level causes only a slight increase in its reactivity, which is not sufficient to resolve the discrepancy with these data. Even making the extremely implausible assumption that reaction at a methyl group occurs 100% of the time is insufficient to account for the IntOH reactivity, and this also

results in a significant overprediction of the conversion factor. However, the model is consistent with the data in that it predicts that the effect of this compound on radicals is relatively small.

The model slightly underpredicts (by ~30%) the d(O_3-NO) reactivity of dimethyl ether, though the conversion factor is correctly predicted. Both the model and the experiment are consistent in indicating that the effect of this compound on radicals is small. The discrepancy in d(O_3-NO) reactivities may be due to the highly approximate method used to represent the reactions of methyl formate, its main reaction product (See Appendix A of Carter, 1991). However, this product reacts quite slowly with OH radicals (Atkinson, 1989), and should not photolyze under atmospheric conditions (Calvert and Pitts 1966), so even an incorrect representation of its reactions should not significantly affect model predictions. Thus, we do not have a good explanation of why the model slightly underpredicts the reactivity of dimethyl ether.

These data do not provide an independent test of the mechanisms for MTBE, ethoxyethanol and carbitol, since they were adjusted to optimize the fits to these runs. However, the only parameter adjusted was the organic nitrate yields, which, though important in affecting predictions of d(O_3-NO) and IntOH reactivities, does not significantly affect predicted conversion factors. The model predicts the conversion factors for all these compounds within the experimental errors of the measurements.

f. Siloxanes.

The siloxanes are not represented in the current versions of the SAPRC mechanism. The use of these data to develop possible siloxane mechanisms is discussed elsewhere (Carter et al., 1992).

VI. CONCLUSIONS

We believe that this study was successful in its objective of providing the type of data needed for reducing the chemical mechanistic uncertainties in maximum reactivity scales for ozone formation in the atmosphere. Data were obtained which can test model predictions of maximum reactivities of 35 different VOCs, including a variety of alkanes, alkenes, aromatic hydrocarbons, alcohols, ethers, alcohol ethers, and others. Many of these compounds have never been studied previously in environmental chamber experiments suitable for model evaluation, except perhaps as parts of complex mixtures of many other VOCs, or in experiments whose results are dominated by poorly characterized chamber effects. In particular, this study has provided the only data available concerning the ozone reactivities of representative ethers, alcohol ethers, and siloxanes, has provided the most useful presently available data concerning ozone reactivities of alkanes, and has provided a unique and valuable addition to the existing data set for the other VOCs, most of which have not been previously studied in this way.

Note that the reactivities measured in these experiments should not be extrapolated to the atmosphere without taking into account the differences in conditions between these experiments and the atmosphere. These differences include differences in spectral characteristics of the light sources, higher absolute pollutant concentrations, the lack of dilution and continuous emissions, the lack of background or entrained pollutants, and the highly simplified base ROG surrogate in the experiments. The extrapolation to atmospheric conditions can be carried out by using these data to evaluate the chemical mechanisms used in the airshed models to calculate atmospheric reactivity, or by using models to derive relationships which can be used to estimate atmospheric reactivities from those measured in the chamber. The discussion in this report has focused on the use of these data for evaluating mechanisms. We are in the process of examining the potential utility of the second approach, but, since this effort is not complete, a discussion of this is beyond the scope of this report.

The ultimate practical benefit of these data will come when the mechanisms used to calculate VOC reactivity scales are updated to take these results into account. The preliminary mechanism evaluation discussed in this report showed that while the mechanism performs reasonably well in simulating the general reactivity trends and rankings among the VOCs, there are a number of discrepancies which will need to be addressed when the mechanism is updated.

It is important to recognize, however, that this study does not provide all the data needed to adequately evaluate the chemical mechanisms used to predict atmospheric reactivities. The present experiments are only suitable for testing mechanisms under high NO_x, maximum reactivity conditions. While this is obviously important, it is also important that the mechanism be tested under conditions where NO_x is limited. Chemical factors involving VOC NO_x sinks, which have essentially no effect on maximum reactivities, become important under NO_x limited conditions, and experiments are needed to test this aspect of the mechanisms. In addition, experiments are needed to determine how reactivities are affected by changes in the composition of the base case ROG mixture, and to determine if reactivities are obtained if sunlight, or light sources with a visible spectrum more closely resembling sunlight, are used. The next phase of our experimental reactivity studies will address at least some of these additional data needs.

VII. REFERENCES

Atkinson, R. and J. N. Pitts, Jr. (1977): "Absolute Rate Constants for the Reaction of O(^{3}P) Atoms with a Series of Olefins over the Temperature Range 298-439 K., J. chem. Phys. 67, 38.

Atkinson, R. and W. P. L. Carter (1984): "Kinetics and Mechanisms of the Gas-Phase Reactions of Ozone with Organic Compounds under Atmospheric Conditions," Chem. Rev. 1984, 437-470.

Atkinson, R. and S. M. Aschmann (1985): "Kinetics of the Gas-Phase Reaction of Cl Atoms with a Series of Organics at 296±2 K and Atmospheric Pressure," Int. J. Chem. Kinet., 17, 33-41.

Atkinson, R. (1986); "Kinetics and Mechanisms of the Gas Phase Reactions of the Hydroxyl Radical with Organic Compounds Under Atmospheric Conditions", Chem Rev., 86, 69-201.

Atkinson, R. (1987): "A Structure-Activity Relationship for the Estimation of Rate Constants for the Gas-Phase Reactions of OH Radicals with Organic Compounds," Int. J. Chem. Kinet., 19, 799-828.

Atkinson, R. (1989): "Kinetics and Mechanisms of the Gas-Phase Reactions of the Hydroxyl Radical with Organic Compounds," J. Phys. Chem. Ref. Data, Monograph no 1.

Atkinson, R., D. L. Baulch, R. A. Cox, R. F. Hampson, Jr., J. A. Kerr, and J. Troe (1989): "Evaluated Kinetic and Photochemical Data for Atmospheric Chemistry. Supplement III, J. Phys. Chem. Ref. Data 18, 881-1097.

Atkinson, R. (1990): "Gas-Phase Tropospheric Chemistry of Organic Compounds: A Review," Atmos. Environ., 24A, 1-24.

Atkinson, R. (1991a): "Kinetics and Mechanisms of the Gas-Phase Reactions of the NO_3 Radical with Organic Compounds," J. Phys. Chem. Ref. Data, 20, 459-507.

Atkinson, R. (1991b): "Kinetics of the Gas-Phase Reactions of Organosilicon compounds with OH and NO_3 Radicals at 297 ± 2 K," Environ. Sci. Technol. 25, 863-866.

Atkinson, R. and W. P. L. Carter (1992): "Reactions of Alkoxy Radicals under Atmospheric Conditions: The Relative Importance of Decomposition versus Reaction with O_2," J. Atm. Chem., 13, 195-210.

Atkinson, R. (1992): "Gas-Phase Tropospheric Chemistry of Organic Compounds," to be submitted to J. Phys. Chem. Ref. Data

Atkinson, R., S. M. Aschmann, J. Arey and B. Shorees (1992): "Formation of OH Radicals in the Gas-Phase Reactions of Ozone with a Series of Terpenes," J. Geophys. Res. 97, 6065-6073.

Bass, A. M., L. C. Glasgow, C. Miller, J. P. Jesson, and D. L. Filken (1980): "Temperature Dependent Absorption Cross Sections for Formaldehyde: the Effect of formaldehyde on Stratospheric Chlorine Chemistry," Planet. Space Sci. 28, 675-679.

Batt, L., M. W. M. Hisham and M. MacKay (1989): "Decomposition of the t-Butoxy Radical: II Studies over the Temperature Range 303-393 K," Int. J. Chem. Kinet., 21, 535-546

Bridier, I., H. Caralp, R. Loirat, B. Lesclaux and B. Veyret (1991): "Kinetic and Theoretical Studies of the Reactions of $CH_3C(O)O_2$ + NO_2 + M <=> $CH_3C(O)O_2NO_2$ + M between 248 and 393 K and between 30 and 760 Torr," J. Phys. Chem. 95, 3594-3600.

Calvert, J. G., and J. N. Pitts, Jr. (1966): Photochemistry, John Wiley and Sons, New York.

Cantrell, C. A., J. A. Davidson, A. H. McDaniel, R. E. Shetter and J. G. Calvert (1990): "Temperature-Dependent Formaldehyde Cross Sections in the Near Ultraviolet Spectral Region," J. Phys. Chem. 94, 3902-3908.

CARB (1991): "Proposed Reactivity Adjustment Factors for Transitional Low-Emissions Vehicles: Technical Support Document," California Air Resources Board, Sacramento, CA., September 27.

Carter, W. P. L., R. Atkinson, A. M. Winer, and J. N. Pitts, Jr. (1982): "Experimental Investigation of Chamber-Dependent Radical Sources," Int. J. Chem. Kinet., 14, 1071.

Carter, W. P. L., Winer, A. M., Atkinson, R., Dodd, M. C. and Aschmann, S. A. (1984a): Atmospheric Photochemical Modeling of Turbine Engine Fuels. Phase I. Experimental studies. Volume I of II. Results and Discussion. Final Report to the U. S. Air Force, ESL-TR-84-32, September.

Carter, W. P. L., and R. Atkinson (1985): "Atmospheric Chemistry of Alkanes", J. Atmos. Chem., 3, 377-405, 1985.

Carter, W. P. L., W. D. Long, L. N. Parker, and M. C. Dodd (1986a): "Effects of Methanol Fuel Substitution on Multi-Day Air Pollution Episodes," Final Report on California Air Resources Board Contract No. A3-125-32, April.

Carter, W. P. L., F. W. Lurmann, R. Atkinson, and A. C. Lloyd (1986b): "Development and Testing of a Surrogate Species Chemical Reaction Mechanism," EPA-600/3-86-031, August.

Carter, W. P. L., A. M. Winer, R. Atkinson, S. E. Heffron, M. P. Poe, and M. A. Goodman (1987): "Atmospheric Photochemical Modeling of Turbine Engine Fuels. Phase II. Computer Model Development," Report on USAF Contract no. F08635-83-0278, Engineering and Services Laboratory, Air Force Engineering and Services Center, Tyndall Air Force Base, Florida, August.

Carter, W. P. L. (1987): "An Experimental and Modeling Study of the Photochemical Reactivity of Heatset Printing Oils," Report #2 on U. S. EPA Cooperative Agreement No. CR810214-01

Carter, W. P. L. and R. Atkinson (1987): "An Experimental Study of Incremental Hydrocarbon Reactivity," Environ. Sci. Technol., 21, 670-679

Carter, W. P. L. and R. Atkinson (1989a): "A Computer Modeling Study of Incremental Hydrocarbon Reactivity", Environ. Sci. and Technol., 23, 864.

Carter, W. P. L. and R. Atkinson (1989b): "Alkyl Nitrate Formation from the Atmospheric Photooxidation of Alkanes; a Revised Estimation Method," J. Atm. Chem. 8, 165-173.

Carter, W. P. L. (1990): "A Detailed Mechanism for the Gas-Phase Atmospheric Reactions of Organic Compounds," Atm. Environ., 24A, 481-518.

Carter, W. P. L., and F. W. Lurmann (1990): "Evaluation of the RADM Gas-Phase Chemical Mechanism," Final Report, EPA-600/3-90-001.

Carter, W. P. L., E. C. Tuazon, and S. M. Aschmann (1990): "Investigation of the Atmospheric Chemistry of Methyl t-Butyl Ether (MTBE)," Draft report to the Coordinating Research Council, inc, for the Automotive Emissions Cooperative Research Program, Atlanta, GA, October.

Carter, W. P. L. (1991): "Development of Ozone Reactivity Scales for Volatile Organic Compounds", EPA-600/3-91/050, August.

Carter, W. P. L. and F. W. Lurmann (1991): "Evaluation of a Detailed Gas-Phase Atmospheric Reaction Mechanism using Environmental Chamber Data," Atm. Environ. 25A, 2771-2806.

Carter, W. P. L., E. C. Tuazon, and S. M. Aschmann (1991): "Investigation of the Atmospheric Chemistry of Methyl t-Butyl Ether (MTBE)," Final Report to the Coordinating Research Council, inc, for the Auto/Oil Air Quality Improvement Research Program, Atlanta, GA, January.

Carter, W. P. L., J. A. Pierce, and I. L. Malkina (1992): "Investigation of the Ozone Formation Potential of Selected Volatile Silicone Compounds," Report to Dow Corning Corporation, Midland MI, November.

Chang, T. Y. and S. J. Rudy (1990): "Ozone-Forming Potential of Organic Emissions from Alternative-Fueled Vehicles," Atmos. Environ., 24A, 2421-2430.

Daguat, P., T. J. Wallington, R. Liu and M. J. Kurylo (1988): 22nd International Symposium on Combustion, Seattle, August 14-19.

Dasgupta, P.K, Dong, S. and Hwang, H. (1990): Aerosol Science and Technology 12, 98-104

Dasgupta, P. K, Dong, S. and Hwang, H. (1988): "Continuous Liquid Phase Fluorometry Coupled to a Diffusion Scrubber for the Determination of Atmospheric Formaldehyde, Hydrogen Peroxide, and Sulfur Dioxide," Atmos. Environ. 22, 949-963.

DeMore, W. B,, R. F. Hampson, S. P. Sander, M. J. Kurylo, D. M. Golden, C. J. Howard, A. R. Ravishankara, and M. J. Molina (1990): "Chemical Kinetics and Photochemical Data for Use in Stratospheric Modeling. Evaluation Number 9," JPL Publication 90-1, January.

Dodge, M. C. (1984): "Combined Effects of Organic Reactivity and NMHC/NO_x Ratio on Photochemical Oxidant Formation -- A Modeling Study," Atmos. Environ., 18, 1657.

Dong, S. and Dasgupta, P. K. (1987): "Fast Fluorometric Flow Analysis of Formaldehyde," Environ. Sci. and Technol. 21, 581-588.

Doyle, G. J., P. J. Bekowies, A. M. Winer, and J. N. Pitts, Jr. (1977): Environ. Sci. Technol. 11, 45

Gardner, E. P., P. D. Sperry, and J. G. Calvert (1987): "Photodecomposition of Acrolein in O_2-N_2 Mixtures," J. Phys. Chem. 91, 1922.

Gery, M. W., G. Z. Whitten, and J. P. Killus (1988): "Development and Testing of the CBM-IV For Urban and Regional Modeling,", EPA-600/ 3-88-012, January.

Gery, M. W. (1991): "Review of the SAPRC-90 Chemical Mechanism," Report to the California Air Resources Board, Contract No. A132-055, Sacramento, CA.

Hartmann, D., A. Gedra, D. Rhasa, and R. Zellner (1987): Proceedings, 4th European Symposium on the Physico-Chemical Behavior of Atmospheric Pollutants, 1986; D. Riedel Publishing Co., Dordrecht, Holland, p. 225.

Jeffries H. E., K. G. Sexton, J. R. Arnold, and T. L. Kale (1989): "Validation Testing of New Mechanisms with Outdoor Chamber Data. Volume 2: Analysis of VOC Data for the CB4 and CAL Photochemical Mechanisms," Final Report, EPA-600/3-89-010b.

Jeffries, H. E., K. G. Sexton, J. R. Arnold, Y. Bai, J. L. Li, and R. Crouse (1990): "A Chamber and Modeling Study to Assess the Photochemistry of Formaldehyde," Report on EPA Cooperative Agreement CR-813964, Atmospheric Research and Exposure Assessment Laboratory, EPA, Research Triangle Park, NC.

Jeffries, H. E. and R. Crouse (1991): "Scientific and Technical Issues Related to the Application of Incremental Reactivity. Part II: Explaining Mechanism Differences," Report prepared for Western States Petroleum Association, Glendale, CA, October.

Johnson, G. M. (1983): "Factors Affecting Oxidant Formation in Sydney Air," in "The Urban Atmosphere -- Sydney, a Case Study." Eds. J. N. Carras and G. M. Johnson (CSIRO, Melbourne), pp. 393-408.

Lurmann, F. W., H. H. Main, K. T. Knapp, L. Stockburrger, R. A. Rasmussen and K. Fung (1992): "Analysis of Ambient VOC Data Collected in the Southern California Air Quality Study," Final Report to California Air Resources Board Contract No. A382-130; Research Division, Sacramento, CA, February.

MathSoft (1992): "Mathcad 3.1 Users Guide Windows Version," MathSoft, Inc., 201 Broadway, Cambridge, Mass.

Moortgat, G. K., W. Seiler and P. Warneck (1983): "Photodissociation of HCHO in Air: CO and H2 Quantum Yields at 220 and 300 K," J. Chem. Phys. 78, 1185-1190.

Rogers, J. D. (1990): "Ultraviolet Absorption Cross Sections and Atmospheric Photodissociation Rate Constants of Formaldehyde," J. Phys. Chem., 90, 4011-4015.

Russell, A. G. (1990): "Air Quality Modeling of Alternative Fuel Use in Los Angeles, CA: Sensitivity of Pollutant Formation to Individual Pollutant Compounds," the AWMA 83rd Annual Meeting, June 24-29.

SAS (1985): "SAS User's Guide: Statistics. Version 5 Edition," SAS Institute, Inc., Cary, NC.

Snedecor, G. W. and W. G. Cochran (1967): "Statistical Methods", sixth edition, Iowa State University Press, Ames Iowa.

Stephens, E. R., F. R. Burleson and E. A. Cardiff (1965): "The Production of Pure Peroxyacyl Nitrates," J. Air Pollut. Control Assoc., 15, 87.

Stockwell, W. R., P. Middleton, J. S. Chang, and X. Tang (1990): "The Second Generation Regional Acid Deposition Model Chemical Mechanism for Regional Air Quality Modeling," J. Geophys. Res. 95, 16343-16376.

Tuazon, E. C., R. Atkinson, A. M. Winer and J. N. Pitts, Jr. (1984): Arch. Environ. Contam. Toxicol. 13, 691.

Tuazon, E. C., R. Atkinson, S. M. Aschmann, M. A. Goodman and A. M. Winer (1988): Int J. Chem. Kinet. 20, 241.

Tuazon, E. C., W. P. L. Carter and R. Atkinson (1991a): "Thermal Decomposition of Peroxyacetyl Nitrate and Reactions of Acetyl Peroxy Radicals with NO and NO_2 Over the Temperature Range 283-313 K," J. Phys. Chem., in 95, 2434.

Tuazon, E. C., W. P. L. Carter, S. M. Aschmann, and R. Atkinson (1991b): "Products of the Gas-Phase Reaction of Methyl tert-Butyl Ether with the OH Radical in the Presence of NO_x," Int. J. Chem. Kinet., 23, 1003-1015.

Wallington, T. J. and S. M. Japar (1991): "Atmospheric Chemistry of Diethyl-ether and Ethyl-t-butylether," Environ. Sci. Technol., 25, 410-414.

Zafonte, L., P. L. Rieger, and J. R. Holmes (1977): "Nitrogen Dioxide Photolysis in the Los Angeles Atmosphere," Environ. Sci. Technol. 11, 483-487.

APPENDIX A

DETAILED DATA TABULATIONS AND PLOTS

Table A-1. Derivation of Reactivities with Respect to Hourly Ozone Formation and NO Oxidation for All Test VOC Experiments.

Run Set	Added (ppm)	Time (hr)	Reacted [a] (ppm)	Deriv.	$d(O_3\text{-NO})$ (ppm) Test	Base Fit	Change	Reactivity (mol/mol) Incremental	Mechanistic
Carbon Monoxide									
418	110.	1	0.081 ±0.032	IntOH	0.081	0.050 ±0.009	0.031 ±0.012	0.0003 ± 39%	0.38 ± 55%
3		2	0.173 ±0.032	IntOH	0.269	0.167 ±0.016	0.102 ±0.023	0.0009 ± 23%	0.59 ± 29%
		3	0.278 ±0.033	IntOH	0.452	0.309 ±0.024	0.143 ±0.034	0.0013 ± 24%	0.52 ± 26%
		4	0.395 ±0.035	IntOH	0.644	0.445 ±0.035	0.199 ±0.049	0.0018 ± 25%	0.50 ± 26%
		5	0.523 ±0.037	IntOH	0.864	0.566 ±0.040	0.298 ±0.056	0.0027 ± 19%	0.57 ± 20%
		6	0.662 ±0.040	IntOH	1.120	0.694 ±0.048	0.426 ±0.068	0.0039 ± 16%	0.64 ± 17%
416	130.	1	0.061 ±0.037	IntOH	0.229	0.050 ±0.009	0.179 ±0.012	0.0014 ± 7%	2.93 ± 62%
3		2	0.182 ±0.038	IntOH	0.402	0.148 ±0.017	0.254 ±0.024	0.0020 ± 10%	1.39 ± 23%
		3	0.301 ±0.039	IntOH	0.585	0.283 ±0.024	0.302 ±0.034	0.0023 ± 12%	1.00 ± 17%
		4	0.421 ±0.041	IntOH	0.770	0.412 ±0.035	0.358 ±0.050	0.0028 ± 14%	0.85 ± 17%
		5	0.561 ±0.043	IntOH	0.984	0.511 ±0.040	0.473 ±0.057	0.0036 ± 12%	0.84 ± 14%
		6	0.726 ±0.047	IntOH	1.238	0.610 ±0.049	0.628 ±0.070	0.0048 ± 11%	0.86 ± 13%
414	138.	1	0.208 ±0.051	IntOH	0.287	0.050 ±0.008	0.237 ±0.012	0.0017 ± 5%	1.14 ± 25%
3		2	0.371 ±0.054	IntOH	0.480	0.160 ±0.016	0.320 ±0.023	0.0023 ± 8%	0.86 ± 16%
		3	0.558 ±0.056	IntOH	0.676	0.298 ±0.024	0.378 ±0.034	0.0027 ± 9%	0.68 ± 13%
		4	0.810 ±0.057	IntOH	0.910	0.430 ±0.035	0.480 ±0.049	0.0035 ± 10%	0.59 ± 12%
		5	1.102 ±0.061	IntOH	1.152	0.543 ±0.040	0.609 ±0.056	0.0044 ± 9%	0.55 ± 11%
		6	1.370 ±0.069	IntOH	1.356	0.660 ±0.048	0.696 ±0.068	0.0050 ± 10%	0.51 ± 11%
Ethane									
68	10.01	1	0.015 ±0.004	IntOH	0.098	0.082 ±0.017	0.016 ±0.024	(0.002±0.002) (	1.1 ± 1.7)
1	±0.20	2	0.029 ±0.004	IntOH	0.222	0.186 ±0.022	0.036 ±0.032	0.0036 ± 87%	1.26 ± 88%
		3	0.043 ±0.005	IntOH	0.341	0.296 ±0.024	0.045 ±0.034	0.0045 ± 75%	1.04 ± 76%
		4	0.057 ±0.005	IntOH	0.446	0.400 ±0.026	0.046 ±0.037	0.0046 ± 80%	0.81 ± 80%
		5	0.071 ±0.005	IntOH	0.559	0.501 ±0.031	0.058 ±0.043	0.0058 ± 75%	0.81 ± 75%
		6	0.086 ±0.006	IntOH	0.675	0.618 ±0.039	0.057 ±0.056	0.0057 ± 97%	0.67 ± 97%
79	17.6	1	0.022 ±0.006	IntOH	0.123	0.075 ±0.017	0.048 ±0.024	0.0027 ± 51%	2.18 ± 57%
1	±0.4	2	0.043 ±0.006	IntOH	0.243	0.171 ±0.023	0.072 ±0.032	0.0041 ± 45%	1.66 ± 47%
		3	0.063 ±0.006	IntOH	0.356	0.280 ±0.024	0.076 ±0.034	0.0043 ± 45%	1.21 ± 46%
		4	0.084 ±0.006	IntOH	0.477	0.383 ±0.026	0.094 ±0.037	0.0053 ± 40%	1.12 ± 41%
		5	0.104 ±0.007	IntOH	0.591	0.479 ±0.031	0.112 ±0.044	0.0064 ± 39%	1.07 ± 40%
		6	0.127 ±0.007	IntOH	0.724	0.589 ±0.040	0.135 ±0.056	0.0077 ± 42%	1.06 ± 42%
62	17.6	1	0.018 ±0.006	IntOH	0.120	0.087 ±0.017	0.033 ±0.024	0.0019 ± 73%	1.87 ± 80%
1	±0.4	2	0.042 ±0.006	IntOH	0.279	0.195 ±0.023	0.084 ±0.032	0.0048 ± 38%	1.99 ± 41%
		3	0.064 ±0.007	IntOH	0.416	0.307 ±0.024	0.109 ±0.034	0.0062 ± 31%	1.70 ± 33%
		4	0.087 ±0.007	IntOH	0.553	0.411 ±0.026	0.142 ±0.037	0.0081 ± 26%	1.64 ± 27%
		5	0.112 ±0.007	IntOH	0.704	0.516 ±0.031	0.188 ±0.043	0.0107 ± 23%	1.68 ± 24%
		6	0.144 ±0.008	IntOH	0.882	0.637 ±0.039	0.245 ±0.056	0.0139 ± 23%	1.70 ± 23%
73	18.1	1	0.017 ±0.006	IntOH	0.091	0.078 ±0.017	0.013 ±0.024	(0.0007±0.001) (	0.8 ± 1.5)
1	±0.4	2	0.035 ±0.006	IntOH	0.213	0.178 ±0.023	0.035 ±0.032	0.0019 ± 91%	1.00 ± 93%
		3	0.055 ±0.006	IntOH	0.333	0.287 ±0.024	0.046 ±0.034	0.0025 ± 75%	0.83 ± 76%
		4	0.076 ±0.007	IntOH	0.448	0.391 ±0.026	0.057 ±0.037	0.0032 ± 65%	0.75 ± 65%
		5	0.098 ±0.007	IntOH	0.562	0.489 ±0.031	0.072 ±0.043	0.0040 ± 60%	0.74 ± 60%
		6	0.122 ±0.007	IntOH	0.696	0.603 ±0.040	0.093 ±0.056	0.0052 ± 60%	0.77 ± 60%
88	24.4	1	0.027 ±0.008	IntOH	0.150	0.070 ±0.018	0.080 ±0.025	0.0033 ± 31%	2.91 ± 43%
1	±0.5	2	0.056 ±0.009	IntOH	0.297	0.162 ±0.023	0.135 ±0.033	0.0055 ± 24%	2.42 ± 29%
		3	0.082 ±0.009	IntOH	0.428	0.269 ±0.025	0.159 ±0.035	0.0065 ± 22%	1.95 ± 25%
		4	0.108 ±0.009	IntOH	0.558	0.372 ±0.027	0.186 ±0.038	0.0076 ± 21%	1.72 ± 22%
		5	0.142 ±0.010	IntOH	0.719	0.465 ±0.032	0.254 ±0.045	0.0104 ± 18%	1.79 ± 19%
		6	0.178 ±0.011	IntOH	0.881	0.570 ±0.041	0.311 ±0.058	0.0127 ± 19%	1.74 ± 20%

Table A-1 (continued)

Run Set	Added (ppm)	Time (hr)	Reacted [a] (ppm)	Deriv.	d(O_3-NO) (ppm) Test	Base Fit	Change	Reactivity (mol/mol) Incremental	Mechanistic
99	16.6	1	0.008 ±0.009	IntOH	0.050	0.034 ±0.007	0.016 ±0.010	0.0010 ± 60%	(1.9 ± 2.5)
2	±0.9	2	0.024 ±0.009	IntOH	0.140	0.097 ±0.011	0.043 ±0.016	0.0026 ± 38%	1.78 ± 55%
		3	0.041 ±0.010	IntOH	0.240	0.179 ±0.014	0.061 ±0.020	0.0036 ± 33%	1.48 ± 40%
		4	0.060 ±0.010	IntOH	0.347	0.274 ±0.014	0.073 ±0.020	0.0044 ± 28%	1.22 ± 33%
		5	0.078 ±0.011	IntOH	0.452	0.359 ±0.016	0.093 ±0.023	0.0056 ± 25%	1.19 ± 28%
		6	0.096 ±0.012	IntOH	0.562	0.443 ±0.018	0.119 ±0.025	0.0071 ± 22%	1.23 ± 24%
92	17.1	1	0.010 ±0.008	IntOH	0.039	0.034 ±0.007	0.005 ±0.010	(0.0003±.0006)	(0.5 ± 1.1)
2	±0.5	2	0.023 ±0.009	IntOH	0.131	0.100 ±0.012	0.031 ±0.017	0.0018 ± 53%	1.37 ± 65%
		3	0.038 ±0.009	IntOH	0.230	0.185 ±0.014	0.045 ±0.020	0.0026 ± 45%	1.18 ± 51%
		4	0.056 ±0.009	IntOH	0.345	0.285 ±0.015	0.060 ±0.021	0.0035 ± 34%	1.08 ± 38%
		5	0.077 ±0.009	IntOH	0.451	0.375 ±0.016	0.076 ±0.023	0.0044 ± 31%	0.99 ± 33%
		6	0.100 ±0.010	IntOH	0.581	0.463 ±0.018	0.118 ±0.025	0.0069 ± 22%	1.18 ± 24%
332	20.0	1	0.012 ±0.007	IntOH	0.104	0.057 ±0.008	0.047 ±0.012	0.0023 ± 25%	3.93 ± 61%
3	±0.4	2	0.040 ±0.007	IntOH	0.320	0.195 ±0.016	0.125 ±0.023	0.0063 ± 18%	3.11 ± 25%
		3	0.070 ±0.007	IntOH	0.518	0.363 ±0.023	0.155 ±0.033	0.0078 ± 21%	2.22 ± 23%
		4	0.102 ±0.007	IntOH	0.708	0.517 ±0.034	0.191 ±0.048	0.0095 ± 25%	1.87 ± 26%
		5	0.139 ±0.008	IntOH	0.909	0.678 ±0.039	0.231 ±0.055	0.0115 ± 24%	1.66 ± 24%
		6	0.180 ±0.009	IntOH	1.115	0.858 ±0.047	0.257 ±0.067	0.0129 ± 26%	1.43 ± 26%
333	21.0	1	0.033 ±0.007	IntOH	0.269	0.058 ±0.008	0.211 ±0.012	0.0100 ± 6%	6.42 ± 22%
3	±0.4	2	0.068 ±0.007	IntOH	0.501	0.195 ±0.016	0.306 ±0.023	0.0146 ± 8%	4.48 ± 13%
		3	0.106 ±0.007	IntOH	0.703	0.363 ±0.023	0.340 ±0.033	0.0162 ± 10%	3.20 ± 12%
		4	0.146 ±0.008	IntOH	0.910	0.518 ±0.034	0.392 ±0.048	0.0186 ± 12%	2.67 ± 13%
		5	0.189 ±0.009	IntOH	1.125	0.680 ±0.039	0.445 ±0.055	0.021 ± 12%	2.35 ± 13%
		6	0.235 ±0.010	IntOH	1.299	0.860 ±0.047	0.439 ±0.067	0.021 ± 15%	1.87 ± 16%
235	43.7	1	0.021 ±0.014	IntOH	0.072	0.040 ±0.008	0.032 ±0.012	0.0007 ± 37%	1.51 ± 78%
3	±1.3	2	0.071 ±0.015	IntOH	0.236	0.151 ±0.016	0.085 ±0.022	0.0019 ± 27%	1.20 ± 34%
		3	0.124 ±0.015	IntOH	0.409	0.294 ±0.023	0.115 ±0.032	0.0026 ± 28%	0.93 ± 31%
		4	0.178 ±0.016	IntOH	0.586	0.435 ±0.033	0.151 ±0.047	0.0034 ± 31%	0.85 ± 33%
		5	0.239 ±0.018	IntOH	0.788	0.586 ±0.038	0.202 ±0.054	0.0046 ± 27%	0.85 ± 28%
		6	0.306 ±0.020	IntOH	1.006	0.754 ±0.047	0.252 ±0.066	0.0058 ± 26%	0.83 ± 27%
Propane									
226	11.57	1	0.009 ±0.016	IntOH	0.046	0.035 ±0.008	0.011 ±0.012	(0.0009±0.001)	(1.2 ± 2.4)
3	±0.23	2	0.033 ±0.016	IntOH	0.146	0.135 ±0.016	0.011 ±0.023	(0.0010±0.002)	(0.3 ± 0.7)
		3	0.069 ±0.017	IntOH	0.276	0.261 ±0.023	0.015 ±0.033	(0.001±0.003)	(0.2 ± 0.5)
		4	0.110 ±0.017	IntOH	0.408	0.390 ±0.034	0.018 ±0.048	(0.002±0.004)	(0.2 ± 0.4)
		5	0.163 ±0.018	IntOH	0.560	0.518 ±0.038	0.042 ±0.054	(0.004±0.005)	(0.3 ± 0.3)
		6	0.231 ±0.019	IntOH	0.736	0.658 ±0.047	0.078 ±0.066	0.0068 ± 85%	0.34 ± 85%
305	20.1	1	0.021 ±0.052	IntOH	0.060	0.040 ±0.008	0.020 ±0.012	0.0010 ± 60%	(0.9 ± 2.4)
3	±0.5	2	0.073 ±0.052	IntOH	0.191	0.138 ±0.016	0.053 ±0.023	0.0027 ± 43%	0.74 ± 83%
		3	0.138 ±0.053	IntOH	0.353	0.272 ±0.023	0.081 ±0.033	0.0040 ± 41%	0.59 ± 56%
		4	0.209 ±0.055	IntOH	0.530	0.406 ±0.034	0.124 ±0.048	0.0061 ± 39%	0.59 ± 47%
		5	0.298 ±0.058	IntOH	0.752	0.543 ±0.039	0.209 ±0.055	0.0104 ± 26%	0.70 ± 33%
		6	0.405 ±0.062	IntOH	1.018	0.695 ±0.047	0.323 ±0.067	0.0160 ± 21%	0.80 ± 26%
230	28.8	1	0.057 ±0.040	IntOH	0.085	0.040 ±0.008	0.045 ±0.012	0.0016 ± 26%	0.79 ± 75%
3	±0.6	2	0.162 ±0.044	IntOH	0.249	0.133 ±0.016	0.116 ±0.023	0.0040 ± 20%	0.72 ± 34%
		3	0.265 ±0.048	IntOH	0.438	0.266 ±0.023	0.172 ±0.033	0.0060 ± 19%	0.65 ± 26%
		4	0.360 ±0.050	IntOH	0.648	0.399 ±0.034	0.249 ±0.048	0.0086 ± 19%	0.69 ± 24%
		5	0.445 ±0.050	IntOH	0.900	0.522 ±0.039	0.378 ±0.055	0.0131 ± 15%	0.85 ± 18%
		6	0.505 ±0.052	IntOH	1.180	0.654 ±0.048	0.526 ±0.067	0.0183 ± 13%	1.04 ± 16%

Table A-1 (continued)

Run Set	Added (ppm)	Time (hr)	Reacted [a] (ppm)	Deriv.	d(O_3-NO) (ppm) Test	Base Fit	Change	Reactivity (mol/mol) Incremental	Mechanistic
n-Butane									
59	1.82	1	0.015 ±0.006	IntOH	0.108	0.090 ±0.017	0.018 ±0.024	(0.010±0.013)	(1.2 ± 1.6)
1	±0.04	2	0.033 ±0.006	IntOH	0.223	0.201 ±0.023	0.022 ±0.032	(0.012 ±0.02)	(0.7 ± 1.0)
		3	0.053 ±0.006	IntOH	0.355	0.314 ±0.024	0.041 ±0.034	0.023 ± 83%	0.78 ± 83%
		4	0.072 ±0.006	IntOH	0.471	0.418 ±0.026	0.053 ±0.037	0.029 ± 70%	0.75 ± 70%
		5	0.093 ±0.006	IntOH	0.602	0.525 ±0.031	0.077 ±0.044	0.042 ± 56%	0.83 ± 57%
		6	0.120 ±0.007	IntOH	0.761	0.648 ±0.040	0.113 ±0.056	0.062 ± 50%	0.94 ± 50%
51	2.31	1	0.018 ±0.008	IntOH	0.097	0.099 ±0.018	-0.002 ±0.025	(-.0009±0.011)	(-0.1 ± 1.4)
1	±0.07	2	0.041 ±0.009	IntOH	0.225	0.219 ±0.024	0.006 ±0.034	(0.003±0.015)	(0.1 ± 0.8)
		3	0.065 ±0.009	IntOH	0.359	0.334 ±0.025	0.025 ±0.036	(0.011 ±0.02)	(0.4 ± 0.6)
		4	0.089 ±0.010	IntOH	0.494	0.439 ±0.028	0.055 ±0.039	0.024 ± 71%	0.62 ± 72%
		5	0.116 ±0.010	IntOH	0.647	0.552 ±0.032	0.095 ±0.046	0.041 ± 49%	0.82 ± 49%
		6	0.148 ±0.011	IntOH	0.830	0.684 ±0.042	0.146 ±0.059	0.063 ± 41%	0.99 ± 41%
53	5.21	1	0.035 ±0.027	IntOH	0.105	0.097 ±0.018	0.008 ±0.025	(0.002±0.005)	(0.2 ± 0.7)
1	±0.11	2	0.079 ±0.029	IntOH	0.229	0.214 ±0.023	0.015 ±0.033	(0.003±0.006)	(0.2 ± 0.4)
		3	0.139 ±0.030	IntOH	0.382	0.329 ±0.025	0.053 ±0.035	0.0102 ± 66%	0.38 ± 70%
		4	0.194 ±0.031	IntOH	0.518	0.433 ±0.027	0.085 ±0.038	0.0163 ± 45%	0.44 ± 48%
		5	0.264 ±0.031	IntOH	0.678	0.545 ±0.032	0.133 ±0.045	0.026 ± 34%	0.50 ± 36%
		6	0.357 ±0.032	IntOH	0.878	0.675 ±0.041	0.203 ±0.058	0.039 ± 29%	0.57 ± 30%
82	6.75	1	0.033 ±0.021	IntOH	0.098	0.073 ±0.017	0.025 ±0.025	0.0037 ± 98%	(0.8 ± 0.9)
1	±0.14	2	0.069 ±0.021	IntOH	0.208	0.168 ±0.023	0.041 ±0.032	0.0060 ± 80%	0.58 ± 86%
		3	0.115 ±0.022	IntOH	0.343	0.276 ±0.024	0.067 ±0.035	0.0100 ± 51%	0.59 ± 55%
		4	0.154 ±0.023	IntOH	0.461	0.379 ±0.027	0.082 ±0.038	0.0122 ± 46%	0.54 ± 48%
		5	0.203 ±0.025	IntOH	0.611	0.473 ±0.031	0.138 ±0.044	0.020 ± 32%	0.68 ± 34%
		6	0.257 ±0.027	IntOH	0.775	0.582 ±0.040	0.193 ±0.057	0.029 ± 30%	0.75 ± 31%
86	7.00	1	0.024 ±0.027	IntOH	0.112	0.071 ±0.018	0.041 ±0.025	0.0058 ± 61%	(1.7 ± 2.2)
1	±0.14	2	0.055 ±0.029	IntOH	0.225	0.164 ±0.023	0.061 ±0.033	0.0088 ± 54%	1.11 ± 75%
		3	0.096 ±0.030	IntOH	0.348	0.271 ±0.025	0.077 ±0.035	0.0110 ± 45%	0.80 ± 55%
		4	0.145 ±0.031	IntOH	0.472	0.374 ±0.027	0.098 ±0.038	0.0140 ± 39%	0.67 ± 44%
		5	0.202 ±0.031	IntOH	0.637	0.468 ±0.032	0.169 ±0.045	0.024 ± 26%	0.84 ± 30%
		6	0.266 ±0.032	IntOH	0.813	0.574 ±0.041	0.239 ±0.057	0.034 ± 24%	0.90 ± 27%
135	6.06	1	0.017 ±0.035	IntOH	0.044	0.026 ±0.007	0.018 ±0.010	0.0029 ± 54%	(1.1 ± 2.4)
2	±0.12	2	0.041 ±0.035	IntOH	0.109	0.079 ±0.011	0.030 ±0.016	0.0049 ± 55%	(0.7 ± 0.7)
		3	0.083 ±0.036	IntOH	0.212	0.155 ±0.014	0.057 ±0.020	0.0094 ± 35%	0.69 ± 55%
		4	0.123 ±0.037	IntOH	0.312	0.244 ±0.014	0.068 ±0.020	0.0113 ± 30%	0.56 ± 42%
		5	0.163 ±0.039	IntOH	0.416	0.321 ±0.016	0.095 ±0.023	0.0157 ± 24%	0.58 ± 34%
		6	0.209 ±0.041	IntOH	0.534	0.402 ±0.018	0.132 ±0.025	0.022 ± 19%	0.63 ± 27%
97	6.12	1	0.017 ±0.032	IntOH	0.058	0.033 ±0.007	0.025 ±0.010	0.0040 ± 39%	(1.4 ± 2.7)
2	±0.12	2	0.044 ±0.032	IntOH	0.144	0.098 ±0.012	0.046 ±0.016	0.0075 ± 35%	1.05 ± 82%
		3	0.073 ±0.033	IntOH	0.238	0.180 ±0.014	0.058 ±0.020	0.0094 ± 34%	0.79 ± 57%
		4	0.107 ±0.034	IntOH	0.347	0.276 ±0.014	0.071 ±0.020	0.0116 ± 29%	0.66 ± 43%
		5	0.142 ±0.035	IntOH	0.461	0.363 ±0.016	0.098 ±0.023	0.0161 ± 23%	0.69 ± 34%
		6	0.191 ±0.038	IntOH	0.618	0.448 ±0.018	0.170 ±0.025	0.028 ± 15%	0.89 ± 25%
94	7.16	1	0.020 ±0.022	IntOH	0.050	0.033 ±0.008	0.017 ±0.012	0.0023 ± 70%	(0.9 ± 1.1)
2	±0.14	2	0.047 ±0.022	IntOH	0.127	0.100 ±0.014	0.027 ±0.020	0.0037 ± 74%	0.56 ± 88%
		3	0.084 ±0.023	IntOH	0.220	0.180 ±0.017	0.040 ±0.024	0.0055 ± 60%	0.47 ± 66%
		4	0.131 ±0.023	IntOH	0.330	0.284 ±0.017	0.046 ±0.025	0.0065 ± 53%	0.35 ± 56%
		5	0.184 ±0.024	IntOH	0.451	0.364 ±0.020	0.087 ±0.028	0.0121 ± 32%	0.47 ± 34%
		6	0.247 ±0.025	IntOH	0.574	0.450 ±0.021	0.124 ±0.030	0.0173 ± 25%	0.50 ± 27%
224	9.76	1	0.053 ±0.042	IntOH	0.067	0.036 ±0.008	0.031 ±0.012	0.0031 ± 38%	0.58 ± 88%
3	±0.41	2	0.105 ±0.043	IntOH	0.197	0.141 ±0.016	0.056 ±0.023	0.0058 ± 40%	0.53 ± 57%
		3	0.157 ±0.044	IntOH	0.354	0.276 ±0.023	0.078 ±0.033	0.0079 ± 42%	0.49 ± 51%
		4	0.208 ±0.046	IntOH	0.532	0.412 ±0.034	0.120 ±0.048	0.0122 ± 40%	0.58 ± 46%
		5	0.258 ±0.048	IntOH	0.726	0.546 ±0.038	0.180 ±0.054	0.0185 ± 30%	0.70 ± 36%
		6	0.309 ±0.052	IntOH	0.953	0.691 ±0.047	0.262 ±0.067	0.027 ± 26%	0.85 ± 30%

Table A-1 (continued)

Run Set	Added (ppm)	Time (hr)	Reacted [a] (ppm)	Deriv.	d(O_3-NO) (ppm) Test	Base Fit	Change	Reactivity (mol/mol) Incremental	Mechanistic
393	3.46	1	0.011 ±0.017	IntOH	0.054	0.058 ±0.008	-0.004 ±0.019	(-0.001±0.006)	(-0.4 ± 1.8)
4	±0.07	2	0.045 ±0.018	IntOH	0.189	0.233 ±0.020	-0.044 ±0.040	-0.0127 ± 90%	-0.99 ± 99%
		3	0.100 ±0.020	IntOH	0.381	0.430 ±0.042	-0.049 ±0.065	(-0.014 ±0.02)	(-0.5 ± 0.7)
		4	0.161 ±0.019	IntOH	0.562	0.561 ±0.030	0.001 ±0.078	(0.0002 ±0.02)	(0.0 ± 0.5)
		5	0.204 ±0.018	IntOH	0.681	0.621 ±0.030	0.060 ±0.088	(0.02 ±0.03)	(0.3 ± 0.4)
		6	0.226 ±0.018	IntOH	0.739	0.639 ±0.034	0.100 ±0.106	(0.03 ±0.03)	(0.4 ± 0.5)
389	3.60	1	0.012 ±0.023	IntOH	0.052	0.060 ±0.008	-0.008 ±0.020	(-0.002±0.006)	(-0.7 ± 2.1)
4	±0.07	2	0.037 ±0.025	IntOH	0.193	0.240 ±0.021	-0.047 ±0.041	-0.0132 ± 86%	(-1.3 ± 1.4)
		3	0.075 ±0.026	IntOH	0.372	0.445 ±0.045	-0.073 ±0.067	-0.020 ± 92%	-0.98 ± 99%
		4	0.124 ±0.025	IntOH	0.544	0.571 ±0.032	-0.026 ±0.080	(-0.007 ±0.02)	(-0.2 ± 0.7)
		5	0.184 ±0.024	IntOH	0.654	0.626 ±0.032	0.028 ±0.090	(0.008 ±0.03)	(0.2 ± 0.5)
		6	0.256 ±0.025	IntOH	0.718	0.641 ±0.037	0.077 ±0.109	(0.02 ±0.03)	(0.3 ± 0.4)
Isobutane									
228	2.72	1	0.007 ±0.013	IntOH	0.044	0.038 ±0.008	0.006 ±0.012	(0.002±0.004)	(0.9 ± 2.4)
3	±0.05	2	0.023 ±0.013	IntOH	0.140	0.135 ±0.016	0.005 ±0.023	(0.002±0.008)	(0.2 ± 1.0)
		3	0.045 ±0.013	IntOH	0.273	0.266 ±0.023	0.007 ±0.033	(0.002±0.012)	(0.1 ± 0.7)
		4	0.069 ±0.013	IntOH	0.412	0.399 ±0.034	0.013 ±0.048	(0.005 ±0.02)	(0.2 ± 0.7)
		5	0.093 ±0.014	IntOH	0.560	0.523 ±0.039	0.037 ±0.054	(0.014 ±0.02)	(0.4 ± 0.6)
		6	0.123 ±0.015	IntOH	0.739	0.656 ±0.047	0.083 ±0.067	0.030 ± 81%	0.67 ± 81%
303	6.62	1	0.011 ±0.080	IntOH	0.039	0.040 ±0.008	-0.001 ±0.012	(-.0001±0.002)	(-0.1 ± 1.1)
3	±0.16	2	0.046 ±0.080	IntOH	0.136	0.138 ±0.016	-0.002 ±0.023	(-.0004±0.003)	(-0.1 ± 0.5)
		3	0.097 ±0.082	IntOH	0.278	0.270 ±0.023	0.008 ±0.033	(0.001±0.005)	(0.1 ± 0.3)
		4	0.157 ±0.085	IntOH	0.443	0.403 ±0.034	0.040 ±0.048	(0.006±0.007)	(0.3 ± 0.3)
		5	0.233 ±0.092	IntOH	0.656	0.538 ±0.038	0.118 ±0.054	0.0179 ± 46%	0.51 ± 60%
		6	0.333 ±0.103	IntOH	0.937	0.687 ±0.047	0.250 ±0.067	0.038 ± 27%	0.75 ± 41%
241	10.21	1	0.009 ±0.029	IntOH	0.051	0.037 ±0.008	0.014 ±0.012	0.0013 ± 86%	(1.5 ± 4.7)
3	±0.21	2	0.039 ±0.029	IntOH	0.164	0.145 ±0.016	0.019 ±0.023	(0.002±0.002)	(0.5 ± 0.7)
		3	0.084 ±0.030	IntOH	0.321	0.277 ±0.023	0.044 ±0.033	0.0044 ± 74%	0.53 ± 82%
		4	0.153 ±0.030	IntOH	0.533	0.410 ±0.034	0.123 ±0.048	0.0120 ± 39%	0.80 ± 44%
		5	0.267 ±0.032	IntOH	0.842	0.552 ±0.039	0.290 ±0.055	0.028 ± 19%	1.09 ± 22%
		6	0.418 ±0.034	IntOH	1.209	0.710 ±0.047	0.499 ±0.067	0.049 ± 14%	1.19 ± 16%
232	20.9	1	0.021 ±0.212	IntOH	0.069	0.038 ±0.008	0.031 ±0.012	0.0015 ± 38%	(1.5 ±14.7)
3	±0.4	2	0.074 ±0.213	IntOH	0.210	0.134 ±0.016	0.076 ±0.023	0.0037 ± 30%	(1.0 ± 3.0)
		3	0.148 ±0.215	IntOH	0.399	0.264 ±0.023	0.135 ±0.033	0.0064 ± 25%	(0.9 ± 1.3)
		4	0.244 ±0.219	IntOH	0.642	0.396 ±0.034	0.246 ±0.048	0.0117 ± 20%	1.00 ± 91%
		5	0.381 ±0.229	IntOH	0.981	0.518 ±0.039	0.463 ±0.055	0.022 ± 12%	1.22 ± 61%
		6	0.539 ±0.245	IntOH	1.373	0.647 ±0.047	0.726 ±0.067	0.035 ± 9%	1.35 ± 46%
n-Hexane									
201	1.168	1	0.003 ±0.041	IntOH	0.045	0.038 ±0.008	0.007 ±0.012	(0.006±0.010)	(2.4 ±34.2)
3	±0.031	2	0.007 ±0.041	IntOH	0.110	0.135 ±0.016	-0.025 ±0.022	-0.022 ± 89%	(-3.4 ±19.5)
		3	0.014 ±0.041	IntOH	0.207	0.266 ±0.023	-0.059 ±0.032	-0.051 ± 55%	(-4.1 ±11.9)
		4	0.023 ±0.042	IntOH	0.313	0.398 ±0.033	-0.085 ±0.047	-0.073 ± 56%	(-3.8 ± 7.3)
		5	0.031 ±0.044	IntOH	0.424	0.527 ±0.038	-0.103 ±0.054	-0.088 ± 53%	(-3.3 ± 5.0)
		6	0.041 ±0.046	IntOH	0.558	0.667 ±0.047	-0.109 ±0.066	-0.093 ± 60%	(-2.7 ± 3.4)
209	1.58	1	0.014 ±0.013	IntOH	0.055	0.038 ±0.008	0.017 ±0.012	0.0108 ± 69%	(1.2 ± 1.4)
3	±0.04	2	0.026 ±0.013	IntOH	0.102	0.128 ±0.016	-0.026 ±0.023	-0.0165 ± 87%	(-1.0 ± 1.0)
		3	0.039 ±0.013	IntOH	0.162	0.258 ±0.023	-0.096 ±0.033	-0.061 ± 34%	-2.45 ± 49%
		4	0.064 ±0.014	IntOH	0.284	0.388 ±0.034	-0.104 ±0.048	-0.066 ± 46%	-1.62 ± 51%
		5	0.076 ±0.014	IntOH	0.359	0.509 ±0.039	-0.150 ±0.055	-0.095 ± 36%	-1.98 ± 41%
		6	0.092 ±0.015	IntOH	0.480	0.640 ±0.047	-0.160 ±0.067	-0.101 ± 42%	-1.75 ± 45%

Table A-1 (continued)

Run Set	Added (ppm)	Time (hr)	Reacted [a] (ppm)	Deriv.	d(O_3-NO) (ppm) Test	Base Fit	Change	Reactivity (mol/mol) Incremental	Mechanistic
Isooctane									
291	10.14	1	0.007 ±0.086	IntOH	0.044	0.043 ±0.009	0.001 ±0.012	(0.0001±0.001)	(0.1 ± 2.4)
3	±0.20	2	0.026 ±0.086	IntOH	0.131	0.168 ±0.016	-0.037 ±0.023	-0.0036 ± 64%	(-1.4 ± 4.7)
		3	0.063 ±0.087	IntOH	0.265	0.333 ±0.024	-0.068 ±0.034	-0.0067 ± 50%	(-1.1 ± 1.6)
		4	0.115 ±0.089	IntOH	0.449	0.489 ±0.035	-0.040 ±0.049	(-0.004±0.005)	(-0.3 ± 0.5)
		5	0.189 ±0.094	IntOH	0.707	0.666 ±0.040	0.041 ±0.056	(0.004±0.006)	(0.2 ± 0.3)
		6	0.294 ±0.101	IntOH	1.060	0.870 ±0.048	0.190 ±0.069	0.0188 ± 36%	0.65 ± 50%
293	10.64	1	0.014 ±0.100	IntOH	0.050	0.040 ±0.008	0.010 ±0.012	(0.0010±0.001)	(0.8 ± 5.6)
3	±0.22	2	0.041 ±0.099	IntOH	0.131	0.160 ±0.016	-0.029 ±0.023	-0.0028 ± 78%	(-0.7 ± 1.8)
		3	0.087 ±0.100	IntOH	0.261	0.318 ±0.024	-0.057 ±0.033	-0.0054 ± 58%	(-0.7 ± 0.8)
		4	0.153 ±0.102	IntOH	0.438	0.470 ±0.034	-0.032 ±0.049	(-0.003±0.005)	(-0.2 ± 0.3)
		5	0.248 ±0.108	IntOH	0.685	0.636 ±0.039	0.049 ±0.055	(0.005±0.005)	(0.2 ± 0.2)
		6	0.382 ±0.118	IntOH	1.033	0.825 ±0.048	0.208 ±0.068	0.0195 ± 33%	0.54 ± 45%
n-Octane									
239	1.55	1	0.011 ±0.016	IntOH	0.025	0.043 ±0.008	-0.018 ±0.012	-0.0116 ± 67%	(-1.6 ± 2.6)
3	±0.03	2	0.022 ±0.016	IntOH	0.060	0.142 ±0.016	-0.082 ±0.023	-0.053 ± 28%	-3.74 ± 80%
		3	0.033 ±0.017	IntOH	0.112	0.284 ±0.024	-0.172 ±0.033	-0.111 ± 20%	-5.26 ± 54%
		4	0.043 ±0.017	IntOH	0.175	0.424 ±0.034	-0.249 ±0.049	-0.160 ± 20%	-5.80 ± 44%
		5	0.053 ±0.017	IntOH	0.252	0.561 ±0.039	-0.309 ±0.056	-0.20 ± 18%	-5.79 ± 37%
		6	0.064 ±0.018	IntOH	0.334	0.712 ±0.048	-0.378 ±0.068	-0.24 ± 18%	-5.93 ± 33%
237	1.66	1	0.004 ±0.018	IntOH	0.022	0.039 ±0.008	-0.017 ±0.012	-0.0100 ± 71%	(-3.7 ±14.9)
3	±0.03	2	0.014 ±0.018	IntOH	0.059	0.149 ±0.016	-0.090 ±0.023	-0.054 ± 25%	(-6.3 ± 7.8)
		3	0.030 ±0.018	IntOH	0.114	0.286 ±0.023	-0.172 ±0.033	-0.104 ± 19%	-5.69 ± 62%
		4	0.049 ±0.018	IntOH	0.180	0.423 ±0.034	-0.243 ±0.048	-0.147 ± 20%	-4.93 ± 41%
		5	0.072 ±0.018	IntOH	0.257	0.570 ±0.038	-0.313 ±0.054	-0.189 ± 17%	-4.33 ± 31%
		6	0.098 ±0.019	IntOH	0.345	0.734 ±0.047	-0.389 ±0.066	-0.23 ± 17%	-3.96 ± 26%
Ethene									
203	0.217	1	0.004 ±0.026	D(d3)	0.056	0.039 ±0.008	0.017 ±0.012	0.077 ± 70%	(4.3 ±29.1)
3	±0.019	2	0.016 ±0.026	D(d3)	0.201	0.150 ±0.016	0.051 ±0.023	0.23 ± 45%	(3.1 ± 5.1)
		3	0.031 ±0.025	D(d3)	0.362	0.298 ±0.023	0.064 ±0.033	0.30 ± 52%	2.09 ± 97%
		4	0.047 ±0.025	D(d3)	0.538	0.441 ±0.034	0.097 ±0.048	0.45 ± 50%	2.06 ± 73%
		5	0.065 ±0.025	D(d3)	0.727	0.591 ±0.038	0.136 ±0.054	0.63 ± 41%	2.11 ± 55%
		6	0.086 ±0.025	D(d3)	0.956	0.758 ±0.047	0.198 ±0.067	0.91 ± 35%	2.31 ± 44%
199	0.386	1	0.005 ±0.036	D(d3)	0.063	0.037 ±0.008	0.026 ±0.012	0.067 ± 46%	(4.8 ±31.6)
3	±0.026	2	0.026 ±0.037	D(d3)	0.237	0.148 ±0.016	0.089 ±0.023	0.23 ± 27%	(3.4 ± 5.0)
		3	0.053 ±0.038	D(d3)	0.434	0.291 ±0.023	0.143 ±0.033	0.37 ± 24%	2.69 ± 76%
		4	0.086 ±0.037	D(d3)	0.653	0.431 ±0.034	0.222 ±0.048	0.58 ± 23%	2.58 ± 49%
		5	0.131 ±0.035	D(d3)	0.933	0.584 ±0.039	0.349 ±0.055	0.91 ± 17%	2.68 ± 31%
		6	0.172 ±0.034	D(d3)	1.198	0.759 ±0.047	0.439 ±0.067	1.14 ± 17%	2.55 ± 25%
Propene									
65	0.083	1	0.002 ±0.020	D(d3)	0.087	0.085 ±0.017	0.002 ±0.024	(0.03 ± 0.3)	(1.0 ±14.0)
1	±0.014	2	0.012 ±0.020	D(d3)	0.223	0.190 ±0.022	0.033 ±0.032	0.40 ± 99%	(2.7 ± 5.3)
		3	0.026 ±0.019	D(d3)	0.358	0.302 ±0.024	0.056 ±0.034	0.68 ± 62%	2.14 ± 94%
		4	0.042 ±0.017	D(d3)	0.494	0.405 ±0.026	0.089 ±0.037	1.07 ± 45%	2.12 ± 58%
		5	0.056 ±0.015	D(d3)	0.629	0.508 ±0.031	0.121 ±0.043	1.46 ± 40%	2.17 ± 45%
		6	0.067 ±0.015	D(d3)	0.776	0.627 ±0.039	0.149 ±0.056	1.80 ± 41%	2.23 ± 43%
72	0.120	1	0.008 ±0.008	D(t3)	0.068	0.079 ±0.017	-0.011 ±0.024	(-0.09 ± 0.2)	(-1.4 ± 3.3)
1	±0.005	2	0.022 ±0.007	D(t3)	0.180	0.180 ±0.022	0.000 ±0.032	(0.0008 ± 0.3)	(0.0 ± 1.4)
		3	0.040 ±0.007	D(t3)	0.316	0.290 ±0.024	0.026 ±0.034	(0.2 ± 0.3)	(0.7 ± 0.8)
		4	0.059 ±0.006	D(t3)	0.432	0.393 ±0.026	0.039 ±0.037	0.33 ± 95%	0.66 ± 95%
		5	0.076 ±0.006	D(t3)	0.553	0.492 ±0.031	0.061 ±0.043	0.51 ± 72%	0.79 ± 72%
		6	0.090 ±0.006	D(t3)	0.695	0.606 ±0.039	0.089 ±0.056	0.74 ± 63%	0.98 ± 63%

Table A-1 (continued)

Run Set	Added (ppm)	Time (hr)	Reacted [a] (ppm)	Deriv.	d(O_3-NO) (ppm) Test	Base Fit	Change	Reactivity (mol/mol) Incremental	Mechanistic
110	0.070	1	0.002 ±0.013	D(d3)	0.043	0.032 ±0.007	0.011 ±0.010	0.156 ± 90%	(6.3 ±46.1)
2	±0.009	2	0.007 ±0.013	D(d3)	0.132	0.090 ±0.012	0.042 ±0.016	0.60 ± 41%	(6.1 ±11.7)
		3	0.015 ±0.013	D(d3)	0.248	0.171 ±0.014	0.077 ±0.020	1.09 ± 29%	4.97 ± 86%
		4	0.025 ±0.012	D(d3)	0.363	0.257 ±0.014	0.106 ±0.020	1.51 ± 23%	4.26 ± 51%
		5	0.035 ±0.011	D(d3)	0.481	0.343 ±0.016	0.138 ±0.023	1.96 ± 21%	3.98 ± 35%
		6	0.045 ±0.010	D(d3)	0.624	0.424 ±0.018	0.200 ±0.025	2.8 ± 18%	4.41 ± 25%
106	0.081	1	0.003 ±0.005	D(d3)	0.045	0.033 ±0.007	0.012 ±0.010	0.147 ± 83%	(4.6 ±10.2)
2	±0.004	2	0.010 ±0.005	D(d3)	0.142	0.095 ±0.012	0.047 ±0.017	0.57 ± 36%	4.63 ± 64%
		3	0.022 ±0.005	D(d3)	0.267	0.177 ±0.014	0.090 ±0.020	1.10 ± 23%	4.09 ± 33%
		4	0.034 ±0.005	D(d3)	0.390	0.275 ±0.015	0.115 ±0.021	1.42 ± 19%	3.37 ± 23%
		5	0.046 ±0.004	D(d3)	0.513	0.359 ±0.016	0.155 ±0.023	1.90 ± 16%	3.36 ± 18%
		6	0.057 ±0.004	D(d3)	0.655	0.442 ±0.018	0.212 ±0.026	2.6 ± 13%	3.71 ± 14%
108	0.085	1	0.004 ±0.003	D(t3)	0.053	0.033 ±0.007	0.020 ±0.010	0.24 ± 50%	4.49 ± 91%
2	±0.002	2	0.013 ±0.004	D(t3)	0.143	0.091 ±0.012	0.052 ±0.017	0.61 ± 33%	4.08 ± 43%
		3	0.023 ±0.003	D(t3)	0.249	0.174 ±0.014	0.075 ±0.020	0.89 ± 27%	3.22 ± 31%
		4	0.035 ±0.003	D(t3)	0.366	0.260 ±0.015	0.106 ±0.021	1.25 ± 20%	3.02 ± 22%
		5	0.047 ±0.003	D(t3)	0.489	0.347 ±0.017	0.142 ±0.024	1.68 ± 17%	3.05 ± 18%
		6	0.057 ±0.003	D(t3)	0.596	0.428 ±0.018	0.168 ±0.026	1.98 ± 16%	2.95 ± 16%
118	0.148	1	0.003 ±0.008	D(d3)	0.041	0.029 ±0.008	0.012 ±0.011	0.082 ± 91%	(4.1 ±11.9)
2	±0.006	2	0.015 ±0.008	D(d3)	0.145	0.094 ±0.013	0.051 ±0.019	0.35 ± 37%	3.35 ± 64%
		3	0.035 ±0.008	D(d3)	0.267	0.176 ±0.016	0.091 ±0.022	0.62 ± 25%	2.59 ± 33%
		4	0.059 ±0.007	D(d3)	0.395	0.288 ±0.016	0.107 ±0.023	0.73 ± 22%	1.83 ± 25%
		5	0.085 ±0.007	D(d3)	0.542	0.369 ±0.018	0.173 ±0.026	1.17 ± 16%	2.03 ± 17%
		6	0.108 ±0.006	D(d3)	0.702	0.461 ±0.020	0.241 ±0.029	1.63 ± 12%	2.22 ± 13%
Isobutene									
257	0.108	1	0.013 ±0.003	D(t3)	0.072	0.039 ±0.008	0.033 ±0.012	0.30 ± 35%	2.45 ± 41%
3	±0.002	2	0.039 ±0.003	D(t3)	0.217	0.142 ±0.016	0.075 ±0.023	0.70 ± 30%	1.95 ± 31%
		3	0.065 ±0.002	D(t3)	0.383	0.275 ±0.023	0.108 ±0.033	1.00 ± 30%	1.66 ± 30%
		4	0.086 ±0.002	D(t3)	0.578	0.408 ±0.034	0.170 ±0.047	1.57 ± 28%	1.98 ± 28%
		5	0.098 ±0.002	D(t3)	0.786	0.548 ±0.038	0.238 ±0.054	2.2 ± 23%	2.43 ± 23%
		6	0.104 ±0.002	D(t3)	0.998	0.703 ±0.047	0.295 ±0.066	2.7 ± 23%	2.85 ± 23%
255	0.195	1	0.024 ±0.030	D(d3)	0.094	0.043 ±0.008	0.051 ±0.012	0.26 ± 26%	(2.1 ± 2.7)
3	±0.022	2	0.086 ±0.028	D(d3)	0.294	0.161 ±0.016	0.133 ±0.023	0.68 ± 21%	1.54 ± 36%
		3	0.148 ±0.024	D(d3)	0.537	0.313 ±0.023	0.225 ±0.033	1.15 ± 19%	1.52 ± 22%
		4	0.182 ±0.023	D(d3)	0.816	0.460 ±0.034	0.356 ±0.048	1.83 ± 18%	1.96 ± 18%
		5	0.191 ±0.022	D(d3)	1.057	0.622 ±0.038	0.435 ±0.054	2.2 ± 17%	2.28 ± 17%
		6	0.192 ±0.022	D(d3)	1.246	0.804 ±0.047	0.442 ±0.067	2.3 ± 19%	2.30 ± 19%
253	0.207	1	0.022 ±0.022	D(d3)	0.096	0.039 ±0.008	0.057 ±0.012	0.27 ± 22%	(2.6 ± 2.6)
3	±0.015	2	0.094 ±0.021	D(d3)	0.293	0.153 ±0.016	0.140 ±0.023	0.68 ± 18%	1.49 ± 27%
		3	0.171 ±0.016	D(d3)	0.554	0.292 ±0.023	0.262 ±0.033	1.26 ± 15%	1.53 ± 16%
		4	0.200 ±0.015	D(d3)	0.832	0.432 ±0.034	0.400 ±0.048	1.93 ± 14%	2.00 ± 14%
		5	0.205 ±0.015	D(d3)	1.079	0.581 ±0.038	0.498 ±0.054	2.4 ± 13%	2.43 ± 13%
		6	0.205 ±0.015	D(d3)	1.259	0.748 ±0.047	0.511 ±0.067	2.5 ± 15%	2.49 ± 15%
trans-2-Butene									
309	0.069	1	0.027 ±0.010	D(t3)	0.162	0.042 ±0.008	0.120 ±0.012	1.75 ± 15%	4.51 ± 38%
3	±0.008	2	0.059 ±0.008	D(t3)	0.441	0.138 ±0.016	0.303 ±0.023	4.4 ± 14%	5.15 ± 15%
		3	0.068 ±0.008	D(t3)	0.618	0.276 ±0.024	0.342 ±0.033	5.0 ± 15%	5.01 ± 15%
		4	0.068 ±0.008	D(t3)	0.761	0.411 ±0.034	0.350 ±0.049	5.1 ± 18%	5.12 ± 18%
		5	0.068 ±0.008	D(t3)	0.917	0.549 ±0.039	0.368 ±0.055	5.4 ± 19%	5.38 ± 19%
		6	0.068 ±0.008	D(t3)	1.079	0.703 ±0.048	0.376 ±0.068	5.5 ± 21%	5.50 ± 21%

Table A-1 (continued)

Run Set	Added (ppm)	Time (hr)	Reacted [a] (ppm)	Deriv.	d(O_3-NO) (ppm) Test	Base Fit	Change	Reactivity (mol/mol) Incremental	Mechanistic
307	0.087	1	0.030 ±0.040	D(d3)	0.219	0.040 ±0.008	0.179 ±0.012	2.1 ± 35%	(5.9 ± 7.8)
3	±0.030	2	0.081 ±0.030	D(d3)	0.531	0.137 ±0.016	0.394 ±0.023	4.5 ± 35%	4.88 ± 37%
		3	0.086 ±0.030	D(d3)	0.695	0.272 ±0.023	0.423 ±0.033	4.9 ± 35%	4.91 ± 35%
		4	0.086 ±0.030	D(d3)	0.833	0.406 ±0.034	0.427 ±0.048	4.9 ± 36%	4.95 ± 36%
		5	0.086 ±0.030	D(d3)	0.987	0.539 ±0.039	0.448 ±0.055	5.2 ± 36%	5.20 ± 37%
		6	0.086 ±0.030	D(d3)	1.126	0.685 ±0.047	0.441 ±0.067	5.1 ± 38%	5.11 ± 38%
Isoprene									
277	0.076	1	0.016 ±0.002	D(d2)	0.079	0.043 ±0.008	0.036 ±0.012	0.48 ± 32%	2.23 ± 34%
3	±0.002	2	0.043 ±0.002	D(d2)	0.268	0.163 ±0.016	0.105 ±0.023	1.38 ± 22%	2.46 ± 22%
		3	0.058 ±0.002	D(d2)	0.476	0.320 ±0.023	0.156 ±0.033	2.1 ± 21%	2.68 ± 21%
		4	0.075 ±0.002	D(d2)	0.701	0.471 ±0.034	0.230 ±0.048	3.0 ± 21%	3.06 ± 21%
		5	0.075 ±0.002	D(d2)	0.944	0.639 ±0.039	0.305 ±0.055	4.0 ± 18%	4.05 ± 18%
		6	0.075 ±0.002	D(d2)	1.167	0.829 ±0.047	0.338 ±0.067	4.4 ± 20%	4.48 ± 20%
275	0.108	1	0.028 ±0.003	D(d2)	0.097	0.041 ±0.008	0.056 ±0.012	0.52 ± 21%	2.02 ± 23%
3	±0.002	2	0.064 ±0.002	D(d2)	0.297	0.153 ±0.016	0.144 ±0.023	1.33 ± 16%	2.24 ± 16%
		3	0.086 ±0.002	D(d2)	0.523	0.301 ±0.023	0.222 ±0.033	2.0 ± 15%	2.58 ± 15%
		4	0.108 ±0.002	D(d2)	0.765	0.446 ±0.034	0.319 ±0.048	2.9 ± 15%	2.97 ± 15%
		5	0.108 ±0.002	D(d2)	1.010	0.601 ±0.038	0.409 ±0.054	3.8 ± 13%	3.80 ± 13%
		6	0.108 ±0.002	D(d2)	1.217	0.776 ±0.047	0.441 ±0.066	4.1 ± 15%	4.10 ± 15%
273	0.139	1	0.035 ±0.006	D(d2)	0.103	0.039 ±0.008	0.064 ±0.012	0.46 ± 18%	1.83 ± 24%
3	±0.004	2	0.084 ±0.005	D(d2)	0.334	0.151 ±0.016	0.183 ±0.022	1.31 ± 13%	2.16 ± 14%
		3	0.111 ±0.005	D(d2)	0.580	0.297 ±0.023	0.283 ±0.032	2.0 ± 12%	2.54 ± 12%
		4	0.138 ±0.004	D(d2)	0.840	0.441 ±0.033	0.399 ±0.047	2.9 ± 12%	2.89 ± 12%
		5	0.138 ±0.004	D(d2)	1.076	0.592 ±0.038	0.484 ±0.054	3.5 ± 12%	3.50 ± 12%
		6	0.138 ±0.004	D(d2)	1.262	0.762 ±0.047	0.500 ±0.066	3.6 ± 14%	3.62 ± 14%
271	0.157	1	0.039 ±0.009	D(d2)	0.101	0.036 ±0.008	0.065 ±0.012	0.42 ± 18%	1.66 ± 29%
3	±0.007	2	0.091 ±0.008	D(d2)	0.303	0.133 ±0.016	0.170 ±0.022	1.09 ± 14%	1.87 ± 16%
		3	0.123 ±0.007	D(d2)	0.540	0.261 ±0.023	0.279 ±0.032	1.78 ± 12%	2.27 ± 13%
		4	0.139 ±0.007	D(d2)	0.788	0.391 ±0.033	0.397 ±0.047	2.5 ± 13%	2.85 ± 13%
		5	0.147 ±0.007	D(d2)	1.021	0.519 ±0.038	0.502 ±0.054	3.2 ± 12%	3.41 ± 12%
		6	0.150 ±0.007	D(d2)	1.207	0.661 ±0.047	0.546 ±0.066	3.5 ± 13%	3.63 ± 13%
2-Chloromethyl-3-chloropropene									
343	0.103	1	0.012 ±0.006	D(t3)	0.085	0.055 ±0.009	0.030 ±0.012	0.29 ± 41%	2.59 ± 65%
3	±0.004	2	0.028 ±0.006	D(t3)	0.288	0.202 ±0.017	0.086 ±0.024	0.84 ± 28%	3.10 ± 34%
		3	0.045 ±0.005	D(t3)	0.524	0.364 ±0.025	0.160 ±0.035	1.56 ± 22%	3.54 ± 24%
		4	0.062 ±0.005	D(t3)	0.786	0.516 ±0.036	0.270 ±0.051	2.6 ± 19%	4.37 ± 20%
		5	0.075 ±0.004	D(t3)	1.062	0.684 ±0.041	0.378 ±0.058	3.7 ± 16%	5.02 ± 16%
		6	0.085 ±0.004	D(t3)	1.260	0.873 ±0.050	0.387 ±0.071	3.8 ± 19%	4.53 ± 19%
342	0.108	1	0.006 ±0.003	D(t3)	0.081	0.061 ±0.009	0.020 ±0.012	0.187 ± 60%	3.31 ± 78%
3	±0.002	2	0.020 ±0.003	D(t3)	0.308	0.190 ±0.017	0.118 ±0.023	1.09 ± 20%	6.03 ± 25%
		3	0.037 ±0.003	D(t3)	0.567	0.359 ±0.024	0.208 ±0.034	1.93 ± 16%	5.59 ± 18%
		4	0.056 ±0.003	D(t3)	0.833	0.512 ±0.035	0.321 ±0.049	3.0 ± 15%	5.74 ± 16%
		5	0.072 ±0.002	D(t3)	1.116	0.669 ±0.040	0.447 ±0.056	4.1 ± 13%	6.17 ± 13%
		6	0.085 ±0.002	D(t3)	1.335	0.844 ±0.049	0.491 ±0.069	4.5 ± 14%	5.76 ± 14%
350	0.113	1	0.015 ±0.008	D(t3)	0.096	0.061 ±0.008	0.035 ±0.012	0.31 ± 34%	2.33 ± 65%
3	±0.006	2	0.034 ±0.008	D(t3)	0.341	0.205 ±0.016	0.136 ±0.023	1.21 ± 18%	3.95 ± 29%
		3	0.054 ±0.007	D(t3)	0.613	0.379 ±0.023	0.234 ±0.033	2.1 ± 15%	4.32 ± 20%
		4	0.072 ±0.007	D(t3)	0.922	0.538 ±0.034	0.384 ±0.048	3.4 ± 14%	5.32 ± 16%
		5	0.086 ±0.006	D(t3)	1.211	0.707 ±0.039	0.504 ±0.055	4.5 ± 12%	5.85 ± 13%
		6	0.096 ±0.006	D(t3)	1.386	0.893 ±0.048	0.493 ±0.067	4.4 ± 15%	5.12 ± 15%

Table A-1 (continued)

Run Set	Added (ppm)	Time (hr)	Reacted [a] (ppm)	Deriv.	d(O_3-NO) (ppm) Test	Base Fit	Change	Reactivity (mol/mol) Incremental	Mechanistic
Benzene									
265	5.78	1	0.030 ±0.046	IntOH	0.068	0.037 ±0.008	0.031 ±0.012	0.0053 ± 38%	(1.0 ± 1.6)
3	±0.12	2	0.072 ±0.050	IntOH	0.226	0.143 ±0.016	0.083 ±0.023	0.0143 ± 27%	1.15 ± 74%
		3	0.126 ±0.051	IntOH	0.423	0.277 ±0.023	0.146 ±0.033	0.025 ± 22%	1.15 ± 46%
		4	0.192 ±0.050	IntOH	0.675	0.412 ±0.034	0.264 ±0.047	0.046 ± 18%	1.37 ± 32%
		5	0.269 ±0.049	IntOH	0.945	0.553 ±0.038	0.392 ±0.054	0.068 ± 14%	1.45 ± 23%
		6	0.357 ±0.048	IntOH	0.989	0.712 ±0.047	0.277 ±0.066	0.048 ± 24%	0.78 ± 27%
263	6.86	1	0.039 ±0.044	IntOH	0.066	0.043 ±0.008	0.023 ±0.012	0.0034 ± 50%	(0.6 ± 0.7)
3	±0.19	2	0.093 ±0.047	IntOH	0.244	0.165 ±0.016	0.079 ±0.023	0.0116 ± 29%	0.86 ± 58%
		3	0.161 ±0.048	IntOH	0.484	0.317 ±0.023	0.167 ±0.033	0.024 ± 20%	1.04 ± 36%
		4	0.243 ±0.048	IntOH	0.836	0.465 ±0.034	0.371 ±0.048	0.054 ± 13%	1.53 ± 24%
		5	0.339 ±0.047	IntOH	0.983	0.635 ±0.039	0.348 ±0.055	0.051 ± 16%	1.03 ± 21%
		6	0.447 ±0.047	IntOH	0.983	0.829 ±0.048	0.154 ±0.067	0.022 ± 44%	0.34 ± 45%
Toluene									
64	0.061	1	0.001 ±0.002	D(d2)	0.080	0.086 ±0.017	-0.006 ±0.024	(-0.09 ± 0.4)	(-4.2 ±18.7)
1	±0.001	2	0.004 ±0.002	D(d2)	0.205	0.192 ±0.022	0.013 ±0.032	(0.2 ± 0.5)	(3.6 ± 9.1)
		3	0.006 ±0.002	D(d2)	0.341	0.304 ±0.024	0.037 ±0.034	0.61 ± 91%	6.34 ± 96%
		4	0.008 ±0.002	D(d2)	0.454	0.408 ±0.026	0.046 ±0.037	0.76 ± 79%	6.05 ± 82%
		5	0.009 ±0.002	D(d2)	0.569	0.511 ±0.031	0.058 ±0.043	0.94 ± 75%	6.11 ± 77%
		6	0.011 ±0.002	D(d2)	0.702	0.631 ±0.039	0.071 ±0.056	1.16 ± 78%	6.22 ± 80%
69	0.095	1	0.003 ±0.003	D(d2)	0.095	0.081 ±0.017	0.014 ±0.024	(0.14 ± 0.3)	(5.4 ±11.0)
1	±0.002	2	0.006 ±0.003	D(d2)	0.224	0.184 ±0.022	0.040 ±0.032	0.42 ± 79%	6.72 ± 90%
		3	0.010 ±0.003	D(d2)	0.366	0.294 ±0.024	0.072 ±0.034	0.76 ± 47%	7.40 ± 54%
		4	0.013 ±0.003	D(d2)	0.487	0.398 ±0.026	0.089 ±0.037	0.94 ± 41%	7.09 ± 46%
		5	0.016 ±0.003	D(d2)	0.629	0.498 ±0.031	0.131 ±0.043	1.37 ± 33%	8.15 ± 37%
		6	0.020 ±0.003	D(d2)	0.785	0.614 ±0.039	0.171 ±0.056	1.80 ± 33%	8.74 ± 35%
61	0.175	1	0.005 ±0.005	D(d3)	0.119	0.088 ±0.017	0.031 ±0.024	0.178 ± 78%	(6.4 ± 8.2)
1	±0.004	2	0.012 ±0.005	D(d3)	0.298	0.197 ±0.023	0.101 ±0.032	0.58 ± 32%	8.22 ± 51%
		3	0.019 ±0.005	D(d3)	0.457	0.309 ±0.024	0.148 ±0.034	0.85 ± 23%	7.88 ± 35%
		4	0.026 ±0.005	D(d3)	0.624	0.413 ±0.026	0.211 ±0.037	1.21 ± 18%	8.17 ± 26%
		5	0.034 ±0.005	D(d3)	0.813	0.519 ±0.031	0.294 ±0.043	1.69 ± 15%	8.76 ± 21%
		6	0.043 ±0.005	D(d3)	1.041	0.641 ±0.040	0.400 ±0.056	2.3 ± 14%	9.31 ± 18%
101	0.170	1	0.003 ±0.005	D(t3)	0.039	0.033 ±0.007	0.006 ±0.010	(0.03 ±0.06)	(1.9 ± 4.7)
2	±0.003	2	0.007 ±0.005	D(t3)	0.128	0.097 ±0.012	0.031 ±0.017	0.184 ± 53%	4.68 ± 90%
		3	0.012 ±0.005	D(t3)	0.256	0.177 ±0.014	0.079 ±0.020	0.46 ± 26%	6.86 ± 49%
		4	0.017 ±0.005	D(t3)	0.395	0.274 ±0.015	0.121 ±0.021	0.71 ± 17%	7.08 ± 33%
		5	0.023 ±0.005	D(t3)	0.508	0.356 ±0.017	0.152 ±0.023	0.89 ± 15%	6.51 ± 26%
		6	0.030 ±0.005	D(t3)	0.647	0.439 ±0.018	0.208 ±0.026	1.22 ± 13%	6.89 ± 21%
103	0.174	1	0.002 ±0.005	D(d2)	0.046	0.032 ±0.007	0.014 ±0.009	0.083 ± 65%	(6.8 ±16.7)
2	±0.004	2	0.007 ±0.005	D(d2)	0.138	0.094 ±0.011	0.044 ±0.016	0.25 ± 36%	6.42 ± 80%
		3	0.013 ±0.005	D(d2)	0.261	0.177 ±0.014	0.084 ±0.019	0.49 ± 23%	6.32 ± 43%
		4	0.020 ±0.005	D(d2)	0.396	0.274 ±0.014	0.122 ±0.020	0.70 ± 16%	6.05 ± 29%
		5	0.027 ±0.005	D(d2)	0.532	0.360 ±0.016	0.172 ±0.022	0.99 ± 13%	6.41 ± 23%
		6	0.034 ±0.005	D(d2)	0.680	0.447 ±0.017	0.234 ±0.024	1.34 ± 11%	6.97 ± 18%
Ethylbenzene									
313	0.092	1	0.000 ±0.001	IntOH	0.032	0.031 ±0.008	0.001 ±0.012	(0.006 ±0.13)	(1.5 ±30.4)
3	±0.003	2	0.002 ±0.001	IntOH	0.124	0.116 ±0.016	0.008 ±0.023	(0.09 ± 0.2)	(4.7 ±13.5)
		3	0.004 ±0.001	IntOH	0.255	0.229 ±0.023	0.026 ±0.033	(0.3 ± 0.4)	(6.4 ± 8.5)
		4	0.007 ±0.001	IntOH	0.377	0.348 ±0.034	0.029 ±0.048	(0.3 ± 0.5)	(4.1 ± 6.9)
		5	0.011 ±0.001	IntOH	0.503	0.459 ±0.039	0.044 ±0.055	(0.5 ± 0.6)	(4.1 ± 5.1)
		6	0.015 ±0.001	IntOH	0.649	0.581 ±0.048	0.068 ±0.067	0.74 ± 99%	(4.5 ± 4.4)

Table A-1 (continued)

Run Set	Added (ppm)	Time (hr)	Reacted [a] (ppm)	Reacted [a] Deriv.	d(O_3-NO) (ppm) Test	d(O_3-NO) (ppm) Base Fit	d(O_3-NO) (ppm) Change	Reactivity (mol/mol) Incremental	Reactivity (mol/mol) Mechanistic
311	0.098	1	0.000 ±0.001	IntOH	0.030	0.029 ±0.008	0.001 ±0.012	(0.008 ±0.12)	(2.8 ±46.1)
3	±0.004	2	0.001 ±0.001	IntOH	0.108	0.111 ±0.016	-0.003 ±0.023	(-0.03 ± 0.2)	(-2.1 ±16.0)
		3	0.004 ±0.001	IntOH	0.229	0.219 ±0.024	0.010 ±0.034	(0.10 ± 0.3)	(2.5 ± 8.4)
		4	0.008 ±0.001	IntOH	0.354	0.334 ±0.035	0.020 ±0.049	(0.2 ± 0.5)	(2.7 ± 6.5)
		5	0.011 ±0.001	IntOH	0.470	0.436 ±0.039	0.034 ±0.056	(0.3 ± 0.6)	(3.0 ± 4.9)
		6	0.017 ±0.001	IntOH	0.608	0.546 ±0.048	0.062 ±0.068	(0.6 ± 0.7)	(3.7 ± 4.1)
315	0.215	1	0.001 ±0.006	D(t3)	0.034	0.034 ±0.008	0.000 ±0.012	(-0.001 ±0.06)	(-0.2 ± 9.0)
3	±0.004	2	0.005 ±0.006	D(t3)	0.141	0.113 ±0.016	0.028 ±0.023	0.130 ± 83%	(6.2 ± 9.8)
		3	0.009 ±0.006	D(t3)	0.301	0.232 ±0.024	0.069 ±0.033	0.32 ± 48%	7.61 ± 83%
		4	0.015 ±0.006	D(t3)	0.457	0.352 ±0.034	0.104 ±0.049	0.48 ± 47%	6.90 ± 62%
		5	0.022 ±0.006	D(t3)	0.622	0.461 ±0.039	0.161 ±0.056	0.75 ± 35%	7.16 ± 44%
		6	0.031 ±0.006	D(t3)	0.806	0.578 ±0.048	0.228 ±0.068	1.06 ± 30%	7.35 ± 36%
o-Xylene									
259	0.064	1	0.002 ±0.004	D(d2)	0.058	0.037 ±0.008	0.021 ±0.012	0.32 ± 57%	(13.0 ±30.8)
3	±0.003	2	0.006 ±0.004	D(d2)	0.208	0.140 ±0.016	0.068 ±0.023	1.07 ± 33%	11.14 ± 67%
		3	0.011 ±0.003	D(d2)	0.382	0.272 ±0.023	0.110 ±0.033	1.73 ± 30%	10.14 ± 44%
		4	0.015 ±0.003	D(d2)	0.554	0.405 ±0.034	0.149 ±0.047	2.3 ± 32%	9.83 ± 39%
		5	0.020 ±0.003	D(d2)	0.750	0.544 ±0.038	0.206 ±0.054	3.2 ± 27%	10.48 ± 32%
		6	0.024 ±0.003	D(d2)	0.962	0.701 ±0.047	0.261 ±0.066	4.1 ± 26%	10.92 ± 29%
261	0.064	1	0.002 ±0.003	D(d2)	0.065	0.038 ±0.008	0.027 ±0.012	0.42 ± 44%	(13.2 ±22.0)
3	±0.002	2	0.007 ±0.003	D(d2)	0.212	0.152 ±0.016	0.060 ±0.023	0.93 ± 38%	8.89 ± 61%
		3	0.012 ±0.003	D(d2)	0.392	0.293 ±0.023	0.099 ±0.033	1.55 ± 33%	8.32 ± 42%
		4	0.017 ±0.003	D(d2)	0.579	0.432 ±0.034	0.147 ±0.048	2.3 ± 33%	8.71 ± 37%
		5	0.022 ±0.003	D(d2)	0.801	0.586 ±0.038	0.215 ±0.054	3.4 ± 26%	9.72 ± 29%
		6	0.027 ±0.003	D(d2)	1.028	0.761 ±0.047	0.267 ±0.067	4.2 ± 25%	9.97 ± 27%
m-Xylene									
207	0.038	1	0.001 ±0.004	D(d3)	0.056	0.037 ±0.009	0.019 ±0.012	0.50 ± 65%	(13.1 ±38.5)
3	±0.003	2	0.006 ±0.004	D(d3)	0.213	0.127 ±0.017	0.086 ±0.024	2.3 ± 29%	15.01 ± 78%
		3	0.011 ±0.004	D(d3)	0.408	0.261 ±0.024	0.147 ±0.034	3.9 ± 25%	13.60 ± 45%
		4	0.015 ±0.004	D(d3)	0.590	0.393 ±0.035	0.197 ±0.050	5.2 ± 26%	13.08 ± 36%
		5	0.019 ±0.004	D(d3)	0.772	0.521 ±0.040	0.251 ±0.057	6.6 ± 24%	13.22 ± 30%
		6	0.023 ±0.004	D(d3)	0.977	0.665 ±0.049	0.312 ±0.070	8.2 ± 24%	13.69 ± 27%
301	0.053	1	0.002 ±0.008	D(d3)	0.043	0.037 ±0.008	0.006 ±0.012	(0.12 ± 0.2)	(3.8 ±20.0)
3	±0.006	2	0.008 ±0.008	D(d3)	0.198	0.140 ±0.016	0.058 ±0.022	1.10 ± 40%	(7.3 ± 8.0)
		3	0.015 ±0.008	D(d3)	0.395	0.271 ±0.023	0.124 ±0.032	2.3 ± 28%	8.10 ± 58%
		4	0.022 ±0.008	D(d3)	0.585	0.404 ±0.033	0.181 ±0.047	3.4 ± 28%	8.38 ± 44%
		5	0.028 ±0.007	D(d3)	0.797	0.539 ±0.038	0.258 ±0.054	4.9 ± 24%	9.30 ± 33%
		6	0.033 ±0.007	D(d3)	1.014	0.688 ±0.047	0.326 ±0.066	6.2 ± 23%	9.87 ± 29%
196	0.057	1	0.002 ±0.004	D(d2)	0.040	0.033 ±0.009	0.007 ±0.012	(0.11 ± 0.2)	(3.1 ± 8.5)
3	±0.003	2	0.009 ±0.004	D(d2)	0.175	0.140 ±0.016	0.035 ±0.023	0.61 ± 68%	3.71 ± 81%
		3	0.017 ±0.004	D(d2)	0.343	0.268 ±0.024	0.075 ±0.034	1.32 ± 45%	4.41 ± 51%
		4	0.024 ±0.004	D(d2)	0.518	0.398 ±0.035	0.120 ±0.049	2.1 ± 41%	5.09 ± 44%
		5	0.029 ±0.004	D(d2)	0.694	0.539 ±0.040	0.155 ±0.056	2.7 ± 37%	5.35 ± 38%
		6	0.034 ±0.004	D(d2)	0.892	0.698 ±0.048	0.194 ±0.069	3.4 ± 36%	5.69 ± 37%
344	0.081	1	0.006 ±0.020	D(d2)	0.111	0.059 ±0.008	0.052 ±0.012	0.64 ± 29%	(8.5 ±27.3)
3	±0.014	2	0.021 ±0.018	D(d2)	0.411	0.201 ±0.016	0.210 ±0.023	2.6 ± 21%	10.14 ± 88%
		3	0.032 ±0.017	D(d2)	0.688	0.370 ±0.023	0.318 ±0.033	3.9 ± 21%	10.06 ± 56%
		4	0.041 ±0.017	D(d2)	0.983	0.527 ±0.034	0.456 ±0.048	5.7 ± 21%	11.14 ± 42%
		5	0.047 ±0.016	D(d2)	1.209	0.690 ±0.039	0.519 ±0.055	6.4 ± 21%	11.10 ± 36%
		6	0.049 ±0.016	D(d2)	1.329	0.869 ±0.048	0.460 ±0.067	5.7 ± 23%	9.29 ± 36%

Table A-1 (continued)

Run Set	Added (ppm)	Time (hr)	Reacted [a] (ppm)	Deriv.	d(O_3-NO) (ppm) Test	Base Fit	Change	Reactivity (mol/mol) Incremental	Mechanistic
p-Xylene									
348	0.075	1	0.003 ±0.001	IntOH	0.065	0.059 ±0.008	0.006 ±0.012	(0.08 ± 0.2)	(2.0 ± 4.1)
3	±0.002	2	0.008 ±0.001	IntOH	0.233	0.203 ±0.016	0.030 ±0.023	0.40 ± 78%	3.85 ± 79%
		3	0.014 ±0.001	IntOH	0.431	0.371 ±0.024	0.060 ±0.034	0.80 ± 56%	4.36 ± 56%
		4	0.021 ±0.001	IntOH	0.626	0.527 ±0.035	0.099 ±0.049	1.32 ± 49%	4.74 ± 50%
		5	0.028 ±0.001	IntOH	0.845	0.689 ±0.040	0.156 ±0.056	2.1 ± 36%	5.47 ± 36%
		6	0.036 ±0.001	IntOH	1.066	0.868 ±0.048	0.198 ±0.068	2.6 ± 35%	5.51 ± 35%
346	0.080	1	0.002 ±0.001	IntOH	0.074	0.054 ±0.009	0.020 ±0.013	0.24 ± 66%	8.14 ± 82%
3	±0.002	2	0.009 ±0.001	IntOH	0.252	0.208 ±0.018	0.044 ±0.025	0.54 ± 57%	5.04 ± 59%
		3	0.016 ±0.001	IntOH	0.459	0.371 ±0.026	0.088 ±0.036	1.09 ± 41%	5.43 ± 42%
		4	0.024 ±0.001	IntOH	0.684	0.525 ±0.037	0.159 ±0.053	1.97 ± 33%	6.54 ± 34%
		5	0.033 ±0.001	IntOH	0.932	0.699 ±0.042	0.233 ±0.060	2.9 ± 26%	7.08 ± 26%
		6	0.039 ±0.001	IntOH	1.130	0.895 ±0.052	0.235 ±0.074	2.9 ± 31%	5.99 ± 31%
135-trimethyl-Benzene									
251	0.045	1	0.008 ±0.004	D(t3)	0.068	0.038 ±0.008	0.030 ±0.012	0.68 ± 40%	3.83 ± 66%
3	±0.003	2	0.018 ±0.004	D(t3)	0.278	0.120 ±0.016	0.158 ±0.023	3.5 ± 16%	8.87 ± 26%
		3	0.027 ±0.004	D(t3)	0.483	0.239 ±0.023	0.244 ±0.033	5.4 ± 15%	8.94 ± 19%
		4	0.035 ±0.003	D(t3)	0.677	0.362 ±0.034	0.315 ±0.048	7.0 ± 17%	9.11 ± 18%
		5	0.039 ±0.003	D(t3)	0.923	0.473 ±0.039	0.450 ±0.055	10.1 ± 14%	11.44 ± 15%
		6	0.042 ±0.003	D(t3)	1.029	0.591 ±0.048	0.438 ±0.067	9.8 ± 17%	10.42 ± 17%
249	0.047	1	0.008 ±0.007	IntOH	0.096	0.041 ±0.008	0.055 ±0.012	1.17 ± 24%	7.10 ± 97%
3	±0.005	2	0.019 ±0.006	IntOH	0.353	0.144 ±0.016	0.209 ±0.023	4.5 ± 15%	11.13 ± 33%
		3	0.030 ±0.005	IntOH	0.602	0.280 ±0.023	0.322 ±0.033	6.9 ± 15%	10.87 ± 19%
		4	0.038 ±0.005	IntOH	0.871	0.416 ±0.034	0.455 ±0.048	9.7 ± 15%	12.07 ± 16%
		5	0.043 ±0.005	IntOH	1.128	0.555 ±0.038	0.573 ±0.054	12.3 ± 15%	13.48 ± 15%
		6	0.045 ±0.005	IntOH	1.305	0.707 ±0.047	0.598 ±0.067	12.8 ± 16%	13.31 ± 16%
124-trimethyl-Benzene									
267	0.037	1	0.002 ±0.001	D(d2)	0.059	0.038 ±0.008	0.021 ±0.012	0.57 ± 56%	9.85 ± 86%
3	±0.001	2	0.007 ±0.001	D(d2)	0.203	0.140 ±0.016	0.063 ±0.023	1.68 ± 36%	8.91 ± 41%
		3	0.012 ±0.001	D(d2)	0.363	0.269 ±0.023	0.094 ±0.033	2.5 ± 35%	8.03 ± 37%
		4	0.016 ±0.001	D(d2)	0.539	0.401 ±0.034	0.138 ±0.048	3.7 ± 35%	8.68 ± 36%
		5	0.020 ±0.001	D(d2)	0.729	0.536 ±0.039	0.192 ±0.055	5.2 ± 28%	9.79 ± 29%
		6	0.023 ±0.001	D(d2)	0.952	0.686 ±0.047	0.266 ±0.067	7.1 ± 25%	11.44 ± 26%
269	0.041	1	0.003 ±0.002	D(d2)	0.063	0.040 ±0.008	0.023 ±0.012	0.57 ± 50%	8.31 ± 80%
3	±0.001	2	0.009 ±0.002	D(d2)	0.224	0.157 ±0.016	0.067 ±0.023	1.64 ± 34%	7.24 ± 38%
		3	0.015 ±0.002	D(d2)	0.413	0.303 ±0.023	0.110 ±0.033	2.7 ± 30%	7.14 ± 31%
		4	0.020 ±0.001	D(d2)	0.600	0.447 ±0.034	0.153 ±0.047	3.8 ± 31%	7.55 ± 32%
		5	0.025 ±0.001	D(d2)	0.821	0.606 ±0.038	0.215 ±0.054	5.3 ± 25%	8.69 ± 26%
		6	0.028 ±0.001	D(d2)	1.049	0.785 ±0.047	0.264 ±0.066	6.5 ± 25%	9.32 ± 26%
123-trimethyl-Benzene									
299	0.035	1	0.004 ±0.005	D(t3)	0.069	0.037 ±0.008	0.032 ±0.012	0.91 ± 39%	(7.7 ± 9.5)
3	±0.003	2	0.009 ±0.005	D(t3)	0.311	0.159 ±0.016	0.152 ±0.023	4.4 ± 18%	16.24 ± 52%
		3	0.015 ±0.004	D(t3)	0.550	0.312 ±0.024	0.238 ±0.033	6.9 ± 17%	15.81 ± 32%
		4	0.020 ±0.004	D(t3)	0.794	0.461 ±0.034	0.333 ±0.049	9.6 ± 18%	16.35 ± 24%
		5	0.025 ±0.004	D(t3)	1.035	0.623 ±0.039	0.412 ±0.055	11.9 ± 17%	16.65 ± 20%
		6	0.028 ±0.004	D(t3)	1.221	0.804 ±0.048	0.417 ±0.068	12.0 ± 19%	14.78 ± 21%
297	0.044	1	0.004 ±0.001	D(d2)	0.085	0.038 ±0.008	0.047 ±0.012	1.08 ± 25%	11.84 ± 39%
3	±0.001	2	0.015 ±0.001	D(d2)	0.364	0.164 ±0.016	0.200 ±0.023	4.6 ± 12%	13.37 ± 14%
		3	0.022 ±0.001	D(d2)	0.629	0.320 ±0.024	0.309 ±0.033	7.1 ± 11%	13.76 ± 12%
		4	0.028 ±0.001	D(d2)	0.897	0.471 ±0.034	0.426 ±0.049	9.7 ± 12%	15.20 ± 12%
		5	0.032 ±0.001	D(d2)	1.133	0.638 ±0.039	0.495 ±0.056	11.3 ± 11%	15.62 ± 12%
		6	0.033 ±0.001	D(d2)	1.273	0.828 ±0.048	0.445 ±0.068	10.1 ± 15%	13.32 ± 16%

Table A-1 (continued)

Run Set	Added (ppm)	Time (hr)	Reacted [a] (ppm)	Deriv.	d(O_3-NO) (ppm) Test	Base Fit	Change	Reactivity (mol/mol) Incremental	Mechanistic
Methanol									
287	0.816	1	0.001 ±0.001	IntOH	0.043	0.042 ±0.008	0.001 ±0.012	(0.0008±0.014)	(0.7 ±13.4)
3	±0.031	2	0.004 ±0.001	IntOH	0.174	0.166 ±0.016	0.008 ±0.023	(0.009 ±0.03)	(1.9 ± 5.6)
		3	0.009 ±0.002	IntOH	0.338	0.327 ±0.023	0.011 ±0.033	(0.013 ±0.04)	(1.3 ± 3.9)
		4	0.013 ±0.002	IntOH	0.500	0.481 ±0.034	0.019 ±0.048	(0.02 ±0.06)	(1.4 ± 3.6)
		5	0.020 ±0.002	IntOH	0.686	0.654 ±0.039	0.032 ±0.055	(0.04 ±0.07)	(1.7 ± 2.8)
		6	0.027 ±0.002	IntOH	0.886	0.850 ±0.048	0.036 ±0.067	(0.04 ±0.08)	(1.3 ± 2.5)
289	2.29	1	0.003 ±0.003	IntOH	0.048	0.044 ±0.009	0.004 ±0.012	(0.002±0.005)	(1.4 ± 4.1)
3	±0.10	2	0.014 ±0.003	IntOH	0.205	0.184 ±0.017	0.021 ±0.023	(0.009±0.010)	(1.4 ± 1.7)
		3	0.029 ±0.004	IntOH	0.397	0.357 ±0.024	0.040 ±0.034	0.0175 ± 85%	1.38 ± 85%
		4	0.045 ±0.004	IntOH	0.606	0.521 ±0.035	0.085 ±0.049	0.037 ± 58%	1.87 ± 59%
		5	0.066 ±0.005	IntOH	0.847	0.713 ±0.040	0.134 ±0.056	0.058 ± 42%	2.04 ± 43%
		6	0.087 ±0.005	IntOH	1.093	0.934 ±0.049	0.159 ±0.069	0.070 ± 43%	1.83 ± 44%
285	7.64	1	0.009 ±0.014	IntOH	0.062	0.043 ±0.008	0.019 ±0.012	0.0025 ± 63%	(2.2 ± 3.8)
3	±0.19	2	0.039 ±0.014	IntOH	0.239	0.171 ±0.016	0.068 ±0.023	0.0089 ± 34%	1.76 ± 50%
		3	0.082 ±0.016	IntOH	0.456	0.336 ±0.024	0.120 ±0.033	0.0157 ± 28%	1.46 ± 34%
		4	0.145 ±0.016	IntOH	0.721	0.493 ±0.034	0.228 ±0.049	0.030 ± 21%	1.57 ± 24%
		5	0.230 ±0.017	IntOH	1.029	0.670 ±0.039	0.359 ±0.055	0.047 ± 16%	1.56 ± 17%
		6	0.316 ±0.018	IntOH	1.302	0.871 ±0.048	0.431 ±0.068	0.056 ± 16%	1.37 ± 17%
Ethanol									
133	2.91	1	0.006 ±0.013	IntOH	0.038	0.024 ±0.008	0.014 ±0.011	0.0049 ± 75%	(2.5 ± 6.0)
2	±0.14	2	0.025 ±0.014	IntOH	0.128	0.078 ±0.013	0.050 ±0.018	0.0172 ± 36%	1.97 ± 67%
		3	0.059 ±0.016	IntOH	0.248	0.159 ±0.015	0.089 ±0.022	0.030 ± 25%	1.50 ± 36%
		4	0.103 ±0.016	IntOH	0.375	0.245 ±0.016	0.130 ±0.022	0.044 ± 18%	1.26 ± 23%
		5	0.144 ±0.017	IntOH	0.479	0.335 ±0.018	0.144 ±0.025	0.049 ± 18%	1.00 ± 21%
		6	0.199 ±0.019	IntOH	0.600	0.423 ±0.019	0.177 ±0.027	0.061 ± 16%	0.89 ± 18%
138	3.01	1	0.020 ±0.016	IntOH	0.045	0.026 ±0.007	0.019 ±0.010	0.0063 ± 54%	0.96 ± 99%
2	±0.18	2	0.045 ±0.018	IntOH	0.124	0.074 ±0.012	0.050 ±0.017	0.0165 ± 35%	1.11 ± 53%
		3	0.075 ±0.019	IntOH	0.233	0.149 ±0.015	0.083 ±0.021	0.028 ± 25%	1.11 ± 35%
		4	0.110 ±0.019	IntOH	0.345	0.232 ±0.015	0.113 ±0.021	0.038 ± 20%	1.03 ± 26%
		5	0.149 ±0.020	IntOH	0.452	0.309 ±0.017	0.143 ±0.024	0.048 ± 18%	0.96 ± 21%
		6	0.193 ±0.021	IntOH	0.553	0.387 ±0.019	0.166 ±0.026	0.055 ± 17%	0.86 ± 19%
131	3.15	1	0.021 ±0.012	IntOH	0.042	0.024 ±0.007	0.018 ±0.010	0.0057 ± 55%	0.85 ± 81%
2	±0.06	2	0.048 ±0.012	IntOH	0.138	0.076 ±0.012	0.062 ±0.017	0.0195 ± 27%	1.29 ± 37%
		3	0.080 ±0.013	IntOH	0.256	0.157 ±0.014	0.099 ±0.020	0.031 ± 20%	1.23 ± 26%
		4	0.118 ±0.013	IntOH	0.370	0.245 ±0.015	0.125 ±0.021	0.040 ± 17%	1.06 ± 20%
		5	0.161 ±0.014	IntOH	0.480	0.333 ±0.016	0.147 ±0.023	0.047 ± 16%	0.92 ± 18%
		6	0.208 ±0.014	IntOH	0.598	0.420 ±0.018	0.178 ±0.026	0.057 ± 14%	0.86 ± 16%
Isopropanol									
148	3.63	1	0.038 ±0.023	IntOH	0.059	0.024 ±0.007	0.035 ±0.010	0.0097 ± 30%	0.91 ± 66%
2	±0.30	2	0.094 ±0.024	IntOH	0.185	0.077 ±0.012	0.108 ±0.017	0.030 ± 18%	1.15 ± 30%
		3	0.166 ±0.027	IntOH	0.327	0.154 ±0.015	0.173 ±0.021	0.048 ± 15%	1.04 ± 20%
		4	0.253 ±0.031	IntOH	0.472	0.239 ±0.015	0.233 ±0.021	0.064 ± 12%	0.92 ± 15%
		5	0.353 ±0.037	IntOH	0.630	0.321 ±0.017	0.309 ±0.024	0.085 ± 11%	0.88 ± 13%
		6	0.466 ±0.045	IntOH	0.816	0.405 ±0.019	0.411 ±0.026	0.113 ± 10%	0.88 ± 12%
157	1.26	1	0.004 ±0.036	D(d3)	0.060	0.043 ±0.008	0.017 ±0.014	0.0138 ± 82%	(4.3 ±38.9)
3	±0.03	2	0.024 ±0.036	D(d3)	0.186	0.138 ±0.016	0.048 ±0.025	0.038 ± 53%	(2.0 ± 3.2)
		3	0.054 ±0.036	D(d3)	0.323	0.272 ±0.023	0.051 ±0.033	0.041 ± 65%	0.94 ± 93%
		4	0.095 ±0.036	D(d3)	0.463	0.404 ±0.034	0.059 ±0.048	0.047 ± 81%	0.62 ± 90%
		5	0.145 ±0.037	D(d3)	0.608	0.533 ±0.039	0.075 ±0.055	0.060 ± 73%	0.52 ± 77%
		6	0.212 ±0.037	D(d3)	0.774	0.674 ±0.047	0.100 ±0.067	0.080 ± 67%	0.47 ± 69%

Table A-1 (continued)

Run Set	Added (ppm)	Time (hr)	Reacted [a] (ppm)	Reacted [a] Deriv.	d(O_3-NO) (ppm) Test	d(O_3-NO) (ppm) Base Fit	d(O_3-NO) (ppm) Change	Reactivity (mol/mol) Incremental	Reactivity (mol/mol) Mechanistic
159	1.61	1	0.016 ±0.010	IntOH	0.057	0.043 ±0.008	0.014 ±0.015	(0.009±0.009)	(0.9 ± 1.1)
3	±0.10	2	0.044 ±0.012	IntOH	0.183	0.149 ±0.016	0.034 ±0.026	0.021 ± 79%	0.76 ± 83%
		3	0.084 ±0.013	IntOH	0.330	0.285 ±0.023	0.045 ±0.034	0.028 ± 77%	0.53 ± 79%
		4	0.135 ±0.014	IntOH	0.472	0.421 ±0.034	0.051 ±0.048	0.032 ± 94%	0.38 ± 95%
		5	0.196 ±0.016	IntOH	0.630	0.555 ±0.039	0.075 ±0.054	0.046 ± 73%	0.38 ± 74%
		6	0.265 ±0.020	IntOH	0.811	0.701 ±0.047	0.110 ±0.067	0.069 ± 61%	0.41 ± 61%
155	1.74	1	0.016 ±0.022	IntOH	0.075	0.042 ±0.008	0.033 ±0.015	0.0187 ± 45%	(2.0 ± 2.9)
3	±0.08	2	0.052 ±0.024	IntOH	0.219	0.146 ±0.016	0.073 ±0.026	0.042 ± 36%	1.40 ± 58%
		3	0.099 ±0.025	IntOH	0.382	0.282 ±0.023	0.100 ±0.034	0.058 ± 34%	1.02 ± 42%
		4	0.150 ±0.026	IntOH	0.545	0.417 ±0.033	0.128 ±0.047	0.074 ± 37%	0.85 ± 41%
		5	0.211 ±0.025	IntOH	0.720	0.549 ±0.038	0.171 ±0.054	0.099 ± 32%	0.81 ± 34%
		6	0.290 ±0.025	IntOH	0.927	0.692 ±0.047	0.235 ±0.066	0.135 ± 29%	0.81 ± 29%
Dimethyl Ether									
283	2.10	1	0.008 ±0.015	IntOH	0.065	0.043 ±0.008	0.022 ±0.012	0.0107 ± 52%	(2.9 ± 5.7)
3	±0.04	2	0.032 ±0.016	IntOH	0.238	0.171 ±0.016	0.067 ±0.023	0.032 ± 34%	2.09 ± 60%
		3	0.062 ±0.017	IntOH	0.432	0.333 ±0.023	0.099 ±0.033	0.047 ± 33%	1.60 ± 43%
		4	0.101 ±0.017	IntOH	0.659	0.488 ±0.034	0.171 ±0.048	0.081 ± 28%	1.69 ± 33%
		5	0.150 ±0.017	IntOH	0.923	0.663 ±0.039	0.260 ±0.055	0.123 ± 21%	1.73 ± 24%
		6	0.206 ±0.017	IntOH	1.196	0.863 ±0.047	0.333 ±0.067	0.159 ± 20%	1.62 ± 22%
295	2.12	1	0.008 ±0.008	IntOH	0.060	0.039 ±0.008	0.021 ±0.012	0.0099 ± 56%	(2.7 ± 3.2)
3	±0.06	2	0.032 ±0.008	IntOH	0.221	0.157 ±0.016	0.064 ±0.023	0.030 ± 36%	2.01 ± 43%
		3	0.062 ±0.008	IntOH	0.402	0.310 ±0.023	0.092 ±0.033	0.043 ± 36%	1.47 ± 38%
		4	0.097 ±0.008	IntOH	0.591	0.459 ±0.034	0.132 ±0.048	0.062 ± 36%	1.36 ± 37%
		5	0.142 ±0.009	IntOH	0.817	0.620 ±0.039	0.197 ±0.055	0.093 ± 28%	1.39 ± 28%
		6	0.197 ±0.010	IntOH	1.069	0.802 ±0.047	0.267 ±0.067	0.126 ± 25%	1.36 ± 26%
281	3.41	1	0.023 ±0.016	IntOH	0.072	0.043 ±0.008	0.029 ±0.012	0.0085 ± 40%	1.26 ± 80%
3	±0.07	2	0.059 ±0.017	IntOH	0.248	0.167 ±0.016	0.081 ±0.023	0.024 ± 28%	1.37 ± 40%
		3	0.109 ±0.018	IntOH	0.443	0.327 ±0.023	0.116 ±0.033	0.034 ± 29%	1.07 ± 33%
		4	0.170 ±0.018	IntOH	0.677	0.481 ±0.034	0.196 ±0.048	0.058 ± 25%	1.15 ± 27%
		5	0.243 ±0.018	IntOH	0.965	0.653 ±0.039	0.312 ±0.055	0.092 ± 18%	1.28 ± 19%
		6	0.326 ±0.019	IntOH	1.248	0.849 ±0.047	0.399 ±0.067	0.117 ± 17%	1.22 ± 18%
279	4.04	1	0.023 ±0.027	IntOH	0.088	0.043 ±0.008	0.045 ±0.012	0.0113 ± 26%	(2.0 ± 2.4)
3	±0.08	2	0.064 ±0.029	IntOH	0.283	0.164 ±0.016	0.119 ±0.023	0.029 ± 19%	1.84 ± 48%
		3	0.125 ±0.030	IntOH	0.500	0.323 ±0.023	0.177 ±0.033	0.044 ± 19%	1.42 ± 30%
		4	0.203 ±0.029	IntOH	0.769	0.475 ±0.034	0.294 ±0.048	0.073 ± 16%	1.45 ± 22%
		5	0.298 ±0.029	IntOH	1.081	0.644 ±0.039	0.437 ±0.055	0.108 ± 13%	1.47 ± 16%
		6	0.407 ±0.029	IntOH	1.361	0.835 ±0.047	0.526 ±0.067	0.130 ± 13%	1.29 ± 15%
MTBE									
120	2.04	1	0.008 ±0.007	IntOH	0.043	0.027 ±0.007	0.016 ±0.010	0.0079 ± 60%	(2.0 ± 2.1)
2	±0.04	2	0.024 ±0.007	IntOH	0.119	0.083 ±0.012	0.036 ±0.016	0.0175 ± 46%	1.51 ± 54%
		3	0.044 ±0.007	IntOH	0.219	0.163 ±0.014	0.056 ±0.020	0.027 ± 36%	1.27 ± 39%
		4	0.065 ±0.007	IntOH	0.325	0.261 ±0.014	0.064 ±0.020	0.031 ± 32%	0.98 ± 34%
		5	0.083 ±0.008	IntOH	0.423	0.344 ±0.016	0.079 ±0.023	0.039 ± 29%	0.95 ± 30%
		6	0.108 ±0.008	IntOH	0.555	0.430 ±0.018	0.125 ±0.025	0.061 ± 20%	1.16 ± 22%
125	2.49	1	0.006 ±0.010	IntOH	0.031	0.026 ±0.007	0.005 ±0.010	(0.002±0.004)	(0.8 ± 2.0)
2	±0.05	2	0.022 ±0.010	IntOH	0.104	0.084 ±0.012	0.020 ±0.017	0.0079 ± 84%	0.89 ± 95%
		3	0.043 ±0.010	IntOH	0.200	0.164 ±0.014	0.036 ±0.020	0.0144 ± 56%	0.83 ± 60%
		4	0.069 ±0.010	IntOH	0.314	0.265 ±0.015	0.049 ±0.021	0.0197 ± 42%	0.72 ± 45%
		5	0.091 ±0.011	IntOH	0.417	0.346 ±0.016	0.071 ±0.023	0.028 ± 33%	0.78 ± 35%
		6	0.120 ±0.012	IntOH	0.552	0.434 ±0.018	0.118 ±0.025	0.047 ± 22%	0.98 ± 24%

Table A-1 (continued)

Run Set	Added (ppm)	Time (hr)	Reacted [a] (ppm)	Deriv.	d(O_3-NO) (ppm) Test	Base Fit	Change	Reactivity (mol/mol) Incremental	Mechanistic
127	2.51	1	0.008 ±0.009	IntOH	0.038	0.026 ±0.007	0.012 ±0.009	0.0048 ± 77%	(1.4 ± 1.8)
2	±0.05	2	0.021 ±0.009	IntOH	0.121	0.081 ±0.011	0.040 ±0.016	0.0160 ± 39%	1.88 ± 56%
		3	0.038 ±0.009	IntOH	0.224	0.160 ±0.013	0.064 ±0.019	0.025 ± 30%	1.66 ± 38%
		4	0.060 ±0.009	IntOH	0.338	0.252 ±0.014	0.086 ±0.020	0.034 ± 23%	1.43 ± 28%
		5	0.085 ±0.009	IntOH	0.439	0.336 ±0.016	0.103 ±0.022	0.041 ± 21%	1.21 ± 24%
		6	0.115 ±0.010	IntOH	0.579	0.422 ±0.017	0.157 ±0.024	0.063 ± 16%	1.37 ± 18%
123	2.98	1	0.012 ±0.011	IntOH	0.050	0.022 ±0.009	0.028 ±0.013	0.0092 ± 48%	(2.4 ± 2.5)
2	±0.06	2	0.032 ±0.011	IntOH	0.160	0.091 ±0.016	0.069 ±0.022	0.023 ± 33%	2.14 ± 48%
		3	0.062 ±0.012	IntOH	0.290	0.180 ±0.019	0.110 ±0.027	0.037 ± 25%	1.77 ± 32%
		4	0.100 ±0.012	IntOH	0.437	0.298 ±0.020	0.139 ±0.028	0.047 ± 20%	1.38 ± 23%
		5	0.147 ±0.012	IntOH	0.587	0.396 ±0.022	0.191 ±0.031	0.064 ± 17%	1.30 ± 18%
		6	0.202 ±0.013	IntOH	0.812	0.502 ±0.024	0.310 ±0.034	0.104 ± 11%	1.53 ± 13%
Ethoxyethanol									
175	0.401	1	0.013 ±0.035	D(d2)	0.053	0.037 ±0.008	0.016 ±0.012	0.041 ± 72%	(1.3 ± 3.7)
3	±0.025	2	0.043 ±0.034	D(d2)	0.177	0.128 ±0.016	0.049 ±0.023	0.122 ± 47%	1.14 ± 92%
		3	0.075 ±0.033	D(d2)	0.323	0.249 ±0.023	0.074 ±0.033	0.184 ± 45%	0.98 ± 63%
		4	0.108 ±0.032	D(d2)	0.486	0.374 ±0.034	0.112 ±0.048	0.28 ± 43%	1.04 ± 52%
		5	0.143 ±0.031	D(d2)	0.681	0.484 ±0.039	0.197 ±0.055	0.49 ± 29%	1.38 ± 36%
		6	0.178 ±0.031	D(d2)	0.905	0.600 ±0.048	0.305 ±0.067	0.76 ± 23%	1.71 ± 28%
171	0.730	1	0.006 ±0.029	D(d3)	0.063	0.040 ±0.008	0.023 ±0.015	0.031 ± 66%	(3.8 ±18.6)
3	±0.020	2	0.031 ±0.029	D(d3)	0.214	0.138 ±0.016	0.076 ±0.026	0.104 ± 35%	(2.5 ± 2.5)
		3	0.074 ±0.030	D(d3)	0.398	0.269 ±0.023	0.129 ±0.034	0.176 ± 27%	1.74 ± 49%
		4	0.138 ±0.030	D(d3)	0.616	0.400 ±0.034	0.215 ±0.048	0.29 ± 22%	1.57 ± 31%
		5	0.237 ±0.027	D(d3)	0.910	0.536 ±0.039	0.374 ±0.055	0.51 ± 15%	1.58 ± 19%
		6	0.342 ±0.026	D(d3)	1.208	0.687 ±0.047	0.521 ±0.067	0.71 ± 13%	1.52 ± 15%
163	0.859	1	0.023 ±0.024	IntOH	0.083	0.042 ±0.008	0.041 ±0.058	(0.05 ±0.07)	(1.8 ± 3.1)
3	±0.078	2	0.080 ±0.023	IntOH	0.272	0.164 ±0.016	0.108 ±0.097	0.125 ± 91%	1.34 ± 95%
		3	0.165 ±0.025	IntOH	0.496	0.310 ±0.024	0.186 ±0.118	0.22 ± 64%	1.12 ± 66%
		4	0.267 ±0.030	IntOH	0.798	0.455 ±0.034	0.343 ±0.124	0.40 ± 37%	1.28 ± 38%
		5	0.376 ±0.038	IntOH	1.148	0.607 ±0.039	0.541 ±0.140	0.63 ± 27%	1.44 ± 28%
		6	0.480 ±0.046	IntOH	1.424	0.773 ±0.048	0.651 ±0.155	0.76 ± 25%	1.36 ± 26%
Carbitol									
169	0.412	1	0.018 ±0.012	D(t3)	0.057	0.043 ±0.008	0.014 ±0.014	0.035 ± 98%	(0.8 ± 0.9)
3	±0.008	2	0.051 ±0.011	D(t3)	0.164	0.143 ±0.016	0.021 ±0.025	(0.05 ±0.06)	(0.4 ± 0.5)
		3	0.094 ±0.011	D(t3)	0.291	0.277 ±0.023	0.014 ±0.033	(0.03 ±0.08)	(0.2 ± 0.4)
		4	0.142 ±0.010	D(t3)	0.438	0.410 ±0.034	0.028 ±0.048	(0.07 ±0.12)	(0.2 ± 0.3)
		5	0.192 ±0.010	D(t3)	0.613	0.537 ±0.039	0.076 ±0.055	0.185 ± 72%	0.40 ± 72%
		6	0.239 ±0.010	D(t3)	0.817	0.672 ±0.048	0.145 ±0.067	0.35 ± 46%	0.61 ± 46%
166	0.503	1	0.024 ±0.020	D(d2)	0.067	0.050 ±0.009	0.017 ±0.017	(0.03 ±0.03)	(0.7 ± 0.9)
3	±0.015	2	0.068 ±0.020	D(d2)	0.191	0.183 ±0.016	0.008 ±0.030	(0.02 ±0.06)	(0.1 ± 0.4)
		3	0.120 ±0.020	D(d2)	0.355	0.349 ±0.024	0.006 ±0.039	(0.013 ±0.08)	(0.1 ± 0.3)
		4	0.175 ±0.019	D(d2)	0.556	0.507 ±0.035	0.049 ±0.049	(0.10 ±0.10)	(0.3 ± 0.3)
		5	0.235 ±0.019	D(d2)	0.816	0.686 ±0.040	0.130 ±0.056	0.26 ± 43%	0.55 ± 44%
		6	0.289 ±0.018	D(d2)	1.109	0.888 ±0.049	0.221 ±0.069	0.44 ± 31%	0.76 ± 32%
173	0.946	1	0.050 ±0.055	IntOH	0.051	0.039 ±0.008	0.012 ±0.017	(0.012 ±0.02)	(0.2 ± 0.4)
3	±0.019	2	0.106 ±0.052	IntOH	0.151	0.141 ±0.016	0.010 ±0.029	(0.010 ±0.03)	(0.1 ± 0.3)
		3	0.168 ±0.049	IntOH	0.274	0.275 ±0.023	-0.001 ±0.038	(-0.001 ±0.04)	(0.0 ± 0.2)
		4	0.233 ±0.046	IntOH	0.423	0.410 ±0.033	0.013 ±0.047	(0.014 ±0.05)	(0.1 ± 0.2)
		5	0.299 ±0.044	IntOH	0.615	0.540 ±0.038	0.075 ±0.054	0.079 ± 72%	0.25 ± 73%
		6	0.365 ±0.041	IntOH	0.871	0.681 ±0.047	0.190 ±0.066	0.20 ± 35%	0.52 ± 37%

Table A-1 (continued)

Run Set	Added (ppm)	Time (hr)	Reacted [a] (ppm)	Deriv.	d(O_3-NO) (ppm) Test	Base Fit	Change	Reactivity (mol/mol) Incremental	Mechanistic
Formaldehyde									
352	0.104	1	[b]		0.147	0.057 ±0.008	0.090 ±0.012	0.86 ± 13%	
3	±0.002	2	[b]		0.350	0.199 ±0.016	0.151 ±0.023	1.46 ± 15%	
		3	[b]		0.528	0.366 ±0.023	0.162 ±0.033	1.56 ± 20%	
		4	[b]		0.715	0.520 ±0.034	0.195 ±0.048	1.87 ± 25%	
		5	[b]		0.913	0.683 ±0.039	0.230 ±0.055	2.2 ± 24%	
		6	[b]		1.110	0.863 ±0.048	0.247 ±0.067	2.4 ± 27%	
357	0.267	1	[b]		0.225	0.058 ±0.008	0.167 ±0.012	0.62 ± 7%	
3	±0.005	2	[b]		0.461	0.193 ±0.016	0.268 ±0.023	1.00 ± 9%	
		3	[b]		0.659	0.358 ±0.023	0.301 ±0.033	1.13 ± 11%	
		4	[b]		0.866	0.511 ±0.034	0.355 ±0.048	1.33 ± 14%	
		5	[b]		1.056	0.669 ±0.039	0.387 ±0.055	1.45 ± 14%	
		6	[b]		1.206	0.844 ±0.047	0.362 ±0.067	1.35 ± 19%	
Acetaldehyde									
335	0.696	1	0.044 ±0.019	D(d3)	0.206	0.058 ±0.008	0.148 ±0.012	0.21 ± 8%	3.37 ± 45%
3	±0.014	2	0.094 ±0.019	D(d3)	0.410	0.200 ±0.016	0.210 ±0.023	0.30 ± 11%	2.24 ± 23%
		3	0.132 ±0.019	D(d3)	0.562	0.371 ±0.023	0.191 ±0.033	0.27 ± 17%	1.44 ± 22%
		4	0.171 ±0.018	D(d3)	0.709	0.529 ±0.034	0.180 ±0.048	0.26 ± 27%	1.05 ± 29%
		5	0.216 ±0.018	D(d3)	0.870	0.695 ±0.039	0.175 ±0.055	0.25 ± 31%	0.81 ± 32%
		6	0.261 ±0.018	D(d3)	1.036	0.879 ±0.047	0.157 ±0.067	0.23 ± 43%	0.60 ± 43%
338	1.31	1	0.090 ±0.036	D(d3)	0.269	0.055 ±0.008	0.214 ±0.012	0.163 ± 6%	2.38 ± 41%
3	±0.03	2	0.169 ±0.036	D(d3)	0.459	0.199 ±0.016	0.260 ±0.023	0.199 ± 9%	1.54 ± 23%
		3	0.230 ±0.035	D(d3)	0.596	0.365 ±0.024	0.231 ±0.033	0.176 ± 15%	1.00 ± 21%
		4	0.297 ±0.035	D(d3)	0.734	0.519 ±0.034	0.215 ±0.049	0.164 ± 23%	0.72 ± 26%
		5	0.371 ±0.035	D(d3)	0.878	0.685 ±0.039	0.193 ±0.055	0.147 ± 29%	0.52 ± 30%
		6	0.444 ±0.035	D(d3)	1.020	0.872 ±0.048	0.148 ±0.068	0.113 ± 46%	0.33 ± 46%
Acetone									
243	0.847	1	[b]		0.047	0.039 ±0.008	0.008 ±0.012	(0.010±0.014)	
3	±0.017	2	[b]		0.161	0.151 ±0.016	0.010 ±0.023	(0.012 ±0.03)	
		3	[b]		0.304	0.289 ±0.023	0.015 ±0.033	(0.02 ±0.04)	
		4	[b]		0.447	0.427 ±0.034	0.020 ±0.048	(0.02 ±0.06)	
		5	[b]		0.598	0.578 ±0.038	0.020 ±0.054	(0.02 ±0.06)	
		6	[b]		0.770	0.748 ±0.047	0.022 ±0.067	(0.03 ±0.08)	
245	2.19	1	[b]		0.068	0.042 ±0.008	0.026 ±0.012	0.0117 ± 46%	
3	±0.09	2	[b]		0.222	0.155 ±0.016	0.067 ±0.023	0.031 ± 34%	
		3	[b]		0.376	0.301 ±0.023	0.075 ±0.033	0.035 ± 44%	
		4	[b]		0.521	0.444 ±0.034	0.077 ±0.048	0.035 ± 63%	
		5	[b]		0.694	0.593 ±0.039	0.101 ±0.055	0.046 ± 54%	
		6	[b]		0.886	0.757 ±0.047	0.129 ±0.067	0.059 ± 52%	
247	4.14	1	[b]		0.091	0.039 ±0.008	0.052 ±0.012	0.0124 ± 23%	
3	±0.08	2	[b]		0.253	0.150 ±0.016	0.102 ±0.022	0.025 ± 22%	
		3	[b]		0.410	0.293 ±0.023	0.117 ±0.032	0.028 ± 28%	
		4	[b]		0.564	0.433 ±0.033	0.131 ±0.047	0.031 ± 36%	
		5	[b]		0.742	0.586 ±0.038	0.156 ±0.054	0.038 ± 35%	
		6	[b]		0.942	0.757 ±0.047	0.185 ±0.066	0.045 ± 36%	
Hexamethyldisiloxane									
183	6.71	1	0.008 ±0.011	IntOH	0.036	0.032 ±0.008	0.004 ±0.012	(0.0005±0.002)	(0.5 ± 1.6)
3	±0.17	2	0.018 ±0.011	IntOH	0.083	0.136 ±0.016	-0.053 ±0.023	-0.0079 ± 44%	-2.92 ± 76%
		3	0.030 ±0.011	IntOH	0.137	0.264 ±0.024	-0.127 ±0.034	-0.0190 ± 26%	-4.26 ± 46%
		4	0.044 ±0.012	IntOH	0.184	0.394 ±0.035	-0.210 ±0.049	-0.031 ± 23%	-4.80 ± 35%
		5	0.059 ±0.012	IntOH	0.238	0.525 ±0.039	-0.287 ±0.056	-0.043 ± 20%	-4.85 ± 28%
		6	0.076 ±0.013	IntOH	0.282	0.671 ±0.048	-0.389 ±0.068	-0.058 ± 18%	-5.08 ± 24%

Table A-1 (continued)

Run Set	Added (ppm)	Time (hr)	Reacted [a] (ppm)	Deriv.	d(O_3-NO) (ppm) Test	Base Fit	Change	Reactivity (mol/mol) Incremental	Mechanistic
179	9.13	1	0.009 ±0.024	IntOH	0.038	0.036 ±0.008	0.002 ±0.012	(0.0002±0.001)	(0.2 ± 1.4)
3	±0.24	2	0.020 ±0.024	IntOH	0.082	0.122 ±0.016	-0.040 ±0.023	-0.0044 ± 58%	(-1.9 ± 2.6)
		3	0.035 ±0.025	IntOH	0.136	0.239 ±0.024	-0.103 ±0.033	-0.0113 ± 33%	-2.95 ± 79%
		4	0.045 ±0.026	IntOH	0.179	0.360 ±0.034	-0.181 ±0.049	-0.0199 ± 27%	-3.99 ± 63%
		5	0.053 ±0.027	IntOH	0.214	0.462 ±0.039	-0.248 ±0.056	-0.027 ± 23%	-4.65 ± 56%
		6	0.064 ±0.029	IntOH	0.257	0.566 ±0.048	-0.309 ±0.068	-0.034 ± 22%	-4.84 ± 50%
396	2.83	1	0.016 ±0.011	IntOH	0.034	0.054 ±0.008	-0.020 ±0.020	-0.0071 ± 98%	(-1.3 ± 1.6)
4	±0.06	2	0.031 ±0.011	IntOH	0.098	0.216 ±0.019	-0.118 ±0.040	-0.042 ± 34%	-3.80 ± 50%
		3	0.046 ±0.012	IntOH	0.168	0.394 ±0.041	-0.226 ±0.065	-0.080 ± 29%	-4.88 ± 38%
		4	0.062 ±0.012	IntOH	0.246	0.541 ±0.030	-0.295 ±0.080	-0.104 ± 27%	-4.80 ± 33%
		5	0.076 ±0.012	IntOH	0.334	0.610 ±0.030	-0.276 ±0.090	-0.097 ± 33%	-3.61 ± 36%
		6	0.091 ±0.013	IntOH	0.420	0.634 ±0.034	-0.214 ±0.109	-0.076 ± 51%	-2.35 ± 53%
391	3.99	1	0.004 ±0.009	IntOH	0.030	0.055 ±0.008	-0.025 ±0.020	-0.0063 ± 78%	(-6.2 ±13.9)
4	±0.08	2	0.012 ±0.009	IntOH	0.078	0.220 ±0.019	-0.142 ±0.040	-0.036 ± 28%	-11.62 ± 79%
		3	0.023 ±0.010	IntOH	0.131	0.402 ±0.040	-0.271 ±0.065	-0.068 ± 24%	-11.91 ± 48%
		4	0.035 ±0.010	IntOH	0.181	0.546 ±0.029	-0.365 ±0.079	-0.091 ± 22%	-10.50 ± 35%
		5	0.052 ±0.010	IntOH	0.243	0.612 ±0.029	-0.369 ±0.089	-0.093 ± 24%	-7.16 ± 30%
		6	0.072 ±0.010	IntOH	0.307	0.635 ±0.033	-0.328 ±0.108	-0.082 ± 33%	-4.58 ± 36%
Octamethylcyclotetrasiloxane									
194	2.15	1	0.002 ±0.003	IntOH	0.027	0.035 ±0.008	-0.008 ±0.012	(-0.004±0.006)	(-4.1 ± 9.2)
3	±0.31	2	0.007 ±0.003	IntOH	0.083	0.142 ±0.016	-0.059 ±0.023	-0.027 ± 42%	-8.87 ± 65%
		3	0.013 ±0.004	IntOH	0.160	0.272 ±0.024	-0.112 ±0.033	-0.052 ± 33%	-8.58 ± 42%
		4	0.019 ±0.004	IntOH	0.232	0.403 ±0.034	-0.171 ±0.049	-0.079 ± 32%	-9.00 ± 37%
		5	0.025 ±0.005	IntOH	0.310	0.547 ±0.039	-0.237 ±0.056	-0.110 ± 27%	-9.33 ± 31%
		6	0.032 ±0.006	IntOH	0.387	0.710 ±0.048	-0.323 ±0.068	-0.150 ± 25%	-10.22 ± 28%
185	4.31	1	0.008 ±0.008	IntOH	0.025	0.035 ±0.008	-0.010 ±0.012	(-0.002±0.003)	(-1.2 ± 1.9)
3	±0.17	2	0.016 ±0.008	IntOH	0.067	0.119 ±0.016	-0.052 ±0.023	-0.0122 ± 43%	-3.25 ± 68%
		3	0.024 ±0.009	IntOH	0.124	0.239 ±0.023	-0.115 ±0.033	-0.027 ± 29%	-4.71 ± 46%
		4	0.032 ±0.009	IntOH	0.179	0.361 ±0.034	-0.182 ±0.048	-0.042 ± 27%	-5.63 ± 39%
		5	0.040 ±0.010	IntOH	0.237	0.472 ±0.039	-0.235 ±0.054	-0.055 ± 23%	-5.85 ± 33%
		6	0.048 ±0.010	IntOH	0.278	0.593 ±0.047	-0.315 ±0.067	-0.073 ± 22%	-6.52 ± 30%
181	10.08	1	0.002 ±0.012	IntOH	0.020	0.037 ±0.008	-0.017 ±0.012	-0.0017 ± 69%	(-9.5 ±64.2)
3	±0.20	2	0.005 ±0.012	IntOH	0.046	0.122 ±0.016	-0.076 ±0.023	-0.0076 ± 30%	(-15.6 ±39.5)
		3	0.009 ±0.013	IntOH	0.077	0.244 ±0.023	-0.167 ±0.033	-0.0166 ± 20%	(-18.0 ±24.7)
		4	0.014 ±0.013	IntOH	0.111	0.367 ±0.034	-0.256 ±0.048	-0.025 ± 19%	-18.86 ± 98%
		5	0.019 ±0.014	IntOH	0.146	0.481 ±0.039	-0.336 ±0.055	-0.033 ± 16%	-17.91 ± 77%
		6	0.024 ±0.015	IntOH	0.183	0.606 ±0.047	-0.423 ±0.067	-0.042 ± 16%	-17.72 ± 65%
406	1.35	1	0.005 ±0.002	IntOH	0.026	0.054 ±0.008	-0.028 ±0.020	-0.021 ± 71%	-5.38 ± 78%
4	±0.03	2	0.011 ±0.002	IntOH	0.089	0.214 ±0.020	-0.125 ±0.040	-0.093 ± 32%	-11.68 ± 36%
		3	0.017 ±0.002	IntOH	0.164	0.390 ±0.042	-0.226 ±0.065	-0.168 ± 29%	-13.56 ± 31%
		4	0.023 ±0.002	IntOH	0.246	0.539 ±0.030	-0.293 ±0.079	-0.22 ± 27%	-12.69 ± 28%
		5	0.030 ±0.002	IntOH	0.338	0.609 ±0.030	-0.271 ±0.089	-0.20 ± 33%	-9.07 ± 34%
		6	0.037 ±0.002	IntOH	0.429	0.634 ±0.034	-0.205 ±0.108	-0.152 ± 53%	-5.54 ± 53%
402	1.77	1	0.003 ±0.002	IntOH	0.023	0.053 ±0.008	-0.030 ±0.021	-0.0169 ± 70%	-9.28 ± 88%
4	±0.04	2	0.008 ±0.002	IntOH	0.072	0.211 ±0.020	-0.139 ±0.042	-0.078 ± 31%	-17.15 ± 38%
		3	0.015 ±0.002	IntOH	0.136	0.382 ±0.043	-0.246 ±0.069	-0.139 ± 28%	-16.89 ± 31%
		4	0.023 ±0.002	IntOH	0.209	0.534 ±0.031	-0.325 ±0.085	-0.184 ± 26%	-14.32 ± 27%
		5	0.032 ±0.002	IntOH	0.287	0.606 ±0.031	-0.319 ±0.095	-0.181 ± 30%	-9.85 ± 30%
		6	0.044 ±0.002	IntOH	0.360	0.633 ±0.035	-0.273 ±0.115	-0.154 ± 42%	-6.26 ± 43%
398	2.62	1	0.000 ±0.008	IntOH	0.025	0.057 ±0.008	-0.032 ±0.020	-0.0124 ± 62%	[c]
4	±0.05	2	0.002 ±0.008	IntOH	0.071	0.229 ±0.019	-0.158 ±0.041	-0.060 ± 26%	[c]
		3	0.003 ±0.008	IntOH	0.125	0.422 ±0.041	-0.297 ±0.066	-0.113 ± 22%	[c]
		4	0.004 ±0.008	IntOH	0.179	0.557 ±0.030	-0.378 ±0.082	-0.144 ± 22%	[c]
		5	0.006 ±0.008	IntOH	0.244	0.619 ±0.029	-0.375 ±0.092	-0.143 ± 25%	(-59.8 ±82.4)
		6	0.008 ±0.009	IntOH	0.319	0.638 ±0.033	-0.319 ±0.112	-0.122 ± 35%	(-38.0 ±43.1)

Table A-1 (continued)

Run Set	Added (ppm)	Time (hr)	Reacted [a] (ppm)	Reacted [a] Deriv.	d(O_3-NO) (ppm) Test	d(O_3-NO) (ppm) Base Fit	d(O_3-NO) (ppm) Change	Reactivity (mol/mol) Incremental	Reactivity (mol/mol) Mechanistic
Decamethylcyclopentasiloxane									
190	1.55	1	0.001 ±0.003	IntOH	0.018	0.031 ±0.009	-0.013 ±0.013	-0.0084 ± 97%	(-9.0 ±23.2)
3	±0.03	2	0.004 ±0.003	IntOH	0.052	0.142 ±0.017	-0.090 ±0.024	-0.058 ± 27%	-20.56 ± 83%
		3	0.009 ±0.004	IntOH	0.101	0.271 ±0.025	-0.170 ±0.035	-0.110 ± 21%	-18.77 ± 45%
		4	0.013 ±0.004	IntOH	0.146	0.402 ±0.036	-0.256 ±0.051	-0.165 ± 20%	-19.42 ± 35%
		5	0.018 ±0.004	IntOH	0.199	0.548 ±0.041	-0.349 ±0.058	-0.23 ± 17%	-19.34 ± 27%
		6	0.023 ±0.004	IntOH	0.257	0.716 ±0.051	-0.459 ±0.071	-0.30 ± 16%	-19.55 ± 24%
192	1.85	1	0.005 ±0.004	IntOH	0.018	0.031 ±0.009	-0.013 ±0.012	-0.0071 ± 95%	(-2.6 ± 3.1)
3	±0.27	2	0.010 ±0.004	IntOH	0.055	0.137 ±0.017	-0.082 ±0.024	-0.044 ± 33%	-8.25 ± 48%
		3	0.015 ±0.004	IntOH	0.101	0.262 ±0.024	-0.161 ±0.035	-0.087 ± 26%	-10.79 ± 36%
		4	0.020 ±0.005	IntOH	0.158	0.389 ±0.036	-0.231 ±0.050	-0.125 ± 26%	-11.69 ± 33%
		5	0.025 ±0.005	IntOH	0.214	0.529 ±0.041	-0.315 ±0.058	-0.170 ± 23%	-12.76 ± 29%
		6	0.029 ±0.006	IntOH	0.271	0.687 ±0.050	-0.416 ±0.070	-0.23 ± 22%	-14.13 ± 27%
187	4.93	1	0.007 ±0.009	IntOH	0.010	0.034 ±0.008	-0.024 ±0.012	-0.0049 ± 49%	(-3.7 ± 5.5)
3	±0.10	2	0.013 ±0.009	IntOH	0.038	0.145 ±0.016	-0.107 ±0.023	-0.022 ± 22%	-8.17 ± 74%
		3	0.020 ±0.009	IntOH	0.076	0.283 ±0.024	-0.207 ±0.033	-0.042 ± 16%	-10.60 ± 51%
		4	0.026 ±0.010	IntOH	0.123	0.420 ±0.034	-0.297 ±0.049	-0.060 ± 17%	-11.44 ± 41%
		5	0.032 ±0.010	IntOH	0.166	0.569 ±0.039	-0.403 ±0.056	-0.082 ± 14%	-12.46 ± 34%
		6	0.039 ±0.010	IntOH	0.211	0.739 ±0.048	-0.528 ±0.068	-0.107 ± 13%	-13.66 ± 30%
Pentamethyldisiloxanol									
412	0.712	1	0.005 ±0.001	IntOH	0.040	0.048 ±0.009	-0.008 ±0.012	(-0.012 ±0.02)	(-1.6 ± 2.4)
3	±0.014	2	0.010 ±0.001	IntOH	0.124	0.161 ±0.017	-0.037 ±0.023	-0.052 ± 63%	-3.53 ± 65%
		3	0.016 ±0.001	IntOH	0.227	0.298 ±0.024	-0.071 ±0.034	-0.099 ± 48%	-4.35 ± 49%
		4	0.022 ±0.001	IntOH	0.330	0.429 ±0.035	-0.099 ±0.049	-0.140 ± 50%	-4.45 ± 50%
		5	0.029 ±0.002	IntOH	0.425	0.546 ±0.040	-0.121 ±0.056	-0.170 ± 47%	-4.20 ± 47%
		6	0.036 ±0.002	IntOH	0.526	0.670 ±0.049	-0.144 ±0.069	-0.20 ± 48%	-4.04 ± 48%
409	2.17	1	0.002 ±0.007	IntOH	0.029	0.053 ±0.008	-0.024 ±0.012	-0.0110 ± 50%	(-14.8 ±64.6)
3	±0.04	2	0.008 ±0.008	IntOH	0.088	0.158 ±0.016	-0.070 ±0.023	-0.032 ± 33%	(-9.2 ±10.0)
		3	0.018 ±0.008	IntOH	0.161	0.298 ±0.024	-0.137 ±0.034	-0.063 ± 25%	-7.52 ± 50%
		4	0.033 ±0.008	IntOH	0.232	0.431 ±0.035	-0.199 ±0.049	-0.091 ± 25%	-5.99 ± 34%
		5	0.052 ±0.008	IntOH	0.303	0.542 ±0.039	-0.239 ±0.056	-0.110 ± 23%	-4.57 ± 28%
		6	0.075 ±0.009	IntOH	0.370	0.657 ±0.048	-0.287 ±0.068	-0.132 ± 24%	-3.81 ± 26%
404	1.20	1	0.005 ±0.002	IntOH	0.023	0.053 ±0.008	-0.030 ±0.018	-0.025 ± 59%	-6.32 ± 73%
4	±0.03	2	0.010 ±0.002	IntOH	0.078	0.212 ±0.020	-0.134 ±0.037	-0.112 ± 27%	-12.93 ± 34%
		3	0.017 ±0.002	IntOH	0.144	0.386 ±0.042	-0.242 ±0.061	-0.20 ± 26%	-14.47 ± 28%
		4	0.024 ±0.002	IntOH	0.213	0.537 ±0.031	-0.324 ±0.072	-0.27 ± 22%	-13.56 ± 24%
		5	0.032 ±0.002	IntOH	0.288	0.607 ±0.030	-0.319 ±0.080	-0.27 ± 25%	-10.06 ± 26%
		6	0.040 ±0.003	IntOH	0.375	0.633 ±0.034	-0.258 ±0.097	-0.21 ± 38%	-6.40 ± 38%
400	2.70	1	0.003 ±0.006	IntOH	0.025	0.055 ±0.008	-0.030 ±0.021	-0.0111 ± 70%	(-9.6 ±19.0)
4	±0.07	2	0.009 ±0.006	IntOH	0.061	0.220 ±0.019	-0.159 ±0.042	-0.059 ± 27%	-16.80 ± 70%
		3	0.019 ±0.006	IntOH	0.103	0.402 ±0.040	-0.299 ±0.068	-0.111 ± 23%	-15.62 ± 41%
		4	0.031 ±0.007	IntOH	0.147	0.546 ±0.029	-0.399 ±0.085	-0.147 ± 21%	-12.68 ± 30%
		5	0.046 ±0.007	IntOH	0.192	0.612 ±0.029	-0.420 ±0.095	-0.156 ± 23%	-9.04 ± 27%
		6	0.066 ±0.007	IntOH	0.241	0.635 ±0.033	-0.394 ±0.116	-0.146 ± 30%	-6.00 ± 31%

[a] Codes for methods for deriving amounts reacted are as follows: "IntOH" = derived using IntOH and the OH radical rate constant for the VOC; "D(tn)" or "D(dn)" = amounts reacted determined directly from the measured data for the VOC, where the data was smoothed by fitting to linear (n=2) or quadratic (n=3) functions of time "(tn)" or d(O3-NO) "(dn)".
[b] Amounts reacted could not be determined for this VOC.
[c] Mechanistic reactivities could not be determined because amount reacted is too uncertain.

Table A-2. Derivation of Reactivities with Respect to Hourly Integrated OH Radical Levels for All Test VOC Experiments.

Run Set	Added (ppm)	Time (hr)	Reacted (ppm)	IntOH (ppt-min)			Reactivity (ppt-min/ppm)	
				Test Run	Base Fit	Change	Incremental	Mechanistic
Carbon Monoxide								
418	110.	1	0.081 ±0.032	2.1 ±0.8	1.5 ±0.6	0.6 ±1.0	(0.005 ±0.009) (	7. ± 13.)
		2	0.173 ±0.032	4.5 ±0.9	4.2 ±0.9	0.3 ±1.3	(0.003 ±0.012) (	2. ± 8.)
		3	0.278 ±0.033	7.2 ±1.2	7.7 ±1.2	-0.4 ±1.6	(-0.004 ±0.015) (	-2. ± 6.)
		4	0.395 ±0.035	10.3 ±1.4	11.7 ±1.4	-1.4 ±2.0	(-0.013 ±0.02) (	-4. ± 5.)
		5	0.523 ±0.037	13.7 ±1.6	16.0 ±1.6	-2.3 ±2.2	(-0.02 ±0.02) (	-4. ± 4.)
		6	0.662 ±0.040	17.4 ±1.9	20.8 ±1.9	-3.4 ±2.7	-0.031 ± 80%	-5. ± 80%
416	130.	1	0.061 ±0.037	1.3 ±0.8	1.6 ±0.6	-0.2 ±1.0	(-0.002 ±0.008) (	-4. ± 17.)
		2	0.182 ±0.038	4.0 ±1.0	3.9 ±1.0	0.1 ±1.4	(0.0009 ±0.010) (	1. ± 7.)
		3	0.301 ±0.039	6.6 ±1.2	7.1 ±1.2	-0.5 ±1.7	(-0.004 ±0.013) (	-2. ± 6.)
		4	0.421 ±0.041	9.3 ±1.5	10.8 ±1.5	-1.5 ±2.1	(-0.011 ±0.02) (	-4. ± 5.)
		5	0.561 ±0.043	12.4 ±1.6	14.3 ±1.6	-1.9 ±2.3	(-0.015 ±0.02) (	-3. ± 4.)
		6	0.726 ±0.047	16.1 ±2.0	18.3 ±2.0	-2.1 ±2.8	(-0.02 ±0.02) (	-3. ± 4.)
414	138.	1	0.208 ±0.051	4.3 ±1.1	1.5 ±0.6	2.8 ±1.2	0.021 ± 43%	14. ± 50%
		2	0.371 ±0.054	7.7 ±1.1	4.0 ±0.9	3.7 ±1.4	0.027 ± 39%	10. ± 41%
		3	0.558 ±0.056	11.6 ±1.2	7.4 ±1.2	4.2 ±1.7	0.031 ± 39%	8. ± 40%
		4	0.810 ±0.057	16.9 ±1.4	11.3 ±1.4	5.6 ±2.0	0.041 ± 35%	7. ± 36%
		5	1.102 ±0.061	23.1 ±1.6	15.3 ±1.6	7.8 ±2.2	0.056 ± 29%	7. ± 29%
		6	1.370 ±0.069	28.8 ±1.9	19.9 ±1.9	8.9 ±2.7	0.065 ± 31%	6. ± 31%
Ethane								
68	10.01	1	0.015 ±0.004	3.6 ±1.1	3.3 ±0.6	0.3 ±1.2	(0.03 ±0.12) (	20. ± 85.)
		2	0.029 ±0.004	7.2 ±1.1	6.8 ±1.0	0.4 ±1.5	(0.04 ±0.15) (	14. ± 51.)
		3	0.043 ±0.005	10.8 ±1.2	10.6 ±1.2	0.2 ±1.7	(0.02 ± 0.2) (	4. ± 40.)
		4	0.057 ±0.005	14.4 ±1.3	14.8 ±1.3	-0.4 ±1.9	(-0.04 ± 0.2) (	-7. ± 32.)
		5	0.071 ±0.005	18.0 ±1.4	19.3 ±1.4	-1.3 ±1.9	(-0.13 ± 0.2) (	-18. ± 27.)
		6	0.086 ±0.006	21.6 ±1.8	23.8 ±1.8	-2.2 ±2.6	(-0.2 ± 0.3) (	-25. ± 31.)
79	17.6	1	0.022 ±0.006	3.1 ±0.8	3.0 ±0.6	0.2 ±1.0	(0.009 ±0.06) (	7. ± 46.)
		2	0.043 ±0.006	6.1 ±0.9	6.1 ±0.9	0.0 ±1.3	(-.0001 ±0.08) (	0. ± 31.)
		3	0.063 ±0.006	9.0 ±1.2	9.7 ±1.2	-0.7 ±1.6	(-0.04 ±0.09) (	-11. ± 26.)
		4	0.084 ±0.006	12.1 ±1.3	13.5 ±1.3	-1.5 ±1.8	(-0.08 ±0.10) (	-18. ± 21.)
		5	0.104 ±0.007	14.9 ±1.3	17.5 ±1.3	-2.5 ±1.9	-0.143 ± 75%	-24. ± 75%
		6	0.127 ±0.007	18.3 ±1.8	21.5 ±1.8	-3.2 ±2.5	-0.181 ± 79%	-25. ± 79%
62	17.6	1	0.018 ±0.006	2.5 ±0.8	3.7 ±0.6	-1.2 ±1.0	-0.066 ± 88%	-67. ± 94%
		2	0.042 ±0.006	6.0 ±1.0	7.4 ±1.0	-1.4 ±1.4	(-0.08 ±0.08) (	-32. ± 33.)
		3	0.064 ±0.007	9.1 ±1.2	11.3 ±1.2	-2.2 ±1.7	-0.124 ± 79%	-34. ± 80%
		4	0.087 ±0.007	12.4 ±1.3	15.6 ±1.3	-3.3 ±1.9	-0.185 ± 58%	-38. ± 58%
		5	0.112 ±0.007	16.1 ±1.4	20.2 ±1.4	-4.1 ±2.0	-0.23 ± 48%	-37. ± 48%
		6	0.144 ±0.008	20.7 ±1.9	24.7 ±1.9	-4.0 ±2.6	-0.22 ± 67%	-28. ± 67%
73	18.1	1	0.017 ±0.006	2.3 ±0.8	2.7 ±0.5	-0.4 ±1.0	(-0.02 ±0.05) (	-23. ± 59.)
		2	0.035 ±0.006	4.8 ±0.9	5.9 ±0.9	-1.0 ±1.2	(-0.06 ±0.07) (	-29. ± 36.)
		3	0.055 ±0.006	7.6 ±1.1	9.5 ±1.1	-1.9 ±1.5	-0.104 ± 82%	-34. ± 82%
		4	0.076 ±0.007	10.5 ±1.2	13.3 ±1.2	-2.8 ±1.7	-0.152 ± 60%	-36. ± 61%
		5	0.098 ±0.007	13.6 ±1.2	17.3 ±1.2	-3.6 ±1.7	-0.20 ± 48%	-37. ± 49%
		6	0.122 ±0.007	17.0 ±1.7	21.7 ±1.7	-4.8 ±2.3	-0.26 ± 49%	-39. ± 50%
88	24.4	1	0.027 ±0.008	2.8 ±0.8	2.4 ±0.6	0.4 ±1.0	(0.02 ±0.04) (	15. ± 37.)
		2	0.056 ±0.009	5.7 ±0.9	5.3 ±0.9	0.5 ±1.3	(0.02 ±0.05) (	8. ± 23.)
		3	0.082 ±0.009	8.4 ±1.1	8.7 ±1.1	-0.3 ±1.6	(-0.011 ±0.07) (	-3. ± 19.)
		4	0.108 ±0.009	11.1 ±1.2	12.3 ±1.2	-1.1 ±1.7	(-0.05 ±0.07) (	-10. ± 16.)
		5	0.142 ±0.010	14.7 ±1.3	15.9 ±1.3	-1.2 ±1.8	(-0.05 ±0.07) (	-9. ± 13.)
		6	0.178 ±0.011	18.5 ±1.7	20.1 ±1.7	-1.6 ±2.4	(-0.06 ±0.10) (	-9. ± 14.)

Table A-2 (continued)

Run Set	Added (ppm)	Time (hr)	Reacted (ppm)	IntOH (ppt-min) Test Run	Base Fit	Change	Reactivity (ppt-min/ppm) Incremental	Mechanistic
99	16.6	1	0.008 ±0.009	1.2 ±1.4	1.3 ±0.5	0.0 ±1.5	(-.0003 ±0.09)	(-1. ±178.)
		2	0.024 ±0.009	3.6 ±1.4	3.4 ±0.7	0.2 ±1.6	(0.011 ±0.09)	(8. ± 66.)
		3	0.041 ±0.010	6.2 ±1.4	6.3 ±0.8	0.0 ±1.6	(-0.003 ±0.10)	(-1. ± 40.)
		4	0.060 ±0.010	9.0 ±1.5	9.6 ±0.6	-0.6 ±1.6	(-0.03 ±0.10)	(-10. ± 27.)
		5	0.078 ±0.011	11.8 ±1.6	12.9 ±0.5	-1.1 ±1.7	(-0.07 ±0.10)	(-14. ± 22.)
		6	0.096 ±0.012	14.7 ±1.7	16.5 ±0.7	-1.8 ±1.8	(-0.11 ±0.11)	(-19. ± 19.)
92	17.1	1	0.010 ±0.008	1.5 ±1.1	1.3 ±0.5	0.2 ±1.3	(0.012 ±0.07)	(20. ±124.)
		2	0.023 ±0.009	3.3 ±1.2	3.4 ±0.7	-0.1 ±1.4	(-0.006 ±0.08)	(-4. ± 63.)
		3	0.038 ±0.009	5.6 ±1.3	6.2 ±0.8	-0.7 ±1.5	(-0.04 ±0.09)	(-17. ± 41.)
		4	0.056 ±0.009	8.3 ±1.3	9.7 ±0.6	-1.5 ±1.5	(-0.09 ±0.09)	(-26. ± 27.)
		5	0.077 ±0.009	11.3 ±1.3	13.2 ±0.5	-1.9 ±1.4	-0.110 ± 75%	-24. ± 76%
		6	0.100 ±0.010	14.8 ±1.3	17.0 ±0.7	-2.2 ±1.5	-0.127 ± 70%	-22. ± 70%
332	20.0	1	0.012 ±0.007	1.5 ±0.8	1.5 ±0.6	0.0 ±1.0	(0.0010 ±0.05)	(2. ± 86.)
		2	0.040 ±0.007	5.0 ±0.9	4.6 ±0.9	0.4 ±1.3	(0.02 ±0.06)	(11. ± 32.)
		3	0.070 ±0.007	8.8 ±1.2	8.8 ±1.2	-0.1 ±1.6	(-0.003 ±0.08)	(-1. ± 23.)
		4	0.102 ±0.007	12.8 ±1.4	13.4 ±1.4	-0.6 ±2.0	(-0.03 ±0.10)	(-6. ± 19.)
		5	0.139 ±0.008	17.5 ±1.6	18.7 ±1.6	-1.2 ±2.2	(-0.06 ±0.11)	(-9. ± 16.)
		6	0.180 ±0.009	22.8 ±1.9	25.0 ±1.9	-2.1 ±2.7	(-0.11 ±0.14)	(-12. ± 15.)
333	21.0	1	0.033 ±0.007	3.9 ±0.8	1.4 ±0.6	2.5 ±1.0	0.117 ± 41%	75. ± 46%
		2	0.068 ±0.007	8.1 ±0.9	4.6 ±0.9	3.5 ±1.3	0.169 ± 37%	52. ± 38%
		3	0.106 ±0.007	12.7 ±1.2	8.8 ±1.2	3.8 ±1.6	0.183 ± 43%	36. ± 43%
		4	0.146 ±0.008	17.6 ±1.4	13.4 ±1.4	4.2 ±2.0	0.199 ± 47%	29. ± 48%
		5	0.189 ±0.009	22.8 ±1.6	18.7 ±1.6	4.1 ±2.2	0.195 ± 55%	22. ± 55%
		6	0.235 ±0.010	28.4 ±1.9	25.0 ±1.9	3.4 ±2.7	0.160 ± 81%	14. ± 81%
235	43.7	1	0.021 ±0.014	1.2 ±0.8	1.1 ±0.6	0.1 ±1.0	(0.002 ±0.02)	(5. ± 49.)
		2	0.071 ±0.015	4.1 ±0.9	3.9 ±0.9	0.2 ±1.3	(0.004 ±0.03)	(2. ± 18.)
		3	0.124 ±0.015	7.1 ±1.1	7.8 ±1.1	-0.7 ±1.6	(-0.02 ±0.04)	(-5. ± 13.)
		4	0.178 ±0.016	10.2 ±1.4	12.1 ±1.4	-1.9 ±2.0	(-0.04 ±0.04)	(-10. ± 11.)
		5	0.239 ±0.018	13.8 ±1.6	17.1 ±1.6	-3.2 ±2.2	-0.074 ± 68%	-14. ± 69%
		6	0.306 ±0.020	17.7 ±1.9	23.0 ±1.9	-5.3 ±2.7	-0.120 ± 51%	-17. ± 52%
Propane								
226	11.57	1	0.009 ±0.016	0.5 ±0.8	1.1 ±0.6	-0.6 ±1.0	(-0.05 ±0.09)	(-66. ±159.)
		2	0.033 ±0.016	1.7 ±0.9	3.6 ±0.9	-1.9 ±1.3	-0.165 ± 68%	-58. ± 84%
		3	0.069 ±0.017	3.5 ±1.2	7.1 ±1.2	-3.6 ±1.6	-0.31 ± 46%	-52. ± 52%
		4	0.110 ±0.017	5.6 ±1.4	11.0 ±1.4	-5.4 ±2.0	-0.47 ± 36%	-49. ± 40%
		5	0.163 ±0.018	8.4 ±1.6	15.4 ±1.6	-7.0 ±2.2	-0.61 ± 32%	-43. ± 33%
		6	0.231 ±0.019	12.0 ±1.9	20.5 ±1.9	-8.6 ±2.7	-0.74 ± 32%	-37. ± 33%
305	20.1	1	0.021 ±0.052	0.6 ±1.5	0.9 ±0.6	-0.3 ±1.6	(-0.013 ±0.08)	(-13. ± 84.)
		2	0.073 ±0.052	2.1 ±1.5	3.4 ±0.9	-1.3 ±1.8	(-0.06 ±0.09)	(-18. ± 28.)
		3	0.138 ±0.053	4.0 ±1.6	7.1 ±1.2	-3.1 ±2.0	-0.152 ± 64%	-22. ± 75%
		4	0.209 ±0.055	6.2 ±1.6	11.2 ±1.4	-5.0 ±2.1	-0.25 ± 43%	-24. ± 50%
		5	0.298 ±0.058	8.8 ±1.7	15.7 ±1.6	-6.9 ±2.3	-0.34 ± 34%	-23. ± 39%
		6	0.405 ±0.062	12.1 ±1.9	21.1 ±1.9	-9.0 ±2.7	-0.45 ± 30%	-22. ± 34%
230	28.8	1	0.057 ±0.040	1.2 ±0.8	1.2 ±0.6	-0.1 ±1.0	(-0.002 ±0.04)	(-1. ± 18.)
		2	0.162 ±0.044	3.3 ±0.9	3.7 ±0.9	-0.4 ±1.3	(-0.02 ±0.04)	(-3. ± 8.)
		3	0.265 ±0.048	5.5 ±1.2	7.3 ±1.2	-1.8 ±1.6	-0.064 ± 90%	-7. ± 91%
		4	0.360 ±0.050	7.4 ±1.4	11.3 ±1.4	-3.8 ±2.0	-0.133 ± 52%	-11. ± 53%
		5	0.445 ±0.050	9.2 ±1.6	15.5 ±1.6	-6.2 ±2.2	-0.22 ± 36%	-14. ± 37%
		6	0.505 ±0.052	10.5 ±1.9	20.3 ±1.9	-9.8 ±2.7	-0.34 ± 28%	-20. ± 30%

Table A-2 (continued)

Run Set	Added (ppm)	Time (hr)	Reacted (ppm)	IntOH (ppt-min) Test Run	Base Fit	Change	Reactivity (ppt-min/ppm) Incremental	Mechanistic
n-Butane								
59	1.82	1	0.015 ±0.006	2.3 ±0.8	2.3 ±0.7	-0.1 ±1.1	(-0.04 ± 0.6)	(-5. ± 71.)
		2	0.033 ±0.006	4.8 ±1.1	5.7 ±1.1	-0.8 ±1.6	(-0.5 ± 0.9)	(-26. ± 50.)
		3	0.053 ±0.006	7.9 ±1.4	9.4 ±1.4	-1.5 ±2.0	(-0.8 ± 1.1)	(-29. ± 38.)
		4	0.072 ±0.006	10.8 ±1.5	13.3 ±1.5	-2.6 ±2.2	-1.40 ± 85%	-36. ± 85%
		5	0.093 ±0.006	14.1 ±1.6	17.6 ±1.6	-3.6 ±2.3	-1.95 ± 64%	-38. ± 64%
		6	0.120 ±0.007	18.4 ±2.2	23.1 ±2.2	-4.6 ±3.0	-2.5 ± 66%	-39. ± 66%
51	2.31	1	0.018 ±0.008	2.0 ±1.0	4.1 ±0.6	-2.0 ±1.2	-0.88 ± 57%	-116. ± 75%
		2	0.041 ±0.009	4.8 ±1.0	8.2 ±1.0	-3.4 ±1.4	-1.46 ± 41%	-82. ± 46%
		3	0.065 ±0.009	7.6 ±1.2	12.3 ±1.2	-4.7 ±1.7	-2.0 ± 36%	-72. ± 39%
		4	0.089 ±0.010	10.5 ±1.3	16.8 ±1.3	-6.2 ±1.8	-2.7 ± 30%	-70. ± 31%
		5	0.116 ±0.010	13.9 ±1.4	21.5 ±1.4	-7.6 ±1.9	-3.3 ± 26%	-65. ± 27%
		6	0.148 ±0.011	17.8 ±1.8	26.1 ±1.8	-8.3 ±2.6	-3.6 ± 32%	-56. ± 32%
53	5.21	1	0.035 ±0.027	1.8 ±1.4	3.1 ±0.6	-1.3 ±1.5	(-0.2 ± 0.3)	(-36. ± 52.)
		2	0.079 ±0.029	4.1 ±1.5	6.8 ±1.0	-2.7 ±1.8	-0.51 ± 67%	-34. ± 77%
		3	0.139 ±0.030	7.2 ±1.6	10.7 ±1.2	-3.4 ±2.0	-0.66 ± 58%	-25. ± 62%
		4	0.194 ±0.031	10.2 ±1.6	14.6 ±1.3	-4.4 ±2.1	-0.84 ± 48%	-23. ± 50%
		5	0.264 ±0.031	14.0 ±1.6	18.7 ±1.4	-4.7 ±2.1	-0.91 ± 45%	-18. ± 46%
		6	0.357 ±0.032	19.2 ±1.8	23.5 ±1.8	-4.4 ±2.6	-0.84 ± 59%	-12. ± 60%
82	6.75	1	0.033 ±0.021	1.3 ±0.8	2.5 ±0.6	-1.2 ±1.0	-0.177 ± 83%	(-36. ± 38.)
		2	0.069 ±0.021	2.8 ±0.9	5.5 ±0.9	-2.7 ±1.3	-0.40 ± 47%	-39. ± 56%
		3	0.115 ±0.022	4.6 ±1.1	9.0 ±1.1	-4.4 ±1.6	-0.65 ± 36%	-38. ± 41%
		4	0.154 ±0.023	6.2 ±1.2	12.7 ±1.2	-6.5 ±1.7	-0.96 ± 26%	-42. ± 30%
		5	0.203 ±0.025	8.2 ±1.3	16.6 ±1.3	-8.4 ±1.8	-1.24 ± 21%	-41. ± 25%
		6	0.257 ±0.027	10.5 ±1.7	20.9 ±1.7	-10.5 ±2.4	-1.55 ± 23%	-41. ± 25%
86	7.00	1	0.024 ±0.027	0.9 ±1.0	2.4 ±0.6	-1.5 ±1.2	-0.21 ± 80%	(-62. ± 86.)
		2	0.055 ±0.029	2.1 ±1.1	5.2 ±0.9	-3.1 ±1.4	-0.45 ± 46%	-56. ± 70%
		3	0.096 ±0.030	3.7 ±1.2	8.6 ±1.1	-4.9 ±1.6	-0.70 ± 33%	-51. ± 46%
		4	0.145 ±0.031	5.6 ±1.2	12.1 ±1.2	-6.5 ±1.7	-0.93 ± 27%	-45. ± 34%
		5	0.202 ±0.031	7.9 ±1.3	15.8 ±1.3	-7.9 ±1.8	-1.13 ± 23%	-39. ± 28%
		6	0.266 ±0.032	10.5 ±1.7	19.9 ±1.7	-9.4 ±2.4	-1.35 ± 26%	-35. ± 28%
135	6.06	1	0.017 ±0.035	0.7 ±1.6	1.1 ±0.5	-0.3 ±1.6	(-0.05 ± 0.3)	(-20. ±108.)
		2	0.041 ±0.035	1.8 ±1.6	3.1 ±0.7	-1.3 ±1.7	(-0.2 ± 0.3)	(-30. ± 49.)
		3	0.083 ±0.036	3.7 ±1.6	6.0 ±0.8	-2.3 ±1.8	-0.38 ± 77%	-28. ± 89%
		4	0.123 ±0.037	5.5 ±1.7	9.5 ±0.6	-4.0 ±1.8	-0.66 ± 45%	-33. ± 54%
		5	0.163 ±0.039	7.3 ±1.8	12.6 ±0.5	-5.2 ±1.8	-0.86 ± 35%	-32. ± 43%
		6	0.209 ±0.041	9.5 ±1.9	15.9 ±0.7	-6.4 ±2.0	-1.06 ± 31%	-31. ± 37%
97	6.12	1	0.017 ±0.032	0.8 ±1.4	1.2 ±0.5	-0.4 ±1.5	(-0.07 ± 0.2)	(-24. ± 96.)
		2	0.044 ±0.032	1.9 ±1.4	3.3 ±0.7	-1.4 ±1.6	(-0.2 ± 0.3)	(-32. ± 43.)
		3	0.073 ±0.033	3.2 ±1.4	6.2 ±0.8	-3.0 ±1.6	-0.49 ± 55%	-41. ± 71%
		4	0.107 ±0.034	4.7 ±1.5	9.7 ±0.6	-4.9 ±1.6	-0.80 ± 33%	-46. ± 46%
		5	0.142 ±0.035	6.3 ±1.6	13.0 ±0.5	-6.7 ±1.7	-1.09 ± 25%	-47. ± 35%
		6	0.191 ±0.038	8.6 ±1.7	16.7 ±0.7	-8.1 ±1.9	-1.32 ± 23%	-42. ± 30%
94	7.16	1	0.020 ±0.022	0.7 ±0.8	1.3 ±0.6	-0.5 ±1.0	(-0.07 ±0.14)	(-27. ± 60.)
		2	0.047 ±0.022	1.8 ±0.8	3.6 ±0.8	-1.8 ±1.2	-0.26 ± 65%	-39. ± 80%
		3	0.084 ±0.023	3.2 ±0.9	6.5 ±0.9	-3.3 ±1.3	-0.46 ± 39%	-40. ± 48%
		4	0.131 ±0.023	4.9 ±0.9	10.3 ±0.8	-5.4 ±1.1	-0.75 ± 21%	-41. ± 28%
		5	0.184 ±0.024	7.0 ±0.9	13.4 ±0.6	-6.3 ±1.1	-0.89 ± 17%	-34. ± 21%
		6	0.247 ±0.025	9.5 ±0.9	17.1 ±0.8	-7.6 ±1.3	-1.06 ± 17%	-31. ± 19%
224	9.76	1	0.053 ±0.042	1.5 ±1.1	1.4 ±0.6	0.0 ±1.3	(0.002 ±0.13)	(0. ± 25.)
		2	0.105 ±0.043	2.9 ±1.2	4.2 ±0.9	-1.3 ±1.5	(-0.13 ± 0.2)	(-12. ± 15.)
		3	0.157 ±0.044	4.4 ±1.2	7.7 ±1.2	-3.4 ±1.7	-0.35 ± 49%	-22. ± 57%
		4	0.208 ±0.046	5.8 ±1.4	11.8 ±1.4	-6.0 ±2.0	-0.62 ± 33%	-29. ± 39%
		5	0.258 ±0.048	7.2 ±1.6	16.3 ±1.6	-9.1 ±2.2	-0.93 ± 25%	-35. ± 31%
		6	0.309 ±0.052	8.7 ±1.9	21.4 ±1.9	-12.8 ±2.7	-1.31 ± 22%	-41. ± 27%

Table A-2 (continued)

Run Set	Added (ppm)	Time (hr)	Reacted (ppm)	IntOH (ppt-min) Test Run	Base Fit	Change	Reactivity (ppt-min/ppm) Incremental	Mechanistic
393	3.46	1	0.011 ±0.017	0.9 ±2.7	3.6 ±2.7	-2.7 ±3.9	(-0.8 ± 1.1)	(-245. ±503.)
		2	0.045 ±0.018	3.5 ±3.1	9.9 ±3.1	-6.5 ±4.4	-1.87 ± 68%	-146. ± 80%
		3	0.100 ±0.020	7.9 ±2.6	18.2 ±2.6	-10.4 ±3.7	-3.0 ± 36%	-103. ± 41%
		4	0.161 ±0.019	12.8 ±2.4	25.8 ±2.4	-13.0 ±3.5	-3.8 ± 27%	-81. ± 29%
		5	0.204 ±0.018	16.4 ±2.6	31.2 ±2.4	-14.8 ±3.6	-4.3 ± 24%	-73. ± 26%
		6	0.226 ±0.018	18.2 ±5.0	35.1 ±5.0	-16.9 ±7.0	-4.9 ± 42%	-75. ± 42%
389	3.60	1	0.012 ±0.023	0.9 ±2.9	4.0 ±2.9	-3.1 ±4.2	(-0.9 ± 1.2)	(-251. ±588.)
		2	0.037 ±0.025	2.8 ±3.3	10.3 ±3.3	-7.5 ±4.7	-2.1 ± 63%	-201. ± 92%
		3	0.075 ±0.026	5.6 ±2.8	18.3 ±2.8	-12.7 ±3.9	-3.5 ± 31%	-170. ± 47%
		4	0.124 ±0.025	9.4 ±2.6	25.7 ±2.6	-16.3 ±3.7	-4.5 ± 23%	-132. ± 31%
		5	0.184 ±0.024	14.2 ±2.7	31.3 ±2.6	-17.1 ±3.7	-4.8 ± 22%	-93. ± 25%
		6	0.256 ±0.025	19.9 ±5.3	35.7 ±5.3	-15.8 ±7.5	-4.4 ± 48%	-62. ± 49%
Isobutane								
228	2.72	1	0.007 ±0.013	0.7 ±1.4	1.3 ±0.6	-0.6 ±1.5	(-0.2 ± 0.5)	(-83. ±266.)
		2	0.023 ±0.013	2.4 ±1.4	3.9 ±0.9	-1.4 ±1.7	(-0.5 ± 0.6)	(-62. ± 81.)
		3	0.045 ±0.013	4.9 ±1.4	7.4 ±1.2	-2.5 ±1.8	-0.91 ± 74%	-54. ± 79%
		4	0.069 ±0.013	7.5 ±1.5	11.4 ±1.4	-3.9 ±2.0	-1.42 ± 52%	-56. ± 56%
		5	0.093 ±0.014	10.2 ±1.6	15.6 ±1.6	-5.4 ±2.2	-1.99 ± 41%	-58. ± 44%
		6	0.123 ±0.015	13.6 ±1.9	20.5 ±1.9	-7.0 ±2.7	-2.6 ± 39%	-57. ± 41%
303	6.62	1	0.011 ±0.080	0.5 ±3.5	0.8 ±0.6	-0.3 ±3.6	(-0.05 ± 0.5)	(-31. ±383.)
		2	0.046 ±0.080	2.0 ±3.5	3.4 ±0.9	-1.3 ±3.7	(-0.2 ± 0.6)	(-29. ± 94.)
		3	0.097 ±0.082	4.3 ±3.6	7.0 ±1.2	-2.7 ±3.8	(-0.4 ± 0.6)	(-28. ± 46.)
		4	0.157 ±0.085	7.0 ±3.8	11.1 ±1.4	-4.1 ±4.1	(-0.6 ± 0.6)	(-26. ± 30.)
		5	0.233 ±0.092	10.5 ±4.2	15.7 ±1.6	-5.2 ±4.5	-0.78 ± 87%	-22. ± 95%
		6	0.333 ±0.103	15.1 ±4.8	21.1 ±1.9	-6.0 ±5.2	-0.90 ± 86%	-18. ± 92%
241	10.21	1	0.009 ±0.029	0.3 ±0.8	0.9 ±0.6	-0.6 ±1.0	(-0.06 ±0.10)	(-66. ±232.)
		2	0.039 ±0.029	1.1 ±0.9	3.5 ±0.9	-2.4 ±1.3	-0.24 ± 53%	-62. ± 92%
		3	0.084 ±0.030	2.4 ±1.2	7.3 ±1.2	-4.8 ±1.6	-0.47 ± 34%	-57. ± 49%
		4	0.153 ±0.030	4.4 ±1.4	11.4 ±1.4	-7.0 ±2.0	-0.69 ± 28%	-46. ± 34%
		5	0.267 ±0.032	7.7 ±1.6	16.2 ±1.6	-8.5 ±2.2	-0.83 ± 26%	-32. ± 29%
		6	0.418 ±0.034	12.3 ±1.9	22.0 ±1.9	-9.7 ±2.7	-0.95 ± 28%	-23. ± 29%
232	20.9	1	0.021 ±0.212	0.3 ±2.9	1.4 ±0.6	-1.1 ±3.0	(-0.05 ±0.14)	(-50. ±522.)
		2	0.074 ±0.213	1.0 ±3.0	3.9 ±0.9	-2.9 ±3.1	(-0.14 ±0.15)	(-39. ±122.)
		3	0.148 ±0.215	2.1 ±3.0	7.4 ±1.2	-5.3 ±3.2	-0.25 ± 61%	(-36. ± 57.)
		4	0.244 ±0.219	3.4 ±3.1	11.3 ±1.4	-7.9 ±3.4	-0.38 ± 43%	(-32. ± 32.)
		5	0.381 ±0.229	5.4 ±3.3	15.5 ±1.6	-10.2 ±3.6	-0.49 ± 36%	-27. ± 70%
		6	0.539 ±0.245	7.7 ±3.5	20.3 ±1.9	-12.7 ±4.0	-0.61 ± 32%	-23. ± 55%
n-Hexane								
201	1.168	1	0.003 ±0.041	0.3 ±3.2	1.1 ±0.6	-0.8 ±3.2	(-0.7 ± 3.)	
		2	0.007 ±0.041	0.8 ±3.2	3.6 ±0.9	-2.8 ±3.3	(-2. ± 3.)	
		3	0.014 ±0.041	1.5 ±3.3	7.1 ±1.1	-5.6 ±3.5	-4.8 ± 62%	
		4	0.023 ±0.042	2.4 ±3.4	11.1 ±1.4	-8.7 ±3.7	-7.5 ± 42%	(-385. ±737.)
		5	0.031 ±0.044	3.3 ±3.5	15.4 ±1.6	-12.1 ±3.9	-10.4 ± 32%	(-392. ±569.)
		6	0.041 ±0.046	4.4 ±3.8	20.5 ±1.9	-16.1 ±4.2	-13.8 ± 26%	(-391. ±453.)
209	1.58	1	0.014 ±0.013	1.1 ±0.8	1.2 ±0.6	-0.1 ±1.0	(-0.04 ± 0.6)	(-5. ± 71.)
		2	0.026 ±0.013	2.0 ±0.9	3.6 ±0.9	-1.6 ±1.3	-1.02 ± 80%	-63. ± 95%
		3	0.039 ±0.013	3.1 ±1.2	7.0 ±1.2	-4.0 ±1.6	-2.5 ± 41%	-102. ± 54%
		4	0.064 ±0.014	5.1 ±1.4	10.9 ±1.4	-5.9 ±2.0	-3.7 ± 34%	-91. ± 40%
		5	0.076 ±0.014	6.0 ±1.6	15.0 ±1.6	-9.0 ±2.2	-5.7 ± 25%	-119. ± 31%
		6	0.092 ±0.015	7.3 ±1.9	19.7 ±1.9	-12.4 ±2.7	-7.8 ± 22%	-135. ± 27%

Table A-2 (continued)

Run Set	Added (ppm)	Time (hr)	Reacted (ppm)	IntOH (ppt-min) Test Run	Base Fit	Change	Reactivity (ppt-min/ppm) Incremental	Mechanistic
Isooctane								
291	10.14	1	0.007 ±0.086	0.1 ±1.6	1.4 ±0.6	-1.3 ±1.7	(-0.13 ± 0.2)	
		2	0.026 ±0.086	0.5 ±1.6	4.7 ±0.9	-4.2 ±1.8	-0.41 ± 43%	(-161. ±532.)
		3	0.063 ±0.087	1.1 ±1.6	9.0 ±1.2	-7.8 ±2.0	-0.77 ± 25%	(-125. ±175.)
		4	0.115 ±0.089	2.1 ±1.6	13.6 ±1.4	-11.5 ±2.2	-1.13 ± 19%	-100. ± 80%
		5	0.189 ±0.094	3.5 ±1.7	19.1 ±1.6	-15.6 ±2.3	-1.54 ± 15%	-82. ± 52%
		6	0.294 ±0.101	5.5 ±1.9	25.6 ±1.9	-20.2 ±2.7	-2.0 ± 14%	-69. ± 37%
293	10.64	1	0.014 ±0.100	0.2 ±1.7	1.6 ±0.6	-1.3 ±1.8	(-0.12 ± 0.2)	(-96. ±709.)
		2	0.041 ±0.099	0.7 ±1.7	4.7 ±0.9	-4.0 ±2.0	-0.38 ± 49%	(-98. ±244.)
		3	0.087 ±0.100	1.5 ±1.8	8.8 ±1.2	-7.3 ±2.1	-0.68 ± 29%	(-83. ± 98.)
		4	0.153 ±0.102	2.7 ±1.8	13.2 ±1.4	-10.6 ±2.3	-0.99 ± 22%	-69. ± 70%
		5	0.248 ±0.108	4.4 ±1.9	18.5 ±1.6	-14.1 ±2.5	-1.33 ± 18%	-57. ± 47%
		6	0.382 ±0.118	6.8 ±2.1	24.6 ±1.9	-17.8 ±2.9	-1.67 ± 16%	-46. ± 35%
n-Octane								
239	1.55	1	0.011 ±0.016	0.6 ±0.8	1.2 ±0.6	-0.6 ±1.0	(-0.4 ± 0.7)	(-55. ±123.)
		2	0.022 ±0.016	1.1 ±0.9	3.8 ±0.9	-2.7 ±1.3	-1.75 ± 48%	-124. ± 88%
		3	0.033 ±0.017	1.7 ±1.2	7.6 ±1.2	-5.9 ±1.6	-3.8 ± 28%	-182. ± 57%
		4	0.043 ±0.017	2.2 ±1.4	11.8 ±1.4	-9.6 ±2.0	-6.2 ± 21%	-223. ± 44%
		5	0.053 ±0.017	2.7 ±1.6	16.3 ±1.6	-13.6 ±2.2	-8.7 ± 17%	-254. ± 36%
		6	0.064 ±0.018	3.3 ±1.9	21.7 ±1.9	-18.4 ±2.7	-11.9 ± 15%	-289. ± 32%
237	1.66	1	0.004 ±0.018	0.2 ±0.8	1.0 ±0.6	-0.8 ±1.0	(-0.5 ± 0.6)	(-173. ±720.)
		2	0.014 ±0.018	0.7 ±0.9	3.7 ±0.9	-3.1 ±1.3	-1.84 ± 42%	(-213. ±275.)
		3	0.030 ±0.018	1.4 ±1.2	7.5 ±1.2	-6.1 ±1.6	-3.7 ± 27%	-202. ± 64%
		4	0.049 ±0.018	2.4 ±1.4	11.8 ±1.4	-9.4 ±2.0	-5.7 ± 21%	-191. ± 42%
		5	0.072 ±0.018	3.5 ±1.6	16.7 ±1.6	-13.2 ±2.2	-8.0 ± 17%	-183. ± 30%
		6	0.098 ±0.019	4.8 ±1.9	22.6 ±1.9	-17.8 ±2.7	-10.7 ± 15%	-181. ± 24%
Ethene								
203	0.217	1	0.004 ±0.026	1.1 ±0.8	1.4 ±0.6	-0.3 ±1.0	(-1.4 ± 5.)	(-77. ±581.)
		2	0.016 ±0.026	4.5 ±0.9	4.3 ±0.9	0.2 ±1.3	(0.9 ± 6.)	(12. ± 80.)
		3	0.031 ±0.025	8.7 ±1.2	8.1 ±1.2	0.6 ±1.6	(3. ± 8.)	(18. ± 55.)
		4	0.047 ±0.025	13.8 ±1.4	12.4 ±1.4	1.4 ±2.0	(6. ± 9.)	(29. ± 44.)
		5	0.065 ±0.025	19.9 ±1.6	17.2 ±1.6	2.7 ±2.2	12.2 ± 84%	41. ± 92%
		6	0.086 ±0.025	28.0 ±1.9	22.8 ±1.9	5.2 ±2.7	24. ± 53%	61. ± 59%
199	0.386	1	0.005 ±0.036	0.8 ±2.6	1.1 ±0.6	-0.3 ±2.6	(-0.8 ± 7.)	(-60. ±626.)
		2	0.026 ±0.037	3.8 ±2.7	3.9 ±0.9	-0.2 ±2.9	(-0.4 ± 7.)	(-7. ±110.)
		3	0.053 ±0.038	8.0 ±2.9	7.7 ±1.2	0.2 ±3.1	(0.6 ± 8.)	(5. ± 59.)
		4	0.086 ±0.037	13.7 ±3.0	11.9 ±1.4	1.7 ±3.3	(5. ± 9.)	(20. ± 39.)
		5	0.131 ±0.035	22.6 ±2.9	16.9 ±1.6	5.8 ±3.3	14.9 ± 58%	44. ± 63%
		6	0.172 ±0.034	32.7 ±3.0	22.6 ±1.9	10.1 ±3.6	26. ± 36%	59. ± 40%
Propene								
65	0.083	1	0.002 ±0.020	2.8 ±0.8	3.1 ±0.5	-0.3 ±1.0	(-3. ± 12.)	
		2	0.012 ±0.020	6.2 ±0.9	6.5 ±0.9	-0.3 ±1.2	(-4. ± 15.)	(-25. ±111.)
		3	0.026 ±0.019	10.2 ±1.1	10.3 ±1.1	-0.1 ±1.5	(-1.0 ± 18.)	(-3. ± 58.)
		4	0.042 ±0.017	14.7 ±1.2	14.2 ±1.2	0.6 ±1.7	(7. ± 20.)	(13. ± 40.)
		5	0.056 ±0.015	19.8 ±1.2	18.2 ±1.2	1.6 ±1.7	(19. ± 21.)	(28. ± 32.)
		6	0.067 ±0.015	25.5 ±1.6	22.6 ±1.6	2.9 ±2.3	35. ± 83%	43. ± 84%
72	0.120	1	0.008 ±0.008	2.3 ±1.6	3.1 ±0.6	-0.8 ±1.7	(-7. ± 14.)	(-105. ±238.)
		2	0.022 ±0.007	6.1 ±1.6	6.4 ±0.9	-0.3 ±1.9	(-3. ± 16.)	(-14. ± 84.)
		3	0.040 ±0.007	10.9 ±1.7	10.1 ±1.1	0.7 ±2.0	(6. ± 17.)	(18. ± 50.)
		4	0.059 ±0.006	14.9 ±1.7	14.1 ±1.2	0.8 ±2.1	(6. ± 18.)	(13. ± 36.)
		5	0.076 ±0.006	19.1 ±1.8	18.4 ±1.3	0.7 ±2.2	(6. ± 19.)	(10. ± 29.)
		6	0.090 ±0.006	24.0 ±1.9	22.7 ±1.7	1.4 ±2.6	(11. ± 22.)	(15. ± 29.)

Table A-2 (continued)

Run / Set	Added (ppm)	Time (hr)	Reacted (ppm)	IntOH (ppt-min) Test Run	Base Fit	Change	Reactivity (ppt-min/ppm) Incremental	Mechanistic
110	0.070	1	0.002 ±0.013	0.0 ±2.4	1.1 ±0.5	-1.1 ±2.5	(-16. ± 35.)	
		2	0.007 ±0.013	0.8 ±2.6	3.1 ±0.7	-2.3 ±2.7	(-33. ± 39.)	(-341. ±749.)
		3	0.015 ±0.013	2.8 ±2.8	5.9 ±0.8	-3.1 ±2.9	-44. ± 94%	(-203. ±252.)
		4	0.025 ±0.012	6.0 ±2.9	9.0 ±0.7	-3.0 ±3.0	(-42. ± 42.)	(-119. ±131.)
		5	0.035 ±0.011	10.6 ±2.8	12.4 ±0.5	-1.9 ±2.9	(-27. ± 41.)	(-55. ± 85.)
		6	0.045 ±0.010	17.7 ±2.8	15.9 ±0.7	1.8 ±2.9	(26. ± 42.)	(41. ± 65.)
106	0.081	1	0.003 ±0.005	1.4 ±0.8	1.3 ±0.5	0.0 ±1.0	(0.5 ± 12.)	(16. ±375.)
		2	0.010 ±0.005	4.5 ±0.8	3.5 ±0.7	1.0 ±1.1	(13. ± 14.)	(103. ±122.)
		3	0.022 ±0.005	8.5 ±0.9	6.3 ±0.8	2.3 ±1.2	28. ± 52%	104. ± 57%
		4	0.034 ±0.005	12.5 ±0.9	9.6 ±0.6	2.9 ±1.1	36. ± 39%	85. ± 41%
		5	0.046 ±0.004	16.5 ±1.0	13.0 ±0.5	3.6 ±1.1	44. ± 31%	78. ± 32%
		6	0.057 ±0.004	21.1 ±1.0	16.5 ±0.7	4.6 ±1.3	57. ± 28%	81. ± 28%
108	0.085	1	0.004 ±0.003	1.1 ±0.8	1.2 ±0.5	-0.1 ±1.0	(-0.8 ± 11.)	(-15. ±217.)
		2	0.013 ±0.004	3.4 ±0.9	3.2 ±0.7	0.2 ±1.1	(2. ± 13.)	(16. ± 90.)
		3	0.023 ±0.003	6.4 ±0.9	6.0 ±0.8	0.4 ±1.2	(5. ± 15.)	(16. ± 53.)
		4	0.035 ±0.003	10.1 ±0.9	9.0 ±0.7	1.2 ±1.2	(14. ± 14.)	(33. ± 33.)
		5	0.047 ±0.003	14.6 ±0.9	12.5 ±0.5	2.2 ±1.1	26. ± 50%	47. ± 50%
		6	0.057 ±0.003	19.0 ±0.9	15.9 ±0.7	3.1 ±1.2	37. ± 38%	55. ± 38%
118	0.148	1	0.003 ±0.008	1.7 ±1.7	1.2 ±0.5	0.4 ±1.8	(3. ± 12.)	(147. ±726.)
		2	0.015 ±0.008	4.2 ±1.8	3.5 ±0.8	0.7 ±2.0	(5. ± 13.)	(47. ±133.)
		3	0.035 ±0.008	7.6 ±1.9	6.4 ±0.9	1.3 ±2.1	(9. ± 14.)	(36. ± 60.)
		4	0.059 ±0.007	11.8 ±1.9	10.3 ±0.7	1.6 ±2.0	(11. ± 14.)	(27. ± 35.)
		5	0.085 ±0.007	16.9 ±1.9	13.6 ±0.6	3.3 ±2.0	23. ± 59%	39. ± 60%
		6	0.108 ±0.006	22.9 ±1.9	17.5 ±0.8	5.3 ±2.1	36. ± 40%	49. ± 40%
Isobutene								
257	0.108	1	0.013 ±0.003	1.0 ±1.2	0.9 ±0.6	0.1 ±1.3	(0.8 ± 12.)	(6. ± 99.)
		2	0.039 ±0.003	3.5 ±1.3	3.5 ±0.9	0.1 ±1.6	(0.7 ± 15.)	(2. ± 41.)
		3	0.065 ±0.002	7.3 ±1.4	7.2 ±1.2	0.2 ±1.8	(1.5 ± 17.)	(2. ± 28.)
		4	0.086 ±0.002	12.9 ±1.4	11.3 ±1.4	1.6 ±2.0	(15. ± 18.)	(19. ± 23.)
		5	0.098 ±0.002	20.3 ±1.6	16.0 ±1.6	4.3 ±2.2	39. ± 52%	44. ± 52%
		6	0.104 ±0.002	29.1 ±1.9	21.6 ±1.9	7.6 ±2.7	70. ± 36%	73. ± 36%
255	0.195	1	0.024 ±0.030	2.4 ±1.5	1.1 ±0.6	1.3 ±1.6	(7. ± 8.)	(52. ± 92.)
		2	0.086 ±0.028	6.5 ±1.6	4.1 ±0.9	2.3 ±1.8	12.1 ± 79%	27. ± 84%
		3	0.148 ±0.024	12.2 ±1.6	8.3 ±1.2	3.9 ±2.0	20. ± 52%	27. ± 53%
		4	0.182 ±0.023	19.6 ±1.7	12.7 ±1.4	6.8 ±2.2	35. ± 34%	37. ± 34%
		5	0.191 ±0.022	28.6 ±1.6	18.0 ±1.6	10.5 ±2.3	54. ± 24%	55. ± 25%
		6	0.192 ±0.022	39.3 ±1.9	24.4 ±1.9	14.9 ±2.7	76. ± 22%	77. ± 22%
253	0.207	1	0.022 ±0.022	2.8 ±1.7	1.0 ±0.6	1.8 ±1.8	8.7 ± 98%	(82. ±115.)
		2	0.094 ±0.021	7.1 ±1.8	3.8 ±0.9	3.2 ±2.0	15.6 ± 63%	35. ± 66%
		3	0.171 ±0.016	12.7 ±1.9	7.7 ±1.2	5.0 ±2.2	24. ± 45%	29. ± 45%
		4	0.200 ±0.015	19.8 ±1.9	12.0 ±1.4	7.8 ±2.3	37. ± 31%	39. ± 31%
		5	0.205 ±0.015	28.3 ±1.9	17.1 ±1.6	11.2 ±2.4	54. ± 23%	55. ± 23%
		6	0.205 ±0.015	38.1 ±1.9	23.1 ±1.9	15.0 ±2.7	72. ± 19%	73. ± 20%
trans-2-Butene								
309	0.069	1	0.027 ±0.010	4.6 ±0.9	0.9 ±0.6	3.7 ±1.1	54. ± 31%	138. ± 47%
		2	0.059 ±0.008	9.3 ±0.9	3.4 ±0.9	5.9 ±1.3	86. ± 25%	100. ± 26%
		3	0.068 ±0.008	14.2 ±1.2	7.1 ±1.2	7.0 ±1.7	102. ± 26%	103. ± 26%
		4	0.068 ±0.008	19.2 ±1.4	11.3 ±1.4	8.0 ±2.0	116. ± 27%	117. ± 27%
		5	0.068 ±0.008	24.5 ±1.6	15.8 ±1.6	8.6 ±2.2	126. ± 28%	127. ± 28%
		6	0.068 ±0.008	29.8 ±1.9	21.3 ±1.9	8.6 ±2.7	125. ± 34%	126. ± 34%

Table A-2 (continued)

Run Set	Added (ppm)	Time (hr)	Reacted (ppm)	IntOH (ppt-min) Test Run	Base Fit	Change	Reactivity (ppt-min/ppm) Incremental	Mechanistic
307	0.087	1	0.030 ±0.040	2.9 ±2.4	1.0 ±0.6	1.8 ±2.5	(21. ± 30.)	(61. ±116.)
		2	0.081 ±0.030	9.9 ±2.7	3.6 ±0.9	6.4 ±2.8	73. ± 56%	79. ± 58%
		3	0.086 ±0.030	14.9 ±2.7	7.2 ±1.2	7.7 ±2.9	89. ± 52%	89. ± 52%
		4	0.086 ±0.030	19.9 ±2.7	11.3 ±1.4	8.6 ±3.0	99. ± 49%	100. ± 49%
		5	0.086 ±0.030	26.2 ±2.6	15.7 ±1.6	10.4 ±3.1	120. ± 45%	121. ± 45%
		6	0.086 ±0.030	32.5 ±2.7	21.0 ±1.9	11.5 ±3.3	133. ± 45%	134. ± 45%
Isoprene								
277	0.076	1	0.016 ±0.002	1.0 ±0.8	1.3 ±0.6	-0.2 ±1.0	(-3. ± 13.)	(-14. ± 63.)
		2	0.043 ±0.002	3.7 ±0.9	4.4 ±0.9	-0.7 ±1.3	(-9. ± 17.)	(-16. ± 30.)
		3	0.058 ±0.002	7.9 ±1.2	8.6 ±1.2	-0.7 ±1.6	(-9. ± 21.)	(-12. ± 28.)
		4	0.075 ±0.002	13.7 ±1.4	13.1 ±1.4	0.6 ±2.0	(8. ± 26.)	(8. ± 26.)
		5	0.075 ±0.002	21.0 ±1.6	18.5 ±1.6	2.6 ±2.2	34. ± 87%	34. ± 87%
		6	0.075 ±0.002	30.0 ±1.9	24.8 ±1.9	5.1 ±2.7	67. ± 53%	68. ± 53%
275	0.108	1	0.028 ±0.003	0.2 ±2.3	1.2 ±0.6	-1.0 ±2.3	(-9. ± 21.)	(-36. ± 84.)
		2	0.064 ±0.002	2.0 ±2.4	4.1 ±0.9	-2.1 ±2.6	(-19. ± 24.)	(-33. ± 41.)
		3	0.086 ±0.002	5.9 ±2.6	8.1 ±1.1	-2.1 ±2.9	(-20. ± 26.)	(-25. ± 33.)
		4	0.108 ±0.002	12.4 ±2.7	12.4 ±1.4	0.0 ±3.0	(-0.07 ± 28.)	(0. ± 28.)
		5	0.108 ±0.002	21.4 ±2.6	17.4 ±1.6	4.0 ±3.0	36. ± 76%	37. ± 76%
		6	0.108 ±0.002	30.8 ±2.6	23.3 ±1.9	7.4 ±3.2	68. ± 43%	69. ± 43%
273	0.139	1	0.035 ±0.006	1.3 ±2.1	1.3 ±0.6	0.0 ±2.2	(0.2 ± 15.)	(1. ± 62.)
		2	0.084 ±0.005	4.1 ±2.2	4.2 ±0.9	-0.1 ±2.4	(-0.4 ± 17.)	(-1. ± 29.)
		3	0.111 ±0.005	8.4 ±2.3	8.1 ±1.1	0.3 ±2.6	(2. ± 19.)	(3. ± 23.)
		4	0.138 ±0.004	14.2 ±2.4	12.4 ±1.4	1.9 ±2.7	(13. ± 20.)	(13. ± 20.)
		5	0.138 ±0.004	21.5 ±2.3	17.3 ±1.6	4.2 ±2.8	30. ± 66%	30. ± 66%
		6	0.138 ±0.004	30.3 ±2.3	23.1 ±1.9	7.2 ±3.0	52. ± 42%	52. ± 42%
271	0.157	1	0.039 ±0.009	1.3 ±1.5	1.0 ±0.6	0.3 ±1.6	(2. ± 10.)	(7. ± 40.)
		2	0.091 ±0.008	4.0 ±1.6	3.5 ±0.9	0.5 ±1.8	(3. ± 12.)	(5. ± 20.)
		3	0.123 ±0.007	8.1 ±1.6	7.0 ±1.2	1.1 ±2.0	(7. ± 13.)	(9. ± 16.)
		4	0.139 ±0.007	13.6 ±1.7	11.0 ±1.4	2.6 ±2.2	16.4 ± 84%	18. ± 84%
		5	0.147 ±0.007	20.4 ±1.6	15.3 ±1.6	5.0 ±2.3	32. ± 45%	34. ± 45%
		6	0.150 ±0.007	28.6 ±1.9	20.4 ±1.9	8.1 ±2.7	52. ± 33%	54. ± 34%
2-Chloromethyl-3-chloropropene								
343	0.103	1	0.012 ±0.006	2.6 ±1.3	1.2 ±0.6	1.4 ±1.4	(14. ± 14.)	(123. ±136.)
		2	0.028 ±0.006	6.8 ±1.4	4.4 ±0.9	2.5 ±1.7	24. ± 67%	89. ± 70%
		3	0.045 ±0.005	12.7 ±1.4	8.7 ±1.2	4.0 ±1.8	39. ± 46%	89. ± 47%
		4	0.062 ±0.005	20.2 ±1.4	13.3 ±1.4	6.9 ±2.0	67. ± 29%	111. ± 30%
		5	0.075 ±0.004	29.3 ±1.6	19.0 ±1.6	10.3 ±2.3	100. ± 22%	136. ± 23%
		6	0.085 ±0.004	40.0 ±1.9	25.8 ±1.9	14.2 ±2.8	138. ± 20%	166. ± 20%
342	0.108	1	0.006 ±0.003	1.3 ±0.6	1.3 ±0.6	0.0 ±0.9	(-0.3 ± 8.)	(-6. ±145.)
		2	0.020 ±0.003	4.3 ±0.9	4.3 ±0.9	0.0 ±1.3	(0.4 ± 12.)	(2. ± 68.)
		3	0.037 ±0.003	9.2 ±1.2	8.5 ±1.2	0.7 ±1.7	(6. ± 16.)	(19. ± 45.)
		4	0.056 ±0.003	16.0 ±1.4	13.0 ±1.4	2.9 ±2.0	27. ± 69%	52. ± 69%
		5	0.072 ±0.002	24.5 ±1.6	18.2 ±1.6	6.3 ±2.3	59. ± 36%	88. ± 36%
		6	0.085 ±0.002	34.9 ±2.0	24.4 ±2.0	10.6 ±2.8	98. ± 26%	124. ± 27%
350	0.113	1	0.015 ±0.008	3.1 ±1.7	1.5 ±0.6	1.7 ±1.8	(15. ± 16.)	(109. ±133.)
		2	0.034 ±0.008	7.9 ±1.8	4.8 ±0.9	3.1 ±2.1	27. ± 67%	90. ± 71%
		3	0.054 ±0.007	14.3 ±1.9	9.2 ±1.2	5.0 ±2.2	44. ± 45%	92. ± 47%
		4	0.072 ±0.007	22.3 ±1.9	14.0 ±1.4	8.3 ±2.4	74. ± 29%	116. ± 30%
		5	0.086 ±0.006	31.9 ±1.9	19.6 ±1.6	12.4 ±2.5	109. ± 21%	143. ± 21%
		6	0.096 ±0.006	43.2 ±1.9	26.3 ±1.9	16.9 ±2.8	150. ± 17%	175. ± 18%

Table A-2 (continued)

Run Set	Added (ppm)	Time (hr)	Reacted (ppm)	IntOH (ppt-min) Test Run	Base Fit	Change	Reactivity (ppt-min/ppm) Incremental	Mechanistic
Benzene								
265	5.78	1	0.030 ±0.046	2.8 ±4.3	1.0 ±0.6	1.8 ±4.3	(0.3 ± 0.7)	(60. ±171.)
		2	0.072 ±0.050	6.7 ±4.6	3.6 ±0.9	3.0 ±4.7	(0.5 ± 0.8)	(42. ± 71.)
		3	0.126 ±0.051	11.8 ±4.8	7.3 ±1.2	4.5 ±4.9	(0.8 ± 0.9)	(35. ± 42.)
		4	0.192 ±0.050	18.1 ±4.8	11.5 ±1.4	6.6 ±5.0	1.14 ± 76%	34. ± 80%
		5	0.269 ±0.049	25.5 ±4.7	16.2 ±1.6	9.3 ±4.9	1.61 ± 53%	35. ± 56%
		6	0.357 ±0.048	34.2 ±4.7	21.9 ±1.9	12.4 ±5.1	2.1 ± 41%	35. ± 43%
263	6.86	1	0.039 ±0.044	3.0 ±3.4	1.0 ±0.6	2.1 ±3.5	(0.3 ± 0.5)	(53. ±107.)
		2	0.093 ±0.047	7.2 ±3.7	4.0 ±0.9	3.2 ±3.8	(0.5 ± 0.6)	(35. ± 44.)
		3	0.161 ±0.048	12.6 ±3.8	8.2 ±1.2	4.4 ±4.0	0.65 ± 90%	28. ± 95%
		4	0.243 ±0.048	19.3 ±3.8	12.8 ±1.4	6.5 ±4.1	0.96 ± 62%	27. ± 65%
		5	0.339 ±0.047	27.1 ±3.7	18.3 ±1.6	8.9 ±4.1	1.29 ± 46%	26. ± 48%
		6	0.447 ±0.047	36.2 ±3.8	25.0 ±1.9	11.2 ±4.2	1.64 ± 38%	25. ± 39%
Toluene								
64	0.061	1	0.001 ±0.002	2.3 ±0.8	3.6 ±0.6	-1.3 ±1.0	-21. ± 81%	
		2	0.004 ±0.002	6.3 ±1.0	7.2 ±1.0	-1.0 ±1.4	(-16. ± 22.)	(-269. ±405.)
		3	0.006 ±0.002	11.0 ±1.2	11.1 ±1.2	-0.1 ±1.7	(-2. ± 28.)	(-24. ±288.)
		4	0.008 ±0.002	15.1 ±1.3	15.3 ±1.3	-0.2 ±1.8	(-3. ± 30.)	(-26. ±239.)
		5	0.009 ±0.002	19.6 ±1.4	19.7 ±1.4	-0.2 ±1.9	(-3. ± 32.)	(-18. ±204.)
		6	0.011 ±0.002	25.1 ±1.8	24.0 ±1.8	1.1 ±2.6	(18. ± 42.)	(95. ±227.)
69	0.095	1	0.003 ±0.003	3.6 ±2.0	2.9 ±0.6	0.7 ±2.0	(7. ± 21.)	(261. ±846.)
		2	0.006 ±0.003	8.5 ±2.0	6.2 ±0.9	2.3 ±2.2	24. ± 96%	(376. ±400.)
		3	0.010 ±0.003	13.8 ±2.1	9.9 ±1.1	3.9 ±2.3	41. ± 59%	406. ± 65%
		4	0.013 ±0.003	18.4 ±2.1	13.8 ±1.2	4.6 ±2.4	49. ± 53%	366. ± 57%
		5	0.016 ±0.003	23.8 ±2.2	18.0 ±1.2	5.8 ±2.6	61. ± 44%	364. ± 47%
		6	0.020 ±0.003	29.8 ±2.4	22.5 ±1.7	7.2 ±2.9	76. ± 40%	370. ± 42%
61	0.175	1	0.005 ±0.005	3.4 ±0.8	3.6 ±0.6	-0.2 ±1.0	(-1.1 ± 6.)	(-41. ±213.)
		2	0.012 ±0.005	8.8 ±1.0	7.2 ±1.0	1.6 ±1.3	8.9 ± 86%	127. ± 95%
		3	0.019 ±0.005	14.0 ±1.2	11.2 ±1.2	2.8 ±1.7	16.2 ± 59%	151. ± 64%
		4	0.026 ±0.005	19.9 ±1.3	15.4 ±1.3	4.4 ±1.8	25. ± 41%	171. ± 45%
		5	0.034 ±0.005	26.9 ±1.3	20.0 ±1.3	7.0 ±1.9	40. ± 27%	207. ± 31%
		6	0.043 ±0.005	36.2 ±1.8	24.5 ±1.8	11.7 ±2.5	67. ± 22%	271. ± 25%
101	0.170	1	0.003 ±0.005	1.9 ±0.8	1.3 ±0.5	0.6 ±1.0	(3. ± 6.)	(197. ±470.)
		2	0.007 ±0.005	4.5 ±0.8	3.5 ±0.7	1.0 ±1.1	(6. ± 7.)	(153. ±199.)
		3	0.012 ±0.005	8.0 ±0.8	6.4 ±0.8	1.6 ±1.2	9.5 ± 73%	141. ± 84%
		4	0.017 ±0.005	12.3 ±0.9	9.8 ±0.7	2.4 ±1.1	14.2 ± 45%	142. ± 53%
		5	0.023 ±0.005	17.3 ±0.9	13.0 ±0.5	4.3 ±1.0	25. ± 25%	183. ± 32%
		6	0.030 ±0.005	23.1 ±0.9	16.5 ±0.7	6.6 ±1.2	39. ± 18%	218. ± 24%
103	0.174	1	0.002 ±0.005	1.5 ±1.0	1.2 ±0.5	0.3 ±1.1	(1.5 ± 7.)	(120. ±610.)
		2	0.007 ±0.005	4.6 ±1.0	3.3 ±0.7	1.3 ±1.3	(7. ± 7.)	(184. ±226.)
		3	0.013 ±0.005	8.9 ±1.1	6.2 ±0.8	2.7 ±1.3	15.5 ± 49%	202. ± 61%
		4	0.020 ±0.005	13.5 ±1.1	9.7 ±0.6	3.9 ±1.3	22. ± 33%	192. ± 41%
		5	0.027 ±0.005	18.2 ±1.2	13.0 ±0.5	5.2 ±1.3	30. ± 25%	193. ± 31%
		6	0.034 ±0.005	23.3 ±1.3	16.7 ±0.7	6.6 ±1.5	38. ± 22%	198. ± 27%
Ethylbenzene								
313	0.092	1	0.000 ±0.001	0.4 ±1.1	0.9 ±0.6	-0.5 ±1.2	(-5. ± 13.)	
		2	0.002 ±0.001	1.8 ±1.2	3.0 ±0.9	-1.2 ±1.5	(-13. ± 16.)	(-702. ±962.)
		3	0.004 ±0.001	4.3 ±1.2	6.1 ±1.2	-1.9 ±1.7	-20. ± 90%	-472. ± 94%
		4	0.007 ±0.001	7.7 ±1.4	9.8 ±1.4	-2.1 ±2.0	-23. ± 96%	-296. ± 97%
		5	0.011 ±0.001	12.1 ±1.6	13.6 ±1.6	-1.5 ±2.3	(-16. ± 24.)	(-137. ±209.)
		6	0.015 ±0.001	17.6 ±1.9	18.0 ±1.9	-0.4 ±2.8	(-4. ± 30.)	(-27. ±181.)

Table A-2 (continued)

Run Set	Added (ppm)	Time (hr)	Reacted (ppm)	IntOH (ppt-min) Test Run	Base Fit	Change	Reactivity (ppt-min/ppm) Incremental	Mechanistic
311	0.098	1	0.000 ±0.001	0.3 ±1.1	1.0 ±0.6	-0.7 ±1.3	(-7. ± 13.)	
		2	0.001 ±0.001	1.5 ±1.2	3.1 ±0.9	-1.6 ±1.5	-16.5 ± 93%	
		3	0.004 ±0.001	4.1 ±1.3	6.0 ±1.2	-1.9 ±1.7	-19.6 ± 91%	-474. ± 96%
		4	0.008 ±0.001	7.8 ±1.4	9.6 ±1.4	-1.8 ±2.0	(-18. ± 21.)	(-238. ±272.)
		5	0.011 ±0.001	12.0 ±1.6	13.2 ±1.6	-1.2 ±2.3	(-12. ± 23.)	(-104. ±202.)
		6	0.017 ±0.001	18.1 ±2.0	17.3 ±2.0	0.8 ±2.8	(9. ± 29.)	(51. ±169.)
315	0.215	1	0.001 ±0.006	0.4 ±0.8	1.0 ±0.6	-0.6 ±1.0	(-3. ± 5.)	
		2	0.005 ±0.006	2.1 ±0.9	3.2 ±0.9	-1.0 ±1.3	(-5. ± 6.)	(-228. ±422.)
		3	0.009 ±0.006	5.2 ±1.2	6.3 ±1.2	-1.0 ±1.7	(-5. ± 8.)	(-112. ±197.)
		4	0.015 ±0.006	8.9 ±1.4	9.9 ±1.4	-1.0 ±2.0	(-5. ± 9.)	(-68. ±135.)
		5	0.022 ±0.006	13.3 ±1.6	13.5 ±1.6	-0.2 ±2.3	(-1.0 ± 10.)	(-10. ±100.)
		6	0.031 ±0.006	19.0 ±1.9	17.7 ±1.9	1.3 ±2.8	(6. ± 13.)	(42. ± 89.)
o-Xylene								
259	0.064	1	0.002 ±0.004	1.1 ±2.1	0.9 ±0.6	0.2 ±2.2	(4. ± 35.)	
		2	0.006 ±0.004	4.6 ±2.3	3.5 ±0.9	1.1 ±2.5	(17. ± 39.)	(181. ±420.)
		3	0.011 ±0.003	9.1 ±2.5	7.1 ±1.2	1.9 ±2.7	(30. ± 43.)	(179. ±258.)
		4	0.015 ±0.003	14.0 ±2.5	11.2 ±1.4	2.8 ±2.9	(44. ± 46.)	(184. ±196.)
		5	0.020 ±0.003	20.3 ±2.5	15.9 ±1.6	4.4 ±2.9	69. ± 67%	224. ± 69%
		6	0.024 ±0.003	27.8 ±2.5	21.4 ±1.9	6.4 ±3.2	100. ± 50%	266. ± 52%
261	0.064	1	0.002 ±0.003	1.8 ±2.8	1.0 ±0.6	0.9 ±2.8	(13. ± 45.)	
		2	0.007 ±0.003	6.1 ±2.8	3.8 ±0.9	2.3 ±3.0	(36. ± 46.)	(346. ±470.)
		3	0.012 ±0.003	11.4 ±2.9	7.7 ±1.2	3.7 ±3.1	58. ± 83%	312. ± 87%
		4	0.017 ±0.003	16.9 ±3.0	12.0 ±1.4	4.9 ±3.3	77. ± 67%	291. ± 69%
		5	0.022 ±0.003	23.5 ±3.1	17.1 ±1.6	6.4 ±3.5	100. ± 55%	289. ± 56%
		6	0.027 ±0.003	30.2 ±3.3	23.2 ±1.9	7.0 ±3.8	110. ± 55%	262. ± 56%
m-Xylene								
207	0.038	1	0.001 ±0.004	0.7 ±3.5	1.2 ±0.6	-0.5 ±3.5	(-14. ± 93.)	
		2	0.006 ±0.004	3.3 ±3.7	3.6 ±0.9	-0.3 ±3.8	(-9. ±101.)	(-59. ±669.)
		3	0.011 ±0.004	7.5 ±4.0	7.0 ±1.2	0.4 ±4.1	(12. ±110.)	(41. ±385.)
		4	0.015 ±0.004	12.3 ±4.0	10.9 ±1.4	1.4 ±4.2	(38. ±112.)	(94. ±283.)
		5	0.019 ±0.004	18.1 ±3.9	15.0 ±1.6	3.1 ±4.2	(83. ±112.)	(165. ±224.)
		6	0.023 ±0.004	25.8 ±4.0	19.7 ±1.9	6.0 ±4.4	160. ± 74%	265. ± 75%
301	0.053	1	0.002 ±0.008	0.9 ±1.6	1.1 ±0.6	-0.1 ±1.7	(-3. ± 31.)	
		2	0.008 ±0.008	4.7 ±1.6	3.7 ±0.9	1.0 ±1.9	(20. ± 35.)	(131. ±271.)
		3	0.015 ±0.008	10.0 ±1.8	7.3 ±1.2	2.7 ±2.1	50. ± 80%	175. ± 95%
		4	0.022 ±0.008	15.4 ±1.8	11.4 ±1.4	4.0 ±2.3	76. ± 58%	186. ± 67%
		5	0.028 ±0.007	21.9 ±1.8	15.9 ±1.6	6.0 ±2.4	112. ± 42%	214. ± 47%
		6	0.033 ±0.007	29.0 ±1.9	21.3 ±1.9	7.7 ±2.7	146. ± 37%	234. ± 40%
196	0.057	1	0.002 ±0.004	1.1 ±0.8	0.9 ±0.6	0.2 ±1.0	(4. ± 18.)	(101. ±527.)
		2	0.009 ±0.004	5.2 ±0.9	3.5 ±0.9	1.7 ±1.3	30. ± 77%	184. ± 89%
		3	0.017 ±0.004	10.3 ±1.2	7.0 ±1.2	3.3 ±1.7	58. ± 51%	195. ± 56%
		4	0.024 ±0.004	15.6 ±1.4	11.1 ±1.4	4.5 ±2.0	80. ± 45%	193. ± 47%
		5	0.029 ±0.004	21.0 ±1.6	15.8 ±1.6	5.2 ±2.3	92. ± 44%	180. ± 45%
		6	0.034 ±0.004	27.1 ±2.0	21.3 ±2.0	5.7 ±2.8	101. ± 49%	168. ± 50%
344	0.081	1	0.006 ±0.020	2.3 ±3.1	1.5 ±0.6	0.8 ±3.2	(10. ± 40.)	(136. ±681.)
		2	0.021 ±0.018	8.7 ±3.2	4.7 ±0.9	4.0 ±3.3	49. ± 86%	(191. ±233.)
		3	0.032 ±0.017	14.5 ±3.3	9.0 ±1.2	5.5 ±3.5	68. ± 66%	174. ± 84%
		4	0.041 ±0.017	20.8 ±3.4	13.7 ±1.4	7.1 ±3.7	89. ± 55%	174. ± 66%
		5	0.047 ±0.016	25.5 ±3.6	19.1 ±1.6	6.4 ±3.9	79. ± 64%	137. ± 70%
		6	0.049 ±0.016	28.0 ±3.7	25.7 ±1.9	2.4 ±4.2	(30. ± 52.)	(48. ± 85.)

Table A-2 (continued)

Run Set	Added (ppm)	Time (hr)	Reacted (ppm)	IntOH (ppt-min) Test Run	Base Fit	Change	Reactivity (ppt-min/ppm) Incremental	Mechanistic
p-Xylene								
348	0.075	1	0.003 ±0.001	1.9 ±0.6	1.4 ±0.6	0.5 ±0.9	(7. ± 11.)	(172. ±295.)
		2	0.008 ±0.001	5.2 ±0.9	4.7 ±0.9	0.5 ±1.3	(7. ± 17.)	(67. ±168.)
		3	0.014 ±0.001	9.8 ±1.2	9.0 ±1.2	0.7 ±1.6	(10. ± 22.)	(52. ±119.)
		4	0.021 ±0.001	15.6 ±1.4	13.7 ±1.4	2.0 ±2.0	(26. ± 26.)	(93. ± 95.)
		5	0.028 ±0.001	22.9 ±1.6	19.3 ±1.6	3.6 ±2.2	48. ± 62%	127. ± 62%
		6	0.036 ±0.001	31.4 ±1.9	25.9 ±1.9	5.5 ±2.7	73. ± 49%	154. ± 49%
346	0.080	1	0.002 ±0.001	1.4 ±0.7	1.2 ±0.6	0.3 ±1.0	(3. ± 12.)	(109. ±400.)
		2	0.009 ±0.001	5.5 ±0.9	4.5 ±0.9	1.0 ±1.3	(12. ± 17.)	(111. ±154.)
		3	0.016 ±0.001	10.8 ±1.2	8.9 ±1.2	1.9 ±1.7	23. ± 90%	116. ± 90%
		4	0.024 ±0.001	17.3 ±1.4	13.6 ±1.4	3.7 ±2.0	46. ± 55%	151. ± 56%
		5	0.033 ±0.001	25.4 ±1.6	19.5 ±1.6	5.9 ±2.3	73. ± 39%	179. ± 39%
		6	0.039 ±0.001	32.6 ±2.0	26.6 ±2.0	6.0 ±2.8	74. ± 47%	152. ± 47%
135-trimethyl-Benzene								
251	0.045	1	0.008 ±0.004	2.5 ±1.8	0.9 ±0.6	1.6 ±1.9	(36. ± 42.)	(202. ±259.)
		2	0.018 ±0.004	6.2 ±1.9	3.0 ±0.9	3.1 ±2.1	70. ± 69%	175. ± 72%
		3	0.027 ±0.004	11.1 ±2.0	6.3 ±1.2	4.8 ±2.3	106. ± 49%	175. ± 50%
		4	0.035 ±0.003	17.2 ±2.0	10.1 ±1.4	7.2 ±2.5	160. ± 35%	207. ± 36%
		5	0.039 ±0.003	24.6 ±1.9	13.9 ±1.6	10.6 ±2.5	238. ± 25%	270. ± 25%
		6	0.042 ±0.003	33.2 ±1.9	18.5 ±1.9	14.7 ±2.8	328. ± 20%	350. ± 20%
249	0.047	1	0.008 ±0.007	2.1 ±2.2	1.0 ±0.6	1.2 ±2.3	(25. ± 49.)	(151. ±327.)
		2	0.019 ±0.006	6.1 ±2.3	3.6 ±0.9	2.5 ±2.5	(54. ± 54.)	(134. ±140.)
		3	0.030 ±0.005	12.0 ±2.5	7.4 ±1.2	4.6 ±2.7	99. ± 60%	156. ± 61%
		4	0.038 ±0.005	19.8 ±2.5	11.5 ±1.4	8.2 ±2.8	176. ± 36%	218. ± 36%
		5	0.043 ±0.005	29.4 ±2.4	16.2 ±1.6	13.1 ±2.9	281. ± 25%	309. ± 25%
		6	0.045 ±0.005	40.8 ±2.4	21.8 ±1.9	19.0 ±3.1	407. ± 20%	423. ± 20%
124-trimethyl-Benzene								
267	0.037	1	0.002 ±0.001	1.0 ±0.8	0.8 ±0.6	0.1 ±1.0	(4. ± 28.)	(66. ±488.)
		2	0.007 ±0.001	3.9 ±0.9	3.4 ±0.9	0.5 ±1.3	(15. ± 35.)	(77. ±185.)
		3	0.012 ±0.001	7.7 ±1.2	7.0 ±1.2	0.7 ±1.6	(18. ± 44.)	(59. ±141.)
		4	0.016 ±0.001	12.4 ±1.4	11.1 ±1.4	1.3 ±2.0	(35. ± 53.)	(83. ±124.)
		5	0.020 ±0.001	18.3 ±1.6	15.8 ±1.6	2.5 ±2.2	67. ± 90%	126. ± 90%
		6	0.023 ±0.001	26.0 ±1.9	21.3 ±1.9	4.7 ±2.7	126. ± 58%	203. ± 58%
269	0.041	1	0.003 ±0.002	2.2 ±0.8	1.1 ±0.6	1.1 ±1.0	26. ± 97%	(378. ±436.)
		2	0.009 ±0.002	5.5 ±0.9	4.1 ±0.9	1.4 ±1.3	35. ± 90%	156. ± 91%
		3	0.015 ±0.002	10.0 ±1.2	8.1 ±1.2	1.9 ±1.6	47. ± 85%	125. ± 86%
		4	0.020 ±0.001	15.7 ±1.4	12.5 ±1.4	3.2 ±2.0	79. ± 62%	158. ± 62%
		5	0.025 ±0.001	22.5 ±1.6	17.7 ±1.6	4.8 ±2.2	118. ± 46%	195. ± 47%
		6	0.028 ±0.001	30.5 ±1.9	23.9 ±1.9	6.6 ±2.7	163. ± 41%	234. ± 41%
123-trimethyl-Benzene								
299	0.035	1	0.004 ±0.005	1.1 ±1.2	1.6 ±0.6	-0.5 ±1.4	(-15. ± 40.)	(-126. ±371.)
		2	0.009 ±0.005	6.3 ±1.4	4.8 ±0.9	1.5 ±1.6	(42. ± 48.)	(157. ±193.)
		3	0.015 ±0.004	12.4 ±1.5	8.8 ±1.2	3.7 ±1.9	106. ± 52%	244. ± 59%
		4	0.020 ±0.004	19.9 ±1.5	13.2 ±1.4	6.7 ±2.0	193. ± 32%	329. ± 36%
		5	0.025 ±0.004	28.4 ±1.6	18.3 ±1.6	10.1 ±2.3	291. ± 25%	407. ± 27%
		6	0.028 ±0.004	35.7 ±2.0	24.2 ±2.0	11.4 ±2.8	330. ± 26%	405. ± 27%
297	0.044	1	0.004 ±0.001	3.4 ±2.0	1.6 ±0.6	1.8 ±2.1	(41. ± 48.)	(444. ±536.)
		2	0.015 ±0.001	8.1 ±2.1	4.8 ±0.9	3.3 ±2.3	75. ± 71%	221. ± 71%
		3	0.022 ±0.001	14.3 ±2.2	8.9 ±1.2	5.4 ±2.5	123. ± 47%	239. ± 47%
		4	0.028 ±0.001	21.8 ±2.3	13.4 ±1.4	8.4 ±2.7	192. ± 32%	300. ± 32%
		5	0.032 ±0.001	30.7 ±2.2	18.8 ±1.6	12.0 ±2.7	273. ± 23%	378. ± 23%
		6	0.033 ±0.001	41.0 ±2.2	25.0 ±2.0	16.0 ±3.0	366. ± 19%	480. ± 19%

Table A-2 (continued)

Run Set	Added (ppm)	Time (hr)	Reacted (ppm)	IntOH (ppt-min) Test Run	Base Fit	Change	Reactivity (ppt-min/ppm) Incremental	Mechanistic
Methanol								
287	0.816	1	0.001 ±0.001	0.8 ±1.2	1.4 ±0.6	-0.6 ±1.4	(-0.8 ± 2.)	
		2	0.004 ±0.001	3.7 ±1.3	4.6 ±0.9	-0.9 ±1.6	(-1.2 ± 2.)	(-232. ±402.)
		3	0.009 ±0.002	7.7 ±1.4	8.8 ±1.2	-1.2 ±1.8	(-1.4 ± 2.)	(-136. ±218.)
		4	0.013 ±0.002	12.1 ±1.5	13.4 ±1.4	-1.3 ±2.0	(-2. ± 3.)	(-98. ±153.)
		5	0.020 ±0.002	17.8 ±1.6	18.9 ±1.6	-1.1 ±2.2	(-1.4 ± 3.)	(-56. ±114.)
		6	0.027 ±0.002	24.5 ±1.9	25.3 ±1.9	-0.8 ±2.7	(-1.0 ± 3.)	(-30. ±102.)
289	2.29	1	0.003 ±0.003	1.0 ±1.0	1.6 ±0.6	-0.6 ±1.2	(-0.3 ± 0.5)	(-192. ±421.)
		2	0.014 ±0.003	4.6 ±1.1	5.1 ±0.9	-0.5 ±1.4	(-0.2 ± 0.6)	(-37. ± 98.)
		3	0.029 ±0.004	9.3 ±1.2	9.7 ±1.2	-0.4 ±1.7	(-0.2 ± 0.7)	(-15. ± 58.)
		4	0.045 ±0.004	14.7 ±1.4	14.6 ±1.4	0.1 ±2.0	(0.05 ± 0.9)	(2. ± 45.)
		5	0.066 ±0.005	21.3 ±1.6	20.7 ±1.6	0.7 ±2.3	(0.3 ± 1.0)	(10. ± 35.)
		6	0.087 ±0.005	28.5 ±2.0	27.9 ±2.0	0.6 ±2.8	(0.3 ± 1.2)	(7. ± 32.)
285	7.64	1	0.009 ±0.014	0.8 ±1.3	1.5 ±0.6	-0.7 ±1.4	(-0.09 ± 0.2)	(-83. ±215.)
		2	0.039 ±0.014	3.7 ±1.4	4.8 ±0.9	-1.1 ±1.7	(-0.15 ± 0.2)	(-29. ± 44.)
		3	0.082 ±0.016	7.9 ±1.5	9.1 ±1.2	-1.2 ±1.9	(-0.2 ± 0.2)	(-15. ± 23.)
		4	0.145 ±0.016	14.0 ±1.6	13.8 ±1.4	0.2 ±2.1	(0.03 ± 0.3)	(1. ± 14.)
		5	0.230 ±0.017	22.4 ±1.6	19.4 ±1.6	3.1 ±2.2	0.40 ± 73%	13. ± 74%
		6	0.316 ±0.018	31.0 ±1.9	26.0 ±1.9	5.1 ±2.7	0.67 ± 54%	16. ± 54%
Ethanol								
133	2.91	1	0.006 ±0.013	0.4 ±0.9	0.8 ±0.6	-0.3 ±1.1	(-0.12 ± 0.4)	(-60. ±235.)
		2	0.025 ±0.014	1.8 ±1.0	2.6 ±0.8	-0.8 ±1.3	(-0.3 ± 0.4)	(-30. ± 54.)
		3	0.059 ±0.016	4.3 ±1.1	5.5 ±0.9	-1.2 ±1.4	(-0.4 ± 0.5)	(-20. ± 25.)
		4	0.103 ±0.016	7.5 ±1.2	8.9 ±0.7	-1.4 ±1.4	-0.47 ± 99%	(-13. ± 13.)
		5	0.144 ±0.017	10.7 ±1.1	12.6 ±0.6	-1.9 ±1.3	-0.65 ± 67%	-13. ± 68%
		6	0.199 ±0.019	14.9 ±1.2	16.3 ±0.8	-1.4 ±1.4	(-0.5 ± 0.5)	(-7. ± 7.)
138	3.01	1	0.020 ±0.016	1.4 ±1.1	1.2 ±0.5	0.2 ±1.2	(0.07 ± 0.4)	(10. ± 64.)
		2	0.045 ±0.018	3.1 ±1.2	3.1 ±0.8	0.0 ±1.5	(0.02 ± 0.5)	(1. ± 33.)
		3	0.075 ±0.019	5.3 ±1.3	6.0 ±0.8	-0.7 ±1.5	(-0.2 ± 0.5)	(-10. ± 21.)
		4	0.110 ±0.019	7.8 ±1.3	9.2 ±0.7	-1.4 ±1.5	(-0.5 ± 0.5)	(-13. ± 14.)
		5	0.149 ±0.020	10.7 ±1.3	12.3 ±0.6	-1.6 ±1.4	-0.52 ± 90%	-10. ± 91%
		6	0.193 ±0.021	14.0 ±1.3	15.4 ±0.8	-1.4 ±1.5	(-0.5 ± 0.5)	(-7. ± 8.)
131	3.15	1	0.021 ±0.012	1.4 ±0.8	1.0 ±0.5	0.4 ±1.0	(0.14 ± 0.3)	(21. ± 48.)
		2	0.048 ±0.012	3.2 ±0.8	2.8 ±0.7	0.4 ±1.1	(0.12 ± 0.4)	(8. ± 23.)
		3	0.080 ±0.013	5.4 ±0.8	5.7 ±0.8	-0.3 ±1.2	(-0.10 ± 0.4)	(-4. ± 15.)
		4	0.118 ±0.013	8.0 ±0.9	9.1 ±0.7	-1.1 ±1.1	(-0.3 ± 0.3)	(-9. ± 9.)
		5	0.161 ±0.014	11.0 ±0.9	12.6 ±0.5	-1.6 ±1.0	-0.50 ± 66%	-10. ± 66%
		6	0.208 ±0.014	14.4 ±0.9	16.2 ±0.7	-1.8 ±1.2	-0.57 ± 66%	-9. ± 67%
Isopropanol								
148	3.63	1	0.038 ±0.023	1.4 ±0.8	0.8 ±0.5	0.6 ±1.0	(0.2 ± 0.3)	(17. ± 27.)
		2	0.094 ±0.024	3.5 ±0.8	2.7 ±0.8	0.8 ±1.1	(0.2 ± 0.3)	(8. ± 12.)
		3	0.166 ±0.027	6.2 ±0.9	5.6 ±0.8	0.6 ±1.2	(0.2 ± 0.3)	(3. ± 7.)
		4	0.253 ±0.031	9.6 ±0.9	9.1 ±0.7	0.5 ±1.1	(0.14 ± 0.3)	(2. ± 4.)
		5	0.353 ±0.037	13.6 ±0.9	12.4 ±0.6	1.1 ±1.1	0.32 ± 92%	3. ± 92%
		6	0.466 ±0.045	18.3 ±0.9	16.0 ±0.8	2.3 ±1.2	0.63 ± 53%	5. ± 53%
157	1.26	1	0.004 ±0.036	1.7 ±3.5	0.9 ±0.6	0.8 ±3.5	(0.6 ± 3.)	
		2	0.024 ±0.036	5.3 ±3.5	3.4 ±0.9	2.0 ±3.6	(2. ± 3.)	(82. ±195.)
		3	0.054 ±0.036	9.4 ±3.6	7.0 ±1.2	2.4 ±3.8	(2. ± 3.)	(44. ± 76.)
		4	0.095 ±0.036	13.5 ±3.7	10.9 ±1.4	2.5 ±4.0	(2. ± 3.)	(27. ± 43.)
		5	0.145 ±0.037	17.8 ±3.9	15.3 ±1.6	2.5 ±4.2	(2. ± 3.)	(17. ± 29.)
		6	0.212 ±0.037	22.6 ±4.1	20.4 ±1.9	2.2 ±4.5	(2. ± 4.)	(11. ± 22.)

Table A-2 (continued)

Run Set	Added (ppm)	Time (hr)	Reacted (ppm)	IntOH (ppt-min) Test Run	Base Fit	Change	Reactivity (ppt-min/ppm) Incremental	Mechanistic
159	1.61	1	0.016 ±0.010	1.3 ±0.9	1.0 ±0.6	0.2 ±1.1	(0.15 ± 0.7)	(15. ± 68.)
		2	0.044 ±0.012	3.7 ±1.0	3.7 ±0.9	0.0 ±1.3	(-0.02 ± 0.8)	(-1. ± 30.)
		3	0.084 ±0.013	7.1 ±1.2	7.4 ±1.2	-0.3 ±1.6	(-0.2 ± 1.0)	(-4. ± 19.)
		4	0.135 ±0.014	11.6 ±1.4	11.6 ±1.4	0.1 ±2.0	(0.05 ± 1.2)	(1. ± 14.)
		5	0.196 ±0.016	17.3 ±1.6	16.2 ±1.6	1.1 ±2.2	(0.7 ± 1.4)	(5. ± 11.)
		6	0.265 ±0.020	24.0 ±1.9	21.7 ±1.9	2.3 ±2.7	(1.4 ± 2.)	(9. ± 10.)
155	1.74	1	0.016 ±0.022	1.2 ±1.6	1.1 ±0.6	0.1 ±1.7	(0.08 ± 1.0)	(8. ±109.)
		2	0.052 ±0.024	4.0 ±1.8	3.7 ±0.9	0.3 ±2.0	(0.2 ± 1.2)	(6. ± 40.)
		3	0.099 ±0.025	7.7 ±2.0	7.4 ±1.1	0.3 ±2.3	(0.2 ± 1.3)	(3. ± 23.)
		4	0.150 ±0.026	12.0 ±2.1	11.4 ±1.4	0.5 ±2.5	(0.3 ± 1.4)	(3. ± 17.)
		5	0.211 ±0.025	17.2 ±2.0	16.0 ±1.6	1.2 ±2.5	(0.7 ± 1.4)	(6. ± 12.)
		6	0.290 ±0.025	24.3 ±1.9	21.3 ±1.9	2.9 ±2.7	1.70 ± 92%	10. ± 92%
Dimethyl Ether								
283	2.10	1	0.008 ±0.015	0.8 ±1.6	1.5 ±0.6	-0.6 ±1.7	(-0.3 ± 0.8)	(-78. ±266.)
		2	0.032 ±0.016	3.5 ±1.7	4.7 ±0.9	-1.2 ±2.0	(-0.6 ± 0.9)	(-38. ± 64.)
		3	0.062 ±0.017	6.8 ±1.8	9.0 ±1.2	-2.2 ±2.2	(-1.0 ± 1.0)	(-35. ± 36.)
		4	0.101 ±0.017	11.2 ±1.9	13.7 ±1.4	-2.4 ±2.4	-1.15 ± 98%	(-24. ± 24.)
		5	0.150 ±0.017	17.0 ±1.9	19.3 ±1.6	-2.3 ±2.5	(-1.1 ± 1.2)	(-15. ± 16.)
		6	0.206 ±0.017	23.6 ±1.9	25.9 ±1.9	-2.3 ±2.7	(-1.1 ± 1.3)	(-11. ± 13.)
295	2.12	1	0.008 ±0.008	0.8 ±0.8	1.5 ±0.6	-0.7 ±1.0	(-0.3 ± 0.5)	(-90. ±162.)
		2	0.032 ±0.008	3.5 ±0.9	4.6 ±0.9	-1.1 ±1.3	(-0.5 ± 0.6)	(-35. ± 41.)
		3	0.062 ±0.008	6.8 ±1.2	8.5 ±1.2	-1.7 ±1.6	-0.82 ± 95%	-28. ± 95%
		4	0.097 ±0.008	10.7 ±1.4	12.9 ±1.4	-2.3 ±2.0	-1.07 ± 87%	-23. ± 88%
		5	0.142 ±0.009	15.9 ±1.6	18.0 ±1.6	-2.2 ±2.2	(-1.0 ± 1.1)	(-15. ± 16.)
		6	0.197 ±0.010	22.4 ±1.9	24.0 ±1.9	-1.7 ±2.7	(-0.8 ± 1.3)	(-8. ± 14.)
281	3.41	1	0.023 ±0.016	1.5 ±1.1	1.4 ±0.6	0.2 ±1.2	(0.05 ± 0.4)	(7. ± 54.)
		2	0.059 ±0.017	4.0 ±1.2	4.6 ±0.9	-0.6 ±1.5	(-0.2 ± 0.4)	(-9. ± 25.)
		3	0.109 ±0.018	7.4 ±1.2	8.8 ±1.2	-1.4 ±1.7	(-0.4 ± 0.5)	(-13. ± 16.)
		4	0.170 ±0.018	11.7 ±1.4	13.4 ±1.4	-1.7 ±2.0	(-0.5 ± 0.6)	(-10. ± 12.)
		5	0.243 ±0.018	16.9 ±1.6	18.9 ±1.6	-1.9 ±2.2	(-0.6 ± 0.7)	(-8. ± 9.)
		6	0.326 ±0.019	23.1 ±1.9	25.4 ±1.9	-2.3 ±2.7	(-0.7 ± 0.8)	(-7. ± 8.)
279	4.04	1	0.023 ±0.027	1.3 ±1.5	1.3 ±0.6	-0.1 ±1.6	(-0.02 ± 0.4)	(-3. ± 72.)
		2	0.064 ±0.029	3.7 ±1.6	4.5 ±0.9	-0.8 ±1.9	(-0.2 ± 0.5)	(-13. ± 30.)
		3	0.125 ±0.030	7.2 ±1.7	8.7 ±1.2	-1.5 ±2.1	(-0.4 ± 0.5)	(-12. ± 17.)
		4	0.203 ±0.029	11.8 ±1.7	13.2 ±1.4	-1.4 ±2.2	(-0.4 ± 0.5)	(-7. ± 11.)
		5	0.298 ±0.029	17.5 ±1.7	18.6 ±1.6	-1.1 ±2.3	(-0.3 ± 0.6)	(-4. ± 8.)
		6	0.407 ±0.029	24.4 ±1.9	25.0 ±1.9	-0.6 ±2.7	(-0.2 ± 0.7)	(-2. ± 7.)
MTBE								
120	2.04	1	0.008 ±0.007	1.0 ±0.8	1.2 ±0.5	-0.3 ±1.0	(-0.13 ± 0.5)	(-33. ±122.)
		2	0.024 ±0.007	2.8 ±0.8	3.3 ±0.7	-0.5 ±1.1	(-0.2 ± 0.5)	(-20. ± 47.)
		3	0.044 ±0.007	5.2 ±0.8	6.2 ±0.8	-0.9 ±1.2	(-0.4 ± 0.6)	(-21. ± 27.)
		4	0.065 ±0.007	7.8 ±0.9	9.7 ±0.7	-1.9 ±1.1	-0.94 ± 56%	-30. ± 57%
		5	0.083 ±0.008	10.1 ±0.9	13.0 ±0.5	-2.9 ±1.0	-1.43 ± 36%	-35. ± 37%
		6	0.108 ±0.008	13.2 ±0.9	16.6 ±0.7	-3.4 ±1.2	-1.69 ± 34%	-32. ± 35%
125	2.49	1	0.006 ±0.010	0.6 ±0.9	1.2 ±0.5	-0.6 ±1.1	(-0.2 ± 0.4)	(-95. ±234.)
		2	0.022 ±0.010	2.2 ±1.0	3.3 ±0.7	-1.1 ±1.2	(-0.4 ± 0.5)	(-50. ± 58.)
		3	0.043 ±0.010	4.2 ±1.0	6.1 ±0.8	-1.9 ±1.3	-0.76 ± 67%	-44. ± 70%
		4	0.069 ±0.010	6.8 ±1.0	9.8 ±0.6	-3.1 ±1.2	-1.24 ± 39%	-45. ± 42%
		5	0.091 ±0.011	9.0 ±1.1	13.1 ±0.5	-4.1 ±1.2	-1.63 ± 30%	-45. ± 32%
		6	0.120 ±0.012	12.0 ±1.2	16.8 ±0.7	-4.8 ±1.4	-1.92 ± 29%	-40. ± 31%

Table A-2 (continued)

Run Set	Added (ppm)	Time (hr)	Reacted (ppm)	IntOH (ppt-min) Test Run	Base Fit	Change	Reactivity (ppt-min/ppm) Incremental	Mechanistic
127	2.51	1	0.008 ±0.009	0.8 ±0.8	1.0 ±0.5	-0.2 ±1.0	(-0.09 ± 0.4)	(-26. ±115.)
		2	0.021 ±0.009	2.1 ±0.8	3.0 ±0.7	-1.0 ±1.1	(-0.4 ± 0.4)	(-45. ± 54.)
		3	0.038 ±0.009	3.7 ±0.9	5.9 ±0.8	-2.2 ±1.2	-0.88 ± 53%	-57. ± 58%
		4	0.060 ±0.009	5.8 ±0.9	9.4 ±0.6	-3.6 ±1.1	-1.42 ± 30%	-60. ± 34%
		5	0.085 ±0.009	8.4 ±0.9	12.8 ±0.5	-4.4 ±1.0	-1.74 ± 24%	-51. ± 26%
		6	0.115 ±0.010	11.4 ±0.9	16.3 ±0.7	-5.0 ±1.2	-1.98 ± 23%	-43. ± 25%
123	2.98	1	0.012 ±0.011	0.9 ±0.9	0.7 ±0.7	0.2 ±1.1	(0.07 ± 0.4)	(18. ± 97.)
		2	0.032 ±0.011	2.6 ±1.0	2.8 ±1.0	-0.2 ±1.4	(-0.08 ± 0.5)	(-7. ± 44.)
		3	0.062 ±0.012	5.1 ±1.1	5.7 ±1.1	-0.6 ±1.5	(-0.2 ± 0.5)	(-10. ± 25.)
		4	0.100 ±0.012	8.3 ±1.0	10.0 ±0.9	-1.7 ±1.3	-0.57 ± 78%	-17. ± 79%
		5	0.147 ±0.012	12.3 ±1.0	14.0 ±0.7	-1.7 ±1.2	-0.58 ± 71%	-12. ± 72%
		6	0.202 ±0.013	17.1 ±1.0	18.8 ±1.0	-1.7 ±1.4	-0.57 ± 83%	-8. ± 83%
Ethoxyethanol								
175	0.401	1	0.013 ±0.035	0.4 ±1.7	1.2 ±0.6	-0.8 ±1.8	(-2. ± 4.)	(-60. ±218.)
		2	0.043 ±0.034	1.8 ±1.8	3.5 ±0.9	-1.7 ±2.0	(-4. ± 5.)	(-40. ± 57.)
		3	0.075 ±0.033	4.2 ±1.9	6.8 ±1.2	-2.6 ±2.2	-6.5 ± 86%	-35. ± 97%
		4	0.108 ±0.032	7.6 ±1.9	10.6 ±1.4	-3.0 ±2.4	-7.5 ± 79%	-28. ± 85%
		5	0.143 ±0.031	11.9 ±1.9	14.6 ±1.6	-2.6 ±2.4	-6.5 ± 94%	-18. ± 96%
		6	0.178 ±0.031	17.3 ±1.9	19.1 ±1.9	-1.8 ±2.7	(-4. ± 7.)	(-10. ± 15.)
171	0.730	1	0.006 ±0.029	0.7 ±0.8	0.7 ±0.6	0.0 ±1.0	(-0.05 ± 1.4)	(-6. ±175.)
		2	0.031 ±0.029	2.4 ±0.9	3.2 ±0.9	-0.8 ±1.3	(-1.1 ± 2.)	(-26. ± 49.)
		3	0.074 ±0.030	5.0 ±1.2	6.8 ±1.2	-1.8 ±1.7	-2.5 ± 92%	(-24. ± 25.)
		4	0.138 ±0.030	8.6 ±1.4	10.9 ±1.4	-2.2 ±2.0	-3.1 ± 89%	-16. ± 91%
		5	0.237 ±0.027	13.1 ±1.6	15.4 ±1.6	-2.2 ±2.2	(-3. ± 3.)	(-9. ± 10.)
		6	0.342 ±0.026	18.7 ±1.9	20.8 ±1.9	-2.1 ±2.7	(-3. ± 4.)	(-6. ± 8.)
163	0.859	1	0.023 ±0.024	0.8 ±3.3	1.3 ±0.6	-0.5 ±3.4	(-0.6 ± 4.)	(-23. ±148.)
		2	0.080 ±0.023	2.8 ±4.8	4.3 ±0.9	-1.5 ±4.9	(-2. ± 6.)	(-18. ± 61.)
		3	0.165 ±0.025	6.2 ±5.2	8.3 ±1.2	-2.1 ±5.4	(-2. ± 6.)	(-13. ± 32.)
		4	0.267 ±0.030	10.9 ±4.3	12.7 ±1.4	-1.8 ±4.5	(-2. ± 5.)	(-7. ± 17.)
		5	0.376 ±0.038	16.9 ±3.5	17.9 ±1.6	-1.0 ±3.8	(-1.2 ± 4.)	(-3. ± 10.)
		6	0.480 ±0.046	24.1 ±4.8	24.0 ±1.9	0.1 ±5.1	(0.2 ± 6.)	(0. ± 11.)
Carbitol								
169	0.412	1	0.018 ±0.012	0.3 ±0.8	1.1 ±0.6	-0.8 ±1.0	(-2. ± 2.)	(-43. ± 62.)
		2	0.051 ±0.011	1.2 ±0.9	3.7 ±0.9	-2.4 ±1.3	-5.9 ± 53%	-48. ± 57%
		3	0.094 ±0.011	2.5 ±1.2	7.3 ±1.2	-4.8 ±1.6	-11.7 ± 34%	-51. ± 36%
		4	0.142 ±0.010	4.3 ±1.4	11.4 ±1.4	-7.1 ±2.0	-17.1 ± 28%	-50. ± 29%
		5	0.192 ±0.010	6.9 ±1.6	15.8 ±1.6	-8.9 ±2.2	-22. ± 25%	-46. ± 26%
		6	0.239 ±0.010	10.5 ±1.9	21.0 ±1.9	-10.5 ±2.7	-25. ± 26%	-44. ± 26%
166	0.503	1	0.024 ±0.020	0.6 ±0.8	1.2 ±0.6	-0.6 ±1.0	(-1.2 ± 2.)	(-26. ± 48.)
		2	0.068 ±0.020	1.7 ±1.0	4.5 ±0.9	-2.7 ±1.4	-5.4 ± 51%	-40. ± 59%
		3	0.120 ±0.020	3.5 ±1.2	9.0 ±1.2	-5.5 ±1.7	-11.0 ± 30%	-46. ± 34%
		4	0.175 ±0.019	6.0 ±1.4	13.8 ±1.4	-7.8 ±2.0	-15.6 ± 26%	-45. ± 28%
		5	0.235 ±0.019	9.6 ±1.6	19.7 ±1.6	-10.1 ±2.3	-20. ± 23%	-43. ± 24%
		6	0.289 ±0.018	14.3 ±2.0	26.8 ±2.0	-12.6 ±2.8	-25. ± 22%	-43. ± 23%
173	0.946	1	0.050 ±0.055	0.7 ±0.8	1.2 ±0.6	-0.5 ±1.0	(-0.5 ± 1.1)	(-10. ± 23.)
		2	0.106 ±0.052	1.6 ±1.0	3.8 ±0.9	-2.2 ±1.3	-2.4 ± 60%	-21. ± 78%
		3	0.168 ±0.049	2.6 ±1.1	7.4 ±1.1	-4.8 ±1.6	-5.1 ± 34%	-28. ± 45%
		4	0.233 ±0.046	3.8 ±1.4	11.5 ±1.4	-7.6 ±2.0	-8.1 ± 26%	-33. ± 32%
		5	0.299 ±0.044	5.2 ±1.6	15.9 ±1.6	-10.7 ±2.2	-11.4 ± 21%	-36. ± 25%
		6	0.365 ±0.041	6.7 ±1.9	21.1 ±1.9	-14.4 ±2.7	-15.2 ± 19%	-39. ± 22%

Table A-2 (continued)

Run Set	Added (ppm)	Time (hr)	Reacted (ppm)	IntOH (ppt-min) Test Run	Base Fit	Change	Reactivity (ppt-min/ppm) Incremental	Mechanistic
Formaldehyde								
352	0.104	1	[a]	3.4 ±0.7	1.4 ±0.6	2.0 ±0.9	18.8 ± 47%	
		2	[a]	8.7 ±0.9	4.6 ±0.9	4.1 ±1.3	39. ± 32%	
		3	[a]	13.9 ±1.2	8.9 ±1.2	5.0 ±1.6	48. ± 33%	
		4	[a]	19.9 ±1.4	13.5 ±1.4	6.4 ±2.0	62. ± 31%	
		5	[a]	27.0 ±1.6	19.0 ±1.6	8.0 ±2.2	77. ± 28%	
		6	[a]	34.6 ±1.9	25.4 ±1.9	9.2 ±2.7	89. ± 30%	
357	0.267	1	[a]	4.9 ±0.9	1.3 ±0.6	3.6 ±1.1	13.6 ± 30%	
		2	[a]	10.7 ±1.0	4.4 ±0.9	6.4 ±1.3	24. ± 21%	
		3	[a]	17.4 ±1.2	8.6 ±1.2	8.8 ±1.6	33. ± 19%	
		4	[a]	24.9 ±1.4	13.1 ±1.4	11.8 ±2.0	44. ± 17%	
		5	[a]	33.3 ±1.6	18.4 ±1.6	14.9 ±2.2	56. ± 15%	
		6	[a]	42.5 ±1.9	24.7 ±1.9	17.8 ±2.7	67. ± 15%	
Acetaldehyde								
335	0.696	1	0.044 ±0.019	2.3 ±0.8	1.5 ±0.6	0.8 ±1.0	(1.1 ± 1.5)	(18. ± 25.)
		2	0.094 ±0.019	5.3 ±0.9	4.8 ±0.9	0.5 ±1.3	(0.8 ± 2.)	(6. ± 14.)
		3	0.132 ±0.019	7.9 ±1.2	9.1 ±1.2	-1.2 ±1.6	(-2. ± 2.)	(-9. ± 13.)
		4	0.171 ±0.018	10.8 ±1.4	13.7 ±1.4	-2.9 ±2.0	-4.2 ± 68%	-17. ± 69%
		5	0.216 ±0.018	14.4 ±1.6	19.2 ±1.6	-4.8 ±2.2	-6.9 ± 47%	-22. ± 47%
		6	0.261 ±0.018	18.5 ±1.9	25.7 ±1.9	-7.1 ±2.7	-10.2 ± 38%	-27. ± 39%
338	1.31	1	0.090 ±0.036	1.7 ±0.8	1.4 ±0.6	0.3 ±1.0	(0.3 ± 0.8)	(4. ± 11.)
		2	0.169 ±0.036	3.7 ±0.9	4.6 ±0.9	-0.9 ±1.3	(-0.7 ± 1.0)	(-5. ± 8.)
		3	0.230 ±0.035	5.5 ±1.2	8.9 ±1.2	-3.4 ±1.6	-2.6 ± 48%	-15. ± 51%
		4	0.297 ±0.035	7.6 ±1.4	13.5 ±1.4	-5.9 ±2.0	-4.5 ± 34%	-20. ± 36%
		5	0.371 ±0.035	10.2 ±1.6	19.0 ±1.6	-8.8 ±2.2	-6.7 ± 25%	-24. ± 27%
		6	0.444 ±0.035	13.1 ±1.9	25.5 ±1.9	-12.4 ±2.7	-9.4 ± 22%	-28. ± 23%
Acetone								
243	0.847	1	[a]	1.1 ±1.0	0.9 ±0.6	0.2 ±1.2	(0.2 ± 1.4)	
		2	[a]	4.1 ±1.1	3.7 ±0.9	0.4 ±1.4	(0.5 ± 2.)	
		3	[a]	8.4 ±1.2	7.6 ±1.2	0.8 ±1.6	(1.0 ± 2.)	
		4	[a]	13.1 ±1.4	11.8 ±1.4	1.3 ±2.0	(2. ± 2.)	
		5	[a]	18.6 ±1.6	16.9 ±1.6	1.7 ±2.2	(2. ± 3.)	
		6	[a]	25.5 ±1.9	22.9 ±1.9	2.6 ±2.7	(3. ± 3.)	
245	2.19	1	[a]	1.9 ±2.1	1.2 ±0.6	0.7 ±2.2	(0.3 ± 1.0)	
		2	[a]	6.5 ±2.1	4.1 ±0.9	2.4 ±2.3	1.09 ± 97%	
		3	[a]	11.1 ±2.2	8.1 ±1.1	3.0 ±2.5	1.36 ± 83%	
		4	[a]	15.3 ±2.3	12.4 ±1.4	2.9 ±2.6	1.33 ± 91%	
		5	[a]	20.5 ±2.3	17.4 ±1.6	3.0 ±2.8	1.38 ± 93%	
		6	[a]	26.2 ±2.5	23.4 ±1.9	2.8 ±3.1	(1.3 ± 1.4)	
247	4.14	1	[a]	2.2 ±1.6	1.1 ±0.6	1.2 ±1.7	(0.3 ± 0.4)	
		2	[a]	5.4 ±1.7	3.9 ±0.9	1.5 ±1.9	(0.4 ± 0.5)	
		3	[a]	9.5 ±1.8	7.7 ±1.2	1.7 ±2.1	(0.4 ± 0.5)	
		4	[a]	14.6 ±1.8	12.0 ±1.4	2.5 ±2.3	0.61 ± 89%	
		5	[a]	20.6 ±1.7	17.0 ±1.6	3.6 ±2.3	0.87 ± 65%	
		6	[a]	27.7 ±1.9	22.9 ±1.9	4.7 ±2.7	1.14 ± 57%	
Hexamethyldisiloxane								
183	6.71	1	0.008 ±0.011	0.6 ±0.8	1.3 ±0.6	-0.7 ±1.0	(-0.11 ± 0.2)	(-89. ±180.)
		2	0.018 ±0.011	1.3 ±0.9	3.9 ±0.9	-2.5 ±1.3	-0.38 ± 52%	-140. ± 81%
		3	0.030 ±0.011	2.2 ±1.2	7.3 ±1.2	-5.1 ±1.7	-0.75 ± 33%	-169. ± 51%
		4	0.044 ±0.012	3.3 ±1.4	11.2 ±1.4	-7.9 ±2.0	-1.18 ± 25%	-181. ± 37%
		5	0.059 ±0.012	4.4 ±1.6	15.6 ±1.6	-11.1 ±2.3	-1.66 ± 21%	-188. ± 29%
		6	0.076 ±0.013	5.7 ±2.0	20.5 ±2.0	-14.8 ±2.8	-2.2 ± 19%	-193. ± 25%

Table A-2 (continued)

Run Set	Added (ppm)	Time (hr)	Reacted (ppm)	IntOH (ppt-min) Test Run	Base Fit	Change	Reactivity (ppt-min/ppm) Incremental	Mechanistic
179	9.13	1	0.009 ±0.024	0.5 ±1.3	1.2 ±0.6	-0.7 ±1.4	(-0.08 ± 0.2)	(-79. ±257.)
		2	0.020 ±0.024	1.1 ±1.3	3.5 ±0.9	-2.4 ±1.6	-0.26 ± 68%	(-116. ±158.)
		3	0.035 ±0.025	1.9 ±1.4	6.6 ±1.2	-4.7 ±1.8	-0.52 ± 38%	-135. ± 82%
		4	0.045 ±0.026	2.5 ±1.4	10.3 ±1.4	-7.8 ±2.0	-0.85 ± 26%	-172. ± 63%
		5	0.053 ±0.027	2.9 ±1.6	14.0 ±1.6	-11.1 ±2.3	-1.21 ± 21%	-208. ± 55%
		6	0.064 ±0.029	3.5 ±1.9	18.1 ±1.9	-14.6 ±2.7	-1.61 ± 19%	-230. ± 49%
396	2.83	1	0.016 ±0.011	2.7 ±2.7	2.8 ±2.7	-0.1 ±3.8	(-0.02 ± 1.3)	(-3. ±245.)
		2	0.031 ±0.011	5.5 ±3.1	9.1 ±3.1	-3.7 ±4.3	(-1.3 ± 2.)	(-118. ±146.)
		3	0.046 ±0.012	8.2 ±2.6	18.0 ±2.6	-9.8 ±3.6	-3.5 ± 37%	-212. ± 45%
		4	0.062 ±0.012	10.9 ±2.4	26.0 ±2.4	-15.1 ±3.4	-5.3 ± 23%	-245. ± 30%
		5	0.076 ±0.012	13.6 ±2.6	31.0 ±2.4	-17.3 ±3.6	-6.1 ± 21%	-227. ± 26%
		6	0.091 ±0.013	16.4 ±4.9	33.9 ±4.9	-17.5 ±6.9	-6.2 ± 39%	-192. ± 42%
391	3.99	1	0.004 ±0.009	0.5 ±2.7	3.0 ±2.7	-2.5 ±3.8	(-0.6 ± 0.9)	
		2	0.012 ±0.009	1.5 ±3.0	9.3 ±3.0	-7.8 ±4.3	-1.95 ± 55%	-637. ± 92%
		3	0.023 ±0.010	2.8 ±2.5	18.1 ±2.5	-15.2 ±3.6	-3.8 ± 23%	-669. ± 48%
		4	0.035 ±0.010	4.3 ±2.4	26.0 ±2.4	-21.6 ±3.4	-5.4 ± 16%	-622. ± 32%
		5	0.052 ±0.010	6.5 ±2.7	31.0 ±2.3	-24.6 ±3.6	-6.2 ± 15%	-476. ± 24%
		6	0.072 ±0.010	9.1 ±4.8	34.2 ±4.8	-25.1 ±6.8	-6.3 ± 27%	-351. ± 30%
Octamethylcyclotetrasiloxane								
194	2.15	1	0.002 ±0.003	0.6 ±1.0	0.8 ±0.6	-0.2 ±1.2	(-0.09 ± 0.6)	(-103. ±638.)
		2	0.007 ±0.003	2.1 ±1.0	3.4 ±0.9	-1.3 ±1.4	(-0.6 ± 0.7)	(-198. ±233.)
		3	0.013 ±0.004	4.1 ±1.2	7.0 ±1.2	-2.9 ±1.7	-1.35 ± 59%	-223. ± 65%
		4	0.019 ±0.004	6.0 ±1.4	11.1 ±1.4	-5.1 ±2.0	-2.4 ± 42%	-268. ± 46%
		5	0.025 ±0.005	8.1 ±1.6	15.9 ±1.6	-7.8 ±2.3	-3.6 ± 32%	-307. ± 35%
		6	0.032 ±0.006	10.1 ±2.0	21.5 ±2.0	-11.4 ±2.8	-5.3 ± 28%	-361. ± 31%
185	4.31	1	0.008 ±0.008	1.3 ±1.3	1.0 ±0.6	0.3 ±1.4	(0.06 ± 0.3)	(31. ±181.)
		2	0.016 ±0.008	2.6 ±1.3	3.2 ±0.9	-0.7 ±1.6	(-0.2 ± 0.4)	(-43. ±103.)
		3	0.024 ±0.009	3.9 ±1.4	6.4 ±1.2	-2.6 ±1.8	-0.60 ± 71%	-105. ± 79%
		4	0.032 ±0.009	5.1 ±1.4	10.1 ±1.4	-5.0 ±2.0	-1.16 ± 40%	-154. ± 49%
		5	0.040 ±0.010	6.4 ±1.6	13.9 ±1.6	-7.5 ±2.2	-1.75 ± 30%	-187. ± 38%
		6	0.048 ±0.010	7.7 ±1.9	18.3 ±1.9	-10.6 ±2.7	-2.5 ± 26%	-220. ± 33%
181	10.08	1	0.002 ±0.012	0.1 ±0.8	0.9 ±0.6	-0.8 ±1.0	(-0.08 ±0.10)	
		2	0.005 ±0.012	0.3 ±0.9	3.1 ±0.9	-2.8 ±1.3	-0.28 ± 47%	
		3	0.009 ±0.013	0.6 ±1.2	6.4 ±1.2	-5.8 ±1.7	-0.57 ± 29%	(-622. ±862.)
		4	0.014 ±0.013	0.9 ±1.4	10.1 ±1.4	-9.2 ±2.0	-0.91 ± 22%	-678. ± 99%
		5	0.019 ±0.014	1.3 ±1.6	14.0 ±1.6	-12.7 ±2.2	-1.26 ± 18%	-680. ± 77%
		6	0.024 ±0.015	1.6 ±1.9	18.5 ±1.9	-16.9 ±2.7	-1.68 ± 16%	-709. ± 65%
406	1.35	1	0.005 ±0.002	2.6 ±2.7	2.7 ±2.7	-0.1 ±3.9	(-0.07 ± 3.)	(-18. ±748.)
		2	0.011 ±0.002	5.4 ±3.1	9.0 ±3.1	-3.6 ±4.4	(-3. ± 3.)	(-337. ±412.)
		3	0.017 ±0.002	8.5 ±2.6	18.0 ±2.6	-9.5 ±3.7	-7.1 ± 38%	-571. ± 40%
		4	0.023 ±0.002	11.8 ±2.4	26.0 ±2.4	-14.3 ±3.4	-10.6 ± 24%	-618. ± 26%
		5	0.030 ±0.002	15.3 ±2.6	31.0 ±2.4	-15.7 ±3.6	-11.6 ± 23%	-526. ± 24%
		6	0.037 ±0.002	19.0 ±4.9	33.8 ±4.9	-14.7 ±7.0	-10.9 ± 48%	-399. ± 48%
402	1.77	1	0.003 ±0.002	1.2 ±2.8	2.5 ±2.8	-1.3 ±4.0	(-0.7 ± 2.)	
		2	0.008 ±0.002	3.1 ±3.2	8.9 ±3.2	-5.7 ±4.5	-3.2 ± 79%	-710. ± 82%
		3	0.015 ±0.002	5.6 ±2.7	18.0 ±2.7	-12.3 ±3.8	-7.0 ± 31%	-845. ± 33%
		4	0.023 ±0.002	8.8 ±2.5	26.0 ±2.5	-17.2 ±3.5	-9.7 ± 21%	-758. ± 22%
		5	0.032 ±0.002	12.6 ±2.8	30.9 ±2.5	-18.3 ±3.7	-10.3 ± 21%	-564. ± 21%
		6	0.044 ±0.002	17.1 ±5.1	33.5 ±5.1	-16.4 ±7.2	-9.3 ± 44%	-376. ± 44%
398	2.62	1	0.000 ±0.008	0.1 ±2.7	3.4 ±2.7	-3.3 ±3.8	(-1.3 ± 1.4)	
		2	0.002 ±0.008	0.4 ±3.0	9.8 ±3.0	-9.3 ±4.3	-3.6 ± 46%	
		3	0.003 ±0.008	0.8 ±2.5	18.2 ±2.5	-17.4 ±3.6	-6.6 ± 21%	
		4	0.004 ±0.008	1.2 ±2.4	25.9 ±2.4	-24.7 ±3.4	-9.4 ± 14%	
		5	0.006 ±0.008	1.6 ±2.7	31.2 ±2.4	-29.5 ±3.6	-11.3 ± 12%	
		6	0.008 ±0.009	2.2 ±4.9	34.9 ±4.9	-32.7 ±6.9	-12.5 ± 21%	

Table A-2 (continued)

Run Set	Added (ppm)	Time (hr)	Reacted (ppm)	IntOH (ppt-min) Test Run	Base Fit	Change	Reactivity (ppt-min/ppm) Incremental	Mechanistic
Decamethylcyclopentasiloxane								
190	1.55	1	0.001 ±0.003	0.4 ±1.0	0.9 ±0.6	-0.5 ±1.2	(-0.3 ± 0.8)	
		2	0.004 ±0.003	1.3 ±1.0	3.6 ±1.0	-2.3 ±1.4	-1.52 ± 59%	-533. ± 98%
		3	0.009 ±0.004	2.6 ±1.2	7.1 ±1.2	-4.6 ±1.7	-2.9 ± 38%	-503. ± 55%
		4	0.013 ±0.004	3.8 ±1.5	11.2 ±1.5	-7.5 ±2.1	-4.8 ± 28%	-567. ± 40%
		5	0.018 ±0.004	5.2 ±1.7	16.1 ±1.7	-10.9 ±2.3	-7.0 ± 22%	-602. ± 31%
		6	0.023 ±0.004	6.8 ±2.0	21.7 ±2.0	-14.9 ±2.9	-9.6 ± 19%	-635. ± 26%
192	1.85	1	0.005 ±0.004	1.2 ±0.8	0.9 ±0.6	0.3 ±1.1	(0.2 ± 0.6)	(64. ±215.)
		2	0.010 ±0.004	2.4 ±0.9	3.4 ±0.9	-1.0 ±1.3	(-0.6 ± 0.7)	(-104. ±140.)
		3	0.015 ±0.004	3.6 ±1.2	6.9 ±1.2	-3.3 ±1.7	-1.78 ± 54%	-221. ± 59%
		4	0.020 ±0.005	4.8 ±1.4	10.9 ±1.4	-6.1 ±2.0	-3.3 ± 37%	-309. ± 41%
		5	0.025 ±0.005	6.0 ±1.6	15.5 ±1.6	-9.5 ±2.3	-5.2 ± 28%	-387. ± 33%
		6	0.029 ±0.006	7.1 ±2.0	20.9 ±2.0	-13.8 ±2.8	-7.4 ± 25%	-468. ± 29%
187	4.93	1	0.007 ±0.009	0.6 ±0.8	1.2 ±0.6	-0.6 ±1.0	(-0.12 ± 0.2)	(-92. ±203.)
		2	0.013 ±0.009	1.2 ±0.9	3.9 ±0.9	-2.8 ±1.3	-0.56 ± 47%	-213. ± 85%
		3	0.020 ±0.009	1.8 ±1.2	7.6 ±1.2	-5.9 ±1.7	-1.19 ± 28%	-300. ± 56%
		4	0.026 ±0.010	2.3 ±1.4	11.8 ±1.4	-9.4 ±2.0	-1.91 ± 21%	-363. ± 43%
		5	0.032 ±0.010	2.9 ±1.6	16.5 ±1.6	-13.6 ±2.2	-2.8 ± 17%	-421. ± 35%
		6	0.039 ±0.010	3.5 ±1.9	22.1 ±1.9	-18.6 ±2.7	-3.8 ± 15%	-481. ± 31%
Pentamethyldisiloxanol								
412	0.712	1	0.005 ±0.001	2.5 ±0.6	1.4 ±0.6	1.2 ±0.9	1.62 ± 75%	229. ± 79%
		2	0.010 ±0.001	5.3 ±0.9	3.9 ±0.9	1.4 ±1.3	1.97 ± 92%	134. ± 93%
		3	0.016 ±0.001	8.3 ±1.2	7.3 ±1.2	1.0 ±1.6	(1.4 ± 2.)	(60. ±101.)
		4	0.022 ±0.001	11.5 ±1.4	11.2 ±1.4	0.3 ±2.0	(0.4 ± 3.)	(12. ± 88.)
		5	0.029 ±0.002	14.9 ±1.6	15.4 ±1.6	-0.4 ±2.2	(-0.6 ± 3.)	(-15. ± 78.)
		6	0.036 ±0.002	18.6 ±1.9	20.1 ±1.9	-1.5 ±2.7	(-2. ± 4.)	(-42. ± 77.)
409	2.17	1	0.002 ±0.007	0.3 ±1.1	1.4 ±0.6	-1.1 ±1.3	(-0.5 ± 0.6)	
		2	0.008 ±0.008	1.3 ±1.3	3.8 ±0.9	-2.6 ±1.6	-1.18 ± 62%	(-338. ±406.)
		3	0.018 ±0.008	3.0 ±1.3	7.3 ±1.2	-4.2 ±1.8	-1.95 ± 42%	-233. ± 61%
		4	0.033 ±0.008	5.5 ±1.4	11.1 ±1.4	-5.6 ±2.0	-2.6 ± 36%	-169. ± 43%
		5	0.052 ±0.008	8.8 ±1.6	15.1 ±1.6	-6.3 ±2.3	-2.9 ± 36%	-121. ± 39%
		6	0.075 ±0.009	12.8 ±2.0	19.6 ±2.0	-6.8 ±2.8	-3.1 ± 41%	-91. ± 42%
404	1.20	1	0.005 ±0.002	1.4 ±2.8	2.6 ±2.8	-1.2 ±3.9	(-1.0 ± 3.)	(-242. ±822.)
		2	0.010 ±0.002	3.1 ±3.1	8.9 ±3.1	-5.8 ±4.4	-4.8 ± 76%	-560. ± 79%
		3	0.017 ±0.002	5.0 ±2.6	18.0 ±2.6	-12.9 ±3.7	-10.7 ± 29%	-773. ± 31%
		4	0.024 ±0.002	7.2 ±2.5	26.0 ±2.5	-18.8 ±3.5	-15.6 ± 19%	-789. ± 21%
		5	0.032 ±0.002	9.7 ±2.4	30.9 ±2.4	-21.3 ±3.5	-17.7 ± 16%	-671. ± 18%
		6	0.040 ±0.003	12.4 ±5.0	33.6 ±5.0	-21.3 ±7.1	-17.7 ± 33%	-527. ± 34%
400	2.70	1	0.003 ±0.006	0.4 ±2.7	3.0 ±2.7	-2.5 ±3.8	(-0.9 ± 1.4)	
		2	0.009 ±0.006	1.3 ±3.0	9.3 ±3.0	-8.0 ±4.3	-3.0 ± 53%	-850. ± 84%
		3	0.019 ±0.006	2.6 ±2.5	18.1 ±2.5	-15.5 ±3.6	-5.7 ± 23%	-810. ± 41%
		4	0.031 ±0.007	4.2 ±2.5	26.0 ±2.4	-21.7 ±3.4	-8.0 ± 16%	-691. ± 26%
		5	0.046 ±0.007	6.3 ±2.8	31.0 ±2.3	-24.8 ±3.7	-9.2 ± 15%	-533. ± 21%
		6	0.066 ±0.007	8.9 ±4.8	34.2 ±4.8	-25.3 ±6.8	-9.3 ± 27%	-384. ± 29%

[a] Amounts reacted could not be determined for this VOC.

Table A-3. Derivation of Conversion Factors for All the Test VOC Experiments.

Set	Run	Added (ppm)	Reacted (ppm)	IntOH (ppt-min)	Base ROG ConvR [a] (10^3 min-1)	d(O_3-NO) (ppm) Total	d(O_3-NO) (ppm) From Base ROG [b]	-Direct Reactivity- Incremental (mol/mol) [c]	Mechanistic (ConvF)
Carbon Monoxide									
3	418	110.	0.662± 6%	17.4±1.9	33.5±3.0	1.120	0.584±0.083	0.0049 ± 16%	0.8 ±17%
3	416	130.	0.726± 6%	16.1±2.0	34.1±3.1	1.238	0.550±0.085	0.0053 ± 12%	0.9 ±14%
3	414	138.	1.370± 5%	28.8±1.9	33.6±3.0	1.356	0.967±0.109	0.0028 ± 28%	0.3 ±28%
Ethane									
1	68	10.01	0.086± 7%	21.6±1.8	26.2±1.6	0.675	0.568±0.060	0.0107 ± 56%	1.2 ±56%
1	79	17.6	0.127± 6%	18.3±1.8	28.0±1.6	0.724	0.513±0.057	0.0120 ± 27%	1.7 ±28%
1	62	17.6	0.144± 5%	20.7±1.9	26.2±1.6	0.882	0.542±0.060	0.0193 ± 18%	2.4 ±18%
1	73	18.1	0.122± 6%	17.0±1.7	27.8±1.5	0.696	0.472±0.052	0.0123 ± 23%	1.8 ±24%
1	88	24.4	0.178± 6%	18.5±1.7	28.5±1.5	0.881	0.529±0.056	0.0144 ± 16%	2.0 ±17%
2	99	16.6	0.096±13%	14.7±1.7	27.2±1.1	0.562	0.399±0.048	0.0098 ± 30%	1.7 ±32%
2	92	17.1	0.100±10%	14.8±1.3	27.7±1.1	0.581	0.410±0.040	0.0100 ± 24%	1.7 ±26%
3	332	20.0	0.180± 5%	22.8±1.9	33.6±3.0	1.115	0.766±0.094	0.0174 ± 27%	1.9 ±27%
3	333	21.0	0.235± 4%	28.4±1.9	33.6±3.0	1.299	0.953±0.107	0.0165 ± 31%	1.5 ±31%
3	235	43.7	0.306± 6%	17.7±1.9	33.0±3.0	1.006	0.584±0.082	0.0096 ± 20%	1.4 ±21%
Propane									
3	226	11.57	0.231± 8%	12.0±1.9	32.9±3.0	0.736	0.393±0.073	0.030 ± 21%	1.5 ±23%
3	305	20.1	0.405±15%	12.1±1.9	33.1±3.0	1.018	0.399±0.073	0.031 ± 12%	1.5 ±19%
3	230	28.8	0.505±10%	10.5±1.9	33.6±3.0	1.180	0.352±0.072	0.029 ± 9%	1.6 ±14%
n-Butane									
1	59	1.82	0.120± 6%	18.4±2.2	27.2±1.9	0.761	0.500±0.068	0.143 ± 26%	2.2 ±27%
1	51	2.31	0.148± 8%	17.8±1.8	26.5±1.6	0.830	0.471±0.056	0.155 ± 16%	2.4 ±17%
1	53	5.21	0.357± 9%	19.2±1.8	28.4±1.6	0.878	0.544±0.061	0.064 ± 18%	0.9 ±20%
1	82	6.75	0.257±10%	10.5±1.7	27.9±1.5	0.775	0.292±0.050	0.071 ± 11%	1.9 ±15%
1	86	7.00	0.266±12%	10.5±1.7	28.9±1.5	0.813	0.303±0.052	0.073 ± 10%	1.9 ±16%
2	135	6.06	0.209±20%	9.5±1.9	25.6±1.1	0.534	0.243±0.049	0.048 ± 17%	1.4 ±26%
2	97	6.12	0.191±20%	8.6±1.7	27.3±1.1	0.618	0.234±0.048	0.063 ± 13%	2.0 ±23%
2	94	7.16	0.247±10%	9.5±0.9	27.5±1.1	0.574	0.260±0.027	0.044 ± 9%	1.3 ±13%
3	224	9.76	0.309±17%	8.7±1.9	33.2±3.0	0.953	0.288±0.069	0.068 ± 11%	2.2 ±20%
4	393	3.46	0.226± 8%	18.2±5.0	18.4±3.1	0.739	0.335±0.108	0.117 ± 27%	1.8 ±28%
4	389	3.60	0.256±10%	19.9±5.3	18.2±3.3	0.718	0.361±0.117	0.099 ± 33%	1.4 ±34%
Isobutane									
3	228	2.72	0.123±12%	13.6±1.9	33.4±3.0	0.739	0.452±0.076	0.105 ± 26%	2.3 ±29%
3	303	6.62	0.333±31%	15.1±4.8	33.0±3.0	0.937	0.499±0.164	0.066 ± 38%	1.3 ±49%
3	241	10.21	0.418± 8%	12.3±1.9	32.6±3.0	1.209	0.400±0.073	0.079 ± 9%	1.9 ±12%
3	232	20.9	0.539±45%	7.7±3.5	33.5±3.0	1.373	0.256±0.120	0.053 ± 11%	2.1 ±47%
n-Hexane									
3	201	1.168	~0.04 [d]	4.4±3.8	33.2±3.0	0.558	0.146±0.126	0.35 ± 31%	[d]
3	209	1.58	0.092±16%	7.3±1.9	33.4±3.0	0.480	0.245±0.068	0.148 ± 29%	2.6 ±33%
Isooctane									
3	291	10.14	0.294±34%	5.5±1.9	33.3±3.0	1.060	0.182±0.066	0.087 ± 8%	3.0 ±35%
3	293	10.64	0.382±31%	6.8±2.1	33.3±3.0	1.033	0.226±0.073	0.076 ± 9%	2.1 ±32%
n-Octane									
3	239	1.55	0.064±28%	3.3±1.9	33.6±3.0	0.334	0.111±0.066	0.144 ± 29%	3.5 ±40%
3	237	1.66	0.098±19%	4.8±1.9	32.8±3.0	0.345	0.157±0.065	0.113 ± 34%	1.9 ±39%
Ethene									
3	203	0.217	0.086±29%	28.0±1.9	33.3±3.0	0.956	0.933±0.105	(0.11 ± 0.5)	(0.3 ±1.2)
3	199	0.386	0.172±20%	32.7±3.0	32.8±3.0	1.198	1.073±0.139	(0.3 ± 0.4)	(0.7 ±0.8)
Propene									
1	65	0.083	0.067±22%	25.5±1.6	27.9±1.5	0.776	0.712±0.059	0.77 ± 94%	(1.0 ±0.9)
1	72	0.120	0.090± 6%	24.0±1.9	27.2±1.5	0.695	0.653±0.064	(0.4 ± 0.5)	(0.5 ±0.7)
2	110	0.070	0.045±22%	17.7±2.8	26.4±1.1	0.624	0.468±0.077	2.2 ± 51%	3.4 ±54%
2	106	0.081	0.057± 7%	21.1±1.0	26.7±1.1	0.655	0.563±0.036	1.13 ± 39%	1.6 ±40%
2	108	0.085	0.057± 5%	19.0±0.9	26.6±1.1	0.596	0.504±0.032	1.08 ± 35%	1.6 ±35%
2	118	0.148	0.108± 6%	22.9±1.9	26.1±1.1	0.702	0.597±0.056	0.71 ± 54%	1.0 ±54%

Table A-3 (continued)

Set	Run	Added (ppm)	Reacted (ppm)	IntOH (ppt-min)	Base ROG ConvR [a] (10^3 min-1)	d(O_3-NO) (ppm) Total	d(O_3-NO) (ppm) From Base ROG [b]	Direct d(O_3-NO) Incremental (mol/mol) [c]	Reactivity-Mechanistic (ConvF)
Isobutene									
3	257	0.108	0.104± 2%	29.1±1.9	32.9±3.0	0.998	0.958±0.108	(0.4 ± 1.0)	(0.4 ±1.0)
3	255	0.195	0.192±12%	39.3±1.9	33.1±3.0	1.246	1.299±0.133	(-0.3 ± 0.7)	(-0.3 ±0.7)
3	253	0.207	0.205± 7%	38.1±1.9	32.8±3.0	1.259	1.250±0.131	(0.04 ± 0.6)	(0.0 ±0.6)
trans-2-Butene									
3	309	0.069	0.068±11%	29.8±1.9	33.3±3.0	1.079	0.992±0.110	(1.3 ± 2.)	(1.3 ±1.6)
3	307	0.087	0.086±35%	32.5±2.7	33.3±3.0	1.126	1.083±0.132	(0.5 ± 2.)	(0.5 ±1.5)
Isoprene									
3	277	0.076	0.075± 2%	30.0±1.9	33.2±3.0	1.167	0.993±0.110	2.3 ± 63%	2.3 ±63%
3	275	0.108	0.108± 2%	30.8±2.6	33.2±3.0	1.217	1.021±0.126	1.81 ± 64%	1.8 ±64%
3	273	0.139	0.138± 3%	30.3±2.3	33.1±3.0	1.262	1.004±0.119	1.85 ± 46%	1.9 ±46%
3	271	0.157	0.150± 5%	28.6±1.9	32.9±3.0	1.207	0.941±0.106	1.70 ± 40%	1.8 ±40%
2-Chloromethyl-3-chloropropene									
3	343	0.103	0.085± 5%	40.0±1.9	32.8±3.0	1.260	1.312±0.136	(-0.5 ± 1.3)	(-0.6 ±1.6)
3	342	0.108	0.085± 3%	34.9±2.0	33.8±3.0	1.335	1.182±0.126	1.42 ± 82%	1.8 ±82%
3	350	0.113	0.096± 7%	43.2±1.9	33.6±3.0	1.386	1.452±0.146	(-0.6 ± 1.3)	(-0.7 ±1.5)
Benzene									
3	265	5.78	0.357±14%	34.2±4.7	32.8±3.0	0.989	1.121±0.185	(-0.02 ±0.03)	(-0.4 ±0.5)
3	263	6.86	0.447±11%	36.2±3.8	32.8±3.0	0.983	1.185±0.164	-0.029 ± 81%	-0.5 ±82%
Toluene									
1	64	0.061	0.011±16%	25.1±1.8	26.8±1.6	0.702	0.673±0.063	(0.5 ± 1.0)	(2.6 ±5.6)
1	69	0.095	0.020±14%	29.8±2.4	27.4±1.5	0.785	0.815±0.078	(-0.3 ± 0.8)	(-1.5 ±4.0)
1	61	0.175	0.043±11%	36.2±1.8	26.4±1.6	1.041	0.955±0.074	0.49 ± 86%	2.0 ±87%
2	101	0.170	0.030±16%	23.1±0.9	27.0±1.1	0.647	0.623±0.035	(0.14 ± 0.2)	(0.8 ±1.2)
2	103	0.174	0.034±15%	23.3±1.3	26.9±1.1	0.680	0.627±0.042	0.31 ± 79%	1.6 ±81%
Ethylbenzene									
3	313	0.092	0.015± 7%	17.6±1.9	32.8±3.0	0.649	0.577±0.083	(0.8 ± 0.9)	(4.7 ±5.5)
3	311	0.098	0.017± 8%	18.1±2.0	32.7±3.0	0.608	0.592±0.084	(0.2 ± 0.9)	(0.9 ±5.1)
3	315	0.215	0.031±21%	19.0±1.9	33.3±3.0	0.806	0.632±0.086	0.81 ± 49%	5.6 ±54%
o-Xylene									
3	259	0.064	0.024±14%	27.8±2.5	32.8±3.0	0.962	0.910±0.117	(0.8 ± 2.)	(2.2 ±4.9)
3	261	0.064	0.027±11%	30.2±3.3	32.7±3.0	1.028	0.985±0.141	(0.7 ± 2.)	(1.6 ±5.3)
m-Xylene									
3	207	0.038	0.023±16%	25.8±4.0	33.4±3.0	0.977	0.860±0.154	(3. ± 4.)	(5.1 ±6.8)
3	301	0.053	0.033±20%	29.0±1.9	32.9±3.0	1.014	0.955±0.107	(1.1 ± 2.)	(1.8 ±3.3)
3	196	0.057	0.034±11%	27.1±2.0	32.3±3.1	0.892	0.875±0.105	(0.3 ± 2.)	(0.5 ±3.1)
3	344	0.081	0.049±33%	28.0±3.7	33.6±3.0	1.329	0.941±0.149	4.8 ± 42%	7.8 ±50%
p-Xylene									
3	348	0.075	0.036± 3%	31.4±1.9	33.4±3.0	1.066	1.050±0.114	(0.2 ± 2.)	(0.4 ±3.2)
3	346	0.080	0.039± 3%	32.6±2.0	32.6±3.0	1.130	1.062±0.118	(0.8 ± 1.5)	(1.7 ±3.0)
135-trimethyl-Benzene									
3	251	0.045	0.042± 7%	33.2±1.9	33.3±3.0	1.029	1.102±0.118	(-2. ± 3.)	(-1.7 ±2.8)
3	249	0.047	0.045±11%	40.8±2.4	33.1±3.0	1.305	1.353±0.147	(-1.0 ± 3.)	(-1.1 ±3.3)
124-trimethyl-Benzene									
3	267	0.037	0.023± 5%	26.0±1.9	32.8±3.0	0.952	0.852±0.101	(3. ± 3.)	(4.3 ±4.3)
3	269	0.041	0.028± 5%	30.5±1.9	32.8±3.0	1.049	1.001±0.111	(1.2 ± 3.)	(1.7 ±3.9)
123-trimethyl-Benzene									
3	299	0.035	0.028±13%	35.7±2.0	33.2±3.0	1.221	1.183±0.125	(1.1 ± 4.)	(1.4 ±4.4)
3	297	0.044	0.033± 3%	41.0±2.2	33.0±3.0	1.273	1.353±0.143	(-2. ± 3.)	(-2.4 ±4.3)
Methanol									
3	287	0.816	0.027± 7%	24.5±1.9	33.2±3.0	0.886	0.815±0.097	(0.09 ±0.12)	(2.6 ±3.6)
3	289	2.29	0.087± 6%	28.5±2.0	33.1±3.0	1.093	0.942±0.107	0.066 ± 71%	1.7 ±72%

Table A-3 (continued)

Set	Run	Added (ppm)	Reacted (ppm)	IntOH (ppt-min)	Base ROG ConvR [a] (10^3 min-1)	d(O_3-NO) (ppm) Total	d(O_3-NO) (ppm) From Base ROG [b]	-Direct d(O_3-NO) Incremental (mol/mol) [c]	Reactivity-Mechanistic (ConvF)
3	285	7.64	0.316± 6%	31.0±1.9	33.3±3.0	1.302	1.034±0.113	0.035 ± 42%	0.8 ±43%
Ethanol									
2	133	2.91	0.199± 9%	14.9±1.2	25.6±1.1	0.600	0.381±0.034	0.075 ± 16%	1.1 ±18%
2	138	3.01	0.193±11%	14.0±1.3	25.5±1.1	0.553	0.356±0.037	0.065 ± 19%	1.0 ±22%
2	131	3.15	0.208± 7%	14.4±0.9	25.7±1.1	0.598	0.371±0.028	0.072 ± 13%	1.1 ±14%
Isopropanol									
2	148	3.63	0.466±10%	18.3±0.9	25.3±1.1	0.816	0.462±0.031	0.098 ± 12%	0.8 ±13%
3	157	1.26	0.212±17%	22.6±4.1	33.3±3.0	0.774	0.753±0.153	(0.02 ±0.12)	(0.1 ±0.7)
3	159	1.61	0.265± 7%	24.0±1.9	33.2±3.0	0.811	0.796±0.096	(0.010 ±0.06)	(0.1 ±0.4)
3	155	1.74	0.290± 9%	24.3±1.9	33.2±3.0	0.927	0.806±0.096	0.070 ± 80%	0.4 ±80%
Dimethyl Ether									
3	283	2.10	0.206± 8%	23.6±1.9	33.2±3.0	1.196	0.783±0.095	0.196 ± 23%	2.0 ±25%
3	295	2.12	0.197± 5%	22.4±1.9	33.2±3.0	1.069	0.742±0.092	0.154 ± 28%	1.7 ±29%
3	281	3.41	0.326± 6%	23.1±1.9	33.2±3.0	1.248	0.767±0.094	0.141 ± 20%	1.5 ±20%
3	279	4.04	0.407± 7%	24.4±1.9	33.2±3.0	1.361	0.810±0.097	0.136 ± 18%	1.4 ±19%
MTBE									
2	120	2.04	0.108± 7%	13.2±0.9	26.0±1.1	0.555	0.342±0.028	0.104 ± 13%	2.0 ±15%
2	125	2.49	0.120±10%	12.0±1.2	25.8±1.1	0.552	0.310±0.033	0.097 ± 14%	2.0 ±17%
2	127	2.51	0.115± 9%	11.4±0.9	25.8±1.1	0.579	0.293±0.027	0.114 ± 10%	2.5 ±13%
2	123	2.98	0.202± 6%	17.1±1.0	25.9±1.1	0.812	0.443±0.032	0.124 ± 9%	1.8 ±11%
Ethoxyethanol									
3	175	0.401	0.178±17%	17.3±1.9	33.2±3.0	0.905	0.574±0.082	0.83 ± 26%	1.9 ±30%
3	171	0.730	0.342± 8%	18.7±1.9	32.9±3.0	1.208	0.614±0.085	0.81 ± 15%	1.7 ±16%
3	163	0.859	0.480±10%	24.1±4.8	33.0±3.0	1.424	0.797±0.174	0.73 ± 29%	1.3 ±29%
Carbitol									
3	169	0.412	0.239± 4%	10.5±1.9	33.4±3.0	0.817	0.350±0.071	1.13 ± 15%	2.0 ±16%
3	166	0.503	0.289± 6%	14.3±2.0	33.2±3.0	1.109	0.473±0.078	1.26 ± 13%	2.2 ±14%
3	173	0.946	0.365±11%	6.7±1.9	33.3±3.0	0.871	0.221±0.066	0.69 ± 10%	1.8 ±15%
Formaldehyde									
3	352	0.104	[e]	34.6±1.9	33.4±3.0	1.110	1.156±0.122	(-0.4 ± 1.2)	
3	357	0.267	[e]	42.5±1.9	33.5±3.0	1.206	1.423±0.143	-0.81 ± 66%	
Acetaldehyde									
3	335	0.696	0.261± 7%	18.5±1.9	33.6±3.0	1.036	0.622±0.086	0.59 ± 21%	1.6 ±22%
3	338	1.31	0.444± 8%	13.1±1.9	33.2±3.0	1.020	0.435±0.075	0.45 ± 13%	1.3 ±15%
Acetone									
3	243	0.847	[e]	25.5±1.9	32.7±3.0	0.770	0.833±0.100	(-0.07 ±0.12)	
3	245	2.19	[e]	26.2±2.5	33.3±3.0	0.886	0.872±0.114	(0.007 ±0.05)	
3	247	4.14	[e]	27.7±1.9	32.9±3.0	0.942	0.910±0.104	(0.008 ±0.03)	
Hexamethyldisiloxane									
3	183	6.71	0.076±17%	5.7±2.0	32.8±3.0	0.282	0.188±0.067	0.0141 ± 71%	1.2 ±72%
3	179	9.13	0.064±45%	3.5±1.9	33.3±3.0	0.257	0.117±0.066	0.0154 ± 47%	2.2 ±65%
4	396	2.83	0.091±14%	16.4±4.9	19.0±3.1	0.420	0.311±0.105	0.039 ± 96%	(1.2 ±1.2)
4	391	3.99	0.072±14%	9.1±4.8	18.9±3.0	0.307	0.171±0.095	0.034 ± 70%	1.9 ±71%
Octamethylcyclotetrasiloxane									
3	194	2.15	0.032±19%	10.1±2.0	32.4±3.1	0.387	0.328±0.071	(0.03 ±0.03)	(1.9 ±2.3)
3	185	4.31	0.048±21%	7.7±1.9	33.1±3.0	0.278	0.256±0.068	(0.005 ±0.02)	(0.5 ±1.4)
3	181	10.08	0.024±63%	1.6±1.9	33.1±3.0	0.183	0.054±0.064	0.0128 ± 50%	5.4 ±80%
4	406	1.35	0.037± 6%	19.0±4.9	19.1±3.1	0.429	0.363±0.111	(0.05 ±0.08)	(1.8 ±3.0)
4	402	1.77	0.044± 5%	17.1±5.1	19.2±3.2	0.360	0.328±0.112	(0.02 ±0.06)	(0.7 ±2.6)
4	398	2.62	~0.008[d]	2.2±4.9	18.5±3.0	0.319	0.041±0.090	0.106 ± 33%	[d]
Decamethylcyclopentasiloxane									
3	190	1.55	0.023±18%	6.8±2.0	32.1±3.1	0.257	0.218±0.068	(0.03 ±0.04)	(1.7 ±2.9)
3	192	1.85	0.029±21%	7.1±2.0	32.2±3.1	0.271	0.230±0.068	(0.02 ±0.04)	(1.4 ±2.3)

Table A-3 (continued)

Set	Run	Added (ppm)	Reacted (ppm)	IntOH (ppt-min)	Base ROG ConvR [a] (10^3 min-1)	—— d(O_3-NO) (ppm) —— Total	From Base ROG [b]	-Direct d(O_3-NO) Incremental (mol/mol) [c]	Reactivity-Mechanistic (ConvF)
3	187	4.93	0.039±27%	3.5±1.9	32.7±3.0	0.211	0.114±0.064	0.0196 ± 67%	2.5 ±72%
Pentamethyldisiloxanol									
3	412	0.712	0.036± 5%	18.6±1.9	33.4±3.0	0.526	0.619±0.085	-0.131 ± 91%	(-2.6 ±2.4)
3	409	2.17	0.115±46%	19.6±9.2	33.9±3.1	0.370	0.664±0.316	(-0.14 ±0.15)	(-2.6 ±3.0)
4	404	1.20	0.040± 6%	12.4±5.0	19.1±3.1	0.375	0.236±0.103	0.115 ± 74%	3.4 ±75%
4	400	2.70	0.066±11%	8.9±4.8	18.9±3.0	0.241	0.168±0.095	(0.03 ±0.04)	(1.1 ±1.4)

[a] Conversion ratio from base case runs for the conditions of this experiment.
[b] Estimated from $ConvR^{base}$ x $IntOH^{test}$ as discussed in the text.
[c] $IR[d(O_3\text{-}NO)]^{direct} = [d(O_3\text{-}NO)^{test} - d(O_3\text{-}NO)^{from\ base\ ROG}]/[VOC]_0$.
[d] Amount reacted highly uncertain. Mechanistic reactivities could not be determined.
[e] Amounts reacted could not be determined for this VOC.

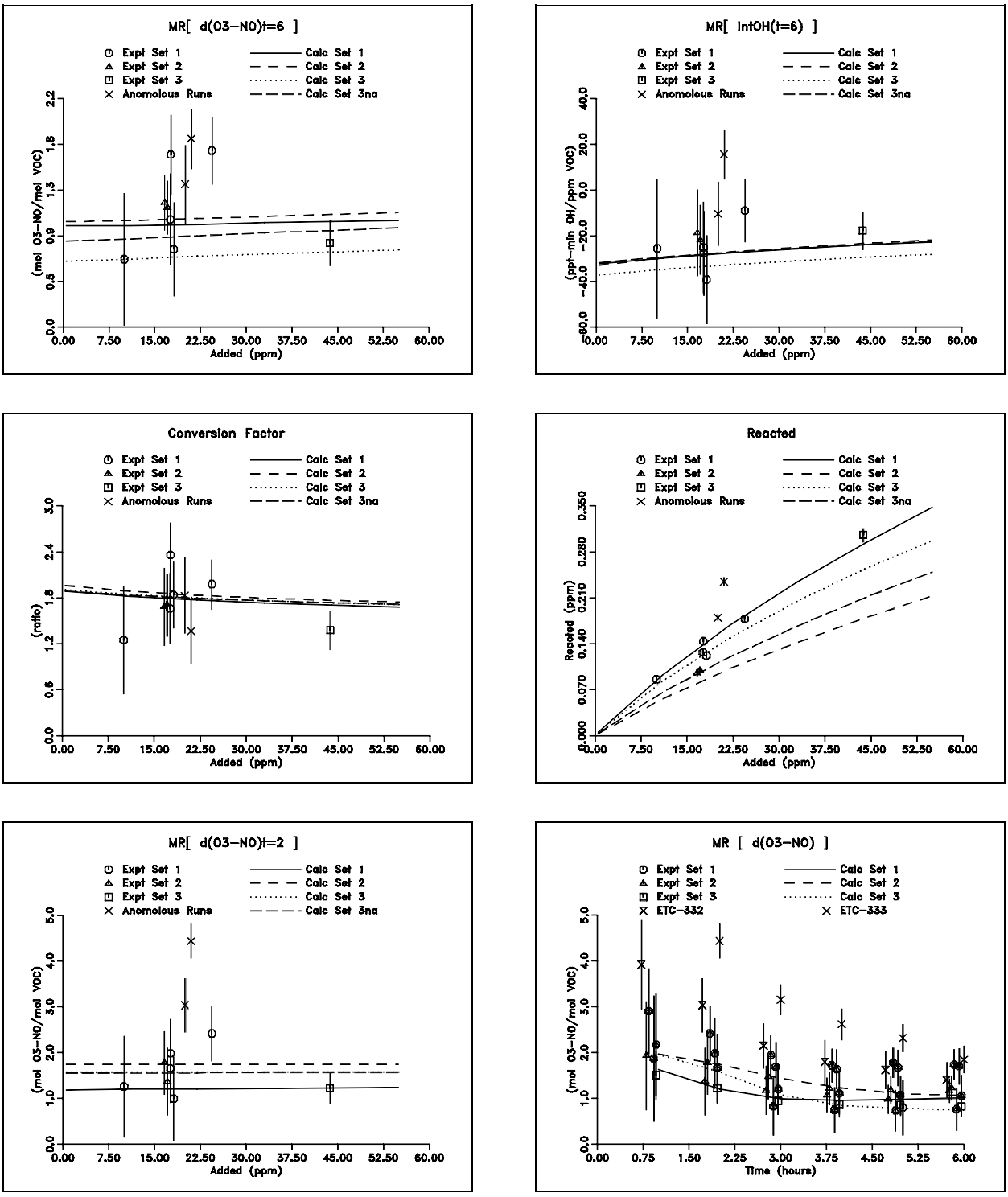

Figure A-1. Plots of experimental and calculated reactivity results for **Ethane**.

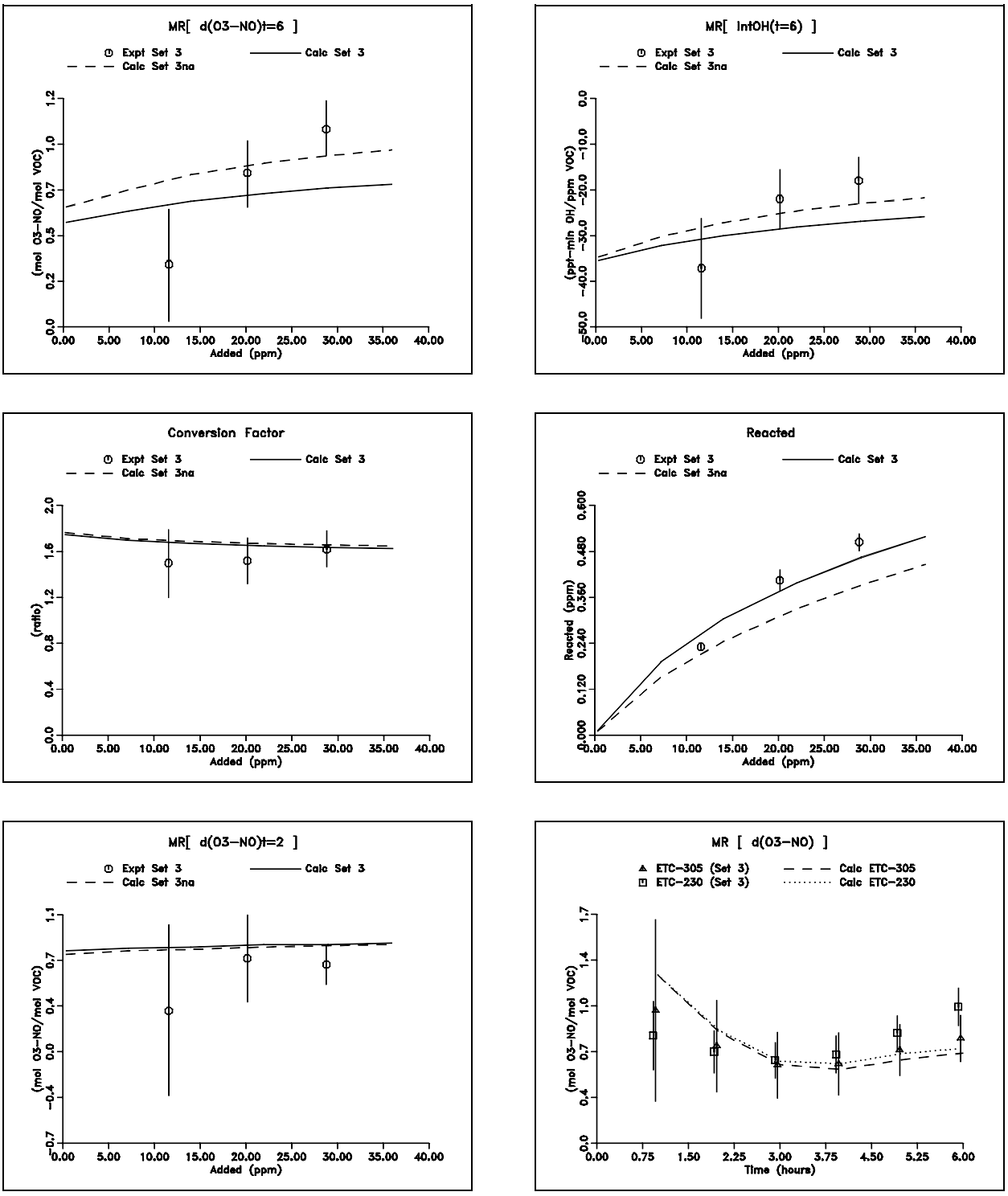

Figure A-2. Plots of experimental and calculated reactivity results for **Propane**.

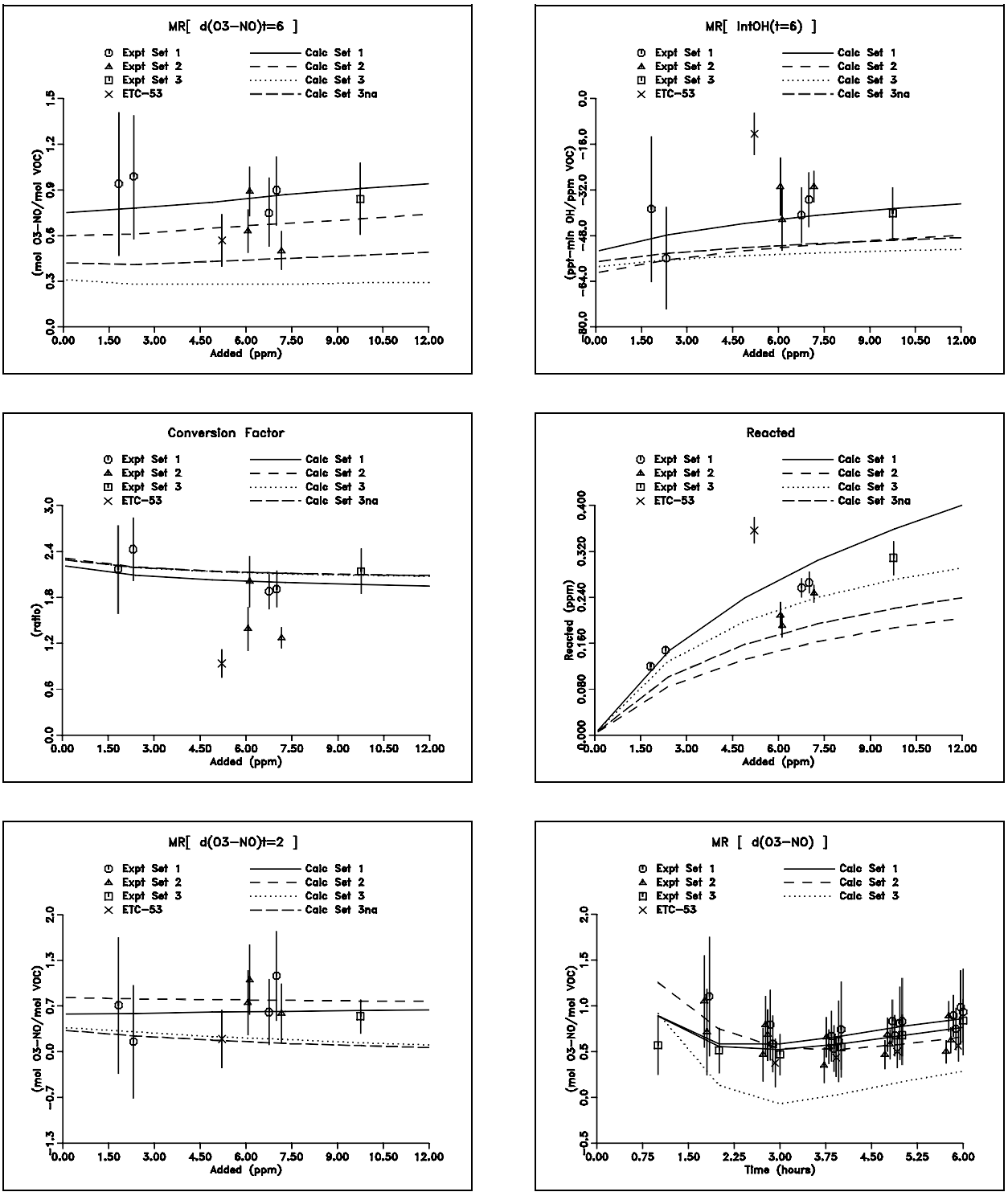

Figure A-3. Plots of experimental and calculated reactivity results for **n-Butane**.

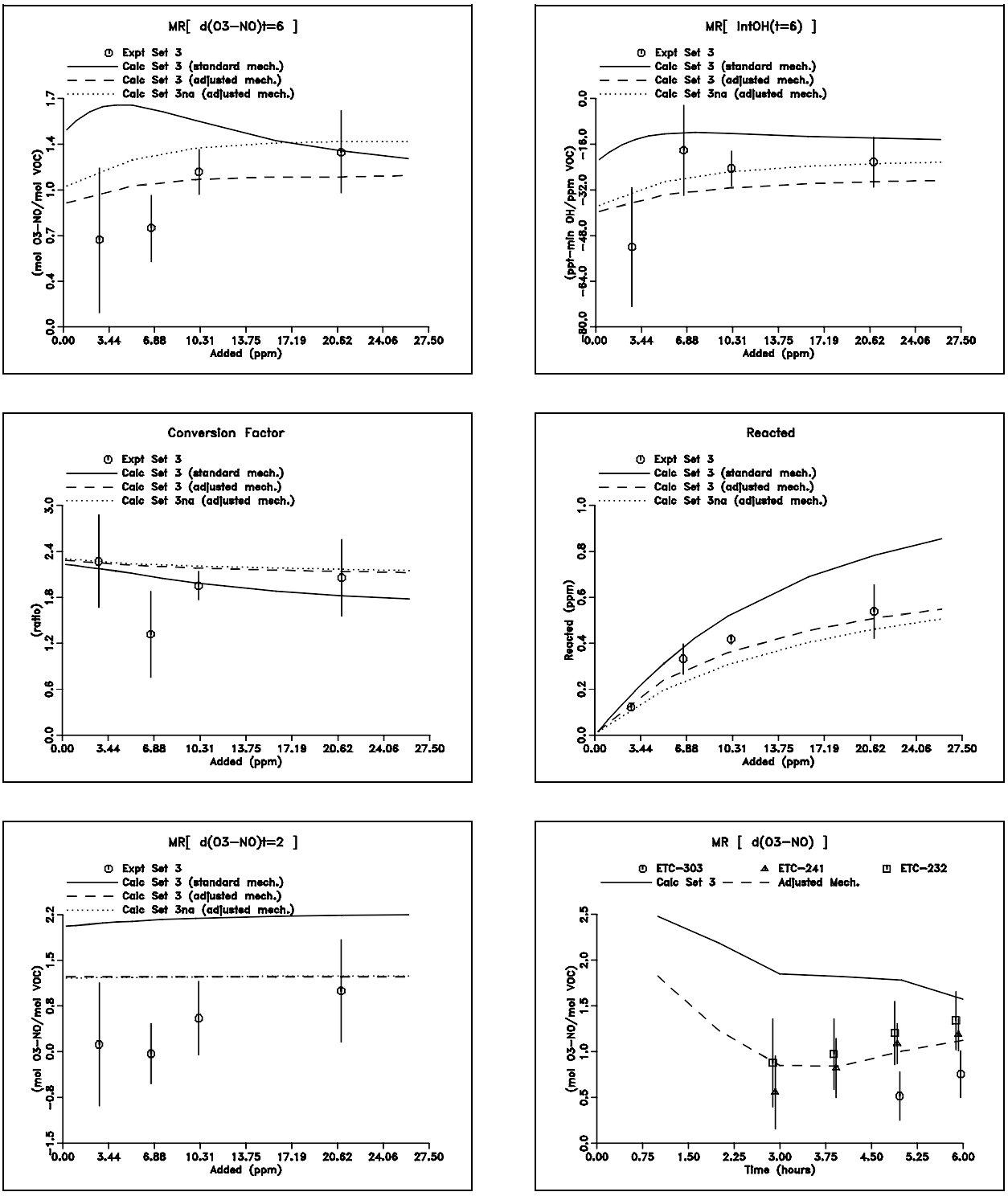

Figure A-4. Plots of experimental and calculated reactivity results for **Isobutane**.

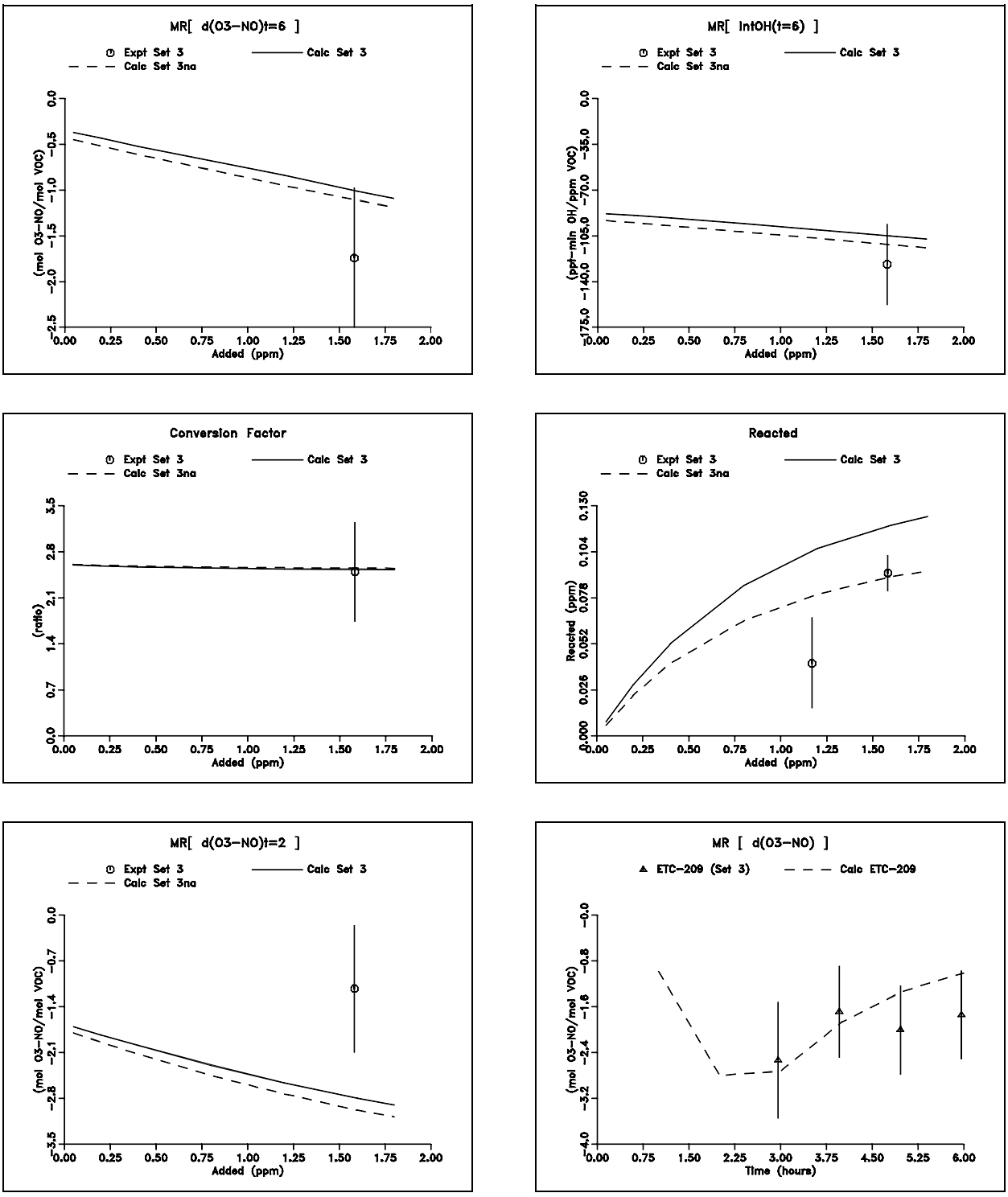

Figure A-5. Plots of experimental and calculated reactivity results for **n-Hexane**.

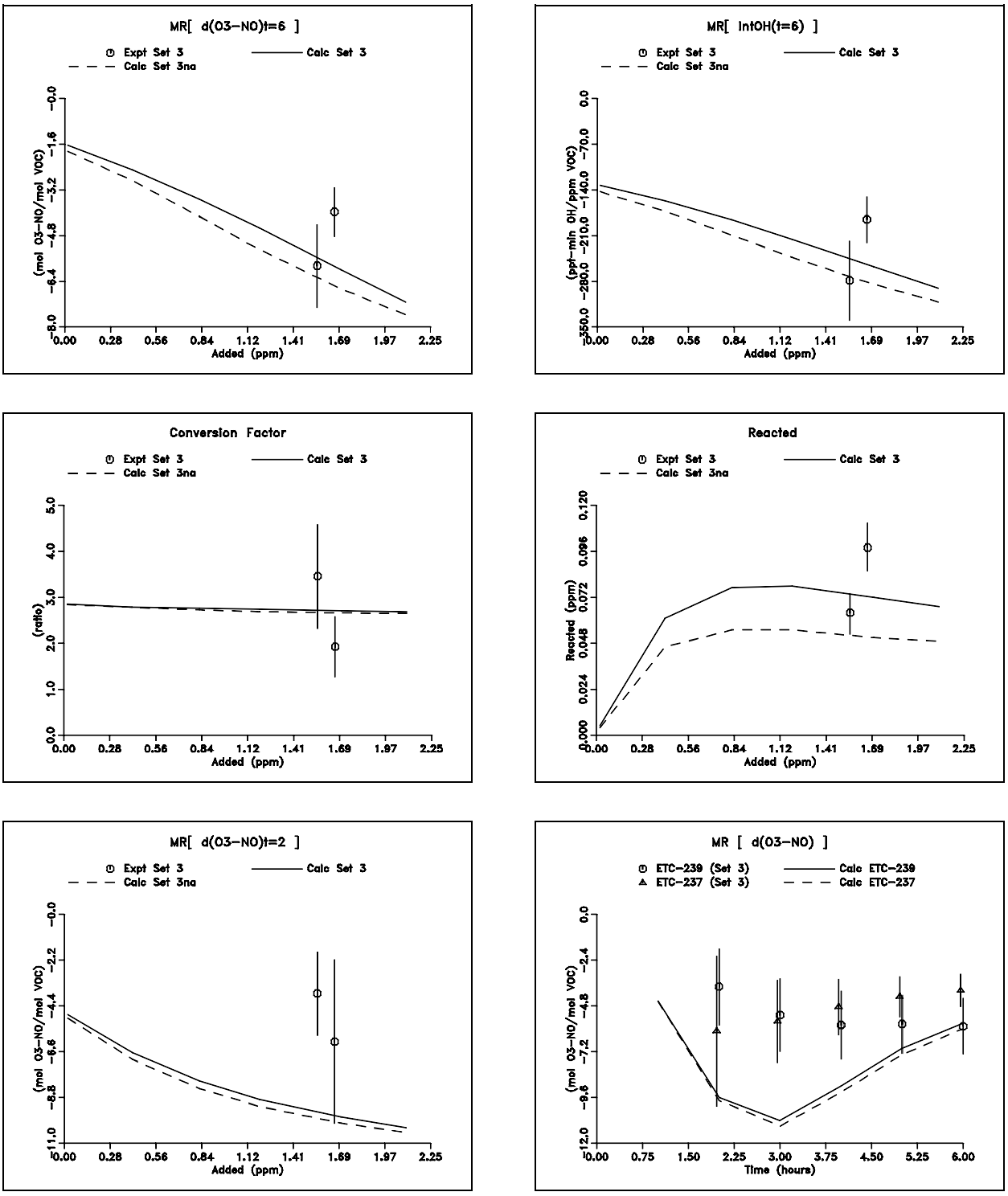

Figure A-6. Plots of experimental and calculated reactivity results for **n-Octane**.

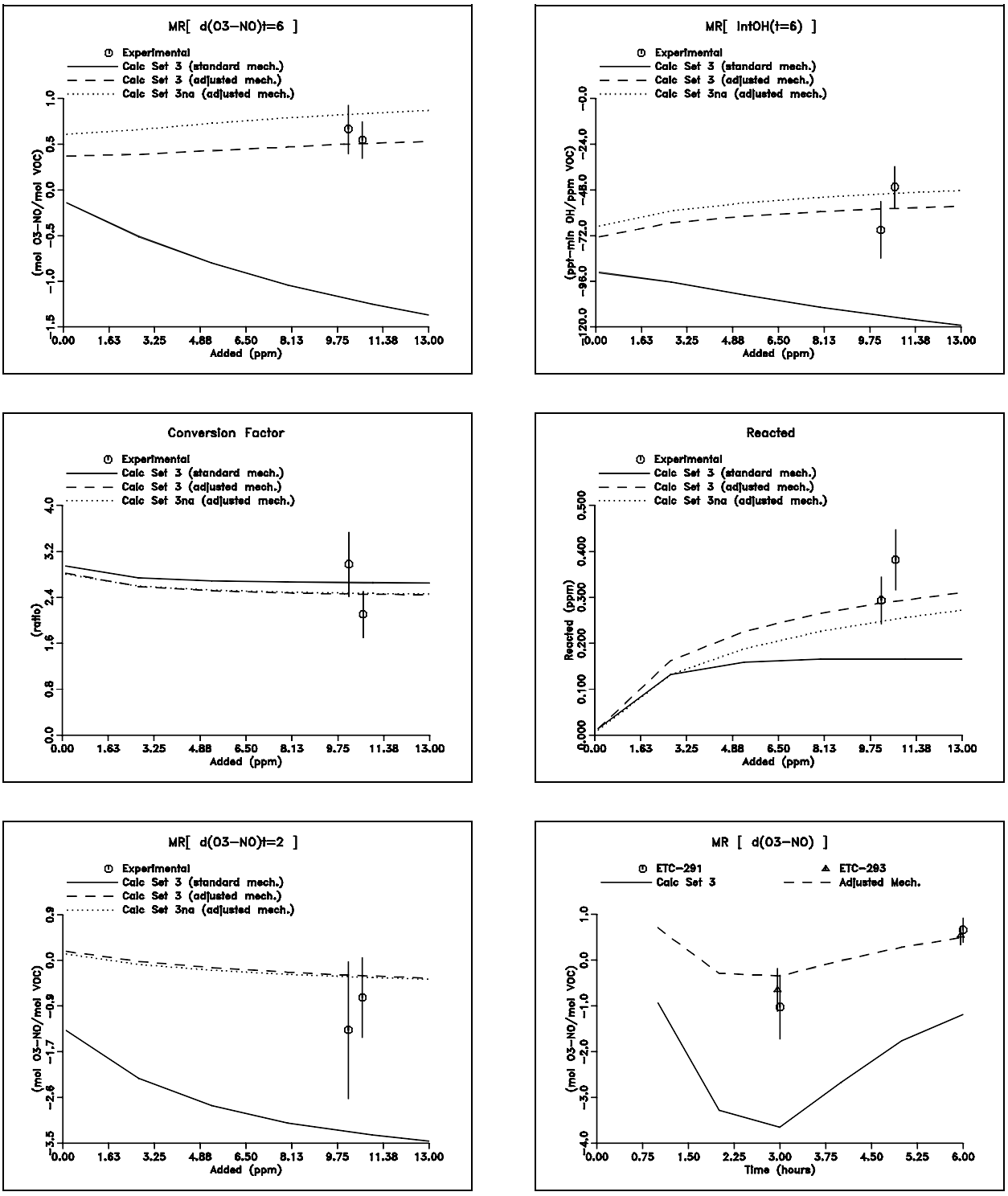

Figure A-7. Plots of experimental and calculated reactivity results for **Isooctane**.

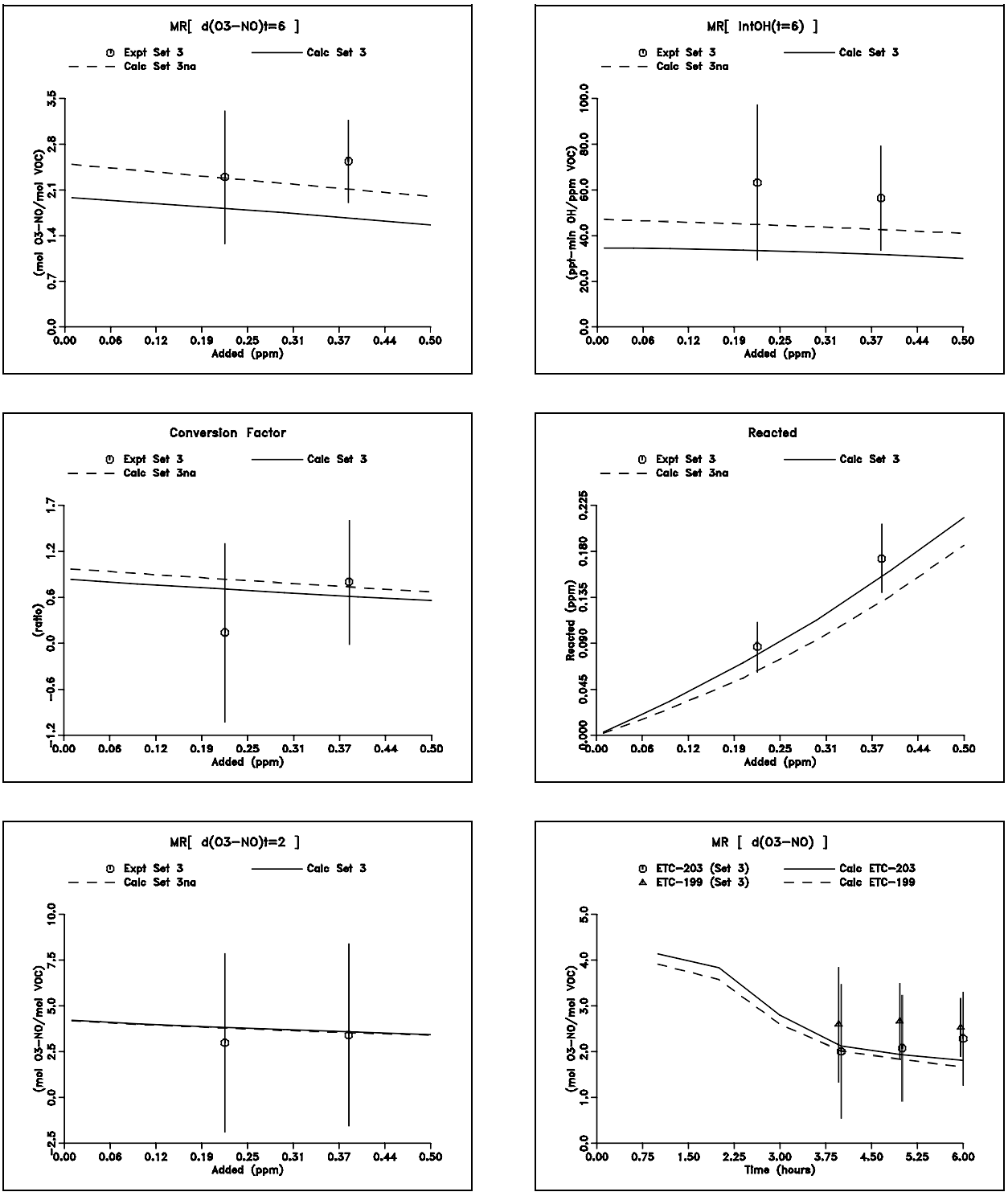

Figure A-8. Plots of experimental and calculated reactivity results for **Ethene**.

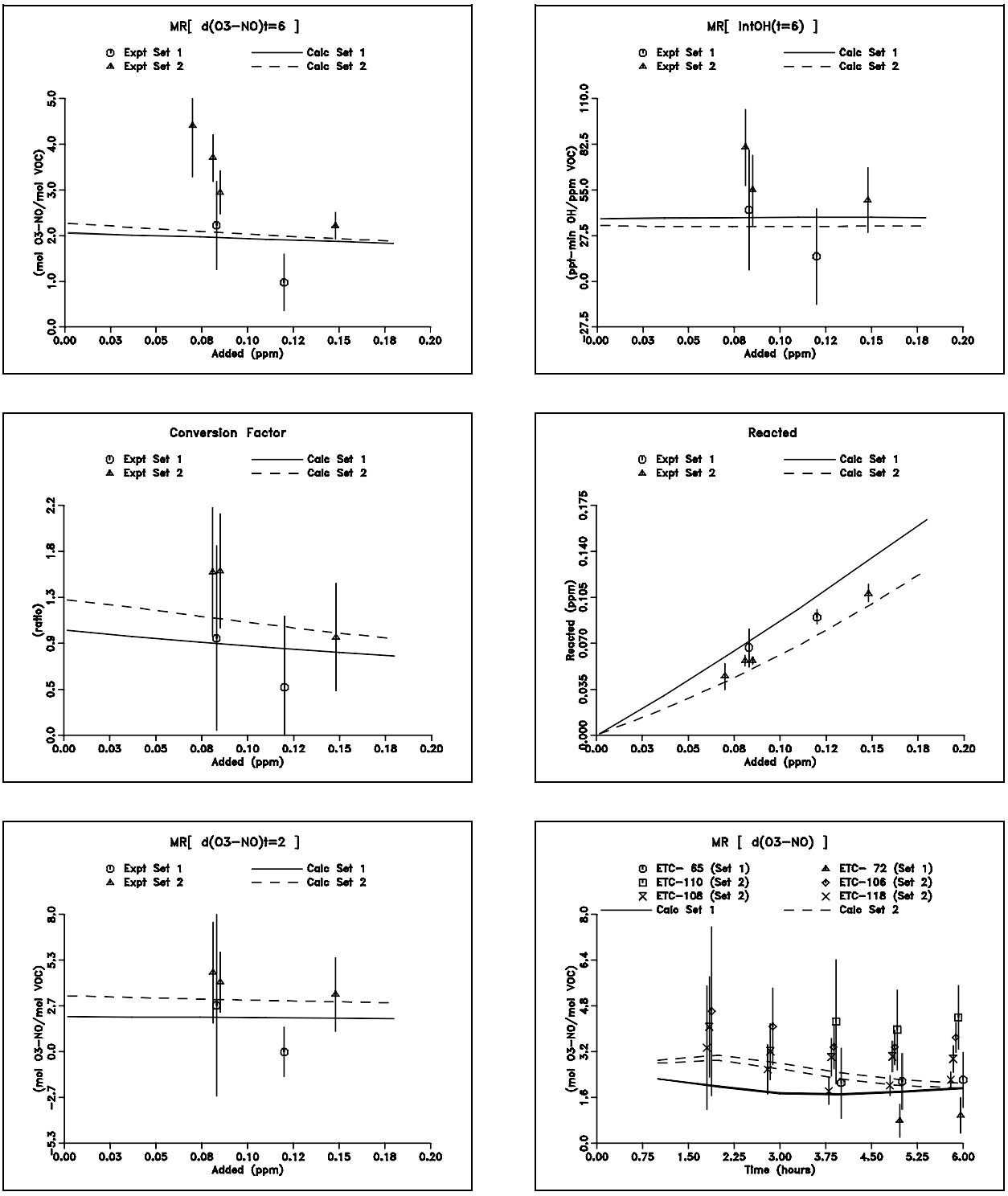

Figure A-9. Plots of experimental and calculated reactivity results for **Propene**.

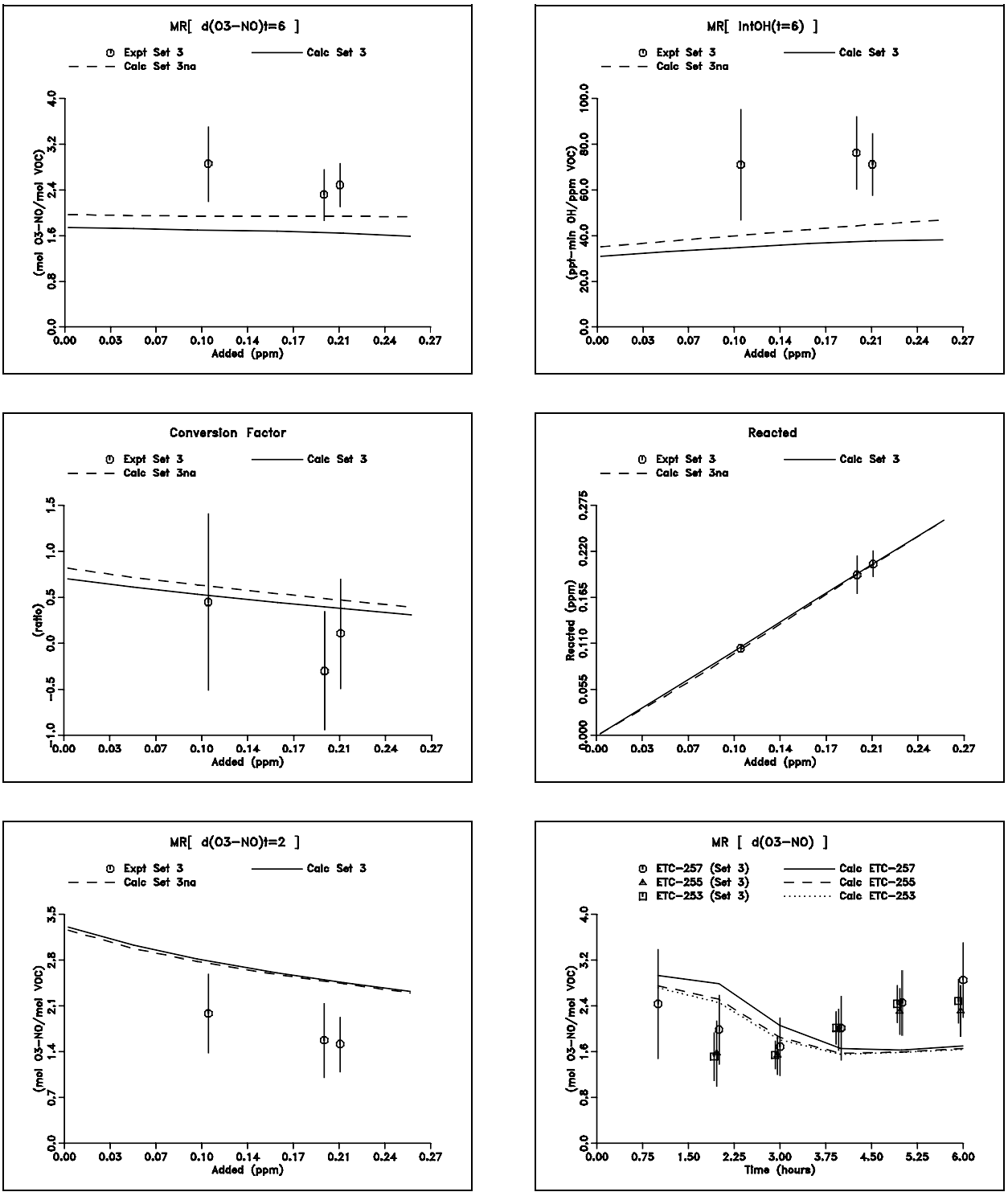

Figure A-10. Plots of experimental and calculated reactivity results for **Isobutene**.

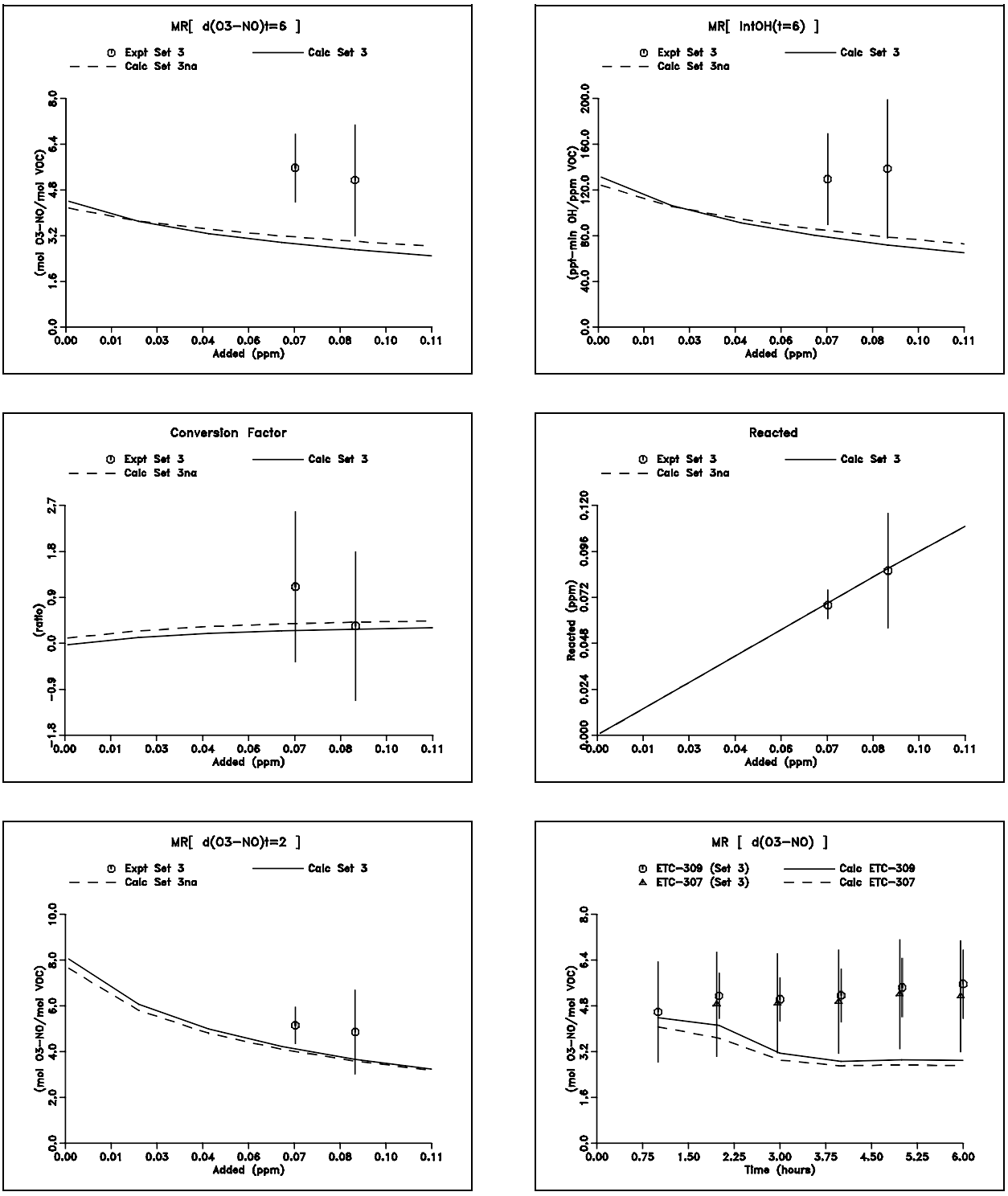

Figure A-11. Plots of experimental and calculated reactivity results for **trans-2-Butene**.

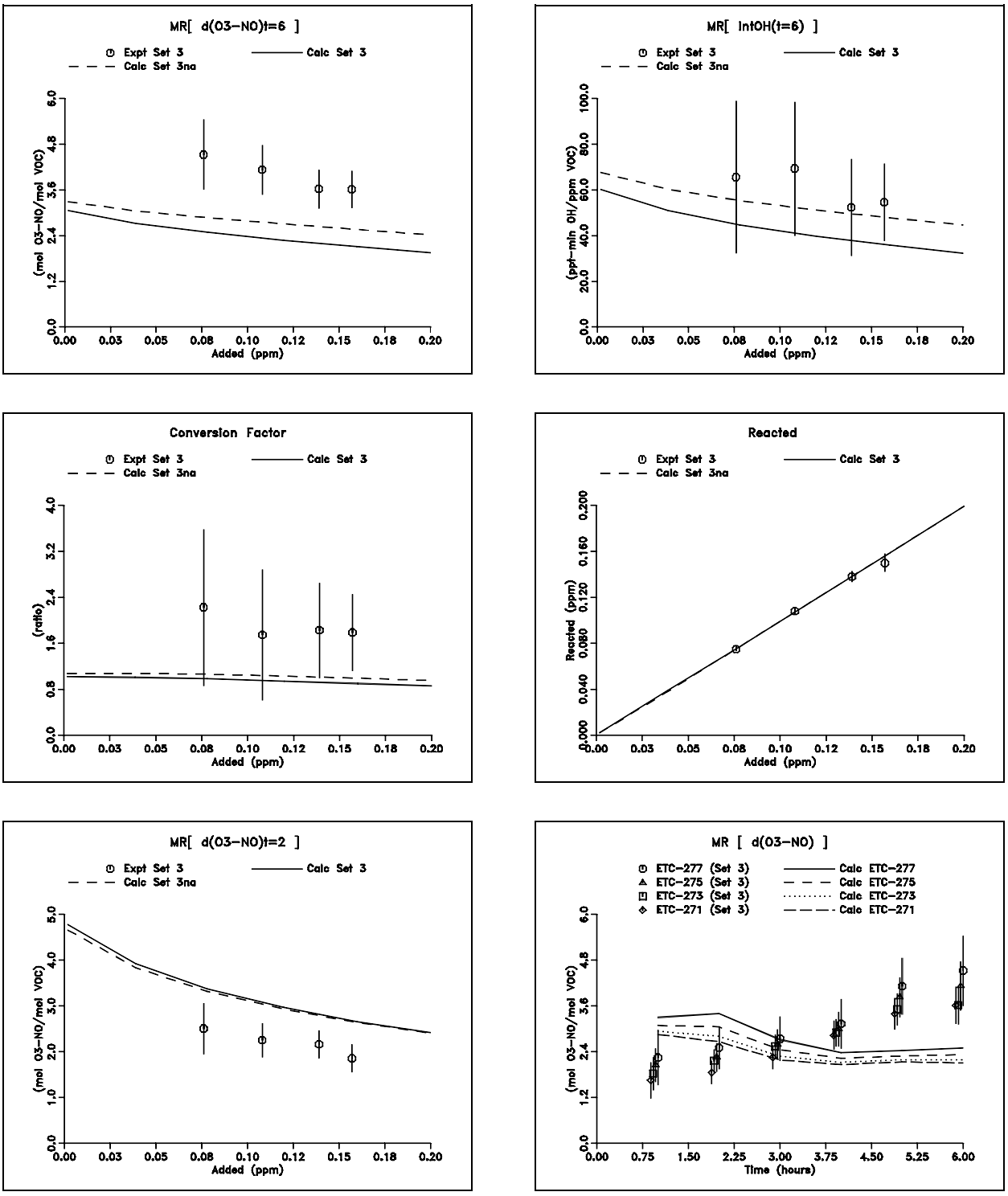

Figure A-12. Plots of experimental and calculated reactivity results for **Isoprene**.

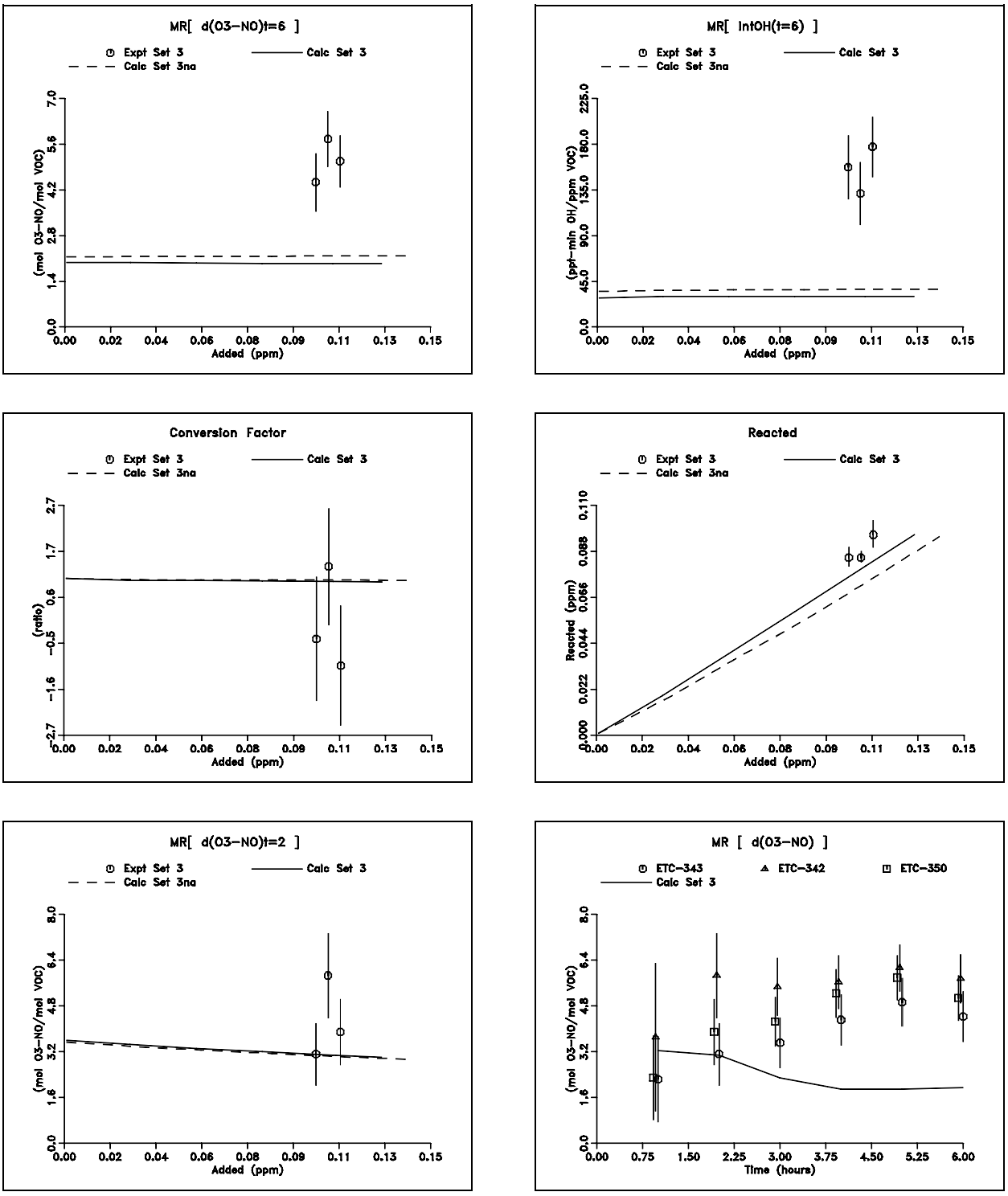

Figure A-13. Plots of experimental and calculated reactivity results for **2-Chloromethyl-3-Chloropropene**.

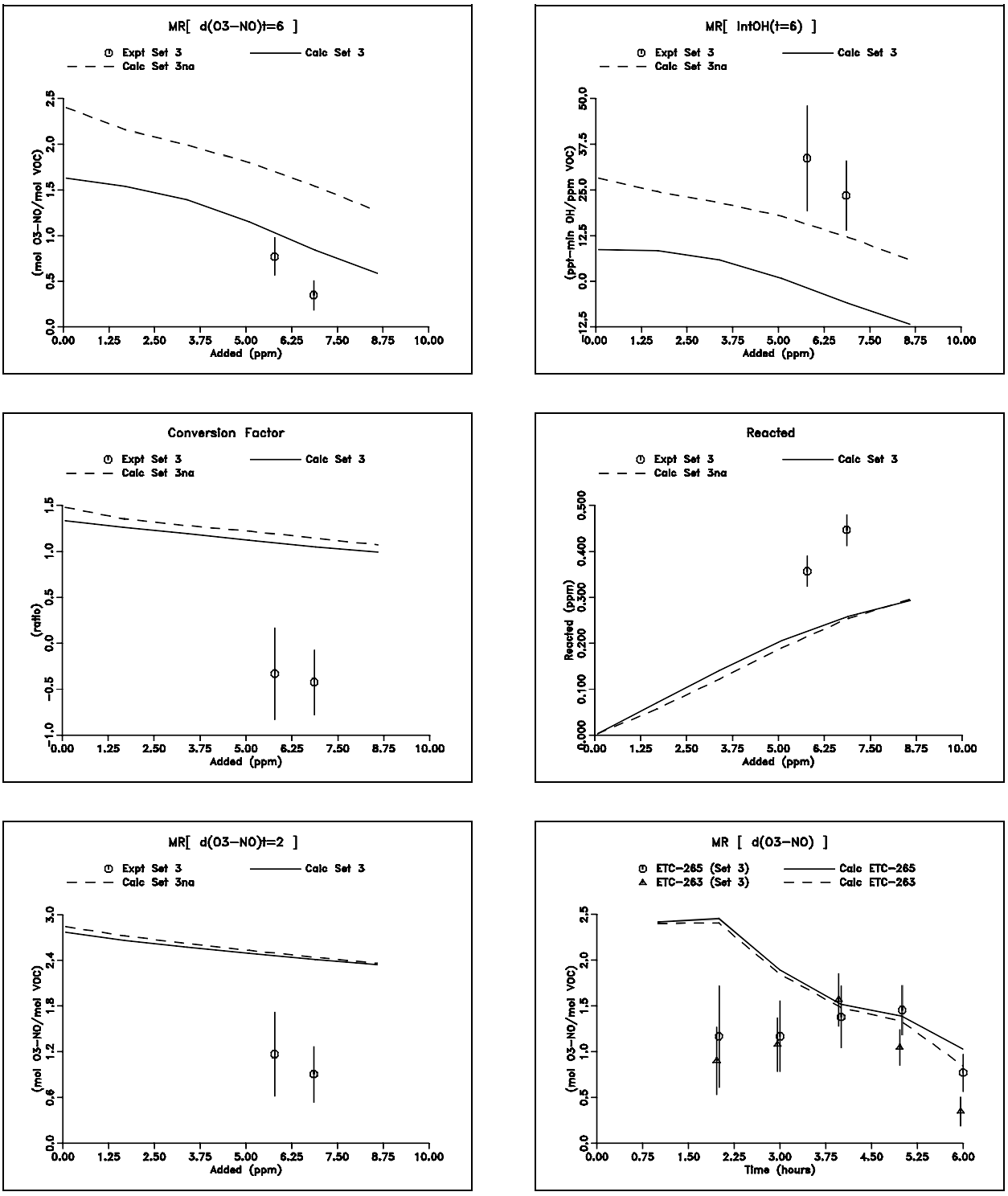

Figure A-14. Plots of experimental and calculated reactivity results for **Benzene**.

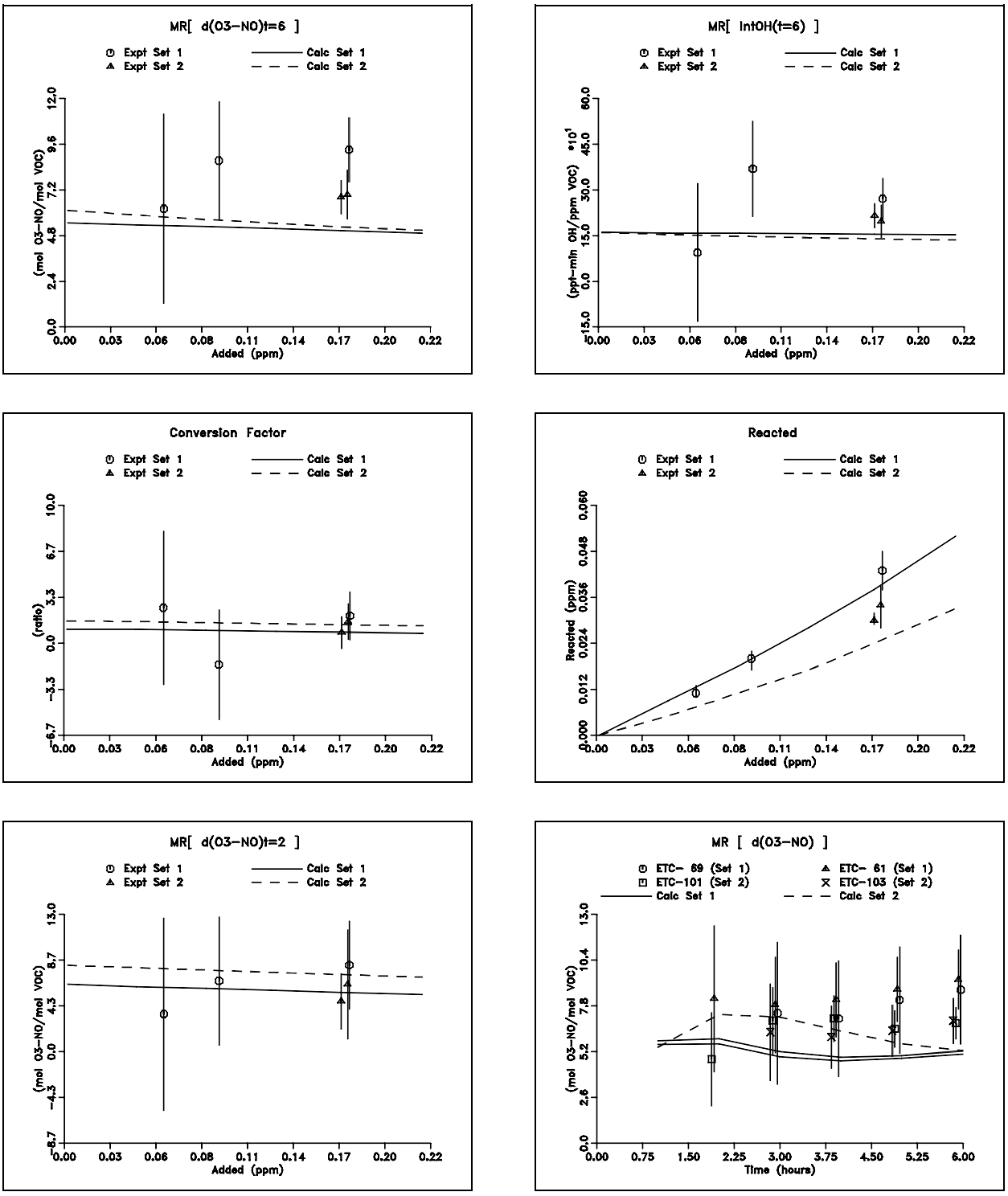

Figure A-15. Plots of experimental and calculated reactivity results for **Toluene**.

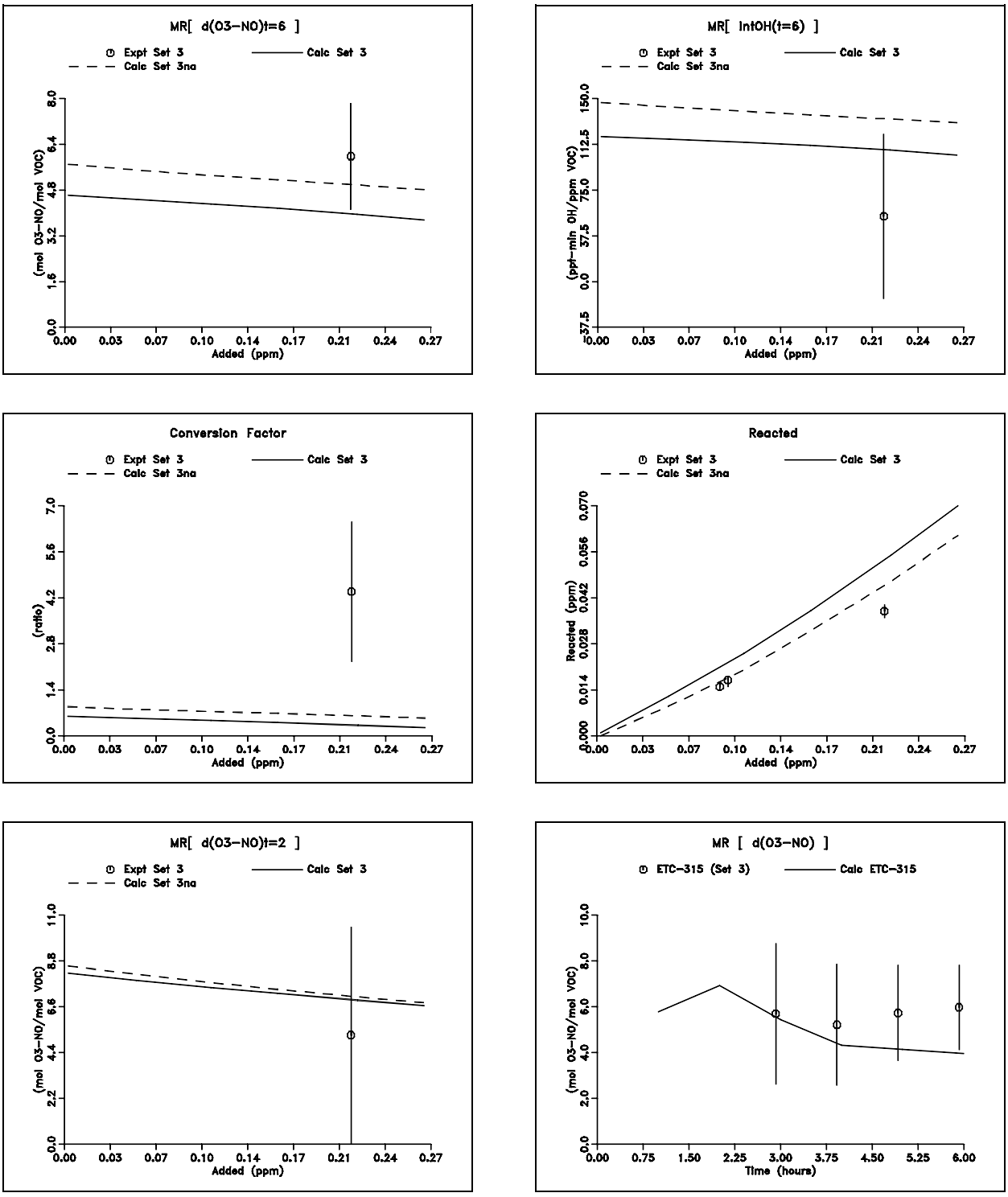

Figure A-16. Plots of experimental and calculated reactivity results for **Ethylbenzene**.

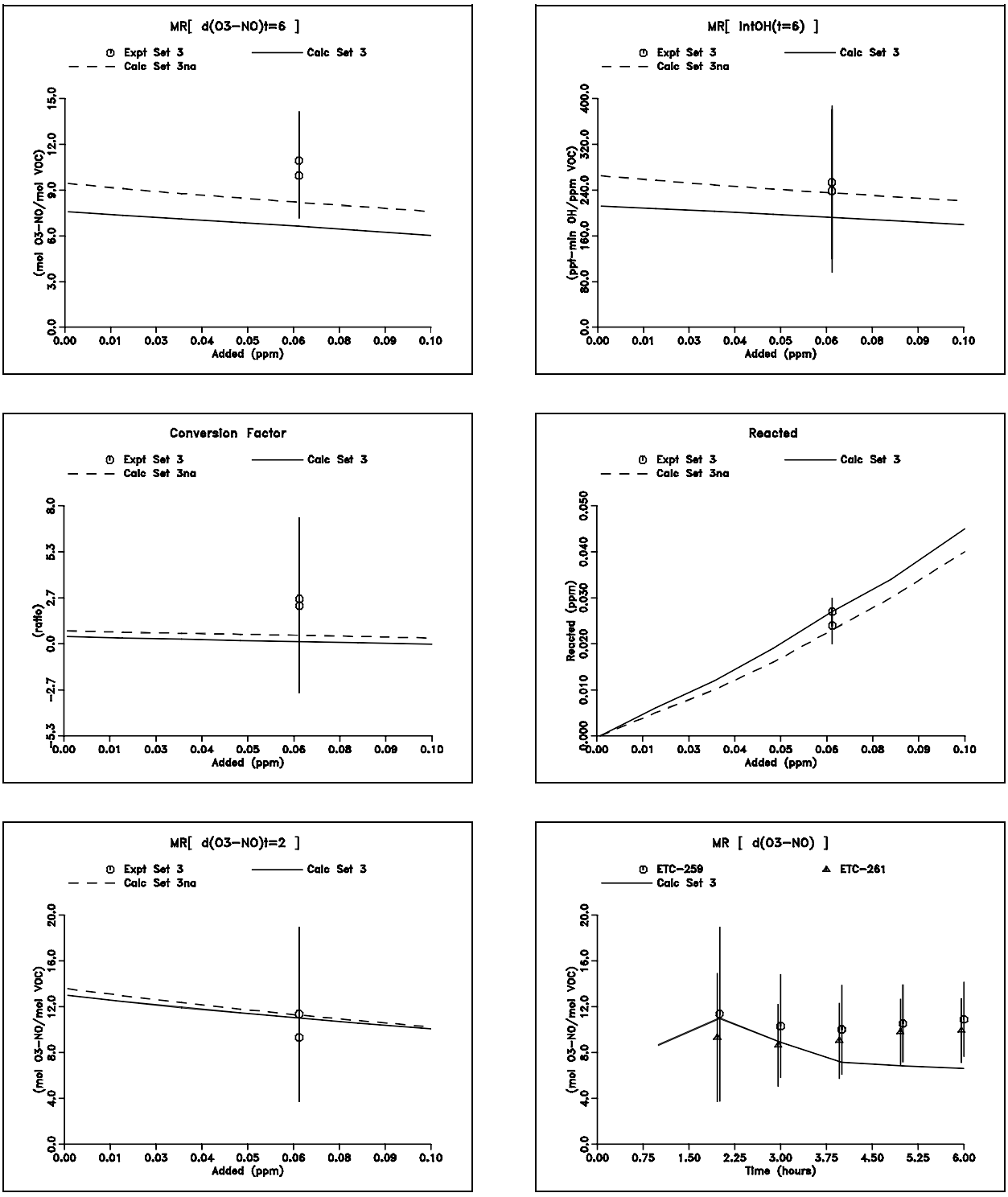

Figure A-17. Plots of experimental and calculated reactivity results for **o-Xylene**.

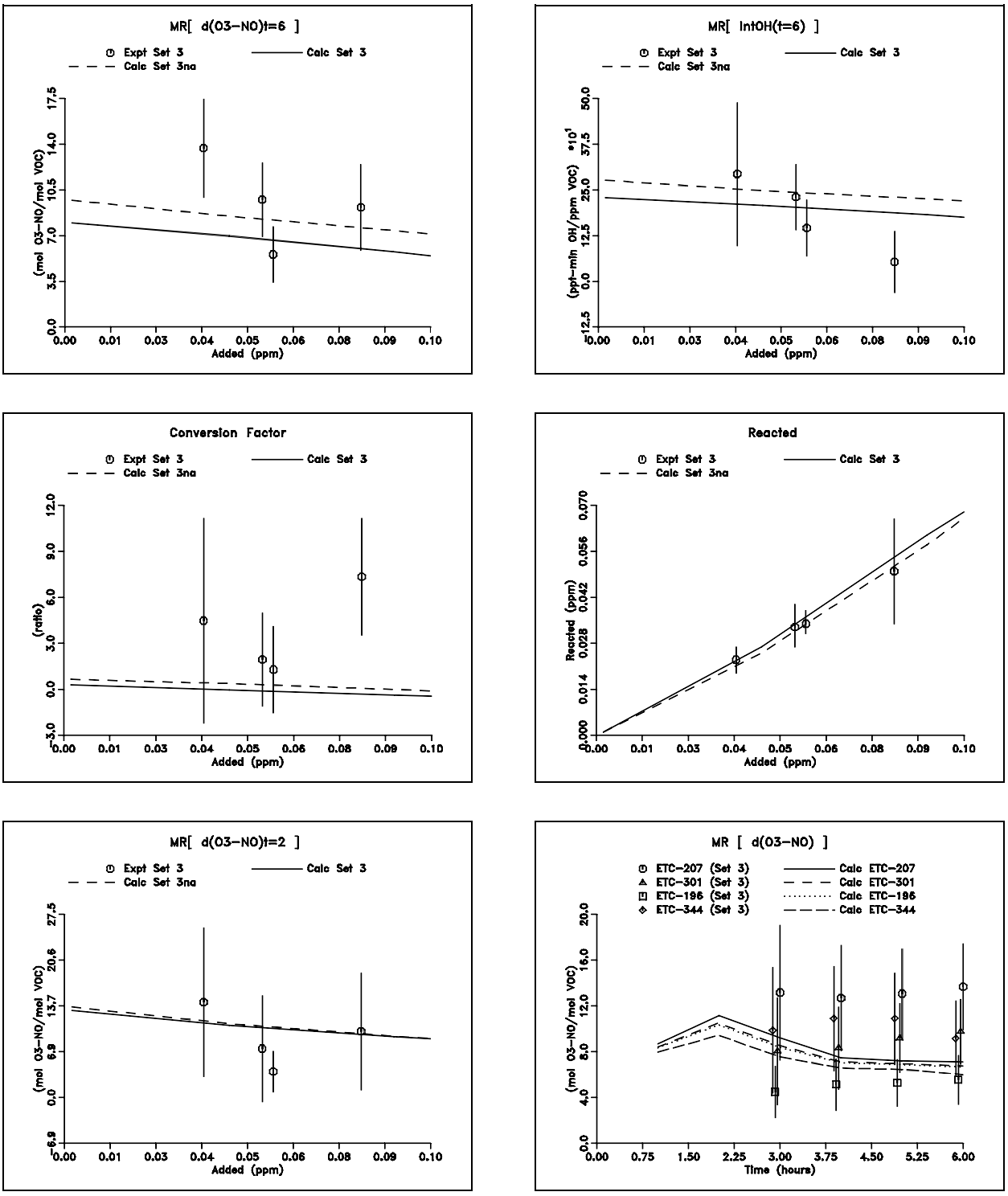

Figure A-18. Plots of experimental and calculated reactivity results for **m-Xylene**.

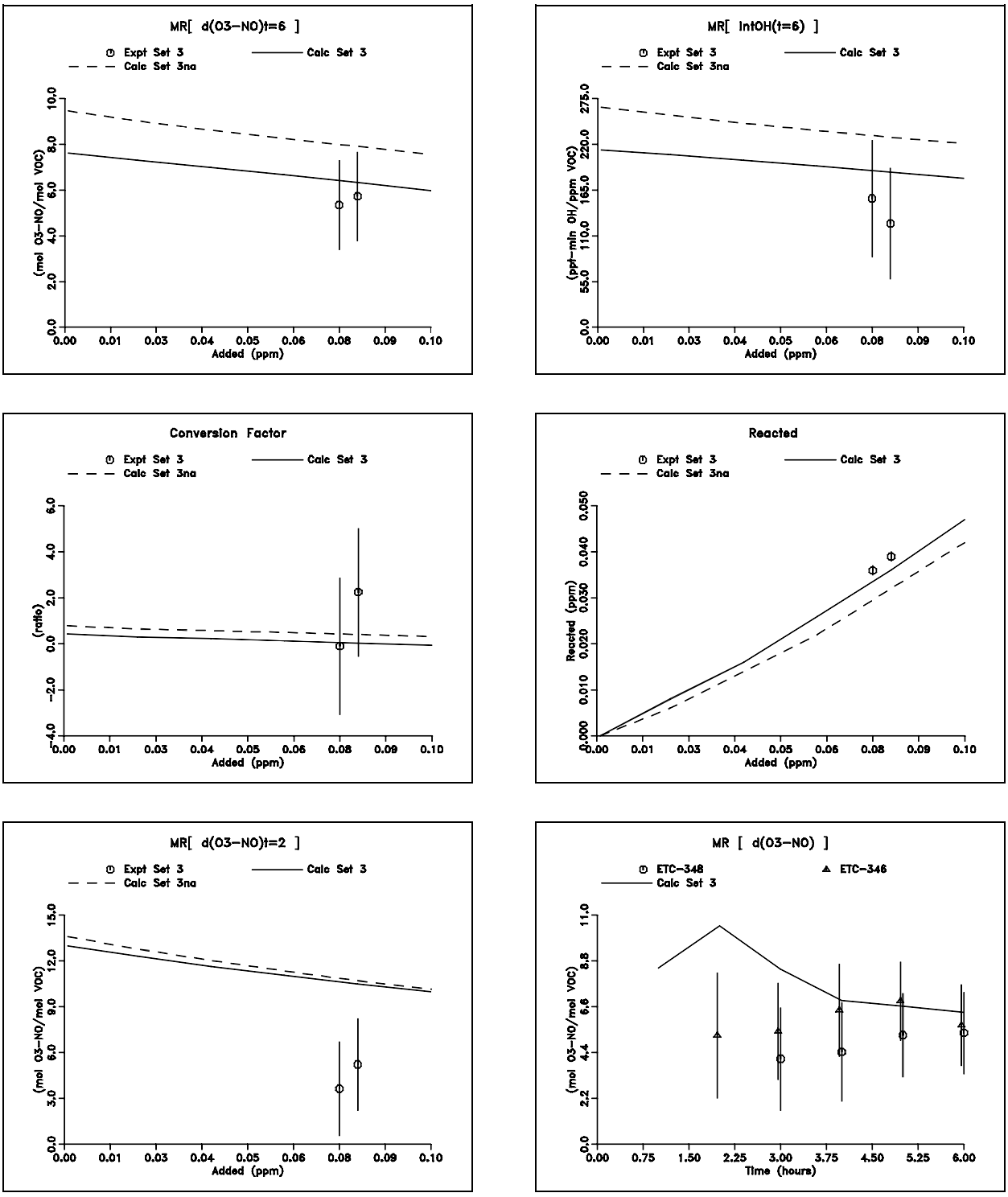

Figure A-19. Plots of experimental and calculated reactivity results for **p-Xylene**.

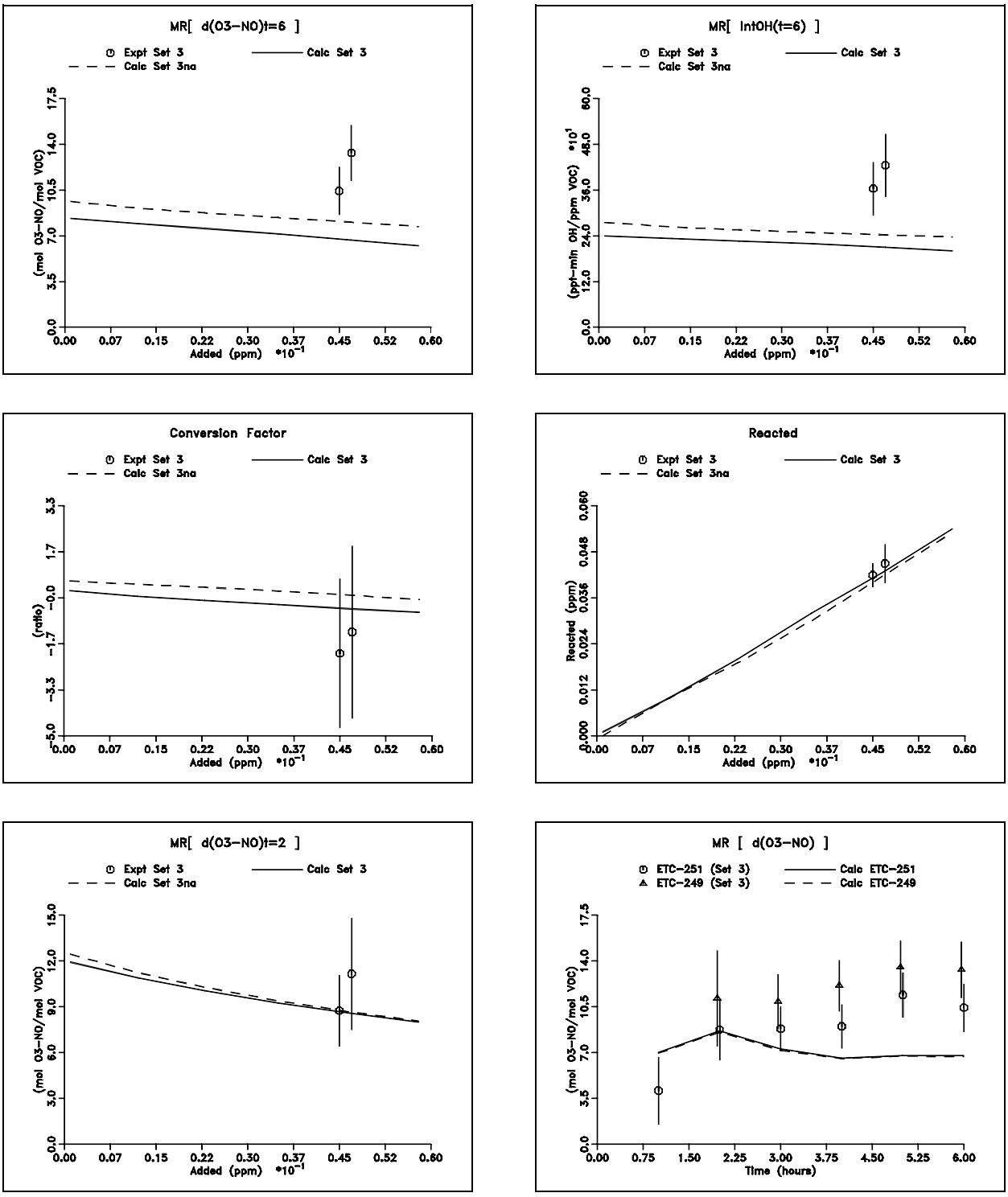

Figure A-20. Plots of experimental and calculated reactivity results for **135-trimethyl Benzene**.

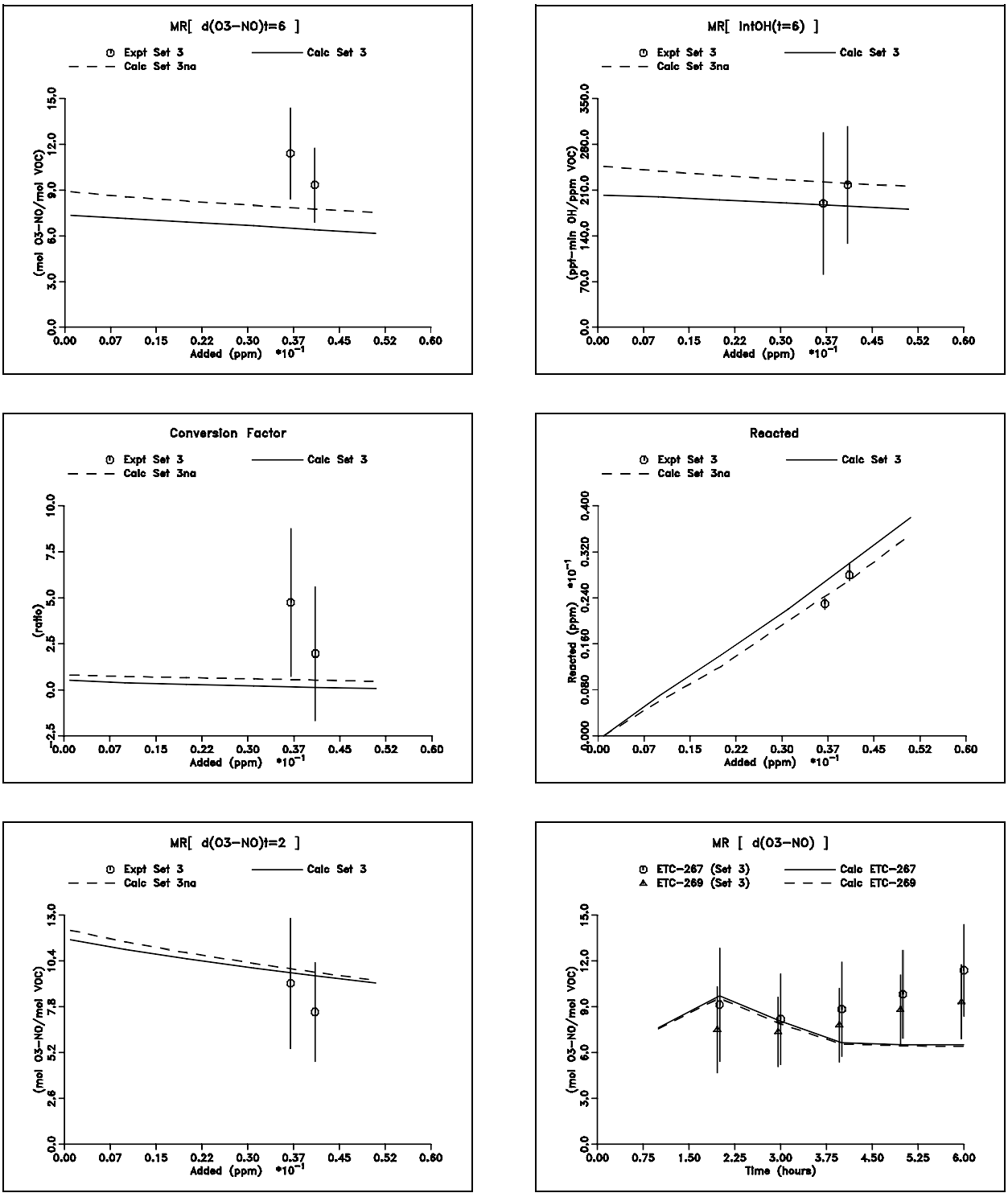

Figure A-21. Plots of experimental and calculated reactivity results for **124-trimethyl Benzene**.

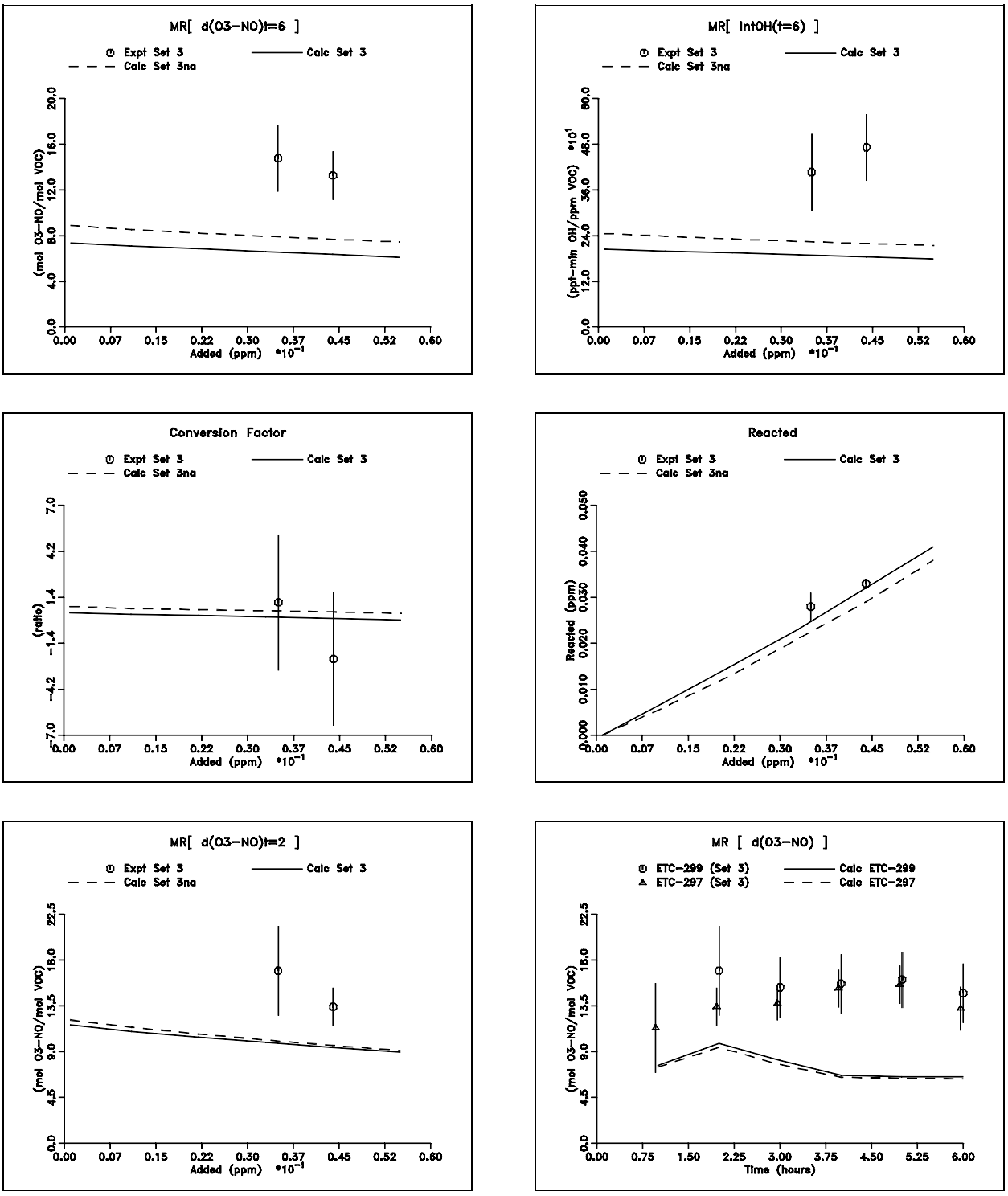

Figure A-22. Plots of experimental and calculated reactivity results for **123-trimethyl Benzene**.

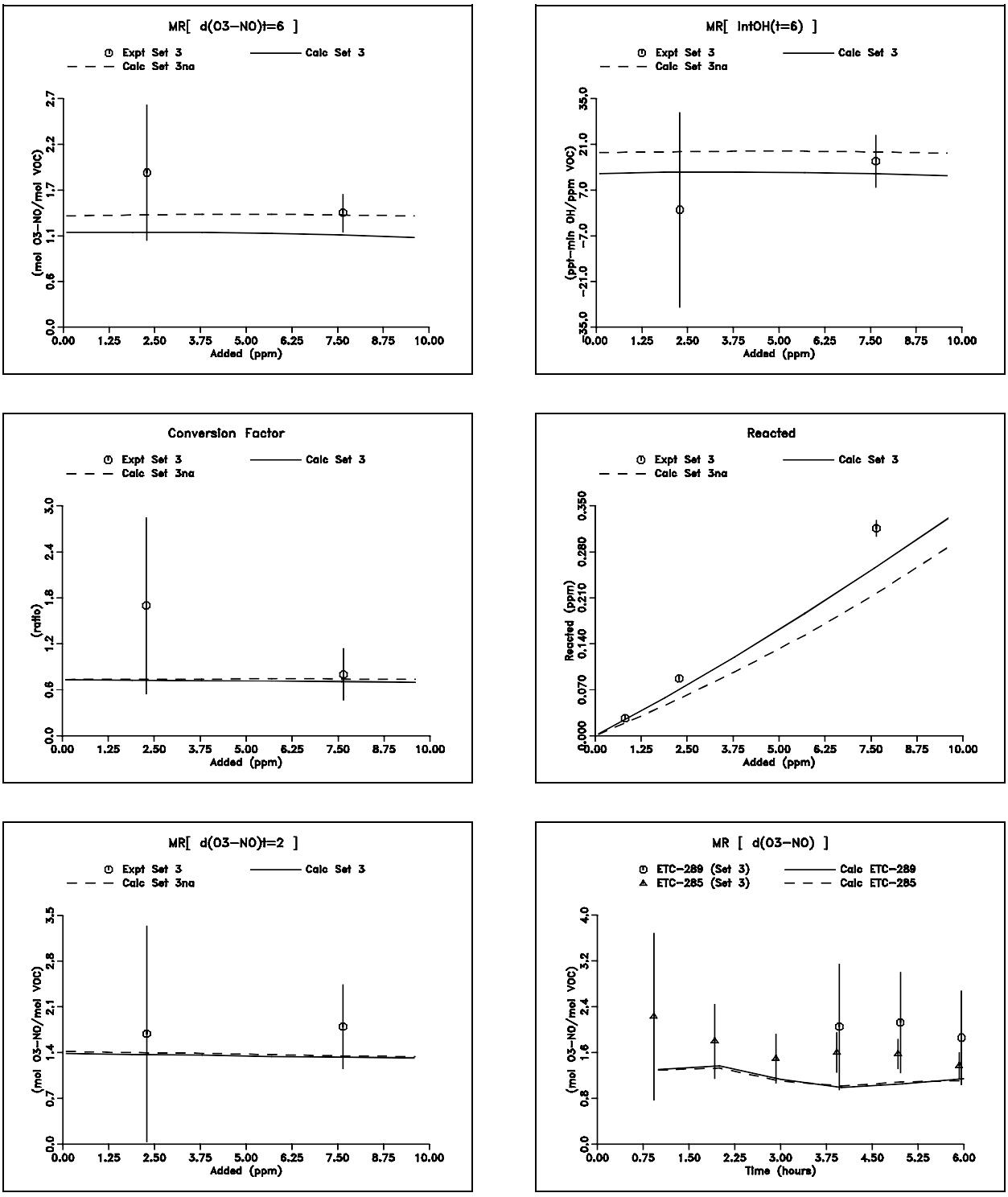

Figure A-23. Plots of experimental and calculated reactivity results for **Methanol**.

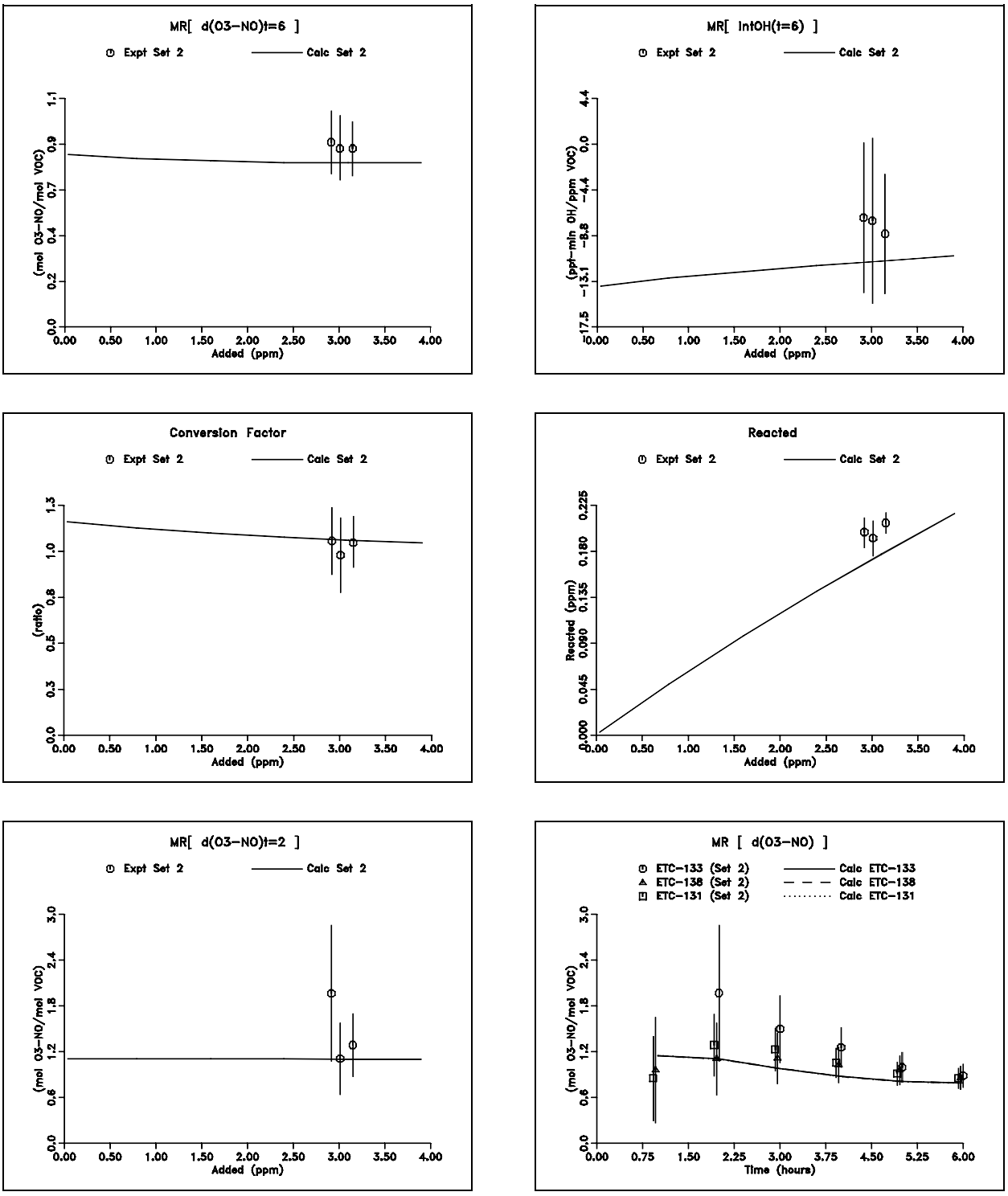

Figure A-24. Plots of experimental and calculated reactivity results for **Ethanol**.

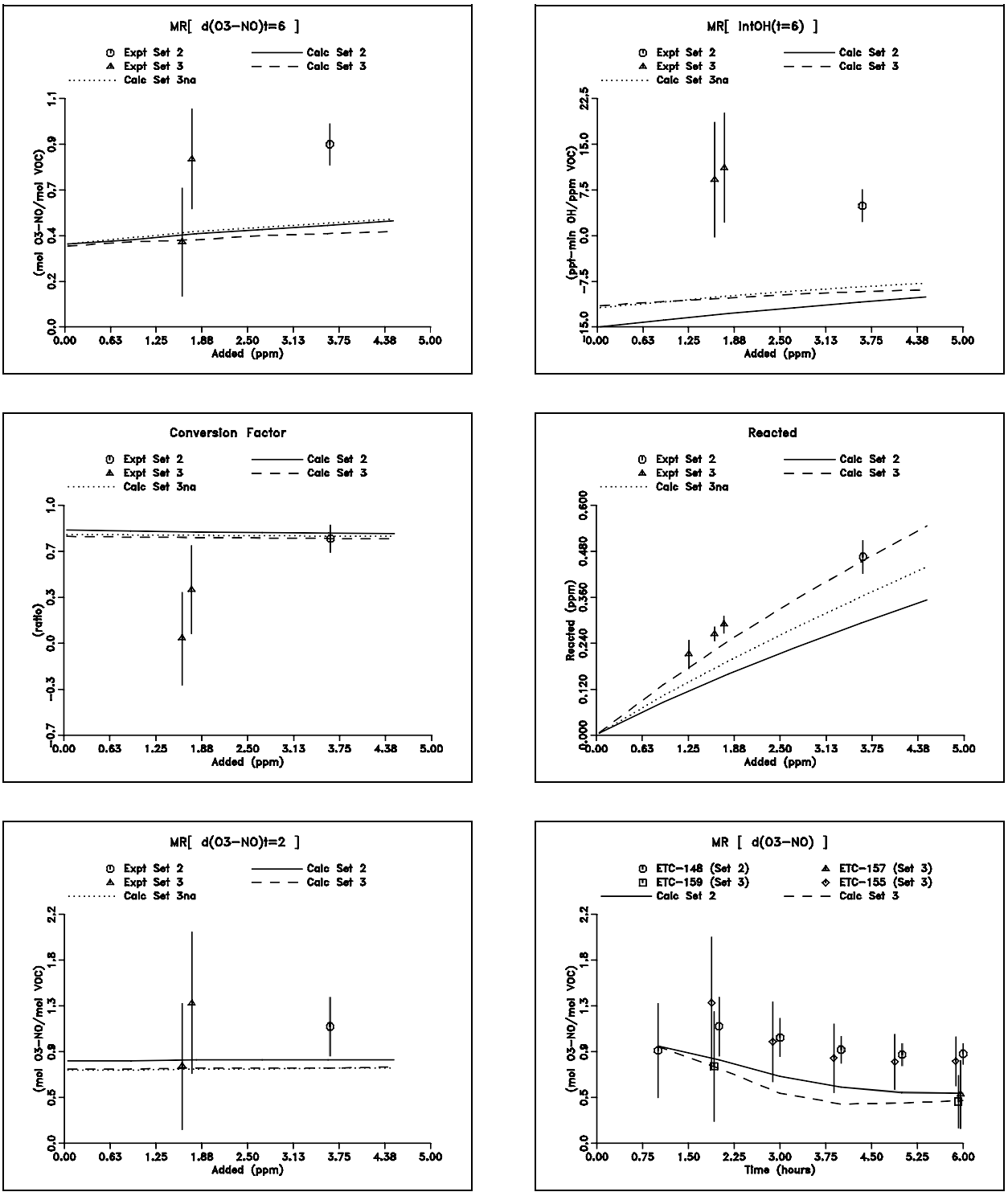

Figure A-25. Plots of experimental and calculated reactivity results for **Isopropanol**.

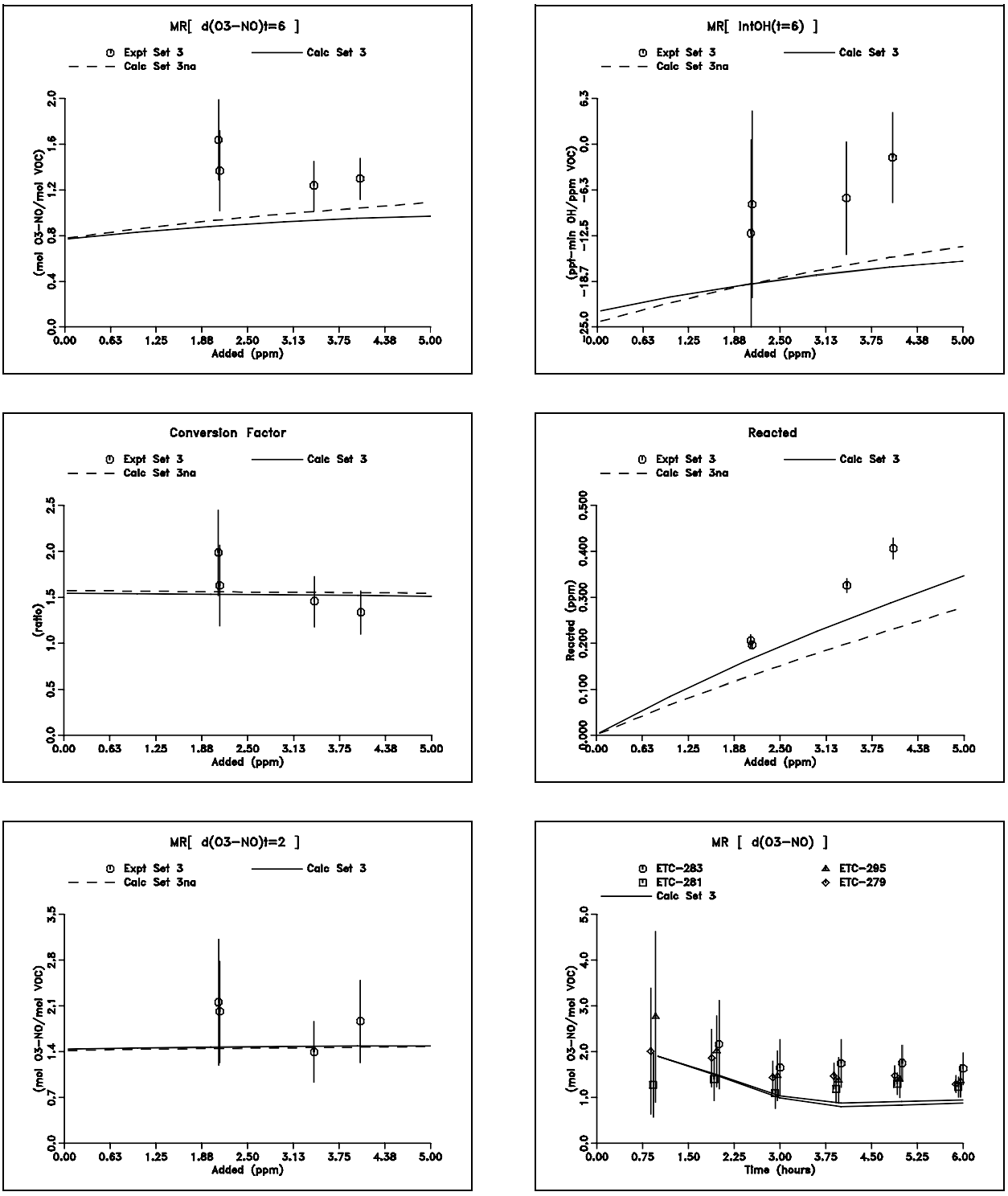

Figure A-26. Plots of experimental and calculated reactivity results for **Dimethyl Ether**.

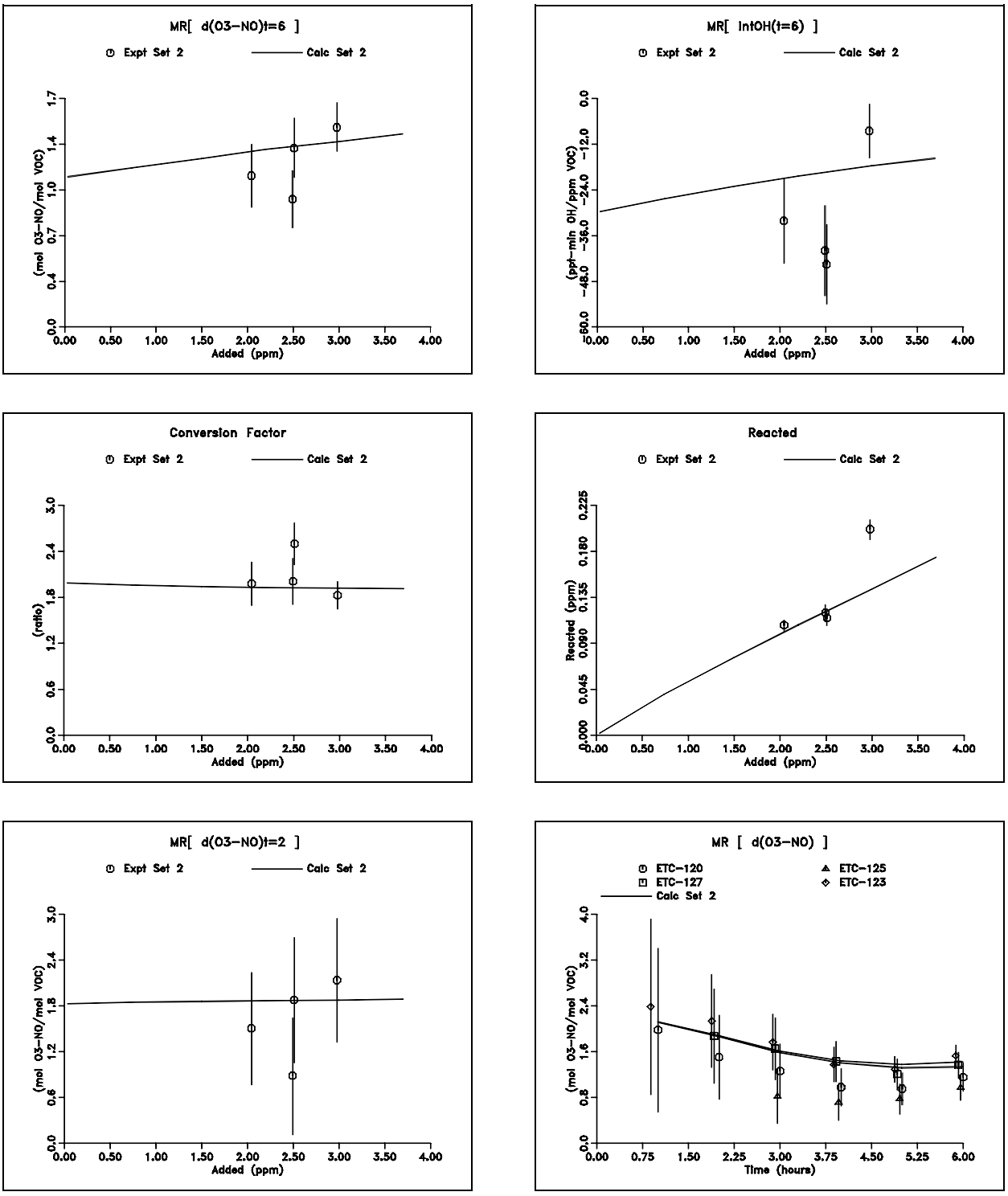

Figure A-27. Plots of experimental and calculated reactivity results for **MTBE**.

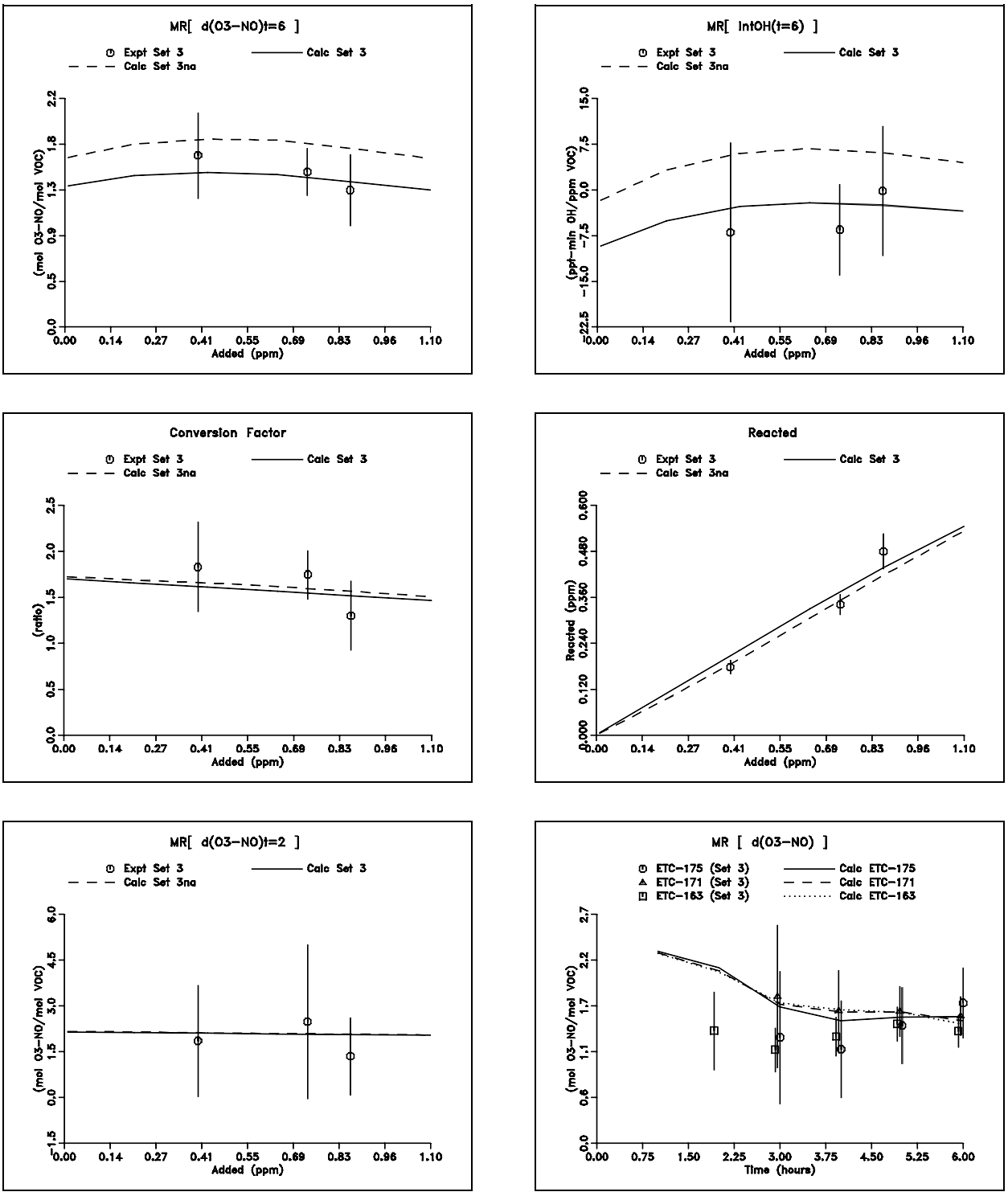

Figure A-28. Plots of experimental and calculated reactivity results for **Ethoxyethanol**.

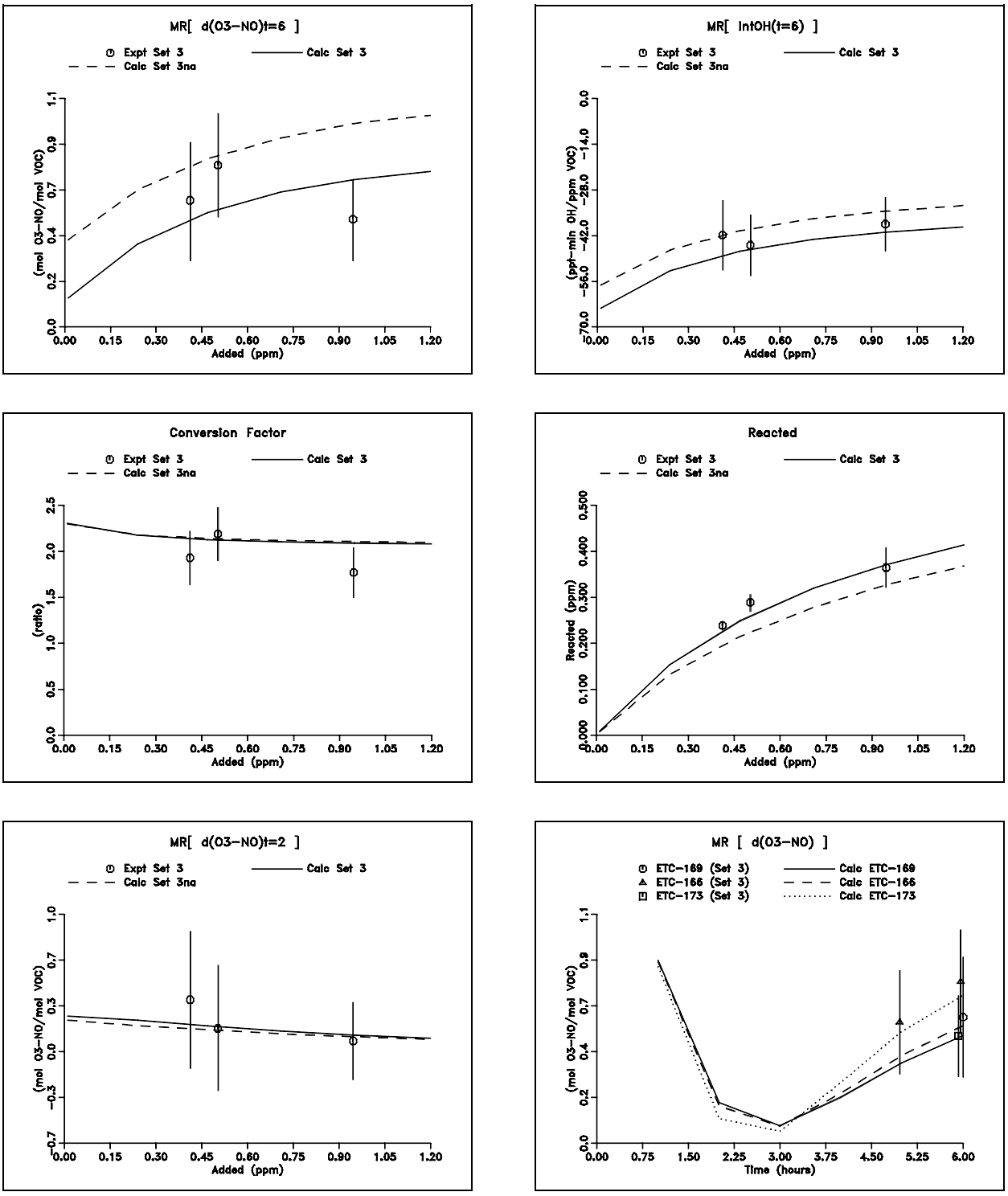

Figure A-29. Plots of experimental and calculated reactivity results for **Carbitol**.

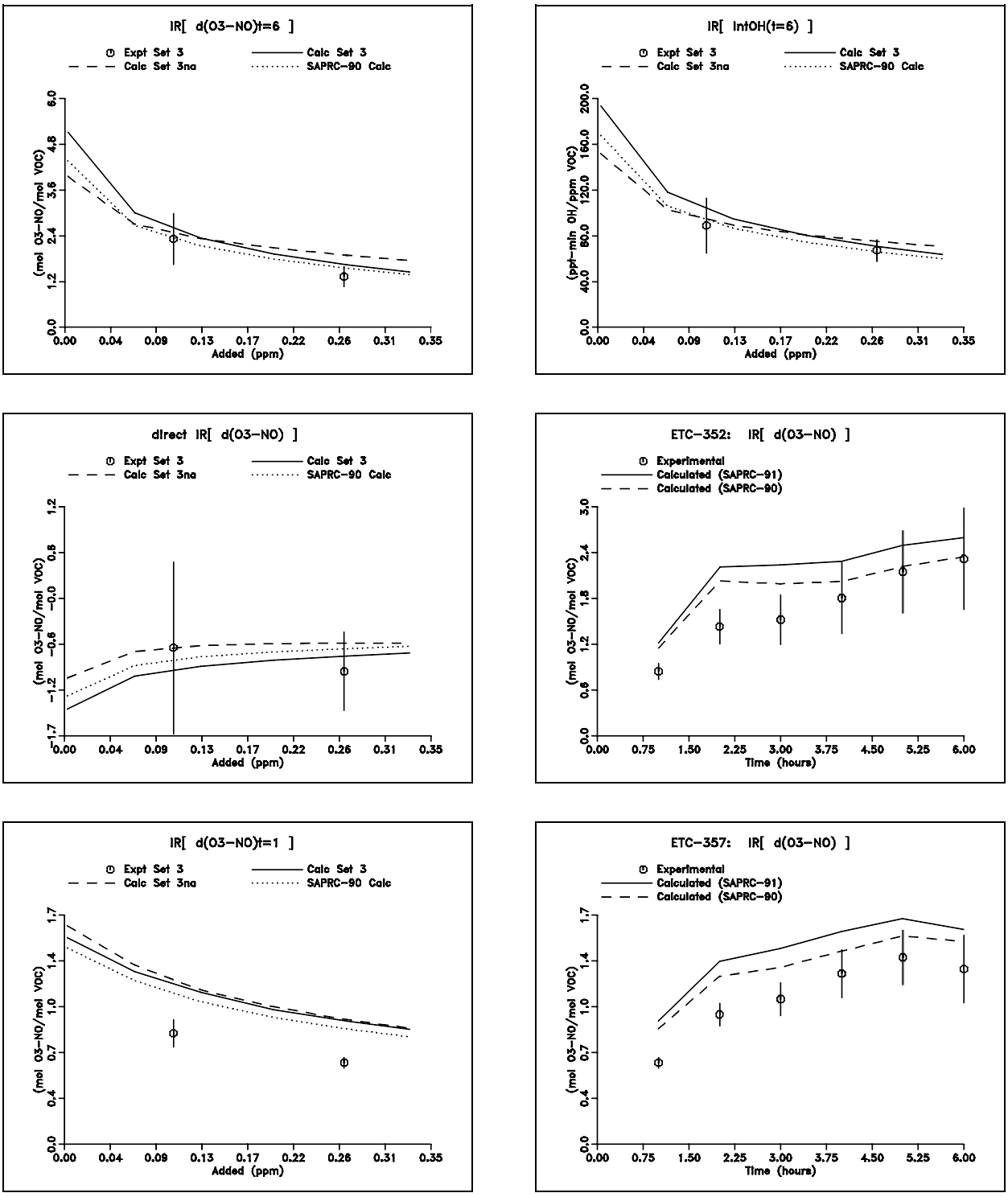

Figure A-30. Plots of experimental and calculated reactivity results for **Formaldehyde**.

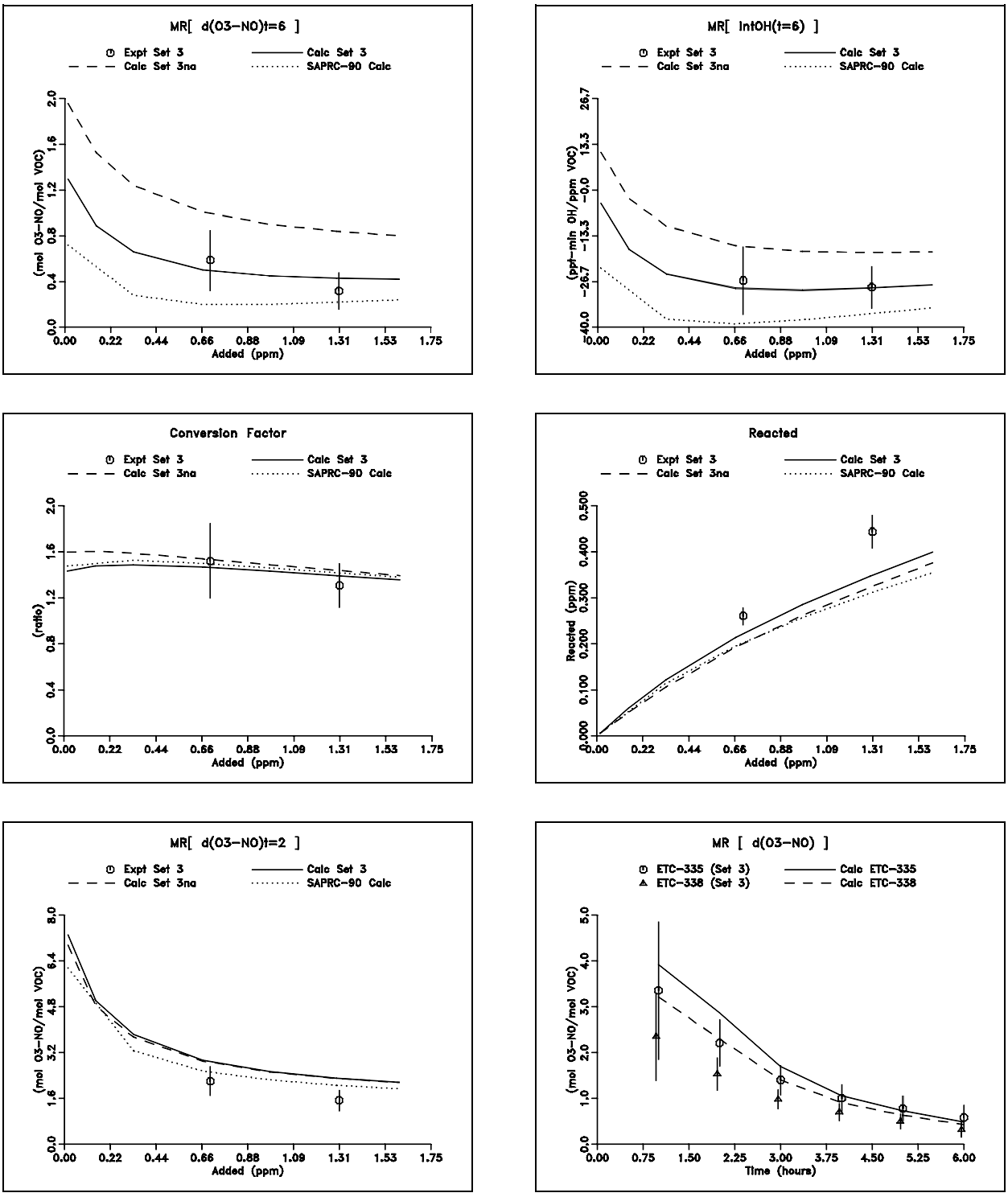

Figure A-31. Plots of experimental and calculated reactivity results for **Acetaldehyde**.

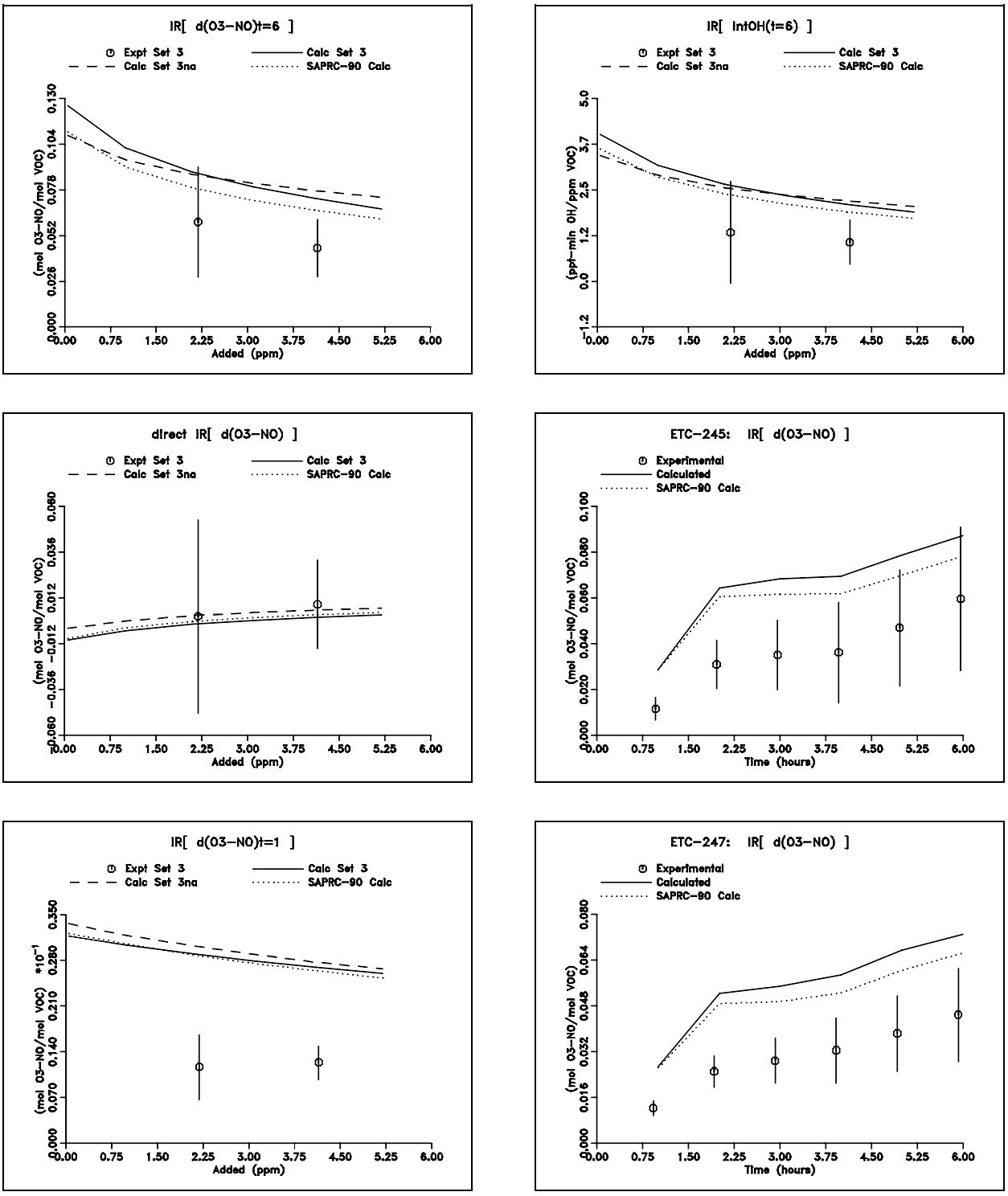

Figure A-32. Plots of experimental and calculated reactivity results for **Acetone**.

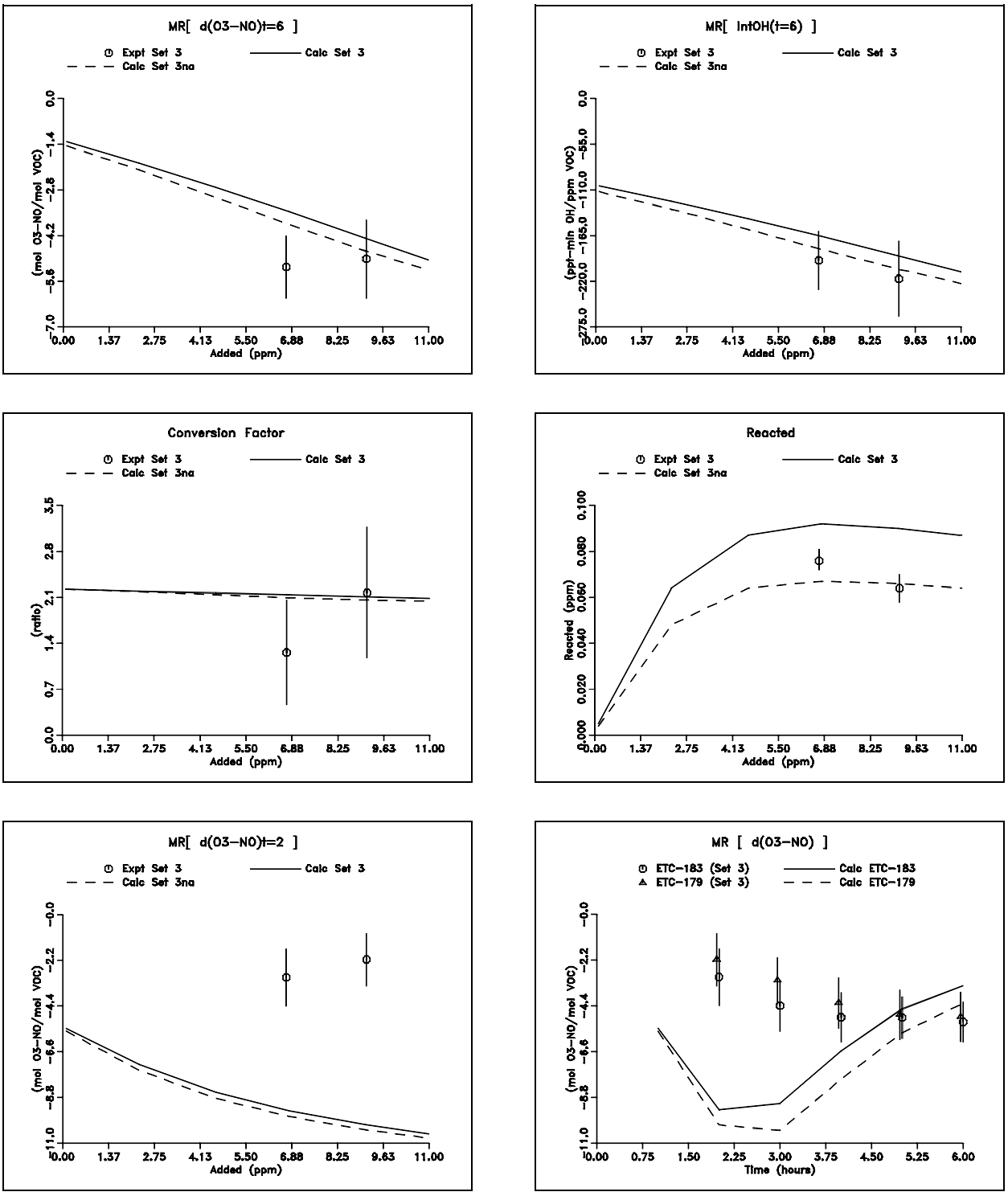

Figure A-33. Plots of experimental and calculated reactivity results for **Hexamethyldisiloxane**.

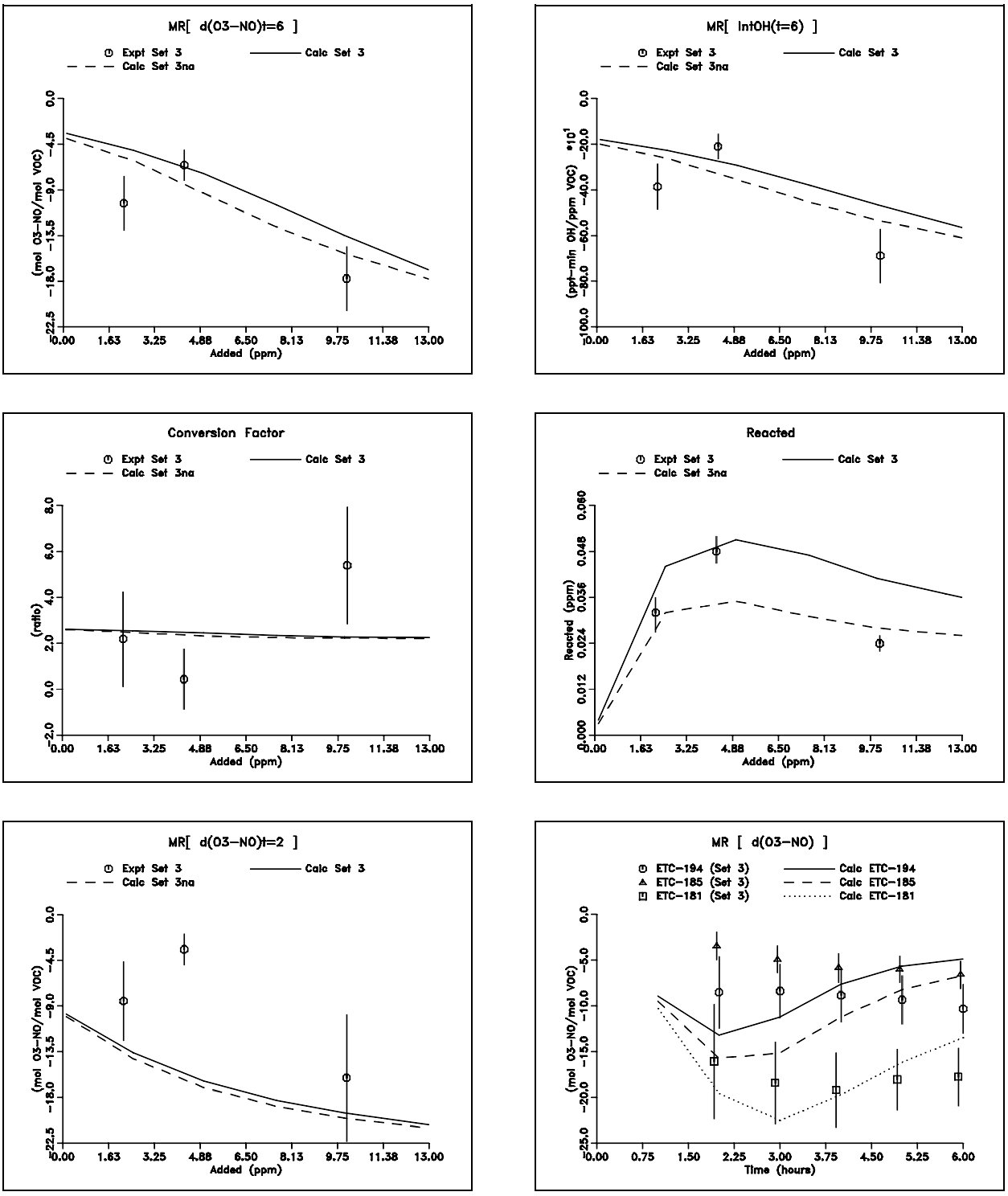

Figure A-34. Plots of experimental and calculated reactivity results for **Octamethylcyclotetrasiloxane**.

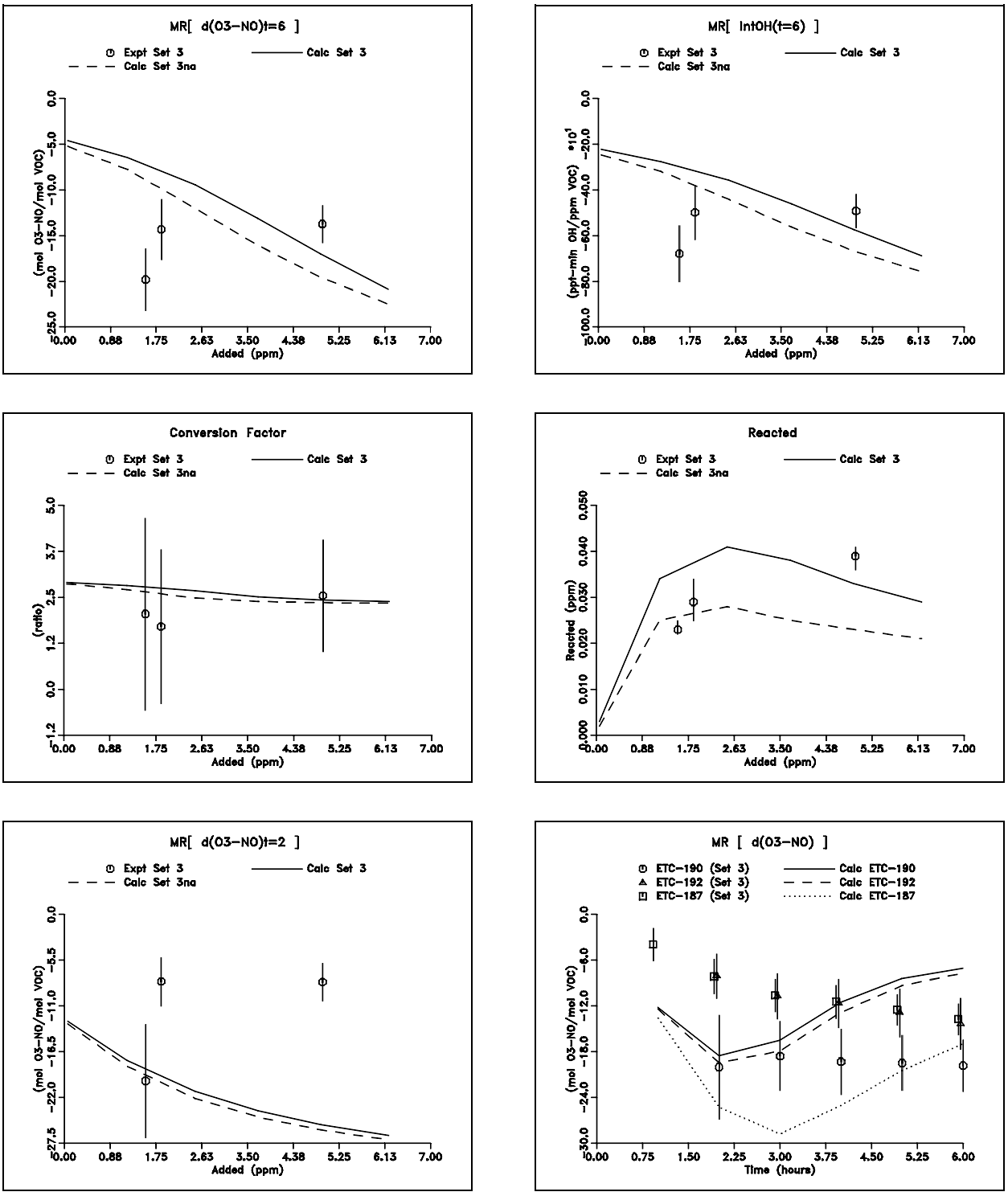

Figure A-35. Plots of experimental and calculated reactivity results for **Decamethylcyclopentasiloxane**.

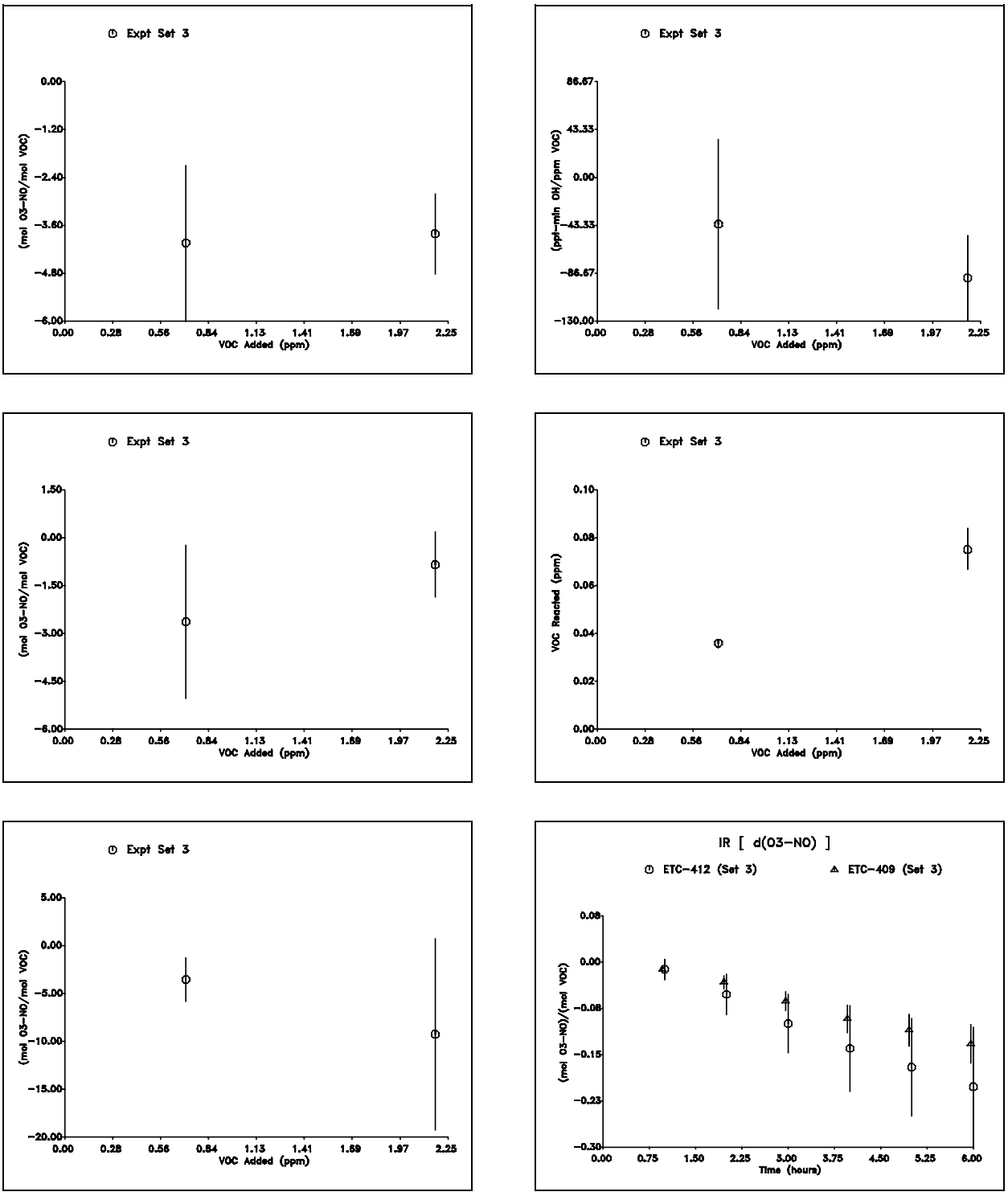

Figure A-36. Plots of experimental reactivity results for **Pentamethyldisiloxanol**.

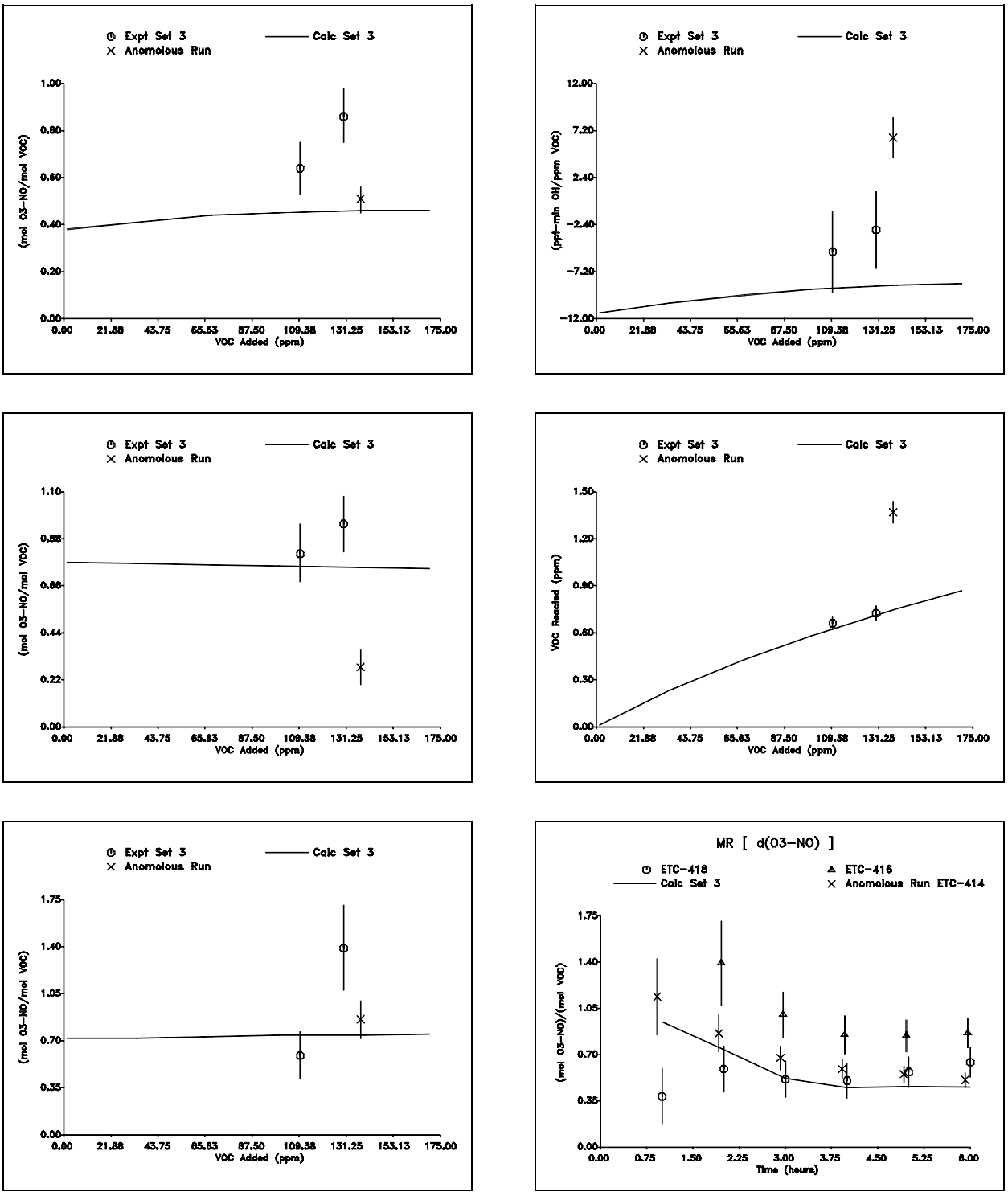

Figure A-37. Plots of experimental and calculated reactivity results for **Carbon Monoxide**.

APPENDIX B

EXAMPLE OF DATA CALCULATIONS: ETC-226

This Appendix provides an illustration of how all the experimentally derived quantities were calculated for a selected added test VOC experiment. This includes calculations of the 6-hour d(O_3-NO), IntOH, amount of test VOC reacted, base case results, the incremental and mechanistic d(O_3-NO), IntOH, and direct reactivities, and the estimated uncertainties in all these quantities. This appendix was generated using the Mathcad 3.1 computer program (MathSoft, 1992). The example run chosen was added propane run ETC-226, where the amount reacted was estimated using the IntOH method.

The format of this appendix is as follows: Text in **bold font** are comments which are ignored by the Mathcad program. Expressions of the form

function(var1,var2,...):=expression

give definitions of functions. Expressions of the form

variable:=expression

assign a variable the value which is the result of the mathematical operations and/or function evaluations in the expression. Expressions of the form

variable=value

give the current value of the variable. The numerical value on the right of the "=" is output by the program, and can be compared with the results for this run in the data tabulations. Slight differences may be due to roundoff error — the Mathcad program is used for illustrative purposes only; the actual data were processed using FORTRAN programs.

The names of the variables could not be the same as used in the text to avoid confusion of subscripts and superscripts with exponentiation. However, they should be reasonably self-explanatory, or obvious from the comments preceding them. The prefix "u" is used to indicate the uncertainty of the variable.

Constants For Set 3 Runs

$Dt := .029$	**Dilution x Time (6 hrs x 0.48%/hr)**
$uDt := .0150$	**Uncertainty in Dt (6 hrs x 0.26%/hr)**
$kOHxyl := 3.46 \cdot 10^4$	**kOH for tracer (m-xylene) (ppm-1 min-1 units)**
$kOHvoc := 1.71 \cdot 10^3$	**kOH for Propane**
$Xyl0avg := .0999$	**Average Initial m-Xylene (ppm)**
$Hex0avg := .387$	**Average Initial n-Hexane (ppm)**
$NO0avg := .391$	**Average Initial NO (ppm)**
$k1avg := .320$	**Average of Assigned NO2 photolysis rate (min-1)**
$avgTavg := 301.4$	**Average of Run's Average Temperatures**

Initial Concentrations and Run Conditions

$VOC0 := 11.57$	**Initial propane (ppm)**
$uVOC0 := .23$	**Uncertainty in initial propane (precision only)**
$Xyl0 := .1017$	**Initial m-Xylene (ppm)**
$Hex0 := .403$	**Initial n-Hexane (ppm)**
$NO0 := .372$	**Initial NO (ppm)**
$k1 := .315$	**Assigned NO2 photolysis rate (min-1)**
$avgT := 300.0$	**Average Temperature**
$lnXyl0 := 2.29$	**Initial -ln[m-Xylene (ppm)] (from fit to data using eq. (XXVI)**
$ulnXyl0 := 0.02$	**Uncertainty in initial ln[m-Xylene] (from fit to eq. XXVI)**

Final (t = 6 hour) Concentrations

$VOC6 := 11.112$	**Final propane (ppm)**
$uVOC6 := .304$	**Uncertainty in final propane (ppm)**
$lnXyl6 := 2.735$	**Final -ln[m-Xylene] (from fit to eq. XXVI)**
$ulnXyl6 := 0.02$	**Uncertainty in final -ln[m-Xylene]**
$dO3NOtest := 0.736$	**Final d(O3-NO) (ppm)**

Computation of IntOH.

$$dlnXyl := lnXyl6 - lnXyl0 \qquad dlnXyl = 0.445$$

$$udlnXyl := \sqrt{ulnXyl0^2 + ulnXyl6^2} \qquad udlnXyl = 0.028$$

$$IntOH(dlnXyl, Dt) := \frac{dlnXyl - Dt}{kOHxyl}$$

$$uIntOH := \frac{\sqrt{ulnXyl6^2 + ulnXyl0^2 + uDt^2}}{kOHxyl}$$

Determine amount of propane reacted: Direct method

$$TstRcdD := VOC0 - VOC6 - Dt \cdot \frac{VOC0 + VOC6}{2} \qquad TstRcdD = 0.129$$

$$uTstRcdD := \sqrt{uVOC0^2 + uVOC6^2 + \left(uDt \cdot \frac{VOC0 + VOC6}{2}\right)^2} \qquad uTstRcdD = 0.417$$

Determine amount of propane reacted: IntOH method (Eq. XXIX):

$$TstRcdI(VOC0, dlnXyl, Dt, kOHvoc) := \frac{VOC0 \cdot kOHvoc \cdot IntOH(dlnXyl, Dt)}{kOHvoc \cdot IntOH(dlnXyl, Dt) + Dt} \cdot \left(1 - e^{-kOHvoc \cdot IntOH(dlnXyl, Dt) - Dt}\right)$$

$$TstRcdI(VOC0, dlnXyl, Dt, kOHvoc) = 0.232$$

$$uTstRcdI := \sqrt{\begin{aligned} &\left(uVOC0 \cdot \frac{d}{dVOC0} TstRcdI(VOC0, dlnXyl, Dt, kOHvoc)\right)^2 ... \\ &+ \left(udlnXyl \cdot \frac{d}{ddlnXyl} TstRcdI(VOC0, dlnXyl, Dt, kOHvoc)\right)^2 ... \\ &+ \left(uDt \cdot \frac{d}{dDt} TstRcdI(VOC0, dlnXyl, Dt, kOHvoc)\right)^2 \end{aligned}}$$

$$uTstRcdI = 0.019$$

Use least uncertain estimate for amount reacted. But add 20% uncertainty in kOHvoc to uTstRcd for the purposes of comparison.

$$uTstRcdIchk := \sqrt{uTstRcdI^2 + \left(0.2 \cdot kOHvoc \cdot \frac{d}{dkOHvoc} TstRcdI(VOC0, dlnXyl, Dt, kOHvoc)\right)^2}$$

$uTstRcdIchk = 0.05$ **Uncertainty in IntOH method**

$uTstRcdD = 0.417$ **Uncertainty in direct method**

IntOH method has least uncertainty, so amount propane reacted and its uncertaity are:

$TstRcd := TstRcdI(VOC0, dlnXyl, Dt, kOHvoc)$ $TstRcd = 0.232$

$uTstRcd := uTstRcdI$ $uTstRcd = 0.019$

Base case estimates for t=6 (Regression coefficients from Table 4.)

$$dO3NObase := .7356 + .0558\cdot(avgT - avgTavg) + 2.90\cdot(Xyl0 - Xyl0avg) \ldots + 1.26\cdot(k1 - k1avg) - 0.42\cdot(NO0 - NO0avg) - 0.37\cdot(Hex0 - Hex0avg)$$

$dO3NObase = 0.658$ **(ppm)**

$udO3NObase := .047$ **Uncertainty of regression estimate**

$IntOHbase := 22.26 + 84.13\cdot(Xyl0 - Xyl0avg) - 16.04\cdot(NO0 - NO0avg) + 1.56\cdot(avgT - avgTavg)$

$IntOHbase = 20.532$ **(ppb-min)**

$uIntOHbase := 1.9$ **Uncertainty of regression estimate**

$ConvRbase := 17.08\cdot(NO0 - NO0avg) + 33.18$

$ConvRbase = 32.855$ **(10^3 min^-1)**

$uConvRbase := 3.0$ **Uncertainty of regression estimate**

Computation of d(O3-NO) incremental and mechanistic reactivities

$Change := dO3NOtest - dO3NObase$ $Change = 0.078$

$udO3NOtest := udO3NObase$ **Test run d(O3-NO) uncertainty estimated from variability in base case runs**

$uChange := \sqrt{udO3NOtest^2 + udO3NObase^2}$ $uChange = 0.066$

Incremental Reactivity (mol O3-NO/mol VOC added)

$IRdO3NO := \frac{Change}{VOC0}$ $IRdO3NO = 0.007$

$uIRdO3NO := \left| IRdO3NO\cdot\sqrt{\left(\frac{uChange}{Change}\right)^2 + \left(\frac{uVOC0}{VOC0}\right)^2}\right|$ $uIRdO3NO = 0.006$

Mechanistic Reactivity (mol O3-NO/mol VOC reacted)

$MRdO3NO := \frac{Change}{TstRcd}$ $MRdO3NO = 0.334$

$uMRdO3NO := \left| MRdO3NO\cdot\sqrt{\left(\frac{uChange}{Change}\right)^2 + \left(\frac{uTstRcd}{TstRcd}\right)^2}\right|$ $uMRdO3NO = 0.288$

Convert to ppt-min units

$IntOHtest := 10^6 \cdot IntOH(dlnXyl, Dt)$ $IntOHtest = 12.023$

$uIntOHtest := 10^6 \cdot uIntOH$ $uIntOHtest = 0.925$

Computation of IntOH Reactivities

Test run uncertainty must be at least as great as base run estimate, to account for uncertainty due to run to run variability. So set uIntOHtest to larger of uIntOHbase uIntOHtest..

$uIntOHtest := if(uIntOHtest > uIntOHbase, uIntOHtest, uIntOHbase)$

$uIntOHtest = 1.9$

$Change := IntOHtest - IntOHbase$ $Change = -8.509$

$uChange := \sqrt{uIntOHtest^2 + uIntOHbase^2}$ $uChange = 2.687$

Incremental Reactivity (ppt-min IntOH/ppm VOC added)

$$IRIntOH := \frac{Change}{VOC0} \qquad IRIntOH = -0.735$$

$$uIRIntOH := \left| IRIntOH \cdot \sqrt{\left(\frac{uChange}{Change}\right)^2 + \left(\frac{uVOC0}{VOC0}\right)^2} \right| \qquad uIRIntOH = 0.233$$

Mechanistic Reactivity (ppt-min IntOH/ppm VOC reacted)

$$MRIntOH := \frac{Change}{TstRcd} \qquad MRIntOH = -36.665$$

$$uMRIntOH := \left| MRIntOH \cdot \sqrt{\left(\frac{uChange}{Change}\right)^2 + \left(\frac{uTstRcd}{TstRcd}\right)^2} \right| \qquad uMRIntOH = 11.966$$

Computation of Direct Reactivity

O3-NO due to reactions of base ROG in test run (Eq. XIV)
(10^-3 converts units back to ppm, since IntOH is in ppt-min, and ConvR is in 10^3 min-1)

$$dO3NObaseROGtest := ConvRbase \cdot IntOHtest \cdot 10^{-3} \qquad dO3NObaseROGtest = 0.395$$

$$udO3NObaseROGtest := dO3NObaseROGtest \cdot \sqrt{\left(\frac{uConvRbase}{ConvRbase}\right)^2 + \left(\frac{uIntOHtest}{IntOHtest}\right)^2}$$

$$udO3NObaseROGtest = 0.072$$

Direct Incremental Reactivity (mol O3-NO/mol VOC added)

$$IRdirect := \frac{dO3NOtest - dO3NObaseROGtest}{VOC0} \qquad IRdirect = 0.029$$

$$uIRdirect := \left| IRdirect \cdot \sqrt{\left(\frac{udO3NObaseROGtest}{dO3NOtest - dO3NObaseROGtest}\right)^2 + \left(\frac{uVOC0}{VOC0}\right)^2} \right|$$

$$uIRdirect = 0.006$$

Direct Mechanistic Reactivity, ConvF (mol O3-NO/mol VOC reacted)

$$ConvF := \frac{dO3NOtest - dO3NObaseROGtest}{TstRcd} \qquad ConvF = 1.469$$

$$uConvF := \left| ConvF \cdot \sqrt{\left(\frac{udO3NObaseROGtest}{dO3NOtest - dO3NObaseROGtest}\right)^2 + \left(\frac{uVOC0}{VOC0}\right)^2} \right|$$

$$uConvF = 0.312$$